Synthesis and biodegradation of marine cyclopeptides derived from laxaphycin B

Laurine Darcel

THÈSE

Pour obtenir le grade de

Docteur

Délivré par

UNIVERSITE DE PERPIGNAN VIA DOMITIA

Préparée au sein de l'école doctorale

ED 305 Énergie et Environnement

Et de l'unité de recherche

USR 3278 – CRIOBE – EPHE-CNRS-UPVD

Spécialité : **Chimie**

Présentée par

Laurine DARCEL

Synthèse et biotransformation de cyclopeptides d'origine marine dérivés de la laxaphycine B

Soutenue le **6 septembre 2021** devant le jury composé de

Mme. Aurélie TASIEMSKI, Maître de conférences, HDR. *Université de Lille*	Examinateur
Mme. Céline LANDON, Chargée de recherche, HDR. *Centre National de la Recherche Scientifique, Orléans*	Présidente
Mr. Sébastien DUTERTRE, Chargé de recherche, HDR. *Université de Montpellier*	Rapporteur
Mr. Didier BOTURYN, Directeur de recherche, HDR. *Centre National de la Recherche Scientifique, Grenoble*	Rapporteur
Mr. Gilles SUBRA, Professeur des Universités. Université de Montpellier	Examinateur
Mr. Joël RICHARD, Chief Development Officer, HDR. *Medincell, Jacou*	Examinateur
Mr. Bernard BANAIGS, Chargé de recherche, HDR. *Université de Perpignan Via Domitia*	Directeur de thèse
Mr. Nicolas INGUIMBERT, Professeur des Universités. *Université de Perpignan Via Domitia*	Co-directeur

Thesis submitted for the degree of
Doctor of Philosophy

Delivered by
UNIVERSITE DE PERPIGNAN VIA DOMITIA

Prepared at the doctoral school
ED 305 Energie et Environnement
And the research unit
USR 3278 – CRIOBE – EPHE-CNRS-UPVD

Major
CHEMISTRY

By
Laurine DARCEL

THESIS TITLE
Synthesis and biotransformation of marine cyclopeptides derived from laxaphycin B

Defended on September 6, 2021

Before the jury composed of

Mme. Aurélie TASIEMSKI, Maître de conférences, HDR. *Université de Lille*	Examiner
Mme. Céline LANDON, Chargée de recherche, HDR. *Centre National de la Recherche Scientifique, Orléans*	President
Mr. Sébastien DUTERTRE, Chargé de recherche, HDR. *Université de Montpellier*	Reporter
Mr. Didier BOTURYN, Directeur de recherche, HDR. *Centre National de la Recherche Scientifique, Grenoble*	Reporter
Mr. Gilles SUBRA, Professeur des Universités. Université de Montpellier	Examiner
Mr. Joël RICHARD, Chief Development Officer, HDR. *Medincell, Jacou*	Examiner
Mr. Bernard BANAIGS, Chargé de recherche, HDR. *Université de Perpignan Via Domitia*	Thesis director
Mr. Nicolas INGUIMBERT, Professeur des Universités. *Université de Perpignan Via Domitia*	Co-director

Je dédie cette thèse aux étoiles qui m'ont soutenue et éclairée de loin, à mon grand-père Michel, à mon frère de cœur Mikaly...

Avant-propos

Ce mémoire de thèse est rédigé en anglais et comprend deux articles publiés ainsi qu'une revue scientifique publiée. Le contenu de la revue scientifique fait l'objet du chapitre 1 bibliographique. Les deux articles ont été intégrés dans les chapitres 2 et 3, et complétés par des informations décrivant le processus d'évolution du travail de thèse. Le chapitre 4 vient compléter les travaux effectués dans les chapitres 2 et 3, mais n'a cependant pas été publié. Chaque chapitre contient sa propre partie expérimentale avec les caractérisations des produits étudiés dans le chapitre. Une partie annexe nommée « Supporting Information » reprend les protocoles et paramètres communs à tous les chapitres. Enfin, les références sont toutes listées à la fin de ce manuscrit.

Ce travail de thèse a été réalisé au sein du Centre de Recherches Insulaires et Observatoire de l'Environnement (CRIOBE, USR CNRS-EPHE-UPVD 3278), sur une durée de 3 ans, financé par l'Université de Perpignan sous forme d'un contrat doctoral de l'école doctorale Énergie et Environnement 305. Un soutien financier de la Fédération de Recherche Énergie Environnement (FREE) a également permis à l'avancement du projet.

Les analyses LC-MSn et RMN ont été réalisées sur le plateau technique de la plateforme Bio2Mar, à Perpignan.

Les récoltes du matériel biologique, ainsi que les dissections ont été effectuées au sein du CRIOBE à Moorea (Polynésie Française) par des collaborateurs du projet.

Remerciements

Je souhaite tout d'abord remercier Sébastien Dutertre, Didier Boturyn, Céline Landon, Aurélie Tasiemski, Gilles Subra et Joël Richard pour m'avoir fait l'honneur de juger mon travail de thèse.

J'aimerai également remercier les membres de mon comité de suivi de thèse, Gilles Subra, Gérald Culioli et Julio Sáez-Vásquez pour leurs conseils aussi bien sur mon travail que sur mon projet professionnel. Un grand merci à Gilles Subra, qui en plus de ses conseils avisés pendant ma thèse, m'a accompagnée auprès de Sonia Cantel pendant mon stage de fin d'étude en me transmettant ses connaissances toujours avec une passion communicative.

Je remercie chaleureusement mes directeurs de thèse, Nicolas Inguimbert et Bernard Banaigs, de m'avoir fait confiance pour travailler sur ce projet et d'avoir été disponibles au quotidien malgré leurs emplois du temps chargés. Ils ont su me transmettre leurs connaissances scientifiques et m'accompagner au mieux tout au long de ce travail, aussi bien professionnellement que personnellement. Je les remercie également pour leurs corrections avisées sur mes articles et ce manuscrit de thèse.

Je tiens également à remercier Isabelle Bonnard et Suzanne Mills pour avoir apporté leur vision et leur aide pendant la rédaction de mes articles. Malgré la distance entre Perpignan et Moorea, Suzanne Mills a été un des piliers de ce travail de thèse, en permettant la récolte du matériel biologique nécessaire à mon travail.

Je remercie le Laboratoire Génome et Développement des Plantes, et plus particulièrement Julio Sáez-Vásquez, pour l'accueil et l'aide matérielle apportés dans ce projet.

Je souhaite également remercier Delphine Raviglione et Jennifer Sola, pour m'avoir permis d'effectuer mes analyses dans les meilleures conditions possibles et d'avoir toujours été présentes en soutien de notre travail.

J'aimerai remercier tous mes collègues du laboratoire pour m'avoir si bien accueillie et intégrée. Je me rappellerai nos repas pleins de rires et de votre bonne humeur au quotidien. Une mention spéciale pour mes collègues doctorants, Mélanie, Christelle, Slimane, Christian, Hikmat et Mélina, pour avoir contribué à cette bonne ambiance au sein du laboratoire. La crise sanitaire liée au Covid ne nous a pas épargné dans nos projets, mais malgré les moments de doute, nous avons gardé le sourire !

Plus généralement, je souhaiterai remercier toutes les personnes dont j'ai croisé la route pendant mon cursus scolaire, ceux qui ont cru en moi, pour leur soutien, et ceux qui ont eu des doutes, pour m'avoir permis de me dépasser et leur prouver qu'ils avaient tort.

Enfin, je remercie profondément ma famille, et plus particulièrement mes parents qui m'ont soutenue tout au long de mes études, moralement et financièrement, et m'ont toujours poussée à faire mieux, alors quoi de plus beau pour eux aujourd'hui que de me voir arriver aux portes du titre de docteur. Je remercie mon frère pour la relation extraordinaire que nous avons tous les deux, qui nous permet de rester soudés à toute épreuve. Je souhaiterai également remercier Pierre, de m'avoir supportée au quotidien dans toutes les émotions qu'apporte une thèse, d'avoir été un pilier pour moi dans les bons comme les mauvais moments, et de m'avoir transmis sa positivité et sa bonne humeur sans faille.

Au cours de ces trois années de thèse, j'ai traversé plusieurs épreuves, tant sur les points psychologique et physique que sur les points professionnel et scientifique. J'ai affronté chacune d'elles et me suis enrichie grâce à toutes les personnes que j'ai pu rencontrer.

Alors une dernière fois, à vous tous, Merci !

Publications

Darcel, L.; Djibo, M.; Gaillard, M.; Raviglione, D.; Bonnard, I.; Banaigs, B.; Inguimbert, N. Trichormamide C Structural Confirmation through Total Synthesis and Extension to Analogs. *Org. Lett.* **2020**, *22*, 145–149, doi:10.1021/acs.orglett.9b04064.

Darcel, L.; Bornancin, L.; Raviglione, D.; Bonnard, I.; Mills, S.C.; Sáez-Vásquez, J.; Banaigs, B.; Inguimbert, N. D-Peptidase Activity in a Marine Mollusk Detoxifies a Nonribosomal Cyclic Lipopeptide: An Ecological Model to Study Antibiotic Resistance. *J. Med. Chem.* **2021**, 64, 6198–6208, doi:10.1021/acs.jmedchem.1c00249.

Darcel, L.; Das, S.; Bonnard, I.; Banaigs, B.; Inguimbert, N. Thirtieth Anniversary of the Discovery of Laxaphycins. Intriguing Peptides Keeping a Part of Their Mystery. *Marine Drugs.* **2021**, 19, 9, 473.

Communications

Darcel, L. Non-ribosomal peptides from cyanobacteria: from synthesis to biodegradation. *Poster presentation at GFPP21 (Groupe Français des Peptides et Protéines) meeting*, Amboise, France, **2019**.

Darcel, L. Synthèse et biotransformation de cyclopeptides d'origine marine dérivés de la laxaphycin B. *Video presentation at PhD students' congress of Occitania*, Perpignan, France, **2019**. **Winner of the best video thesis presentation.**

Darcel, L. Participation in the competition « Ma thèse en 180 secondes », Montpellier, France, **2020**.

Résumé

En raison du changement climatique, le lagon de Moorea en Polynésie Française est impacté par des efflorescences de cyanobactéries asphyxiant les coraux, causant la dégradation de récif et diminuant les ressources en nourriture. *Lyngbya majuscula* et *Anabaena torulosa* sont deux cyanobactéries benthiques filamenteuses qui prolifèrent sur le sable et les coraux. Elles produisent de nombreux métabolites secondaires pouvant être toxiques. *Anabaena torulosa* produit notamment des lipopeptides cycliques tels que les laxaphycins A et B, composés de 11 et 12 acides aminés, respectivement. Cette cyanobactérie a pu développer des stratégies chimiques de protection contre les brouteurs, pouvant être repoussés par les molécules toxiques produites telle que la laxaphycin B. A leur tour, les herbivores doivent contourner ces défenses et dans certains cas, ils en profitent même pour se mettre à l'abri de leurs propres prédateurs. C'est le cas de *Stylocheilus striatus*, un lièvre de mer qui se nourrit de *Lyngbya majuscula* et *Anabaena torulosa* et qui semble moins exposé à la prédation sur *Anabaena torulosa*. *Stylocheilus striatus* consomme cette dernière sans être affecté par la toxicité de la laxaphycin B. Afin de contourner cette toxicité, le lièvre de mer a mis en place un mécanisme d'adaptation permettant la biotransformation de la laxaphycin B en laxaphycin B acyclique non toxique. Alors que la laxaphycin A non toxique est bio-accumulée dans sa glande digestive, la laxaphycin B subit deux clivages successifs en position C-terminale de deux hydroxyleucines. Afin d'étudier le mécanisme enzymatique engagé dans cette biotransformation, nous avons synthétisé divers analogues de la laxaphycin B. Dans un premier temps, nous avons optimisé leur synthèse chimique, nous permettant également de confirmer la structure du trichormamide C, un peptide naturel analogue à la laxaphycin B. Dans un second temps, les analogues synthétisés ont pu être soumis à l'enzyme étudiée et ont montré la reproductibilité du clivage sur différentes séquences. Des premières caractéristiques de l'enzyme ont pu être identifiées, telles que ses spécificités de clivage. Enfin, nos efforts se sont concentrés sur le design d'une séquence peptidique minimale pour la reconnaissance de l'enzyme, afin d'envisager différentes stratégies pour l'isoler.

Mots-clés: Biotransformation ; Peptidase ; Lipopeptide cyclique ; Synthèse peptidique ; Cyanobactérie

Abstract

Due to climate change, the lagoon of Moorea in French Polynesia is impacted by cyanobacteria blooms asphyxiating corals, causing reef degradation and decreasing food resources. *Lyngbya majuscula* and *Anabaena torulosa* are two filamentous benthic cyanobacteria that proliferate on sand and corals. They produce many secondary metabolites that can be toxic. *Anabaena torulosa* produces cyclic lipopeptides such as laxaphycins A and B, composed of 11 and 12 amino acids, respectively. This cyanobacterium has been able to develop chemical strategies of protection against grazers, which can be repelled by the toxic molecules produced such as laxaphycin B. In turn, herbivores must circumvent these defenses and in some cases even take advantage of them to protect themselves from their own predators. This is the case of *Stylocheilus striatus*, a sea hare that feeds on *Lyngbya majuscula* and *Anabaena torulosa*, and appears to be less susceptible to predation on *Anabaena torulosa*. *Stylocheilus striatus* consumes the latter without being affected by laxaphycin B toxicity. To overcome this toxicity, the sea hare has developed an adaptive mechanism that allows the biotransformation of laxaphycin B into non-toxic acyclic laxaphycin B. While non-toxic laxaphycin A is bioaccumulated in its digestive gland, laxaphycin B undergoes two successive cleavages at the C-terminal position of two hydroxyleucines. In order to study the enzymatic mechanism involved in this biotransformation, we have synthesized various analogues of laxaphycin B. First, we optimized their chemical synthesis, allowing us to confirm the structure of trichormamide C, a natural peptide analogous to laxaphycin B. In a second step, the synthesized analogues could be submitted to the studied enzyme and showed the reproducibility of the cleavage on different sequences. First characteristics of the enzyme could be identified, such as its cleavage specificities. Finally, our efforts focused on the design of a minimal peptide sequence for the recognition of the enzyme, in order to consider different strategies to isolate it.

Keywords: Biotransformation ; Peptidase ; Cyclic lipopeptide ; Peptide synthesis ; Cyanobacteria

Résumé du projet

En raison du changement climatique, le lagon de Moorea en Polynésie Française est impacté par des efflorescences de cyanobactéries asphyxiant les coraux, causant la dégradation de récif et diminuant les ressources en nourriture. *Lyngbya majuscula* et *Anabaena torulosa* sont deux cyanobactéries benthiques filamenteuses qui prolifèrent sur le sable et les coraux. Elles produisent de nombreux métabolites secondaires pouvant être toxiques. *Anabaena torulosa* produit notamment des lipopeptides cycliques tels que les laxaphycins A et B, composés de 11 et 12 acides aminés, respectivement. Cette cyanobactérie a pu développer des stratégies chimiques de protection contre les brouteurs, pouvant être repoussés par les molécules toxiques produites telle que la laxaphycin B. A leur tour, les herbivores doivent contourner ces défenses et dans certains cas, ils en profitent même pour se mettre à l'abri de leurs propres prédateurs. C'est le cas de *Stylocheilus striatus*, un lièvre de mer qui se nourrit de *Lyngbya majuscula* et *Anabaena torulosa* et qui semble moins exposé à la prédation sur *Anabaena torulosa*. *Stylocheilus striatus* consomme cette dernière sans être affecté par la toxicité de la laxaphycin B. Afin de contourner cette toxicité, le lièvre de mer a mis en place un mécanisme d'adaptation permettant la biotransformation de la laxaphycin B en laxaphycin B acyclique non toxique. Alors que la laxaphycin A non toxique est bio-accumulée dans sa glande digestive, la laxaphycin B subit deux clivages successifs en position C-terminale de deux hydroxyleucines.

Le premier chapitre de cette thèse décrit l'état de l'art sur les laxaphycins et leurs dérivés. Ce travail bibliographique a permis de vérifier si un tel mécanisme de dégradation des laxaphycins avait déjà été décrit et étudié auparavant. De plus, la description de la biosynthèse de ces peptides cycliques a notamment appuyé l'hypothèse d'un processus enzymatique menant à l'obtention de laxaphycins B acycliques.

Afin d'étudier le mécanisme enzymatique engagé dans cette biotransformation, le travail de thèse a été mené en 4 axes. Le premier axe, constituant le chapitre deux de la thèse, a consisté en la synthèse d'analogues de la laxaphycin B. La synthèse chimique de la laxaphycin B ayant déjà été décrite, il s'agissait d'optimiser la synthèse, notamment en économisant les quantités d'acide 3-aminodecanoique, préalablement obtenu au laboratoire via une synthèse complexe et couteuse. Pour cela, nous avons travaillé à l'obtention d'analogues cycliques ayant une séquence d'acide aminés simplifiée par rapport à la laxaphycin B. Les conditions d'obtention du peptide linéaire ont été optimisées, ainsi que les techniques de cyclisation et de purification. Une fois l'obtention d'une méthode de synthèse adaptée à ces peptides, nous avons pu synthétiser le trichormamide C, un analogue naturel de la laxaphycin B. Le trichormamide C n'ayant jamais été synthétisé auparavant, nous avons pu confirmer sa structure en comparant les analyses RMN du produit naturel avec le produit de synthèse. La méthode de synthèse développée pourra être appliquée à l'obtention d'autres peptides de la même famille, notamment pour confirmer leur structure, souvent complexe à identifier par l'analyse du produit naturel seul.

Le deuxième axe, constituant le chapitre trois de la thèse, s'est orienté sur l'étude de l'enzyme et ses spécificités de clivage. Cet axe s'est divisé en deux points, la reproductibilité du clivage enzymatique, d'une part, et ses conditions d'application, d'autre part. Tout d'abord, les conditions expérimentales ont été définies, avec notamment le choix de la température et du pH appliqués, ainsi que le modèle d'étude constitué du mollusque et de la cyanobactérie sur lequel il se nourrissait (*S. Striatus* sur *L. majuscula*). Afin d'évaluer la reproductibilité du clivage, la première étape était de vérifier la stabilité des laxaphycins face à des enzymes connues. Puis, nous avons reproduit le clivage de la laxaphycin B avec différents échantillons de notre modèle d'étude. Enfin, nous avons appliqué le modèle d'étude aux différents analogues synthétisés dans le cadre de notre premier axe. Nous avons ainsi pu montrer une reproductibilité du clivage des laxaphycins de type B, avec un double clivage en position C-terminale des positions 3 et 5 de la séquence, c'est-à-dire des hydroxyleucines dans le cas de la laxaphycin B et du trichormamide C. L'étape suivante visait l'étude des conditions limitantes pour reproduire ce clivage. Pour cela, nous avons synthétisé divers analogues cycliques et acycliques. Des modifications ont été apportées sur la structure (cyclique/acyclique), le type d'acide aminés utilisés (modifications autour du point de clivage) et leur stéréochimie (L ou D). Ces changements nous ont permis d'établir un premier profil de l'enzyme, spécifique des acides aminés D et dépendante notamment de la présence de l'acide 3-aminodecanoique. En parallèle, nous avons déterminé le sens d'action de l'enzyme, en étudiant les deux possibilités d'ouverture du peptide ainsi qu'en bloquant spécifiquement son accès à l'une des deux positions 3 et 5 par changement de stéréochimie. La détermination du sens de clivage a donné des informations importantes sur le rôle des acides aminés autour des points de clivage. L'impact de la stéréochimie des acides aminés sur le clivage enzymatique a permis de mettre en lumière une potentielle D-peptidase, famille d'enzymes peu connue à ce jour mais qui pourrait être notamment impliquée dans la résistance des bactéries aux antibiotiques. Dans ce cadre, le modèle d'étude a été appliqué à des antibiotiques connus ayant des structures cycliques, cependant aucun peptide n'a été impacté par cette enzyme.

Le troisième axe, constituant le chapitre quatre de la thèse, a visé au design d'une séquence peptidique minimale pour la reconnaissance de l'enzyme. La séquence a ainsi été réduite et optimisée afin d'en simplifier la synthèse tout en gardant des conditions adéquates pour le suivi de la dégradation enzymatique et une reconnaissance de l'enzyme face au substrat. Ce travail nous a mené à une séquence simplifiée intéressante mais néanmoins encore optimisable, pour envisager différentes stratégies pour isoler l'enzyme. Dans cet optique, différentes solutions ont été envisagées et notamment des voies chimique et biochimique. Nous avons ainsi produit, sur la base de la séquence optimisée, un peptide modèle qui après modifications pourrait se lier de manière covalente à l'enzyme par photo-activation. Cependant, ce peptide n'est pas clivé par l'enzyme et ne semble pas agir comme inhibiteur de cette dernière. Nous avons également envisagé une pré-purification de l'extrait contenant l'enzyme par le biais de colonnes échangeuses d'ions et par l'utilisation de filtres par poids moléculaire, nous permettant d'avoir une première idée des interactions ioniques de l'enzyme et de son poids moléculaire.

Le dernier axe, travaillé parallèlement aux autres, a permis l'obtention de résultats préliminaires quant à l'origine de l'enzyme recherchée. Ainsi, les différents compartiments du tractus digestif de *S. striatus* ont été étudiés afin de localiser l'activité enzymatique. Cette dernière semble être plus importante au sein du gésier et de la glande digestive du mollusque. De plus, *S. striatus* a été étudié après avoir été nourris sur différentes cyanobactéries ou non. Les premiers résultats montrent une capacité du mollusque à biotransformer la laxaphycin B quel que soit son type de nourriture, suggérant une « auto-production » de l'enzyme ou la récupération de cette dernière dans un environnement plus global.

En conclusion, ce travail de thèse a contribué, à son échelle, à l'avancée des recherches sur les laxaphycins. Ces lipopeptides cycliques sont connus depuis une trentaine d'années et les chercheurs sont capables de les isoler, les synthétiser et les caractériser. Cependant, leur biosynthèse n'a été décrite que très récemment. Dans ce projet de thèse, leur synthèse chimique a pu être optimisée et la spécificité de leur biotransformation étudiée. Alors que certaines questions restent à élucider quant à leur origine, leurs rôles biologiques et écologiques, l'étude des laxaphycins a ouvert de nouvelles possibilités telles que la découverte d'une D-peptidase impliquée dans leur biotransformation.

Table of contents

List of abbreviations

A domain	Adenylation domain
ACP domain	Acyl carrier protein domain
At	*Anabaena torulosa*
AT domain	Acyltransferase domain
AMP	Adenosine monophosphate
ATP	Adenosine triphosphate
C domain	Condensation domain
Dg	Digestive gland
Dg-Ss-At	Digestive gland of *Stylocheilus striatus* fed on *Anabaena torulosa*
Dg-Ss-Lm	Digestive gland of *Stylocheilus striatus* fed on *Lyngbya majuscula*
Dg-Ss-Turf	Digestive gland of *Stylocheilus striatus* fed on algal turf
DH	Dehydratase
E domain	Epimerization domain
ER	Enoyl reductase
FAAL	Fatty acyl-AMP ligase
FAD	Flavin adenine dinucleotide
Gizz-Ss-Lm	Gizzard of *Stylocheilus striatus* fed on *Lyngbya majuscula*
HPLC	High performance liquid chromatography
IC50	Half maximal inhibitory concentration
KG	ketoglutarate
KR domain	Ketoreductase domain
KS domain	Ketosynthase domain
lax	Laxaphycin
LC-MS	Liquid chromatography-Mass spectrometry
LD50	Median lethal dose
LDH	Lactate dehydrogenase
Lm	*Lyngbya majuscula*
MIC	Minimum inhibitory concentration
Mouth-Ss-Lm	Mouth of *Stylocheilus striatus* fed on *Lyngbya majuscula*
MS-MS	Tandem mass spectrometry
MTT test	Test with MTT tetrazolium salt
NCL	Native chemical ligation
NMR	Nuclear magnetic resonance
NMT domain	Methylation domain
NRPS	Non-ribosomal peptide synthetases
OG	Oxoglutarate
ORF	Open reading frame
PCP	Peptidyl carrier protein domain (or T = thiolation domain)
PKS	Polyketide synthase
Ppant	4'-phospho-pantethine
SPPS	Solid phase peptide synthesis
Ss	*Stylocheilus striatus*
TE domain	Thioesterase domain

List of abbreviated amino acids

Ade	3-aminodecanoic acid
Aoc	3-aminooctanoic acid
Dhb	Dehydrobutyrine
Hasn	Hydroxy asparagine
Hle	Hydroxy leucine
Hse	Homoserine
Hthr	Hydroxy threonine
Hyp	Hydroxy proline
(*N*)-MeIle	N-methylisoleucine

List of figures

List of tables

Introduction

For the past 30 years, chemists and ecologists have pooled their knowledge to link the discovery of new bioactive molecules to chemical mediation mechanisms across different ecosystems. Marine chemical ecology has demonstrated the role of secondary metabolites in defense against predators, in the evolution of food preferences and many other interactions. It is thus possible to study prey-predator trophic relationships between several species, such as carnivore-herbivore-cyanobacteria interactions.

Cyanobacteria are a phylum of prokaryotic bacteria, often called blue-green algae, that obtain their energy through photosynthesis. Despite the prefix "cyano", associated with their blue-green color due to chlorophyll, cyanobacteria can actually be of different colors depending on the proportions of pigments or carotenoids, although blue-green remains the most common color [1]. Climate change is inducing a rapid transition from an ecosystem initially dominated by corals to one now increasingly dominated by algae and cyanobacteria. We are therefore experiencing an increase in the frequency and intensity of cyanobacteria blooms [2]. This algal bloom raises many problems on a global scale. Ecologically speaking, cyanobacteria lead to the asphyxiation of corals and thus to a degradation of the reef and its occupants. The degradation of this habitat also impacts resources and tourism. Finally, these cyanobacteria produce toxins that can affect not only animals but also humans. In 1996, in Caruaru, Brazil, dozens of patients died as a result of hemodialysis using water contaminated with microcystin, a cyanotoxin mainly found in freshwater [3]. Shaw *et al*. reported a significant number of cases of human exposure to cyanobacteria and their associated toxins between 1934 and 2003, with consequences ranging from simple skin or gastrointestinal symptoms to much more serious cases that could lead to death [4,5].

Marine herbivores select their habitat based on their need for food and protection. Depending on the chosen environment, they are able to reduce their risk of being predated by other marine organisms [6]. Most marine herbivores have generalist feeding behaviors, however some develop host-specific preferences. This is the case for some amphipods and opisthobranch mollusks that feed on algae having a wide chemical diversity as weapons to defend themselves. They are able to sequester chloroplasts that provide them energy through photosynthesis, to use these algae to hide themselves, to hijack the algae produced secondary metabolites as chemical shields for their own protection [7].

Benthic cyanobacteria are abundant, especially on coral reefs (Figure 1). They are therefore an important food resource for the grazers of these reefs as well as a shelter of choice for small animals. In the lagoon of Moorea in French Polynesia, *Lyngbya majuscula* and *Anabaena torulosa* are two filamentous benthic cyanobacteria which develop on sand and corals.

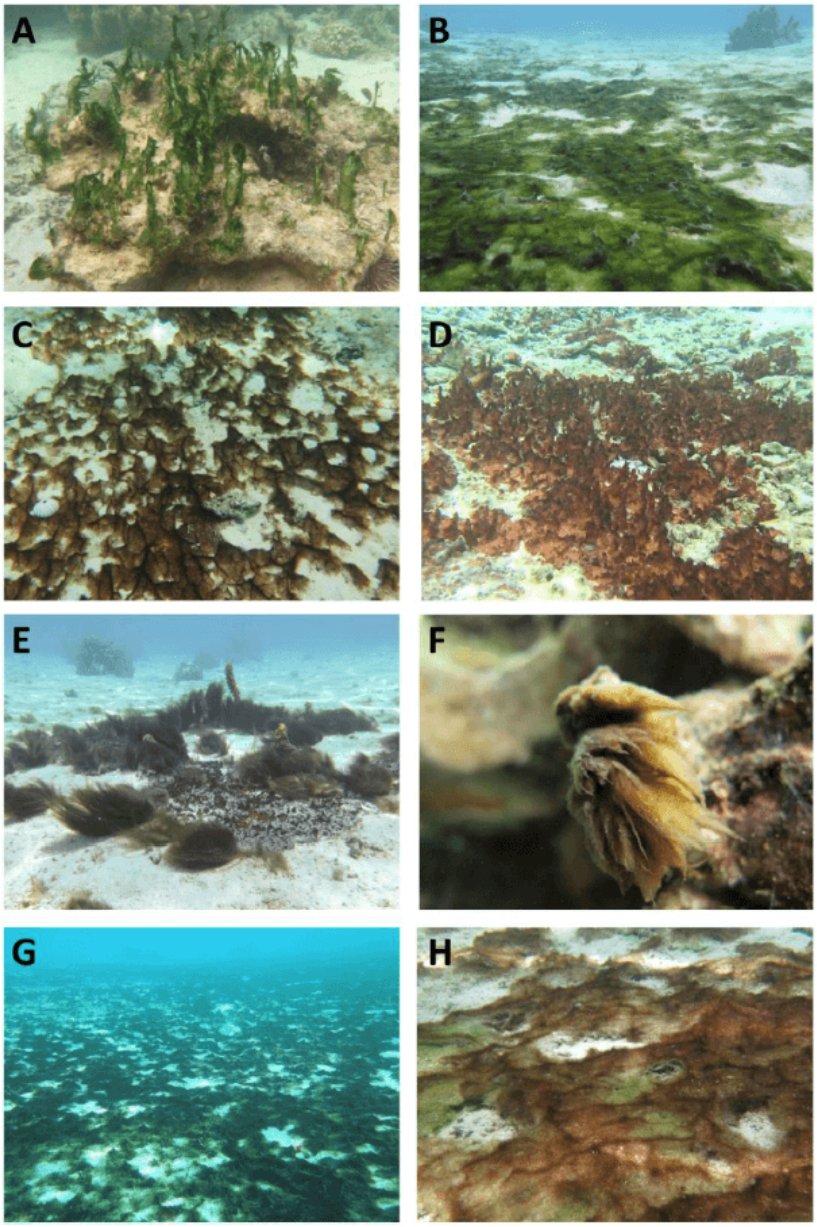

Figure 1. In situ photographs of benthic cyanobacteria mats. A) *Anabaena* sp.1. B) *Anabaena* sp.2. C) *Hydrocoleum majus*-B. D) *Leptolyngbya* sp.2. E) *Lyngbya majuscule*. F) *Phormidium* sp.1. G–H) Plurispecific mats frequently occurring in channels of Moorea lagoon and composed of three major species, *Anabaena* sp.1, *Anabaena* sp.2 and *H. majus*-B.

This image was taken from the article of Bonnard *et al* [8]. (Bonnard, I.; Bornancin, L.; Dalle, K.; Chinain, M.; Zubia, M.; Banaigs, B.; Roué, M. Assessment of the Chemical Diversity and Potential Toxicity of Benthic Cyanobacterial Blooms in the Lagoon of Moorea Island (French Polynesia). J. Mar. Sci. Eng. 2020, 8, 406, doi:10.3390/jmse8060406.)

Lyngbya majuscula produces a large number of secondary metabolites that can be toxic, such as lyngbyatoxin-a [9]. Yet some herbivores are able to feed on these cyanobacteria because they adapted to these toxic environments. In a study by Paul *et al*. on the relationships between different cyanobacteria and marine organisms, *Lyngbya majuscula* showed a strong interaction with different species, including the sea hare *Stylocheilus striatus*, which seems to

be attracted to the secondary metabolites produced by the cyanobacterium [10]. However, some secondary metabolites may be more or less accepted by these herbivores or more or less tolerated depending on concentrations. Pitipeptolide A is a peptide secondary metabolite produced by *Lyngbya majuscula*. This compound has shown its ability to repel 4 grazers with general feeding habits on macroalgae, while *Stylocheilus striatus*, with a more specific diet, was attracted to this peptide, at natural concentrations [11]. This mollusk is now recognized as a specialist grazer of cyanobacteria such as *Lyngbya majuscula*, and is capable of sequestering and detoxifying the secondary metabolites produced such as lyngbyatoxin-a or debromoaplysiatoxin [12,13].

More generally, sea hares detect various smells and pheromones thanks to their rhinophores located at the front of their head [14]. This allows them to follow what is called a chemical cue, mainly produced by secondary metabolites excreted by the algae. Other marine organisms have developed chemical attraction and resistance to the secondary metabolites produced by some algae. As an example, the chlorodesmin produced by *Chlorodesmis fastigiata* repels most fish but not the crab *Caphyra rotundifrons*, which is stimulated by this chemical compound [15].

Slowly moving marine gastropods are easy prey forced to develop defense tools. Thus, some have chosen to adapt to a toxic environment, as some cyanobacteria may propose. This adaptation process involves managing the secondary metabolites produced by these bacteria. Once the metabolite is ingested, it can be sequestered or follow a process of absorption, distribution, metabolization and excretion (ADME). In the case of *Stylocheilus striatus*, the secondary metabolites produced by *Lyngbya majuscula* are either sequestered in its digestive gland as is the case for tiahuramides, or biotransformed into non-toxic compounds [16,17]. Although *Stylocheilus striatus* is a specialist in *Lyngbya majuscula*, it has also been found on *Anabaena torulosa*. The latter produces cyclic lipopeptides such as laxaphycins A and B [18,19].

Toxicity tests for laxaphycin A and B were conducted on *Artemia salina*. Laxaphycin A (laxA) shows no toxicity while laxaphycin B (laxB) already induces mortality at 20 μg/mL on *A. salina* [8]. Furthermore, laxB shows cytotoxicity against a wide variety of cancer cell lines with an IC50 ranging from 0.2 to 6 μM [20]. The toxicity of laxB does not prevent *Stylocheilus striatus* from feeding on *Anabaena torulosa*, but seems to repel its predators *Gymnodoris ceylocia* and *Thalamita coeruleipes* (Figure 2). Questions about the uses of these toxins by *Stylocheilus striatus* to avoid predation have been partially answered by Louis Bornancin, a former doctoral student at CRIOBE [16]. Indeed, he has highlighted the physiological mechanism developed by *Stylocheilus striatus* to adapt to this toxic environment and particularly the degradation of laxaphycin B into non-toxic linear peptides by a yet unstudied mechanism.

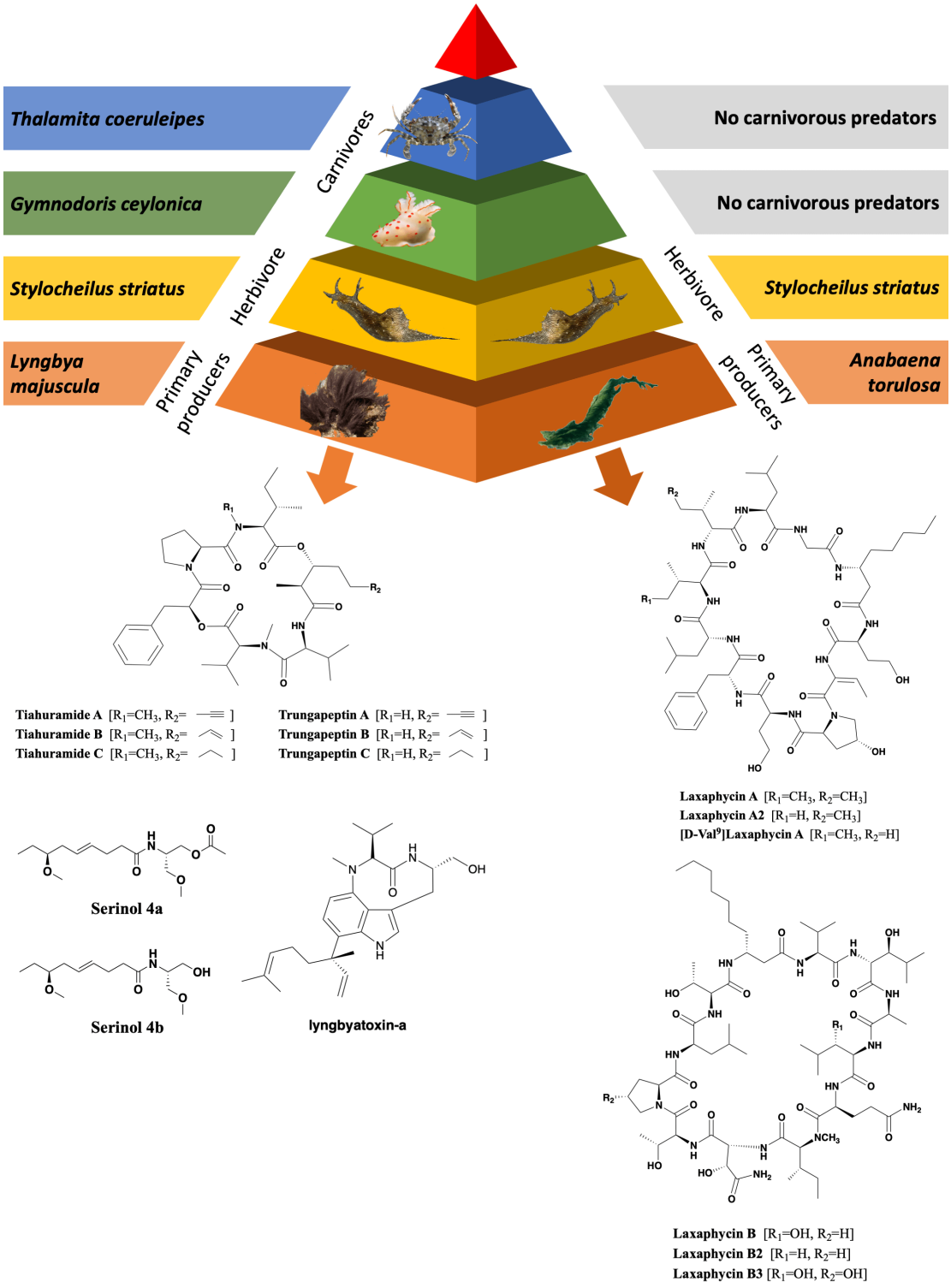

Figure 2. Interspecies relationships between carnivores, herbivores and cyanobacteria, and examples of secondary metabolites produced by the cyanobacteria *Lyngbya majuscula* and *Anabaena torulosa*.

Indeed, non-ribosomal produced peptides such as laxaphycins [21] are believed to be stable in animal organisms due to the presence of non-proteinogenic amino acids such as β-hydroxy amino acids, dehydro amino acids, N-methylated amino acids, D-amino acids or long chain β-amino acids with 8 to 10 carbons.

Such a structure gives them stability to hydrolysis and to proteases, compared to more conventional amino acid-containing linear peptides. However, laxaphycin B was found in the open state within the digestive gland of *Stylocheilus striatus,* raising the question of how the peptide was degraded. Indeed, the opening occurs specifically in C-ter of two D-hydroxyleucine in positions 3 and 5 (Figure 3).

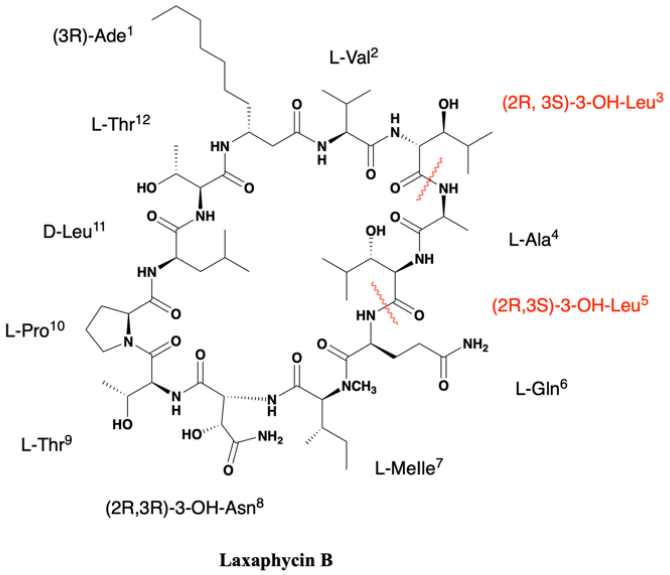

Figure 3. Structure of laxaphycin B showing the two observed cleavage points.

It is possible that *Stylocheilus striatus* may have adapted through the implementation of an enzymatic degradation process allowing it to detoxify laxaphycin B into a more manageable compound. This potential enzyme could be produced by the organism itself or within an associated microbiome at the intestinal level. To date, little is known about the microbiomes associated with sea hares. Most studies show the involvement of bacteria in the degradation and fermentation of polysaccharides [22], but none report bacteria involved in the enzymatic cleavage of secondary metabolites such as cyclic peptides.

To our knowledge, few examples of enzymes with this ability to linearize cyclic peptides have been reported. Microcystinase would allow the cleavage of cyclopeptides of the microcystin family between an Adda group and an arginine (Figure 4). Microcystinase was first described as a possible metalloprotease encoded by the *mlr*A gene [23,24]. The degradation mechanism of microcystin-LR as well as the *mlrA* gene have been studied recently, suggesting that the enzyme belongs rather to the intramembrane glutamate protease family [25,26]. Although various patents mention the possibility of treating polluted water with microcystin by bacteria of the genus *Pseudomonas* or *Sphingomonas* that would secrete enzymes capable of detoxifying it, microcystins and laxaphycins have very different structures that may lead us to believe that we are facing a new enzymatic activity.

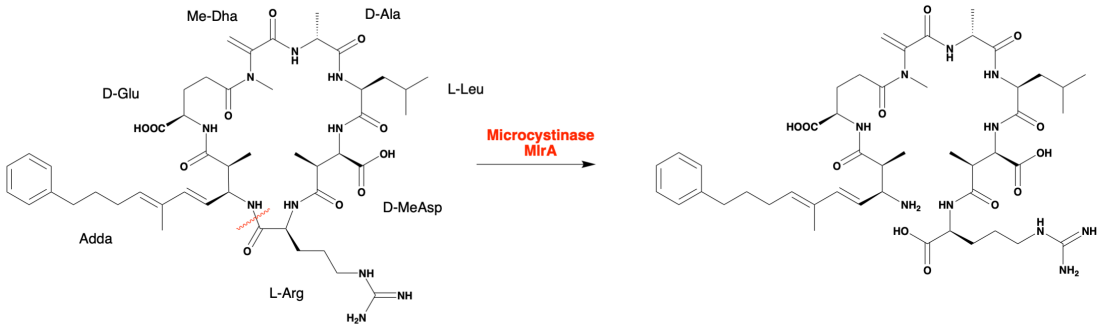

Figure 4. First opening of microcystine by microcystinase.

Understanding these enzymatic phenomena and potentially discovering new enzymes is an important issue for the industrial world, which increasingly uses these enzymes that can be applied in many processes in the food, paper, phytosanitary and pharmaceutical industries [27,28]. The possibility of modifying enzymes by directed evolution, widely studied by the recent Nobel Prize Frances H. Arnold, is paving the way for new and increasingly diversified applications [29]. The specific properties of the marine environment such as its salinity, pH or temperature make it a prime research ground for scientists looking for new bioactive substances.

The aim of this thesis is to understand the mechanism of degradation of cyclic lipopeptides such as laxaphycin B implemented by the mollusk *Stylocheilus striatus*. For this purpose, the thesis objectives have been defined as follows, each of them constituting a chapter:

- A review of the state of the art on laxaphycins and their derivatives since their discovery in the 1990s, allowing us to verify if such a mechanism of degradation had been described. This review will be submitted for publication.
- The synthesis of different cyclic analogues of laxaphycin B in order to study the specificity of the biotransformation. For this purpose, an optimization of the synthesis was performed and resulted in 3 analogous peptides, including trichormamide C another natural peptide isolated from the cyanobacterium *Oscillatoria* sp. This first part of the thesis project resulted in the publication of an article in *Organic Letters* [30].
- A deeper study on the biotransformation phenomenon of B-type laxaphycins within the digestive gland of *Stylocheilus striatus* through the use of the newly synthesized laxB analogues. This study allows the precise determination of the laxaphycin B processing and to determine some of the main enzyme characteristics. These results were published in *Journal of Medicinal Chemistry* [31].
- The design of optimized peptide minimal sequence that could interact with the enzyme in order to consider different methods to recover it. In parallel, other properties of the enzyme were evaluated, such as its molecular weight.

In the rest of this manuscript, many peptides will be defined, with slight structural modifications. A summary of all the structures is available at the end of this manuscript in the "Supporting Information" section (Table 36). The peptides are numbered from **1** to **22**, and their cleavage state is characterized by a letter (Table 37, Table 38, Table 39).

.

Chapter 1.
State of the art: laxaphycins

This chapter constitutes a bibliographical study on laxaphycins, dealing with their discovery, their synthesis and biosynthesis, and what we know about their different properties. This chapter is the subject of a scientific review in preparation.

I. Introduction

The 1970s are considered as the corner stone of the research devoted to secondary metabolites extracted from the marine environment. Since this date, it has been demonstrated that marine secondary metabolites have a high biological activity and a chemodiversity unequalled at the terrestrial level. These natural marine products can be used in applications such as drugs in the fight against cancer, virus or bacterial infections but also as cosmetics [32,33]. Cyanobacteria that represent at least 50% of the aquatic biomass are effective producers of secondary metabolites that can be used as therapeutic agents [34,35], among which peptides isolated from various strains all over the world [36]. These peptides are often synthesized by non-ribosomal peptide synthetase (NRPS) or mixed biosynthetic pathways that involve polyketide synthase (PKS) operating in conjunction with NRPS [37]. These particular biosyntheses allow the assembly of complex peptides containing proteinogenic and non-proteinogenic amino acids such as α,β-dehydro-, *N*-methylated and β-hydroxylated amino acids. The presence of an amino acid bearing a fatty sidechain within the sequence qualified them as lipopeptides. Furthermore, combining these specific amino acids with a cyclic structure confers them a restricted conformation that supports their biological activity and reduces the risk of enzymatic degradation, which makes these peptides very attractive for pharmacological research [38–40]. In addition, β-amino fatty acids induce lipophilicity, which leads to interactions with cell membranes and counterbalance the hydrophilic character of peptides [41]. However, the mechanism of action of cyclic lipopeptides is often not well known. It is therefore necessary to understand the mechanisms of action and to determine potential biological targets. In order to study lipopeptides more extensively, researchers need to have sufficient quantities of them, which is often difficult in the case of natural molecules, either because of their low concentration in cyanobacterial extracts, or because of the difficulty in harvesting these organisms at specific locations and seasons. It is therefore important to develop efficient synthesis routes for these compounds or to express them in host organisms.

Laxaphycins (lax) and their derivatives constitute one example of lipopeptides. The purpose of this review is to summarize the thirty-year history of laxaphycins and their derivatives, from their discovery and characterization to the determination of their different biological activities, including the description of their chemical synthesis and their biosynthesis.

II. Discovery and characterization of laxaphycins and their derivatives

Most of the laxaphycin derivative structures have been determined thanks to a combination approaches based on multidimensional ^{1}H and ^{13}C NMR and high resolution mass spectrometry [42]. Peptide hydrolysis and amino acid derivatization by the advanced Marfey method allowed the determination of amino acid stereochemistry [43].

A. Laxaphycins

a) Cyclic laxaphycins

Laxaphycins were first isolated by Moore's Hawaiian group in 1992 [44,45]. They were extracted from the freshwater cyanobacterium *Anabaena laxa*, collected in mud on the campus of the University of Hawaii. After successive fractionation steps, four major laxaphycins A, B, D, and E were isolated from about thirteen other similar peptides. The raw cyclic structures of the four laxaphycins were determined. These four peptides could already be separated into two subfamilies, laxaphycins with 11 residues (lax A, E) and laxaphycins containing 12 residues (lax B, D), each of them containing in their sequences at least 50% of non-ribosomal amino acids. Laxaphycin A is composed of a 3-aminooctanoic acid residue (Aoc), two homoserine (Hse), a *E*-dehydrobutyrine residue (Dhb), a 4-hydroxyproline (Hyp), and six more standard amino acids with the following sequence (Aoc-Hse-*E*-Dhb-Hyp-Hse-Phe-Leu-Ile-Ile-Leu-Gly). The two isoleucines are diastereoisomers. Laxaphycin E showed a unique difference with laxaphycin A, the substitution of the 3-aminooctanoic acid (Aoc) by a 3-aminodecanoic acid (Ade). Laxaphycin B contains the non-proteinogenic amino acids 3-aminodecanoic acid (Ade), hydroxyleucine (Hle), hydroxyasparagine (Hasn) and N-methylisoleucine ((*N*)-MeIle) as well as six natural amino acids, with the sequence (Ade-Val-Hle-Gln-(*N*)-MeIle-Hasn-Thr-Pro-Leu-Thr). Laxaphycin D differentiated from laxaphycin B by a 3-aminooctanoic acid that replaces the 3-aminodecanoic acid.

It is only in 1997 that Bonnard *et al*. identified the complete structure and assigned the absolute stereochemistry of the amino acids constituting the laxaphycins A and B sequence [46]. The two peptides were extracted from an assemblage of the marine cyanobacteria *Lyngbya majuscula (L. majuscula)* and *Anabaena torulosa (A. torulosa)*, collected in Moorea (French Polynesia), but repeated harvesting at Moorea island highlighted *A. torulosa* as the only producer of laxaphycins. Different experiments including mass spectrometry and NMR confirmed the gross structure, whereas combining the previous results with Marfey's analysis gave access to the stereochemistry of all amino acids. Thus, for laxaphycin A, 3-aminooctanoic, phenylalanine, and leucine in positions 1, 6, and 7,respectively were shown to be of R-configuration. Isoleucine in position 8 is of (2S,3S)-configuration while isoleucine in position 9 has a (2R,3S) configuration, the other amino acids of the sequence having a classical S-configuration. It is worth noting that for laxaphycin A, hydrophobic residues are located on

the same side of the peptide. In laxaphycin B the stereochemistry of hydroxyleucine in position 3 was (2S,3S) while hydroxyleucine in position 5 was (2R,3S). The 3-hydroxyasparagine was stereochemically (2R,2R). An alternation of L and D stereochemistry can be seen along the peptide sequence, with (3R)-Ade^{1}, (2R,3S)-3-OH-Leu^{5}, (2R,3R)-3-OH-Asn^{8} and D-Leu^{11}, and the hydrophobic/hydrophilic character of amino acids is also alternated within the sequence. A further study of the biological activities of laxaphycins produced by cyanobacteria was carried out by the same group in 2007, giving rise at the same time to two new laxaphycins named laxaphycins B2 and B3 (Figure 5) [20]. Laxaphycin B2 differs from laxaphycin B only by the replacement of (2R,3S)-hydroxyleucine to D-leucine in position 5. Laxaphycin B3 contains a (2S,4R)-4-hydroxyproline in position 10 instead of the proline found in laxaphycin B. In these two new laxaphycins, the 3-hydroxyleucine in position 3 is of the (2R,3S) configuration whereas the one described in laxaphycin B is of the (2S,3S) configuration.

In order to further study the ecological role of laxaphycin B and its potential in the discovery of new anti-cancer agents, a total synthesis was achieved in 2013 highlighting a structural misassignment for the absolute configuration of one amino acid [47,48]. Indeed, the comparison of synthetic and natural laxaphycin B showed that laxaphycin B had a (2R,3S)-3-hydroxyleucine in position 3 whereas it had been described with a (2S,3S) configuration.

About a decade later, new analogues of the laxaphycin family were reported, having little difference with the already known laxaphycins [49,50]. Laxaphycins A2 and B4 were discovered in an extract of the cyanobacterium *Hormothamnion enteromorphoides* collected in the Gulf of Mexico. Laxaphycin A2 contains a L-valine in position 8 while laxaphycin A contains an L-isoleucine (Figure 5) [49]. Laxaphycin B4 is analogous to laxaphycin B3, with a homoserine in position 4 replacing the alanine (Figure 5) [49]. Two new peptides laxaphycins B5 and B6 isolated from a freshwater cyanobacterium, *Phormidium* sp., UIC 10484 completed this series [50]. Laxaphycin B5 is derived from laxaphycin B and contains isoleucine instead of valine in position 2, valine in position 4 instead of alanine, asparagine instead of 3-hydroxyasparagine in position 8 and tyrosine in position 11 instead of leucine. Similarly, laxaphycin B6 combines the same four previous modifications observed in laxaphycin B5 and a D-leucine in position 5 that made it the more distant compound from laxaphycin B. It is worth to note that all the observed modifications are made with maintenance of stereochemistry and that the amino acids are often isosteric. The tyrosine and leucine in position 11 are both D-configuration, as are asparagine and hydroxyasparagine in position 8.

One year later, an extract of *Anabaena torulosa* collected in Moorea (French Polynesia) revealed two cyclic laxaphycins-A type peptides, one of which being the previously described laxaphycin A2, revealing the ability of different cyanobacteria strains to produce identical peptides [19]. The other, named [D-Val^{9}]laxaphycin A, showed a very similar structure, but NMR and MSMS analyses suggested the presence of D-valine in position 9 instead of (2R,3S)-isoleucine, while keeping (2S,3S)-isoleucine in position 8 (Figure 5). These two new cyclic laxaphycin A were not found in other samples of *Anabaena* sp. collected at different locations

in the lagoon of Moorea [8]. The production of these peptides cannot yet be explained. Peptides with close structures have been found in other cyanobacteria such as *Hormothamnion enteromorphoides* [51], or *Lyngbya confervoides* [52]. A horizontal gene transfer between cyanobacteria could be an explanation for the presence of these peptides within different cyanobacteria strains [53].

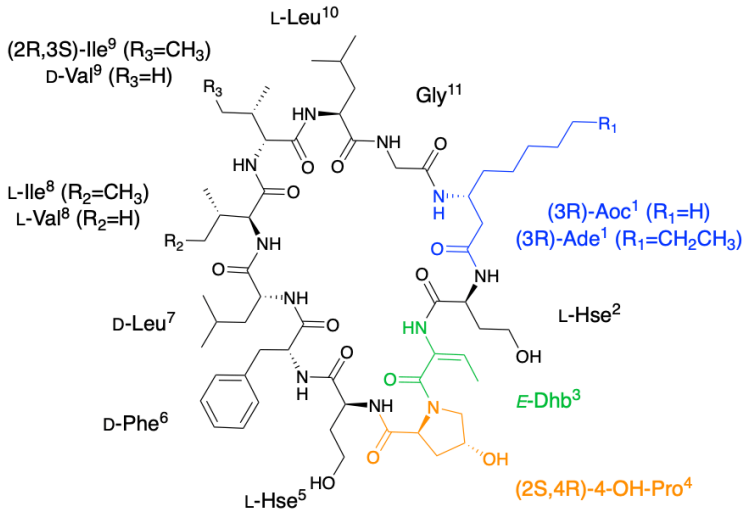

Laxaphycin A [(3R)-Aoc^{1}, L-Ile^{8}, (2R,3S)-Ile^{9}]
Laxaphycin A2 [(3R)-Aoc^{1}, L-Val^{8}, (2R,3S)-Ile^{9}]
Laxaphycin E [(3R)-Ade^{1}, L-Ile^{8}, (2R,3S)-Ile^{9}]
[D-Val^{9}]Laxaphycin A [(3R)-Aoc^{1}, L-Ile^{8}, D-Val^{9}]

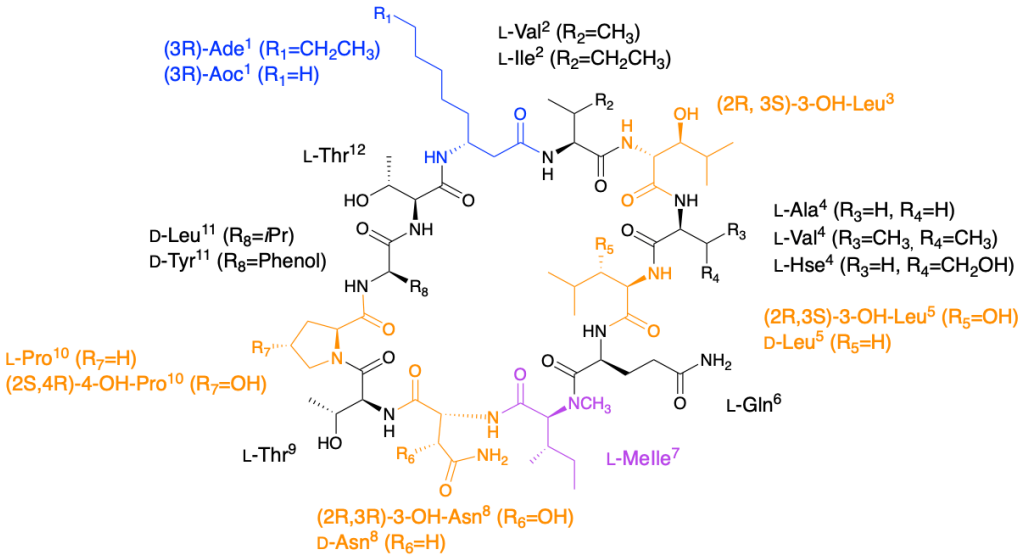

Laxaphycin B [(3R)-Ade^{1}, L-Val^{2}, L-Ala^{4}, (2R,3S)-3-OH-Leu^{5}, (2R,3R)-3-OH-Asn^{8}, L-Pro^{10}, D-Leu^{11}]
Laxaphycin B2 [(3R)-Ade^{1}, L-Val^{2}, L-Ala^{4}, D-Leu^{5}, (2R,3R)-3-OH-Asn^{8}, L-Pro^{10}, D-Leu^{11}]
Laxaphycin B3 [(3R)-Ade^{1}, L-Val^{2}, L-Ala^{4}, (2R,3S)-3-OH-Leu^{5}, (2R,3R)-3-OH-Asn^{8}, (2S,4R)-4-OH-Pro^{10}, D-Leu^{11}]
Laxaphycin B4 [(3R)-Ade^{1}, L-Val^{2}, L-Hse^{4}, (2R,3S)-3-OH-Leu^{5}, (2R,3R)-3-OH-Asn^{8}, (2S,4R)-4-OH-Pro^{10}, D-Leu^{11}]
Laxaphycin B5 [(3R)-Ade^{1}, L-Ile^{2}, L-Val^{4}, (2R,3S)-3-OH-Leu^{5}, D-Asn^{8}, L-Pro^{10}, D-Tyr^{11}]
Laxaphycin B6 [(3R)-Ade^{1}, L-Ile^{2}, L-Val^{4}, D-Leu^{5}, D-Asn^{8}, L-Pro^{10}, D-Tyr^{11}]
Laxaphycin D [(3R)-Aoc^{1}, L-Val^{2}, L-Ala^{4}, (2R,3S)-3-OH-Leu^{5}, (2R,3R)-3-OH-Asn^{8}, L-Pro^{10}, D-Leu^{11}]

Figure 5. Structure of cyclic laxaphycins A and B

b) Acyclic laxaphycins

To complete this set of compounds, three acyclic laxaphycin A type peptides were discovered [19]. Acyclolaxaphycin A is equivalent to laxaphycin A opened between (3R)-Aoc in position 1 and glycine in position 11. NMR and MS spectra of [des-(Gly^{11})]acyclolaxaphycin A show a loss of glycine 11. The [des-(Leu^{10}-Gly^{11})]acyclolaxaphycin A corresponds to acyclolaxaphycin A having lost glycine in position 11 and leucine in position 10 (Figure 6). Like their cyclic structural analogues, laxaphycin A2 and [D-Val^{9}]laxaphycin A, these new acyclolaxaphycins A were not found in samples of *Anabaena* sp. collected by Bonnard *et al*. for their study on the toxicity of cyanobacterial blooms, thus highlighting that laxaphycin production might be seasonally affected or dependent on the environmental conditions [8].

In 2015, upon examination of an extract of *Anabaena torulosa,* Bornancin *et al.* also found two acyclic laxaphycins, B and B3, that differ from their cyclic homologs by an *m/z* value 19 amu higher [18]. Furthermore, both peptides responded positively to the ninhydrin test, confirming an uncapped *N*-terminus. After fragmentation by MS-MS, the peptide is proposed to be open between 3-hydroxyleucine in position 3 and alanine in position 4. Stereochemistry is preserved for all amino acids between the cyclic and acyclic versions (Figure 7). These two new acyclolaxaphycins B were not found in other samples of *Anabaena* sp. collected at different locations in the lagoon of Moorea, as in the case of the new laxaphycins A mentioned above [8].

Recently, two acyclolaxaphycins were isolated from the sea hare *Stylocheilus striatus* that feeds on the cyanobacterium *Anabaena torulosa*, producing laxaphycins [54]. High resolution mass spectrometry (HRMS) analysis allowed to propose [des-(Ala^{4}-Hle^{5})]acyclolaxaphycins B and B3 that result from the loss of the two successive alanine and hydroxyleucine in positions 4 and 5 (Figure 7). NMR analyses sustained this proposal due to the absence of correlations between alanine and a 3-hydroxyleucine. These two compounds undergo a spontaneous cyclization of the *N*-terminal glutamine to form a pyroglutamate, resulting in [des-(Ala^{4}-Hle^{5})]acyclolaxaphycin B1195 and B1211, respectively (Figure 7) [16].

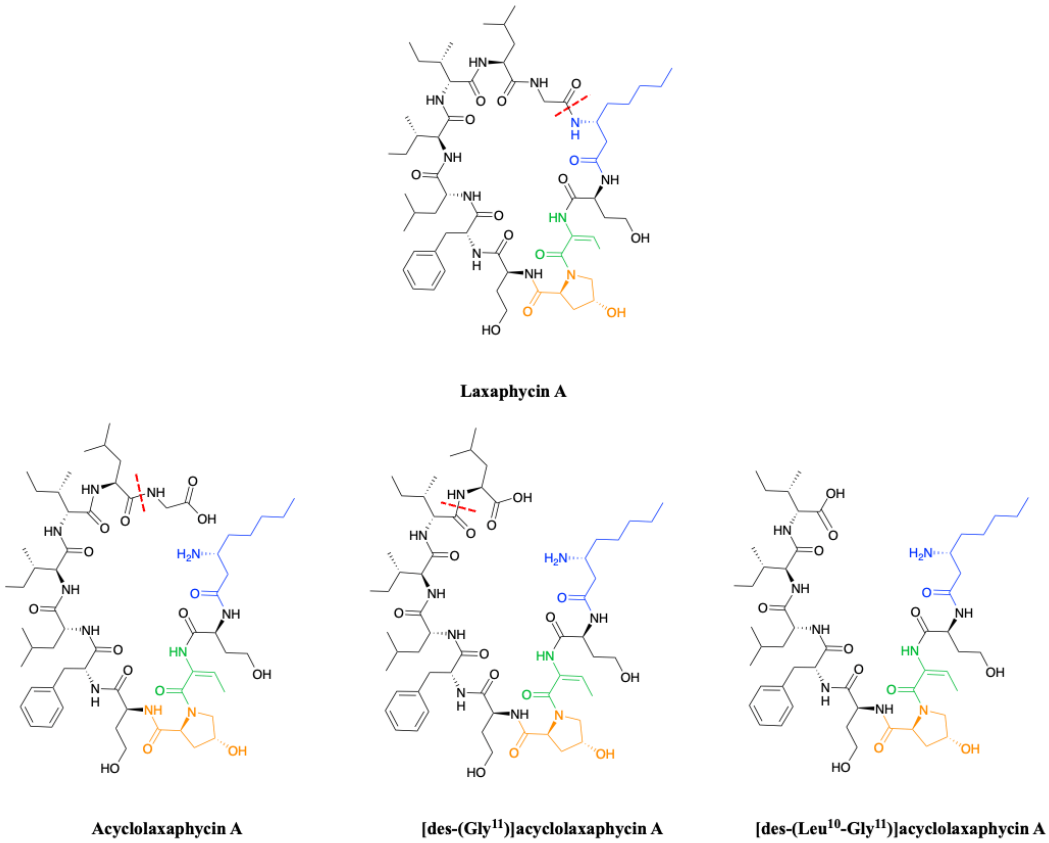

Figure 6. Structure of acyclic laxaphycins A compared to laxaphycin A. Amino acid deletion leading to the next acyclic laxaphycin A are indicated by red marks.

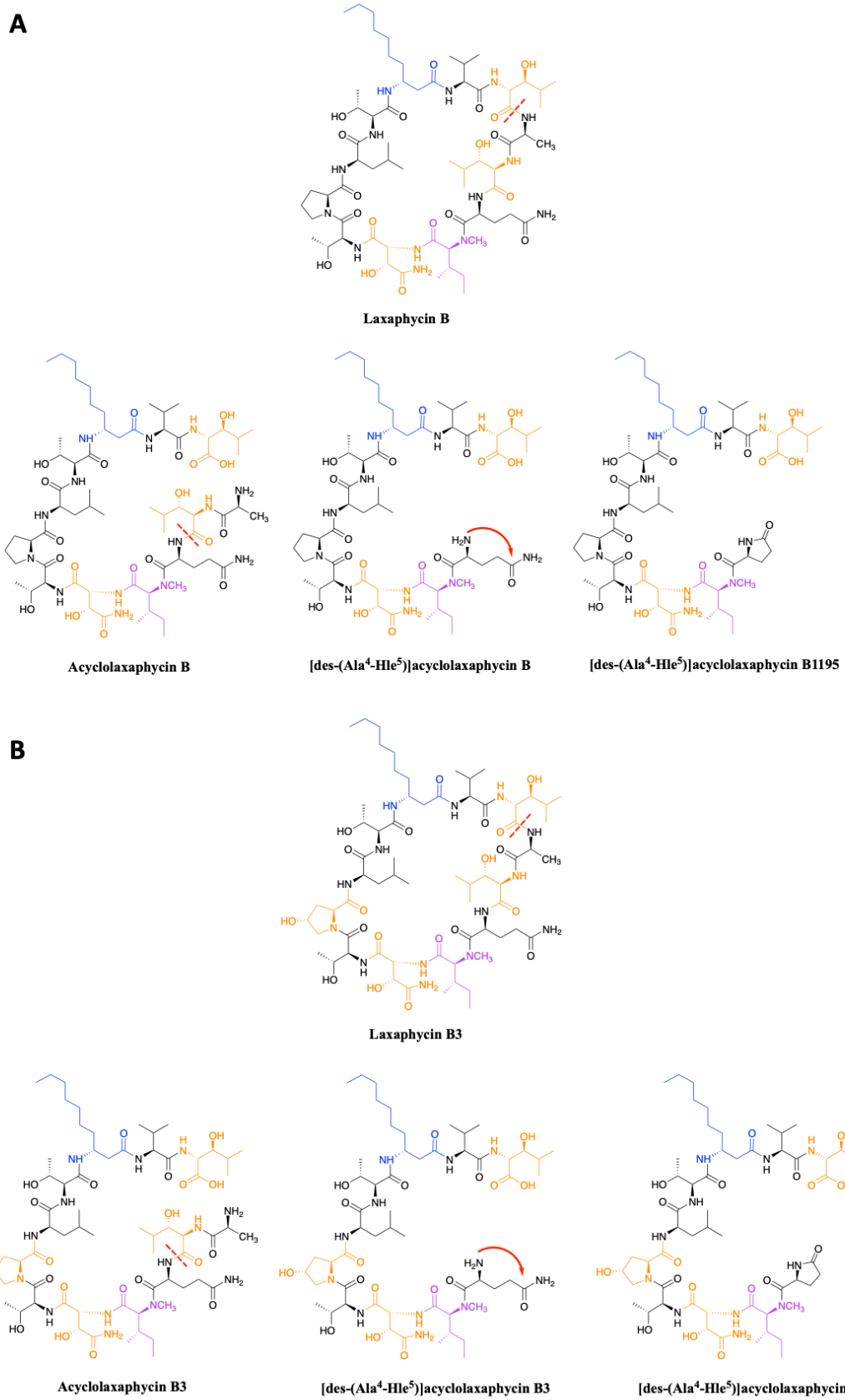

Figure 7. A) Structure of acyclic laxaphycins B compared to cyclic laxaphycin B. B) Structure of acyclic laxaphycins B3 compared to cyclic laxaphycin B3. Positions of ring opening or structural modifications leading to the next acyclic laxaphycins are designated by red marks.

B. Hormothamnin

The first known example of this peptide series was not termed laxaphycin but hormothamnin and was isolated by Gerwick's group in 1989 from the cyanobacterium *Hormothamnion enteromorphoides*, collected in Playa de Luquillo in Puerto Rico [51]. About 15 hormothamnin peptides were detected in the crude extract but only one, hormothamnin A, the major compound and the most lipophilic one was fully characterized. Hormothamnin A contains the same 11 amino acids found in laxaphycin A sequence, albeit NMR analysis identified a *Z*-configuration for dehydrobutyrine (Figure 8) [55,56]. As it is the case for most of the compounds isolated from natural sources, this peptide was named accordingly to the organism from which it was extracted, however, as it was the only example among the 15 peptides detected in the producing organism to be fully characterized it failed to impose its name to the peptide family.

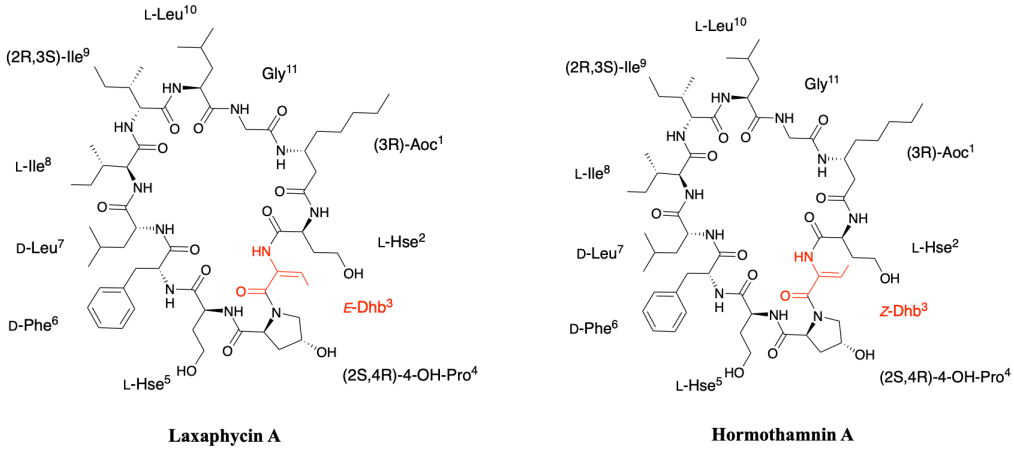

Figure 8. Structure of hormothamnin A compared to laxaphycin A. Changes between structures are marked in red.

C. Lobocyclamides

Lobocyclamides A, B and C were isolated in 2002 from a sample of *Lyngbya confervoides* collected in Cay Lobos, Bahamas [52]. Lobocyclamide A differs from laxaphycin A by a serine in position 2 instead of an homoserine and a D-tyrosine that replaces the D-phenylalanine in position 6 (Figure 9). The article of MacMillan *et al.* suggests a L-*allo*-Ile in position 9 while indicating that is is certainly the same configuration as for laxaphycin A and hormothamnin A, *i.e.*, a D-*allo*-Ile. It can be assumed that lobocyclamide A possesses a D-*allo*-Ile in position 9 and that an error was reported in the article. Differences are observed between the structure proposed in the figure and the text of the article. The figure suggests a Ser in position 2, a Hyp in position 4, a Hse in position 5, and a D-Tyr in position 6 while the text indicates a Hse, Pro, Ser, and D-Tyr in these respective positions. These slight differences in position and stereochemistry show the complexity that chemists face in confirming structures of natural products [36].

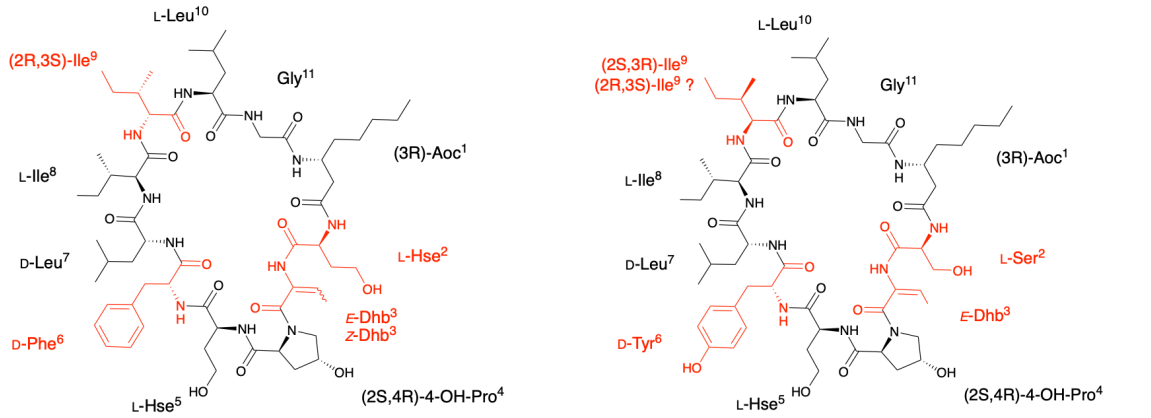

Laxaphycin A [L-Hse^2, (*E*)-Dhb^3, D-Phe^6, (2R,3S)-Ile^9]
Hormothamnin A [L-Hse^2, (*Z*)-Dhb^3, D-Phe^6, (2R,3S)-Ile^9]

Lobocyclamide A [L-Ser^2, (*E*)-Dhb^3, D-Tyr^6, (2S,3R)-Ile^9 or (2R,3S)-Ile^9]

Figure 9. Structure of lobocyclamide A compared to laxaphycin A or hormothamnin A. Changes between structures are marked in red.

Lobocyclamide B structure is very close to the previously reported laxaphycin B and B3 [52]. The main differences are constituted by a (2R,3R)-4-hydroxythreonine replacing the 3-hydroxyasparagine in position 8, which has never been reported in other peptides of the series, and a 4-hydroxyproline in position 10 that replaces the proline. The absolute configurations of the amino acids remain identical with those observed for laxaphycin B despite amino acid variations (Figure 10) [47].

The only difference observed between lobocyclamide B and C is the size of the long carbon chain present in position 1. Indeed, lobocyclamide C contains a β-aminooctanoic acid instead of a β-aminodecanoic acid, bringing it closer to the structure of laxaphycin D.

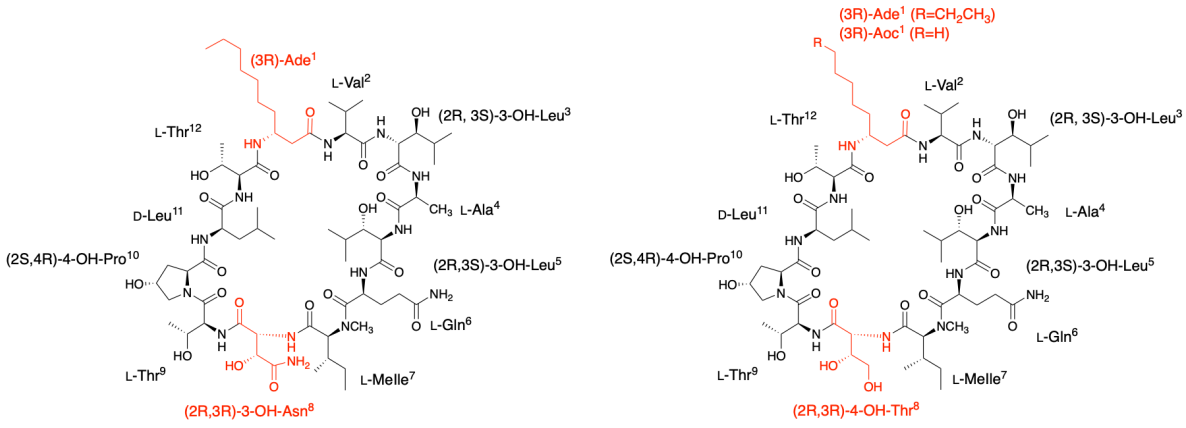

Laxaphycin B3 [(3R)-Ade^1, (2R,3R)-3-OH-Asn^8]

Lobocyclamide B [(3R)-Ade^1, (2R,3R)-4-OH-Thr^8]
Lobocyclamide C [(3R)-Aoc^1, (2R,3R)-4-OH-Thr^8]

Figure 10. Structure of lobocyclamides B and C compared to laxaphycin B3. Changes between structures are marked in red.

D. Scytocyclamides

Scytocyclamides A, B and C were first isolated from the cultivated fresh water *Scytonema hofmanni* PCC 7110 by Jan Christoph Grewe in the early 2000s [57]. This initial study was recently completed by Sivonen's team, which isolated three new scytocyclamides A2, B2 and B3 from the same cyanobacterium [58]. The analysis of the organic extract by UPLC-QToF allowed the isolation of six peaks, three corresponding to the scytocyclamide A-C previously described by Jan Christoph Grewe and three less abundant peaks associated with masses suggesting less hydroxidic peptides. The combination of NMR, PSD spectra, MALDI-ToF mass spectrometry and later MS-MS spectra of the scytocyclamide A-C showed that the amino acid sequence could be recovered from different generated ions in which the proline is always in the N-terminal position. The same fragmentation model was applied to the MS-MS spectra of the new scytocyclamides revealing their sequence and in particular the amino acids having lost a hydroxy group. Within this set of peptides, scytocyclamides A and A2 are related to laxaphycin A and scytocyclamides B, C, B2 and B3 to laxaphycin B. As the later article is focused on the biosynthesis of these peptides, amino acid stereochemistry was deduced from the epimerases found in the biosynthetic gene cluster and from analogy with peptides of the same family (Figure 11A).

Scytocyclamide A is a close analogue of laxaphycin A that differs only by the replacement of homoserine by a glutamine in position 2 [57]. Scytocyclamide A2 differs from scytocyclamide A by replacing 4-hydroxyproline with simple proline in position 4 (Figure 11A) [58].

The scytocyclamide B sequence was determied by homology with analogues such as laxaphycin, hormothamnin or lobocyclamide [57]. This comparison identified that scytocyclamide B has the laxaphycin D (Figure 11B). In the case of scytocyclamide C, MALDI-ToF analysis shows a mass difference of 16 Da with scytocyclamide B, showing a loss of one hydroxy group in the sequence. The very strong similarities with the sequence of scytocyclamide B observed during the analyses accounted for the substitution of the 3-hydroxyleucine in position 5 by a leucine. Thus, the structure of scytocyclamide C is closely related to that of scytocyclamide B (laxaphycin D) (Figure 11B). Similarly, scytocyclamide B2 contains a D-asparagine while scytocyclamide B (laxaphycin D) contains a D-hydroxyasparagine in position 5 (Figure 11B) [58]. Finally, scytocyclamide B3 cumulates the two modifications present in scytocyclamides B2 and C with a D-asparagine in position 8 and a D-leucine in position 5 replacing the hydroxylated counterparts found in scytocyclamide B (Figure 11B).

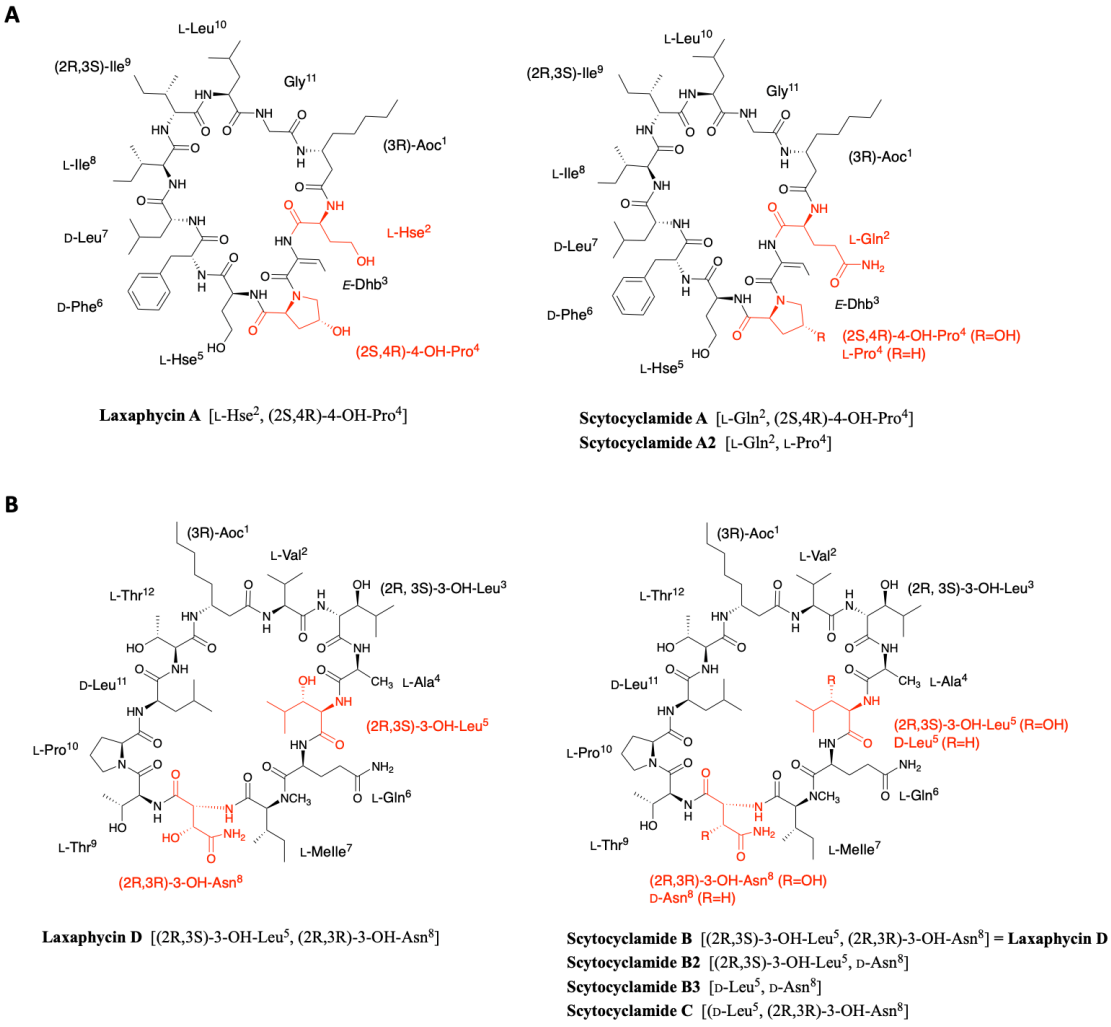

Figure 11. A) Structure of scytocyclamides A and A2 compared to laxaphycin A. B) Structure of scytocyclamides B, B2, B3 and C compared to laxaphycin D. Changes between structures are marked in red.

E. Lyngbyacyclamides

In 2010, a marine cyanobacterium *Lyngbya* sp. collected at the Ishigaki Island in Japan allowed the isolation of two other members related to laxaphycin B, called lyngbyacyclamides A and B [59]. Thanks to NOE and HMBC correlations, the complete structure of both lyngbyacyclamides was established. Lyngbyacyclamide A differs from laxaphycin B by replacing L-alanine in position 4 by L-homoserine, (2R,3S)-hydroxyleucine in position 5 by D-leucine and D-leucine in position 11 by D-phenylalanine (Figure 12). Lyngbyacyclamide B has the same lyngbyacyclamide A sequence except that it contains an 4-hydroxyproline instead of a proline in position 10 (Figure 12).

Stereochemistry of amino acids was partially deduced from Marfey's analysis and comparison with analogous compounds within the laxaphycin B series. This was confirmed by the synthesis of this peptide a few years later, assuming that these non-proteinogenic amino acids were in the same absolute configuration as laxaphycin B [47]. Comparison of the NMR data of the

synthetic peptide with the one reported for natural lyngbyacyclamide A confirmed that the stereochemistry observed within the laxaphycin family is generally conserved.

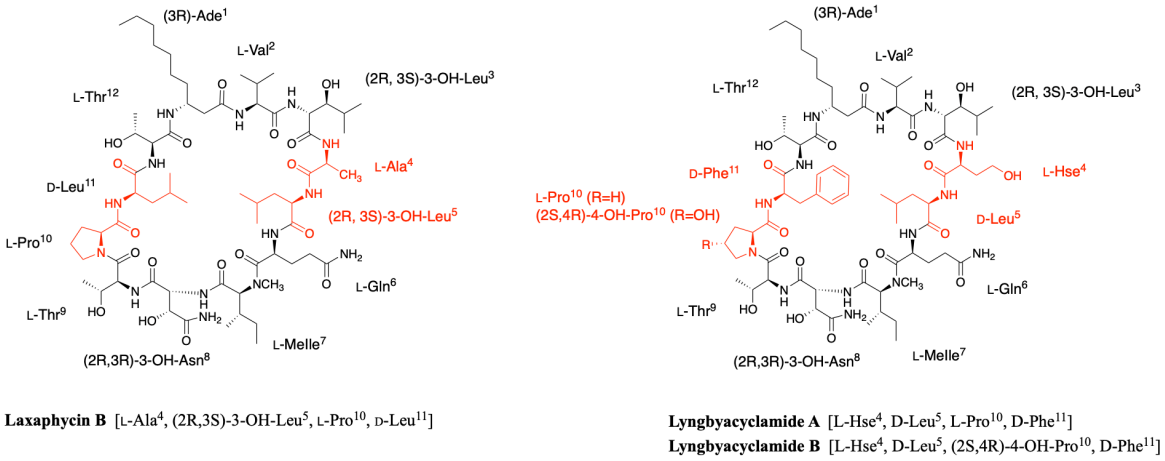

Figure 12. Structure of lyngbyacyclamides A and B compared to laxaphycin B. Changes between structures are marked in red.

F. Trichormamides

In the context of research on natural antiproliferative products from freshwater cyanobacteria, Orjala's group isolated four peptides, trichormamides A-D, from two different cyanobacteria, *Trichormus* sp. UIC 10339 collected in Raven Lake (Wisconsin, USA) and *Oscillatoria* sp. UIC 10045 collected in Downers Grove (Illinois, USA) [60,61]. Trichormamide A complete structure was determined thanks to NMR spectra and was defined as an undecapeptide related to laxaphycin A. Mass fragmentation analysis allowed to fragment the cyclic peptide, with a first cleavage at the N-terminal side of proline, and to confirm a structure with substantial differences with laxaphycin A as almost 60% of the amino acid differs between the two peptides, making it the most distant analogue in terms of sequence identity from laxaphycin A. It is worth noting that trichormamide A is the only example in the laxaphycin A-type peptides lacking the dehydrobutyrine residue. Marfey's analysis enables to assign the absolute configuration of amino acids in the sequence and prove once again the consistency of the series (Figure 13). Trichormamide D is a laxaphycin A analogue isolated from *Oscillatoria* sp. UIC 10045 strain [61]. ROESY correlations enable to confirm a *E*-configuration for the dehydrobutyrine residue. Glutamine, proline, valine and serine were determined as L-configured while tyrosine, phenylalanine and 3-aminodecanoic acid are D-configured. The stereochemistry of the two leucines were more difficult to attribute but was finally assigned as L for leucine in position 10 and D for leucine in position 7, which is consistent with stereochemistry found in laxaphycin A analogues (Figure 13).

Trichormamides B and C are 12-residue laxaphycin analogues isolated from *Trichormus* sp. UIC 10339 and from *Oscillatoria* sp. UIC 10045, respectively [60,61]. While the only difference between trichormamide C and laxaphycin B is the replacement of the (2R,3R)-3-

hydroxyasparagine in position 8 by a simple D-asparagine, the trichormamide B contains three modifications with respect to laxaphycin B (Figure 13). For trichormamide B, the valine in position 2 is replaced by an isosteric isoleucine, the alanine in position 4 by an homoserine and the D-leucine in position 9 by a D-tyrosine. The most striking modification concerns the substitution of the 3-hydroxyasparagine in position 8 by a D-serine that made it a unique representant in this laxaphycin B series.

Some of the modifications contained in the trichormamides made them an attractive group for total synthesis in order to establish further structure activity relationships or simple structure confirmation. For this purpose, trichormamide A was synthesized in 2018 as described by Luo *et al*. [60], along with a diastereoisomer containing a D-*allo*-Ile in position 9 instead of the described L-Ile [62]. Indeed, laxaphycin A and its analogues contain a D-*allo*-Ile in position 9, suggesting an error in the structure of trichormamide A described with an L-Ile. A difference was observed in the resolution and width of the peaks obtained in NMR for the synthetic trichormamide A and the described natural peptide. However, this difference is maintained between the natural peptide and the diastereoisomer containing a D-*allo*-Ile, making it impossible to conclude on the stereochemistry of this amino acid. Furthermore, due to the lack of supply of the natural peptide, comparison between natural and synthetic products was impossible.

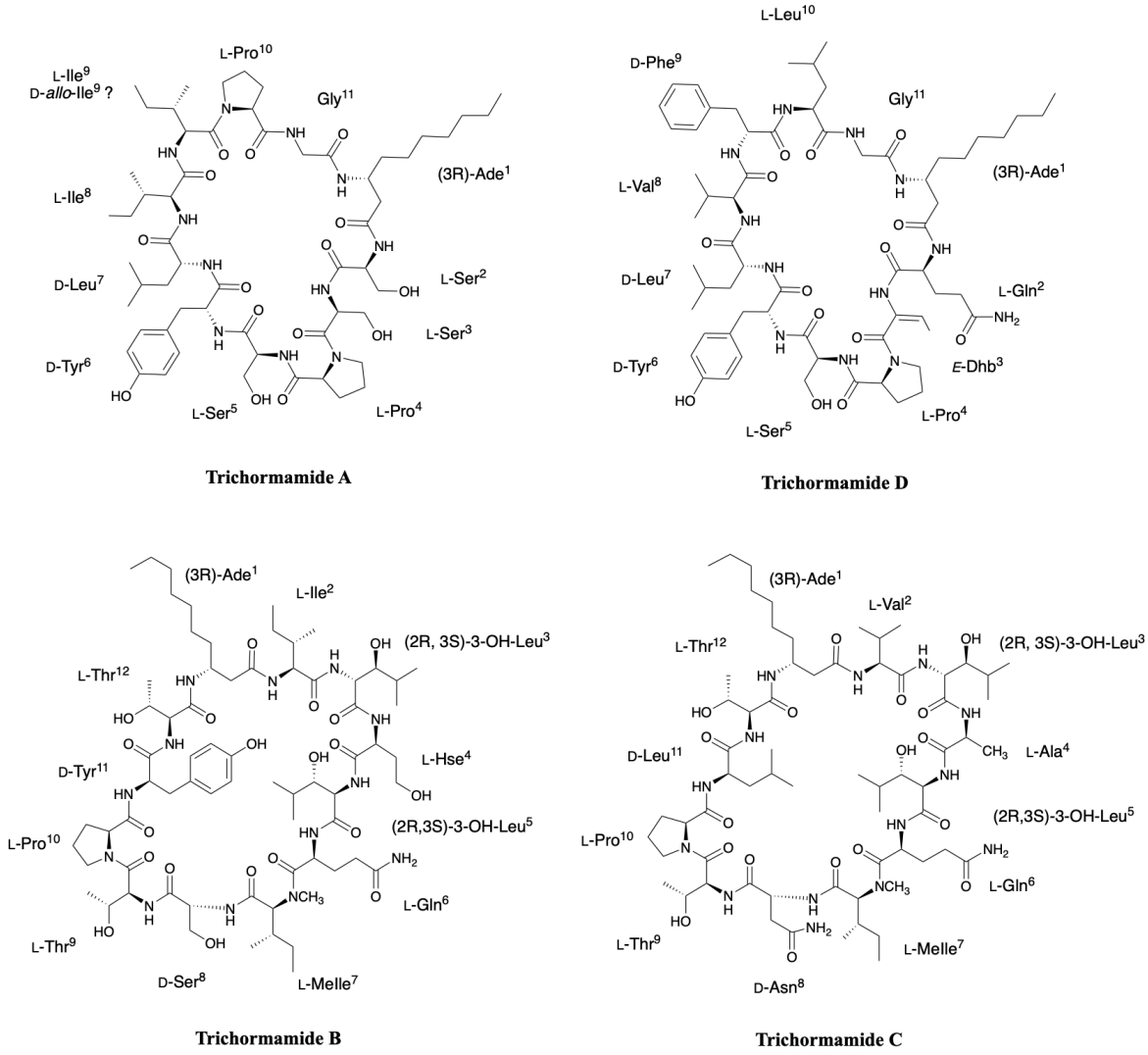

Figure 13. Structure of trichormamide A, B, C and D as described by Luo et al. [60,61].

G. Heinamides

Very recently, Sivonen's group identified eight new laxaphycins from *Nostoc* sp. UHCC 0702 (collected from lake Villähteen Kukkanen) and named heinamides, three of A-type and five of B-type laxaphycins [63]. By cultivating on ^{15}N-containing medium and comparing the masses of the labeled and unlabeled compounds, they showed that heinamides A1, A2, and A3 contain 11 nitrogen atoms, as do the A-type laxaphycins. In contrast, heinamides B1, B2, B3, B4, and B5 contain 14 nitrogen atoms, 1 more than B-type laxaphycins. By recombination of pure and mixed heinamides LC-MS/MS and NMR data, structures for heinamides type A and B could be proposed (Figure 14, Figure 15).

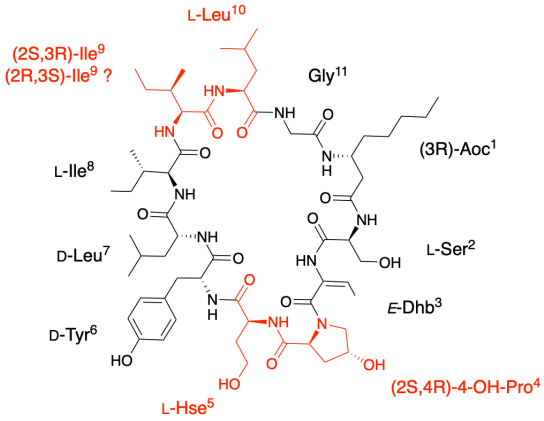

Lobocyclamide A [(2S,4R)-4-OH-Pro^4, L-Hse^5, (2S,3R)-Ile^9 or (2R,3S)-Ile^9, L-Leu^{10}]

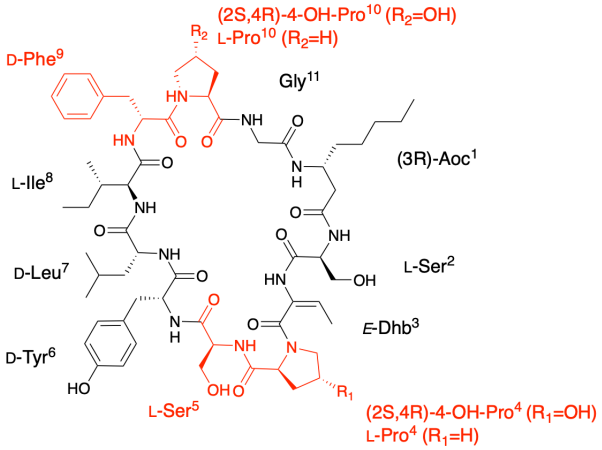

Heinamide A1 [(2S,4R)-4-OH-Pro^4, L-Ser^5, D-Phe^9, (2S,4R)-4-OH-Pro^{10}]
Heinamide A2 [L-Pro^4, L-Ser^5, D-Phe^9, (2S,4R)-4-OH-Pro^{10}]
Heinamide A3 [L-Pro^4, L-Ser^5, D-Phe^9, L-Pro^{10}]

Figure 14. Structure of heinamides A1-A3 compared to lobocyclamide A. Changes between structures are marked in red.

In the case of type A heinamides, no major changes were observed compared to the different type A laxaphycins (Figure 14). On the other hand, type B heinamides have particular features making them quite unique (Figure 15). At position 1, 3-aminooctanoic acid is hydroxylated on carbon 5 with undescribed stereochemistry, whereas this modification has never been reported before. Position 4 is a homoserine, already observed in several type B laxaphycins, but this time containing a carbamoyl group on the alcohol of the side chain, explaining the additional nitrogen atom. This type of amino acid has never been found in other natural peptides. The proline at position 10 can be hydroxylated on carbon 3 and methylated on carbon 4, depending on the different heinamides. The stereochemistry of these two carbons has not been determined. The 3-OH-4-Me-Pro is not much described in the case of natural products from cyanobacteria, but is found in fungi as in the case of echinocandins [64]. Finally, a (2R,3R)-4-OH-Thr occupies position 8 as previously described in lobocyclamide B and C [52]. However, in view of the data obtained in the study of heinamide biosynthesis, it would seem

that it is in fact a homoserine hydroxylated on carbon 3 rather than a threonine hydroxylated on carbon 4 [63]. Therefore, this amino acid will be named (2R,3R)-3-OH-Hse in the rest of this review, although this does not change the final structure.

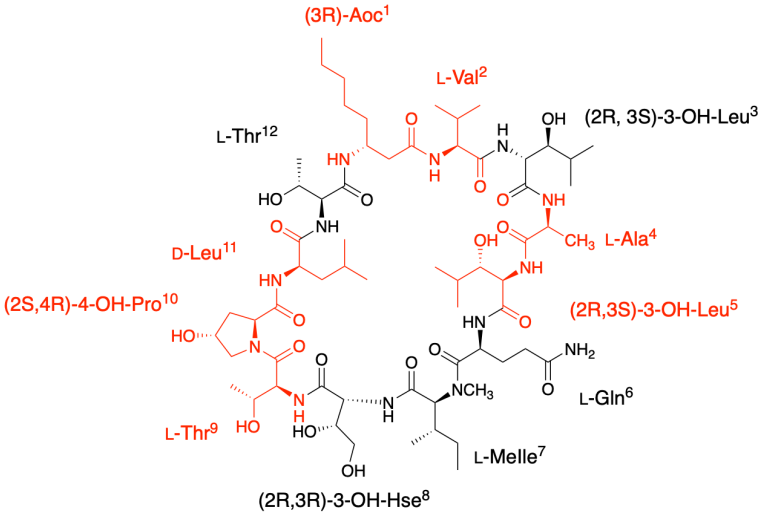

Lobocyclamide C [(3R)-Aoc[1], L-Val[2], L-Ala[4], (2R,3S)-3-OH-Leu[5], L-Thr[9], (2S,4R)-4-OH-Pro[10], D-Leu[11]]

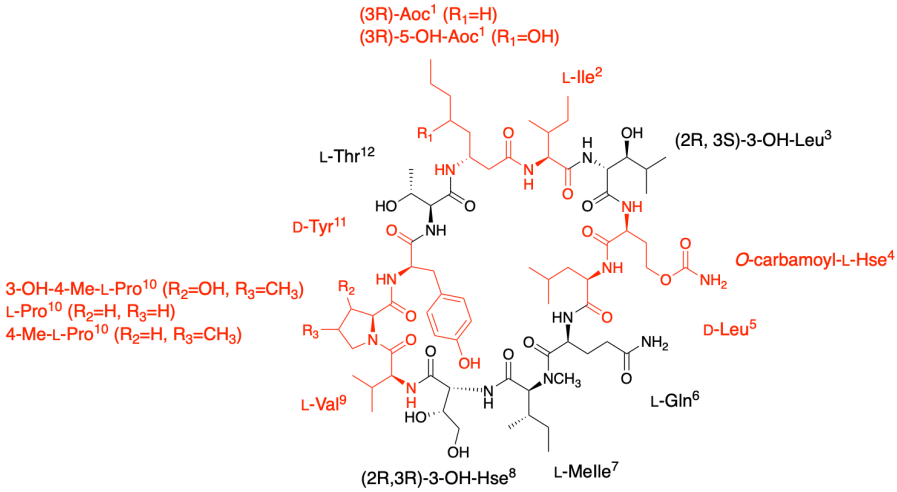

Heinamide B1 [(3R)-5-OH-Aoc[1], L-Ile[2], *O*-carbamoyl-L-Hse[4], D-Leu[5], L-Val[9], 3–OH-4-Me-L-Pro[10], D-Tyr[11]]
Heinamide B2 [(3R)-5-OH-Aoc[1], L-Ile[2], *O*-carbamoyl-L-Hse[4], D-Leu[5], L-Val[9], L-Pro[10], D-Tyr[11]]
Heinamide B3 [(3R)-Aoc[1], L-Ile[2], *O*-carbamoyl-L-Hse[4], D-Leu[5], L-Val[9], L-Pro[10], D-Tyr[11]]
Heinamide B4 [(3R)-Aoc[1], L-Ile[2], *O*-carbamoyl-L-Hse[4], D-Leu[5], L-Val[9], 3–OH-4-Me-L-Pro[10], D-Tyr[11]]
Heinamide B5 [(3R)-5-OH-Aoc[1], L-Ile[2], *O*-carbamoyl-L-Hse[4], D-Leu[5], L-Val[9], 4-Me-L-Pro[10], D-Tyr[11]]

Figure 15. Structure of heinamides B1-B5 compared to lobocyclamide C. Changes between structures are marked in red.

To date, 13 different undecacyclic peptides belonging to the laxaphycin A family (Table 1, Figure 16), and 21 dodecacyclic peptides in the laxaphycin B family are known (

Table 2, Figure 17). Three acyclic laxaphycin A and six acyclic laxaphycin B completed these two groups. Cyclic and acyclic peptides were isolated from marine, freshwater, or terrestrial

cyanobacteria and even from a marine mollusk found at different locations all around the world.

Laxaphycin A analogues are relatively homogeneous in terms of sequence with the notable exception of the trichormamide and heinamide analogues that share less than 50% of their amino acids in common (Table 1).

One of the most frequent modifications observed in laxaphycin B relies on the hydroxylation state. 70% of the analogues are concerned by this modification type, that affects the (2R,3S)-hydroxyleucine in position 5, the (2R,3R)-hydroxyasparagine in position 8 and the proline in position 10 that are often replaced by (2R)-leucine, the (2R)-asparagine or (2S,4R)-hydroxyproline, respectively. Alanine 4 is also concerned and mostly replaced by a homoserine. Among the other observed substitution, valine in position 2 is replaced by its β-branched equivalent isoleucine, whereas (2R)-leucine in position 11 is changed by isosteric amino acids such as (2R)-phenylalanine or (2R)-tyrosine. Thus, most of the time, amino acid variations are made with isosteres but stereochemistry remains preserved (

Table 2). However, the determination of structures and stereochemistry is often complex in the case of natural products, with overlapping or similar signals. Thus, wrong attributions can be made, so that one cannot be sure of the proposed structures until the total synthesis is performed. About 20 of these misassignments have been reported in 2015 on various natural products and laxaphycin does not constitute an exception [48]. In the next part of this review, we described and summarized the efforts that have been pursued to synthesize the laxaphycins.

Table 1. Amino acid sequence and molecular weight of laxaphycin A analogues.

Columns highlighted in orange indicate fully conserved amino acids in all analogues. Columns highlighted in blue show the most conserved amino acids in the analogues relative to the laxaphycin A sequence. When amino acids are different between laxaphycin A and the analogues, the replaced amino acids are reported in a white box. Empty white boxes indicate the absence of the corresponding amino acids compared to laxaphycin A. The grey boxes represent the amino acids for which there is still a doubt about the stereochemistry of the amino acid. Aoc: 3-aminooctanoic acid, Ade: 3-aminodecanoic acid, Hse: homoserine, Dhb: dehydrobutyrine, Hyp: hydroxyproline.

% AA variation vs LaxA		1	2	3	4	5	6	7	8	9	10	11	Exact Mass
54.5 %	Heinamide A3		Ser		Pro	Ser	(2R)Tyr			(2R)Phe	Pro		1186.65122
	Heinamide A2		Ser		Pro	Ser	(2R)Tyr			(2R)Phe	(2S,4R)Hyp		1202.64614
45.5 %	Heinamide A1		Ser			Ser	(2R)Tyr			(2R)Phe	(2S,4R)Hyp		1218.64105
18.2 % or 27.3 %	Lobocyclamide A		Ser				(2R)Tyr			(2R,3S)Ile or (2S,3R)Ile			1197.70091
18.2 %	Scytocyclamide A2		Gln		Pro								1206.73763
	[Des-(Leu^{10}-Gly^{11})]AcyclolaxA												1043,62669
9.1 %	Scytocyclamide A		Gln										1222.73255
	Hormothamnin A			Z-Dhb									1195.72165
	[D-Val^{9}]LaxA									(2R)Val			1181.70599
	LaxA2								Val				1181.70599
	[Des-Gly^{11}]AcyclolaxA												1156,71075
	AcyclolaxA												1213,73221
	LaxA	**Aoc**	**Hse**	**E-Dhb**	**(2S,4R)Hyp**	**Hse**	**(2R)Phe**	**(2R)Leu**	**Ile**	**(2R,3S)Ile**	**Leu**	**Gly**	1195.72165
9.1 %	LaxE	Ade											1223.75295
63.6 %	Trichormamide D	Ade	Gln		Pro	Ser	(2R)Tyr		Val	(2R)Phe			1256.71989
63.6 % or 72.7 %	Trichormamide A	Ade	Ser	Ser	Pro	Ser	(2R)Tyr			(2R,3S)Ile or Ile	Pro		1183.68526

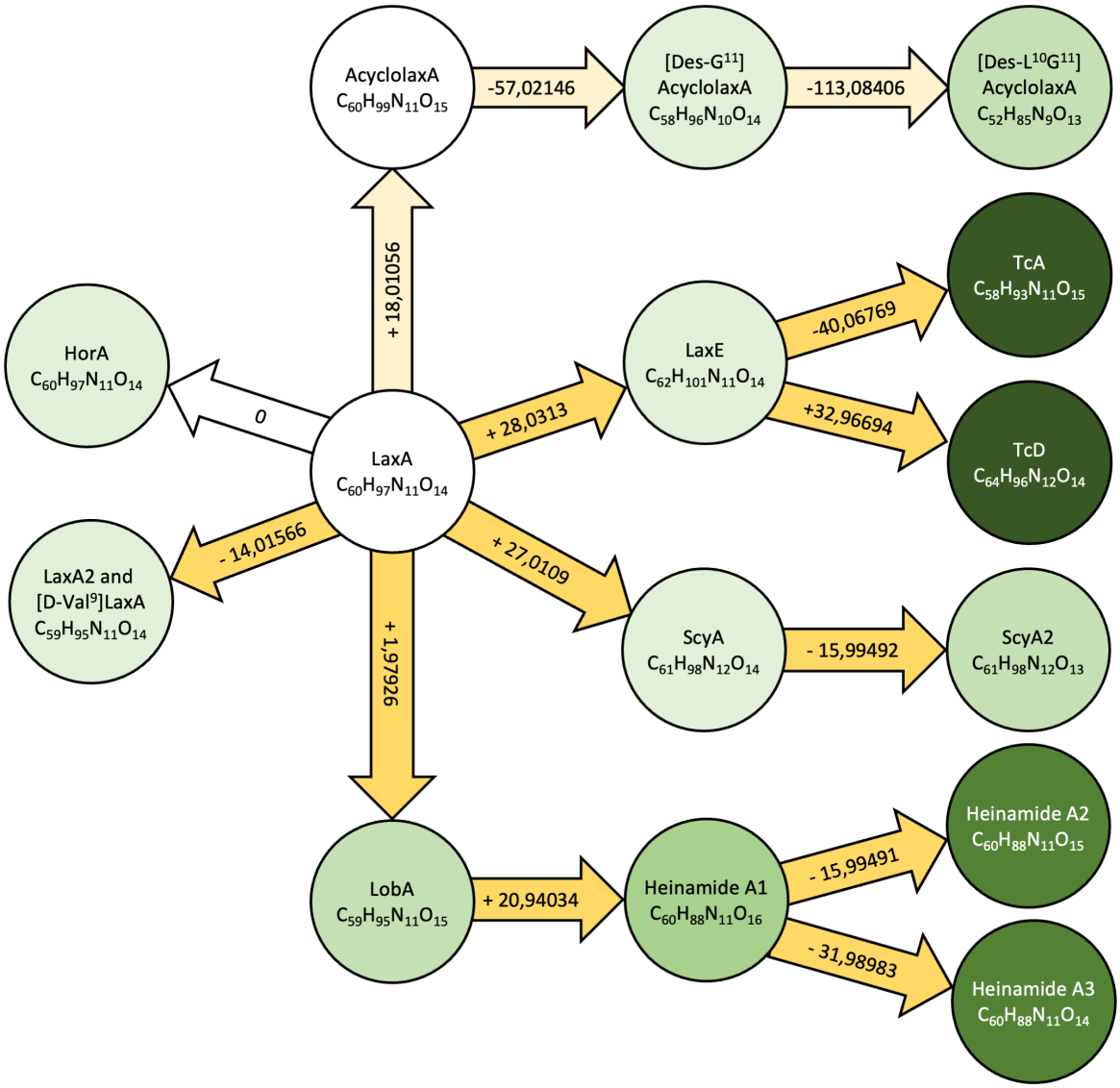

Figure 16. Similarity mass network linking the laxaphycin A analogues.

Dark yellow arrows represent one or more amino acid changes, including loss of hydroxy groups. The light-yellow arrows indicate a ring opening or loss of amino acids without modifications. The white arrow to hormothamnin A shows that there are no modifications or loss of amino acids but simply a change in stereochemistry. Lax: laxaphycin, Hor: hormothamnin, Lob: lobocyclamide, Scy: scytocyclamide, Acyclolax: acyclolaxaphycin, Tc: trichormamide.

Table 2. Amino acid sequence and molecular weight of laxaphycin B analogues.

Columns highlighted in orange indicate fully conserved amino acids in all analogues. Δ sign represents cyclic glutamine and is not consider as a modification in the sequence as the cyclization occurs after the deletion of Ala[4] and Hle[5]. Columns highlighted in blue show the most conserved amino acids in the analogues relative to the laxaphycin B sequence. When amino acids are different between laxaphycin B and the analogues, the replaced amino acids are reported in a white box. Empty white boxes indicate the absence of the corresponding amino acids compared to laxaphycin B. Aoc: 3-aminooctanoic acid, Ade: 3-aminodecanoic acid, Hle: hydroxyleucine, Hse: homoserine, (N)-MeIle: N-methylisoleucine, Hasn: hydroxyasparagine, Hyp: hydroxyproline. * = amino acid first described as (2R,3R)-4-OH-Thr by MacMillan and *al*. but was renamed as 3-OH-Hse after the study of biosynthesis.

% AA variation vs LaxB		1	2	3	4	5	6	7	8	9	10	11	12	Exact Mass
41.7 %	LaxB6		Ile		Val	(2R)Leu			(2R)Asn			(2R)Tyr		1454.87486
33.3 %	LaxB5		Ile		Val				(2R)Asn			(2R)Tyr		1470.86977
	Trichormamide B		Ile		Hse				(2R)Ser			(2R)Tyr		1445.83814
	Lyngbyacyclamide B				Hse	(2R)Leu					(2S,4R)Hyp	(2R)Phe		1458.83338
25 %	Lyngbyacyclamide A				Hse	(2R)Leu						(2R)Phe		1442.83847
	[Des-(Ala[4]-Hle[5])]AcyclolaxB1211						Δ							1211.70131
	[Des-(Ala[4]-Hle[5])]AcyclolaxB3										(2S,4R)Hyp			1228.72786
16.7 %	Lobocyclamide B								3-OHHse*		(2S,4R)Hyp			1397.83814
	LaxB4				Hse						(2S,4R)Hyp			1440.84395
	[Des-(Ala[4]-Hle[5])]AcyclolaxB1195						Δ							1195.70639
	[Des-(Ala[4]-Hle[5])]AcyclolaxB													1212.73294
8.3 %	AcyclolaxB3										(2S,4R)Hyp			1428.84395
	LaxB3										(2S,4R)Hyp			1410.83339
	LaxB2					(2R)Leu								1378.84355
	Trichormamide C								(2R)Asn					1378.84355
	AcyclolaxB													1412.84904
	LaxB	**Ade**	**Val**	**(2R,3S)Hle**	**Ala**	**(2R,3S)Hle**	**Gln**	**(N)-MeIle**	**(2R,3R)Hasn**	**Thr**	**Pro**	**(2R)Leu**	**Thr**	1394.83847
8.3 %	LaxD or Scytocyclamide B	Aoc												1366.80717
16.7 %	Scytocyclamide B2	Aoc							(2R)Asn					1350.81226
	Scytocyclamide C	Aoc				(2R)Leu								1350.81226
25%	Scytocyclamide B3	Aoc				(2R)Leu			(2R)Asn					1334.81734
	Lobocyclamide C	Aoc							3-OHHse*		(2S,4R)Hyp			1369.80684
50.0 %	Heinamide B3	Aoc	Ile		O-carbamoyl-Hse	(2R)Leu			3-OHHse	Val		(2R)Tyr		1472.84903
58.3 %	Heinamide B2	5-OH-Aoc	Ile		O-carbamoyl-Hse	(2R)Leu			3-OHHse	Val		(2R)Tyr		1488.84395
	Heinamide B4	Aoc	Ile		O-carbamoyl-Hse	(2R)Leu			3-OHHse	Val	3-OH-4-MePro	(2R)Tyr		1502.85960
66.7 %	Heinamide B1	5-OH-Aoc	Ile		O-carbamoyl-Hse	(2R)Leu			3-OHHse	Val	3-OH-4-MePro	(2R)Tyr		1518.85451
	Heinamide B5	5-OH-Aoc	Ile		O-carbamoyl-Hse	(2R)Leu			3-OHHse	Val	4-MePro	(2R)Tyr		1502.85960

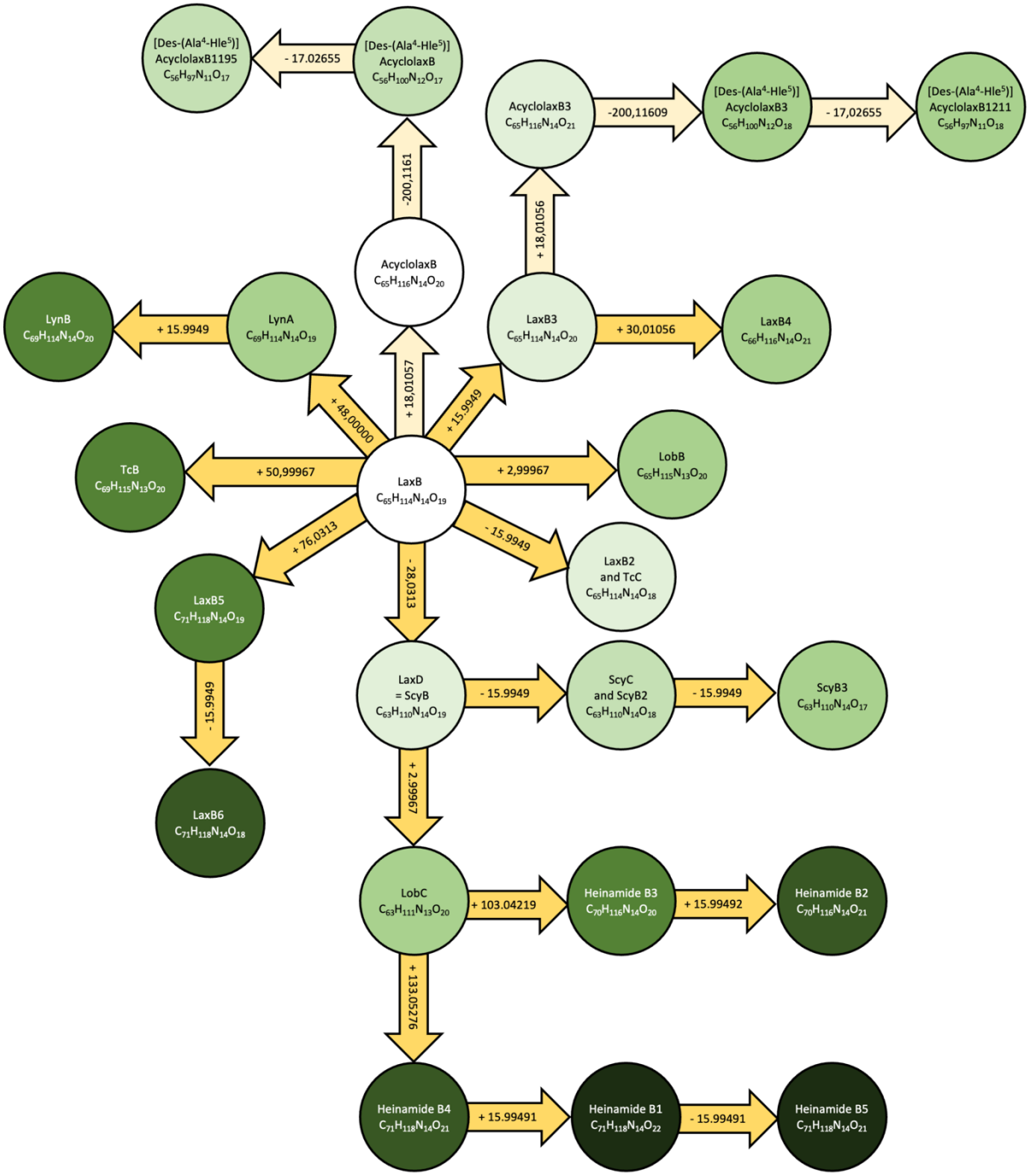

Figure 17. Similarity mass network linking the laxaphycin B analogues.

Dark yellow arrows represent one or more amino acid changes, including loss or gain of hydroxy groups. The light-yellow arrows indicate a ring opening or loss of amino acids without modifications, including the cyclization of glutamine to pyroglutamate. Lax: laxaphycin, Lob: lobocyclamide, Lyn: lyngbyacyclamide, Scy: scytocyclamide, Acyclolax: acyclolaxaphycin, Tc: trichormamide.

III. Chemical synthesis

Cyclic peptides have gained in interest in recent years, in particular due to their resistance to degradation by proteases [65]. Most cyclic peptides have low membrane permeability, but some are able to penetrate the cell membrane, such as cyclosporine [66]. Although many marine peptides are isolated from various organisms, few are studied in clinical research. In the case of cyclic peptides isolated from cyanobacteria, none have been approved as drugs [67,68]. Various reasons can be given for this lack of success, such as the number of steps to be completed in the laboratory beforehand. Indeed, the minute quantities of peptides isolated directly from various organisms preclude their study. It is therefore up to the chemists to produce them on a larger scale. However, it is necessary to develop efficient synthesis methods to obtain these complex molecules. Among the peptides cited in the first part of this review, laxaphycin B was the first of to be fully synthesized [47] along with a very few analogues. In all the cases, the syntheses of the non-classical amino acids included in their sequences are required. This prerequisite concerns the β–hydroxyleucines stereoisomers, the 3-aminodecanoic acid, the 3 amino-octanoic acid and the (2R,3R)-3-hydroxyaspartic acid (Figure 18). Furthermore, for each amino acid relevant protections of the functionality are needed to develop the solid phase peptide synthesis scheme. In this section, we describe the synthetic methods used to obtain these different amino acids as well as the complete syntheses of some laxaphycins and their analogues. The possible synthesis techniques for obtaining dehydrobutyrine are also described, although it is possible to obtain it directly through dehydration of threonine.

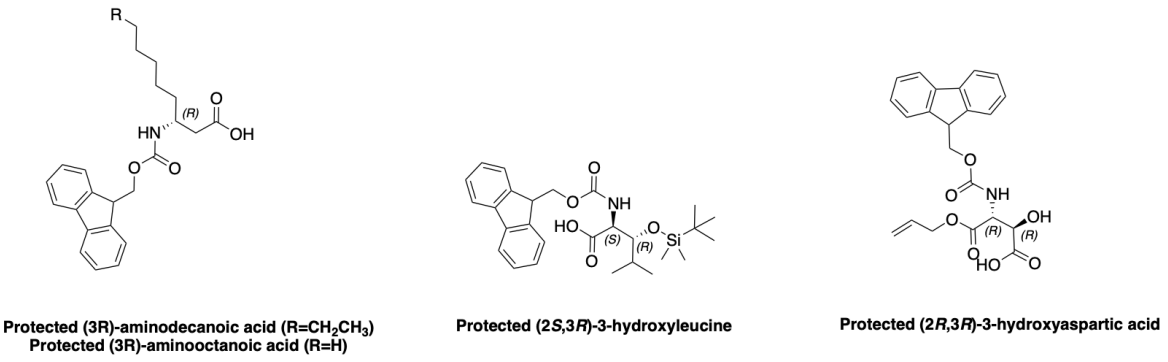

Figure 18. Structure of protected non-proteinogenic amino acids needed for the laxaphycin B synthesis.

A. Synthesis of characteristic amino acids in laxaphycins

a) Synthesis of 3-aminodecanoic acid and 3-aminooctanoic acid

(3R)-aminodecanoic acid (Ade) is obtained from commercially protected aspartic acid following the synthesis method of Buron *et al*. [69]. The carboxylic acid function of *Z*-Asp(OtBu)-OH is converted to anhydride with isobutyl chloroformate. The unsymmetrical anhydride is then reduced to alcohol using $NaBH_4$. The alcohol is transformed to a tosyl group

that allows a nucleophilic substitution with an organocuprate $(Hex)_2CuLi$ to introduce the fatty chain. After successive deprotection of the acid and amine groups, the latter is protected by a Fmoc group in order to use it for solid phase during peptide synthesis (Figure 19). (3R)-aminooctanoic acid (Aoc) is equivalently synthesized using the organocuprate corresponding to the desired chain.

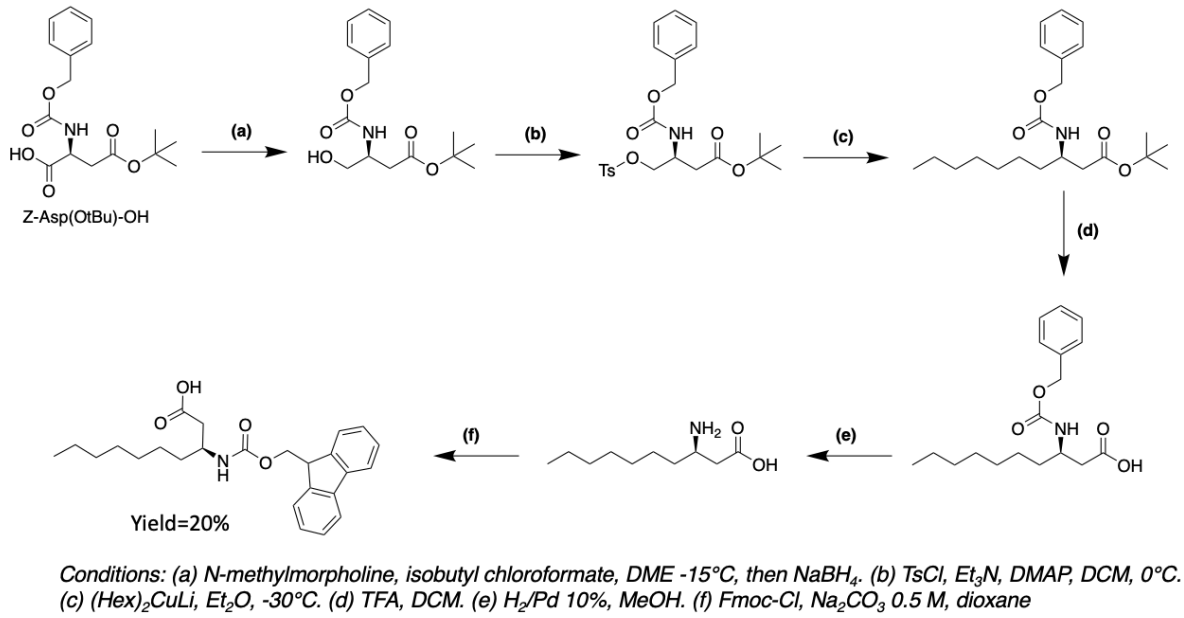

Figure 19. Synthesis of protected (3R)-aminodecanoic acid.

b) Synthesis of hydroxylated amino acids

The biggest challenge encountered by chemists to obtain β-hydroxylated amino acids is the control of the stereochemistry of the asymmetric carbons. It is therefore necessary to go through very stereoselective reactions. The synthesis of (2R,3S)-3-OH-Leu, found notably in laxaphycin B and lobocyclamide B, has been reported in the literature. For the total synthesis of laxaphycin B, Boyaud *et al*. used Sharpless dihydroxylation to obtain (2R,3S)-3-OH-Leu (Figure 20) [47,70]. This method was notably used by Hale *et al*. for the synthesis of the antibiotic depsipeptide A83586C [71]. The first step is a Wittig reaction between isobutyraldehyde and triethylphosphonoacetate to form the corresponding alkene. Next, this alkene is dihydroxylated by the action of AD-mix-α and methane sulfonamide. The two alcohols groups are protected as a cyclic sulfite, later oxidized to cyclic sulfate. Sodium azide reacts according to a nucleophilic substitution on the alpha carbon and the alcohol in the beta position is recovered by hydrolysis. The N_3 group is then reduced in NH_2 function to obtain (2S,3S)-3-OH-Leu. To produce (2R,3S)-3-OH-Leu, an additional step is necessary to modify the stereochemistry. LiBr reacts on the cyclic sulfate in alpha to reverse the stereochemistry of carbon 2. The addition of NaN_3 will then recover the desired stereochemistry to obtain the (2R,3S)-3-OH-Leu after reduction of N_3 to NH_2 function.

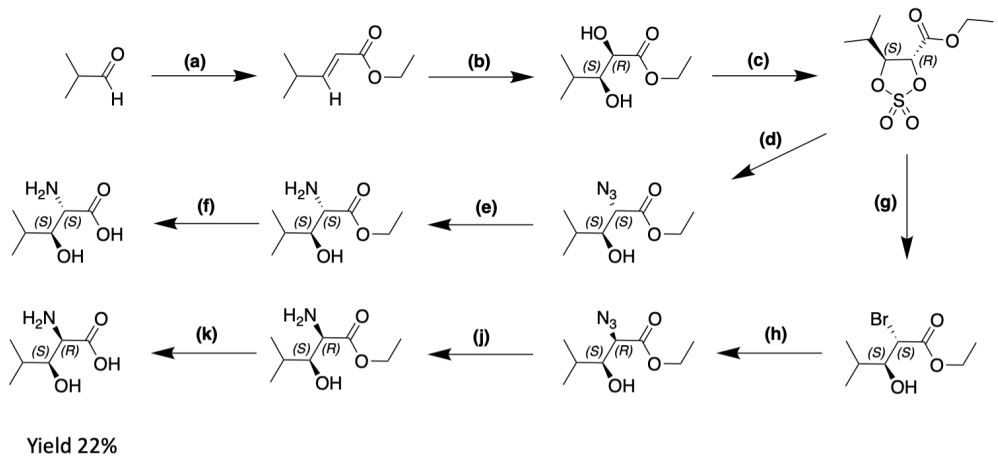

Conditions: (a) triethylphosphonoacetate, NaH, THF, rt, 12h, 97% (b) AD-mix-α, methanesulfonamide, ^{t}BuOH/H_2O 1/1 v/v, 0°C, 48h, 68% (c) (i) $SOCl_2$, CCl_4, reflux (ii) $NaIO_4$, ACN/H_2O, $RuCl_3.3H_2O$, 73% (d) NaN_3, acetone, H_2O, 79% (e) Pd/C, H_2, MeOH, 92% (f) NaOH 1M, THF, 0°C, 100% (g) LiBr, THF, 93% (h) NaN_3, DMSO, 68% (j) Pd/C, H_2, MeOH, 100% (k) NaOH 1M, THF, 0°C, 88%

Figure 20. Synthesis of (2R,3S)-3-OH-Leu by Sharpless dihydroxylation.

Absolute configuration of 3-hydroxyleucine present in lobocyclamide B was determined through a synthesis involving an aldolization reaction (Figure 21) [72]. *N*-(diphenylmethylene)glycine *tert*-butyl ester is transformed into its enolate by the action of *n*-BuLi. The addition of enolate to isobutyraldehyde is assisted by sparteine. Two products are obtained, *threo*-oxazolidine and *erythro*-imine, leading to (2R,3S)-3-OH-Leu and (2R,3R)-3-OH-Leu after hydrolysis, respectively. *threo*-oxazolidine and *erythro*-imine could be obtained in different proportions depending on the base used to form the enolate, *n*-BuLi/sparteine of LDA. MacMillan *et al.* used the same method to obtain 4-hydroxythreonine (or 3-hydroxyhomoserine) with the addition of enolate to *O*-benzylglyoxal. This reaction could be generalized for different β–hydroxylated amino acids, if the right aldehyde is used to create the side chain of the amino acid (Figure 21).

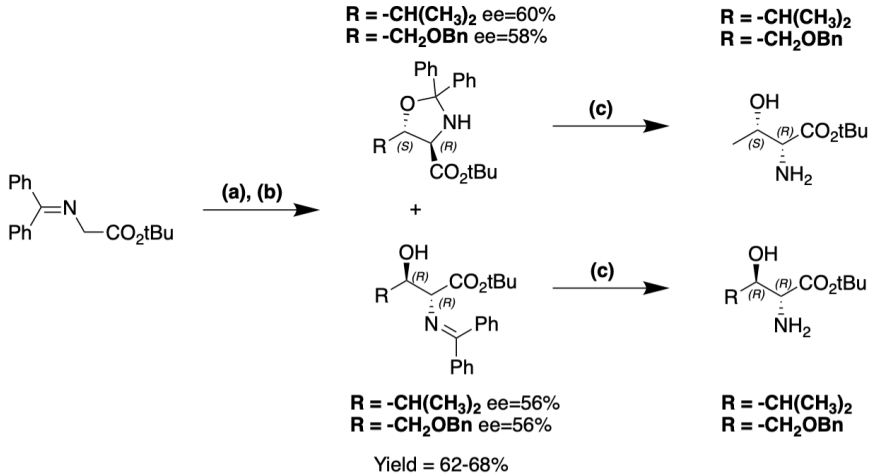

Conditions: (a) n-BuLi, (-)-Sparteine, toluene, -78°C (b) aldehyde RCH=O, -78°C, 3h-6h (c) adequate hydrolysis and deprotection. R = i-Pr, $BnOCH_2$, c-C_6H_{11}, n-C_6H_{13}, Ph, 2-naphthyl, 2-furyl.

Figure 21. Synthesis of (2R,3S)-3-OH-Leu or (2R,3R)-3-OH-Leu by an aldolization reaction.

These two examples are the only ones reported to date in the context of the synthesis of laxaphycins and their derivatives. However, 3-hydroxyleucines are found in other peptides and it is possible to obtain them by different synthetic routes. The (2R,3S)-3-OH-Leu present in skyllamycin is obtained via the Garner aldehyde of S configuration (Figure 22) [73]. A Grignard reaction takes place between Garner aldehyde and isopropylmagnesium bromide to form the corresponding secondary alcohol. The oxazolidine is then hydrolyzed to obtain a primary alcohol which is oxidized to carboxylic acid. The amine can then be deprotected from its Boc to be reprotected by a Fmoc group, more suitable for peptide synthesis. The oxazolidine is then reformed between the amine and the alcohol function in the beta position.

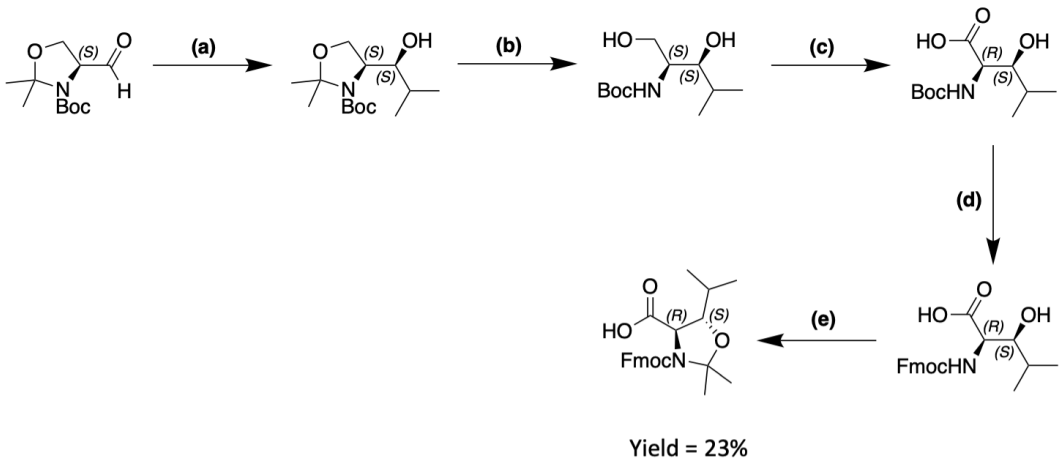

Conditions: (a) iPrMgBr, THF, -78°C, rt, 3h, 44% (b) HCl 0.5M, THF, rt, 16h (c) 10-15% NaOCl, TEMPO, acetone/5% aq $NaHCO_3$ 1/1 v/v, rt, 16h (d) (i) HCl in dioxane, DCM, rt, 3h (ii) Fmoc-Osu, $NaHCO_3$, THF, rt, 16h (e) 2,2-DMP, $BF_3.OEt_2$, acetone, rt, 4h

Figure 22. Synthesis of (2R,3S)-3-OH-Leu using Garner's aldehyde.

Muraymycin C1 [74] as well as alkaloid cyclopeptides [75] contain (2S,3S)-3-OH-Leu obtainable from a protected serine (Figure 23). The ester of the serine is reduced to primary alcohol, which is subsequently oxidized to aldehyde. By a Grignard reaction of isopropylmagnesium bromide on the aldehyde, the corresponding secondary alcohol is obtained. After deprotection of the amine, an oxazolidinone is formed between the amine and the secondary alcohol. The primary alcohol of the serine side chain can then be oxidized to carboxylic acid and the oxazolidinone is hydrolyzed to give (2S,3S)-3-OH-Leu. Several other synthesis routes can be used to obtain these compounds and are referenced in the literature [76–79].

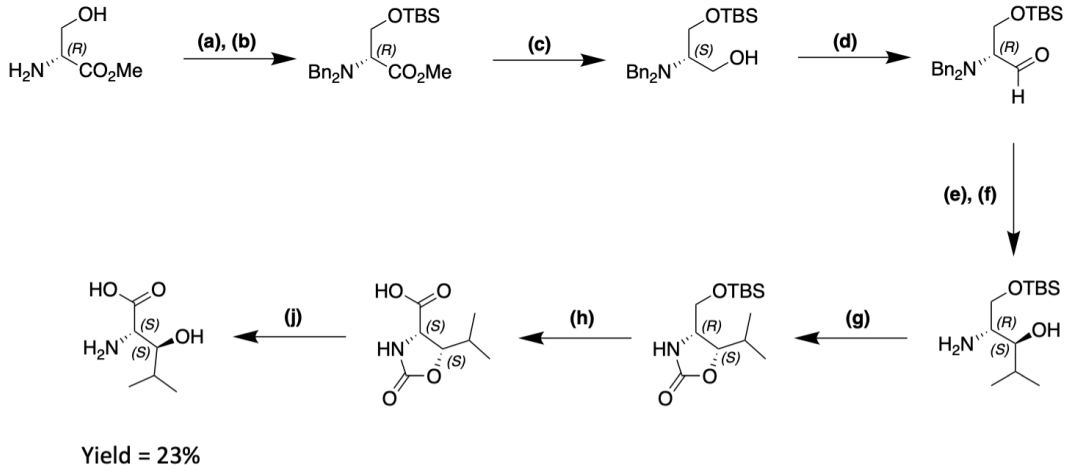

Conditions: (a) $NaHCO_3$, BnBr, DMF/THF 4/1 v/v, 100% (b) TBSCl, DMF, imidazole, 90% (c) $LiBH_4$, Et_2O-MeOH, 99% (d) oxalyl chloride, DCM, 45% (e) iPrMgCl, Et_2O, 88-95% (f) $Pd(OH)_2$, H_2, MeOH, 100% (g) carbonyldiimidazole, THF, DMAP (cat) (h) KF, Jones, 72% (j) HCl conc, 85%

Figure 23. Synthesis of (2S,3S)-3-OH-Leu using chiral derivative of serine.

As part of the synthesis of laxaphycin B, Boyaud *et al.* also had to synthesize 3-hydroxyaspartic acid to graft its side chain on Rink Amide resin [80]. The synthesis starts with a cyclic sulfate derived from dimethylester tartrate (Figure 24). The opening of the sulfate with LiBr gives access to a secondary alcohol and a bromine group. The bromine is then replaced by an azide. The azide is reduced to an amine which is then protected by an Fmoc group. The two ester functions are hydrolyzed to carboxylic acid. An acetonide is formed between the carboxylic acid and the alcohol of the same carbon in order to be able to differentiate the two carboxylic acid groups. The remaining acid can thus be protected by an allyl group, allowing later the hydrolysis of the acetonide and the protection of the alcohol in beta position. This type of synthesis has been used by other groups to obtain 3-hydroxyaspartic acid [81] or 3-hydroxyasparagine [82].

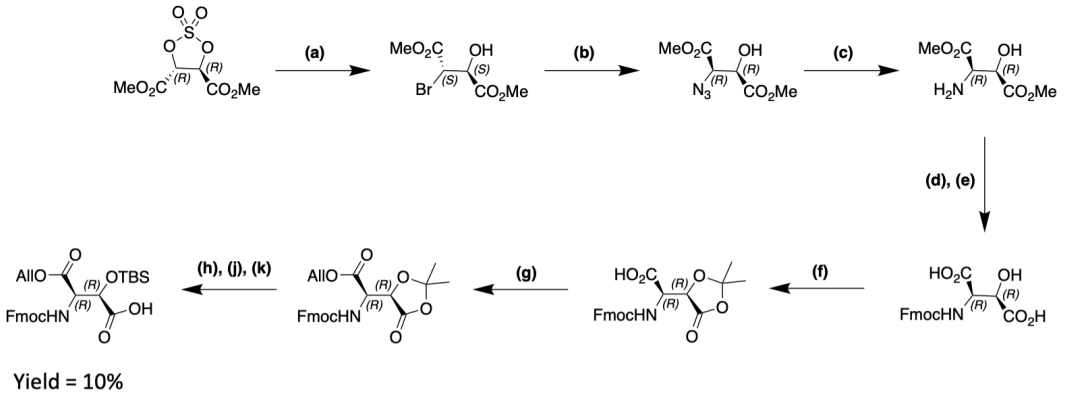

Conditions: (a) (i) LiBr, THF, 25°C, 2h (ii) Et_2O, 20% H_2SO_4 in water, 12h, 82% (b) NaN_3, DMF, 25°C, 90% (c) H_2, Pd/C 10%, ethyl acetate, 25°C, 94% (d) LiOH 0.7M, MeOH (e) HCl 3M, 10% Na_2CO_3, Fmoc-Osu, dioxane, 25°C, 79% (f) $(CH_3O)_2C(CH_3)_2$, ethyl acetate, 70°C, 24h, 63% (g) Allyl bromide, Cs_2CO_3, DMF, 25°C, 98% (h) TFA, H_2O, 70°C, 86% (j) TBSOTf, DIPEA, DCM, 0°C, 4h (k) (i) K_2CO_3, H_2O, 2h (ii) citric acid, 35%

Figure 24. Synthesis of (2R,3R)-3-OH-Asp from dimethylester tartrate.

The aminohydroxylation of Sharpless is also used to obtain 3-hydroxyasparagine or 3-hydroxyaspartic acid in the synthesis of other peptides such as polytheonamide B [83] or Ramoplanin A2 [84]. It is also possible to obtain these compounds via the opening of an oxazoline [85].

Echinocandins are natural peptides found in different ascomycota fungi. They notably contain a 4-OH-Pro and a 3-OH-4-Me-Pro. The 3-OH-4-Me-Pro, which is also found in heinamides, can be synthesized in several ways [86], in particular by starting from a γ-lactam prepared from pyroglutaminol (Figure 25) [87]. The γ-lactam is diastereospecifically transformed into an epoxide. The oxirane is then cleaved to release a secondary alcohol. After a deprotonation/methylation/reprotonation sequence, the *cis*-disubstituted lactam is obtained. This compound is reduced to trisubstituted *N*-benzyl pyrrolidine. The benzyl group is removed by hydrogenolysis and replaced by a Boc protection. The two alcohol functions can thus be protected by a TBDMS group, which will be selectively removed from the primary alcohol only. The latter can then be oxidized by the Sharpless method [88] and the (2S,3S,4S)-3-hydroxy-4-methylproline is recovered by acid hydrolysis (Figure 25).

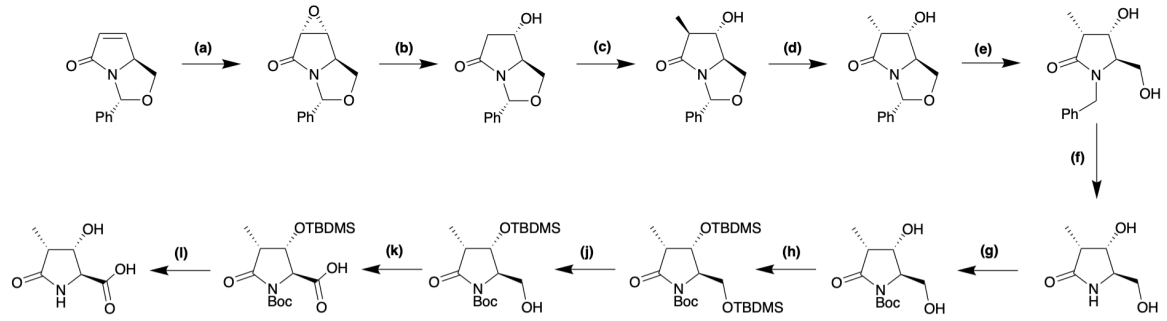

Yield = 12%

Conditions: (a) t-BuOOH, K_2CO_3, DMF, 30 min, $(Bu)_4NF$, rt, 87% (b) SmI_2 , 95% (c) (i) LDA/THF-HMPA, Argon atmosphere, -78°C, 1h at -35°C (ii) MeI, 2h at -78°C, 68% (d) (i) LDA/THF-HMPA, Argon atmosphere, 1h at -78°C then 1h at -35°C (ii) H^+, pivaloic acid, 73% (e) BH_3-DMS in THF, Argon atmosphere, rt then 70°C during 2.25h, 86% (f) H_2, Pd/C 10%, 16h (g) $(Boc)_2O$ in MeOH, 2h at rt, 92% (h) TBDMSCl in DMF, 18h at 40°C, 75% (j) AcOH:THF:H_2O 13:3:7 ,12h at 30°C, 70% (k) $NaIO_4$ / $RuCl_3$ in water, CCl_4/ACN, 30 min at rt, 80% (l) HCl 6N, 30 min at rt then 4h at 118°C, 90%.

Figure 25. Synthesis of (2S,3S,4S)-3-hydroxy-3-methylproline from γ-lactame.

c) Synthesis of dehydro amino acids

Dehydroamino acids are commonly found in cyanobacterial peptides [36] and more generally in peptides of microbial origin [89]. Several studies have shown that these amino acids can structure peptides, similarly to 2-aminoisobutyric acid (Aib) [90,91]. In view of their role in the structure of peptides, it is important to understand how they are biosynthesized and to develop their syntheses for an efficient peptides' production. In this sub-section, we will develop the synthesis pathways used to obtain dehydrobutyrine, present in type A laxaphycins.

Dehydroamino acids are mainly obtained through the dehydration of their β-hydroxylated equivalent amino acid, *i.e.,* threonine for dehydrobutyrine, by an elimination mechanism. Indeed, attempting to insert dehydrobutyrine directly into a peptide sequence brings very low

yield because of the low nucleophilicity of the enamine that impairs its coupling with other amino acids. It is therefore more interesting to insert a threonine into the peptide sequence and then dehydrate it, either once the peptide elongation is completed, or on a smaller sequence of the peptide which will then be inserted into the rest of the sequence. This dehydration reaction has been widely reported in the literature [92]. We report here some cases of dehydration to obtain dehydrobutyrine.

Albericio's group has developed a synthesis method, using EDC/CuCl for the dehydration of threonine, which can be applied both in solution and in solid phase synthesis (Figure 26) [93,94]. The elimination mechanism would be by an E1 or E1cb, with EDC activating the alcohol of the threonine in the presence of CuCl in a DMF/DCM mixture followed by β-elimination of the activated group.

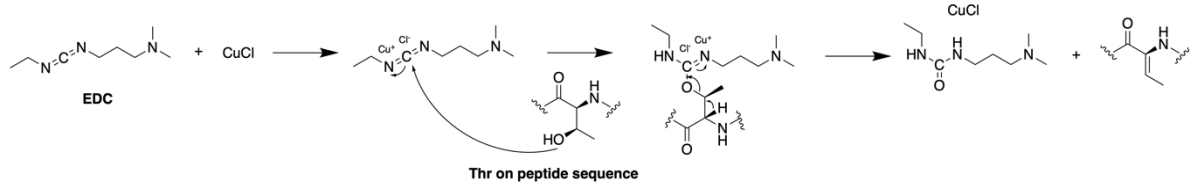

Figure 26. Proposed mechanism of action of EDC on threonine to obtain dehydrobutyrine [93].

The advantage of this technique is that these reagents are inexpensive and simple to use, so the reaction is performed under mild conditions at room temperature. In addition, only the most thermodynamically stable *Z*-isomer of Dhb is produced. In the case of dehydration on a fragment of the peptide, a solution reaction with EDC/CuCl (2:1.2) in solution in DCM/DMF is preferred for a relatively short time (about 20h). For dehydration on the whole peptide, a solid support reaction with EDC/CuCl (2:1.2) in solution in DCM/DMF for a much longer time (several days) is used.

In the case of the synthesis of hormothamnin A, the dehydration reaction was done directly on solid support, but with DIC/CuCl reagents [95]. Indeed, EDC can cause secondary reactions, such as the formation of a cyclic by-product (O-alkyl N-acylisourea) [93] or guanidylation of the N-terminal amino acid, the Fmoc group being sensitive to EDC. Dehydration was therefore performed once the complete linear peptide was obtained, with DIC/CuCl (100:3 equiv) in a DCM/DMF mixture (1:1) for 7 days (Figure 32).

Ferreira *et al*. developed a dehydration method using $(Boc)_2O$/DMAP to protect the side chain alcohol of threonine and the *N,N,N*-tetramethylguanidine base (TMG) to generate removal of the protected alcohol (Figure 27) [96,97]. This method is stereoselective and yields the *Z*-isomer of the dehydro amino acid. Tian's team used the same method to generate dehydrobutyrine one-pot from the threonine already included in the peptide sequence [98].

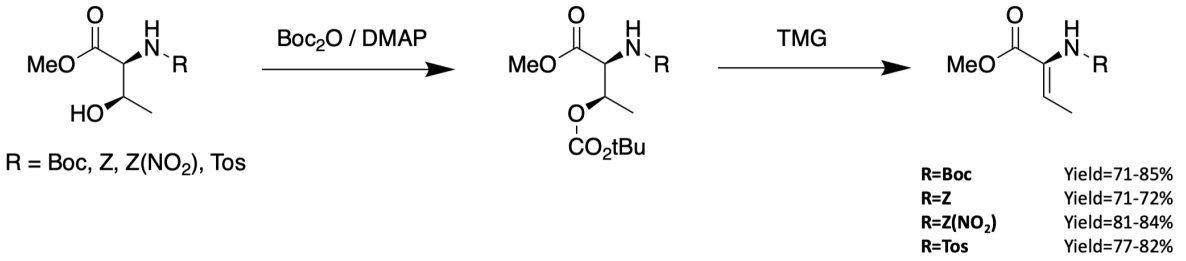

Figure 27. Dehydration of bi-protected threonine by the action of Boc_2O/DMAP and then TMG base [97].

Still with an E1cb elimination reaction, Webster *et al*. showed that it was possible to dehydrate threonine in the presence of pentafluoropyridine and K_2CO_3 base (Figure 28) providing protected dehydrobutyrine [99].

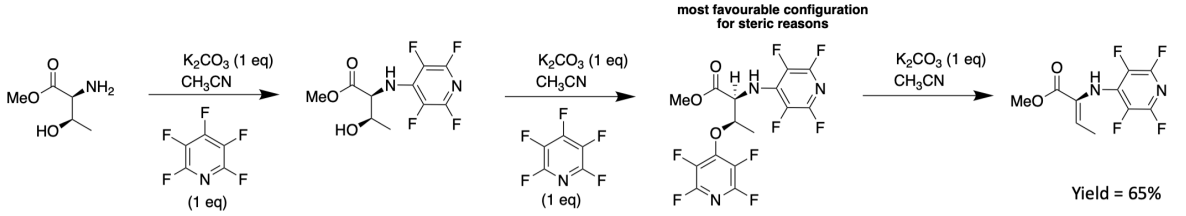

Figure 28. Dehydration of mono-protected threonine by the action of K_2CO_3 base and pentafluoropyridine.

Nagano *et al.* reported an approach for obtaining dehydroamino acids starting from alpha-tosyl glycine and various nitroalkene in the presence of DBU as a base (Figure 29) [100].

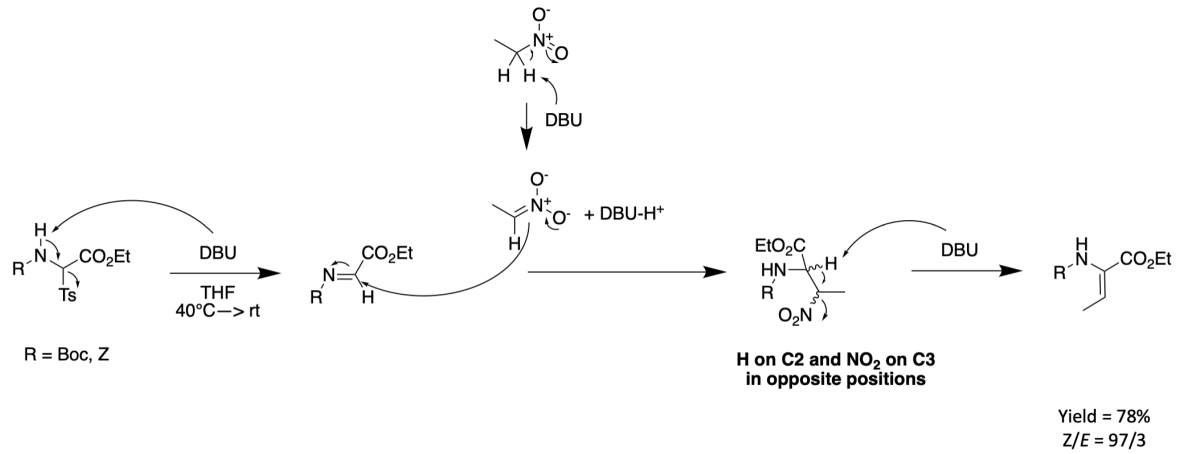

Figure 29. Obtention of dehydrobutyrine from alpha-protected glycine in the presence of DBU base.

To obtain dehydroamino acids other than dehydrobutyrine, other techniques than dehydration are possible and have been reported, notably in a review by Bonauer *et al.* [101].

B. Synthesis of laxaphycin B-type peptides

In order to develop a strategy for the laxaphycin B synthesis, the structure has been simplified to contain only natural amino acids. The 3-hydroxyasparagine and the two 3-hydroxyleucines have been replaced by threonines with the same absolute configuration, and the β-aminodecanoic acid has been replaced by a β-alanine (Figure 30). It is important to note that at the time of the development of this synthesis, the two 3-hydroxyleucines were considered as diastereoisomers and were therefore replaced accordingly by a D-threonine and an L-threonine.

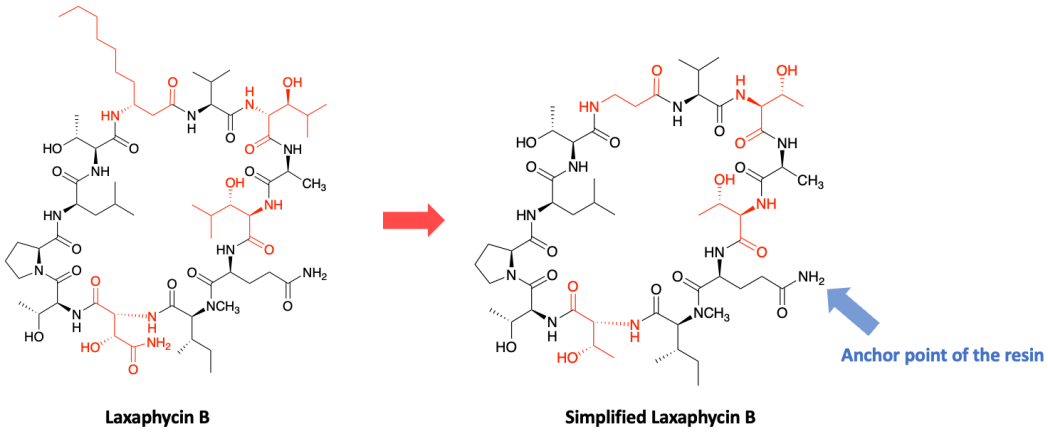

Figure 30. Structure of a simplified laxaphycin B used for the development of laxaphycin B synthesis.

The first trials for the gain of laxaphycin B were based on a head-to-tail cyclization strategy on the solid support to avoid the isolation and purification of an intermediate linear peptide and the risk of dimerization. This cyclization method could be used because the peptide sequence contains an aspartic and a glutamic acid available to be anchored on the resin with their side chain while the acid group is protected with an allyl. Depending on the resin choice, the aspartic and glutamic acid are recovered in their native form in the case of a Wang resin or are transformed into asparagine or glutamine if the synthesis is performed on a rink amide MBHA resin. After preliminary assays, the strategy based on a cyclization between the glutamine and the (*N*)-methylisoleucine was discarded due to the lack of efficiency of the coupling reaction between these two amino acids. The anchoring point of the resin therefore had to be modified, by attaching the side chain of aspartic acid rather than glutamic acid. The elongation of the linear peptide was carried out with HATU/DIEA as coupling reagents to facilitate couplings especially between the glutamine and the (*N*)-methylisoleucine. After the elongation of the peptide, the carboxylic acid of glutamine and the amine of threonine in position 9 were deprotected and subsequently engaged in the cyclization step with DIC/Oxyma. After side chain protections removal under acidic conditions, the simplified laxaphycin B analogue was obtained. Next, this methodology was applied to laxaphycin B. The replacement of β-alanine by β-aminodecanoic acid resulted in a slight decrease in coupling without making synthesis more problematic. Similarly, the addition of 3-hydroxyasparagine

and 3-hydroxyleucine instead of simple asparagine and threonine was not a problem. Laxaphycin B could therefore be obtained by this optimized synthesis method and the LC-MS analysis gave a *m/z* of 1395.8 for $[M+H]^+$ ion. In order to confirm the structure of the synthetic laxaphycin B, HPLC and NMR spectra were compared with the one of the natural laxaphycin B. Significant differences were observed for the proton's chemical shifts but also the retention time of the two molecules were different. Comparison of the amino acid stereochemistry found among the laxaphycin analogues allows to rapidly identify that the 3-hydroxyleucine in position 3 has a stereochemistry (2R,3S) in lobocyclamide B, lyngbyacyclamide B as well as in laxaphycin B2, whereas it had been determined to be (2S,3S) in laxaphycin B. Re-evaluation of Marfey's analyses showed that laxaphycin B contains two 3-hydroxyleucine in (2R,3S) configuration. Laxaphycin B was therefore re-synthesized considering these new stereochemistries and then compared to the natural molecule (Figure 31). Identical signals in HPLC and NMR were observed for both natural and synthetic laxaphycin B, confirming this new structure. The synthesis was then applied to lyngbyacyclamide A, allowing to confirm the stereochemistry of non-proteinogenic amino acids which were postulated by the group of Daisuke Uemura [59].

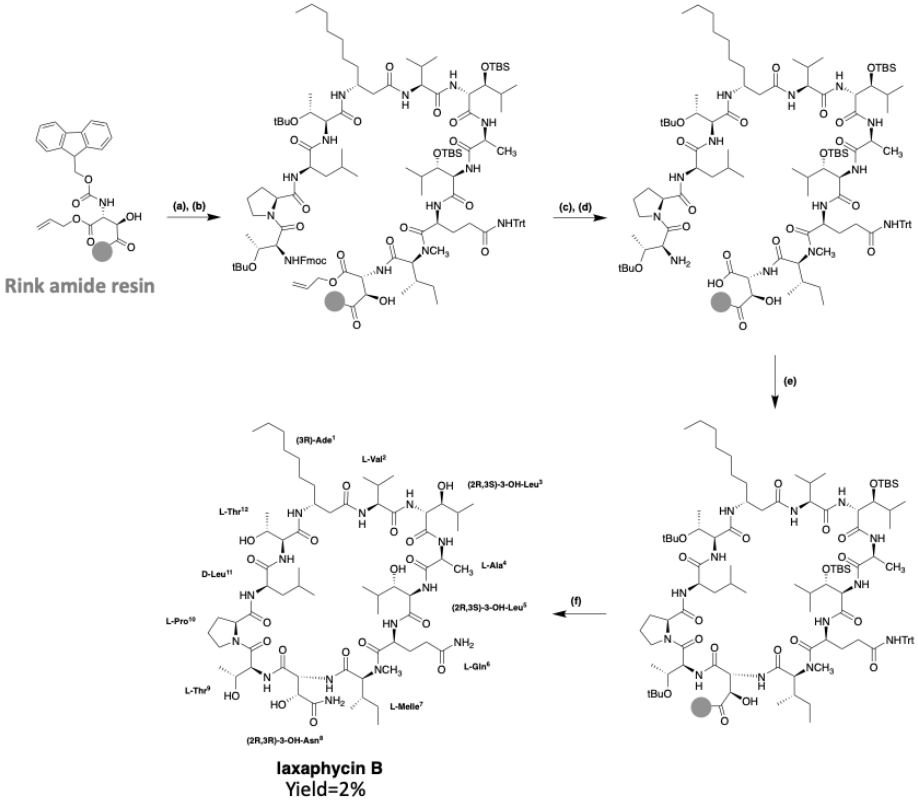

Conditions: (a) (i) 20% v/v piperidine/DMF (ii) Fmoc-NMelle-OH, HATU, DMF, 70°C, 25 W, 5 min. (b) Repeat conditions (a) for all classical amino acids except Fmoc-Gln(Trt)-OH coupled 3 times and capped with 0.5 M acetic anhydride in DMF for 3 min, 60°C, 40 W. Non-proteinogenic amino acids are coupled for 15 min. (c) $Pd(PPh_3)_4$, $CHCl_3$/AcOH/NMM 3.7/0.2/0.1. (d) 20% v/v piperidine/DMF, rt, 2 x 2 min. (e) DIC/Oxyma, DMF, 70°C, 25 W, 3 x 15min. (f) TFA/TIS/H_2O 95/2.5/2.5 v/v/v, rt, 3h.

Figure 31. Optimized synthesis of laxaphycin B.

C. Synthesis of laxaphycin A-type peptides

The synthesis of trichormamide A was investigated in 2018, in order to develop a synthesis method that can be applied to the peptide of the laxaphycin A family [62]. In fact, trichormamide A is a model of choice for the development of this synthesis because it does not contain complex amino acids such as dehydrobutyrine, as other peptides have. Trichormamide A contains the β-aminodecanoic acid (Ade), whose chemical synthesis was already described above. All other amino acids are commercially available. Synthesis was performed at 50°C under microwave irradiations, using DIC/Oxyma coupling agents. The linear peptide was cleaved from the resin by the action of a DCM/TFE/AcOH mixture, while keeping the side chain protections. Cyclization was initiated in solution, under high dilution conditions, in the presence of PyOxim/Oxyma coupling agents, giving good results on this peptide sequence. The cyclic peptide was purified before deprotection of the side chains under strong acidic conditions (Figure 32). HRMS analysis gave a *m/z* of 1184.6919 for $[M+H]^+$ ion while the calculated *m/z* is 1184.6931. The development of the synthesis of this peptide paves the way to obtain other analogous peptides, which would allow the structures to be verified and used for SAR studies. In this article, Gaillard *et al*. applied the synthesis to trichormamide A and a diastereoisomer containing D-*allo*-Ile in position 9 instead of L-Ile. Indeed, all peptides of the laxaphycin A family have been reported with a D-*allo*-Ile[9], except lobocyclamide A which could contain a L-*allo*-Ile, but here again the stereochemistry has not been clearly determined. It could therefore be that lobocyclamide A and trichormamide A both contain a D-*allo*-Ile at this position. The analysis of the NMR spectra of the two diastereoisomers and their comparison with the reported data did not allow structure confirmation in part due to the lack of supply of the natural molecule.

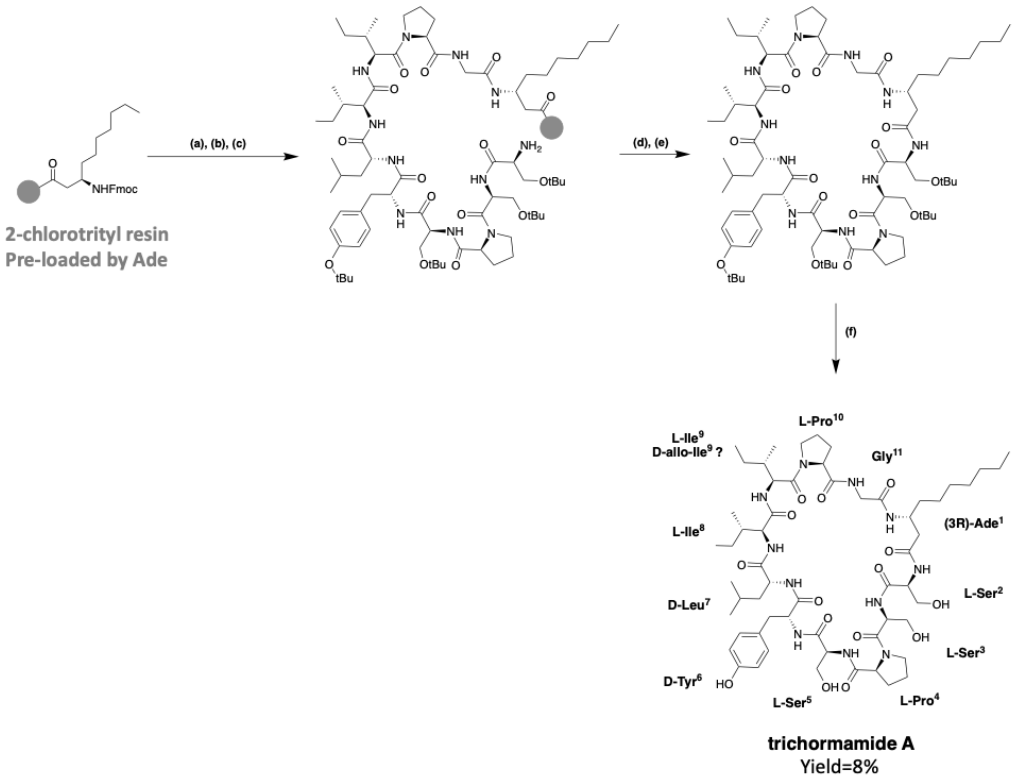

Conditions: (a) 20% v/v piperidine/DMF. (b) (i) Fmoc-Gly-OH, DIC, Oxyma, DMF, 50°C, 20 min (ii) 20% v/v piperidine/DMF. (c) Repeat conditions (b) for amino acids until Fmoc-Ser(tBu)-OH (d) DCM/TFE/AcOH 8/1/1, rt, 2h. (e) PyOxim/Oxyma, DMF, nitrogen atmosphere, rt, overnight. (f) TFA/DCM/H_2O/TIS 4.7/4.7/4/2 v/v/v/v, rt, 1h.

Figure 32. Optimized synthesis of trichormamide A.

After obtaining trichormamide A, the same team undertook the synthesis of hormothamnin A [95]. Hormothamnin A has a *Z*-configuration dehydrobutyrine (*Z*-Dhb) in position 3. In the case of hormothamnin A synthesis, it was chosen to couple a threonine, subsequently dehydrated on the resin. The synthesis is carried out on a 2-chlorotrityl chloride resin preloaded with Aoc. Couplings are done at 50°C with DIC/Oxyma coupling agents. The elongation of the peptide is done until the insertion of homoserine in position 2, and without deprotection of the Fmoc group of the latter. The L-threonine in position 3 introduced without side chain protection was dehydrated on resin, by the action of DIC/CuCl 100/30 in a 50/50 DCM/DMF mixture. The dehydrated peptide is then cleaved from the resin with a DCM/TFE/AcOH 8/1/1 mixture in order to keep the side chain protections. Cyclization is performed with PyOxim/Oxyma under high dilution and then the side chain protections are removed (Figure 33). LC-MS co-injection of the peptide obtained with laxaphycin A revealed 2 distinct peaks, suggesting that the hormothamnin A (*m/z* 1196.48 for $[M+H]^+$ ion) was obtained with the right Dhb configuration (*Z*-Dhb), since this is the only difference with laxaphycin A, which contains an *E*-Dhb [95].

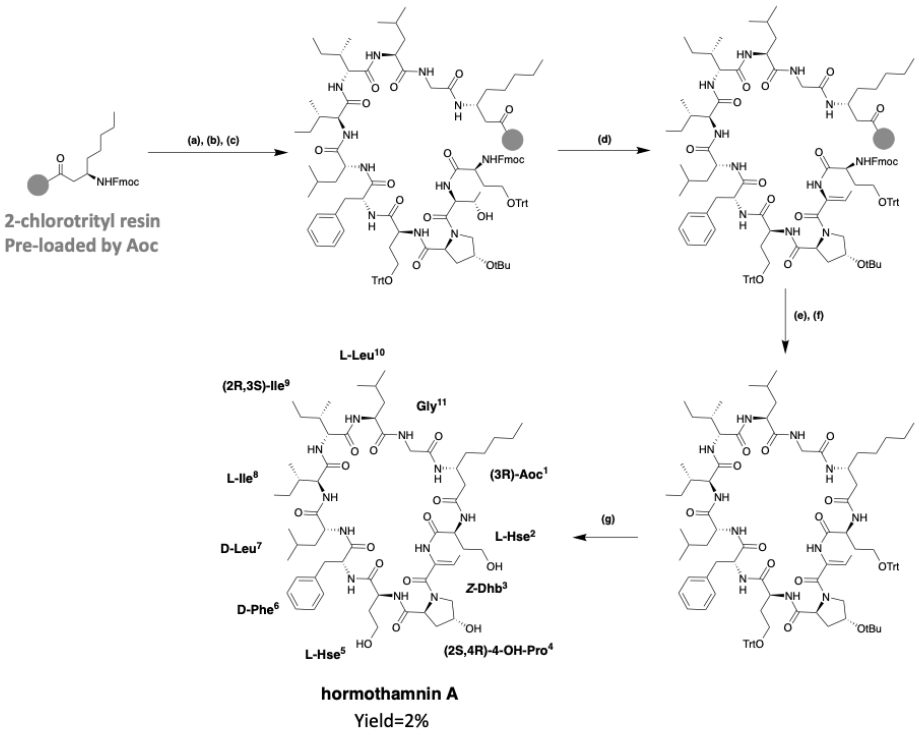

Conditions: (a) 20% v/v piperidine/DMF. (b) (i) Fmoc-Gly-OH, DIC, Oxyma, DMF, 50°C, 10 min (ii) 20% v/v piperidine/DMF. (c) Repeat conditions (b) for amino acids until Fmoc-Thr-OH. Fmoc-Hse(Trt)-OH is not deprotected (d) DIC/CuCl 100/30, DCM/DMF 50/50, nitrogen atmosphere, rt, 7 days. Resin washed with DMF, 5% diethyl thiocarbamate in DMF, DMF and DCM. (e) (i) 20% v/v piperidine/DMF. (ii) DCM/TFE/AcOH 8/1/1, rt, 2h. (f) PyOxim/Oxyma, DMF, nitrogen atmosphere, rt, overnight. (g) TFA/TIS/H_2O 95/2.5/2.5 v/v/v, rt, 2h.

Figure 33. Optimized synthesis of hormothamnin A.

IV. Biosynthesis

Cyanobacteria produce a wide variety of natural bioactive products with high potential for valorization as drugs candidates. Understanding their biosynthesis would allow to consider their production methods through synthetic biology [102]. Natural products from cyanobacteria are mostly synthesized by nonribosomal peptide synthetase (NRPS) and polyketide synthase (PKS) and often by hybrid NRPS/PKS pathways. These large NRPS enzymatic complexes are organized in modules that activate an amino acid, modify it in certain cases before a transfer to the amino acid of the adjacent module to form the amide bond. A module contains at least one adenylation domain (A) which allows the specific recognition of an amino acid and its activation into adenylated aminoacyl, a thiolation domain (T or PCP for peptidyl carrier protein) which retains the peptide during elongation through a thioester bond, and a condensation domain (C) allowing the formation of the peptide bond. The first amino acid is activated by the A domain with ATP co-substrate in the form of an aminoacyl-adenylate (aminoacyl-AMP) and loaded on the 4'-phospho-pantethine (Ppant) side chain of the PCP domain by the action of the thiol group on the -*O*-AMP part of the activated amino acid. At this stage, the substrate can undergo modifications such as epimerization (E domain) or methylation (NMT domain) by optional secondary domains [103]. The E domain possesses a

base that deprotonates the alpha position of the L-amino acid to produce an enolate. During reprotonation, an L/D mixture is obtained, but due to a strong specificity, the following C domain recognizes only the D-amino acids [104]. Different work are underway to share light on the mechanism of action of these enzymes [105].

The amine of the next amino acid, already anchored on its T domain, then attacks the thioester function of the previous amino acid in order to continue the elongation. At the end of the synthesis, the peptide is released by a thioesterase domain (TE) containing a serine that attacks the thioester bond between the peptide and the T domain to form a new intermediate that can either be hydrolyzed to obtain a linear peptide or undergo an intramolecular reaction to give a cyclic peptide (Figure 34). The action of the A domains is specific to the side chains of the substrates while the action of the C domains depends on the stereochemistry of the amino acids. This high specificity ensures the synthesis of the right peptide sequence [106]. Unlike ribosomal peptide synthesis, which leads to peptides containing only natural amino acids, NRPS induce the inclusion of hundreds of non-proteinogenic residues, including D-amino acids, N-methylated or β-hydroxylated amino acids in peptides through the modification of natural amino acids. Hydroxy groups can be used for various modifications, such as glycosylation, and are found in many antibiotic peptides such as lysobactin or skyllamycin [103].

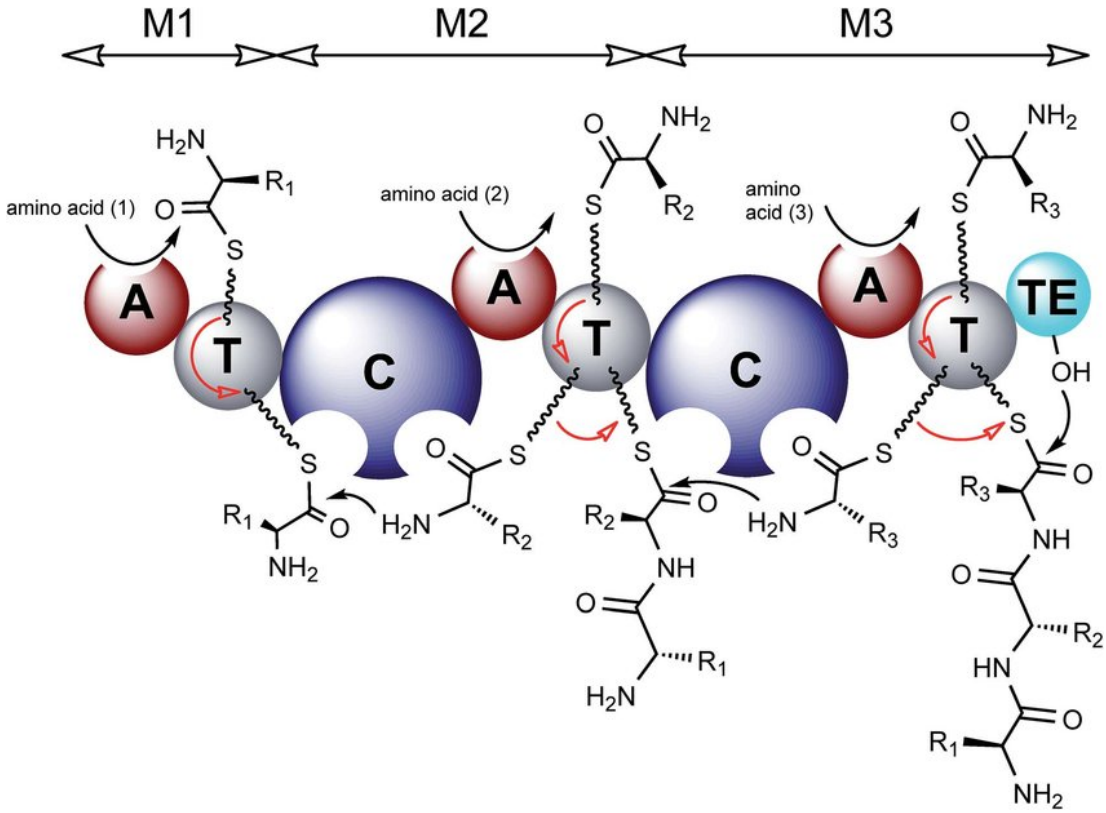

Figure 34. Organization of modules in NRPS synthesis [107]. A = adenylation domain, T = thiolation domain, C = condensation domain. The red arrows represent the movement of residues along the NRPS chain.

This figure was taken from the review of Winn *et al*. [107] (M. Winn, J. K. Fyans, Y. Zhuo and J. Micklefield, Nat. Prod. Rep., 2016, 33, 317 ; DOI: 10.1039/C5NP00099H), published by The Royal Society of Chemistry.

Many natural products are produced by hybrid NRPS/PKS pathways. Polyketide synthases (PKS) assemble small acylated blocks into polyketides via C-C bonds, and NRPS assemble amino acids into peptides via amide bonds. NRPS and PKS use a similar biosynthesis strategy with carrier proteins to attach the growing chain [108]. PKS contain an acyltransferase domain (AT), a ketosynthase domain (KS) and an acyl carrier protein domain (ACP). The AT domain recognizes an acyl unit and catalyzes its transfer to the phosphopanthein arm of the ACP to form a thioester. The KS domain first receives the acyl intermediate from the previous ACP donor via a cysteine. The KS domain then catalyzes the decarboxylation of the growing malonyl substrate attached to the next ACP acceptor and then catalyzes a Claisen condensation between the acyl intermediate and the substrate to form a C-C bond. The resulting substrate can be treated with ketoreductase domains (KR) to form β-hydroxy groups, dehydratase (DH) to create double bonds, and enoyl reductase (ER) to form reduced methylene groups. The polyketide is then released by a thioesterase as in the case of NRPS (Figure 35). When a NRPS module is upstream of a PKS module, the last domain of the NRPS module must be recognized by the first domain of the PKS module, then condensation occurs via the KS domain. On the contrary, when a PKS module is placed before a NRPS module, the C domain of the NRPS must recognize the ACP domain of the PKS module. The combination of the NRPS and PKS systems results in products with a wide structural diversity. Wang's team reported that one third of the PKS and NRPS gene clusters identified were hybrids [109].

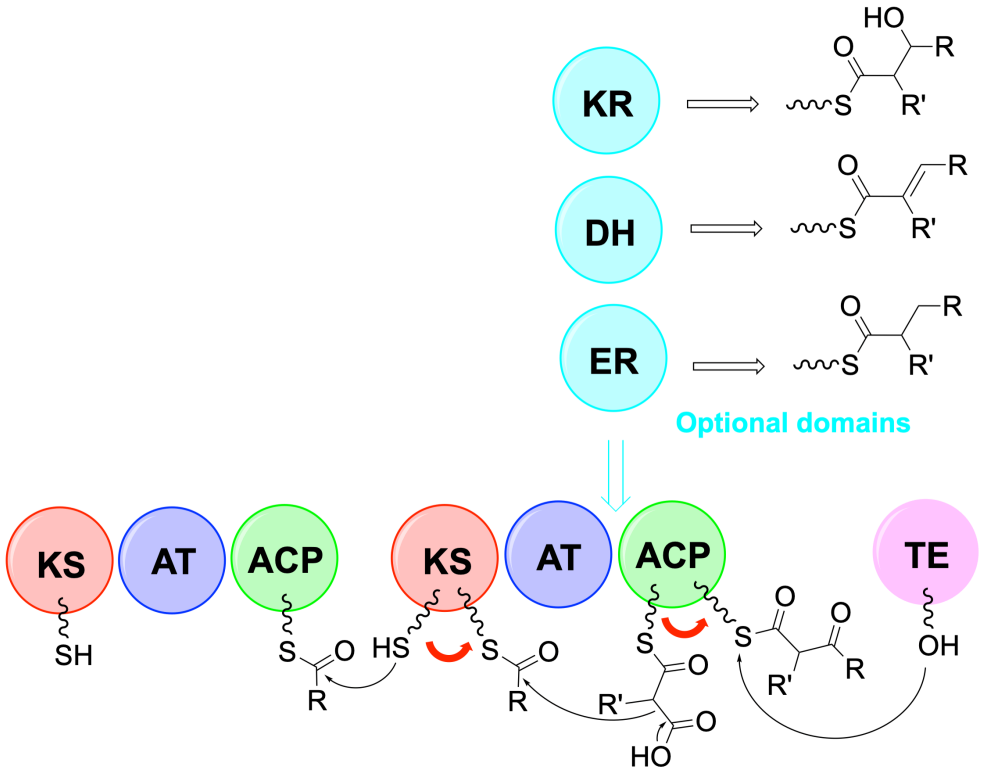

Figure 35. Simplified model of PKS synthesis. KS = ketosynthase domain, AT = acyltransferase domain, ACP = acyl carrier protein domain, KR = ketoreductase domain, DH = dehydratase, ER = enoyl reductase. The red arrows represent the movement of residues along the PKS chain.

A. Biosynthesis of characteristic amino acids found in laxaphycins

a) Biosynthesis of hydroxy-amino acids

In general, the hydroxylation of amino acids can take place via 3 types of enzymes: FAD-dependent monooxygenases, non-heme Fe(II)-oxygenases and heme Fe(II)-oxygenases. These enzymes use different co-factors depending on the reactivity of the amino acid to be hydroxylated. This may be the iron coming either from heme in the case of monooxygenases of the cytochrome P450 family or being in non-heme mononuclear form. Another co-factor is FAD (flavin adenine dinucleotide), which oxidizes in the presence of oxygen to form a less reactive compound, capable of hydroxylating in particular lysine amines, sufficiently nucleophilic for that. In the biosynthesis of peptides, one finds mainly P450 cytochromes or Fe(II)/α-KG-dependent non-heme monooxygenase (KG for ketoglutarate).

The biosynthesis of 3-hydroxyleucine has been reported for several peptides, most recently in the biosynthesis of scytocyclamides [58]. Heinilä *et al*. conducted an experiment to determine whether NRPS modules were specific for the hydroxylated amino acid or not, by supplementing the cyanobacterial culture medium with 3-hydroxyleucine. However, this experiment did not show a higher production of hydroxyleucine-containing scytocyclamide compared to the control without the addition of 3-hydroxyleucine. The two adenylation domains of the $LxaI_2$ and $LxaJ_1$ modules would therefore be specific for leucines and not for 3-hydroxyleucines, which was demonstrated by a comparative analysis on AntiSMASH. In the case of scytocyclamides, the hydroxylation of leucines and asparagine would therefore occur after synthesis of the complete peptide. Besides, the LxaF and LxaG modules code for enzymes of the cupin 8 family that are suspected to be involved in the β-hydroxylation of amino acids as it was described for others peptides [110–112].

In the skyllamycin biosynthetic gene cluster, the monooxygenase P450 (*sky*32) allows the hydroxylation of leucine as well as tyrosine and phenylalanine [113]. This enzyme is capable of hydroxylating 3 different amino acids directly on their respective PCP domains.

In the same way, a P450 monooxygenase (*tem*23) showing similarities with *sky*32 (78% according to Blast searches) is able to specifically β-hydroxylates the leucine found in telomycin antibiotic [114]. The hydroxylation occurs once the complete peptide is assembled and cyclized, thus outside the NRPS assembly line, which is not the case with *sky*32. Another P450 monooxygenase (*tem*29) was found in the gene cluster, allowing the hydroxylation of proline into *trans*-3-OH-Pro. The *tem*32 gene codes for Fe(II)/2-OG-dependent oxygenase, which will be responsible for the hydroxylation of a second proline into *cis*-3-OH-Pro. These two enzymes are also supposed to act post NRPS synthesis.

Parkinson *et al*. combined metabologenomics and molecular networks to discover a new class of peptide, tyrobetaines, which are peptides produced by the NRPS pathway [115]. Among the recognized enzymes, TybP would code for a P450 monooxygenase, showing similarities

with the enzyme coded by *tem*23 (74%). TybP would thus be responsible for the β-hydroxylation of leucine in tyrobetaine. No information is given on the mode and location of action of this enzyme.

Contrary to the case of telomycin biosynthesis where proline is hydroxylated after the complete synthesis of the peptide, peptides of the echinocandin family contain hydroxyprolines obtained before their integration into the peptide chain, in free form. GloF and HytE are 2-OG-dependent proline hydroxylases that are part of the biosynthesis of non-ribosomal peptides. They have been identified in the cluster of pneumocandin genes from *Glarea lozoyensis* (GloF) or echinocandin B from *Aspergillus pachycristatus* [116,117]. These enzymes hydroxylate free proline in positions 3 or 4, before it is loaded on an acyl carrier protein.

The origin of 4-hydroxyproline in scytoclamide A could not be determined since no enzyme allowing this type of reaction has been identified within the cluster of scytocylamide genes [58]. However, the study of heinamides biosynthesis showed that an enzyme in the gene cluster (LxaN) may be responsible for the hydroxylation of proline at position 4 [63].

Cases of hydroxylation of asparagine in free form have also been reported. In the gene cluster for the biosynthesis of occidiofungin B, from the burkholdine family, the *ocf*G gene has been determined as coding for a hydroxylase allowing the β-hydroxylation of asparagine and tyrosine [118]. Asparagine is hydroxylated in the free state and then inserted into the NRPS synthesis chain as the first amino acid of the sequence. Similarly, the lipopeptide CDA (daptomycin-like) is synthesized via NRPS, with a Fe(II)/α-KG-dependent oxygenase (AsnO hydroxylase) that catalyzes the β-hydroxylation of asparagine [111].

This type of Fe(II)/α-KG-dependent enzyme is also found in ribosomal-type synthesis. The linear polytheonamide peptide, composed of 49 residues with high structural diversity, was presumed to be synthesized by NRPS. However, it has recently been shown to be obtained by ribosomal pathway, with no less than 48 post-translational modifications [119]. Among them, the β-hydroxylation of asparagine is performed by a Fe(II)/α-KG-dependent oxidoreductase, encoded by *poy*E in the identified gene cluster.

b) Biosynthesis of dehydroamino acids

The biosynthesis of dehydroamino acids is globally little known. Dehydrobutyrine is mostly described in the case of peptide synthesis by ribosomal pathways. Peptides of the large family of lantibiotics, containing in particular nisin, epidermin or subtilin, are characterized by a lanthionine motif (Figure 36) [120]. This pattern is formed via a dehydroamino acid obtained by dehydration of the corresponding hydroxyamino acid.

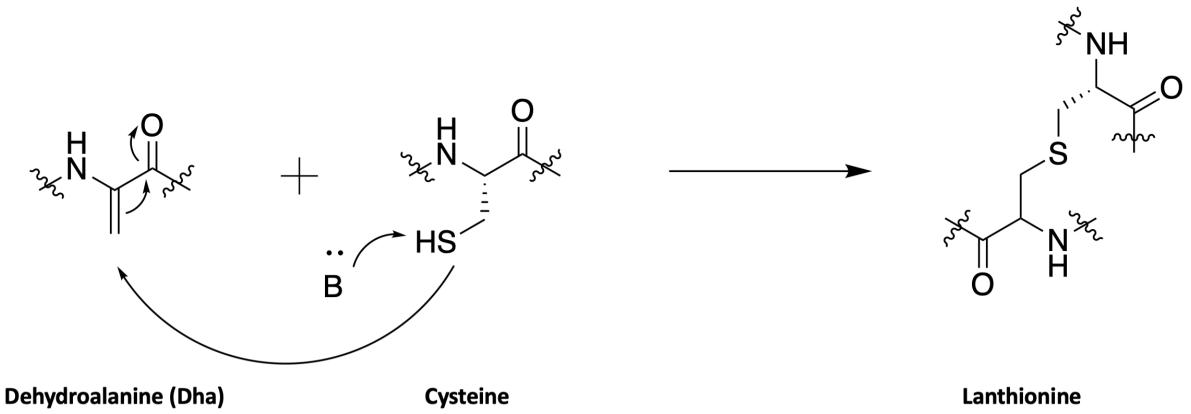

Figure 36. Creation of lanthionine motif via combination of dehydroalanine and a cysteine.

In the case of class I lantibiotics, this dehydration reaction would be catalyzed by lanthionine synthetase lanB (nisB for nisin, epiB for epidermin, spaB for subtilin). Once dehydration has occurred, the addition of the thiol group of a cysteine is catalyzed by lanC, to form the lanthionine motif. In the case of class II lantibiotics, *lan*M gene is a fusion of *lan*B and *lan*C and thus codes for a bifunctional enzyme catalyzing both dehydration and formation of the lanthionine moiety [121,122].

Enzymes similar to lanthionine synthetases have been found in the thiocillin biosynthetic gene cluster. *tcl*K and *tcl*L genes are involved in the dehydration of threonines to dehydrobutyrine [123]. The mechanism of action would imply a phosphorylation of the hydroxyl group followed by its elimination [122]. Similarly, *ber*B and *ber*C from the berninamycin A gene cluster, code for dehydratases of the same type of lanthionine synthetases acting on serine and threonine [124]. Similar enzymes, homologous to LanB, are also found in the gene clusters for the biosynthesis of thiostrepton peptide [125,126] and nosiheptide peptide [127].

Dehydroamino acids are also widely found in non-ribosomal peptides [128,129], but their production mechanism remains unclear [130]. Among them the well-studied microcystin, which contains an N-methyl-dehydroalanine. The N-methyl-serine dehydration is thought to be performed by the first domain of the *Mcy*A module [131]. However, the mechanism of dehydration is still not elucidated, as this is also the case for stenothricin [132].

Concerning the NRPS synthesized puwainaphycins containing two dehydrobutyrines, a strong sequence homology (97%) of both adenylation domains (*puw*F and *puw*G) was shown without evidence for additional enzymes that could cause dehydration of threonine. Thus the adenylation domains are suspected to be specific for dehydrobutyrine [133,134].

In the biosynthesis of scytocyclamides, the adenylation domain $LxaC_2$ recognizes a threonine, then the following condensation domain $LxaC_3$ would be involved in the dehydration of the threonine to dehydrobutyrine [58].

B. Biosynthesis of laxaphycins

In the case of cyanobacteria, the first biosynthetic NRPS/PKS pathway was characterized for microcystin within the freshwater cyanobacterium *Microcystis aeruginosa* [37,135]. After this breakthrough, other peptide biosyntheses have been reported for freshwater, marine and terrestrial cyanobacteria. It is only very recently that the biosynthesis of laxaphycins and their derivatives has been studied [58]. For these lipopeptides, the hypothesis of a hybrid PKS/NRPS biosynthetic pathway has been deciphered [19]. In view of the structural differences between type A and type B laxaphycins, two different biosynthetic pathways are expected. Sivonen's group focused on the biosynthesis of scytocyclamides from the cyanobacterium *Scytonema hofmannii* PCC 7110 [58].

Analysis of the *S. hoffmannii* genome revealed 15 possible NRPS/PKS pathways but only two of them were compatible with the scytocyclamides structures. However, only one enzyme that can initiate biosynthesis was found, suggesting a common initiation step for the two A and B-types scytocyclamides, followed by a separation of the two pathways. The complete gene cluster for the biosynthesis of the two peptides is 96-kb in length and is composed of 13 open reading frames (ORFs) named ORF_1 and *lxa*A-L. The three first PKS modules LxaA-B-E that contains the fatty acyl-AMP ligase (FAAL) transform the hexanoic acid into Aoc^1 (Figure 37) and are analogous to what is observed in the biosynthesis of other peptides such as puwainaphycin [18,133] or mycosubtilin [136].

After this step, the biosynthetic pathway splits into two distinct but parallel NRPS pathways to form either scytocyclamide A or scytocyclamide B. In the case of scytocyclamide A, the $LxaC_i$-D_i modules continue the elongation of the peptide by adding each amino acid. They are composed of the condensation C, adenylation A, and thiolation T domains. $LxaC_5$, $LxaC_6$ and $LxaD_2$ have in addition an epimerization domain E accounting for the D configuration on amino acids Phe^6, Leu^7 and allo-Ile^9, respectively. On the scytocyclamide B side, the $LxaI_i$-L_i modules continue the elongation and are also composed of C, A and T domains. The modules $LxaI_2$, $LxaJ_1$, $LxaJ_3$, and $LxaK_4$ additionally have an epimerization domain E to give an absolute configuration D on the amino acids Leu^3, Leu^5, Asn^8 and Leu^{11}, respectively. $LxaJ_3$ also has a *N*-methylation domain to obtain *N*-methylisoleucine in position 7. At the end of the two NRPS pathways, a thioesterase TE induces a head-to-tail cyclization of the peptide and a subsequent release of the final peptide (Figure 37). LxaH is an ABC-transporter characteristic of NRPS systems that allows the transport of the peptide to its destination within the cell.

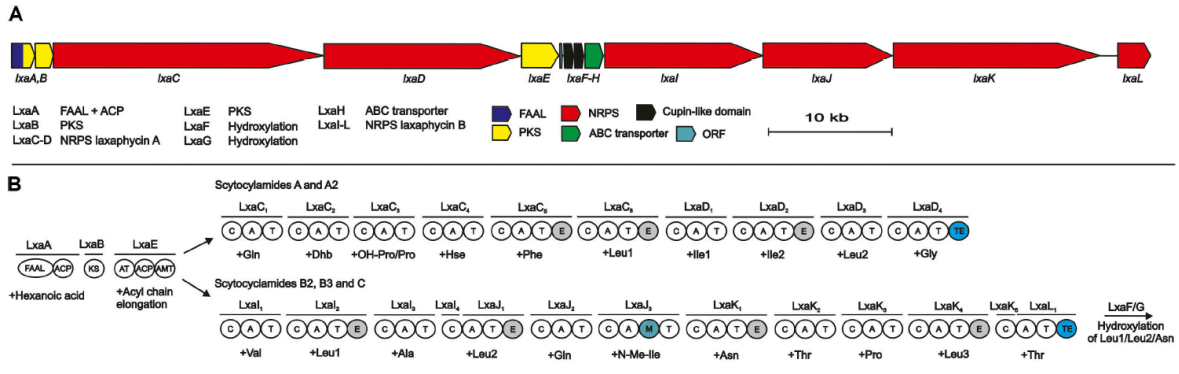

Figure 37. The scytocyclamide (lxa) biosynthetic gene cluster and putative biosynthetic scheme. A. Organization of predicted scytocyclamide biosynthetic genes. B. Proposed biosynthetic pathway of scytocyclamides.

This figure was taken from the article of Heinilä *et al*. [58] (Heinilä, L.M.P.; Fewer, D.P.; Jokela, J.K.; Wahlsten, M.; Jortikka, A.; Sivonen, K. Shared PKS Module in Biosynthesis of Synergistic Laxaphycins. Front. Microbiol. 2020, 11, DOI:10.3389/fmicb.2020.578878)

Some scytocyclamides contain hydroxylated amino acids and others do not. Experience has shown that adding 3-hydroxyleucine to the cyanobacterial culture medium does not favor the production of scytocyclamide B with 3-hydroxyleucines. In accordance with the specificity analysis of the modules, this sustains that the adenylation domains $LxaI_2$, $LxaJ_1$ and $LxaK_1$ are specific for leucines and asparagine but not for their hydroxylated counterparts. Furthermore, these amino acids are epimerized to the D-configuration within the same modules. Thus, hydroxylation would occur after the incorporation and epimerization of the amino acids and would be catalyzed by enzymes of the cupin 8 family encoded in the LxaF-G modules [137], suggesting that the hydroxylation enzymes are specific for D-amino acids, or that epimerases play a role in these hydroxylations. Concerning the obtention of 4-hydroxyproline in scytocyclamide A, no hypothesis has been put forward since no enzyme from the gene cluster has been detected as being suitable for such synthesis. The $LxaC_2$ module would contain a threonine-specific A domain and it would be the C domain of the following $LxaC_3$ module that would induce dehydration of threonine to dehydrobutyrine, as already postulated in the biosynthesis of other peptides such as microcystin [131] or nodularin [128]. Similarities appeared when comparing the condensation domains observed in these peptides with the C domain of the $LxaC_3$ module. Finally, no hypothesis has yet been put forward concerning the obtention of Hse.

In 2021, Heinilä *et al*. reported the biosynthetic gene cluster involved in the biosynthesis of heinamides [63]. The complete gene cluster is 93-kb in length and is also composed of 13 open reading frames (ORFs) named ORF_1 , ORF_2, *lxa*I1-K1, *lxa*A2, ORF_3, *lxa*B, *lxa*C1, *lxa*E-G and *lxa*M (Figure 38).

As it is the case for scytocyclamides, the Aoc^1 is the first residue synthesized. However, no LxaA-like enzyme was found in the heinamide biosynthetic gene cluster. A single ACP domain

LxaA2 was found with 41% similarity to LxaA and a single FAAL domain LxaA1 was designated as possibly involved in the initiation of biosynthesis but is located outside the gene cluster. This separation has already been described in the case of puwainaphycins [134]. The LxaB ketosynthase completed by an acyltransferase, an ACP domain and an aminotransferase in the LxaE module constitute the set of enzymes allowing the Aoc^1 production.

The $LxaC1_i$ modules continue elongation for A-type heinamides, and $LxaI1_i$-$K1_i$ for B-type heinamides. There are again epimerization domains on modules incorporating D-amino acids, as well as a methylation domain for *N*-methylisoleucine addition.

The enzymes LxaF-G and LxaM were identified as cupin-like domain proteins and would be involved in the hydroxylation of Aoc^1, Leu^3 and Hse^8. The adenylation domains corresponding to Hle^3 and Leu^5 being identical, they would be specific to leucine and the hydroxylation of Leu^3 would occur later, either while it is bound to the PCP or after the release of the peptide. It is noteworthy that for the different B-type laxaphycins, position 3 is always hydroxylated, which is not the case for position 5. The $LxaI1_3$ and $LxaJ1_1$ adenylation domains corresponding to Hse and to the carbamoylated homoserine (cHse) are identical, suggesting that both domains are Hse-specific, and that carbamoylation occurs later. Position 8 would therefore correspond to a Hse hydroxylated at position 3, rather than a Thr hydroxylated at position 4, as described in the case of lobocyclamides [52]. Indeed, in other laxaphycins containing a hydroxyasparagine (Hasn), the hydroxylation is done on carbon 3. Lastly, it is not yet known at what point carbamoylation of Hse occurs. Three putative carbamoyltransferases were found in the genome, but none could be assigned to the gene cluster.

As in the case of scytocyclamides, the $LxaC1_3$ condensation domain handles the dehydration of threonine to dehydrobutyrine, with threonine recognized by the preceding $LxaC1_2$ adenylation domain.

The LxaO-P-Q enzymes are described as an L-Leu 5-hydroxylase, a zinc-binding dehydrogenase and a pyrroline-5-carboxylate reductase, respectively. These enzymes are encoded by genes similar to those found in other cyanobacteria and allowing the production of 4-Me-Pro [138], but these enzymes were found outside the gene cluster. LxaN hydroxylates L-Pro to 4-OH-Pro in the case of type A heinamides. While this enzyme was not identified when scytocyclamide biosynthesis was studied, a 93% LxaN-like enzyme was found in the scytocyclamide gene cluster, also hydroxylating L-Pro for type A scytocyclamides. LxaR, on the other hand, would participate in the production of 3-OH-4-Me-Pro for type B heinamides, but does not directly hydroxylate 4-Me-Pro. Indeed, the addition of 4-Me-Pro to the medium does not increase the amount of peptide containing 3-OH-4-Me-Pro, suggesting that 4-Me-Pro is not an intermediate in 3-OH-4-Me-Pro synthesis. LxaR would be assisted by LxaO-P-Q but the direction of action of the 4 enzymes is not defined.

Although the gene clusters for scytocyclamide and heinamide biosynthesis are very similar, there are several differences in their organization (Figure 38A). The biosynthesis of heinamides complements the information already described for the biosynthesis of scytocyclamides, these two families of laxaphycins being the only ones for which the biosynthesis has been described to date.

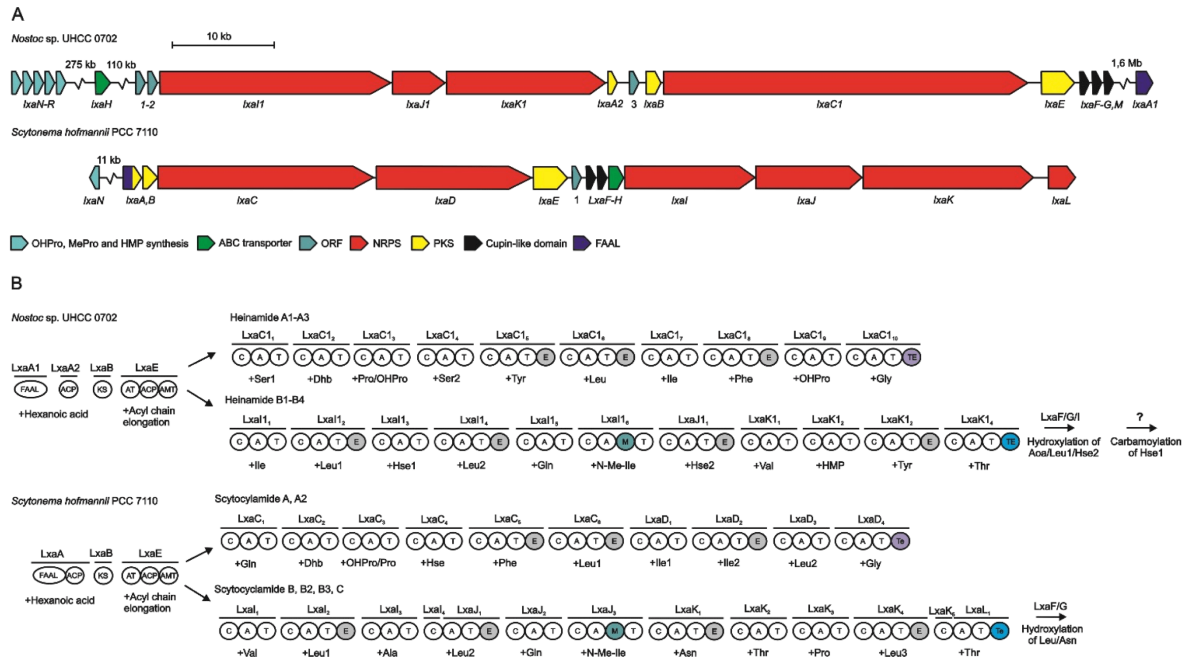

Figure 38. The laxaphycin (lxa) biosynthetic gene clusters and putative biosynthetic schemes in *Nostoc* sp. UHCC 0702 and *S. Hofmannii* PCC 7110. A. Organization of predicted heinamide and scytocyclamide biosynthetic genes. B. Proposed biosynthetic pathway of heinamides and scytocyclamides.

This figure was taken from the article of Heinilä *et al*. [63]. (Heinilä, L.M.P.; Fewer, D.P.; Jokela, J.K.; Wahlsten, M.; Ouyang, X.; Permi, P.; Jortikka, A.; Sivonen, K. The Structure and Biosynthesis of Heinamides A1–A3 and B1–B5, Antifungal Members of the Laxaphycin Lipopeptide Family. *Org. Biomol. Chem*. 2021, doi:10.1039/D1OB00772F). Published by The Royal Society of Chemistry.

The discovery of acyclolaxaphycins raises doubts about their origin. It was first postulated that these linear peptides could be by-products of an incomplete biosynthesis, or products of enzymatic degradations [18,19]. In the case of laxaphycin A, the cyclization would therefore be between Aoc^{1} and Gly^{11} (Figure 6), and in the case of laxaphycin B, between Ala^{4} and hydroxyleucine^{3} (Figure 7). According to the PKS/NRPS architecture proposed by Heinilä *et al*., with the start of biosynthesis by Aoc^{1} (Figure 37), it is possible that acyclolaxaphycins A are an unfinished by-product, having stopped at Leu^{10} or D-allo-Ile^{9}. In contrast, for acyclolaxaphycins B and B3, the opening is described in the middle of the NRPS gene sequence, suggesting instead that these peptides were obtained by enzymatic degradations. Furthermore, if cyclization were to take place between the amine of Ala^{4} and the carboxylic acid of hydroxyleucine^{3}, it would also not be possible to obtain [des-(Ala^{4}-Hle^{5})]acyclolaxaphycin B and [des-(Ala^{4}-Hle^{5})]acyclolaxaphycin B3 as immature products of the biosynthesis.

V. *In situ* and *ex situ* biological activities

Cyanobacteria biosynthesize various secondary metabolites suspected to be involved in UV protection, feeding deterrence or allelopathy [139]. The wide range of biological properties of these metabolites made them attractive compounds for the pharmaceutical, cosmetic, agricultural and energy domains. In this section, we will summarize the studies that have been undertaken on the biological activity of laxaphycins and their derivatives. We will also discuss their impact on the consumption preferences of different herbivores.

A. Biological properties

a) Laxaphycins

After their discovery and structure determination, a first evaluation of the biological activity of laxaphycins was made. The extract containing laxaphycins, isolated from the cyanobacterium *Anabaena laxa*, was tested for its antifungal activity against *Aspergillus oryzae*, *Candida albicans*, *Penicillium notatum*, *Saccharomyces cerevisiae* and *Trichophyton mentagrophytes* and its cytotoxic properties on cancer cell lines, KB (human epidermoid carcinoma) and LoVo (human colorectal adenocarcinoma) [44]. These tests showed that the crude cyanobacterial extract containing all the laxaphycins was active on the five fungi strains tested and cytotoxic on the two cancer cell lines. In addition, the extract was more active than the laxaphycins taken individually as laxaphycin A was not active and laxaphycin B showed less activity than the extract. Combining laxaphycins A and B strongly increased the antifungal activity compared to laxaphycin B alone. However, increasing the proportion of either of the laxaphycins in the mixture had no impact. On *A. oryzae*, Laxaphycin A on its own showed no activity at the maximum dose of 128 μg/mL while laxaphycin B has a minimal inhibitory concentration (MIC) of 64 μg/mL. Together, the two peptides have a MIC of 16 μg/mL, confirming the synergy between the two peptides. Testing of other known antifungal compounds in mixture with laxaphycins did not show such synergy. Moreover, laxaphycin A is not cytotoxic on KB cells at a concentration of 10 μg/mL while laxaphycin B has a MIC of 0.12 μg/mL which is lowered to 0.10 μg/mL when combining with laxaphycin A.

Bonnard *et al.* evaluated the cytotoxicity of laxaphycins A and B, in comparison with adriamycin, on 3 cell lines, the parent drug-sensitive human leukemic lymphoblasts (CCRF-CEM) and the related sublines that express drug resistance associated with overexpression of Pgp (CEM/VLB_{100}) or with alteration of DNA topoisomerase II (CEM/VM1) [46]. Laxaphycin A tested at 20 μM shows no activity on these 3 cell lines. On the other hand, laxaphycin B shows a significant cytotoxicity on the 3 cell lines equally with an IC50 between 1.02 μM and 1.37 μM, whereas adriamycin is more active on drug-sensitive cells than on drug-resistant cells. The synergy between laxaphycins A and B was observed on both drug-sensitive and drug-resistant cells as well as against *Candida albicans*.

The intracellular effect of laxaphycins A and B on the 3 cell lines presented above was further studied using a videomicrofluorometry technique with multiple labelling [140]. No cytotoxicity was found for laxaphycin A used at 4 μM, which is consistent with the previously mentioned results. The different cell lines were subjected to different doses of laxaphycin B with or without combination with laxaphycin A. The growth of CCRF-CEM-WT (wild type) sensitive cells was totally blocked by laxaphycin B at 2 μM or laxaphycin B at 1 μM combined with laxaphycin A at a minimum dose of 0.4 μM. The growth of CEM/VM1 resistant cells is completely blocked if laxaphycin A is raised to 1 μM while the growth of CEM/VLB cells is blocked at only 75%. CEM/VM1 and CEM/VLB cells seem to be slightly more resistant to laxaphycin treatment compared to CCRF-CEM-WT sensitive cells, but their relative resistance remains much lower than the one observed with adriamycin. The inhibition of CCRF-CEM-WT cells growth with laxaphycin B at 2 μM, is coupled with a 23% increase in polyploid cells and an increase in cells with a larger nucleus. However, as the dose of laxaphycin A increases, the amount of polyploid cells decreases. Since laxaphycin A is inactive alone, it potentiates the toxicity of laxaphycin B, but with a different mode of action from the latter. Increased polyploid cell numbers were also observed after treatment of CEM/VM1 cells with laxaphycins but a higher dose of laxaphycin A is required to lower the polyploid cell population. This behavior could be due to the intrinsic low topoisomerase II activity for CEM/VM1 cells coupled with the alteration of topoisomerase II activity by laxaphycin B. In the case of CEM/VLB cells, a similar behavior to CCRF-CEM-WT cells was observed, but with a lesser effect of laxaphycin B which could be attributed to its low intracellular accumulation due to Pgp efflux.

The same cell lines have been used to evaluate the cytotoxicity of laxaphycins A, B, B2 and B3 and thus have first evidence of structure-activity relationships [20]. As mentioned above, laxaphycin A is not active at a concentration of 20 μM (IC50 > 20 μM), however type-B laxaphycins are all active on the 3 cell lines with IC50s ranging from 1.02 to 4.15 μM. Laxaphycin B3 has a similar activity to laxaphycin B on all 3 cell lines (IC50 between 1.35 and 1.5 μM), suggesting that the hydroxy group of proline in position 10 has no impact on cytotoxicity on theses cell lines. On the other hand, laxaphycin B2 is less active than laxaphycins B and B3 (IC50 between 3.33 and 4.15 μM), suggesting that the hydroxy group on leucine in position 5 is important in the activity. The resistance index of CEM/VLB and CEM/VM1 cells, relative to the CCRF-CEM parent cells, is around 1 for all B-type laxaphycins, meaning in the case of CEM/VLB cells that laxaphycins are not Pgp pump substrates.

The antiproliferative activity of laxaphycins A and B was also evaluated on solid cancer cell lines, A549 (non-small cell lung), MCF7 (breast), PA1 (ovary), PC3 (prostate) and DLD1 (colon) [20]. These five human carcinoma cell lines and a human pigmented malignant melanoma line (M4Beu) were used to test the two peptides in comparison to cisplatin. In order to evaluate the specificity of the peptides for cancer cells compared to normal cells, they were also tested on normal human fibroblasts and immortalized murine L-929 cells. These cells are commonly used in screening programs to evaluate the cytotoxicity of chemicals. Laxaphycin A is non-

toxic (IC50 > 20 μM) on these solid cancer lines, whereas laxaphycin B has an IC50 of less than 2 μM on all lines tested except DLD1. Compared to cisplatin (2 μM < IC50 < 24 μM), laxaphycin B is globally more toxic (0.2 μM < IC50 < 6 μM) on all lines with an IC50 of 0.19 μM on PA1, between 0.3 μM and 0.4 μM on M4Beu, between 0.58 μM and 0.8 μM on PC3 and between 0.5 μM and 1 μM on MCF7 (according to RRT or Ho tests). The toxicity of laxaphycin B on these cell lines makes it very interesting, however it is also toxic on normal human fibroblasts. Laxaphycin B at 2 μM caused the death of only 10% of the DLD1 cells, when 55% died in combination with laxaphycin A at 1 μM. As laxaphycin A alone at 5 μM has no effect on these cells, the synergistic effect between these two peptides is demonstrated with the increase of dead cells as the laxaphycin A concentration increases.

Laxaphycin A as well as laxaphycins A2 and B4 were tested on colon cancer cells HCT116 [49]. Type-A laxaphycins are not active, with IC50s of 23 μM for laxaphycin A and 29 μM for laxaphycin A2. Laxaphycin B4, on the other hand, has an antiproliferative action with an IC50 of 1.7 μM.

Type-A laxaphycins were more widely studied by Bornancin *et al*. in 2019, following the discovery of acyclolaxaphycins A [19]. Laxaphycin A, laxaphycin A2 and [D-Val^{9}]laxaphycin A, as well as the 3 acyclolaxaphycins A discovered were tested for their activity on SHSY5Y neuroblastoma cells. Laxaphycin A and [des-(Leu^{10}-Gly^{11})]acyclolaxaphycin A showed no cytotoxicity (IC50 > 10 μM) while [des-Gly^{11}]acyclolaxaphycin A produced slight toxicity (50% decrease in cell viability) at the highest tested concentration of 10 μM. In contrast, laxaphycin A2 and [D-Val^{9}]laxaphycin A completely inhibited cell viability, with laxaphycin A2 being slightly more active than [D-Val^{9}]laxaphycin A, with IC50s of 0.6 μM and 5.6 μM respectively. The ability of these peptides to impact the electrical potential of the mitochondrial membrane of these cells was also studied. Laxaphycin A, [des-(Gly^{11})]acyclolaxaphycin A, laxaphycin A2 and [D-Val^{9}]laxaphycin A slightly affected this potential. [des-(Gly^{11})]acyclolaxaphycin A lowered the potential without affecting cell viability, which is not consistent with the previous result. At the same time, the level of ROS (reactive oxygen species) was measured, after incubation of these laxaphycins with neuroblastoma cells, since mitochondria are the main producers of these species. Only [des-(Gly^{11})]acyclolaxaphycin A and [D-Val^{9}]laxaphycin A lowered the amount of ROS produced, with [des-(Gly^{11})]acyclolaxaphycin A further inhibiting their production. In order to study the type of cell death induced by these compounds, annexin V/propidium iodide staining and flow cytometry analysis were used to label the cells and thus visualize the size, shape and complexity of the cells associated with their type of death. As found previously, laxaphycin A2 and [D-Val^{9}]laxaphycin A showed a decrease in cell viability but without inducing an increase in apoptotic or necrotic cells, a phenomenon of autophagy was therefore considered. The LC3 (microtubule-associated light chain 3) marker level of the autophagosomes was determined. Under stress conditions, LC3 is cleaved by ATG4 proteins to form LC3-I, which will be conjugated with phosphatidylethanolamine to form LC3-II within the autophagosomes. Among the compounds tested, only [des-(Gly^{11})]acyclolaxaphycin A,

laxaphycin A2 and [D-Val^{9}]laxaphycin A increased the LC3-II/I ratio, suggesting death by autophagy. The results obtained on these 3 compounds were confirmed by the study of mTOR (mechanistic target of rapamycin), which notably regulates cell proliferation. Under normal conditions, mTOR is in phosphorylated form and autophagy is inhibited, whereas if mTOR is inactivated and therefore non-phosphorylated, autophagy takes place. The 3 compounds mentioned above induce a decrease from 100% to about 70% in the level of phosphorylated mTOR, confirming that these 3 compounds are involved in the autophagy of neurobastoma cells. Since [des-(Gly^{11})]acyclolaxaphycin A is more toxic than laxaphycin A, it can be hypothesized that [des-(Gly^{11})]acyclolaxaphycin A maintains the secondary structure of laxaphycin A, but the loss of glycine makes it more hydrophilic and improves its biological activity. On the other hand, the loss of the following leucine in [des-(Leu^{10}-Gly^{11})]acyclolaxaphycin A would cause the loss of the secondary structure, which could lead to the loss of activity. Where laxaphycin A2 was not active on colon cancer cells HCT116 [49], it is active on neuroblastoma cells SHSY5Y. In this case, positions 8 and 9 of the peptide sequence could be important in the observed activity, since they are the only changing positions in laxaphycin A2 and [D-Val^{9}]laxaphycin A compared to the non-active laxaphycin A.

Type-B laxaphycins have also been studied for their activity on the same neuroblastoma SHSY5Y cells [54]. Laxaphycins B and B3 are cytotoxic against these cells, with IC50s between 0.3 and 1.8 μM (according to MTT or LDH tests) for laxaphycin B and between 0.15 and 0.8 μM for laxaphycin B3. These two cyclic peptides also depolarize the mitochondrial membrane and reduce the ROS level. Acyclolaxaphycin B and B3 isolated from the cyanobacterium *A. torulosa* do not show cytotoxicity at all concentrations tested between 0.001 and 10 μM. From 0.1 μM of acyclolaxaphycin B, the metabolic activity of the cells increases and the electrical potential of the mitochondrial membrane decreases, while ROS and ATP levels also decrease at high peptide concentrations. However, the ATP levels reduced at 6 hours incubation are recovered after 24 hours incubation. The results obtained with acyclolaxaphycin B3 are similar, although the concentration of acyclolaxaphycin B3 must be higher to depolarize the membrane. However, the metabolic activity of cells with this peptide remains stable. [des-(Ala^{4}-Hle^{5})]acyclolaxaphycin B and [des-(Ala^{4}-Hle^{5})]acyclolaxaphycin B3 isolated from sea hare *Stylocheilus striatus* are not cytotoxic on these cells. [des-(Ala^{4}-Hle^{5})]acyclolaxaphycin B also increases the metabolic activity of the cells, depolarizes the mitochondrial membrane and reduces the level of ROS. As with acyclolaxaphycin B, ATP levels are recovered after 24 hours of incubation. Des-(Ala^{4}-Hle^{5})]acyclolaxaphycin B3 has the same effect on the metabolic activity of the cells and on the reduction of ROS and ATP levels. However, the peptide has no impact on the potential of the mitochondrial membrane. Using the same flow cytometry technique coupled with annexin V/PI labeling, the number of apoptotic and necrotic cells could be calculated, after treatment of the cells with the different laxaphycins B. The addition of laxaphycins B and B3 resulted in a decrease of living cells and an increase of 50% and 46% respectively of apoptotic cells. In contrast, acyclic laxaphycins showed no effect on cell viability. Caspase 3 is an enzyme targeting apoptosis substrates and generating a series of

events leading to cell death. The activity of this caspase is increased by the addition of laxaphycins B and B3 and not by the addition of acyclic laxaphycins, reinforcing the idea that cyclic laxaphycins B are involved in the apoptosis of neuroblastoma cells. Since acyclic laxaphycins show an effect on the potential of the mitochondrial membrane, their involvement in cell autophagy was evaluated. Neuroblastoma cells were treated with different peptides and the expression of different proteins involved in autophagy (rapamycin, compound C AMPK inhibitor, p70 S6 kinase, LC3, p62) was determined. Acyclic laxaphycins B induce an increase in AMPK activation, thus activating autophagy, with [des-(Ala^4-Hle^5)]acyclolaxaphycin B3 being the most impacting. Cyclic laxaphycins have no impact on mTOR activity while acyclic laxaphycin B reduces its activation. Laxaphycin B3 and its two acyclic derivatives show a decrease in p70 S6 phosphorylation, involved in both autophagy and apoptosis activation, suggesting that laxaphycin B3 has a different mechanism of action than laxaphycin B. The hydroxy group on proline in position 10 could therefore have an impact on the inhibition of this enzyme. In addition, the LC3-II/I ratio is increased by the addition of acyclic laxaphycins to the cells. The expression of p62 is decreased by the addition of these acyclic laxaphycins. Treatment of neuroblastoma cells with acyclic laxaphycins B would therefore act on their autophagy.

The newly isolated laxaphycins B5 and B6 from the freshwater cyanobacterium *Phormidium* sp. were tested against three cancer cell lines, MDA-MB-435 (melanoma), MDA-MB-231 (breast cancer) and OVCAR3 (ovarian cancer) [50]. Laxaphycins B5 showed moderate activity against the three cancer cell lines with IC50s of 1.2 μM, 2.2 μM and 1.6 μM, respectively. Laxaphycin B6 is slightly more active with IC50s of 0.58 μM, 0.81 μM and 0.92 μM, respectively. Interestingly, the more active laxaphycin B6 contains a D-Leu in position 5 instead of hydroxyleucine in the case of laxaphycin B5.

Different species of algae and cyanobacteria are used as food supplements. Many potential beneficial uses have been associated with extracts and compounds of cyanobacteria and algae, including antioxidant, immunomodulatory, antimicrobial or antitumor activities [141]. Dussault *et al*. evaluated the antibacterial activity of laxaphycins A, B and B3 against 5 foodborne pathogens, the Gram-positive strains *Listeria monocytogenes*, *Staphylococcus aureus* and *Bacillus cereus*, and the Gram-negative strains *Escherichia coli* and *Salmonella enterica* Typhimurium. Laxaphycins show no activity on Gram-negative strains, a result that can be explained by the hydrophobicity of the structure of these peptides. Indeed, the membrane of Gram-negative strains contains lipopolysaccharides that create a hydrophilic layer to prevent the entry of hydrophobic compounds into the cell. Laxaphycin A inhibits *S. aureus* with a MIC of 125 μg/mL, while it has a moderate activity (MIC = 250 μg/mL) on *B. cereus* and *L. monocytogenes*. Laxaphycin B has moderate activity on all Gram-positive strains (MIC = 250 μg/mL). Laxaphycin B3 has moderate activity on *B. cereus* (MIC = 250 μg/mL) and *S. aureus* (MIC = 500 μg/mL) but is not active on *L. monocytogenes*. It is important to note that the MICs found in this study are much higher than the concentrations tested in previous

cytotoxicity tests with these laxaphycins. The toxicity results obtained in this study on foodborne pathogens are therefore not comparable with toxicities obtained on cells.

b) Hormothamnin A

Gerwick *et al*. isolated hormothamnin A from the cyanobacterium *Hormothamnion enteromorphoides* [51]. This compound is toxic on goldfish *Carassius carassius* with an LD50 of approximately 5 μg/mL, but not on brine shrimp at 20 μg/mL. Hormothamnin A cytotoxicity was examined on different solid cancer cell lines. The peptide has an IC50 of 0.2 μg/mL on SW-1271 (human lung carcinoma cells), 0.16 μg/mL on A529 (human lung carcinoma cells), 0.13 μg/mL on B16-F10 (murine melanoma cells) and 0.72 μg/mL on HCT-116 (human colon carcinoma cells). In comparison, laxaphycin A differing only from hormothamnin A by the Dhb configuration, has an IC50 of 23 μM on HCT-116 cells [20,49]. The peptide is inactive on Gram positive and negative bacteria such as *Staphylococcus aureus*, *Streptococcus faecalis, Escherichia coli* and *Salmonella typhimurium* but is weakly active on *Bacillus subtilis* and *Pseudomonas aeruginosa* with IC50s greater than 100 μg/mL (100 μg/disc). Finally, the peptide is inactive on the fungi *Candida albicans* and on the yeast *Trichophyton mentagrophytes* [51].

c) Lobocyclamides

Lobocyclamides A-C demonstrated moderate antifungal activity against a variety of *Candida* sp. including two strains resistant to floconazole (*Candida albicans* 96-489 and *Candida glabrata*) [52]. Nevertheless, a mixture of lobocyclamides A and B gives a synergy with a high activity and a MIC between 10 and 30 μg/mL for a 50-50% mixture.

d) Scytocyclamides

The antimicrobial activity of scytocyclamides A-C was evaluated on different microorganisms, *Staphylococcus aureus* (ATCC 25923), *Escherichia coli* (ATCC 25922), *Bacillus subtilis* (ATCC 6633), *Streptococcus pyogenes* Gr. A E 12449/98, *Enterococcus faecium* 41769, *Acinetobacter baumannii* (ATCC 19606 T), *Corynebacterium pseudodiphtericum* RV2 / 92, and *Candida albicans* (ATCC 90028) [57]. No activity has been demonstrated for these peptides tested at a maximum concentration of 64 μg/mL. Scytocyclamides A and B were also tested for their toxic properties on two crustaceans, *Thamnocephalus platyurus* and *Daphnia magna*. No toxicity was obtained on *Daphnia magna*. On the other hand, scytocyclamides A and B were lethal on *Thamnocephalus platyurus* after only two hours, with an LD50 of about 18 μmol for scytocyclamide A and 3.7 μmol for scytocyclamide B. The cytotoxic activity of scytocyclamides A and B was then verified on different cell lines, CaCo 2 (human colorectal adenocarcinoma), HeLa (human cervical carcinoma), Swiss 3T3 (mouse embryonic fibroblasts), Ebl (bovine embryonic lung cells), Rbl (basophilic rat leukemia cells), LoVo (human colorectal adenocarcinoma), 293 (human embryonic kidney fibroblasts). Scytocyclamides A and B (10

µg/mL) cause extensive non-specific damage to these cells, with the formation of vesicles and changes in cell structure (observation of "bleeding"). These scytocyclamides could therefore be involved in cell apoptosis, during which this type of "bleeding" can be visualized.

To test for possible membrane damage caused by scytocyclamides A and B, the efflux of radioactive rubidium (86Rb+) from HT-29 cells was measured. Both scytocyclamides damage the membrane and induce a high flux of 86Rb+, up to a 5-fold increase at high peptide concentrations.

Further experiments were undertaken with scytocyclamide B to explain the morphological changes observed on the cells. Fluorescent staining was used to specifically color α-tubulin and F-actin. Fluorescence labeled antibodies with phalloidine were used to visualize F-actin. After treatment with scytocyclamide B (10 µg / 750µL), no changes were observed on F-actin on the cytoskeleton of HeLa cells. On the other hand, treated cells no longer reveal the staining of α-tubulin, suggesting that the mechanism of action of this peptide may be by tubulin degradation, which is commonly observed for many cyanobacterial marine natural products [36].

Scytocyclamide A was tested on mouse embryonic fibroblast cells (MEF-SV40). Under a phase contrast microscope, vesicle formation was observed, which could be a first indication of an apoptotic process. Flow cytometry analysis did indeed show the presence of late apoptotic or necrotic cells. However, no decrease in mitochondrial membrane potential was observed, nor was there an increase in caspase activity, which would exclude these signal transduction pathways for the initiation of apoptosis. Nevertheless, an increase in the rate of ROS was visualized, suggesting their involvement in the apoptosis process. These results complement those obtained on laxaphycins, with in the case of the addition of cyclic laxaphycins of type B, a suggestion of apoptosis process [54], while in the case of acyclic laxaphycins A and B, it would rather be a phenomenon of autophagy [19,54].

Sivonen's group evaluated the antimicrobial activity of organic extracts of *S. hofmannii* PCC 7110 on several fungal strains (*Candida albicans*, *Candida guilliermondii*, *Candida krusei*, *Candida parapsilosis*, *Filobasidiella neoformans*, *Aspergillus niger*, *Aspergillus parasiticus, Aspergillus flavus*) and bacterial strains (*Staphylococcus aureus*, *Enterococcus faecium*, *Bacillus cereus*, *Micrococcus luteus*, *Pseudomonas aeruginosa*, *Escherichia coli*, *Acinetobacter baumannii*, *Enterobacter aerogenes*, *Salmonella enterica*) [58]. The extracts only inhibit the growth of *Aspergillus flavus*, which is consistent with the inactivity found on *Candida albicans* by Jan Christoph Grewe. The inhibition of the growth of *A. flavus* was observed with individual scytocyclamides with inhibition zones of 10 mm for scytocyclamide A (200 µg), 7 mm for scytocyclamide A2 (200 µg), 23 mm for scytocyclamide B (600 µg), 22 mm for scytocyclamide C (160 µg), 10 mm for scytocyclamide B2 (85 µg) and 20 mm for scytocyclamide B3 (85 µg). A synergistic effect was observed between 11 and 12 residue scytocyclamides, with inhibition zones of 36 mm for scytocyclamides A and B (100 µg A + 300 µg B), 33 mm for scytocyclamides

A and C (100 µg A + 80 µg C), 24 mm for scytocyclamides A2 and B2 (100 µg A2 + 43 µg B2), 25 mm for scytocyclamides A2 and B3 (100 µg A2 + 43 µg B3) and 23 mm for scytocyclamides B and C (300 µg B + 80 µg C).

The synergistic activity of laxaphycins and their derivatives would be linked to their shared biosynthesis mode. Indeed, this would suggest simultaneous regulation and expression of synergistic products to interact with the same target via different mechanisms. Such a phenomenon of co-regulation of distinct groups of genes has already been observed with the synergistic antibiotics griseoviridin and viridogrisein in *Streptomyces griseoviridis* [142].

e) Lyngbyacyclamides

Biological study of Lyngbyacyclamides A and B was restricted to cytotoxicity evaluation against B16 mouse melanoma cells (IC50 of 0.7 µM) and toxicity on brine shrimp (not active at 70 µM on *Artemia* genus) [59].

f) Trichormamides

The organic extracts of *Trichormus* sp. and *Oscillatoria* sp. showed antiproliferative activity against human colon cancer cell line HT-29 [60,61]. Trichormamides were tested individually on human melanoma cells MDA-MB-435 and human colon cancer cells HT-29. Trichormamide B is cytotoxic against MDA-MB-435 with an IC50 of 0.8 µM and against HT-29 with an IC50 of 1.5 µM, while trichormamide A is less active with IC50s of 9.9 and 16.9 µM, respectively. Like trichormamide B, trichormamide C is cytotoxic against MDA-MB-435 with an IC50 of 1 µM and against HT-29 with an IC50 of 1.7 µM. Trichormamide D, like trichormamide A, is less active than trichormamide C with IC50s of 11.7 and 11.5 µM, respectively.

Trichormamides C and D were also tested for antibacterial activity against *Mycobacterium tuberculosis*, *Mycobacterium smegmatis*, *Staphylococcus aureus*, *Escherichia coli*, and antifungal activity against *Candida albicans*. Trichormamide C shows moderate activity against *M. tuberculosis* with a MIC of 23.8 µg/mL and no activity against other strains at 50 µg/mL. Trichormamide D is not active against any strain at the same concentration of 50 µg/mL. No synergistic effect was observed between trichormamides C and D, but the lack of peptides did not allow to deepen this result.

g) Heinamides

The heinamides were tested for their antimicrobial and antifungal activity [63]. The crude extract from *Nostoc* sp. inhibited the growth of *Aspergillus flavus* FBCC 2467. Seven other fungi and nine bacterial strains were used but no activity was observed. While heinamide A2 alone and the heinamides mixture (B1+B2) induced a weak inhibition of *A. flavus* growth, a strong synergy was observed with the A2+(B1+B2) mixture.

B. Feeding deterrence as an example of ecological role

Secondary metabolites play an important role in the interactions between different organisms within the trophic chain [10,16]. Some compounds are toxic and have been selected by cyanobacteria as an effective defense strategy against herbivorous predators. But these predators can also develop strategies of resistance to repellent, antiappetant or toxic compounds, allowing them to feed and hide from their own predators. In the previous sub-section, we saw that laxaphycins and their derivatives could show toxicity on certain organisms. It is therefore highly probable that the associated cyanobacteria synthesize them in order to protect themselves from herbivores, competitors or fouling organisms. However, the ecological role of laxaphycins remains unclear [36]. Laxaphycin A, hormothamin A and lyngbyacyclamides are non-toxic on brine shrimp *Artemia*, while laxaphycin B is lethal. Hormothamnin A is, on the other hand, toxic on the goldfish *Carassius carassius* and scytocyclamides are toxic against the crustacean *Thamnocephalus platyurus*. Given the different responses obtained with these peptides on different organisms, the use of all laxaphycins type peptides as chemical defenses cannot be confirmed.

It has been shown that the cyanobacterium *H. enteromorphoides* is chemically defended against most of these predators [143]. Out of eleven cyanobacteria, algae and sea grasses tested, *H. enteromorphoides* was one of the only ones to repel the sea hare *Dolabella auricularia*, suggesting a chemical repulsion phenomenon around this cyanobacterium. This phenomenon of repulsion was also observed on various fish. Indeed, different fractions extracted from this cyanobacterium have been evaluated for their ability to repel predators. The fraction containing cyclic peptides, including laxaphycin A, was able to avoid predation, whereas the fractions containing no cyclic peptides did not. However, not all predators respond in the same way to the mixture of peptides. For example, pufferfish *C. solandri* is weakly impacted by the chemical environment of the cyanobacterium while sea urchin *D. savignyi* is completely repelled by the mixture of peptides. Biosynthesizing several peptides could therefore be a way for the cyanobacterium to repel a wider range of predators, with the hypothesis that each of them has a different sensitivity to each peptide. Moreover, these peptides may have a synergistic effect on each other. However, there is no evidence that the synergism observed in toxicity tests is also observed on the palatability of herbivores. In fact, in this study, laxaphycin A was as effective, or even slightly more effective, in repelling *S. schlegeli* parrotfish as was the mixture of peptides at the same concentration [143].

Although a few studies have been done on the impact of secondary cyanobacterial metabolites on predation [10,12,13,144], very little research has involved laxaphycins and their derivatives. Among these studies, many have shown that the sea hare *Stylocheilus striatus* was not repelled by certain secondary cyanobacterial metabolites. Compared to four other generalist herbivores, *Stylocheilus striatus* is the only one not repelled by the cyclic peptide pitipeptolide A biosynthesized by *Lyngbya majuscula* [11]. Considered as a specialist of *Lyngbya majuscula*, it could have adapted to its chemical environment. However, this

mollusk was also found on *Anabaena torulosa*, known to synthesize laxaphycins in particular [16]. By comparing by LC-MS the chemical fingerprints of *Anabaena torulosa* and *Stylocheilus striatus*, Louis Bornancin discovered that laxaphycin A was sequestered within the digestive gland of the mollusk, while laxaphycins B and B3 were present in the cyanobacterium but no more within the mollusk, presenting new acyclolaxaphycins previously described [16,54], suggesting a degradation of cyclic laxaphycin-B type peptides [18]. *Stylocheilus striatus* would thus be involved in a process of biodegradation of laxaphycin B, allowing it to detoxify this cyclic peptide. The mollusk could have adapted to this unattractive cyanobacterium to hide from its main predators. Indeed, Louis Bornancin observed in the field that *Gymnodoris ceylonica*, specialist predator of *S. striatus*, and *Thalamita coerulipes*, generalist predator of some herbivores, were present on *Lyngbya majuscula* but absent from *Anabaena torulosa*. Secondary metabolites of *A. torulosa* could then repel these two predators [16].

Table 3. Summary of the biological activity of laxaphycins A and their derivatives. For clarity purpose, the intracellular properties of the peptides have not been reported. Dose, Activity, Target. NA=Not active.

Laxaphycin A family (11 residues)	Cytotoxicity	Antimicrobial activity	Antifungal activity	Toxicity on animals	Ref.
Laxaphycin A	10 μg/mL, NA on KB and LoVo cells. 20 μg/mL, NA on CCRF-CEM-WT, CEM/VLB and CEM/VM1 cells. NA on A549, MCF7, PA1, PC3, DLD1, M4Beu, HCT116, SHSY5Y solid cancer lines.	NA on *E. coli* and *S. enterica* Typhimurium. MIC 125 μg/mL on *S. aureus*. MIC 250 μg/mL on *B. cereus*, *L. monocytogenes*.	128 μg/mL, NA on *A. oryzae*, *C. albicans*, *P. notatum*, *S. cerevisiae* and *T. mentagrophytes*. Synergism with laxaphycin B on all strains.	200 μg/mL NA on *A. salina.*	[8,19,20,44,46,49,140,141]
Laxaphycin A2	NA on HCT116. IC50 0.6 μM on SHSY5Y.				[19,49]
[D-Val^{9}]laxaphycin A	IC50 5.6 μM on SHSY5Y.				[19]
[des-Gly^{11}]acyclolaxaphycin A	10 μM, 50% deaths of SHSY5Y.				[19]
[des-(Leu^{10}-Gly^{11})]acyclolaxaphycin A	NA on SHSY5Y.				[19]
Hormothamnin A	IC50 0.2 μg/mL on SW-1271. IC50 0.16 μg/mL on A529. IC50 0.13 μg/mL on B16-F10. IC50 0.72 μg/mL on HCT116.	NA on *S. aureus*, *S. faecalis*, *E. coli* and *S. typhimurium*. IC50 > 100 μg/mL on *B. subtilis.* IC50 > 100 μg/mL on *P. aeruginosa*.	NA on *C. albicans* and *T. mentagrophytes.*	LD50 ~ 5 μg/mL on goldfish *C. carassius*. 20 μg/mL, NA on brine shrimp.	[51]
Lobocyclamide A			MIC 100 μg/disc on *C. albicans* (inhibition zone of 7 mm for 150 μg/disc). Synergy with lobocyclamide B (MIC 10-30 μg/mL, 1:1).		[52]
Scytocyclamide A	10 μg/mL, active on CaCo 2, HeLa, Swiss 3T3, Ebl, Rbl, LoVo and 293 cell lines.	64 μg/mL, NA on *S. aureus*, *S. pyogenes, E. coli, B. subtilis, E. faecium, A. baumannii, C. pseudodiphtericum.*	64 μg/mL, NA on *C. albicans.* Active on *A. flavus* (inhibition zone of 10 mm for 200 μg). Synergy with scytocyclamide B (inhibition zone of 36 mm for 100 μg A + 300 μg B) and with scytocyclamide C (inhibition zone of 33 mm for 100 μg A + 80 μg C).	NA on *D. magna*. LD50 12 μmol on *T. platyurus*.	[57,58]
Scytocyclamide A2			Active on *A. flavus* (inhibition zone of 7 mm for 200 μg). Synergy with scytocyclamide B2 (inhibition zone of 24 mm for 100 μg A2 + 43 μg B2) and with scytocyclamide B3 (inhibition zone of 25 mm for 100 μg A2 + 43 μg B3).		[58]

Trichormamide A	IC50 9.9 μM on MDA-MB-435 cells. IC50 16.9 μM on HT-29 cells.			[60]
Trichormamide D	IC50 11.7 μM on MDA-MB-435 cells. IC50 11.5 μM on HT-29 cells.	50 μg/mL, NA on *M. tuberculosis, M. smegmatis, S. aureus* and *E. coli.*	50 μg/mL, NA on *C. albicans*.	[61]
Heinamides A1-A3		NA on *S. aureus, E. faecium, B. cereus, M. luteus, P. aeruginosa, E. coli, A. baumannii, E. aerogenes, S. enterica.*	Crude extract of heinamides A and B inhibits *A. flavus*. NA on *C. albicans, C. guillermondi, C. krusei, C. parapsilosis, F. neoformans, A. niger, A. parasiticus.*	[63]

Table 4. Summary of the biological activity of laxaphycins B and their derivatives. For clarity purpose, the intracellular properties of the peptides have not been reported. Dose, Activity, Target. NA=Not active.

Laxaphycin B family (12 residues)	Cytotoxicity	Antimicrobial activity	Antifungal activity	Toxicity on animals	Ref.
Laxaphycin B	MIC 0.12 μg/mL on KB cells. Synergy with laxaphycin A (MIC 0.10 μg/mL with 0.06 μg A+ 0.05 μg B). IC50 1.11 μM on CCRF-CEM-WT cells. IC50 1.02 μM on CEM/VLB cells. IC50 1.37 μM on CEM/VM1 cells. Synergy with laxaphycin A (at 1 μM) IC50/3. IC50 0.5 ± 0.07 μM with Ho and 1 ± 0.12 μM with RRT on MCF7. IC50 0.19 ± 0.03 μM on PA1. IC50 0.58 ± 0.03 μM with Ho and 0.8 ± 0.1 μM with RRT on PC3. IC50 between 3 and 6 μM on DLD1. IC50 0.3 ± 0.03 μM with Ho and 0.4 ± 0.03 μM with RRT on M4Beu. IC50 < 2 μM on A549. IC50 < 2 μM on human normal fibroblasts and L-929 murine immortalized cells. IC50 0.3 μM with MTT and 1.8 μM with LDH on SHSY5Y.	NA on *E. coli* and *S. enterica* Typhimurium. MIC 250 μg/mL on *S. aureus*, *B. cereus*, *L. monocytogenes*.	MIC 64 μg/mL on *A. oryzae*. Moderate activity on *C. albicans*, *S. cerevisiae* and *T. mentagrophytes.* Synergism with laxaphycin A (MIC 16 μg/mL with 9.6 μg A+ 6.4 μg B).	200 μg/mL, lethal on *A. salina.*	[8,20,44,46,54,140,141]
Laxaphycin B2	IC50 4.15 ± 0.31 μM on CCRF-CEM-WT cells. IC50 3.33 ± 0.08 μM on CEM/VLB cells. IC50 4.14 ± 0.09 μM on CEM/VM1 cells.				[20]
Laxaphycin B3	IC50 1.50 ± 0.06 μM on CCRF-CEM-WT cells. IC50 1.35 ± 0.05 μM on CEM/VLB cells. IC50 1.45 ± 0.11 μM on CEM/VM1 cells. IC50 0.15 μM with MTT and 0.8 μM with LDH on SHSY5Y.	NA on *E. coli* and *S. enterica* Typhimurium. MIC 500 μg/mL on *S. aureus*. MIC 250 μg/mL on *B. cereus*. NA on *L. monocytogenes*.			[20,54,141]
Laxaphycin B4	IC50 1.7 μM on HCT116 cells.				[49]
Laxaphycin B5	IC50 1.2 μM on MDA-MB-435. IC50 2.2 μM on MDA-MB-231. IC50 1.6 μM on OVCAR3.				[50]
Laxaphycin B6	IC50 0.58 μM on MDA-MB-435. IC50 0.81 μM on MDA-MB-231. IC50 0.92 μM on OVCAR3.				[50]
Laxaphycin D = Scytocyclamide B	10 μg/mL, active on CaCo 2, HeLa, Swiss 3T3, Ebl, Rbl, LoVo and 293 cell lines.	64 μg/mL, NA on *S. aureus*, *S. pyogenes, E. coli, B. subtilis, E.*	64 μg/mL, NA on *C. albicans.* Inhibits *A. flavus* (inhibition zone of 23 mm for 600 μg). Synergy with scytocyclamide A (inhibition	NA on *D. magna*.	[57,58]

		faecium, A. baumannii, C. pseudodiphtericum	zone of 36 mm for 100 μg A + 300 μg B) and with scytocyclamide C (inhibition zone of 23 mm for 300 μg B + 80 μg C).	LD50 4 μmol on *T. platyurus*.	
Acyclolaxaphycin B	Until 10 μM, NA on SHSY5Y cells.				[54]
Acyclolaxaphycin B3	Until 10 μM, NA on SHSY5Y cells.				[54]
[des-(Ala[4]-Hle[5])]acyclolaxaphycin B	NA on SHSY5Y cells.				[54]
[des-(Ala[4]-Hle[5])]acyclolaxaphycin B3	NA on SHSY5Y cells.				[54]
Lobocyclamide B			MIC 30-100 μg/mL on *C. albicans* (inhibition zone of 8 mm for 150 μg/disc). Synergy with lobocyclamide A (MIC 10-30 μg/mL, 1:1). Activity on *C. glabrata* (inhibition zone of 6 mm for 150 μg/disc).		[52]
Lobocyclamide C			Activity on *C. albicans* (inhibition zone of 10 mm for 150 μg/disc). Activity on *C. glabrata* (inhibition zone of 8 mm for 150 μg/disc).		[52]
Scytocyclamide B2			Inhibits *A. flavus* (inhibition zone of 10 mm for 85 μg). Synergy with scytocyclamide A2 (inhibition zone of 24 mm for 100 μg A2 + 43 μg B2).		[58]
Scytocyclamide B3			Inhibits *A. flavus* (inhibition zone of 20 mm for 85 μg). Synergy with scytocyclamide A2 (inhibition zone of 25 mm for 100 μg A2 + 43 μg B3).		[58]
Scytocyclamide C		64 μg/mL, NA on *S. aureus*, *S. pyogenes, E. coli, B. subtilis, E. faecium, A. baumannii, C. pseudodiphtericum*	64 μg/mL, NA on *C. albicans*. Inhibits *A. flavus* (inhibition zone of 22 mm for 160 μg). Synergy with scytocyclamide A (inhibition zone of 33 mm for 100 μg A + 80 μg C) and with scytocyclamide B (inhibition zone of 23 mm for 300 μg B + 80 μg C).		[57,58]
Lyngbyacyclamide A	IC50 0.7 μM on B16 mouse melanoma cells.			70 μM, NA on brine shrimp (*Artemia* genus)	[59]
Lyngbyacyclamide B	IC50 0.7 μM on B16 mouse melanoma cells.			70 μM, NA on brine shrimp (*Artemia* genus)	[59]
Trichormamide B	IC50 0.8 μM on MDA-MB-435 cells. IC50 1.5 μM on HT-29 cells.				[60]

Trichormamide C	IC50 1 μM on MDA-MB-435 cells. IC50 1.7 μM on HT-29 cells.	MIC 23.8 μg/mL on *M. tuberculosis*. 50 μg/mL, NA on *M. smegmatis*, *S. aureus* and *E. coli.*	50 μg/mL, NA on *C. albicans*.	[61]
Heinamides B1-B5		NA on *S. aureus, E. faecium, B. cereus, M. luteus, P. aeruginosa, E. coli, A. baumannii, E. aerogenes, S. enterica.*	Crude extract of heinamides A and B inhibits *A. flavus*. NA on *C. albicans, C. guillermondi, C. krusei, C. parapsilosis, F. neoformans, A. niger, A. parasiticus.*	[63]

VI. Conclusion

To date, the family of laxaphycins includes 16 type-A laxaphycins and 27 type-B laxaphycins, mostly cyclic peptides. Acyclolaxaphycins are either derived from incomplete biosynthesis or are enzymatic degradation products [18,19,58]. Laxaphycins and their derivatives have a wide structural diversity, including many non-proteinogenic amino acids and D-configured amino acids. However, their structures remain very close, with changes in amino acids keeping the same absolute configuration and being mostly isosteric. Since these amino acids have relatively close structures and that the patterns can be repeated within the peptide, researchers have difficulties in determining the structures and stereochemistries with certainty. Although using increasingly precise techniques such as NMR or mass spectrometry, errors in attribution are often observed for natural substances [48]. The chemical synthesis of these peptides is the best way to confirm a proposed structure, since it allows the comparison of the synthetic peptide with the natural molecule. The total synthesis of laxaphycin B was the first to be described [47]. In view of the specific structure of these peptides, the possible synthetic methods are limited and it is necessary to synthesize beforehand the various non-proteinogenic and non-commercial amino acids.

The structural similarities of these peptides suggest that they are biosynthesized in the same way. Since laxaphycins were isolated from various cyanobacteria harvested at different locations, their origin could be the result of horizontal gene transfer between different cyanobacteria [18,53]. The biosynthesis of these peptides has been very little studied, since the only studies identified to date are that of the biosynthesis of scytocyclamides and heinamides, published very recently [58,63]. This study suggests that type-A and -B scytocyclamides and heinamides share common PKS modules to initiate their biosynthesis with β-aminooctanoic acid. Subsequently, two distinct NRPS pathways, matching with the structure of the two peptide types, act in parallel to elongate the rest of the sequence to obtain either type A or B peptides. This result is interesting because the majority of NRPS pathways generally follow the collinearity rule. Most of the genes involved in this biosynthesis have been described, but there are still question marks as to the origin of some amino acids such as dehydrobutyrine. Although some enzymes capable of hydroxylating particular amino acids are known, their mode and location of action are not very detailed. β-hydroxylation can take place on the free amino acid upstream of elongation, directly on the PCP domain during elongation or post-synthesis.

The great diversity of amino acids making up laxaphycins can confer them many biological activities. The vast majority of these peptides have antibacterial and antifungal activities, and can even be cytotoxic on a large number of cancer cell lines [19,20,51,54,59–61]. However, cytotoxic peptides appear to be non-specific between normal and cancerous cell lines [20]. Type-A laxaphycins, showing little or no cytotoxic activity on their own, act in synergy with the more toxic type-B laxaphycins. Type-A laxaphycins potentiate the action of type-B laxaphycins

both on cells and on the growth of bacteria or fungi. However, it seems that these two types of peptides act by different biological pathways. Their toxicity could also help to repel predators of the cyanobacteria that synthesize them in order to protect themselves. Since all peptides have different activities, one might wonder why they synthesize so many peptides, rather than simply synthesizing the peptides that repel predators the most. It has been shown that each predator has a different sensitivity to each molecule, so it would be more interesting for cyanobacteria to synthesize a wide range of peptides to repel more predators [143]. The synergy observed with laxaphycins A and B for cytotoxicity was not found in cases of predation. The diversity of peptides synthesized by cyanobacteria is also related to multiple specificities of adenylation domains in the NRPS chain, allowing the introduction of isosteric amino acids for example [145].

In the 30 years since their first discovery, the laxaphycins family has expanded as researchers have become more knowledgeable about them. We are now able to isolate, synthesize and characterize these peptides. Their complex structures are of great interest as to their origin, ecological and biological roles.

Chapter 2.
Synthesis of laxaphycin B analogues

Section I of this chapter is a brief introduction of peptide synthesis and cyclization methods. Section II covers the extension of the laxaphycin synthesis through the synthesis of trichormamide C and analogues and their structural confirmations by NMR that we published in *Organic Letters* during my thesis [30]:

Darcel, L.; Djibo, M.; Gaillard, M.; Raviglione, D.; Bonnard, I.; Banaigs, B.; Inguimbert, N. Trichormamide C Structural Confirmation through Total Synthesis and Extension to Analogs. *Org. Lett.* **2020**, *22*, 145–149, doi:10.1021/acs.orglett.9b04064.

I. Peptide synthesis

Peptide synthesis is the production of peptides composed of amino acids linked through amide bonds [146,147]. Peptides are obtained by coupling the carboxyl group of an amino acid with the amino group of another amino acid (Figure 39). In order not to induce undesired side reactions, the prior protection of the functional groups of each amino acid is usually necessary. Peptide synthesis starts at the carboxyl end (C-ter) and proceeds towards the amino end (N-ter), i.e., in the opposite direction to biological protein synthesis.

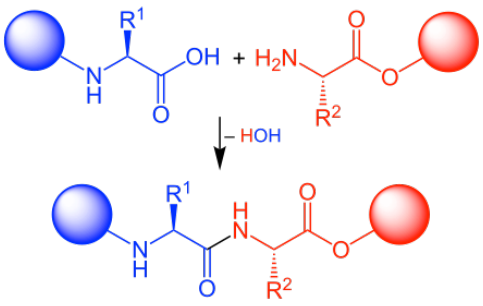

Figure 39. Peptide coupling between an acid and an amine to form an amide bond.

Peptides can be assembled in solution (SPS) or on solid support (SPPS) [148]. When synthesizing in solution, peptide fragments (e.g. tripeptides) are usually prepared upstream and then coupled together to form a longer linear peptide [149]. Many peptides have been synthesized in solution, such as oxytocin [150], or dehydrodidemnin [151]. Solution phase peptide synthesis is generally used for large scale synthesis and is less expensive than solid phase synthesis. However, reaction times are long, couplings are less powerful, and purification is required at each step. Solid phase peptide synthesis has the advantage of being faster (and can be automated), without intermediate purifications, and giving couplings with high conversion. However, this technique is more expensive and less environment-friendly, as a large amount of solvents is needed and reagents are used in excess [152]. More and more research teams and companies are exploring greener peptide chemistry, with less toxic solvents [153,154], and even solvent-free coupling techniques [155,156]. The development of microwave-assisted techniques has allowed the synthesis of longer peptides in high yields. Chemical ligation techniques can also be used to couple peptides fragment of lengths up to 50 amino acids. The native chemical ligation NCL involves the coupling between a C-ter

thioester and a thiol group of an N-ter cysteine of two peptide fragments. The Staudinger ligation proceeds between an azide group and a phosphorus derivative, undergoing a rearrangement to reach the amide function after hydrolysis (Figure 40). Chemical ligation techniques give good yields, high chemoselectivity and allow the synthesis of long and complex peptides difficult to obtain by conventional SPPS [148]. However, they often involve very long reaction times and intermediate purifications [157].

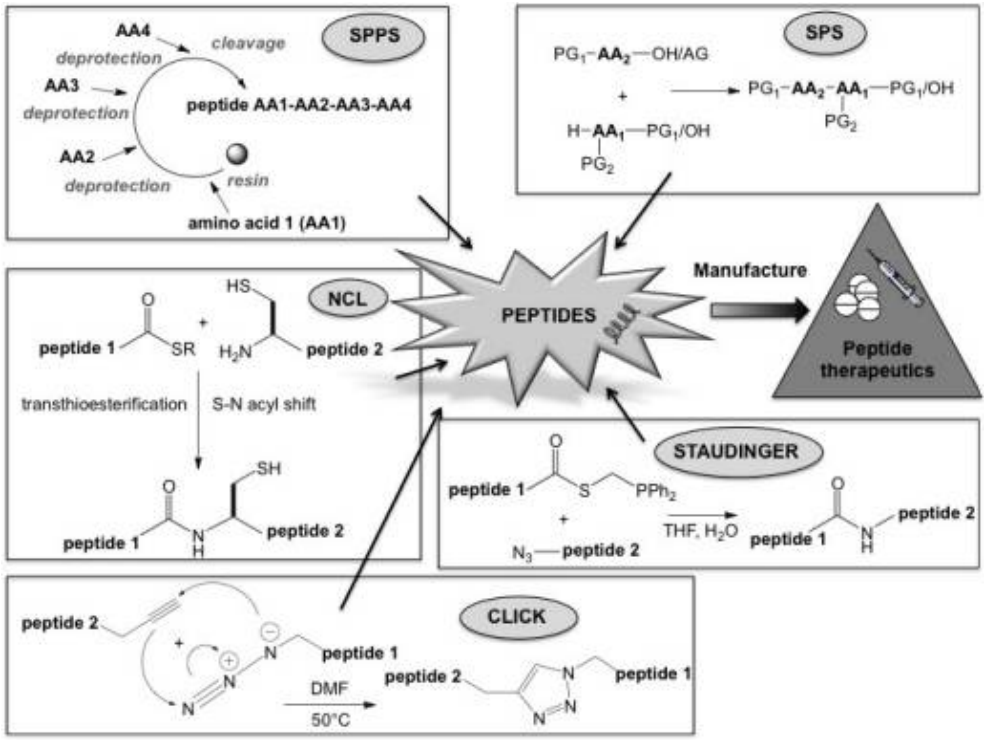

Figure 40. Different strategies to obtain peptide bonds or peptide bond mimics.

This image was taken from the article of Chandrudu *et al*. (Chandrudu S, Simerska P, Toth I. Chemical methods for peptide and protein production. *Molecules.* 2013;18(4):4373-4388. Published 2013 Apr 12. doi:10.3390/molecules18044373) License : http://creativecommons.org/licenses/by/3.0/

A. Solid phase peptide synthesis

Solid phase peptide synthesis (SPPS) consists in grafting an amino acid by its carboxyl group on resin beads. The resins are made of polymers of different nature that confers them suitable swelling and mechanical properties. Resin functionalization by reactive functions allows the grafting of amino acids on it depending on its loading rate which corresponds to the number of moles of available functions per gram of resin. The general principle of SPPS consists in repeating cycles of deprotection, washing and coupling (Figure 41). The terminal amine of the immobilized amino acid is coupled to the acid group of an amino acid whose N-terminus is blocked by a protective group [158]. This new amino acid is then deprotected, revealing a new N-terminal amine to which another amino acid can then be attached. Part of the superiority of this technique is the ability to perform wash cycles after each reaction, removing excess reagent while the peptide of interest remains covalently attached to the solid resin. The most

commonly used strategy in SPPS is the Fmoc/*t*Bu strategy, where the amine is protected by a basic-cleaved Fmoc moiety whereas the orthogonal protections used for the side chains (e.g., Boc, *t*Bu, Trt) and the final cleavage from the resin are performed using acid. Depending on the resin used, it is also possible to cleave the peptide from the resin under milder conditions, without loss of side chain protections.

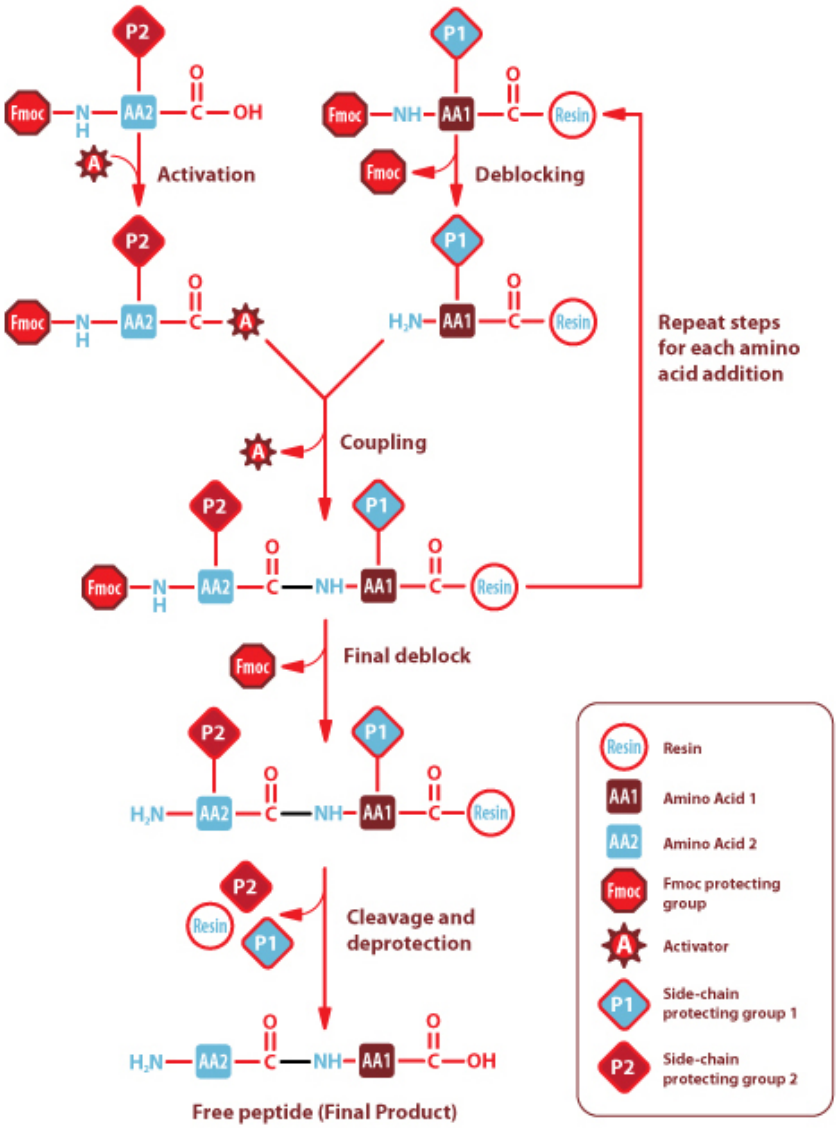

Figure 41. Solid phase peptide synthesis principle.

This image was taken from the website of Sigma Aldrich (consulted in March 2021 at https://www.sigmaaldrich.com/technical-documents/articles/biology/solid-phase-synthesis.html)

B. Cyclization methods

Different cyclization techniques are possible, in solution or directly on solid support, and have been widely reported in the literature [159,160]. To perform cyclization in solution after

synthesizing the linear peptide on solid support, it is necessary to cleave the peptide from the resin without removing side chain protections that may interfere in the coupling. For this, the use of a chlorotrityl resin for example can be considered. Indeed, the treatment of this resin under mild acidic conditions (e.g., 1% TFA) allows to release the peptide without cleaving the side chain protections. The peptide can then be cyclized between its C-ter part and its N-ter part but the cyclization reaction is slow and must be performed at high dilution to avoid intermolecular reactions [161]. In addition, several side reactions can take place such as racemization.

Among the most common solid phase cyclization techniques are “head-to-tail”, “side-chain-to-side-chain”, “head-to-side-chain” or “tail-to-side chain” cyclization’s (Figure 42). In the case of “head-to-tail” cyclization (between the C-ter acid and the N-ter amine), the linear peptide can be cyclized in solution or when attached to the resin by an amino acid side chain. It is then necessary to use an orthogonal protection system to be able to deprotect both ends of the peptide without cleaving other protecting groups. One of the most common cyclization is “side-chain-to-side-chain” cyclization by forming a disulfide bridge between two cysteine residues. In case the peptide contains several cysteines, it is possible to perform selective cyclizations by using adapted orthogonal protections. “Tail-to-side chain” cyclization typically involves the C-terminus and the amine function of a lysine or ornithine side chain and “head-to-side chain” cyclization between the N-terminus and an aspartic acid or glutamic acid side chain.

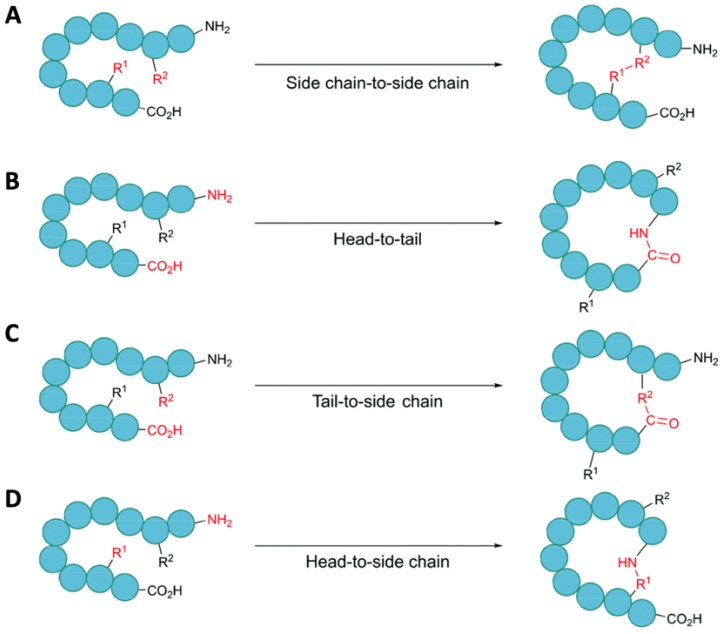

Figure 42. Different strategies of peptide cyclization. A) side chain-to-side chain B) head-to-tail or backbone cyclization C) tail-to-side chain D) head-to-side chain.

This image was taken from the article of Hayes *et al.* [160] (C. Hayes, H.; P. Luk, L.Y.; Tsai, Y.-H. Approaches for Peptide and Protein Cyclisation. *Org. Biomol. Chem*. 2021, 19, 3983–4001, doi:10.1039/D1OB00411E.) License: https://creativecommons.org/licenses/by/3.0/

II. Optimization of the synthesis of laxaphycin B-type peptides through analogues

We recently showed that *Ss* consumed *At* despite LaxB toxicity and turned it into an acyclic compound devoid of any toxicity through a non-characterized biodegradation process [16,54,162]. In contrast, laxaphycin A (named compound **1** hereafter), is bioaccumulated into the digestive gland of *Ss* while only the acyclic form of LaxB is found in the same gland. In order to better understand the biodegradation process involved in the LaxB (named compound **2**) detoxification we searched for an analogous peptide that would allow for the simplification of the previously reported synthesis as well as for new compounds for comparative purposes. Trichormamide C (named compound **4**) that differed by only one amino acid when compared to **2** constituted an appealing alternative (Figure 43). Hence, the (2R,3R)-hydroxyasparagine (HyAsn) of **2** is replaced by a D-Asn but **4** remains as active as the **2** with antiproliferative activities in the µM range on cancer cell lines. Hereafter we present a more flexible synthesis method of **4** which has been extended to two other analogs and avoids racemization problems or secondary reactions. This flexible synthesis will allow to compare LaxB analogs bearing differences at the side chains level that will make it possible to characterize and compare the detoxification process used by *Ss*.

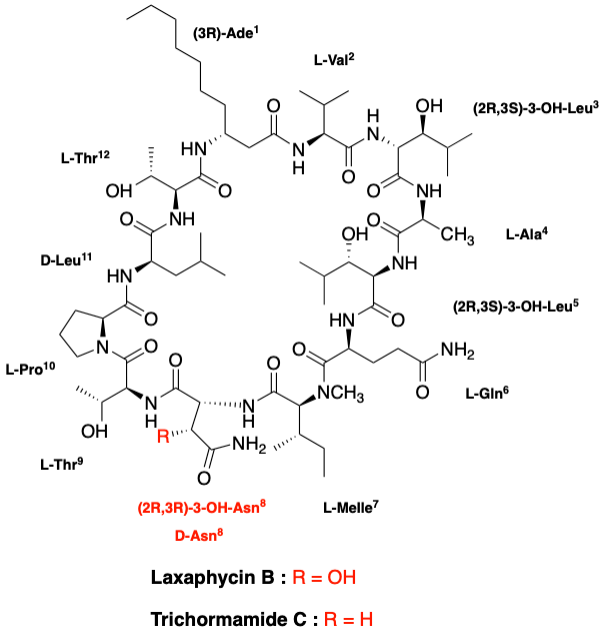

Figure 43. Structure of trichormamide C (4) compared to laxaphycin B (2).

Peptide cyclization is a key step in the synthesis of lipopeptides as racemization issues need to be avoided. Therefore, the carboxylic groups of achiral glycine or the less proned to epimerization proline are often used. This concern led us to choose the (3R)-β-aminodecanoic acid (Ade) as an anchor point on the 2-chlorotrityl chloride resin. Until now, the synthesis of such peptides has been achieved by anchoring hydroxyaspartic acid (HyAsp) on solid support

which is transformed to HyAsn upon the final cleavage. Presence of a chiral center on the activate carboxylic acid of HyAsp might induce epimerization [47,80]. In addition, Ade is expensive and complex to synthesize, requiring a 6-step synthesis for an overall yield of about 20% [69]**.** Grafting this amino acid on a solid support would conserve it by reducing the excess used for the coupling steps.

A. Solid phase peptide synthesis

The first attempts to synthesize the linear peptide were made on a simplified sequence of the peptide, without any hydroxy group (D-Leu^3 and D-Leu^5 instead of HyLeu^3 and HyLeu^5). Once the synthesis was optimized, we used hydroxyleucine to obtain trichormamide C. Both 3-aminodecanoic acid and hydroxyleucine had been synthesized before the beginning of this thesis and by student interns. Among all the techniques presented above to obtain hydroxyleucine, we used Sharpless dihydroxylation.

Ade was added to the 2-chlorotrityl resin with a loading rate of 0.8 mmol/g checked by absorbance measurement when cleaving the Fmoc protecting group of the amino acid [163]**.** The peptide synthesis was done by a standard SPPS protocol using Fmoc/*t*Bu strategy with an automated microwave peptide synthesizer. The synthesis was carried out at 50°C to avoid premature cleavage of the peptide from the 2-chorotrityl resin [164]**.** The conditions optimized for LaxB at a 0.1 mmol scale, i.e., 20-minute couplings with HATU/DIEA and 20% piperidine in DMF for deprotection steps were used. After analyzing the crude peptide cleaved from the resin, different secondary compounds formed during the synthesis were detected by LC-MS. The most important fragment resulted from the formation of a guanidinium capped Thr^9 by HATU reagent (Figure 44, Figure 45).

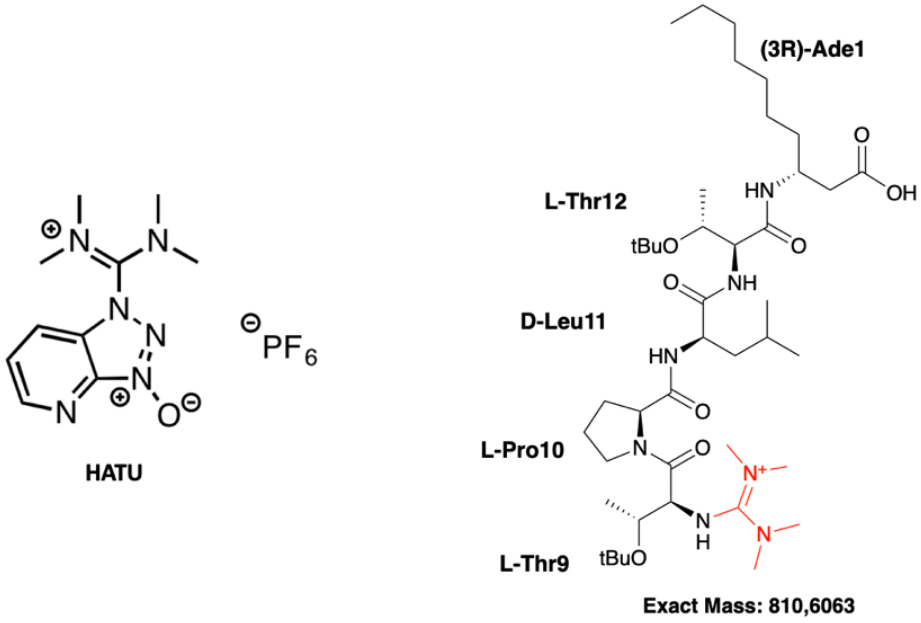

Figure 44. Structure of HATU reagent and the peptide capped by HATU during the synthesis.

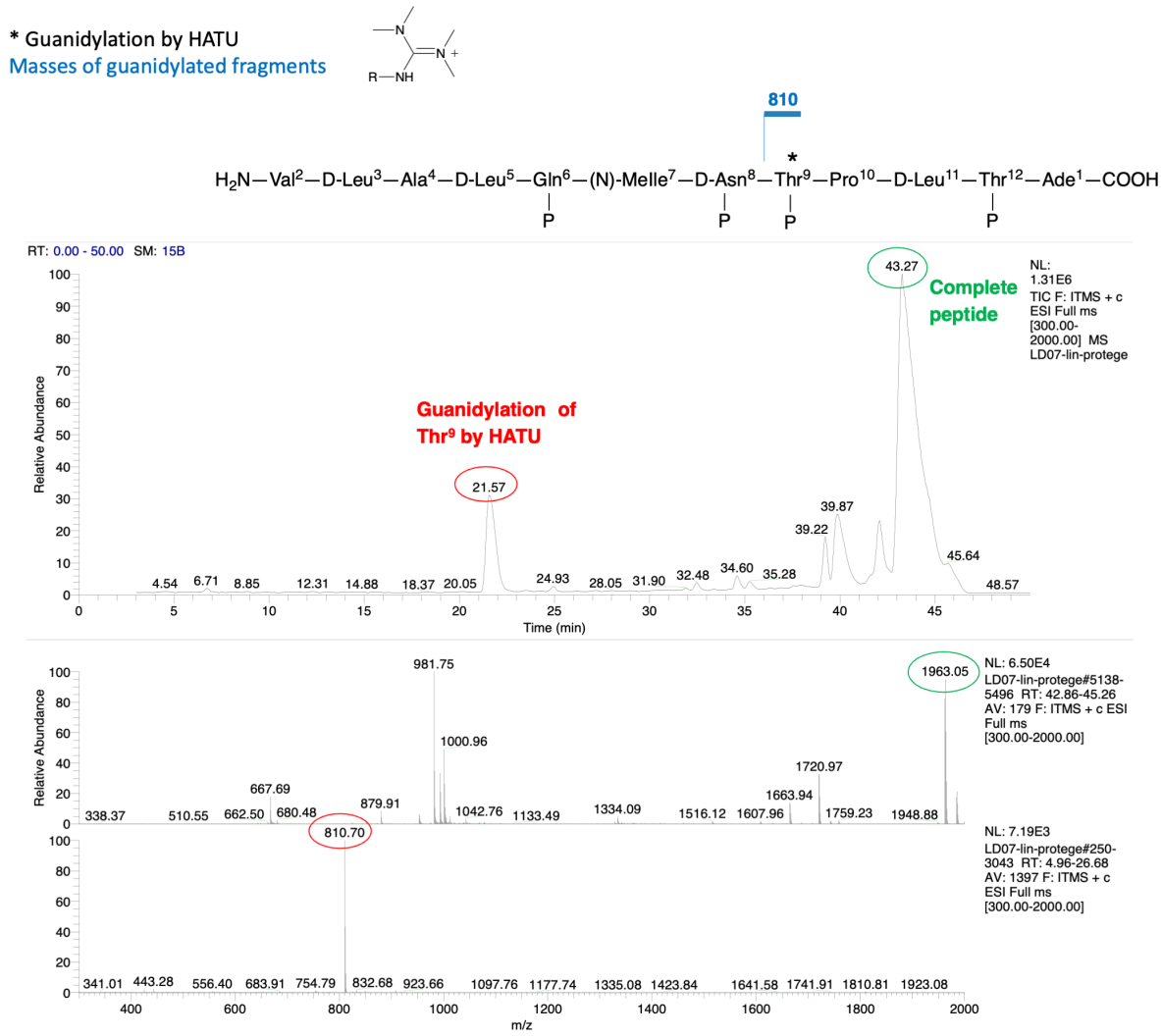

Figure 45. LC-MS chromatogram of the crude peptide with the guanidylation fragment. The asterisk indicates a partial guanidylation site that prevents further extension of the peptide sequence.

Attempts to diminish this side reaction using less HATU with respect to the amino acid were found to be ineffective. The synthesis was then performed using DIC/OxymaPure coupling reagents but the phenomenon of guanidylation has intensified compared to the use of HATU/DIEA (Figure 46). The same kind of guanidylation albeit with direct reaction of the N-terminal amine with the DIC was observed for all amino acids from Ade[1] to N-MeIle[7] thus highlighting an unexpected difficult sequence (Figure 47, Figure 48).

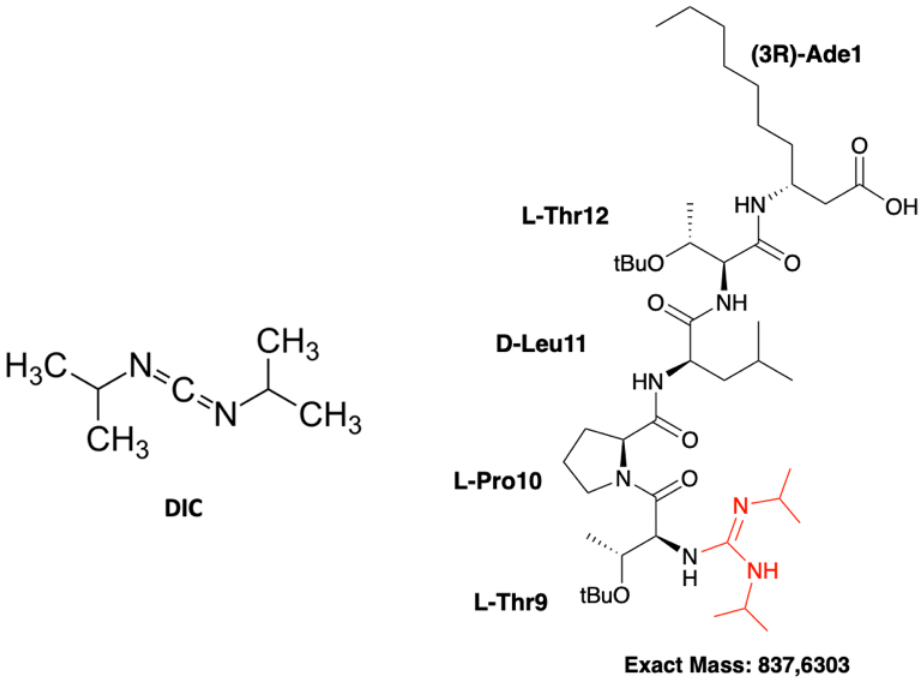

Figure 46. Structure of DIC reagent and the peptide capped by DIC during the synthesis.

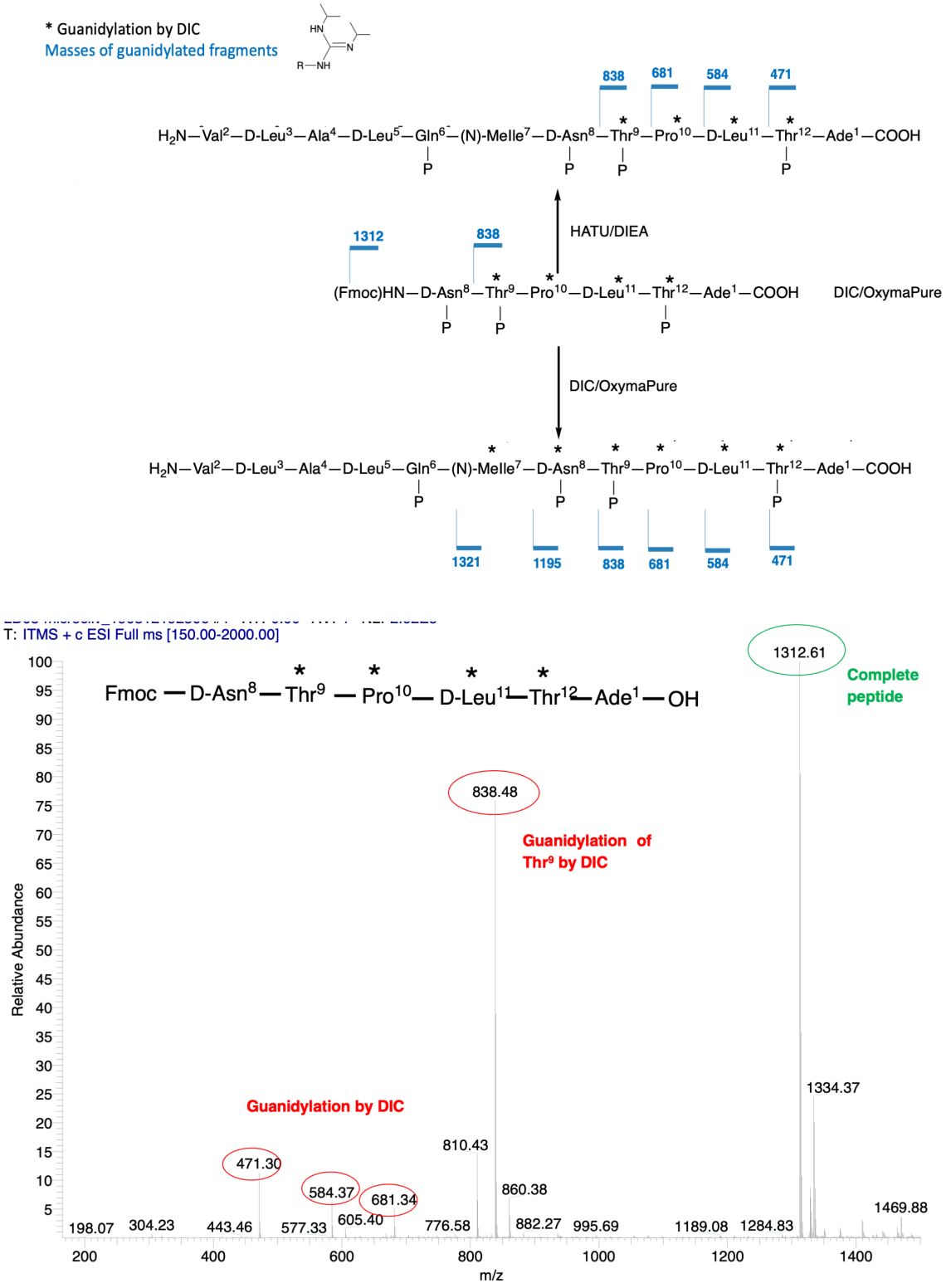

Figure 47. MS spectrum of the crude peptide from Ade[1] to D-Asn[8]. Observation of guanidylated fragments when using DIC/Oxyma as coupling reagents. DIC/Oxyma was used from Ade[1] to D-Asn[8], then the resin was split in two to continue synthesis with either HATU/DIEA or DIC/Oxyma from N-MeIle[7] to Val[2]. The asterisk indicates a partial guanidylation site that prevents further extension of the peptide sequence.

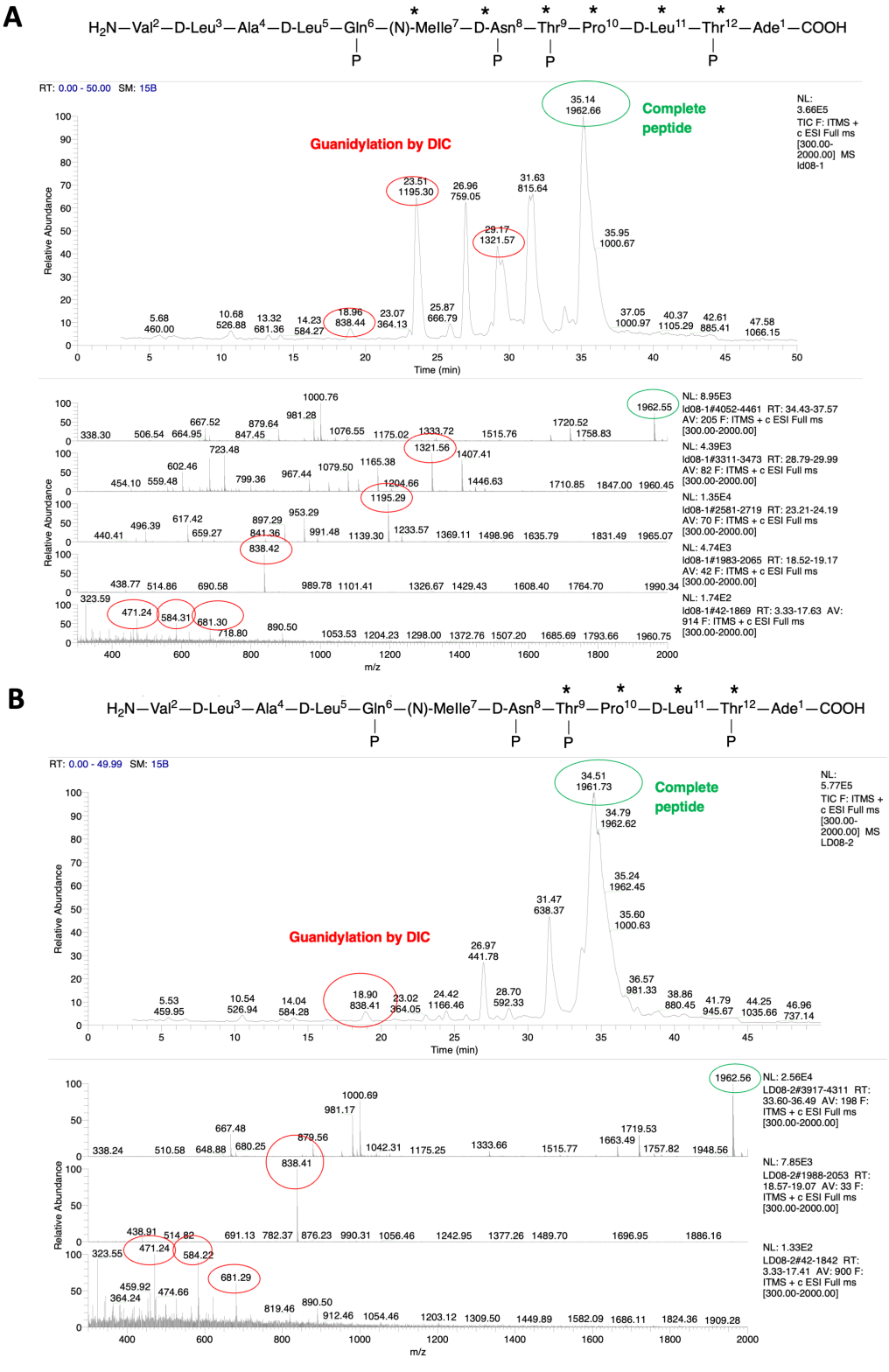

Figure 48. A) LC-MS chromatogram of the complete crude peptide synthesized with DIC/Oxyma only. Observation of guanidylated fragments from Ade[1] to NMeIle[7]. B) LC-MS chromatogram of the complete crude peptide synthesized with DIC/Oxyma from Ade[1] to D-Asn[8] then HATU/DIEA from NMeIle[7] to Val[2]. Observation of guanidylated fragments only from Ade[1] to D-Asn[8].
The asterisk indicates a partial guanidylation site that prevents further extension of the peptide sequence.

We used PyOxim/DIEA coupling reagents for the next synthesis assay, a phosphonium salt which avoids guanidinium formation but one that is less stable than HATU (Figure 49) [165].

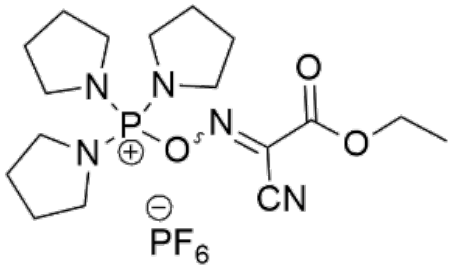

Figure 49. Structure of PyOxim

The most difficult coupling site was located between Gln^{6} and N-MeIle^{7} residues and was best resolved with HATU as observed in the LaxB synthesis. We decided to use PyOxim for couplings between Thr^{12} and Asn^{8} while keeping HATU for the second part containing couplings between N-MeIle^{7} and Val^{2} considering HATU as the most suitable coupling reagent to couple on N-methylated residues [166]. After analyzing the first part of the peptide, no undesired fragments were detected thus validating the potential of PyOxim for this type of sequence. The rest of the synthesis proceeded without difficulties and the peptide was then cleaved from the resin with 20% TFE in DCM allowing us to keep side-chain protections (Figure 50).

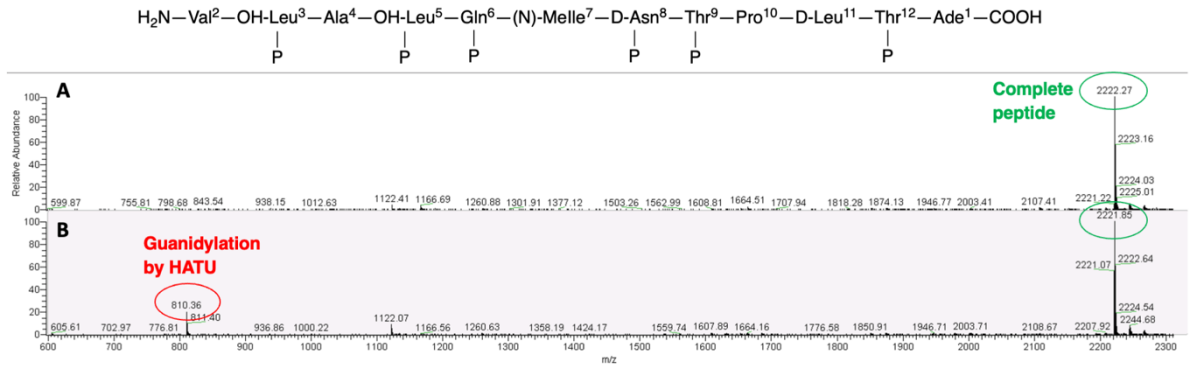

Figure 50. A) MS spectrum of the complete crude peptide (trichormamide C) synthesized with PyOxim/DIEA from Ade^{1} to D-Asn^{8} then HATU/DIEA from NMeIle^{7} to Val^{2}. B) MS spectrum of the complete crude peptide (trichormamide C) synthesized with HATU/DIEA only.

The different tests performed to determine the right cocktail of coupling agents are summarized in the table below (Table 5).

Table 5. Assays performed on the simplified trichormamide sequence without hydroxy groups (assays A-D) and trichormamide C (assay E), with different coupling reagents and times.

Assays	Amino acids	Coupling reagents	Synthesis scale	Coupling steps	Yield of the linear peptide	Observations
A	0.2 M (5eq)	HATU 0.5 M (5eq) + DIEA 2M (10 eq)	0.1 mmol	Gln and NMeIle: Double 20 min + capping Other amino acids: Single 20 min	12%	Lower coupling for Gln Guanidylation of Thr^{9}
B	0.2 M (5eq)	HATU 0.5 M (5eq) + DIEA 2M (10 eq)	0.1 mmol	Gln: Triple 20 min + capping NMeIle: Double 20 min + capping Other amino acids: Single 20 min	19%	Lower coupling for Gln and Asn Guanidylation of Thr^{9}
C	0.2 M (5eq)	HATU 0.45 M (4.5eq) + DIEA 2M (10 eq)	0.1 mmol	Gln: Triple 20 min + capping NMeIle and Asn: Double 20 min + capping Other amino acids: Single 20 min	22%	Lower coupling for Gln Lower coupling for Asn compared to LD06 Guanidylation of Thr^{9}
D	0.2 M (5eq)	From Ade^{1} to Asn^{8}: DIC 0.5 M (5eq) + Oxyma 2 M (10eq) From $NMeIle^{7}$ to Val^{2}: DIC 0.5 M (5eq) + Oxyma 2 M (10eq) OR HATU 0.5 M (5eq) + DIEA 2M (10 eq)	0.1 mmol	Gln: Triple 20 min + capping NMeIle and Asn: Double 20 min + capping Other amino acids: Single 20 min	22% for DIC/Oxyma only 45% for DIC/Oxyma + HATU/DIEA	More guanidylation with DIC/Oxyma only Guanidylation observed from Ade^{1} to $NMeIle^{7}$ for DIC/Oxyma only and from Ade^{1} to Thr^{9} for DIC/Oxyma + HATU/DIEA
E **(on trichormamide C)**	0.2 M (5eq)	From Ade^{1} to Asn^{8}: PyOxim (4.9eq) + DIEA (10eq) From $NMeIle^{7}$ to Val^{2}: HATU (4.9eq) + DIEA (10 eq)	0.1 mmol	Gln: Triple 20 min + capping NMeIle and Asn: Double 20 min + capping Other amino acids: Single 20 min	The linear peptide was not purified. 40% of crude peptide.	No guanidylation observed.

The use of PyOxim/DIEA throughout the whole sequence is also possible despite a slight decrease in glutamine coupling. In all cases, a more or less important by-product of synthesis is observed that corresponds to the peptide without glutamine, due to the weak coupling of glutamine on N-methylisoleucine (Figure 51).

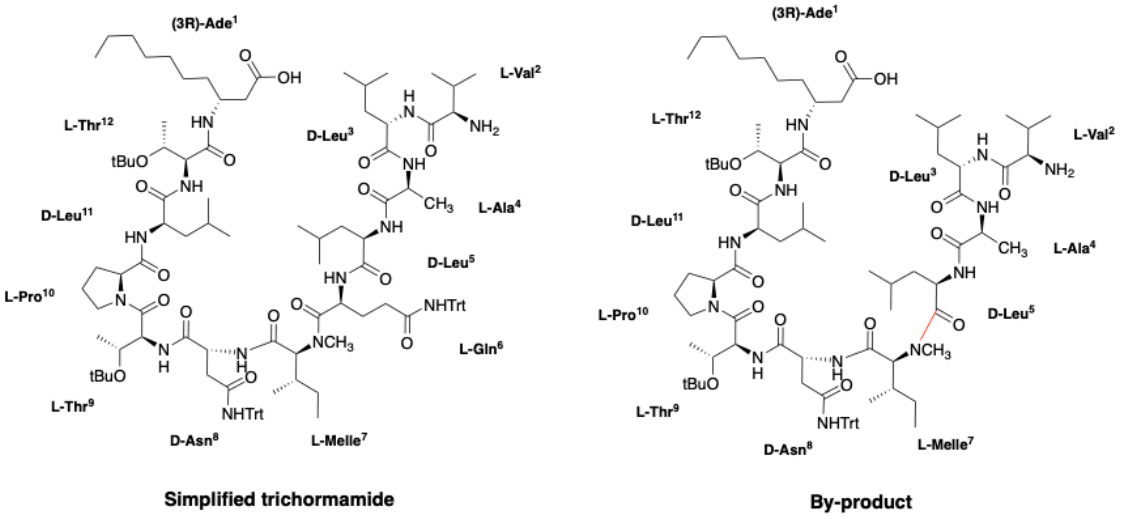

Figure 51. Structure of the by-product obtained during the synthesis of simplified trichormamide (difficult coupling of Gln^6).

The linear peptide obtained with its side chain protections must then be purified before being cyclized (Table 6). Initial purification tests were carried out on C18 Flash chromatography columns (purchased from Agela Technologies). The peptide dragging too much on a C18 column, the purification was not appropriate. We therefore turned to normal phase silica columns. The fragment resulting from the major guanidylation of Thr^9 can thus remain on the column since it is a charged guanidinium, while the desired peptide is recovered from the column after application of a 10% methanol rate. This technique allows easy separation of the peptide from the guanidylation fragments but not from the glutamine-free by-product due to their very close structures. In addition, the use of 10% methanol damages the stationary phase of the column. Ethyl acetate was considered as an alternative to methanol, without success since the peptide was again dragging strongly along the stationary phase. The use of a single commercial silica column for a single purification was not feasible for cost reasons. We could also purify the peptide manually on a silica column in the laboratory. However, due to the difficulty of separating the peptide from its glutamine-free by-product, we decided not to perform any further intermediate purification of the linear peptide and thus cyclized the peptide directly starting from the crude product.

Table 6. Assays performed to purify the protected linear peptide (simplified sequence of trichormamide).

Assays	System used	Elution	Observations
A'	Flash chromatography C18 column	From 50% to 95% of ACN in water (0.1% formic acid)	The peptide remains on the column.
B'	Flash chromatography C18 column	From 90% to 99% of MeOH in water (0.1% formic acid) AND 100% isopropanol	The peptide starts to come out of the column but drags a lot.
C'	Flash chromatography Normal phase silica column	From 5% to 20% of MeOH in DCM	The peptide is released at 10% in methanol. The guanidylation fragment is retained by silica but silica is then degraded.
D'	Flash chromatography Normal phase silica column	From 2% to 10% of MeOH in DCM	The peptide is released at 10% in methanol. The guanidylation fragment is retained by silica but silica is then degraded.
E'	Flash chromatography Normal phase silica column	100% Ethyl acetate	The peptide is dragging on the column.
F'	Manual chromatography with normal phase silica	From 0 to 10% of MeOH in DCM	The peptide is recovered at 10% MeOH. The purification cannot be followed by TLC. → Purification is equal to a simple filtration on silica to remove the guanidylation fragment.

B. Cyclization

In the synthesis of laxaphycin B, cyclization was done directly on solid support, allowed by anchoring the β–hydroxy-aspartic acid side chain on the resin and by an orthogonal protection system. This cyclization technique was no longer feasible in the case of anchoring Ade on the resin. The choice was therefore made to use solution cyclization. In order to limit the intermolecular reactions, the cyclization in solution must be done under high dilution. These reactions can be very slow and generate many by-products. The chosen cyclization technique was that of Malesevic *et al*., already used for the synthesis of trichormamide A by Michel Gaillard [62,161]. The reaction is performed in a tricol flask previously purged with nitrogen and containing a coupling agent (3eq) solubilized in DMF. The linear peptide (1eq, 10^{-3}M) and the complementary coupling agent (3eq) are added drop by drop in parallel in two separate syringes, under inert atmosphere. The addition should be done very slowly, at a rate of 0.01 mL/min. At the end of the addition, the reaction continues for 48h. The PyOxim/OxymaPure

coupling agents were first tested since they had been retained for the synthesis of trichormamide A. However, the cyclization yield was found to be very low or even null (Figure 52, A and C). We therefore turned to the use of EDC/OxymaPure, which after 24h allowed most of the cyclic peptide to be obtained (Figure 52, B and D).

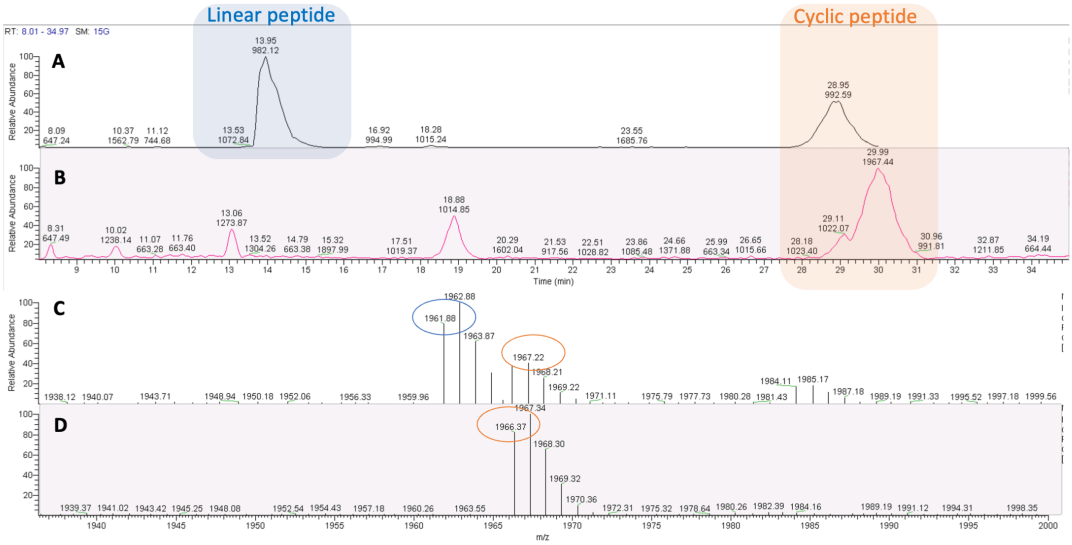

Figure 52. A) LC-MS chromatogram of the cyclization solution after 24h with PyOxim/Oxyma (3eq, into syringe) and PyOxim/DIEA (0.1eq/6eq, into flask). Observation of the linear peptide (13.95min) and the cyclic peptide (28.95min). B) LC-MS chromatogram of the cyclization solution after 24h with EDC (3eq, into syringe) and Oxyma (3eq, into flask). Observation of the cyclic peptide only (29.99min). C) MS spectrum of the direct infusion related to solution A. D) MS spectrum of the direct infusion related to solution B.

At the beginning of the optimization of this synthesis, we used the DCM/TFE/AcOH 8/1/1 mixture to cleave the linear peptide from the resin. However, during the LC/MS analysis of the cyclization reaction crude, we noticed a by-product corresponding to the linear peptide capped by acetic acid. Indeed, the acetic acid used in the resin cleavage cocktail was coupled to the peptide by the addition of EDC during the cyclization step. To overcome this yield loss, acetic acid was removed from the cleavage cocktail for subsequent syntheses (using DCM/TFE 8/2 instead) and the recovered crude linear peptides were lyophilized to remove any traces of TFE.

C. Obtaining final peptide

The cyclic peptide was recovered after DMF evaporation and work-up treatments to remove potential remaining linear peptide. Side-chain protections were removed under acidic conditions for 2 hours (TFA/TIS/H_2O 9.5/0.25/0.25) followed by precipitation of the peptide in diethyl ether in which the protective group residues of the side chains are soluble. The peptide is recovered by centrifugation and purified by semi preparative HPLC (GraceVydac C18 250x10mm column) giving the final pure peptide. The peptide is analyzed by LC/MS, its exact mass is determined and its structure is verified by NMR.

III. Application of the optimized synthesis to compound 4 and two synthesized analogues 5 and 6

The optimization of this synthesis allowed to obtain trichormamide C (**4**), an analogue of laxaphycin B (**2**) (Figure 53). It is interesting to note that **4'** synthesized only with HATU as in the case of laxaphycin B gives a final yield of 2%, while the use of PyOxim to synthesize **4** increases the yield to 7%.

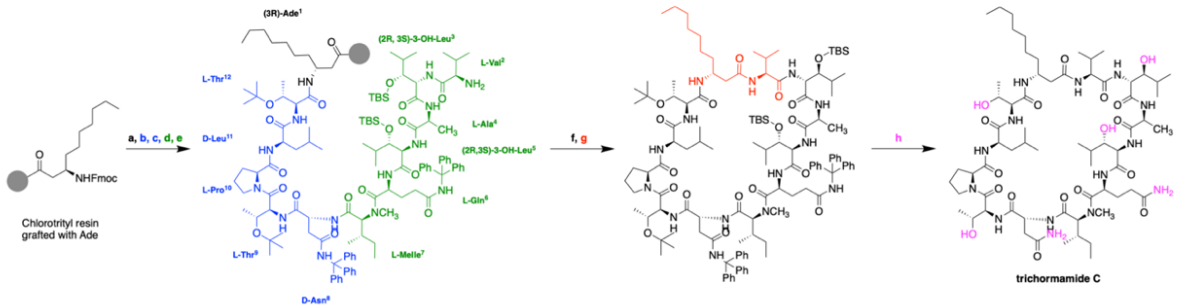

Reagents and conditions: (a) 20% v/v piperidine in DMF, 3 min. (b) (i) Fmoc-Thr(tBu)-OH (5 equiv), PyOxim (4.9 equiv), DIEA (10 equiv), DMF, 20 min. (ii) 20% v/v piperidine in DMF, 3 min. (c) Repeat conditions (b) for other amino acids until Fmoc-Asn(Trt)-OH that is inserted by double coupling for 20 min followed by capping with 0.5 M acetic anhydride (1 equiv), DIEA (0.21 equiv) and HOBt (0.019 equiv) in DMF, 3 min. (d) (i) Fmoc-L-NMeIle-OH (5 equiv), HATU (4.9 equiv), DIEA (10 equiv), DMF, 20 min. (ii) 20% v/v piperidine in DMF, 3 min. (e) Repeat conditions (d) for other amino acids until Fmoc-Val-OH except for Fmoc-L-NMeIle-OH and Fmoc-Gln(Trt)-OH that are added by double and triple coupling for 20 min respectively followed by the same previous capping. (f) DCM/TFE 8:2 (v/v), rt; 2 h. (g) EDC (3 equiv), OxymaPure (3 equiv) in DMF, nitrogen atmosphere, rt, overnight. (h) TFA/TIS/H_2O 95:2.5:2.5, v/v/v, 2 h.

Figure 53. Final synthesis of trichormamide C.

The purified trichormamide C was analyzed by ESI-HRMS resulting in a *m/z* 1401.83530 with a mass error of 1.80 ppm with the theoretical mass (calculated $[M+Na]^+$ *m/z* 1401.83277). Two other analogs were also synthesized, allowing us to test the flexibility of the protocol. The first analog contains D-Leu instead of the two (2R,3S)-3-OH-Leu (compound **5**) in order to modify the hydrophobicity while keeping the stereochemistry. The second one has D-Thr instead of the two (2R,3S)-3-OH-Leu (compound **6**) to modify the side chain while keeping the same stereochemistry and the hydroxy group (Figure 54). Both peptides were analyzed in ESI-HRMS to give *m/z* 1369.8413 for the first one and *m/z* 1345.7698 for the second (calculated $[M+Na]^+$ *m/z* 1369.84294 and *m/z* 1345.77017, respectively) remaining within the accepted mass error range (1.22 ppm and 0.29 ppm, respectively). NMR spectra were obtained thanks to a 500 MHz spectrometer. 1D ^1H, DEPTQ and 2D-homonuclear COSY, TOCSY, ROESY as well as 2D-heteronuclear ^{13}C-HSQC, ^{13}C-HMBC NMR spectra were recorded in DMSO-d_6, allowing for synthesized trichormamide C to be compared with the data reported by Luo and his co-workers on the natural trichormamide C [61].

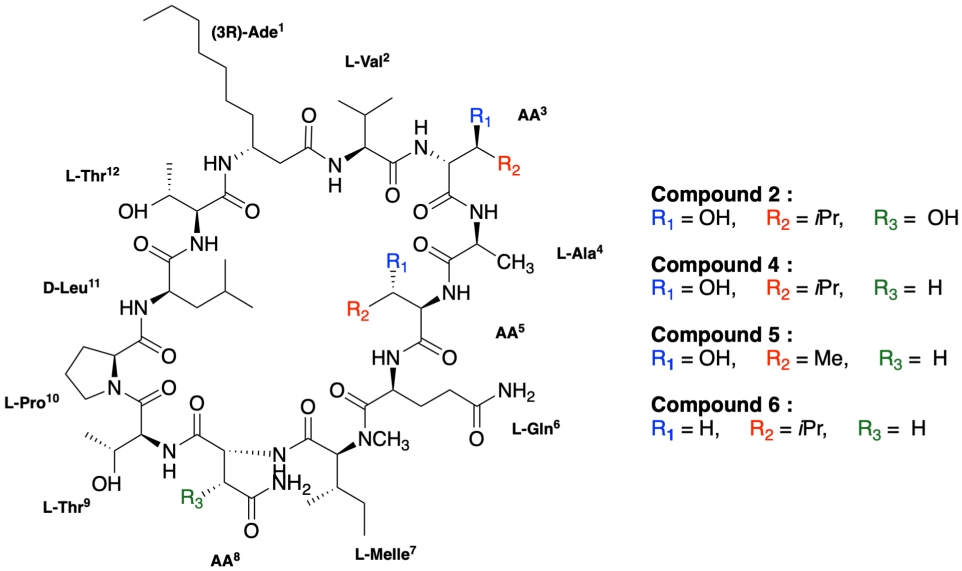

Figure 54. Structure of 2 and its analogues 4, 5 and 6.

As expected, trichormamide C gave comparable spectra, independently of the strategy implemented for its synthesis, i.e., using PyOxim and HATU (compound **4**) or only HATU (compound **4'**) (Figure 55). The spectra of the synthetic compound are identical to those of the natural compound (Table 7). Indeed, α-protons, methylene protons and methyl protons showed the same chemical shifts (Figure 56). Despite a little shift of the resonance that can be attributed to different experimental conditions, we noticed a better resolution of the amide region and the ten doublets, including the Gln^6 and (2R,3S)-3-OH-Leu^5 which are easily distinguished from one another. A perfect match of the data extracted from the publication of Luo was also observed for the DEPTQ spectrum (Figure 57). We were able to assign all non-quaternary carbons except for five peaks at 18.4, 18.6, 18.7, 18.9 and 19.4 ppm. These carbons correspond to methyl groups of Val^2, (2R,3S)-3-OH-Leu^3 and (2R,3S)-3-OH-Leu^5 and give superimposed correlations in all 2D-spectra. Low background noise for COSY, TOCSY and ROESY analyses facilitated interpretation.

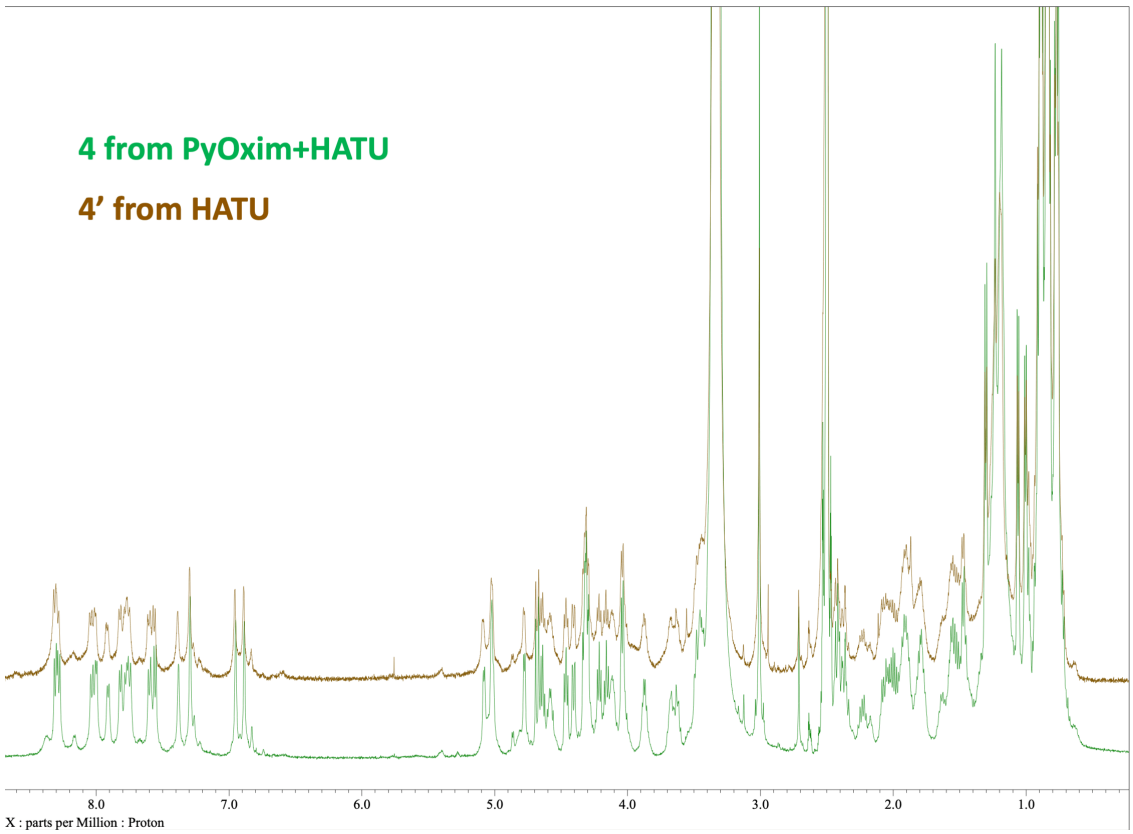

Figure 55. Comparison of ^{1}H spectra of trichormamide C synthesized with PyOxim+HATU (4 in green) or with HATU only (4' in brown).

Table 7. NMR spectroscopic data of 4 in DMSO-d_6 and chemical shift comparison between the synthetic compound and the natural one [61].

entry	position	C, mult., **ΔδC**	H, mult. (J in Hz), **ΔδH**	entry	position	C, mult., **ΔδC**	H, mult. (J in Hz
β-Ade[1]	1	171.5, C, **0**	-		5	174.5, C, **0**	-
	2	40.3, CH_2, **0.4**	2.37, **0.11**		NH	-	7.77, d (7.5), **0.0**
			2.42, **0.09**		NH_2	-	7.38 & 6.95, **0.0**
	3	45.7, CH, **0**	4.11, **0**	**N-MeIle[7]**	1	169.8, C, **0**	-
	4	33.5, CH_2, **0.01**	1.28, **0.07**		2	59.6, CH, **0.03**	4.68, d (10.3), **0**
			1.35, **0.02**		3	32.0, CH, **0**	1.91, **0.02**
	5	25.3, CH_2, **0.02**	1.22, **0.01**		3-Me	15.2, CH_3, **0**	0.77, **0.02**
	6	28.8, CH_2, **0**	1.19, **0.01**		4	23.9, CH_2, **0**	1.27, **0**
	7	28.6, CH_2, **0**	1.19, **0.02**		5	10.5, CH_3, **0.2**	0.77, **0.01**
	8	31.3, CH_2, **0.02**	1.19, **0.02**		N-Me	30.2, CH_3, **0**	3.01, **0.01**
	9	22.1, CH_2, **0**	1.24, **0.07**	**D-Asn[8]**	1	170.6, C, **0.1**	-
	10	14.0, CH_3, **0.1**	0.84, **0.03**		2	49.5, CH, **0**	4.65, **0.01**
	NH	-	7.60, d (8.6), **0**		3	35.9, CH_2, **0.11**	2.41, **0.01**
Val[2]	1	171.5, C, **0**	-				2.52, **0.01**
	2	58.7, CH, **0.09**	4.15, **0.01**		4	171.6, C, **0**	-
	3	29.7, CH, **0,08**	1.99, **0**		NH	-	8.31, d (7.5), **0.0**
	3-Me	19.0, CH_3, **0**	0.85, **0.02**		NH_2	-	7.29 & 6.88, **0.0**
	4	nd	0.88, **0.05**	**Thr[9]**	1	168.5, C, **0**	-
	NH	-	8.28, d (8.0), **0.03**		2	55.5, CH, **0.1**	4.47, t (8.0), **0.0**
3-OH-Leu[3]	1	171.5, C, **0**	-		3	66.7, CH, **0**	3.87, **0.01**
	2	55.2, CH, **0.02**	4.40, d (8.6), **0.01**		4	19.0, CH_3, **0.14**	1.06, d (6.3), **0.0**
	3	76.8, CH, **0**	3.48, **0.01**		3-OH	-	5.02, **0.02**
	4	30.8, CH, **0**	1.55, **0**		NH	-	7.56, d (8.0), **0**
	4-Me	nd	0.77, **0.02**	**Pro[10]**	1	171.5, C, **0**	-
	5	nd	0.90, **0.03**		2	59.6, CH, **0**	4.32, **0.02**
	3-OH	-	5.02, **0.02**		3	29.2, CH_2, **0**	1.78, **0**
	NH	-	8.03, d (9.2), **0.01**				2.03, **0.01**
Ala[4]	1	172.5, C, **0**	-		4	24.3, CH_2, **0**	1.89, **0.01**
	2	49.4, CH, **0.02**	4.21, t (6.8), **0.01**				1.89, **0.02**
	3	17.8, CH_3, **0.03**	1.30, d (7.1), **0**		5	47.2, CH_2, **0**	3.63, **0.02**
	NH	-	8.00, d (5.7), **0**				3.66, **0**
3-OH-Leu[5]	1	170.8, C, **0**	-	**D-Leu[11]**	1	172.0, C, **0**	-
	2	55.5, CH, **0**	4.30, **0.01**		2	51.6, CH, **0**	4.32, **0**
	3	76.0, CH, **0**	3.44, **0.01**		3	40.9, CH_2, **0.02**	1.47, **0**
	4	30.0, CH, **0.05**	1.55, **0**		4	24.2, CH, **0**	1.56, **0.05**
	4-Me	nd	0.77, **0.01**		4-Me	22.1, CH_3, **0**	0.83, **0.02**
	5	nd	0.90, **0.01**		5	22.7, CH_3, **0**	0.89, **0.01**
	3-OH	-	5.08, **0.03**		NH	-	7.91, d (7.5), **0**
	NH	-	7.75, d (8.6), **0.01**	**Thr[12]**	1	168.7, C, **0**	-
Gln[6]	1	172.4, C, **0**	-		2	58.3, CH, **0.28**	4.04, d (6.3), **0.0**
	2	49.0, CH, **0.13**	4.58, **0.01**		3	66.1, CH, **0**	4.04, d (6.3), **0.0**
	3	26.4, CH_2, **0**	1.63, **0.01**		4	19.8, CH_3, **0**	1.00, d (6.3), **0.0**
			1.91, **0.02**		3-OH	-	4.77, **0.03**
	4	30.5, CH_2, **0**	2.07, **0.03**		NH	-	7.82, d (8.0), **0.0**
			2.23, **0.01**				

nd = not determined. The numbering of atoms corresponds to the one used by Luo and his co-workers. ΔδC and ΔδH represent the difference between the chemical shift recorded by Luo *et al.* and the present study, for ^{13}C and ^{1}H NMR, respectively.

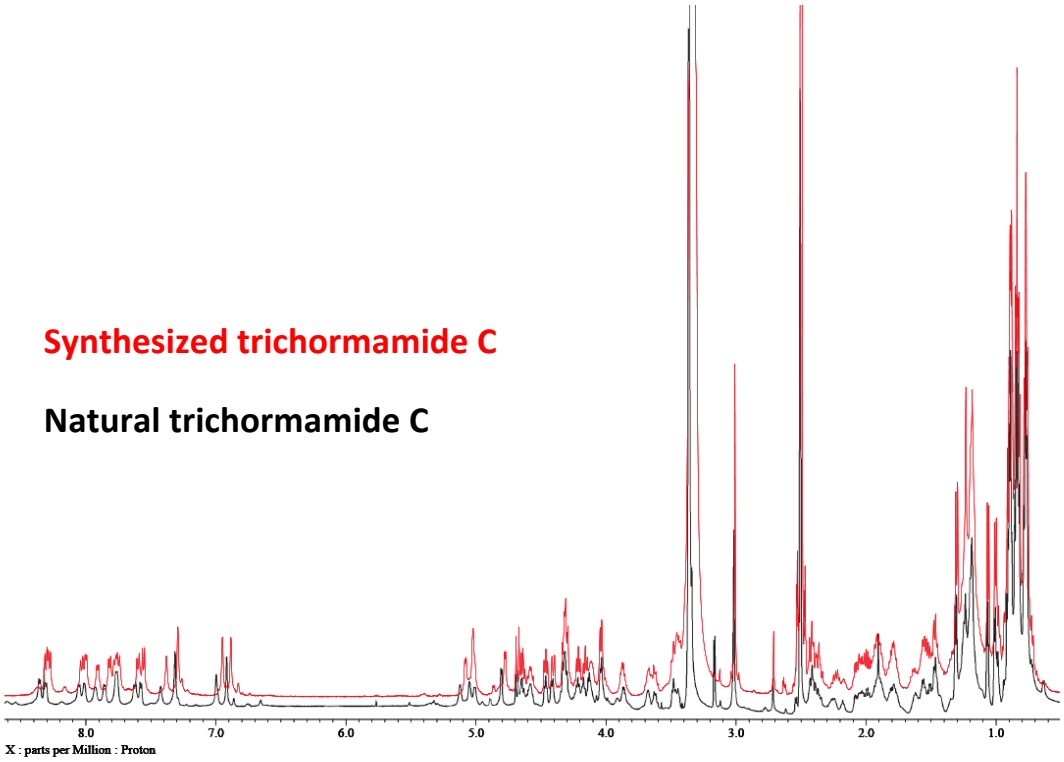

Figure 56. Comparison of ^{1}H spectra of natural (in black) and synthesized (in red) trichormamide C

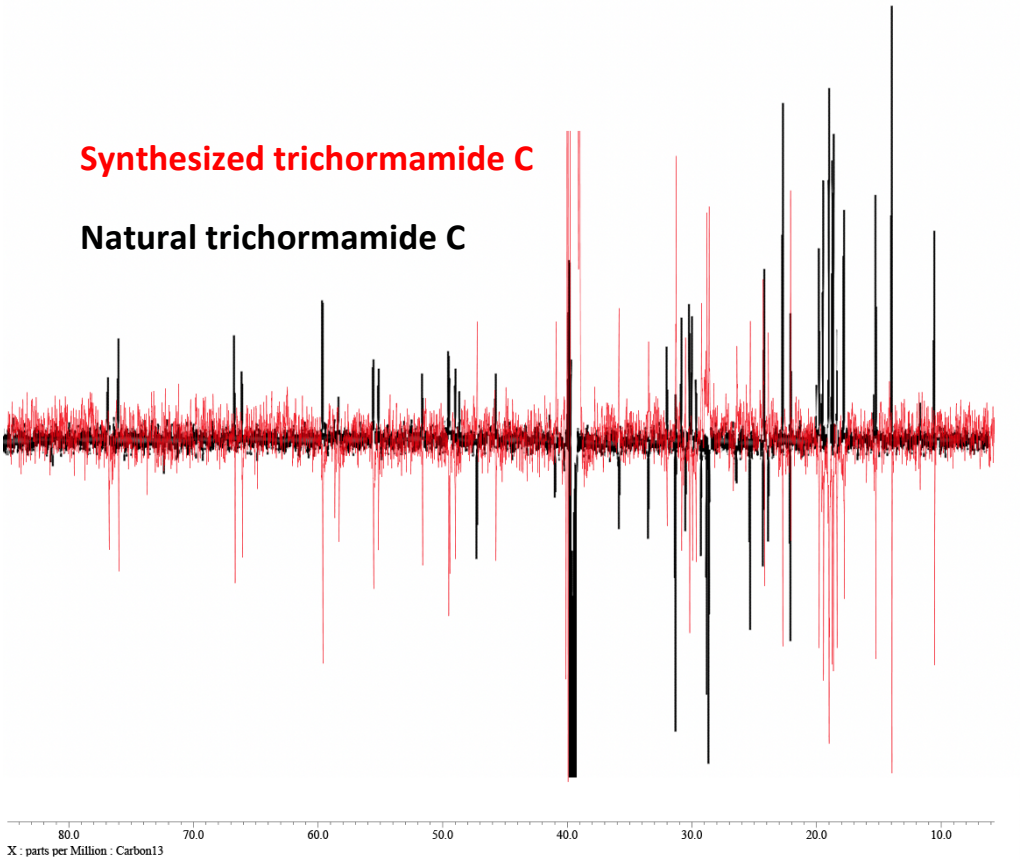

Figure 57. Comparison of DEPTQ spectra of natural (in black) and synthesized (in red) trichormamide C

Table 8. NMR spectroscopic data of 5 in DMSO-d_6

entry	position	δH, mult. (J in Hz)	entry	position	δH, mult. (J in Hz)
β-Ade[1]	1	-	**NMeIle[7]**	1	-
	2	2.35		2	4.66
		2.35		3	1.91
	3	4.06		3-Me	0.77
	4	1.45		4	1.26
		1.45		5	0.85
	5	1.34		N-Me	2.99
	6	1.18	**D-Asn[8]**	1	-
	7	1.18		2	4.63
	8	1.18		3	2.43
	9	1.18			2.53
	10	0.84		4	-
	NH	7.61, d (8.8)		NH	8.23, d (8.0)
Val[2]	1	-		NH_2	7.28 & 6.84
	2	4.06	**Thr[9]**	1	-
	3	1.95		2	4.46
	4	0.84		3	3.89
	4'	0.84		4	1.06, d (6.1)
	NH	8.12, d (5.7)		3-OH	5.04
D-Leu[a]	1	-		NH	7.58, d (8.0)
	2	4.24	**Pro[10]**	1	-
	3	1.46		2	4.30
	4	1.52		3	1.79
	5	0.88			2.03
	5'	0.82		4	1.89
	NH	7.94, d (6.9)			1.89
Ala[4]	1	-		5	3.62
	2	4.16			3.62
	3	1.22	**D-Leu[11]**	1	-
	NH	8.20, d (6.5)		2	4.31
D-Leu[b]	1	-		3	1.46
	2	4.30		4	1.52
	3	1.46		5	0.88
	4	1.52		5'	0.82
	5	0.88		NH	8.25
	5'	0.82	**Thr[12]**	1	-
	NH	7.95, d (6.9)		2	4.04
Gln[6]	1	-		3	4.04
	2	4.60		4	0.99, d (6.5)
	3	1.72		OH	4.76
		1.88		NH	7.77, d (7.6)
	4	2.11			
	5	-			
	NH	7.93, d (8.4)			

a and b are two D-Leu that could not be differentiated within the peptide sequence. We were unable to obtain carbon spectra due to a lack of compound.

Table 9. NMR spectroscopic data of 6 in DMSO-d_6

entry	position	**δ**C, mult	**δ**H, mult. (J in Hz)	entry	position	**δ**C, mult	**δ**H, mult. (J in Hz)
β-Ade[1]	1	*nd*, C	-	NMeIle[7]	1	169.5, C	-
	2	*nd*, CH_2	2.42		2	59.2, CH	4.67
			2.37		3	31.6, CH	1.90
	3	45.6, CH	4.08		3-Me	15.1, CH_3	0.78
	4	33.2, CH_2	1.30		4	*nd*, CH_2	1.27
			1.36		5	10.3, CH_3	0.77
	5	25.1, CH_2	1.19		N-Me	30.0, CH_3	2.98
	6	28.6, CH_2	1.19	D-Asn[8]	1	170.3, C	-
	7	28.4, CH_2	1.19		2	49.2, CH	4.62
	8	31.0, CH_2	1.19		3	35.6, CH_2	2.43
	9	21.8, CH_2	1.23				2.53
	10	13.7, CH_3	0.85		4	171.5, C	-
	NH	-	7.59, d (10.7)		NH	-	8.24, d (7.3)
Val[2]	1	*nd*, C	-		NH_2	-	*nd*
	2	58.7, CH	4.21				6.90
	3	29.7, CH	1.98	L-Thr[9]	1	*nd*, C	-
	4	18.9, CH_3	0.86		2	55.3, CH	4.47
	4'	18.2, CH_3	0.87		3	66.4, CH	3.88
	NH	-	8.18, d (8.0)		4	18.7, CH_3	1.05
Thr[a]	1	*nd*, C	-		3-OH	-	5.02
	2	58.5, CH	4.07		NH	-	7.56, d (8.4)
	3	66.4, CH	3.91	Pro[10]	1	*nd*, C	-
	4	19.3, CH	1.01		2	59.4, CH	4.31
	3-OH	-	4.79		3	29.0, CH_2	1.78
	NH	-	7.80, d (8.8)				2.04
Ala[4]	1	*nd*, C	-		4	24.0, CH_2	1.89
	2	48.7, CH	4.32				1.89
	3	17.8, CH_3	1.27		5	47.0, CH_2	3.66
	NH	-	8.01				3.66
Thr[b]	1	*nd*, C	-	D-Leu[11]	1	*nd*, C	-
	2	58.1, CH	4.04		2	51.4, CH	4.30
	3	66.4, CH	3.91		3	40.5, CH_2	1.47
	4	20.0, CH_3	1.00		4	23.8, CH	1.52
	3-OH	-	4.79		5	21.8, CH_3	0.82
	NH	-	7.82, d (8.0)		5'	22.5, CH_3	0.88
Gln[6]	1	*nd*, C	-		NH	-	7.91, d (6.9)
	2	48.5, CH	4.61	Thr[c]	1	*nd*, C	-
	3	26.2, CH_2	1.66		2	58.1, CH	4.23
			1.92		3	65.8, CH	4.04
	4	30.3, CH_2	2.08		4	19.6, CH_3	1.04
			2.17		OH	-	4.76
	5	174.0, C	-		NH	-	8.02
	NH	-	7.87, d (7.6)				
	NH_2	-	*nd*				

nd = not determined; a, b and c are two D-Thr and one L-Thr that could not be differentiated within the peptide sequence.

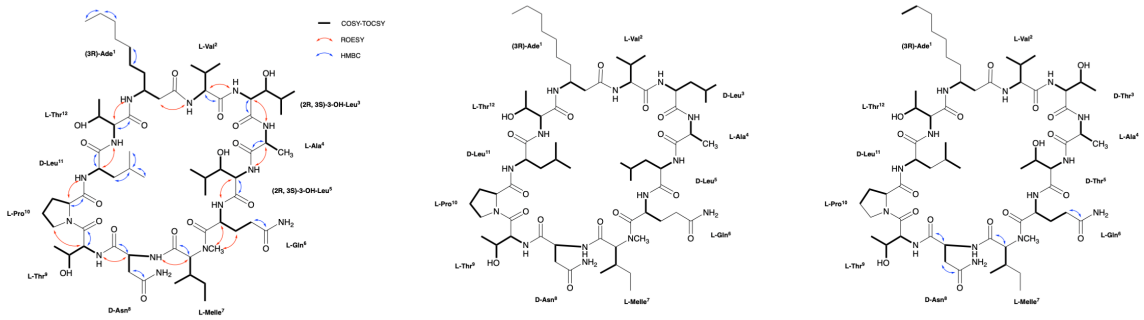

4 **5** **6**

Figure 58. NMR analyses of 4, 5 and 6 structures.

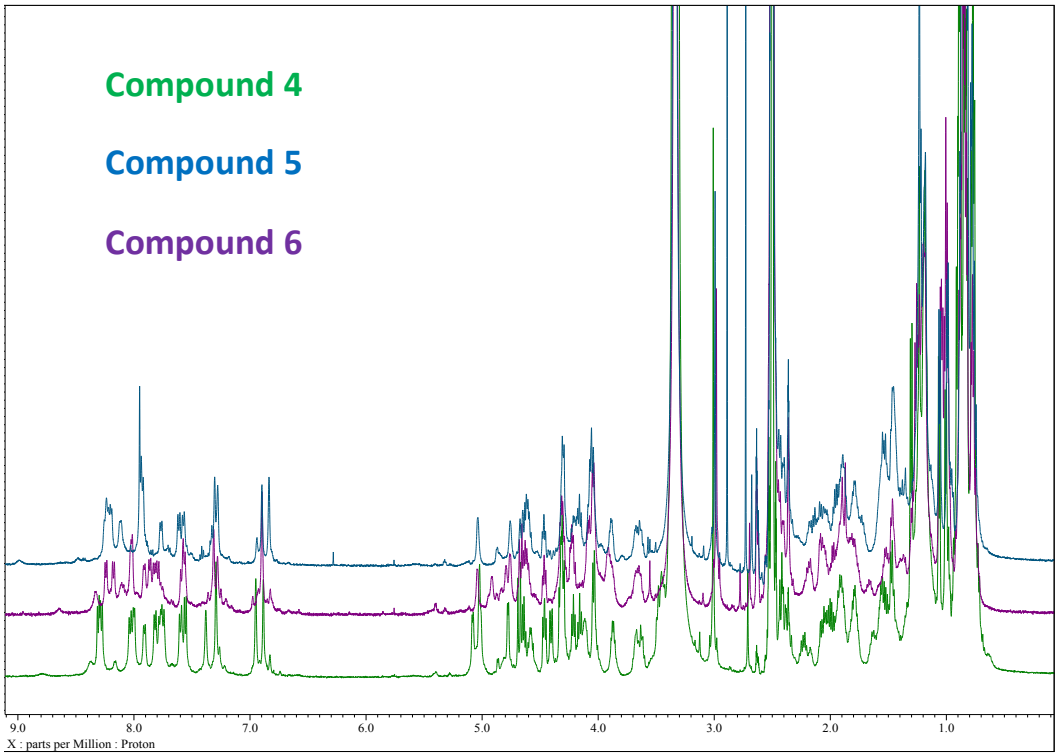

Figure 59. Comparison of ^{1}H NMR spectra of trichormamide C (4 in green), 5 (in blue) and 6 (in purple).

In summary, we reported the total synthesis of the trichormamide C which was demonstrated to be identical to the natural compound by means of NMR and LC/MS. Starting the synthesis by anchoring Ade^{1} instead of the (2R,3R)-3-OH-Asn^{8} or Gln^{6} side chain, as was done for the synthesis of laxaphycin B, was a good alternative and allowed Ade to be conserved while avoiding epimerization. Two other trichormamide C analogs that replaced (2R,3S)-3-OH-Leu with D-Leu (Table 8) and D-Thr (Table 9) were also obtained in this way (Figure 58, Figure 59). Furthermore, the use of PyOxim was advantageous to discard guanidinium formation observed at the aggregation prone sequence ranging from Ade to D-Asn. Additional comparative structure-activity relationship studies within the LaxB family type of peptide could be conducted on trichormamide C and its analogs to further explore biodegradation conditions for those peptides.

IV. Experimental part I

A. Loading of the 2-chlorotrityl chloride resin by (3R)-Fmoc-β-aminodecanoic acid (Ade)

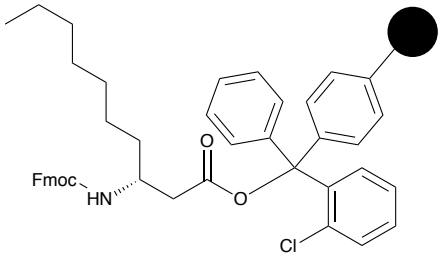

Figure 60. (3R)-Fmoc-β-aminodecanoic acid (Ade) grafted on 2-chlorotrityl chloride resin

(3R)-Fmoc-β-aminodecanoic acid (Ade) was previously synthesized at the laboratory [47]. The amino acid (264 mg, 0.64 mmol, 1.2 equiv relative to the resin) was dissolved in DCM and THF, activated by DIEA (444 μL, 4 equiv relative to the amino acid) and added into a three-neck round-bottom flask previously purged under nitrogen atmosphere. Then the resin (365 mg, 1 equiv) was added to the mixture. The mix was shaken slowly for 4 h under nitrogen atmosphere and then was filtered under *vacuum*. A solution of DCM/MeOH/DIEA 17:2:1 (v/v/v) was put on the resin to cap it. The resin was washed with this mixture three times during 10 min. The filtrate was concentrated *in vacuo* to recover the amino acid that was not loaded on the resin. Then the resin was washed three times with DCM, two times with DMF and two times with DCM again. The resin was dried under vacuum. This filtrate was not recovered. The loading rate of the resin was checked by absorbance measurement when cleaving the Fmoc protecting group of the amino acid. Approximately 5 μmole (with respect to Fmoc amino acid) of the resin were weighed into needles [163]. A solution of 2 mL of 2% DBU in DMF were added on the resin and the mixture was shaken during 60 min. The same process was done in two other needles. A reference solution without the resin was prepared the same way. After shaking, solutions were diluted to 10 mL with ACN. 2 mL of this solution were diluted into a 25-mL graduated flask. The absorbance of these solutions was evaluated with a spectrophotometer (Jasco V-630, Hellma quartz cells) at 304 nm at a rate of three measures per samples. An average of these measurements was made. The loading of the resin was calculated with the following equation: (Abs x 16,4) / mg of resin (mmole/g). The average loading of the resin was 0.8 mmol/g. All the resin was mixed with a solution of 20% piperidine in DMF at a rate of 10 mL per gram of resin. The mixture was shaken 20 min and then filtered. The process was repeated one time then the resin was washed with DMF and DCM. The resin was stored at 4°C.

B. Solid phase synthesis of trichormamide C

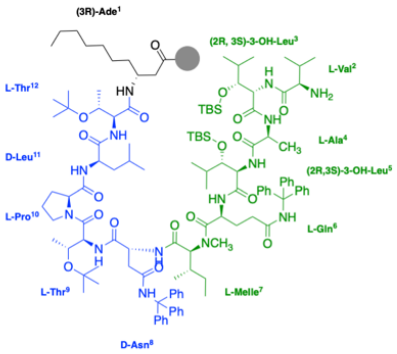

Figure 61. Structure of the protected linear trichormamide C

The linear peptide was synthesized with an automated microwave peptide synthesizer (CEM Liberty One). Proteinogenic amino acids and 2-chlorotrityl chloride resin were purchased from Iris Biotech. Fmoc-D-Asn(Trt)-OH, Fmoc-L-MeIle-OH and HATU were acquired from ABCR while PyOxim was purchased from Novabiochem. HOBt, DIEA, TFE and AcOH were obtained from Sigma-Aldrich while DCM, cyclohexane, MeOH and ACN were obtained from VWR Chemicals. DMF was from Carlo Erba, piperidine from Acros Organics and anhydride acetic from Prolabo. Fmoc-3-O(TBDMS)-Leu-OH was previously synthesized at the laboratory [47]. The synthesis was performed at a 0.1 mmol scale with PyOxim/DIEA and HATU/DIEA as coupling reagents for the first part (Ade^{1} to Asn^{8}) and the second part (N-MeIle^{7} to Val^{2}) of the peptide respectively. 20% piperidine in DMF were used for deprotection steps. 125 mg of the 2-chlorotrityl chloride resin previously loaded by Fmoc-Ade-OH was used at a 0.8 mmol/g substitution level and was swelled overnight in 15 mL of DMF. For each amino acid the standard coupling cycle was as follow: after Fmoc deprotection of the amino acid supported by the resin, 2.5 mL of the requested amino acid at a concentration of 0.2 M in DMF were added to the resin, followed by 1 mL of PyOxim or HATU in DMF at 0.49 M and lastly by 0.5 mL 2 M DIEA in NMP. The resulting mixture was heated at 50°C and 25 W for 20 minutes. The coupling of all amino acids was performed by single coupling except for Fmoc-D-Asn(Trt)-OH and Fmoc-N-MeIle-OH that were coupled twice 20 minutes and Fmoc-L-Gln(Trt)-OH that was coupled three times 20 minutes, followed by a capping with a solution of 30 mL of DMF, 1.5 mL of anhydride acetic (0.5 M, 1 equiv), 0.6 mL of DIEA (0.21 equiv) and 40 mg of HOBt (0.019 equiv) during 3 minutes. Deprotection of Fmoc-group was done by adding 20% piperidine solution in DMF for 3 minutes. All the synthesis steps were carried out at 50°C under microwaves. At the end of the synthesis, the resin was washed three times with DMF and three times with DCM and then was dried under *vacuum*. A cleavage of the peptide from the resin was done using 10 mL of DCM/TFE 8:2 (v/v) under agitation during 2 h. The resin was then filtered and the filtrate was concentrated *in vacuo* with cyclohexane as co-solvent. The peptide was then dried freeze. 1 mg of the solid was dissolved in 1 mL of MeOH to be analyzed by mass spectrometry to verify the presence of the complete peptide. The linear peptide was not purified.

C. In solution cyclization of the protected linear peptide

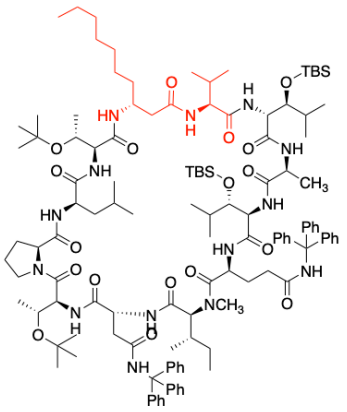

Figure 62. Structure of the protected cyclic trichormamide C

EDC and OxymaPure were purchased from Iris Biotech. The linear peptide (0.083 mmol, 1 equiv) was dissolved in 8.3 mL of DMF into a syringe. EDC (3 equiv) was dissolved in the same amount of DMF (8.3 mL) into another syringe. OxymaPure (3 equiv) was dissolved in 8.3 mL of DMF into a three-neck round-bottom flask purged under nitrogen atmosphere. The two syringes were put both sides of the flask and both solutions were added under nitrogen atmosphere at a rate of 0.01 mL/min. Once the addition was completed, the mixture was stirred overnight under nitrogen atmosphere. The mixture was analyzed by mass spectrometry, showing sodium adduct of the cyclic peptide. There was no trace of the linear peptide. DMF was evaporated using Genevac (T=35°C, Medium BP) during 3 h and the resulting sediments were dissolved with 10 mL of EtOAc. The organic layer was washed three times with 2 mL of citric acid (1M), three times with 2 mL of $NaHCO_3$ (1M) and three times with 2 mL of brine in order to separate the cyclic peptide from potential linear one. The organic layer was dried over magnesium sulfate and then concentrated *in vacuo*.

D. Final deprotection

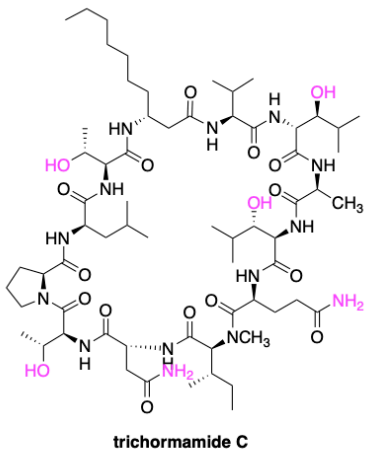

Figure 63. Structure of the final trichormamide C

TFA was purchased from Honeywell and TIS was obtained from Sigma-Aldrich. To allow side-chain deprotection, the resulting white solid was mixed with a solution of TFA/TIS/H_2O 95:2.5:2.5 (v/v) during 2 h. TFA was evaporated under *vacuum* and the peptide was precipitated thanks to ice-cold diethyl ether then was obtained by centrifugation. The peptide was then purified by preparative HPLC with a gradient from 30% to 50% of ACN (0.1% formic acid) during 50 min and an isocratic at 50% ACN (0.1% FA) during 10 min (flow rate = 3 mL/min). The cyclic peptide was recovered between 49% and 50% of ACN (0.1% FA) in 50 min of purification. Fractions were concentrated *in vacuo* and then dried freeze.

E. Analyses

The peptides studied in this chapter are trichormamide C synthesized with PyOxim+HATU (compound **4**), trichormamide C synthesized with only HATU (compound **4'**), and its two synthetic analogues **5** and **6** (Table 10). Hereafter, the HRMS, LCMS and NMR analyses of these four peptides are reported.

Table 10. Summary of peptide studied with the yield of their synthesis and their HRMS mass.

Peptides	Structures	Yields	HRMS
4	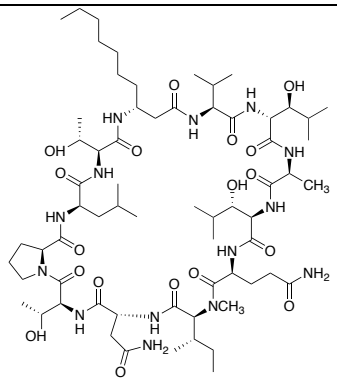	7%	Calculated for $C_{65}H_{114}N_{14}O_{18}Na$ $[M+Na]^+$ *m/z* 1401.83277; Found $[M+Na]^+$ *m/z* 1401.83530; mass error = 1.80 ppm.
4'	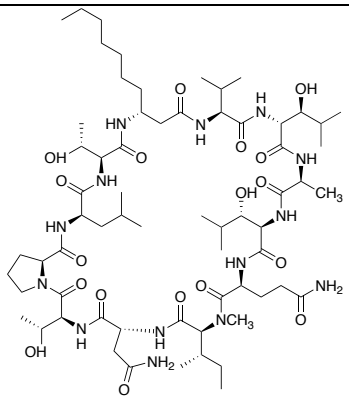	2%	Calculated for $C_{65}H_{114}N_{14}O_{18}Na$ $[M+Na]^+$ m/z 1401.83277; Found $[M+Na]^+$ *m/z* 1401.83222; mass error = 0.40 ppm
5	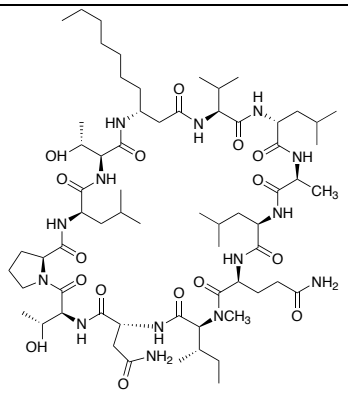	2%	Calculated for $C_{65}H_{114}N_{14}O_{16}Na$ $[M+Na]^+$ *m/z* 1369.84294; Found $[M+Na]^+$ *m/z* 1369.8413; mass error = 1.22 ppm.
6	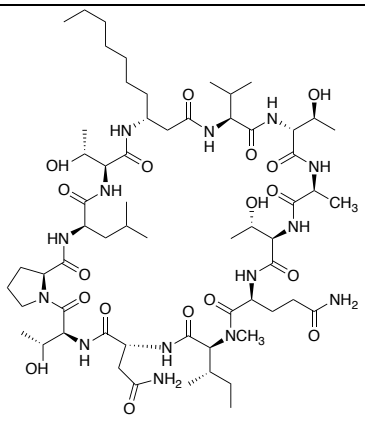	2%	Calculated for $C_{61}H_{106}N_{14}O_{18}Na$ $[M+Na]^+$ *m/z* 1345.77017; Found $[M+Na]^+$ *m/z* 1345.7698; mass error = 0.29 ppm.

a) Compound 4

A

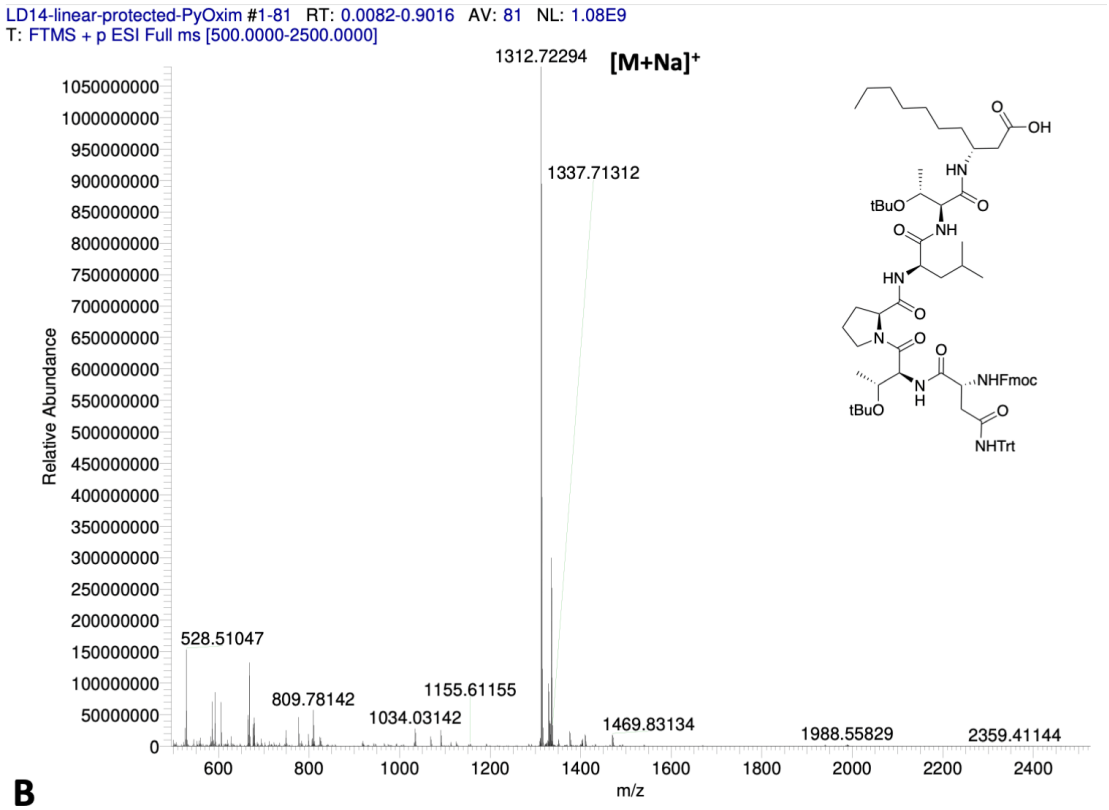

B

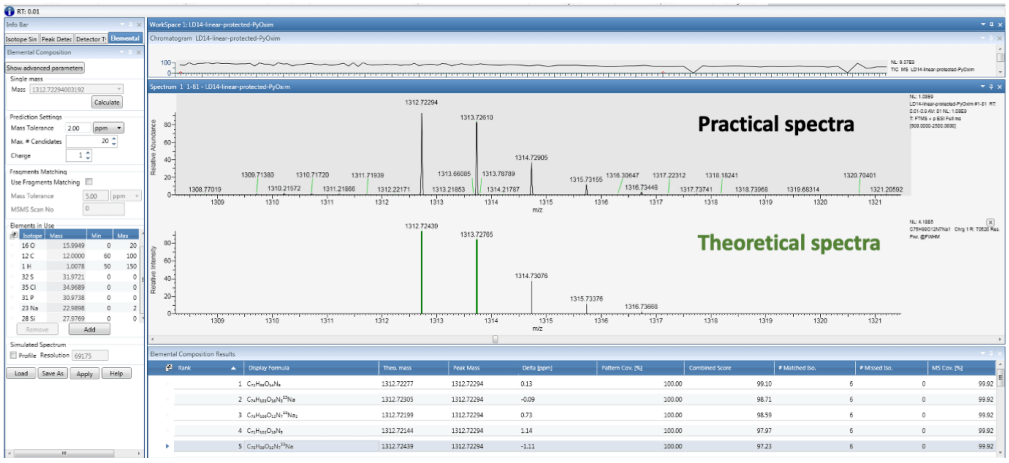

Figure 64. A) ESI-HRMS spectrum of the first part of the protected linear peptide from the synthesis of 4. B) Comparison with the theoretical spectrum. Calculated for $C_{75}H_{99}N_7O_{12}Na$ $[M+Na]^+$ *m/z* 1312.72439; Found $[M+Na]^+$ *m/z* 1312.72294 ; mass error = 1.11 ppm

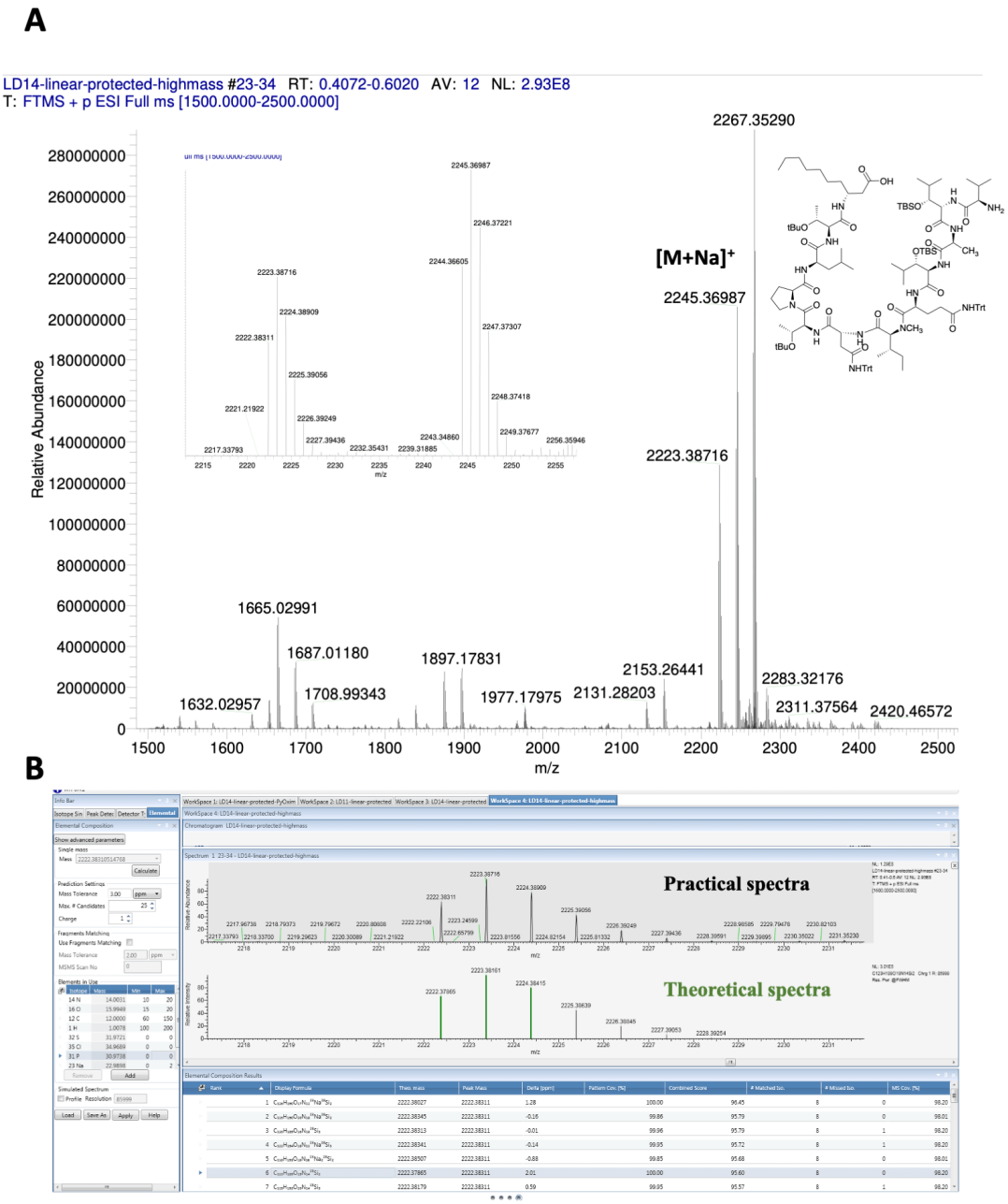

Figure 65. A) ESI-HRMS spectrum of the complete protected linear peptide from the synthesis of 4. B) Comparison with the theoretical spectrum. Calculated for $C_{123}H_{189}N_{14}O_{19}Si_2$ $[M+H]^+$ *m/z* 2222.37865; Found $[M+H]^+$ *m/z* 2222.38311; mass error = 2.01 ppm

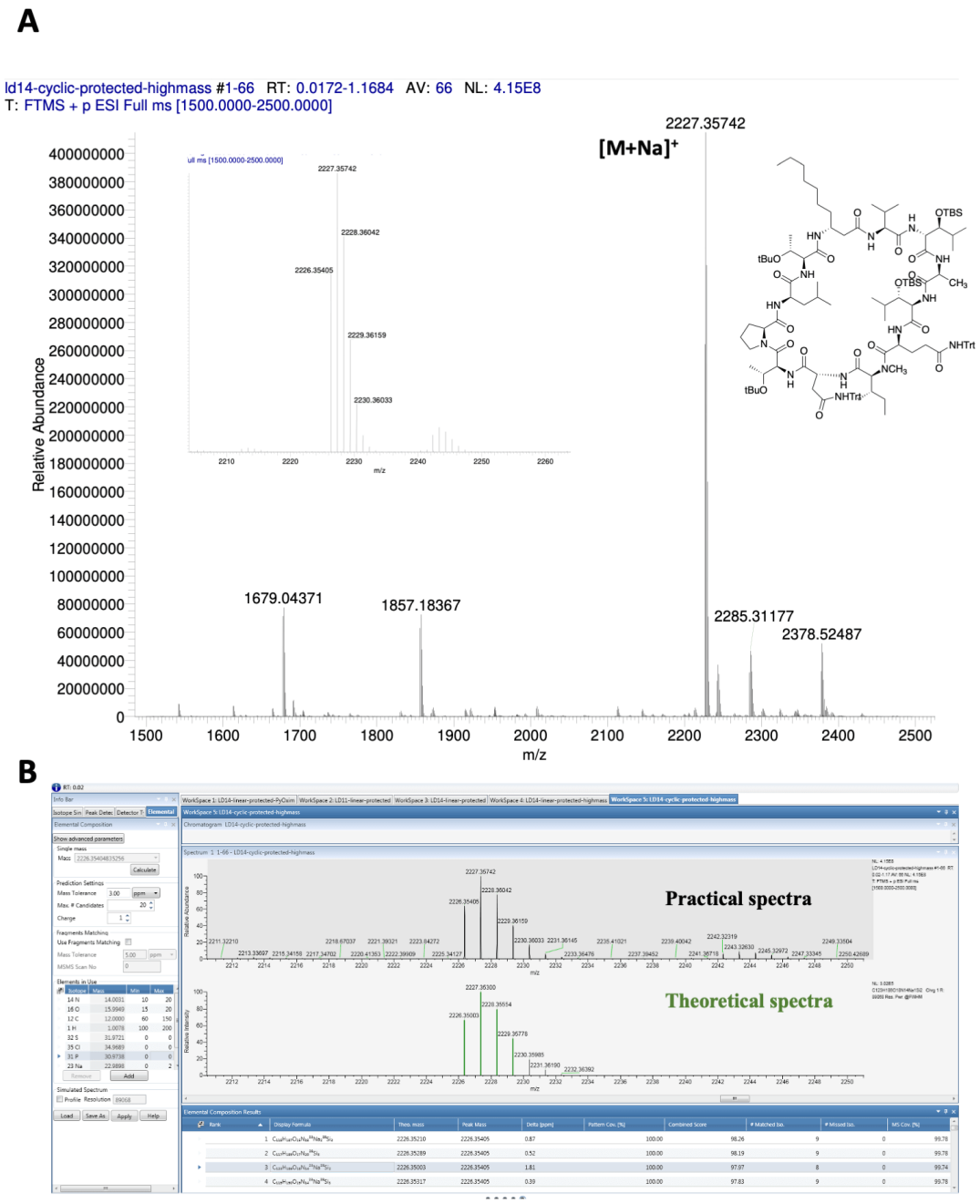

Figure 66. A) ESI-HRMS spectrum of the protected cyclic peptide from the synthesis of 4. B) Comparison with the theoretical spectrum. Calculated for $C_{123}H_{186}N_{14}O_{18}Si_2Na$ $[M+Na]^+$ *m/z* 2226.35003; Found $[M+Na]^+$ *m/z* 2226.35405; mass error = 1.81 ppm

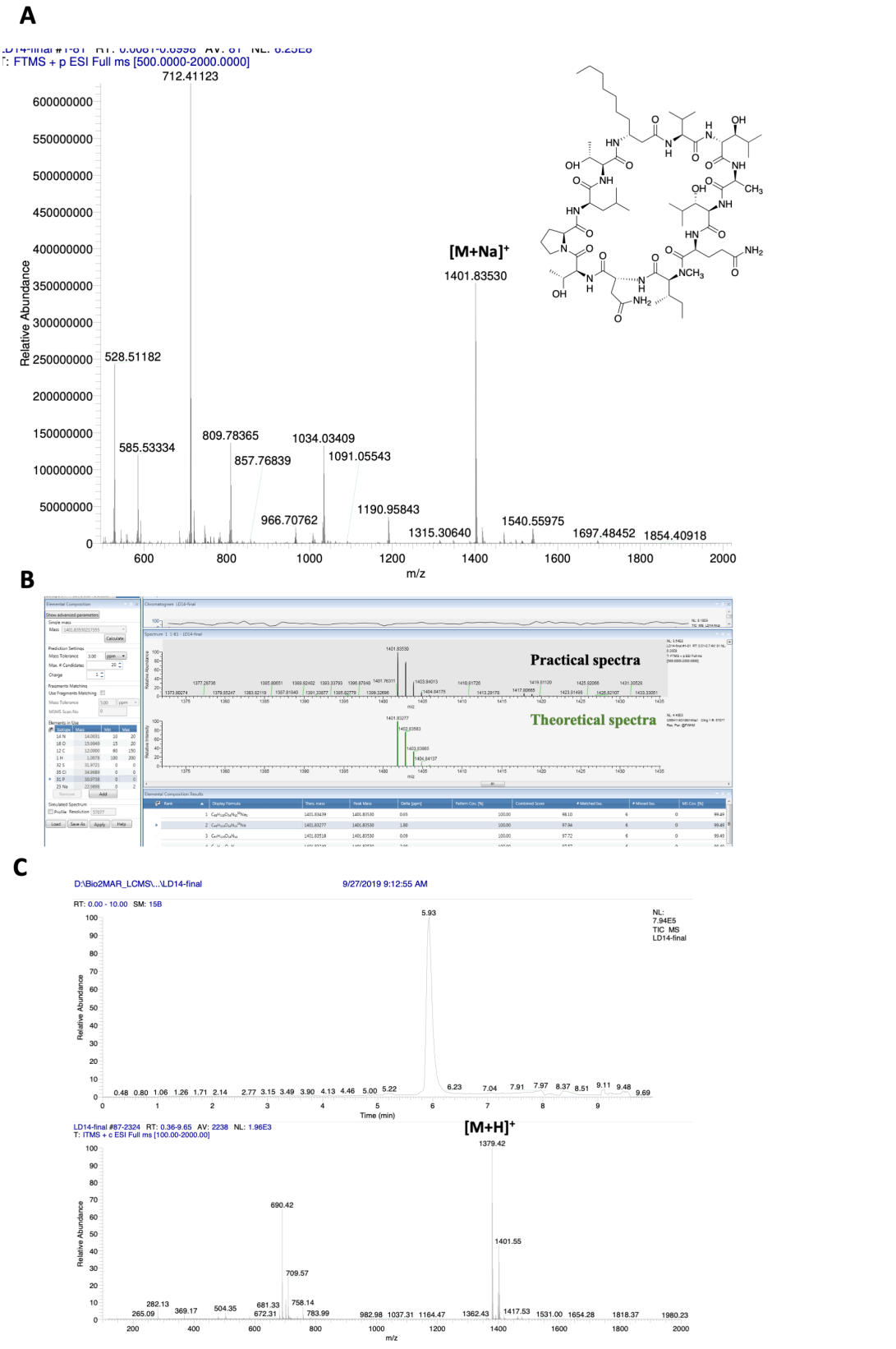

Figure 67. A) ESI-HRMS spectrum of the deprotected purified cyclic peptide from the synthesis of 4. B) Comparison with the theoretical spectrum. Calculated for $C_{65}H_{114}N_{14}O_{18}Na$ $[M+Na]^+$ *m/z* 1401.83277; Found $[M+Na]^+$ *m/z* 1401.83530; mass error = 1.80 ppm. C) LC-MS profile of the purified compound 4.

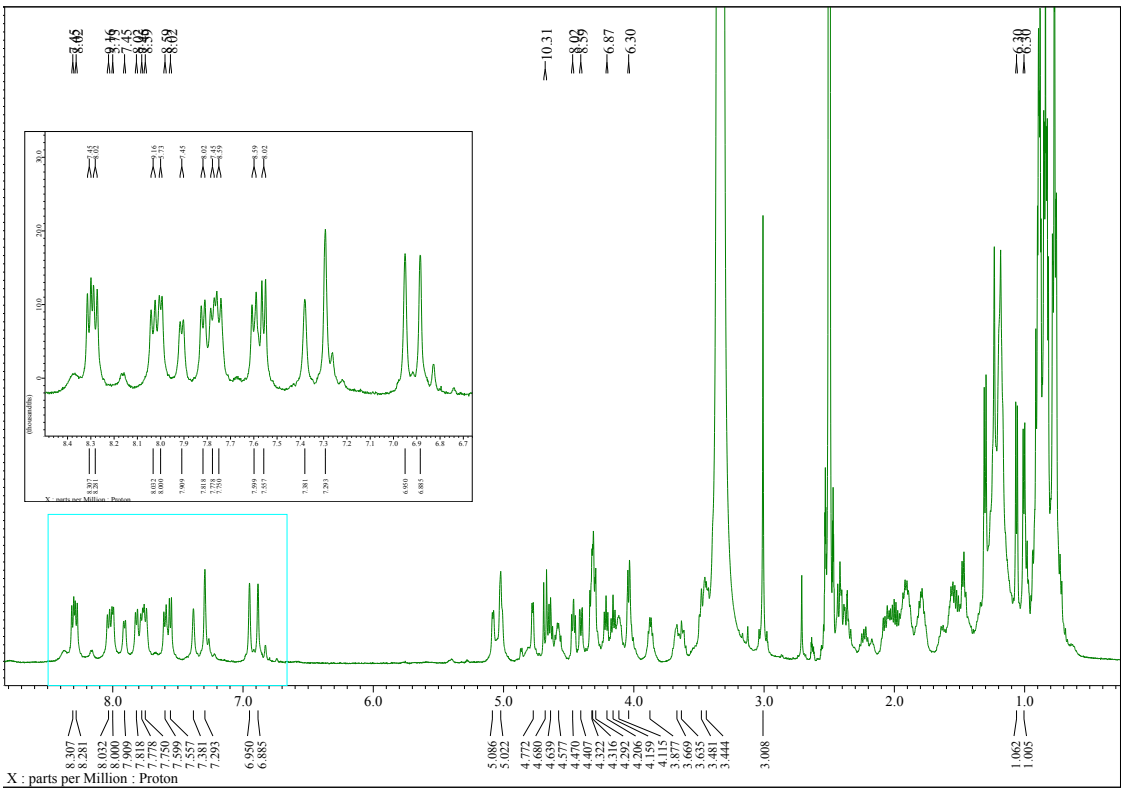

Figure 68. ^{1}H NMR spectrum of compound 4. Solvent : dmso-d_6; T : 23°C; Scans : 32

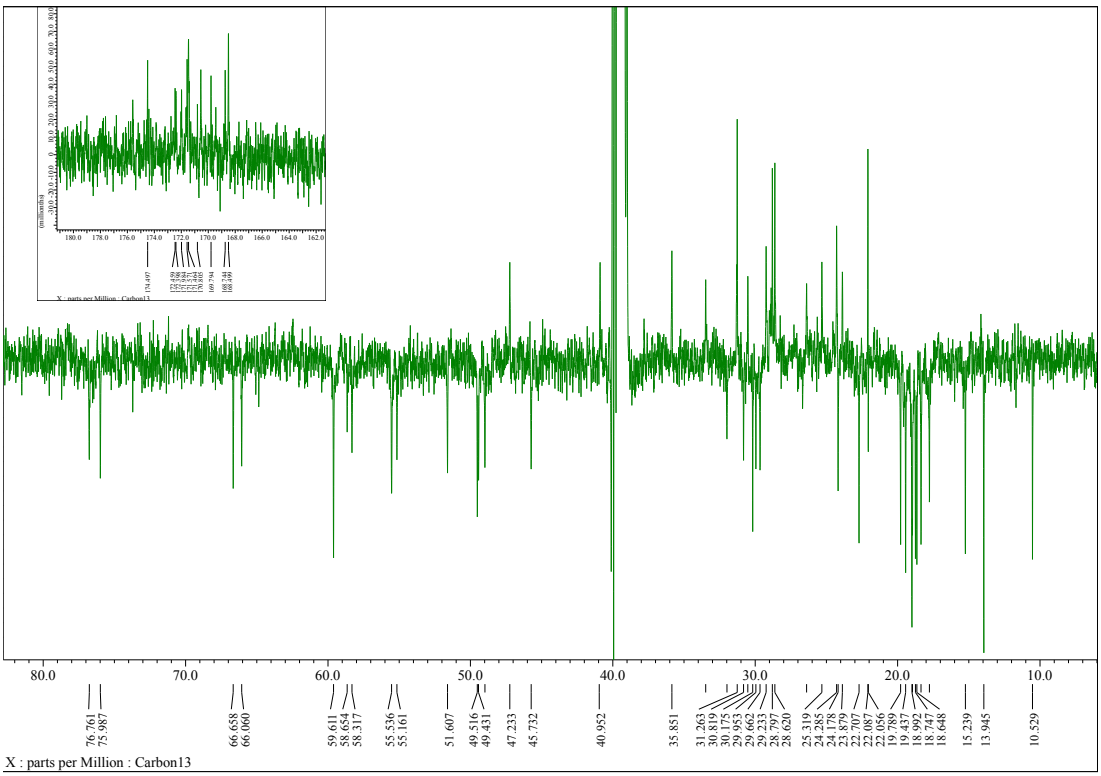

Figure 69. DEPTQ spectrum of compound 4. Solvent : dmso-d_6; T : 23°C; Scans : 10000

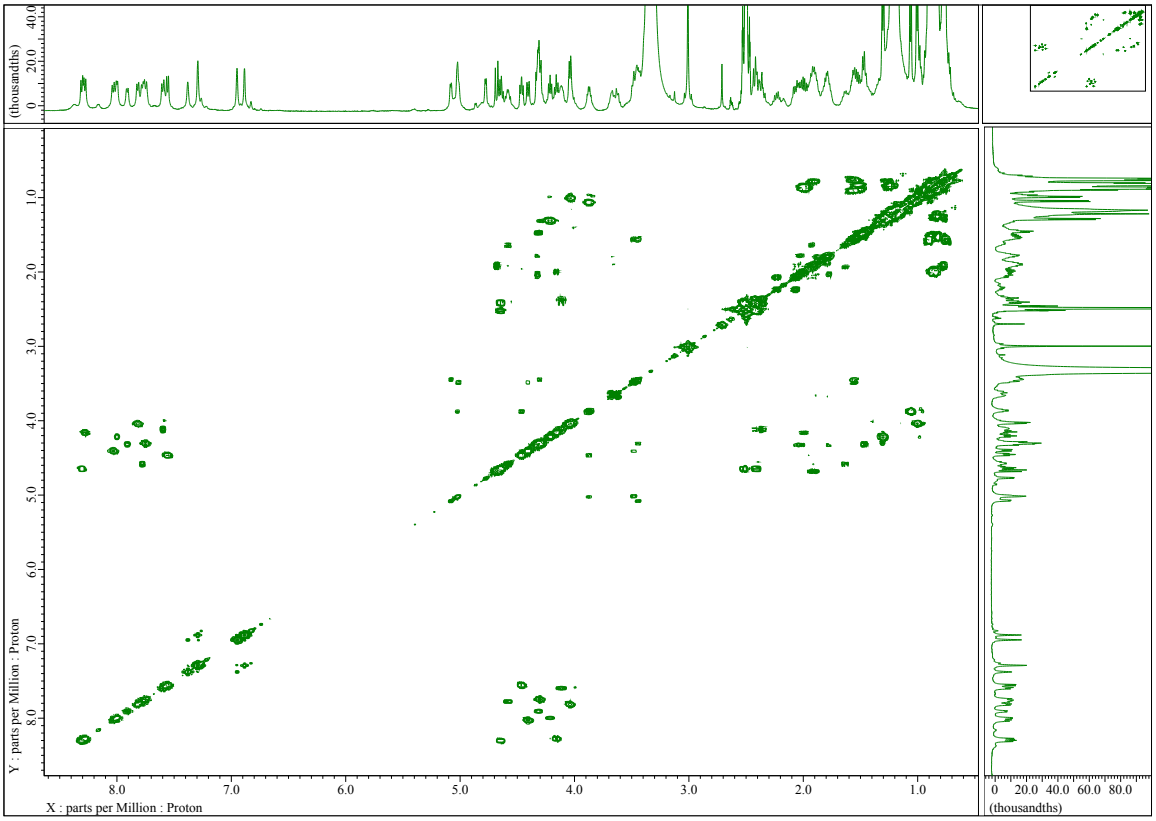

Figure 70. COSY spectrum of compound 4. Solvent : dmso-d_6; T : 23°C; Scans : 8192

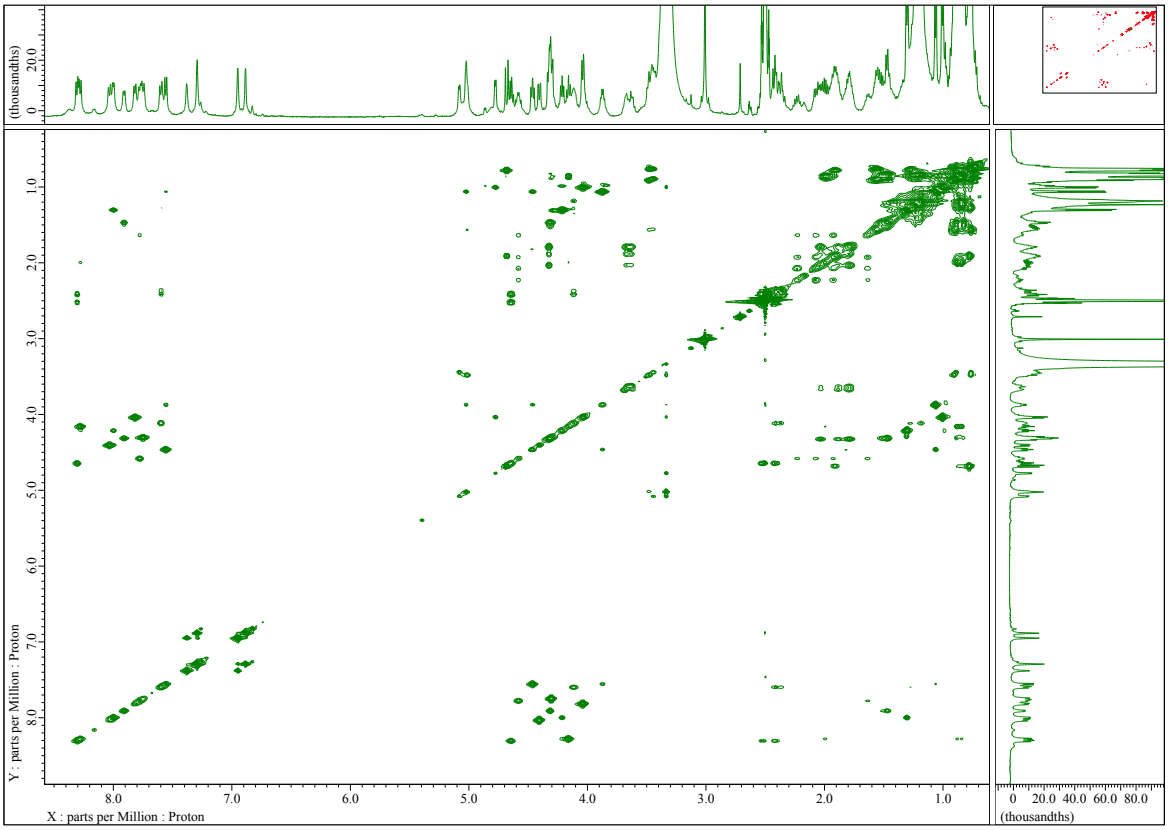

Figure 71. TOCSY spectrum of compound 4. Solvent : dmso-d_6; T : 23°C; Scans : 8192

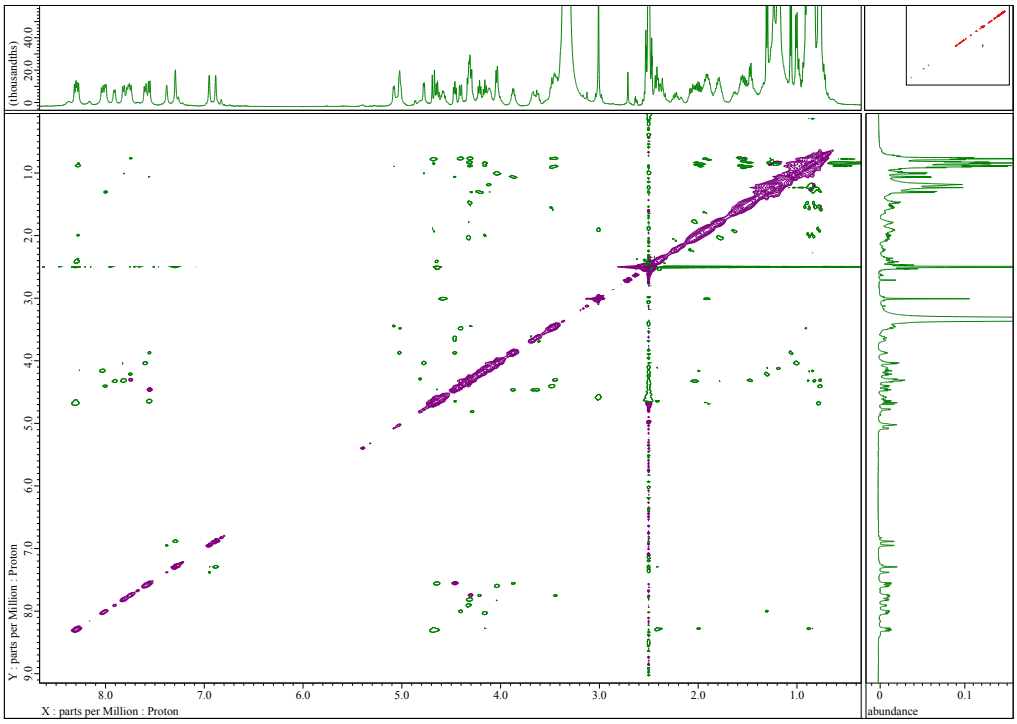

Figure 72. ROESY spectrum of compound 4. Solvent : dmso-d_6; T : 23°C; Scans : 8192

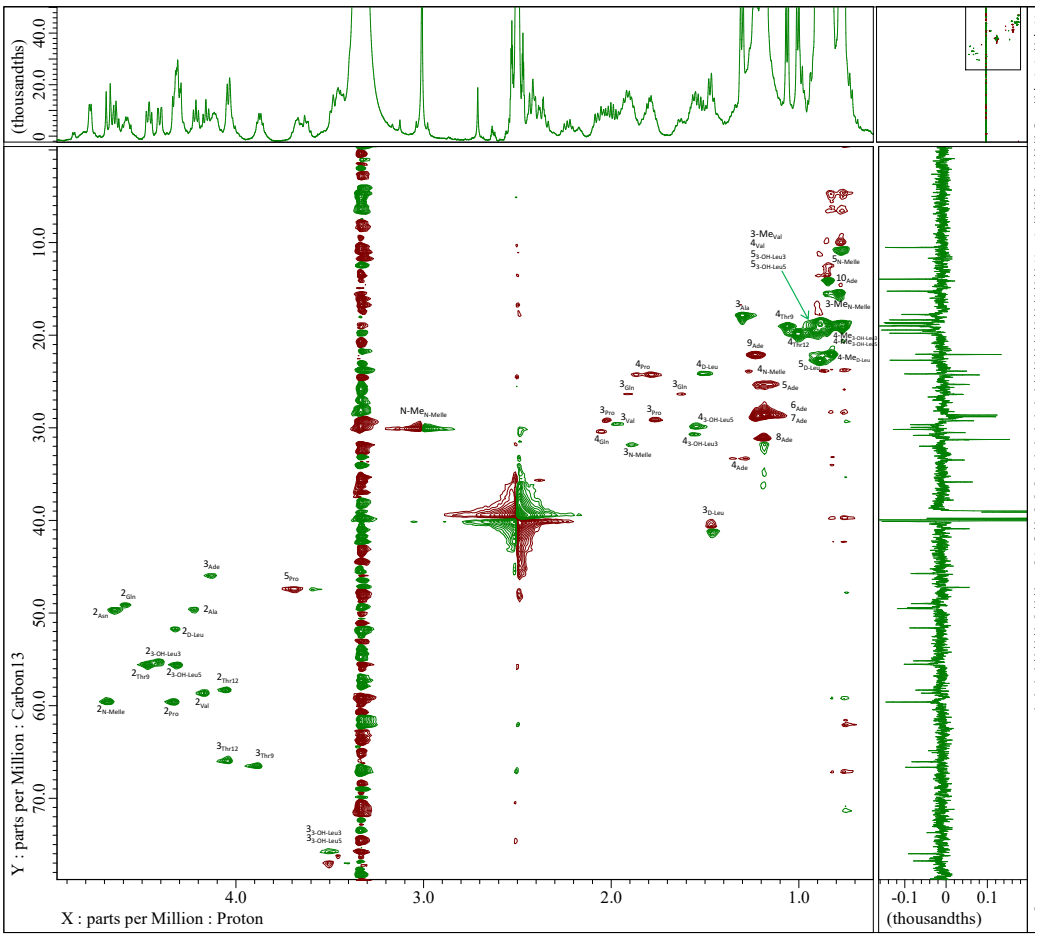

Figure 73. HSQC spectrum of compound 4. Solvent : dmso-d_6; T : 23°C; Scans : 8192

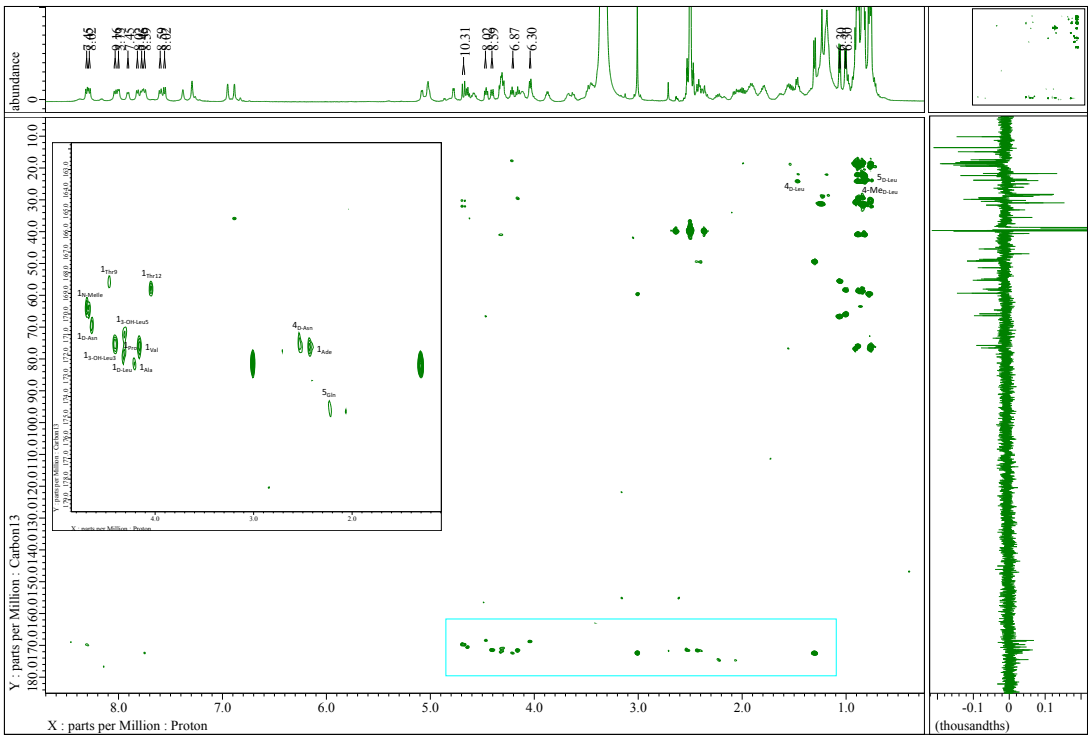

Figure 74. HMBC spectrum of compound 4. Solvent : dmso-d_6; T : 23°C; Scans : 16384

A

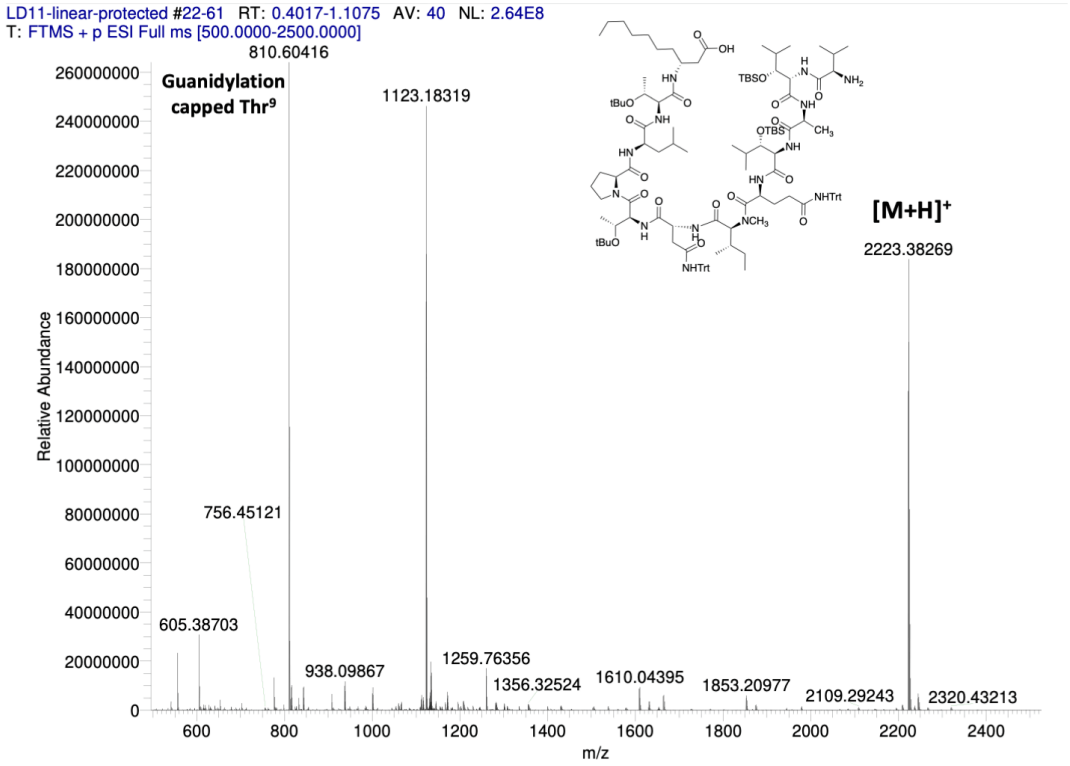

B

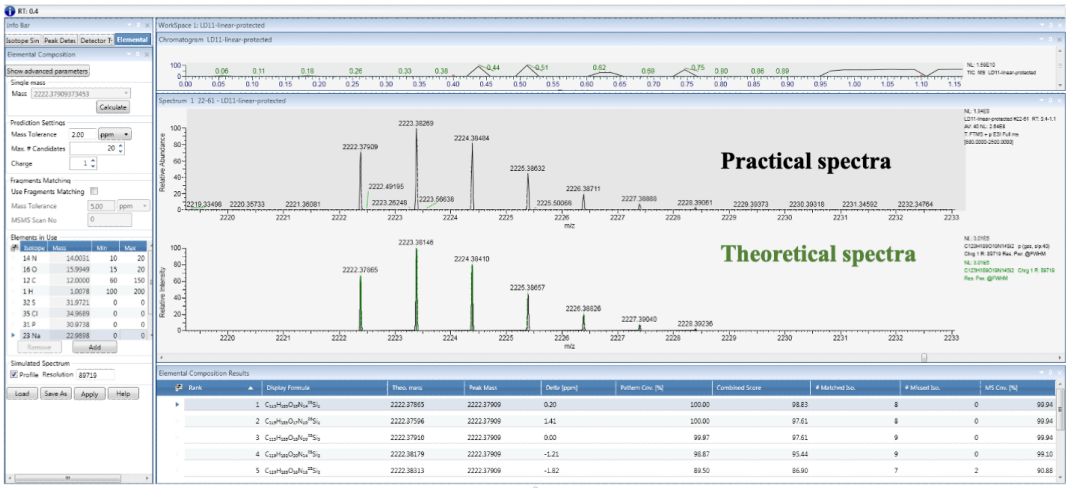

Figure 75. A) ESI-HRMS spectrum of the complete protected linear peptide from the synthesis of 4'. B) Comparison with the theoretical spectrum. Calculated for $C_{123}H_{189}N_{14}O_{19}Si_2$ $[M+H]^+$ *m/z* 2222.37865; Found $[M+H]^+$ *m/z* 2222.37909 ; mass error = 0.20 ppm

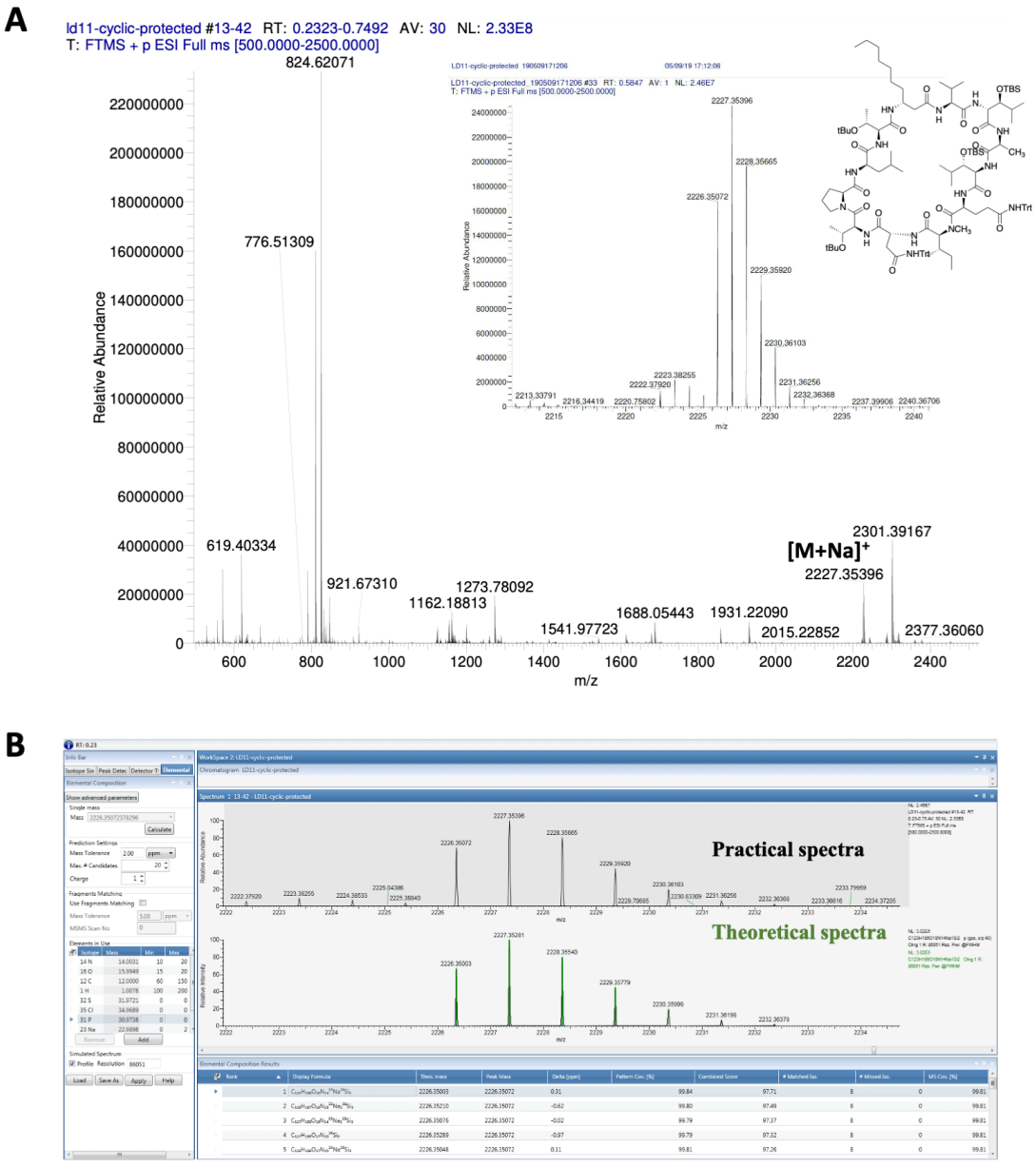

Figure 76. A) ESI-HRMS spectrum of the protected cyclic peptide from the synthesis of 4'. B) Comparison with the theoretical spectrum. Calculated $C_{123}H_{186}N_{14}O_{18}Si_2Na$ $[M+Na]^+$ *m/z* 2226.35003; Found $[M+Na]^+$ *m/z* 2226.35072; mass error = 0.31 ppm

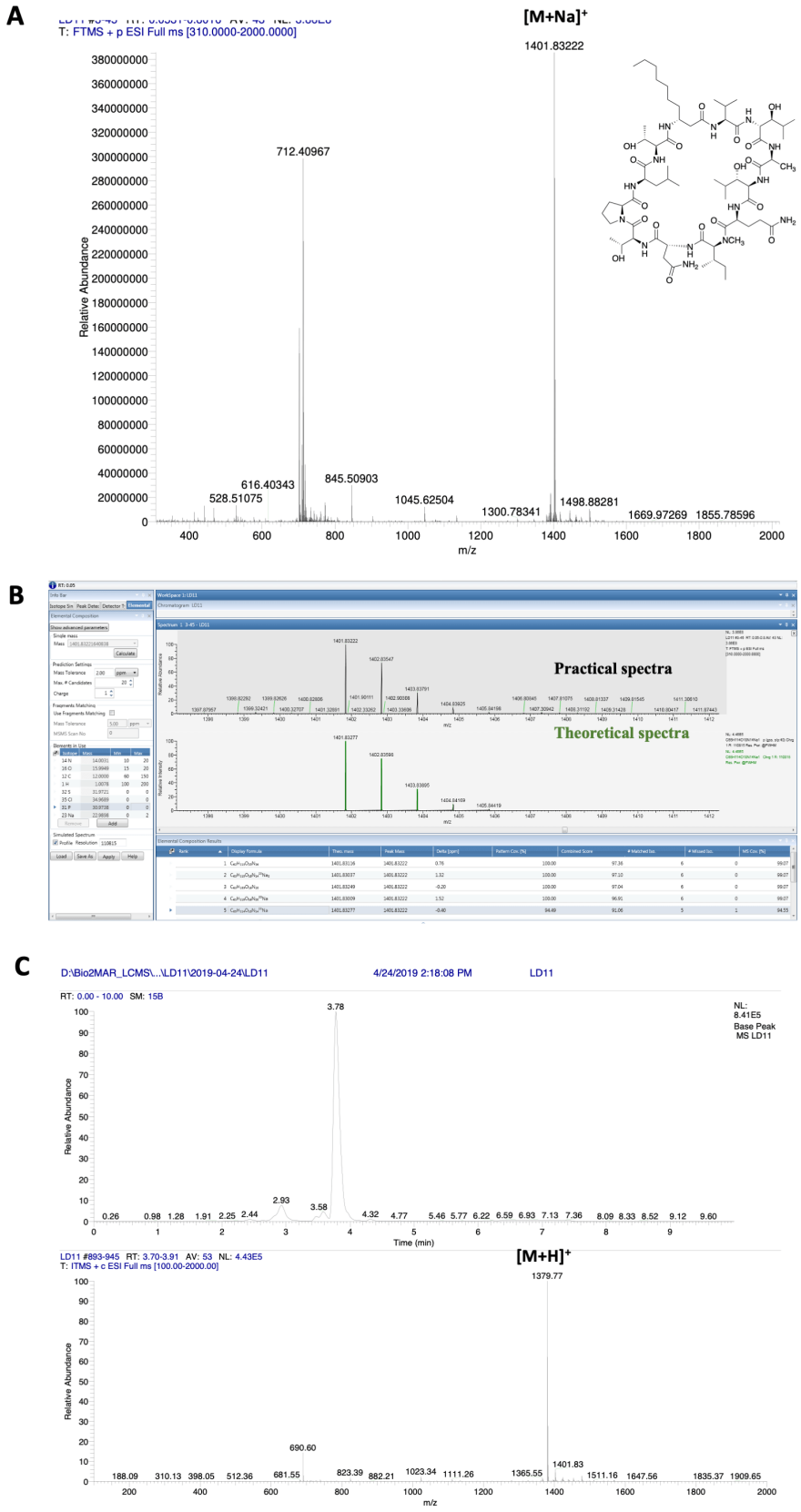

Figure 77. A) ESI-HRMS spectrum of the deprotected purified cyclic peptide from the synthesis of 4'. B) Comparison with the theoretical spectrum. Calculated $C_{65}H_{114}N_{14}O_{18}Na$ $[M+Na]^+$ *m/z* 1401.83277; Found $[M+Na]^+$ *m/z* 1401.83222; mass error = 0.40 ppm. C) LC-MS profile of the purified 4'.

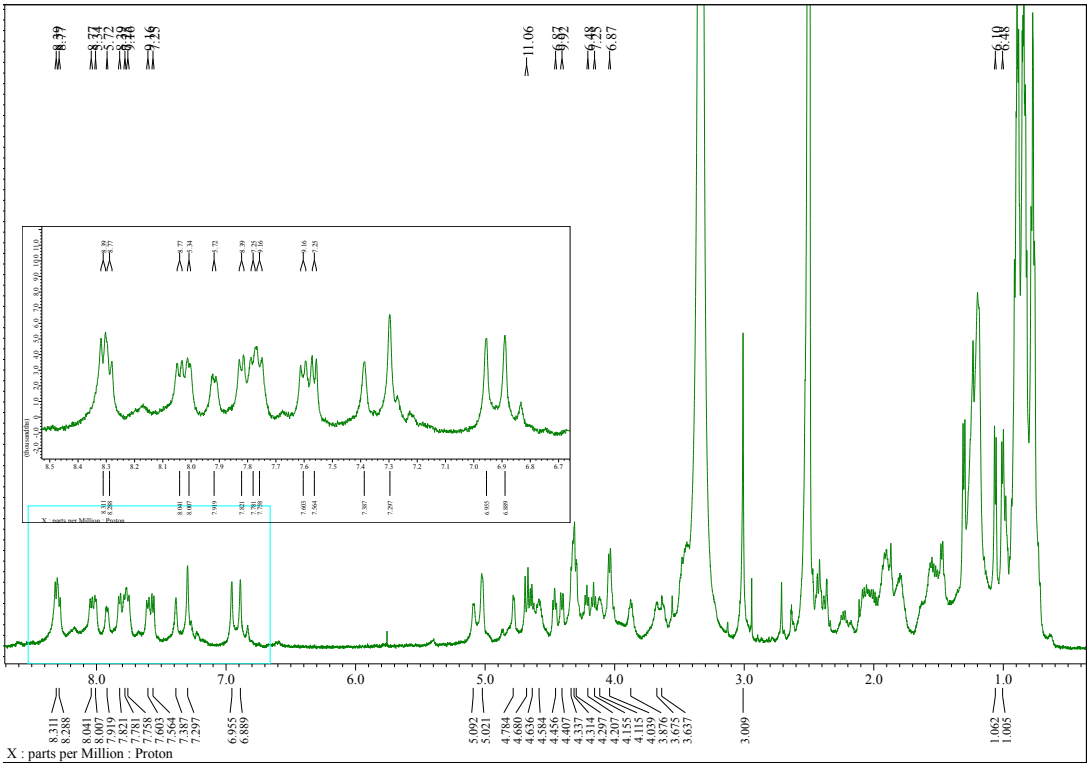

Figure 78. ^{1}H NMR spectrum of compound 4'. Solvent : dmso-d_6; T : 23°C; Scans : 32

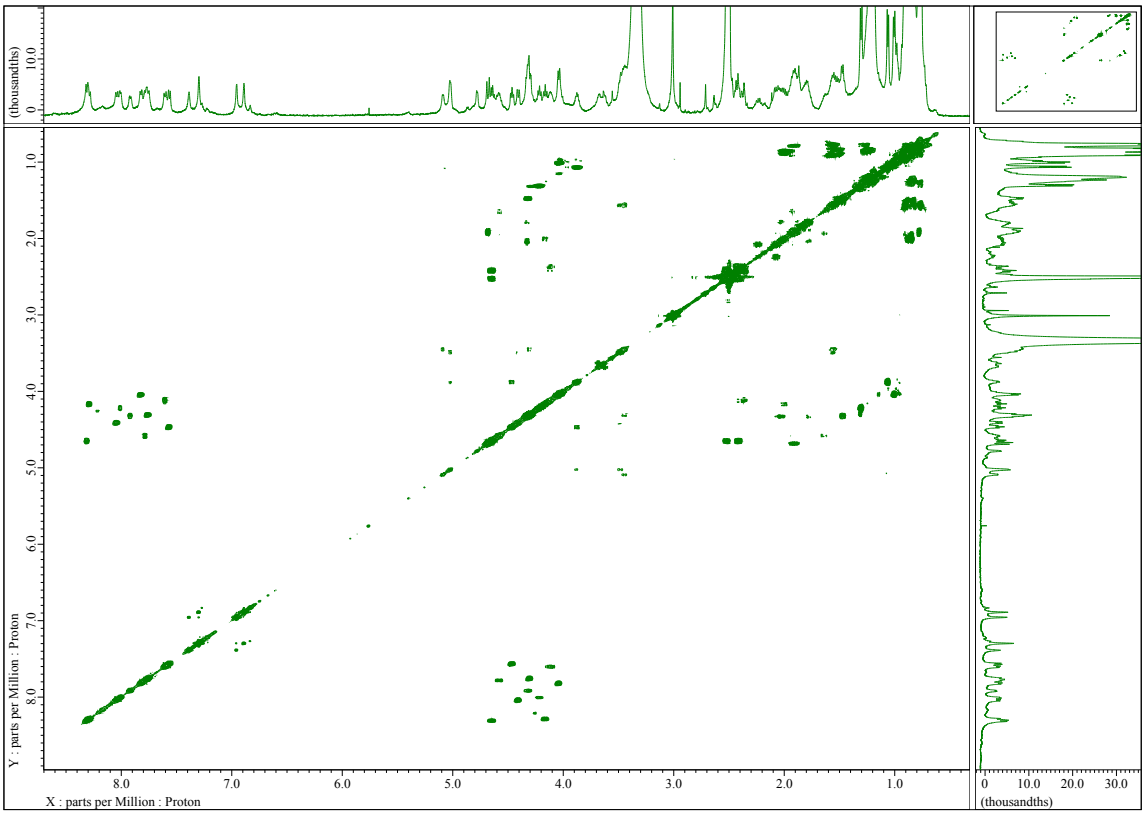

Figure 79. COSY spectrum of compound 4'. Solvent : dmso-d_6; T : 23°C; Scans : 8192

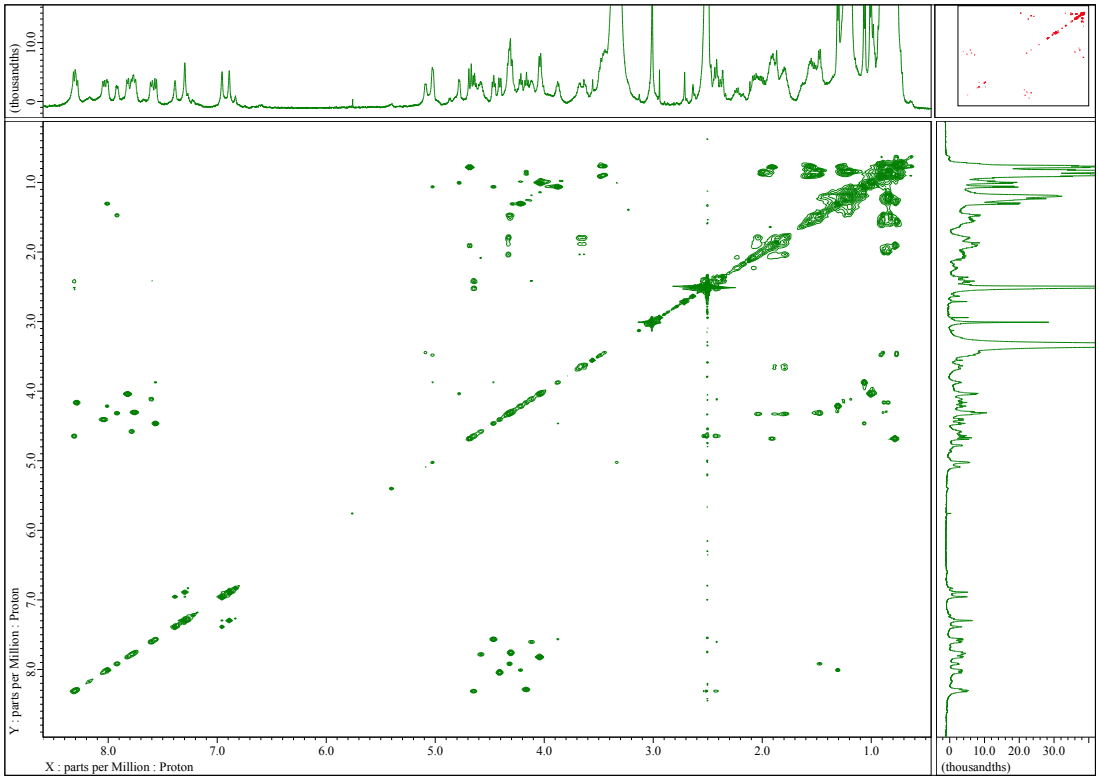

Figure 80. TOCSY spectrum of compound 4'. Solvent : dmso-d_6; T : 23°C; Scans : 8192

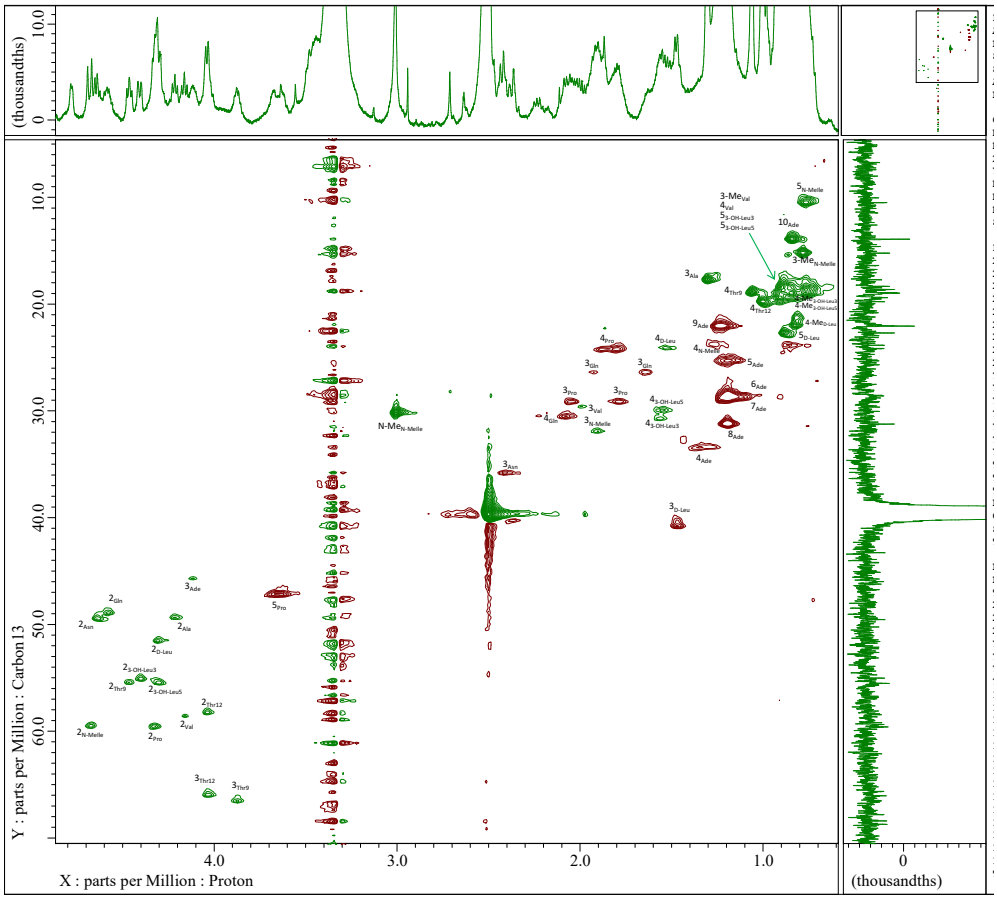

Figure 81. HSQC spectrum of compound 4'. Solvent : dmso-d_6; T : 23°C; Scans : 8192

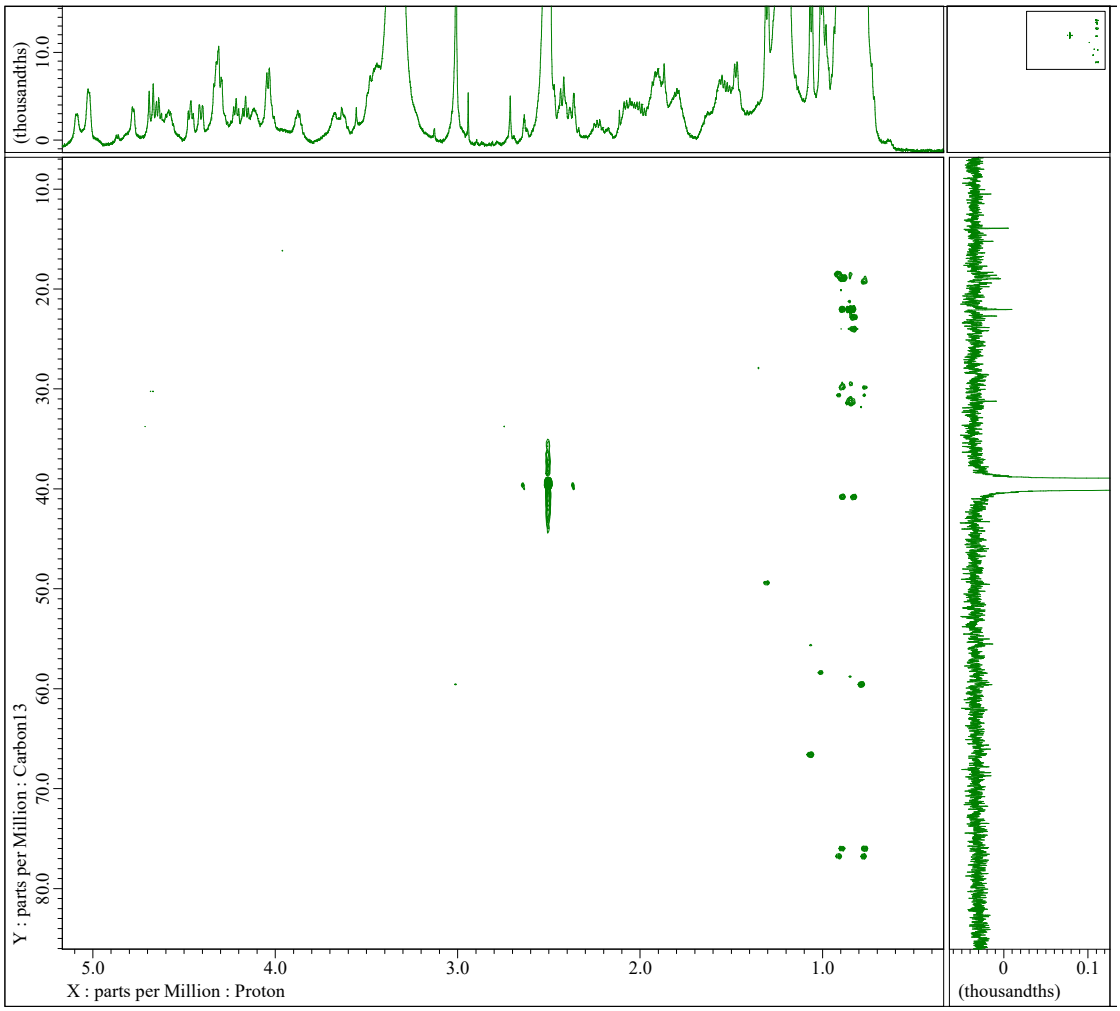

Figure 82. HMBC spectrum of compound 4'. Solvent : dmso-d_6; T : 23°C; Scans : 16384

Table 11. NMR spectroscopic data of trichormamide C in DMSO-d_6. Establishment of the structure by different NMR spectra.

entry	position	**δ**C, mult	**δ**H, mult. (J in Hz)	COSY/TOCSY	ROESY	HMBC
Ade[1]	1	171.5, C	-			
	2	40.3, CH_2	2.37	3	NH_{Val}	
			2.42	3	3, NH_{Val}	
	3	45.7, CH	4.11	2, 4, NH	2, 4	
	4	33.5, CH_2*	1.28	3, 5 overlapped	3	
			1.35	5 overlapped	3	
	5	25.3, CH_2*	1.22	4, 6		6
	6	28.8, CH_2*	1.19	5, 7		5
	7	28.6, CH_2*	1.19			
	8	31.3, CH_2*	1.19			9
	9	22.1, CH_2*	1.24			8, 10
	10	14.0, CH_3*	0.84			9
	NH	-	7.60, d (8.6)	3	2_{Thr12}	
Val[2]	1	171.5, C	-			2
	2	58.7, CH	4.15	3, NH	3, $NH_{3\text{-OH-Leu3}}$	1, 3
	3	29.7, CH	1.99	2, 3-Me, 4	2, 3-Me, 4	2, 3-Me
	3-Me	19.0, CH_3	0.85	3	3	3
	4	nd	0.88	3	3	
	NH	-	8.28, d (8.0)	2	$2_{\beta\text{-Ade}}$	
3-OH-Leu[3]	1	171.5, C	-			2
	2	55.2, CH	4.40, d (8.6)	3, NH	3, 4-Me, NH_{Ala}	1
	3	76.8, CH	3.48	2, 3-OH, 4	2, 4, 4-Me, 5	4
	4	30.8, CH	1.55	3, 4-Me, 5	3, 4-Me, 5	3, 4-Me, 5
	4-Me	nd	0.77	4	2, 3, 4	4
	5	nd	0.90	4	3, 4	4
	3-OH	-	5.02	3		
	NH	-	8.03, d (9.2)	2	2_{Val}	
Ala[4]	1	172.5, C	-			2
	2	49.4, CH	4.21, t (6.8)	3, NH	3, $NH_{3\text{-OH-Leu5}}$	1, 3
	3	17.8, CH_3	1.30, d (7.1)	2	2	2
	NH	-	8.00, d (5.7)	2	$2_{3\text{-OH-Leu3}}$	
3-OH-Leu[5]	1	170.8, C	-			2
	2	55.5, CH	4.30	3, NH	4-Me, NH_{Gln}	1
	3	76.0, CH	3.44	2, 3-OH, 4	3-OH, 4-Me, 5	
	4	30.0, CH	1.55	3, 4-Me, 5	3, 4-Me, 5	4-Me, 5
	4-Me	nd	0.77	4	2, 3, 4	4
	5	nd	0.90	4	2, 3, 3-OH, 4	4
	3-OH	-	5.08	3	3, 5	
	NH	-	7.75, d (8.6)	2	2_{Ala}	
Gln[6]	1	172.4, C	-			
	2	49.0, CH	4.58	3, NH	$N\text{-}Me_{N\text{-}MeIle}$	
	3	26.4, CH_2	1.63	2, 4		

			1.91		$N\text{-}Me_{N\text{-}MeIle}$	
	4	30.5, CH_2	2.07	3		5
			2.23			5
	5	174.5, C	-			4
	NH	-	7.77, d (7.5)	2	$2_{3\text{-}OH\text{-}Leu5}$	
	NH_2	-	7.38 & 6.95			
N-MeIle[7]	1	169.8, C	-			2
	2	59.6, CH	4.68, d (10.3)	3	$3, NH_{D\text{-}Asn}$	1, 3
	3	32.0, CH	1.91	2, 3-Me, 4	2, 3-Me	2
	3-Me	15.2, CH_3	0.77	3	2, 3, 4	
	4	23.9, CH_2	1.27	3, 5		5
	5	10.5, CH_3	0.77	4		4
	N-Me	30.2, CH_3	3.01		2_{Gln}	
D-Asn[8]	1	170.6, C	-			2
	2	49.5, CH	4.65	3, NH	$3, NH_{Thr9}$	1, 3
	3	35.9, CH_2	2.41	2	$2, NH_{Thr9}$	2, 4
			2.52		2	4
	4	171.6, C	-			3
	NH	-	8.31, d (7.5)	2	$2_{N\text{-}MeIle}$	
	NH_2	-	7.29 & 6.88			
Thr[9]	1	168.5, C	-			2
	2	55.5, CH	4.47, t (8.0)	3, NH	$3, 4, 5_{Pro}$	1, 3
	3	66.7, CH	3.87	2, 3-OH, 4	2, 3-OH, 4	2, 4
	4	19.0, CH_3	1.06, d (6.3)	3	2, 3	3
	3-OH	-	5.02	3	4	
	NH	-	7.56, d (8.0)	2	$2_{D\text{-}Asn}$	
Pro[10]	1	171.5, C	-			2
	2	59.6, CH	4.32	3	$3, 4, NH_{D\text{-}Leu}$	1
	3	29.2, CH_2	1.78	2, 4	2, 5	
			2.03		2	
	4	24.3, CH_2	1.89	3, 5	2	
			1.89			
	5	47.2, CH_2	3.63	4	$2_{Thr9}, 3$	
			3.66		$2_{Thr9}, 3$	
D-Leu[11]	1	172.0, C	-			2
	2	51.6, CH	4.32	3, NH	$3, NH_{Thr12}$	1, 3
	3	40.9, CH_2	1.47	2	2	2, 4
	4	24.2, CH	1.56	3, 4-Me, 5	2	3, 4-Me, 5
	4-Me	22.1, CH_3	0.83	4		4
	5	22.7, CH_3	0.89	4		4
	NH	-	7.91, d (7.5)	2	2_{Pro}	
Thr[12]	1	168.7, C	-			2
	2	58.3, CH	4.04, d (6.3)	3, NH	$3\text{-}OH, 4, NH_{\beta\text{-}Ade}$	1
	3	66.1, CH	4.04, d (6.3)	2, 3-OH, 4	3-OH, 4	4
	4	19.8, CH3	1.00, d (6.3)	3	2, 3, 3-OH	3
	3-OH	-	4.77	3	2, 3, 4	
	NH	-	7.82, d (8.0)	2	$2_{D\text{-}Leu}$	

*Most of the information about Ade was found in the HSQC spectrum

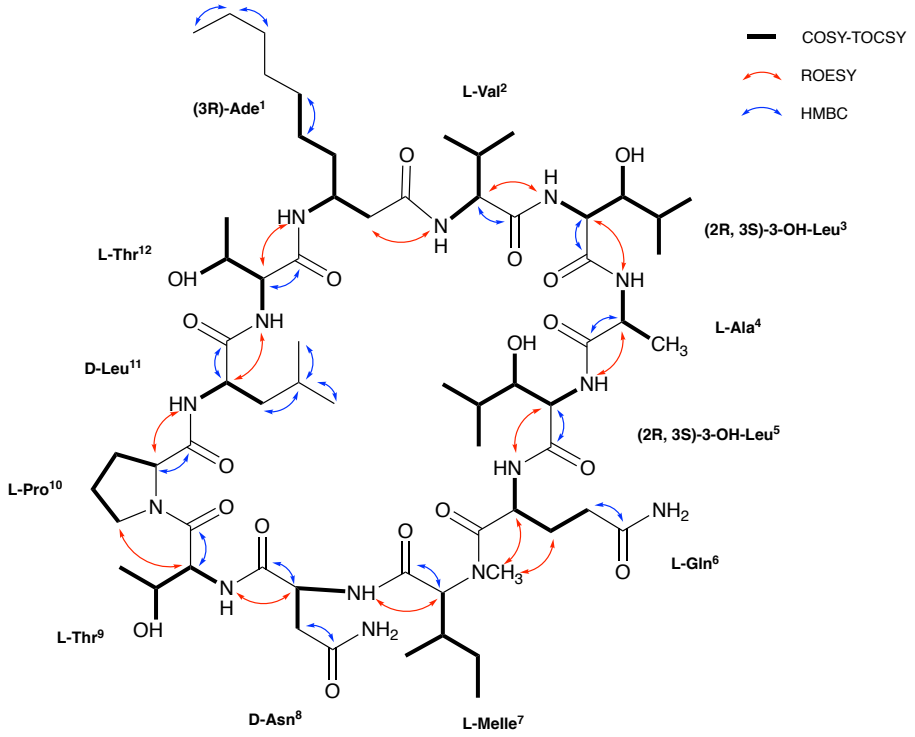

trichormamide C

Figure 83. NMR analysis of trichormamide C structure

b) Compound 5

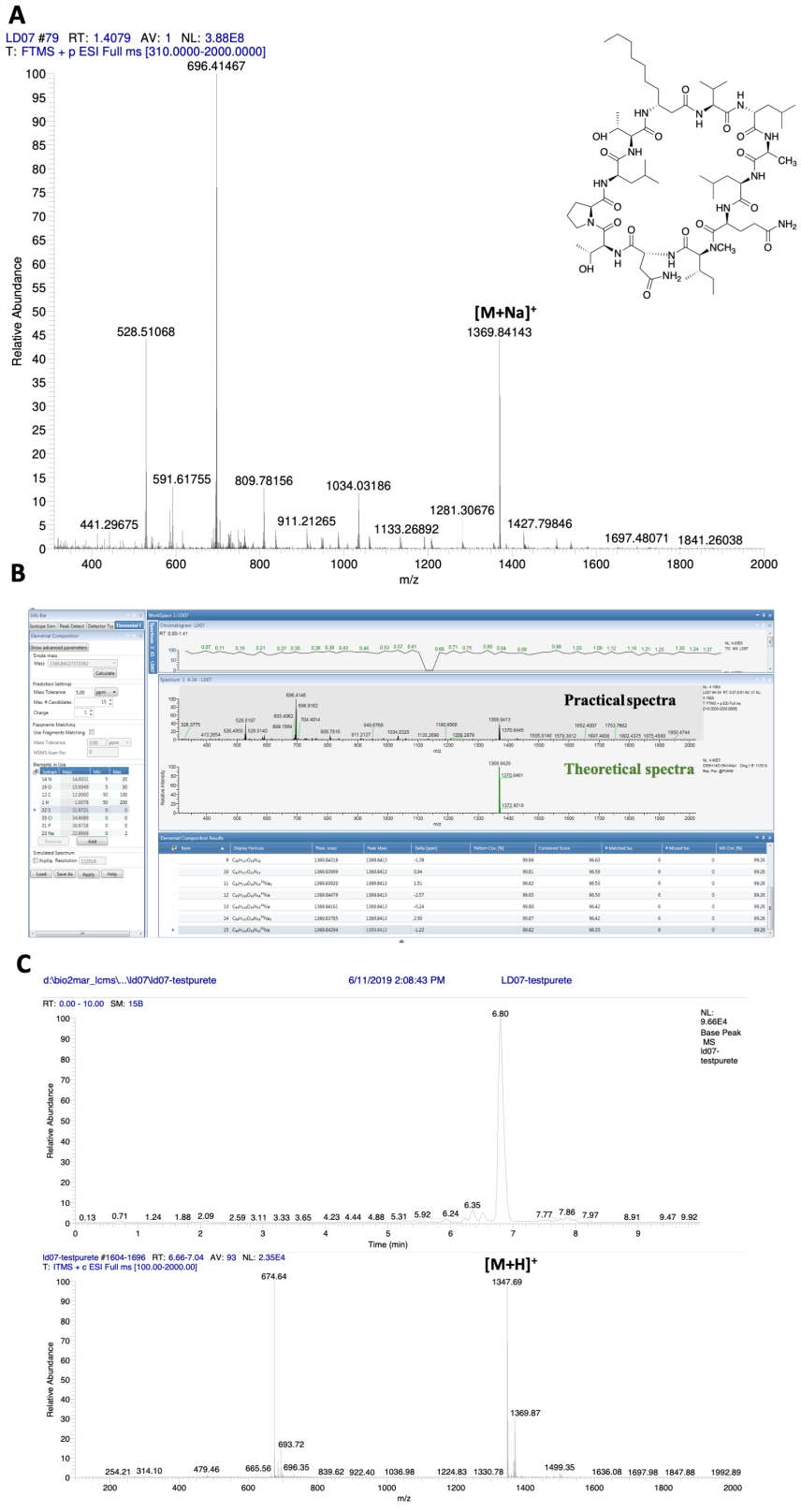

Figure 84. A) ESI-HRMS spectrum of the deprotected purified cyclic peptide from the synthesis of 5. B) Comparison with the theoretical spectrum. Calculated for $C_{65}H_{114}N_{14}O_{16}Na$ $[M+Na]^+$ *m/z* 1369.84294; Found $[M+Na]^+$ *m/z* 1369.8413; mass error = 1.22 ppm. C) LC-MS profile of the purified 5.

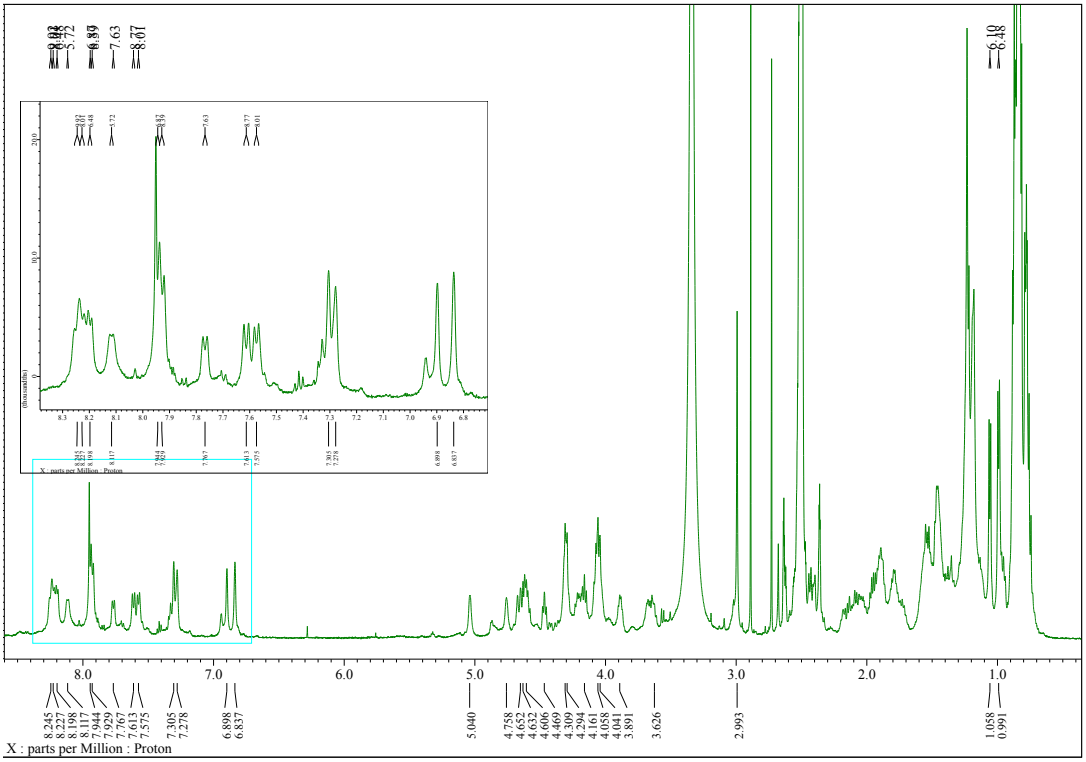

Figure 85. ^{1}H NMR spectrum of 5. Solvent : dmso-d_6; T : 23°C; Scans : 32

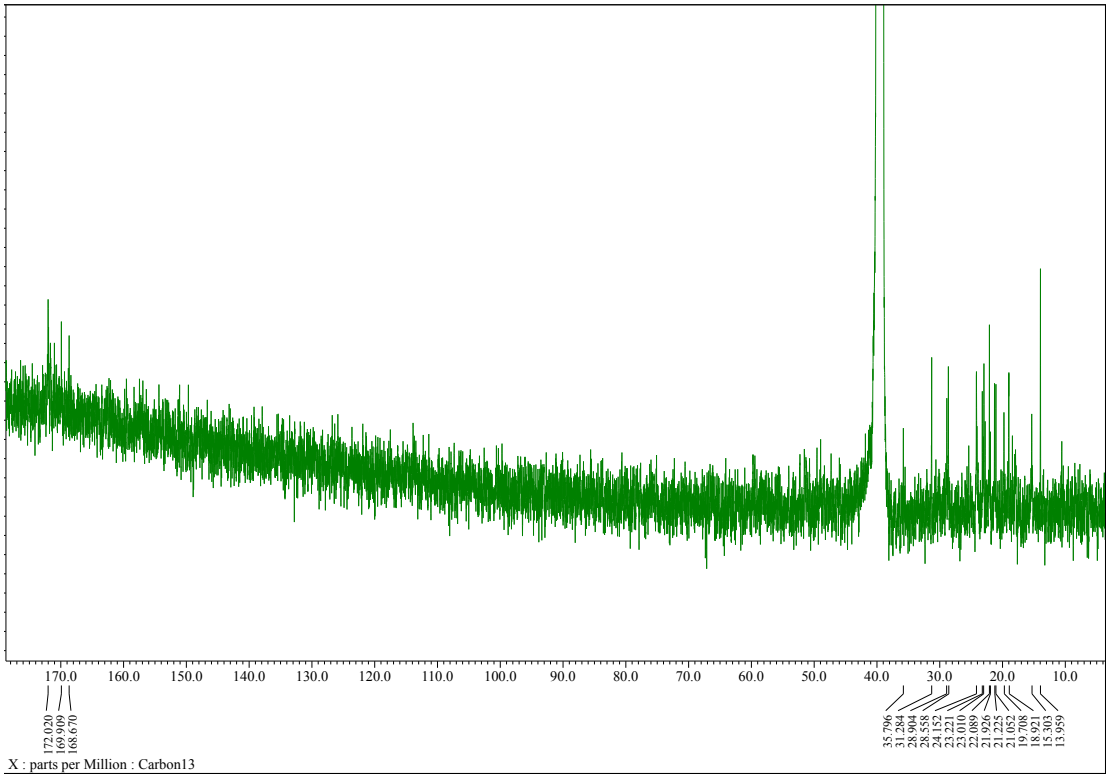

Figure 86. ^{13}C NMR spectrum of 5. Solvent : dmso-d_6; T : 23°C; Scans : 20000

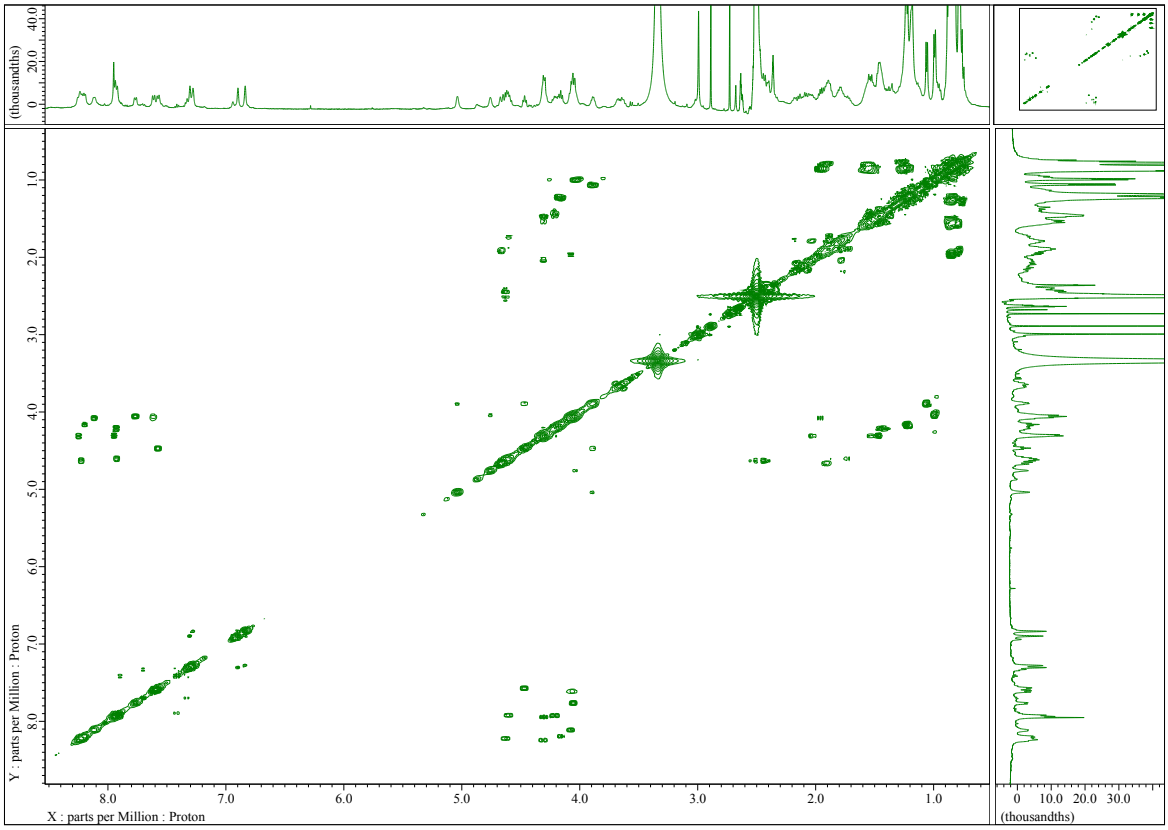

Figure 87. COSY spectrum of 5. Solvent : dmso-d_6; T : 23°C; Scans : 8192

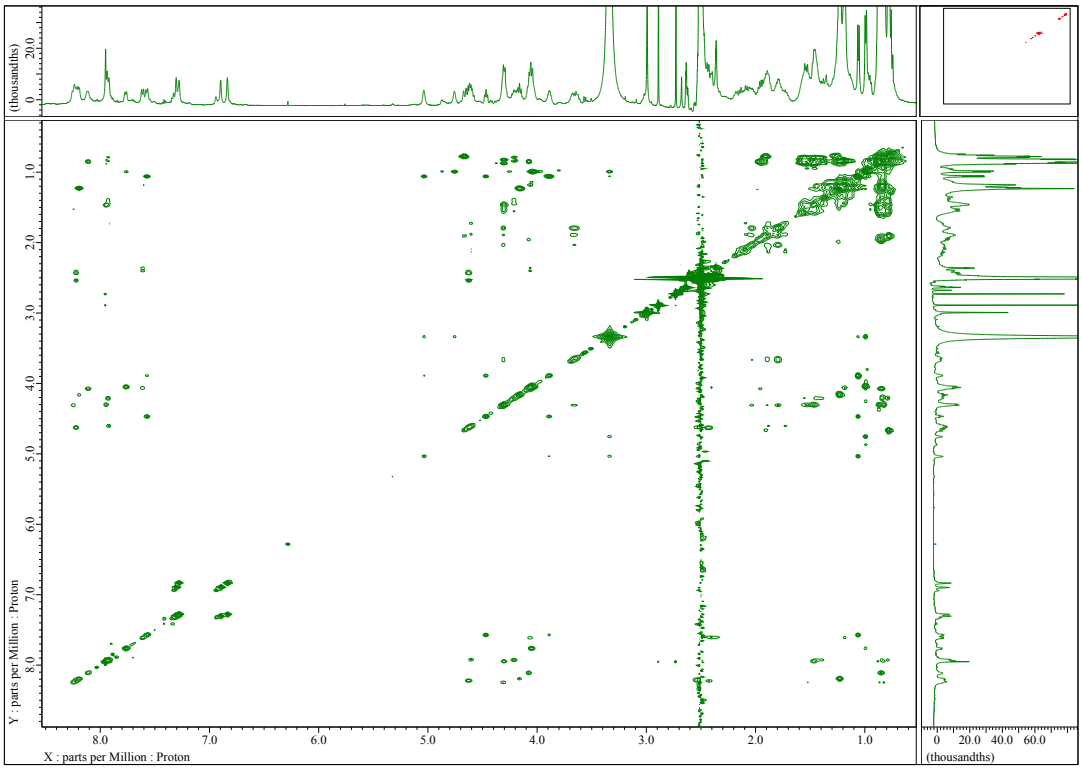

Figure 88. TOCSY spectrum of 5. Solvent : dmso-d_6; T : 23°C; Scans : 8192

c) Compound 6

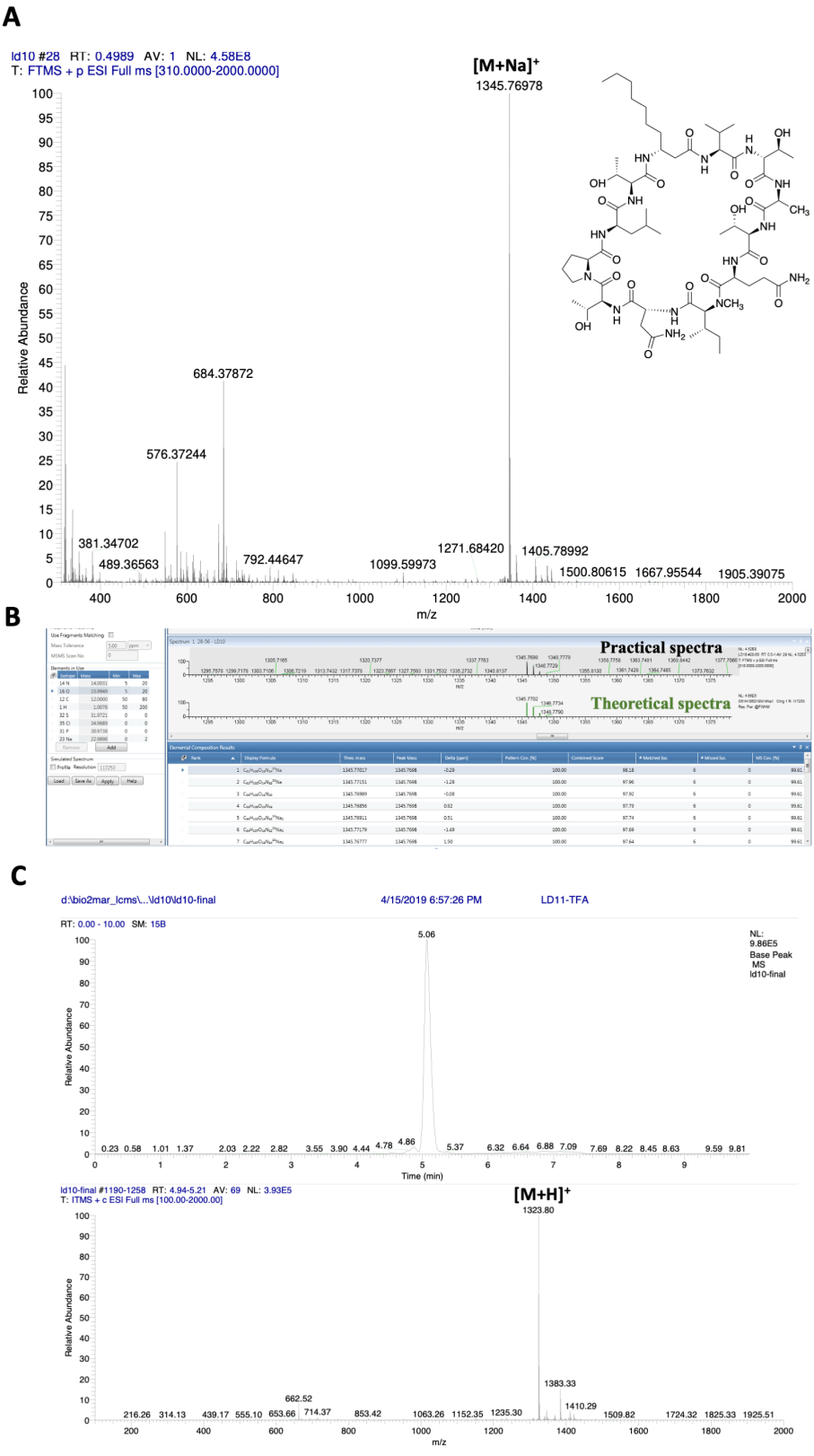

Figure 89. A) ESI-HRMS spectrum of the deprotected purified cyclic peptide from the synthesis of 6. B) Comparison with the theoretical spectrum. Calculated for $C_{61}H_{106}N_{14}O_{18}Na$ $[M+Na]^+$ *m/z* 1345.77017; Found $[M+Na]^+$ *m/z* 1345.7698; mass error = 0.29 ppm. C) LC-MS profile of the purified 6.

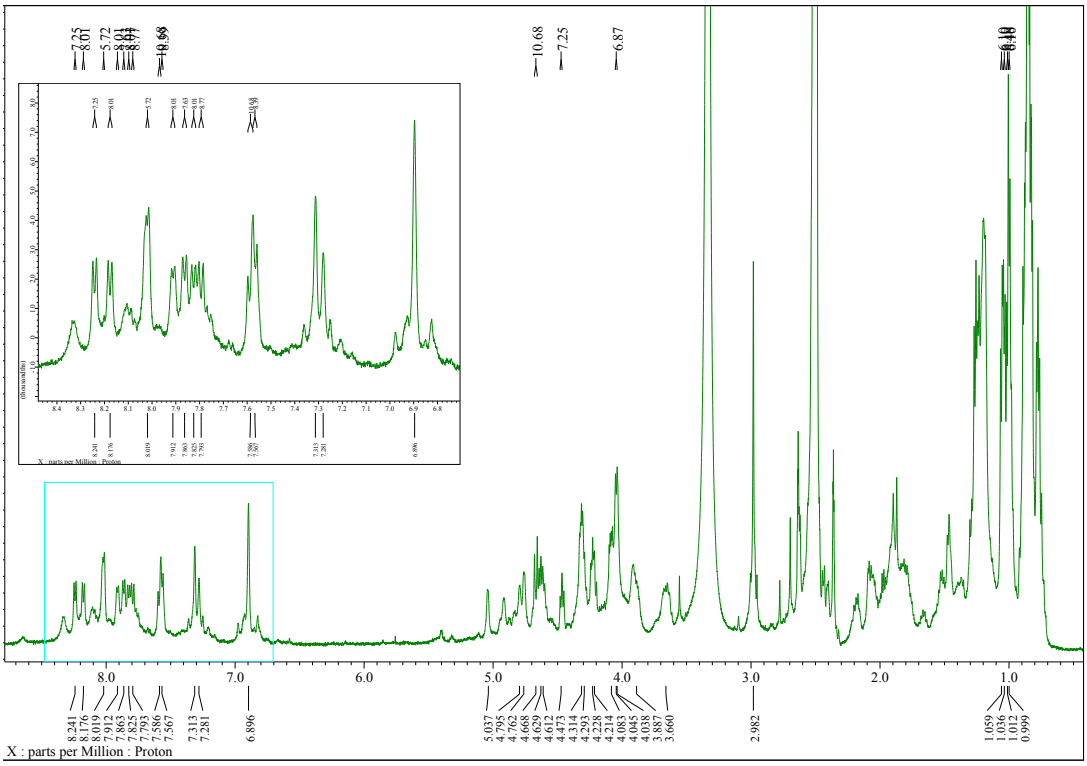

Figure 90. ^{1}H NMR spectrum of 6. Solvent : dmso-d_6; T : 23°C; Scans : 32

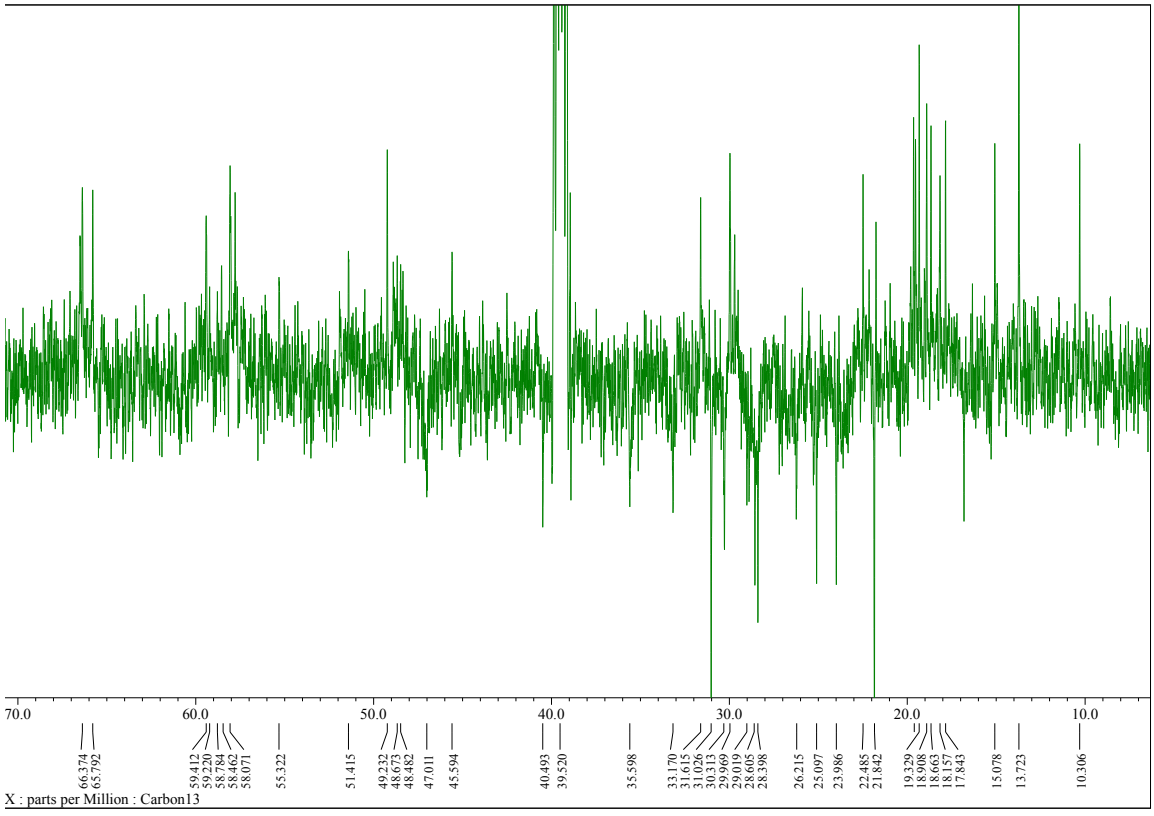

Figure 91. DEPT135 spectrum of 6. Solvent : dmso-d_6; T : 23°C; Scans : 10000

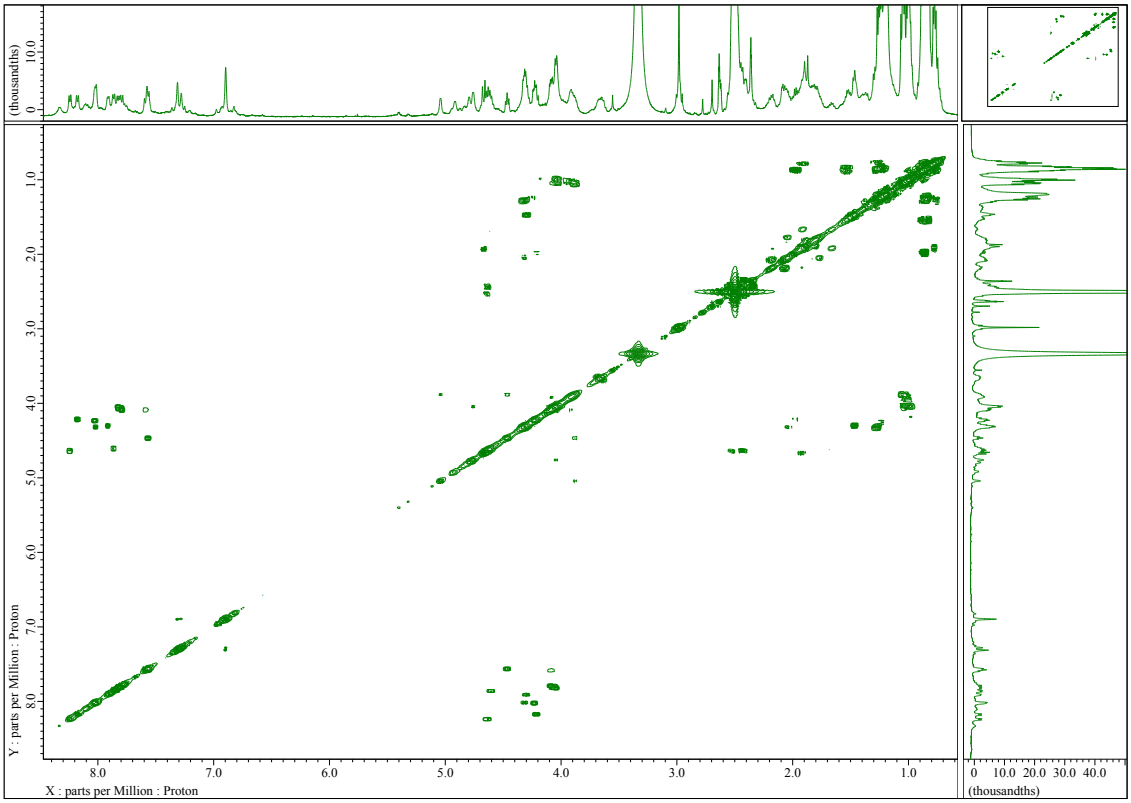

Figure 92. COSY spectrum of 6. Solvent : dmso-d_6; T : 23°C; Scans : 8192

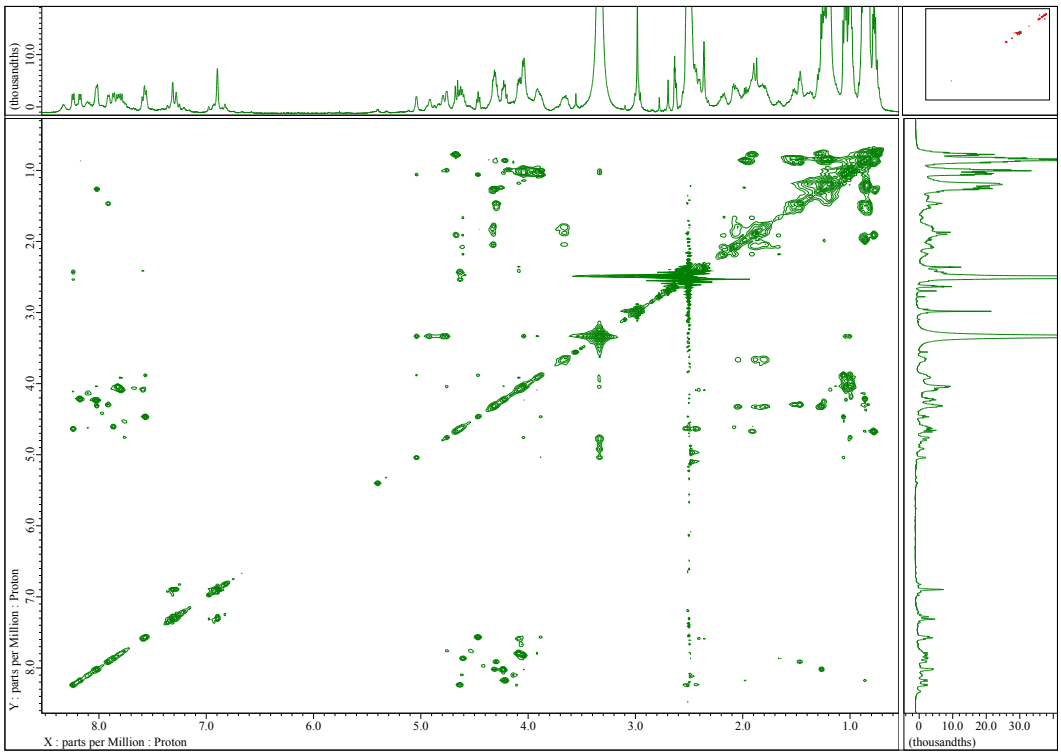

Figure 93. TOCSY spectrum of 6. Solvent : dmso-d_6; T : 23°C; Scans : 8192

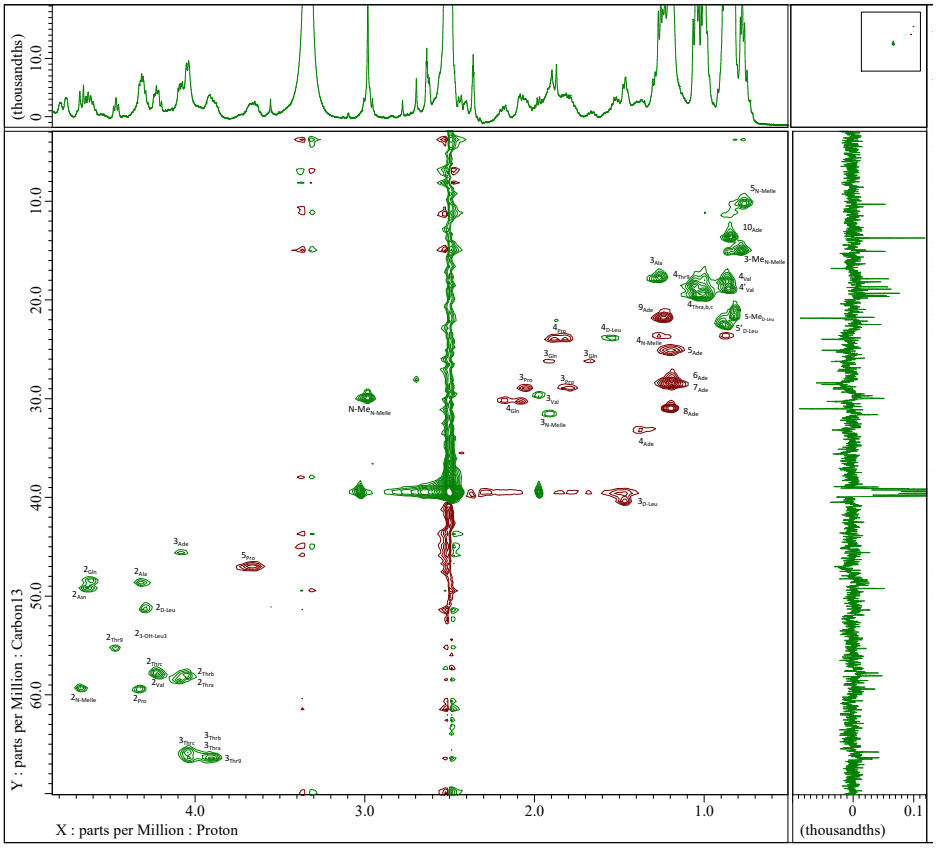

Figure 94. HSQC spectrum of 6. Solvent : dmso-d_6; T : 23°C; Scans : 8192

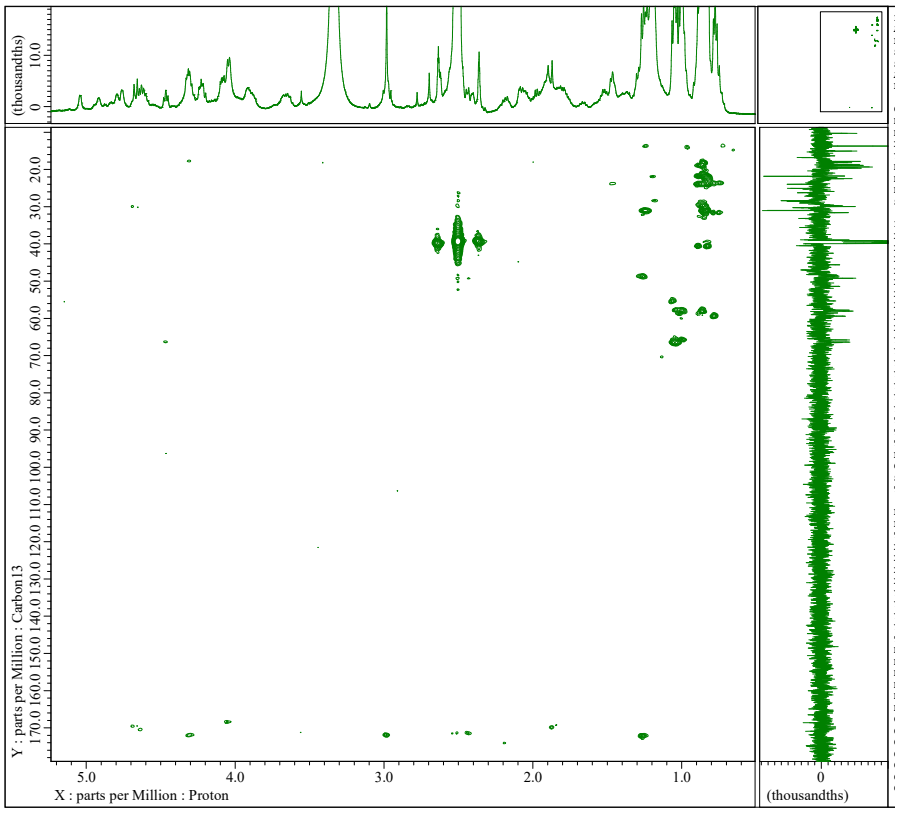

Figure 95. HMBC spectrum of 6. Solvent : dmso-d_6; T : 23°C; Scans : 16384

Chapter 3.
D-peptidase activity in a marine mollusk detoxifies a non-ribosomal cyclic lipopeptide

This chapter is partly based on an article we published in *Journal Of Medicinal Chemistry* [31]:

Darcel, L.; Bornancin, L.; Raviglione, D.; Bonnard, I.; Mills, S.C.; Sáez-Vásquez, J.; Banaigs, B.; Inguimbert, N. D-Peptidase Activity in a Marine Mollusk Detoxifies a Nonribosomal Cyclic Lipopeptide: An Ecological Model to Study Antibiotic Resistance. *J. Med. Chem*. **2021**, 64, 6198–6208, doi:10.1021/acs.jmedchem.1c00249.

In this chapter, a lot of additional information has been added, complementary to the article.

I. Laxaphycin B cleavage

A. Identification of acyclic laxaphycin B

The study of the cyanobacterium *Anabaena torulosa* harvested during a bloom in Moorea in French Polynesia, revealed the presence of acyclolaxaphycin B (acyclolaxB) derived from the toxic laxaphycin B (Figure 96-A). Acyclolaxaphycin B is open between (2R,3S)-HyLeu in position 3 and L-alanine in position 4 [18]. As the starting point of NRPS biosynthesis of laxaphycin B is Ade^{1} and elongation continues to the C-terminal Thr^{12} with the final cyclization mediated by a thioesterase [58], it is unlikely that the acyclolaxaphycin is the result of a malfunction of the NRPS, but more likely results from a biotransformation process of laxaphycin B by external agents. LC-MS analysis of the digestive tract of *S. striatus* showed that acyclolaxaphycin B had lost Ala^{4} and (2R,3S)-$HyLeu^{5}$ confirming a biotransformation process (Figure 96-D) [54], while the non-toxic laxaphycin A (**1**) was bioaccumulated in the same digestive gland (Dg), but not degraded or biotransformed. Subjecting laxaphycin B (**2**) to extracts of the sea hare's digestive gland highlighted that the transformation is a two-steps process beginning with the opening of the macrocycle accompanied with a mass increase of 18 *m/z*, followed by the deletion of Ala^{4} and (2R,3S)-$HyLeu^{5}$ and a loss in mass of 200 *m/z*.

In this chapter, the peptides will be labelled using a number and a letter corresponding to the initial compound and the stage along the cleavage process, respectively. For example, compound **2a** is the cyclic laxaphycin B, compound **2b** is the first intermediate after an increase in mass of 18 *m/z* and **2c** is the final stage of the biotransformation process after a loss in mass of 200 *m/z* (in the case of **2a**).

We hypothesize that the detoxification mechanism involved an enzyme targeting the D-amino acid in positions 3 and 5 of laxaphycin B. Indeed, successive cleavages occur at the C-ter part of two (2R,3S)-HyLeu, suggesting a specificity for these amino acids. However, from this analysis it was difficult to determine if the first cleavage occurred at the C-ter of the (2R,3S)-HyLeu in position 3 resulting in the already known acyclolaxaphycin B (**2d**) (Figure 96-A) or in position 5 producing compound **2b** (Figure 96-C).

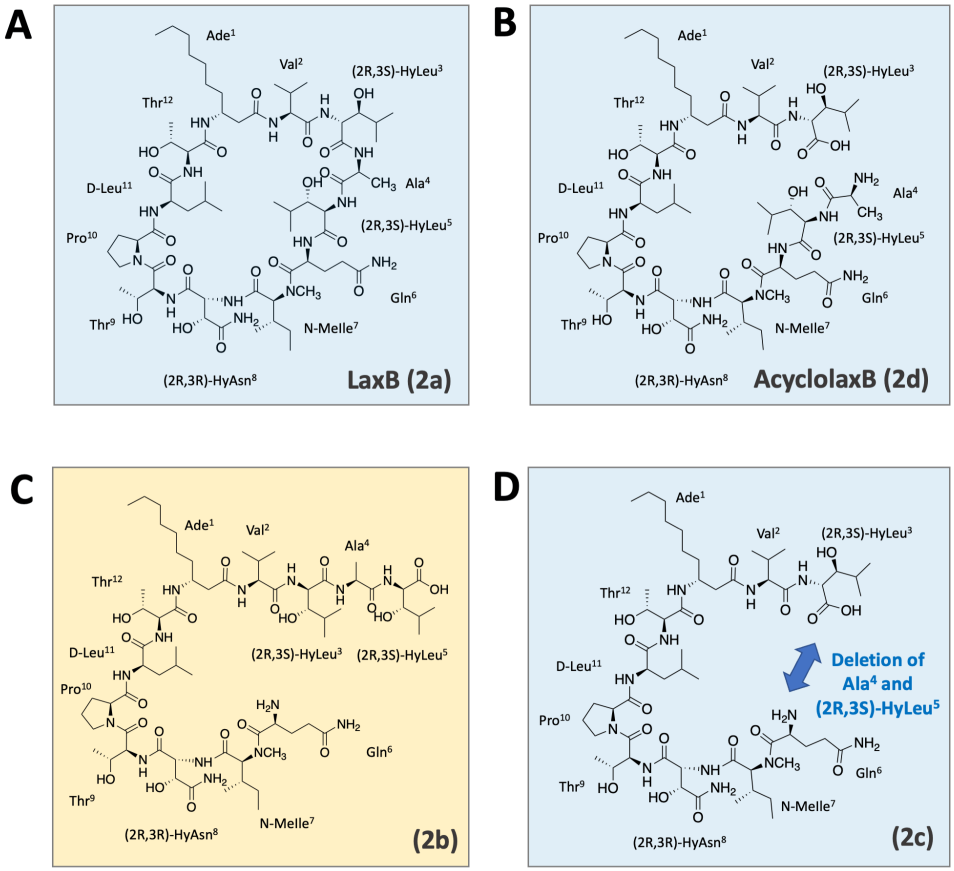

Figure 96. A) Structure of laxaphycin B (2a) isolated from the cyanobacterium *Anabaena torulosa* B) Structure of acyclolaxaphycin B (2d) isolated from the cyanobacterium *Anabaena torulosa*. C) Hypothetical structure of the intermediate acyclic laxaphycin (2b) obtained during the cleavage process of laxaphycin B (2a). D) Structure of acyclic laxaphycin B (2c) isolated from the sea hare *Stylocheilus striatus*.

B. Choice of the study model: *Stylocheilus striatus* fed on *Lyngbya majuscula*

To examine the transformation process of laxaphycin B over time we used *S. striatus* collected from a bloom of *L. majuscula* in Moorea. Unlike *A. torulosa*, *L. majuscula* does not produce laxaphycins and thus *S. striatus* will not be contaminated by acyclic laxaphycins, simplifying the monitoring of laxaphycin B (**2a**) transformation. In order to ensure that *S. striatus* taken from *L. majuscula* has the capacity to transform **2a**, individual *S. striatus* were collected from, and fed on, *L. majuscula* as well as from *A. torulosa* as a comparison. All individuals were dissected and their different organs analyzed. As expected, LC-MS analyses detected acyclic laxaphycin B **2c** within the digestive glands of *S. striatus* collected from *A. torulosa* (*Dg-Ss-At*), but not within the digestive glands of *S. striatus* collected from *L. majuscula* (*Dg-Ss-Lm*) (Figure 97).

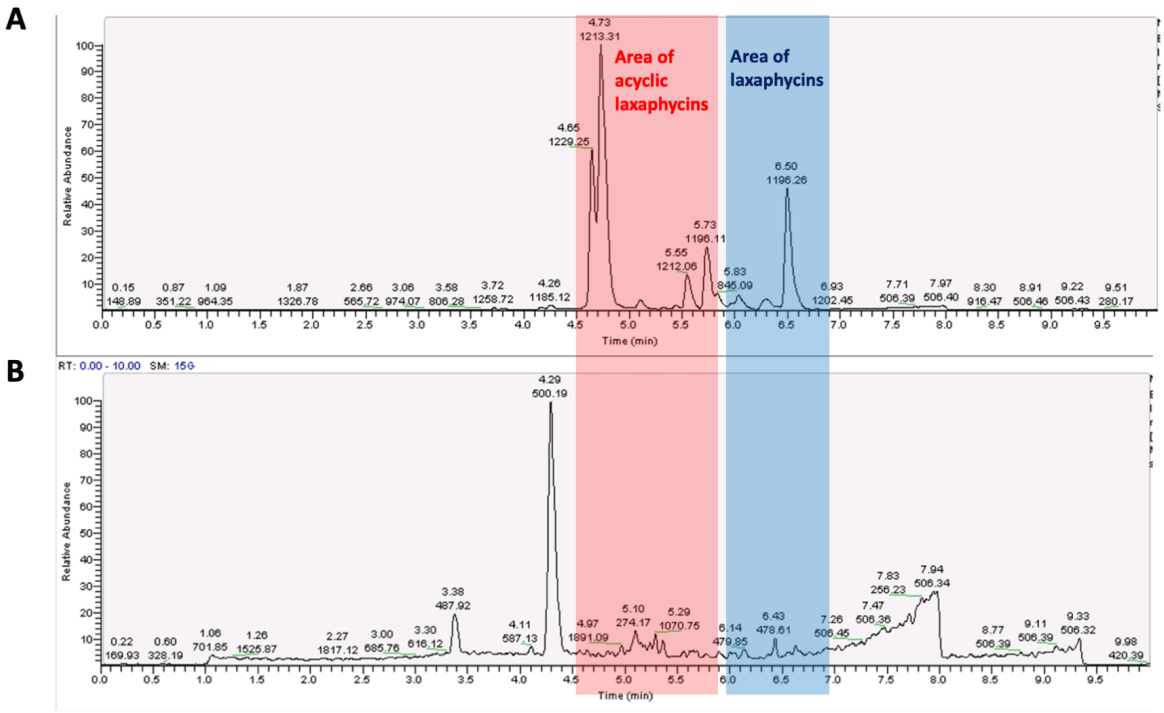

Figure 97. A) Composition of *Dg-Ss-At* extract at 30°C, pH 8. B) Composition of *Dg-Ss-Lm* extract at 30°C, pH 8.

2a is thus detoxified within *Dg-Ss-Lm* to give the non-toxic acyclic laxaphycin **2c** [54]. Furthermore, addition **2a** to digestive gland extracts of *S. striatus* collected from *L. majuscula* confirms that *S. striatus* does have the capacity to cleave **2a** given that we observed the decrease of **2a** to the benefit of acyclic laxaphycin B **2c** by LC-MS (Figure 98). These results were reproduced using different batches of digestive glands from different individuals whose proteins levels were kept constant during each experiment via quantification using the Bradford method [167]. We confirmed that linearization of **2a** occurred with cleavage at the C-terminal position of the two HyLeu and was repeatable over 21 batches of digestive gland extracts obtained from 11 *S. striatus*.

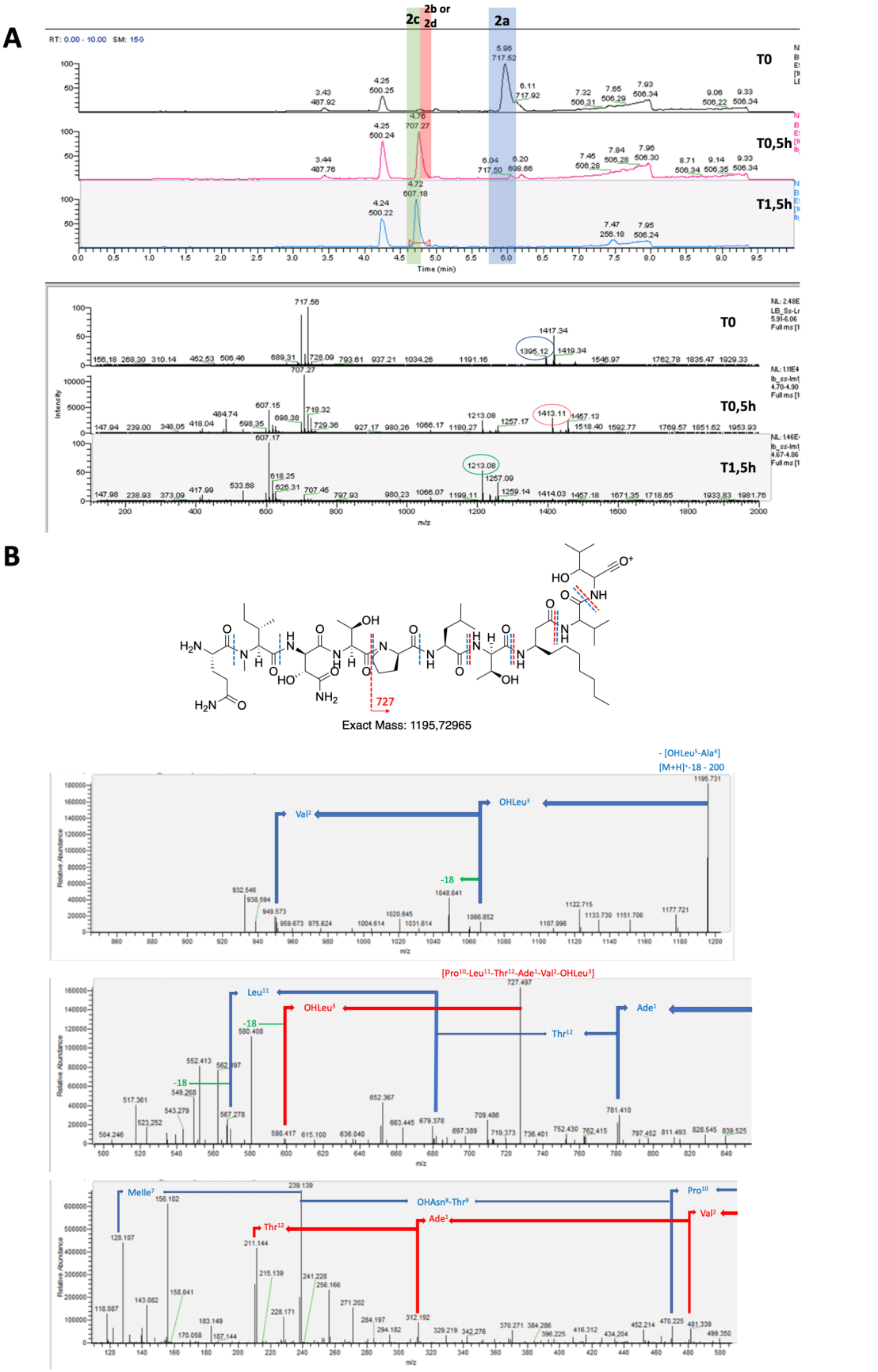

Figure 98. A) LC-MS kinetic monitoring of 2a cleavage with *Dg-Ss*-Lm extract and masses corresponding to the LC-MS peaks of 2a-d. B) MS-MS analysis of 2c confirming its structure.

To better characterize this enzyme, we hereafter used digestive gland extracts of *S. striatus* fed on *L. majuscula* (*Dg-Ss-Lm*) having confirmed its capacity to cleave **2a**.

We tried to degrade **2a** in presence of *Dg-Ss-At* or *Dg-Ss-Lm* at two different pH, pH 5 and pH 8, at a temperature of 30°C which is closer to the temperature conditions in the natural environment. For that purpose, we used Tris buffer at pH 8 and citric acid/Tris sodium citrate buffer at pH 5. The stability of **2a** alone under these same conditions was also tested as a control. At both pH levels, **2a** was stable and no degradation products were observed after 24 hours. At pH 5, no significant degradation was observed whether **2a** was exposed to *Dg-Ss-At* or *Dg-Ss-Lm*. In contrast, at pH 8, a decrease in **2a** to acyclic laxaphycin was observed, with a more rapid total loss of **2a** with *Dg-Ss-Lm* than *Dg-Ss-At* (Figure 99). Since the ocean pH is close to 8, this result is consistent. For further experiments, we chose to perform the cleavage tests at 30°C and pH 8 with *Dg-Ss-Lm* extracts.

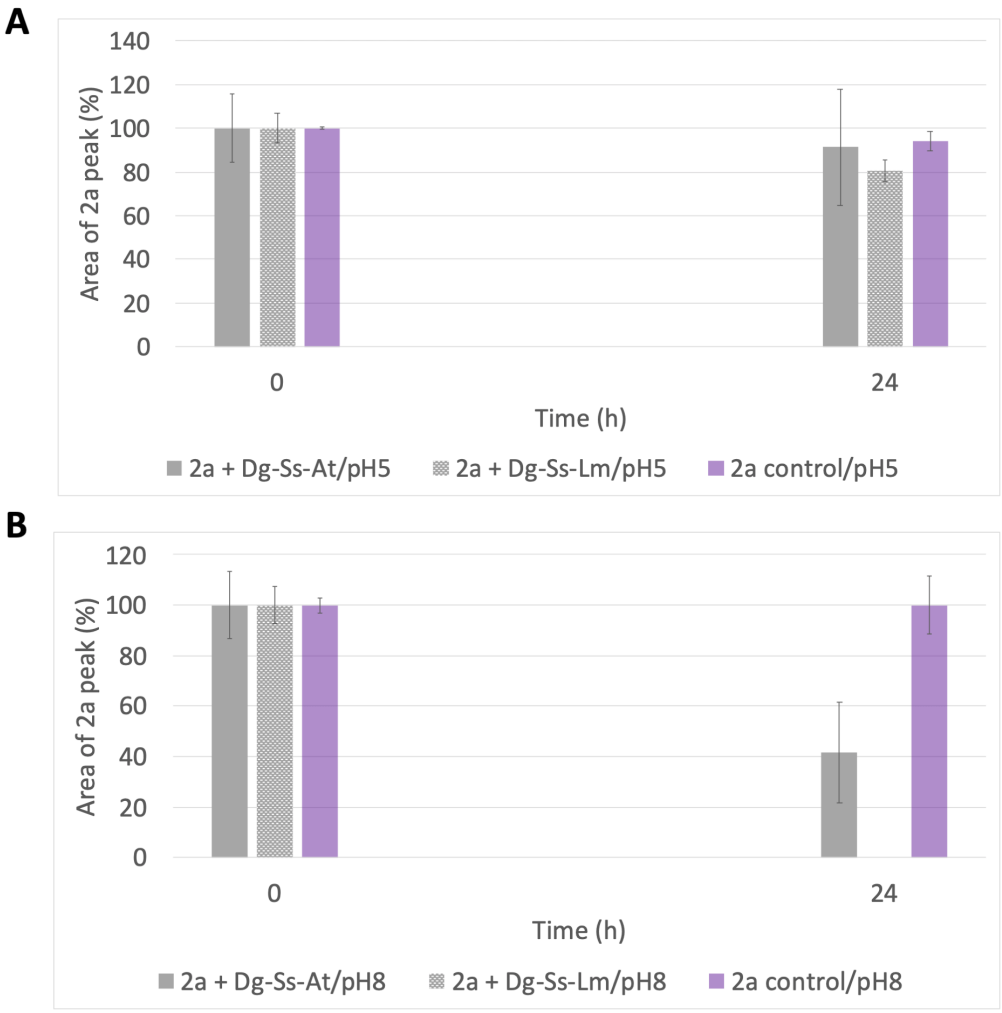

Figure 99. A) Evolution of 2a peak area as a function of incubation time at 30°C, pH = 5, in the presence of *Dg-Ss-At* or *Dg-Ss-Lm*. In solid grey, 2a + *Dg-Ss-At*; in striped grey, laxB + *Dg-Ss-Lm*; in purple, 2a control without *Dg-Ss*. B) Evolution of 2a peak area as a function of incubation time at 30°C, pH = 8, in the presence of *Dg-Ss-At* or *Dg-Ss-Lm*. In solid grey, 2a + *Dg-Ss-At*; in striped grey, 2a + *Dg-Ss-Lm*; in purple, 2a control without *Dg-Ss*.

C. Stability of laxaphycins

As a prerequisite of this study, we verified that laxaphycins **1a** and **2a** do not show any intrinsic susceptibility to cleave when exposed to protease or rat serum even though their cyclic structures and the presence of non-ribosomal amino acids should prevent their cleavage. Both peptides remained stable in Tris buffer at pH 8 when exposed to rat serum at a protein concentration of 10 mg/mL for 24 hours (Figure 100).

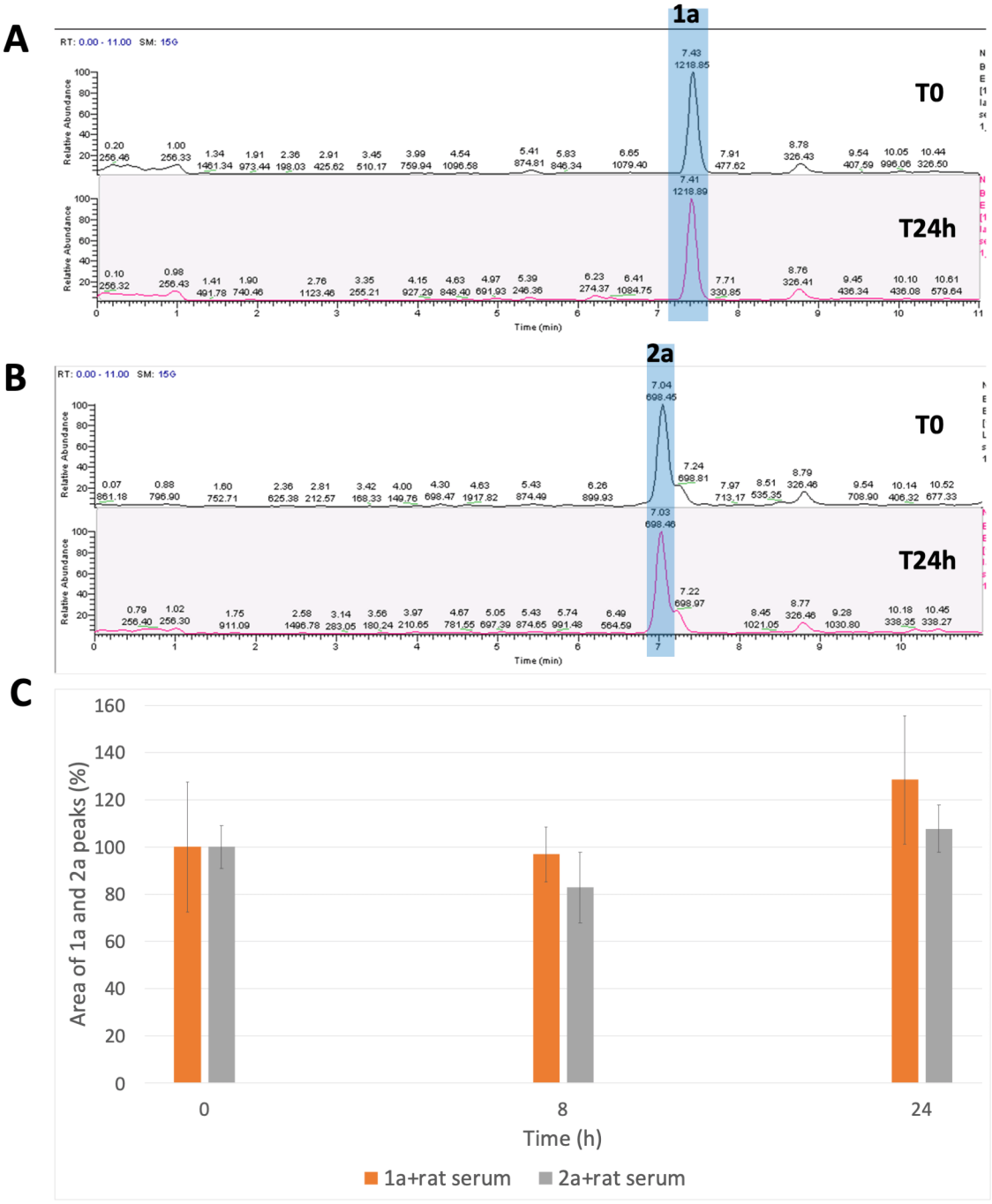

Figure 100. A) 1a evolution over time with rat serum (T=0 and T=24h). B) 2a evolution over time with rat serum (T=0 and T=24h). C) Evolution of 1a and 2a peaks area as a function of incubation time at 37°C, pH = 8, in the presence of rat serum.

To complete this study, compound **2a** was tested against known enzymes with broad substrate specificities: Pepsin, Elastase and Thermolysin (TLN). After a literature investigation, we found an enzyme, Subtilisin, which could cleave gramicidin S, a cyclic peptide used as an antibiotic. This enzyme was therefore added to our pool of tested enzymes.

Table 12. Type of enzymes used and their cleavage preferences.

Enzyme name	Pepsin	Elastase	Thermolysin	Subtilisin
Enzyme type	Aspartic peptidase	Serine protease	Metallo peptidase	Serine protease
Cleavage preference	C-ter of Phe, Leu, Tyr, Trp	C-ter of Ala, Val, Ser, Gly, Leu, Ile	N-ter of Leu, Phe, Val, Ile, Ala, Met	Could cleave in N-ter of Leu

These enzymes were used at their optimal pH and temperature conditions, with an enzyme substrate *E:S* ratio of *1:20*. The stability of laxaphycin B alone under the same conditions was verified and all the tests were performed in triplicate in order to check the reproducibility of the observations.

A certain stability of laxaphycin B is noted, whatever the pH or temperature used. No degradation fragments were observed during these stability tests. The stability of the cyclic peptide at 75°C shows its ability to resist rather extreme conditions (Figure 101-A).

Only TLN at pH 8 and 75°C resulted in the linearization of laxaphycin B **2a** (Figure 101-B), but differed from that observed in *S. striatus*, as cleavage occurred at the C-terminus of proline 10 (Figure 102), and the hydrolysis kinetics were very different. While laxaphycin B was almost completely linearized after 30 minutes in the presence of a digestive gland extracts (Figure 98-A), only 40% of laxaphycin B was consumed after 24 hours by TLN (Figure 101-B). By adding TLN twice during the enzymatic reaction, the degradation of laxaphycin B could be pushed further without being complete, showing again the difficulty to cleave this type of cyclic peptide.

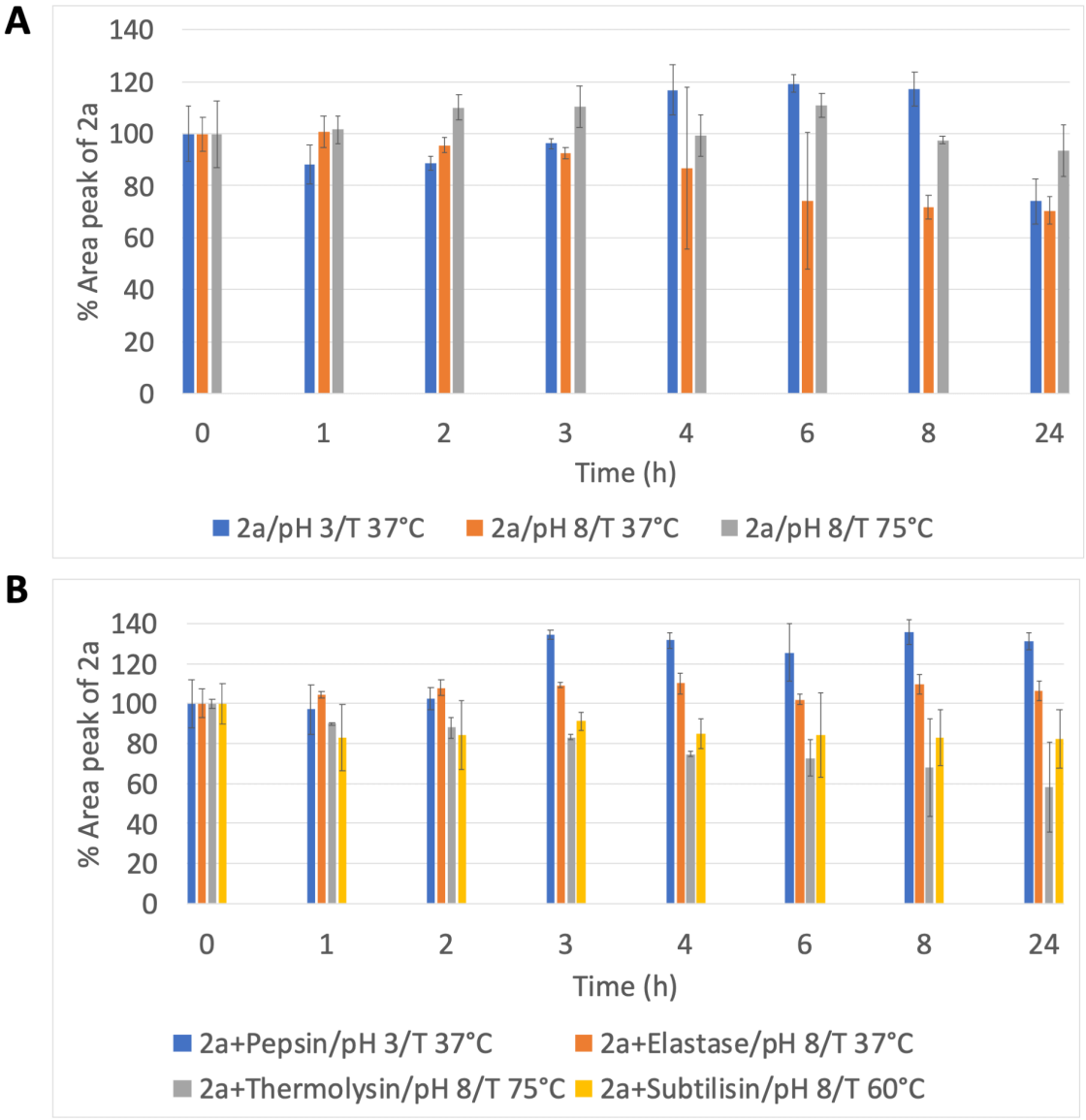

Figure 101. A) Evolution of 2a peak area as a function of incubation time at 37°C pH 3 or 8 and at 75°C pH 8 (control). B) Evolution of 2a peak area as a function of incubation time in the presence of different enzymes.

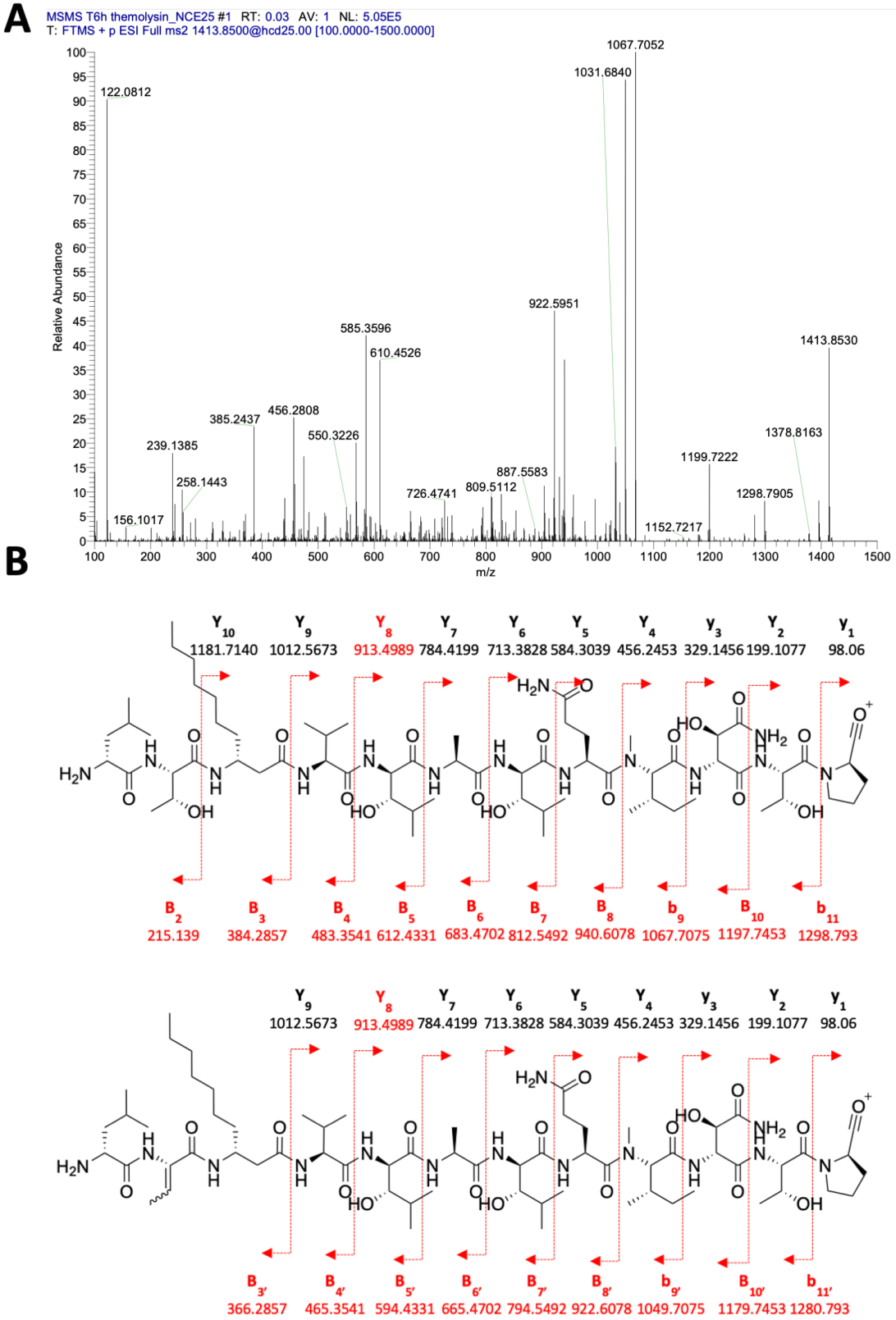

Figure 102. A) MS-MS analysis of the unknown acyclic laxaphycin peak. B) Interpretation of MS-MS analysis. Observed ions are in red color and non-observed ions are in black color.

These experiments support the fact that the two successive cleavages observed at the two HyLeu of **2a** do not correspond to a "classical" opening reproducible by known enzymes. The potential enzyme we are looking for would therefore have very specific characteristics. In addition, some classical protease inhibitor cocktails were tested on *Dg-Ss-Lm* extracts in the presence of **2a**. These inhibitors were used under the conditions recommended by their manufacturer.

Table 13. Protease inhibitor cocktails used with *Dg-Ss-Lm* and their composition or activity against proteases.

Protease inhibitor cocktails	**Composition or activity**	**Remaining % of 2a after 3h**
Control without inhibitors	**-**	0%
P9599 (from Sigma Aldrich)	**AEBSF** acts to inhibit serine proteases, including trypsin, chymotrypsin, and plasmin amongst others. **Bestatin** inhibits aminopeptidases. **E-64** acts against cysteine proteases. **Leupeptin** acts against both serine and cysteine proteases. **Pepstatin A** inhibits acid proteases. **1,10-Phenanthroline** acts against metalloproteases.	10%
MG132	Potent transition-state inhibitor of chymotrypsin like activity of proteasome machinery. **Aldehyde** also known to inhibit certain lysosomal cysteine proteases and the calpains hence MG132 may not be exclusive inhibitor of proteasomal pathway. Inhibitor of chymotrypsin-like, trypsin-like, and peptidylglutamyl peptide hydrolyzing proteasome activities.	0%
Mix of P9599 and MG132	-	17%
cOmplete Mini, EDTA-free (from Merck)	Inhibits a broad spectrum of serine and cysteine proteases Metallo and aspartic proteases are not inhibited.	~20%

None of these cocktails showed an important inhibition of **2a** degradation. Judging from these preliminary results, it would appear that the enzyme sought is not a metalloprotease. However, it should be noted that this experiment was only done once. The enzyme we are

looking for therefore responds very little to these types of inhibitors, making it even more interesting.

Further inspection of the enzyme highlighted that the biotransformation of **2a** was inactivated if the digestive gland extracts from *S. striatus* (*Dg-Ss-Lm*) were denatured at 90°C for 5 minutes. This result reveals that cleavage involves a heat-sensitive protein similar to the enzymes (Figure 103). Indeed, while **2a** was almost completely linearized in 30 minutes in the presence of a digestive gland extract, we still observed 80% of **2a** after 3 hours when mixing with the digestive gland that has been heated. It should also be noted that the control without *Dg-Ss-Lm* was also at 85% at the same period.

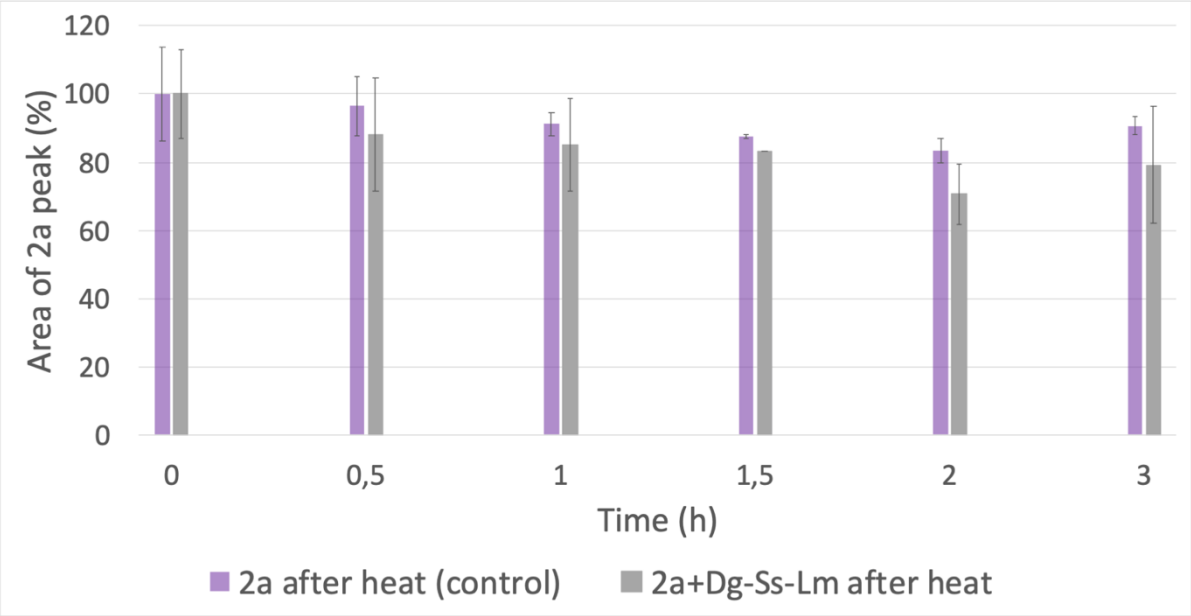

Figure 103. Evolution of 2a peak area as a function of incubation time at 30°C, pH 8, in the presence of *Dg-Ss-Lm* previously heated at 90°C.

II. Cleavage of laxaphycin B cyclic analogues 3a, 4a, 5a and 6a

2a is the archetype of a compound family that includes dozens of analogues slightly differing at the sequence level [18]. In order to define if the observed cleavage is restricted to **2a**, we used isolated natural laxB2 **3a** [18], synthesized trichormamide C **4a** and its analogues **5a** and **6a** (Figure 104) [30] to explore the importance of the nature of the amino acids at the cleavage positions 3 and 5, and also to examine the role of (2R,3R)-HyAsn in position 8, as this amino acid is replaced by a D-Asn in **4a-6a**. The stability of all these compounds alone in the buffer was evaluated as a control. All these peptides are stable at 30°C pH 8 over a tested duration of 24 hours (Figure 105).

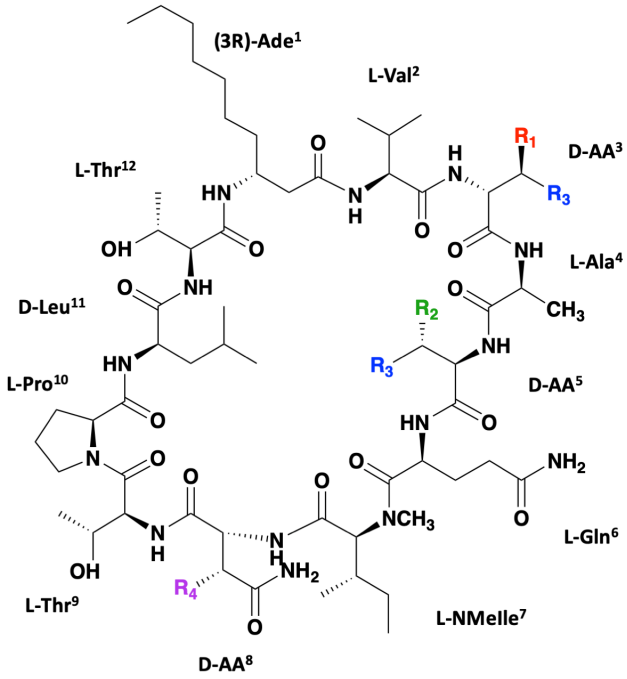

2a: R1=OH, R2=OH, R3=*i*Pr, R4=OH

3a: R1=OH, R2 =H, R3=*i*Pr, R4=OH

4a: R1=OH, R2=OH, R3=*i*Pr, R4 =H

5a: R1=H, R2=H, R3=*i*Pr, R4=H

6a: R1=OH, R2=OH, R3=Me, R4=H

Figure 104. Structure of 2a and its cyclic analogues 3a-6a

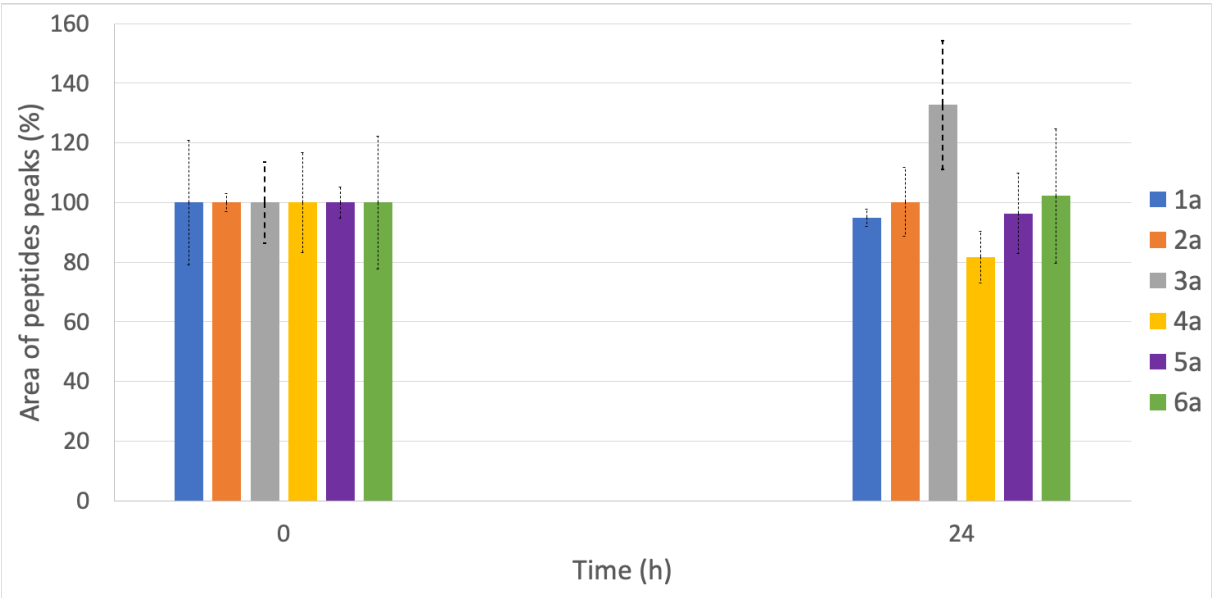

Figure 105. Stability over time of 1a-6a at 30°C in Tris buffer pH 8.

A. Impact of modifications at the cleavage point on the cleavage of laxaphycin B analogues

The structure of **3a** only differs from **2a** by one amino acid, a D-Leu instead of the (2R,3S)-HyLeu in position 5. **4a** possesses a D-Asn in position 8 instead of the (2R,3R)-HyAsn. These slight differences did not affect the outcome of the cleavage of **3a** and **4a** with *Dg-Ss-Lm* extracts and LC-MS analyses confirmed that the linearized compounds **3c** and **4c** were obtained by a cleavage at the C-ter of amino acids in position 3 and 5 (Figure 106, Figure 107). Following this observation, we used compounds **5a** and **6a** that might be considered as **3a** and **4a** hybrids. These fully synthetic compounds **5a** and **6a** have two D-Leu or two D-Thr respectively, instead of the two (2R,3S)-HyLeu present in **2a** and **4a**. For both compounds we observed similar cleavage at the C-ter of the D-Leu or the D-Thr to give **5c** and **6c**, respectively (Figure 108, Figure 109). Thus, **5a** and **6a** are cleaved at the same location as **2a** and **4a** despite the modification of the amino acids at the cleavage site. MS-MS studies confirm the formation of linear fragments noted **c**, following a similar fragmentation pattern for each peptide. While the enzyme has not a strict specificity for hydroxyleucines, since the two synthetic analogues **5a** and **6a** are also recognized, the enzyme shows a preference for D-amino acids bearing an alkyl side chain at P1 position.

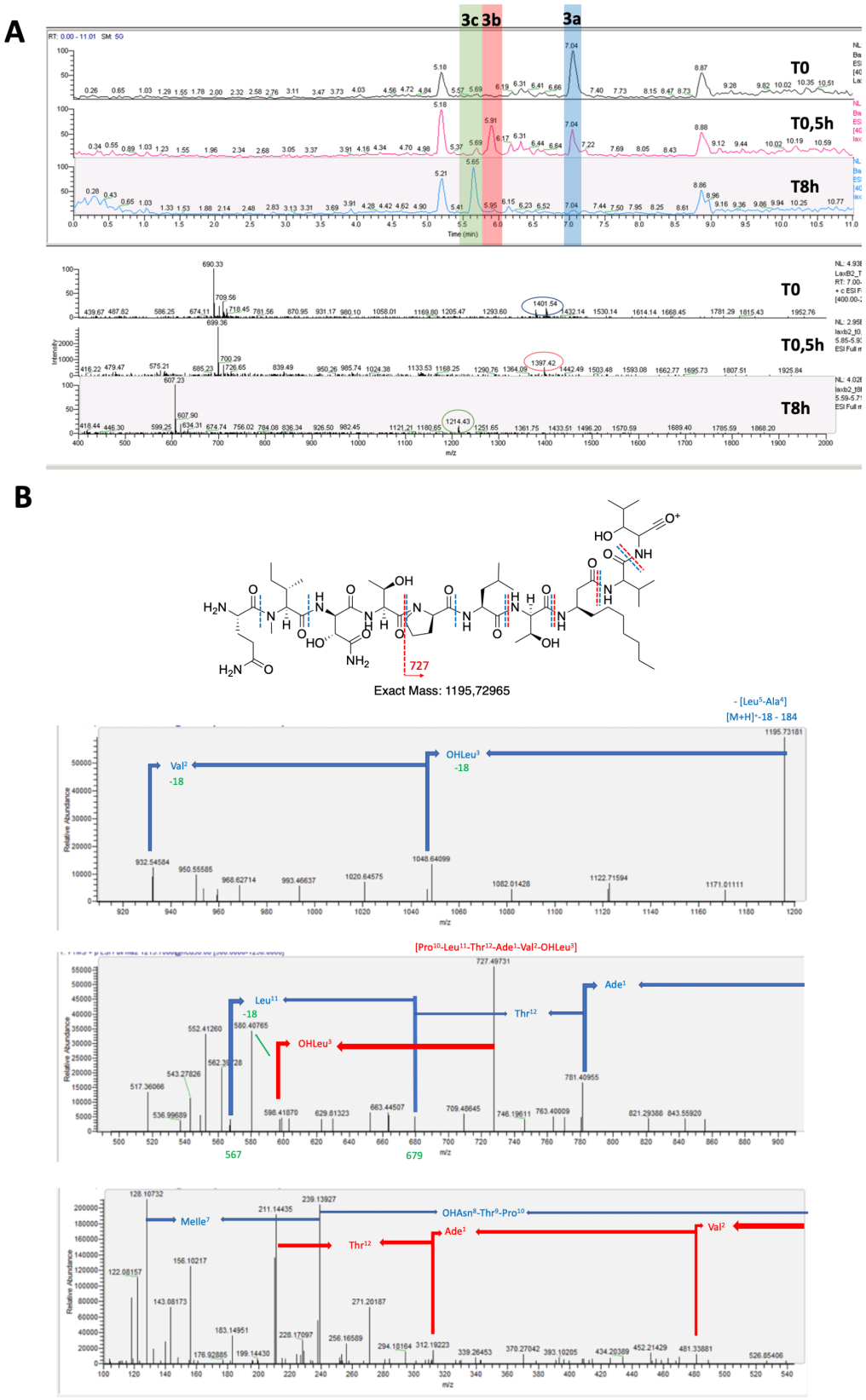

Figure 106. A) LC-MS kinetic monitoring of 3a cleavage with *Dg-Ss-Lm* extract and masses corresponding to the LC-MS peaks of 3a-c. The compound at 5.18 min belongs to the digestive gland extract. B) MS-MS analysis of 3c confirming its structure.

For clarity, the MS-MS spectrum was cut into several mass ranges to allow visualization of all fragmentations.

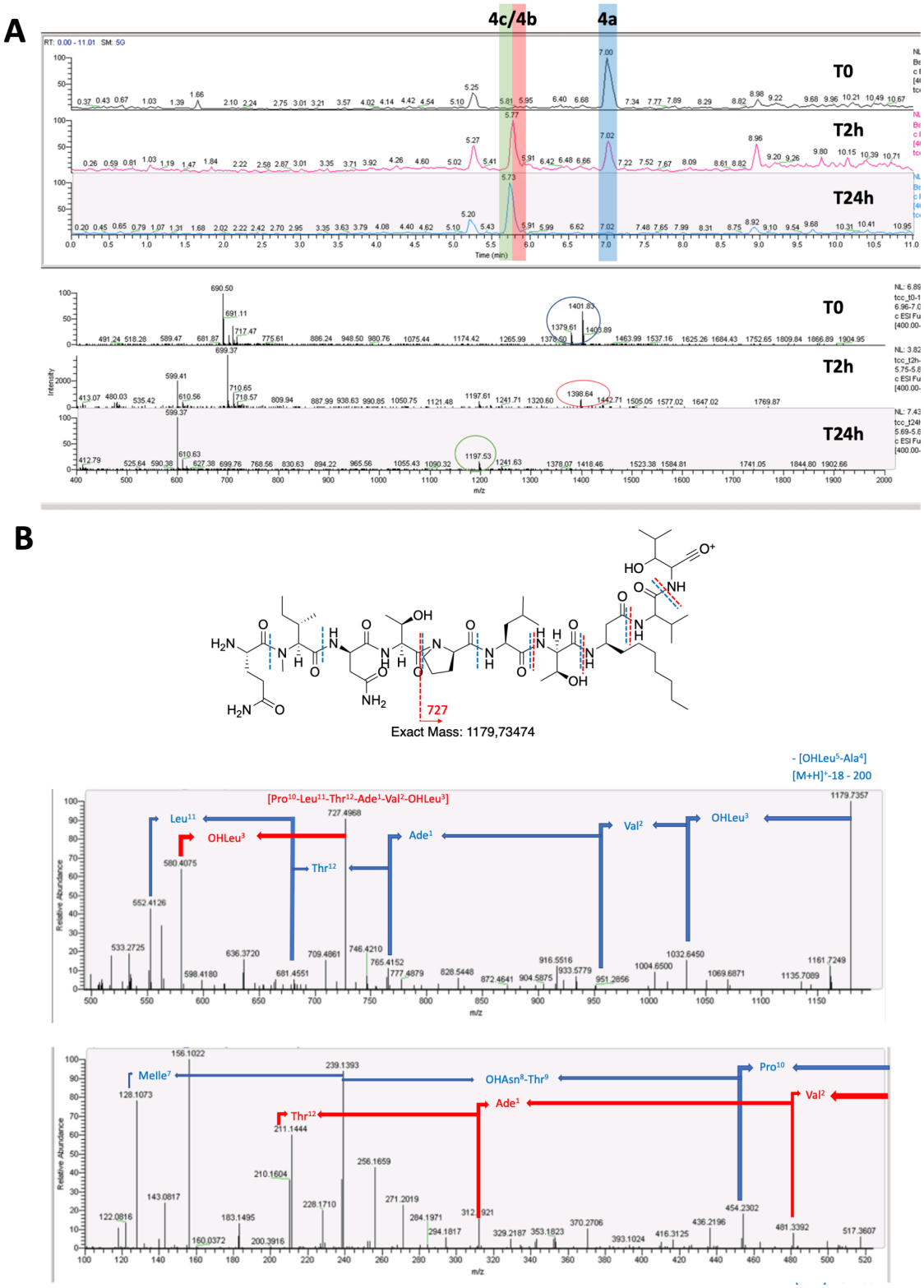

Figure 107. A) LC-MS kinetic monitoring of 4a cleavage with *Dg-Ss-Lm* extract and masses corresponding to the LC-MS peaks of 4a-c. The compound at 5.25 min belongs to the digestive gland extract. B) MS-MS analysis of 4c confirming its structure.

For clarity, the MS-MS spectrum was cut into several mass ranges to allow visualization of all fragmentations.

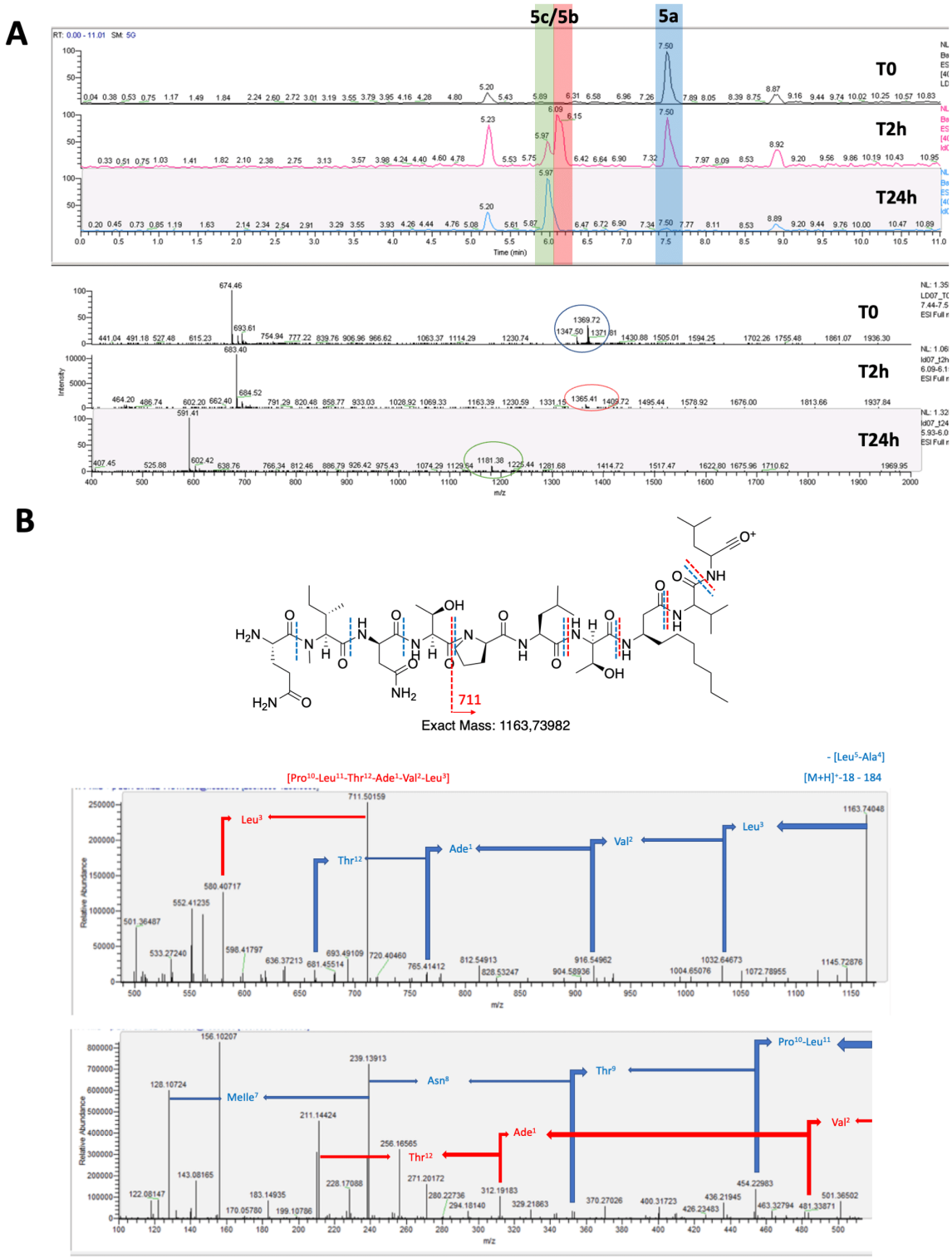

Figure 108. A) LC-MS kinetic monitoring of 5a cleavage with *Dg-Ss-Lm* extract and masses corresponding to the LC-MS peaks of 5a-c. The compound at 5.20 min belongs to the digestive gland extract. B) MS-MS analysis of 5c confirming its structure.

For clarity, the MS-MS spectrum was cut into several mass ranges to allow visualization of all fragmentations.

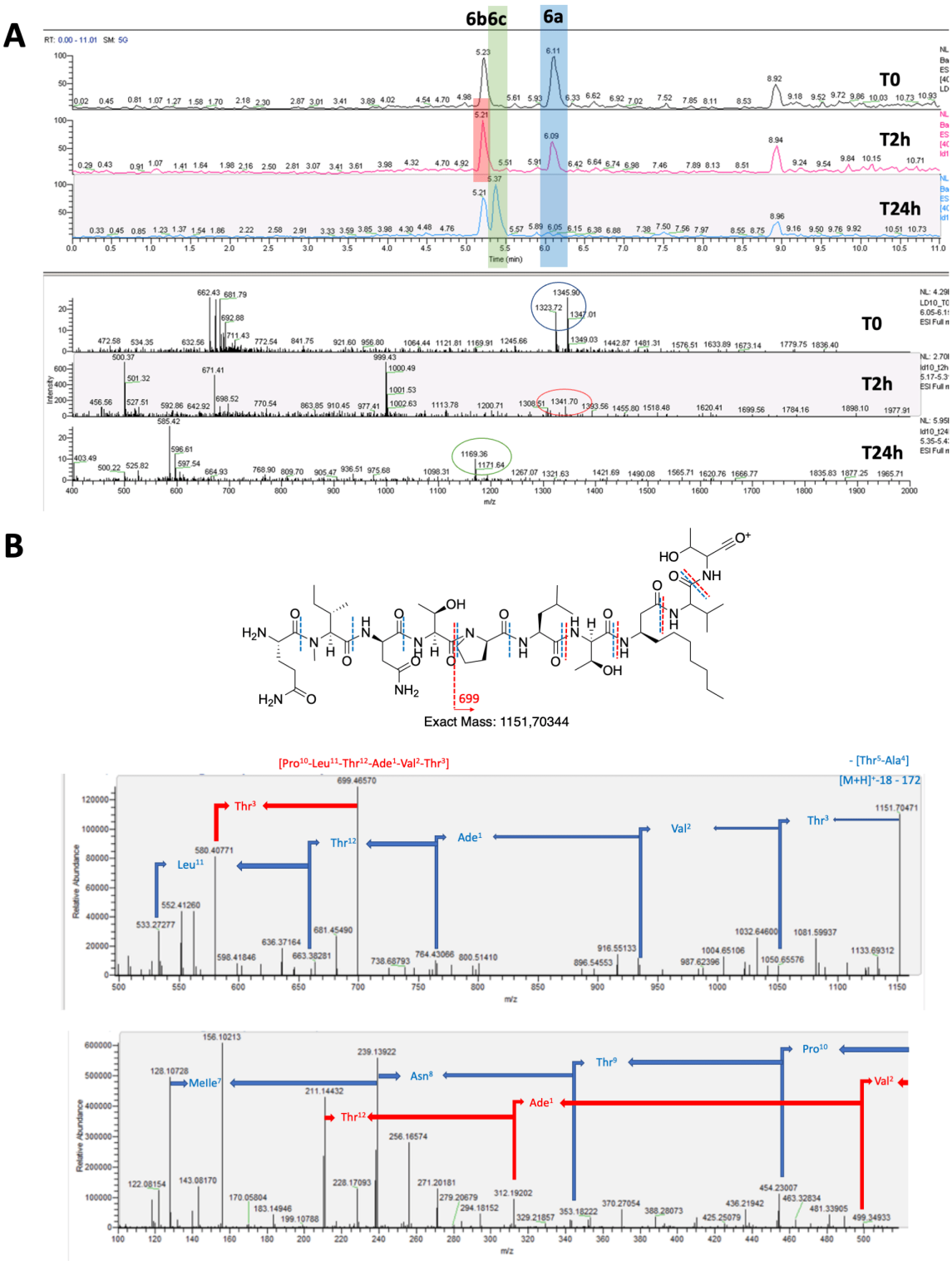

Figure 109. A) LC-MS kinetic monitoring of 6a cleavage with *Dg-Ss-Lm* extract and masses corresponding to the LC-MS peaks of 6a-c. The compound at 5.21 min belongs to the digestive gland extract and co-elute with

**compound 6b .B) MS-MS analysis of 6c confirming its structure.
For clarity, the MS-MS spectrum was cut into several mass ranges to allow visualization of all fragmentations.**

Furthermore, we observed that the cleavage rate of **2a**, **3a**, **4a** and **5a** was similar during the first few hours and 90% or more of the substrate was consumed within four hours. For **6a** the macrocycle opening was slightly slower than the others with as much as 25% of **6a** remaining 8 hours after the beginning of the reaction, while a comparable of cleavage occurred for the other compounds in less than three hours (Figure 110). On the other hand, laxaphycin A having a different structure, is not degraded in the presence of these extracts.

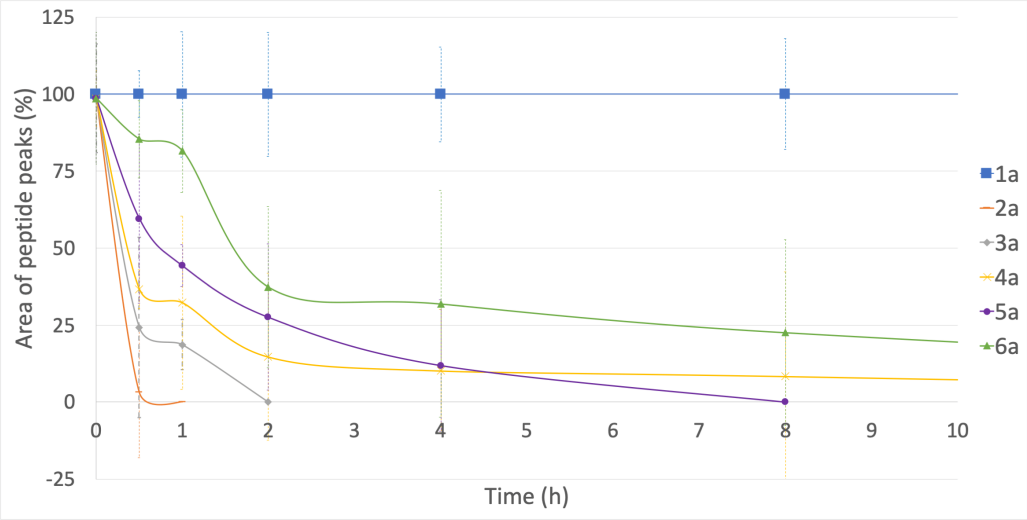

Figure 110. Cleavage rate of laxaphycin B-type peptides 2a-6a, compared to that of laxaphycin A 1a (average rate), as a function of incubation time of the peptide with *Dg-Ss-Lm*

The previous graph shows that the analogue **6a** seems to degrade less rapidly than the others. We therefore decided to put **2a** and **6a** in competition for the enzyme, with **6a** in molar quantity 10 times higher than **2a**. Indeed, **2a** degrades much less quickly in the presence of **6a**, with a loss of 40% of **2a** in 1,5 hours while this rate is normally reached in 15 minutes without competition (Figure 111). **6a** is then able to compete with **2a** despite the fact that it is cleaves more slowly when used alone with Dg-Ss-Lm.

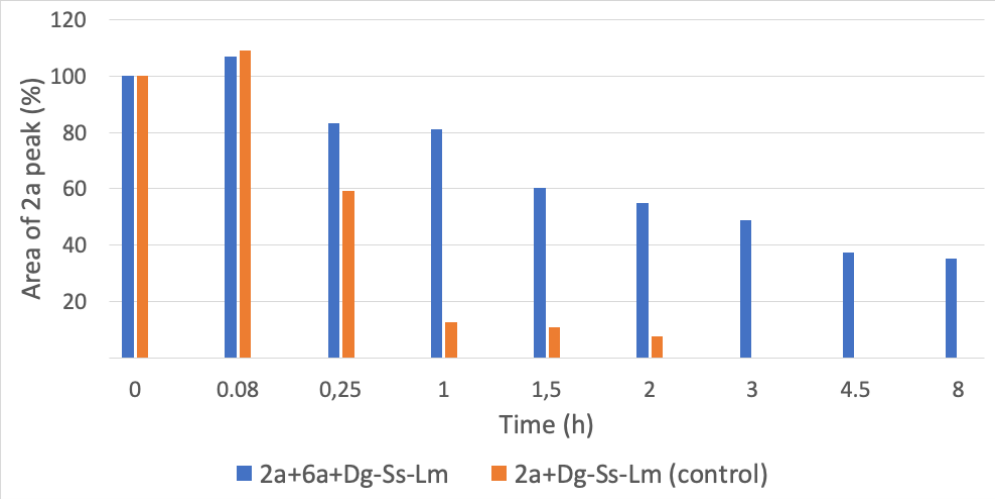

Figure 111. Cleavage rate of 2a with *Dg-Ss-Lm*, with or without competition with 6a. It should be noted that this experiment was done only once.

B. Determination of the cleavage direction

The peptides **3a**-**6a** confirmed that the enzymatic cleavage is a two-step process that deletes the amino acids in positions 4 and 5 of the macrocycle, but defining the location of the first cleavage point using MS-MS was not straightforward due to the observed dehydration of Thr or (2R,3S)-HyLeu that complicated the interpretation of the mass spectra as already reported [62]. To determine the order of the two successive cleavages we focused on compound **5a** to avoid synthesizing hydroxyleucines and hydroxyasparagine contained in **2a**, as these amino acids are not commercially available. However, stereochemistry was respected by using D-leucines and D-asparagine. From **5a**, we produced two linear peptides corresponding to the two possible cleavage points (steps 1' and 2' in path A or steps 1 and 2 in path B; Figure 112-A). Compound **5b** is a linear analogue of **5a** that is disconnected at the C-ter of D-Leu^5. Compound **5d** refers to the open compound **5a** at the C-ter of D-Leu^3. These two candidate peptides allowed us to determine the first cleavage site and subsequently the two-step enzymatic reaction pathway that produces compound **5c**. It is worth noting that when both candidates **5b** and **5d** were exposed to digestive gland extracts, they were cleaved and produced compound **5c** after deletion of compound **5e**. (Figure 113, Figure 114). Optimization of the HPLC conditions enabled us to differentiate between peptides **5b** and **5d** through their retention times of 13.0 and 13.3 min respectively which correlated to their peak mass of *m/z* 1365.6. Subsequently, separation of both peaks remained when co-injected (Figure 112-B). Based on these observations, a solution containing compound **5a** was exposed to digestive gland extracts and LC-MS revealed that only the peak corresponding to **5b** along with the final product **5c** were observed (Figure 112-C, solution B). Mixing solution B with solution A containing compounds **5b** and **5d** in equivalent amounts confirmed that only compound **5b** was formed during the enzymatic process (Figure 112-C). Thus, our test of the enzymatic processing of compound **5a** provided evidence supporting path B that the ring is first cleaved at the C-ter of the amino acid in position 5 delivering compound **5b** (Figure 112-A, step 1 in

red) and then cleaved at the C-ter of the amino acid in position 3 to form **5c** (Figure 112-A, step 2 in red).

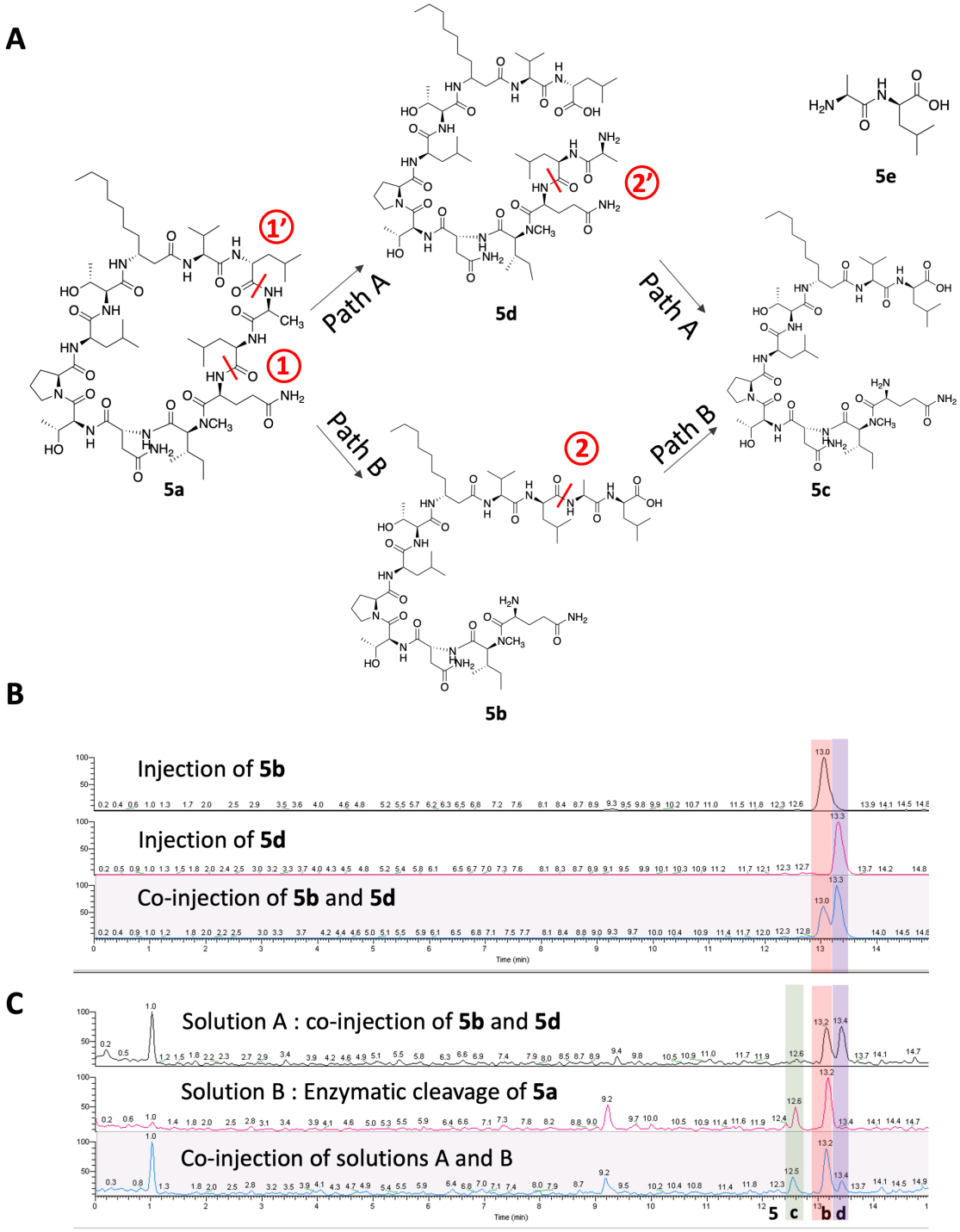

Figure 112. Study of the two possible enzymatic cleavage paths of compound 5a which leads to the formation of compounds 5c and 5e consecutively from the formation of intermediates 5b or 5d. A) Potential intermediates produced by Path A or B. B) LC-MS chromatograms of postulated cleavage intermediates 5b (pink strip) and 5d (purple strip) and their co-injection. C) LC-MS chromatogram of 5a exposed to enzymatic cleavage producing compound 5b as confirmed by co-injection with synthetic 5b and 5d compounds. Compound 5c resulting from the second cleavage is also observed (green strip).

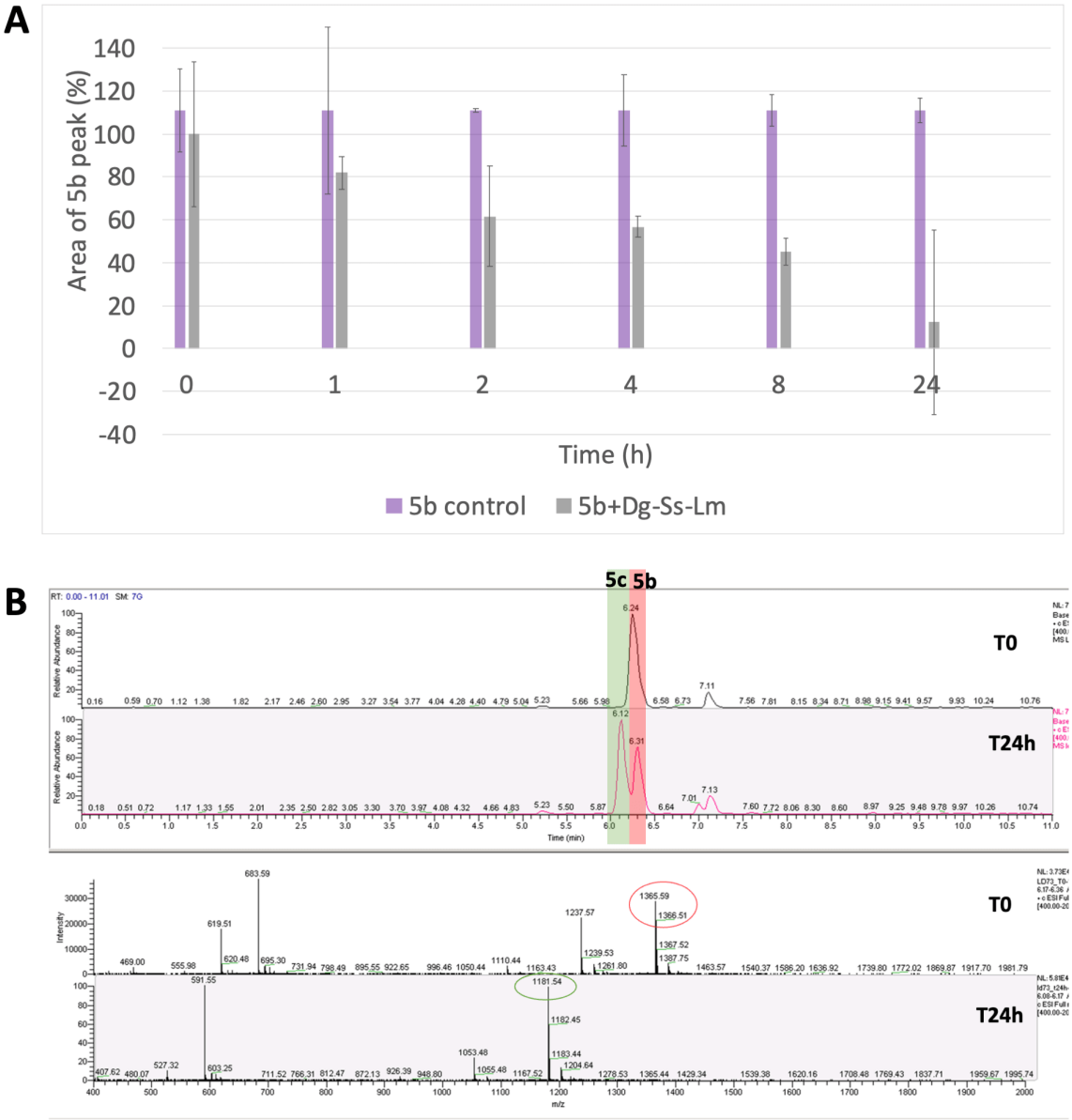

Figure 113. A) Cleavage rate of 5b with *Dg-Ss-Lm*. The control values (in purple) correspond to an average of all the values obtained during the kinetics. B) LC-MS kinetic monitoring of 5b cleavage with *Dg-Ss-Lm* extract at 30°C pH 8 and masses corresponding to the LC-MS peaks of 5b-c

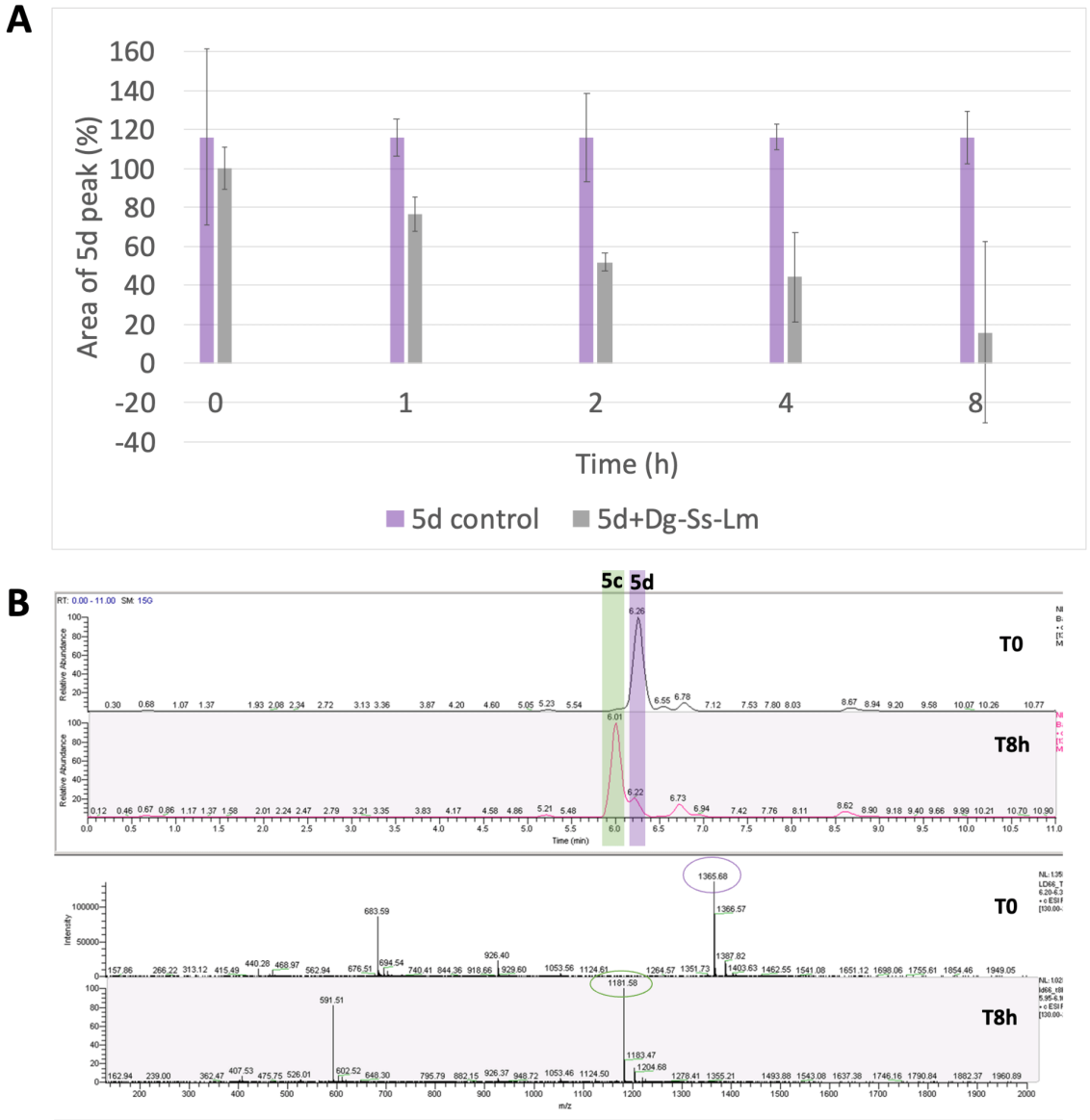

Figure 114. A) Cleavage rate of 5d with *Dg-Ss-Lm*. The control values (in purple) correspond to an average of all the values obtained during the kinetics. B) LC-MS kinetic monitoring of 5d cleavage with *Dg-Ss-Lm* extract at 30°C pH 8 and masses corresponding to the LC-MS peaks of 5c-d

5b and **5d** being able to be cleaved by the digestive gland extract, we decided to place **5a** in competition with **5b** or **5d** for the enzyme, with **5b** and **5d** in molar quantity 10 times higher than **5a**. Whether **5a** is used with **5b** or **5d**, it is cleaved more slowly than alone with *Dg-Ss-Lm*. Indeed, after 3 hours of incubation with *Dg-Ss-Lm*, 17% of **5a** remains when it is in competition with **5d** and 35% when it is with **5b**, whereas it is normally cleaved entirely when it is not in competition (Figure 115). It would thus appear that the enzyme has a preference for linearized peptides, which generally provide more flexibility at the active site. Moreover, **5a** is cleaved more slowly with **5b** than with **5d**, suggesting that the enzyme prefers substrate **5b** and thus again supporting that **5b** would be the intermediate peptide obtained during the two-step cleavage.

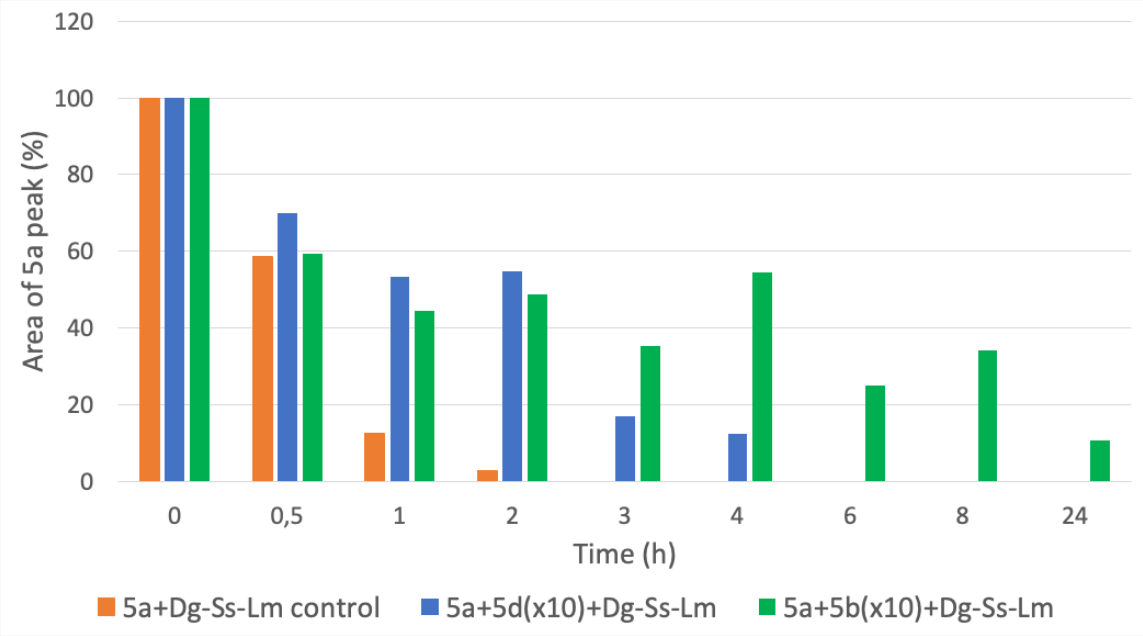

Figure 115. Cleavage rate of 5a with *Dg-Ss-Lm*, with or without competition with 5b or 5d. It should be noted that this experiment was done only once.

The enzyme would therefore not be perturbed by the loss of the ring structure, as long as the peptide sequence remains intact. Indeed, we were also able to put in competition laxaphycin B **2a** with its cleaved derivative **2c**, in molar quantity 10 times higher than **2a**. **2a** is cleaved at almost the same speed whether it is in competition with **2c** or not, showing the preference of the enzyme for the cyclic substrate **2a** (Figure 116). **2c** having lost 2 amino acids, alanine in position 4 and hydroxyleucine in position 5, the linear peptide is not recognized by the enzyme anymore. This supports again the hypothesis of a cleavage site around these 2 amino acids having an importance in the recognition of the enzyme towards its substrate.

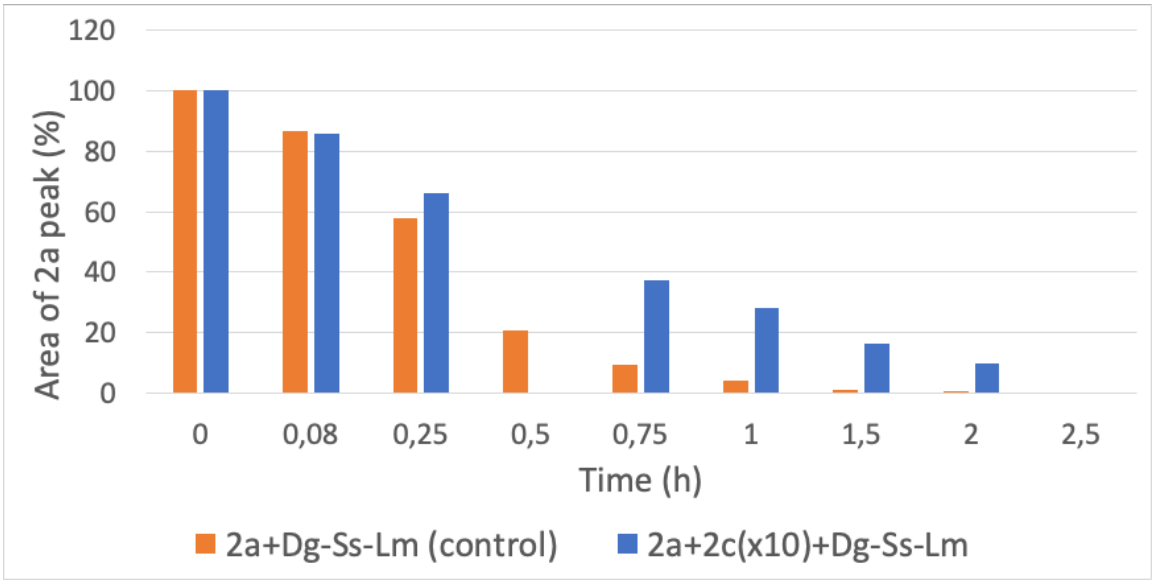

Figure 116. Cleavage rate of 2a with *Dg-Ss-Lm*, with or without competition with 2c. It should be noted that this experiment was done only once.

III. Determination of enzyme substrate preferences

Intrigued by the fact that linear compounds **5b** and **5d** were substrates of the enzyme, we synthesized compound **7a** that corresponds to a linear analogue of **5a** in which the Ade has been replaced by a decanoic acid at the N-terminus (Figure 117-B). Despite a linear structure, the peptide was still cleaved at the same location as its cyclic analogue (Figure 117) indicating that **7a** manages to structure itself in order to be recognized by the enzyme as its cyclic analogue. Furthermore, compound **7a** enabled us to differentiate between the fragments by mass spectrometry and to confirm the order of the two-step cleavage process (Figure 117, Figure 118). The two cleavage studies of **5a** and **7a** demonstrate that **2a** and its cyclic analogues (**3a**, **4a**, **5a** and **6a)** are cleaved in the same way, according to path B (Figure 112-A). The discovery of acyclolaxB **2d** in *Anabaena torulosa* suggests that cleavage of **2a** would produce the intermediates **2d** then **2c**, however, they are in fact **2b** then **2c** (Figure 119). The origin of acyclolaxaphycin B **2d** is still unknown to date.

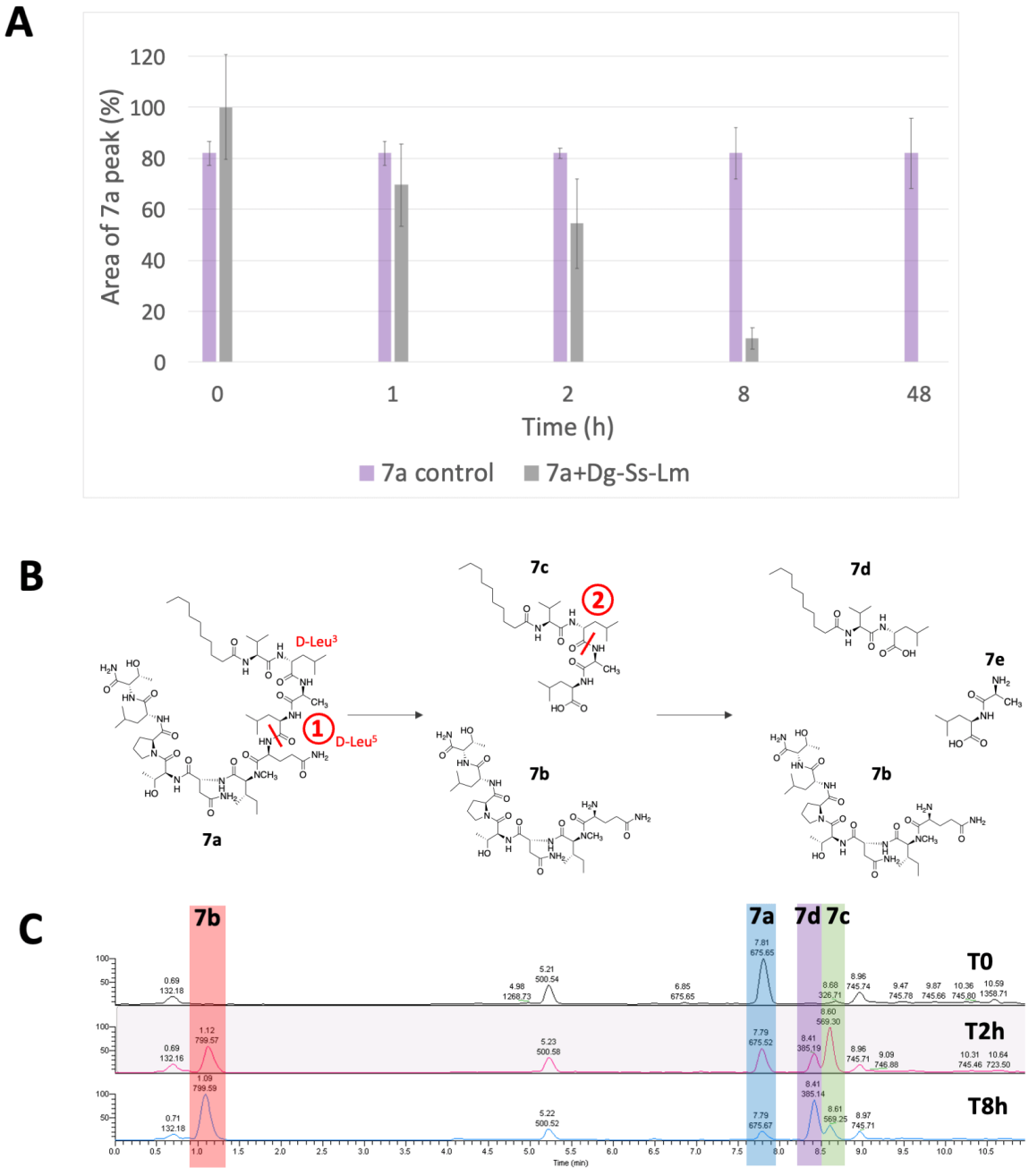

Figure 117. A) Cleavage rate of 7a with *Dg-Ss-Lm*. The control values (in purple) correspond to an average of all the values obtained during the kinetics. B) Successive cleavages observed by LC-MS for compound 7a. C) LC-MS kinetic monitoring of 7a cleavage with *Dg-Ss-Lm* extract at 30°C pH 8 and masses corresponding to the LC-MS peaks of 7a-d. The compound at 5.22 min belongs to the digestive gland extract.

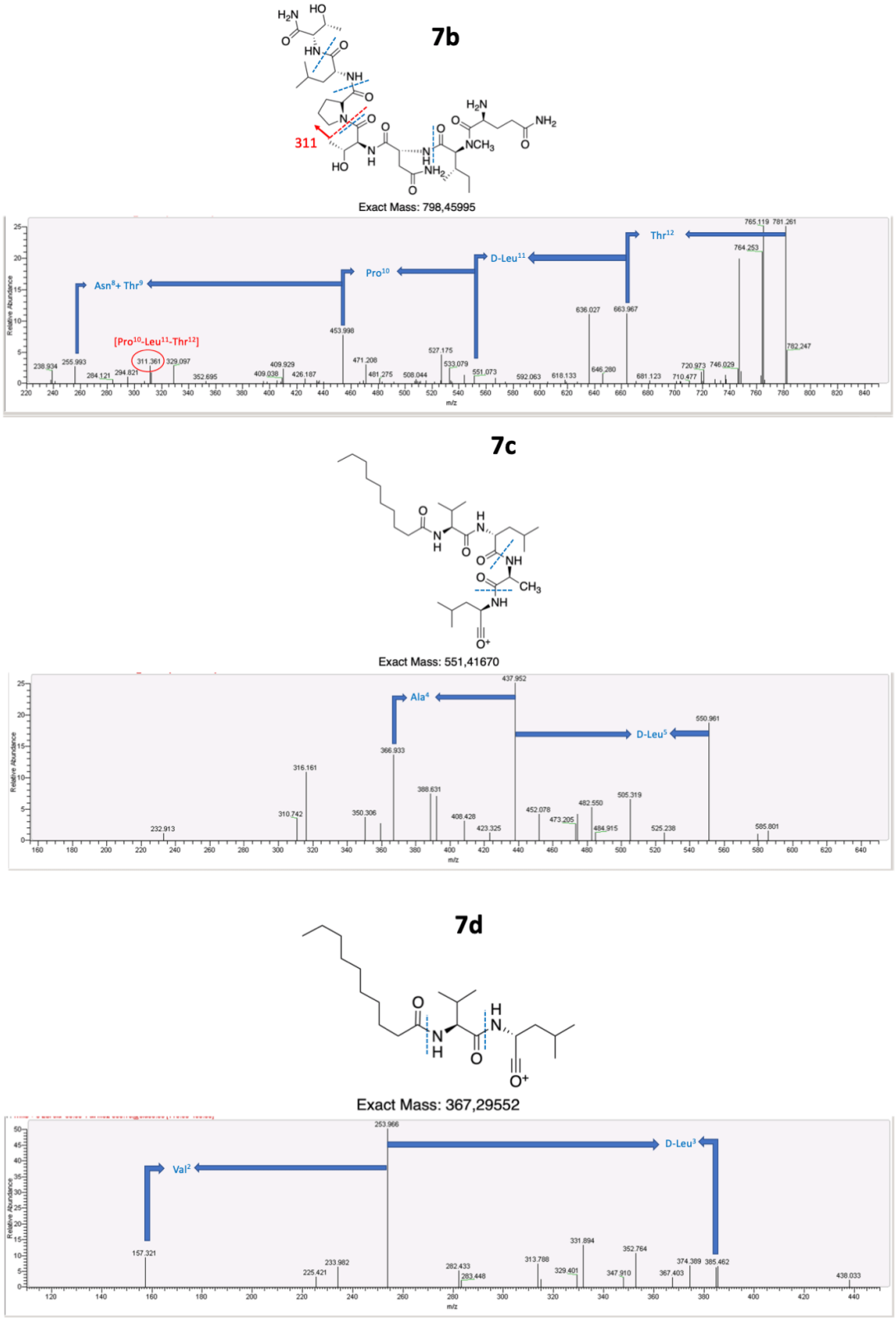

Figure 118. MS-MS analyses of 7b-d fragments obtained during the cleavage of 7a

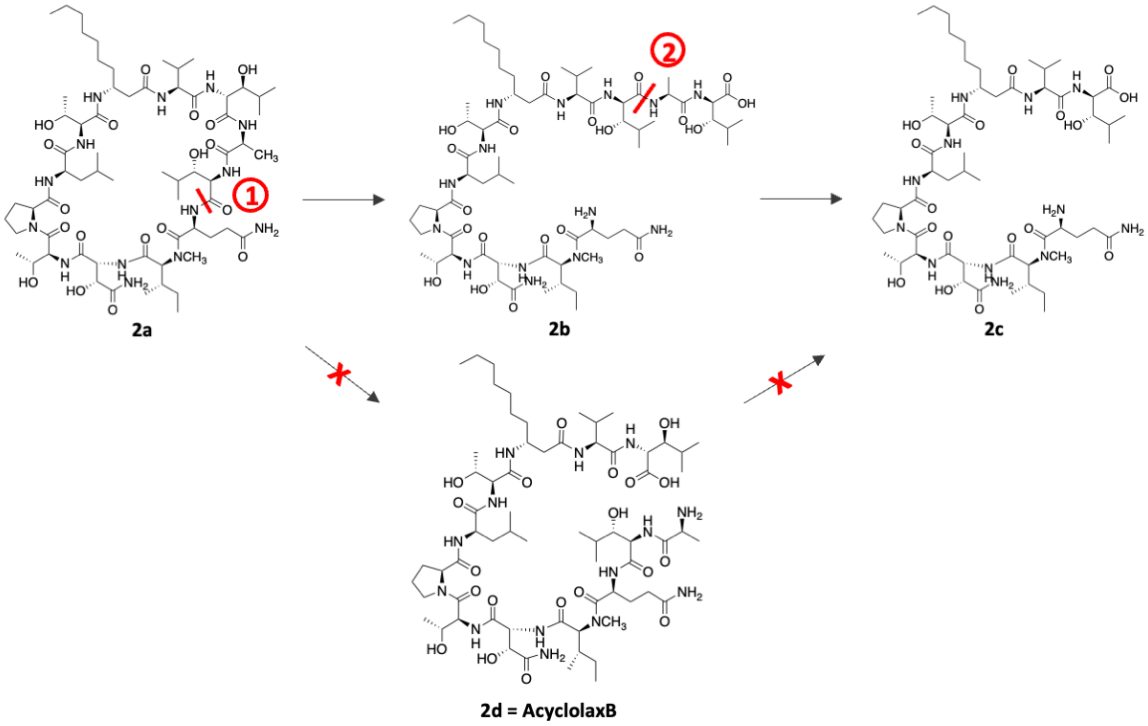

Figure 119. Cleavage path of 2a determined following the studies on 5a and 7a.

Given the length of Ade[1]'s carbon chain, this amino acid could play a crucial role in the enzyme's ability to recognize the substrate. We therefore replaced Ade[1] with β-Alanine and synthesized compound **8a** (Figure 120). This peptide was not cleaved by the digestive gland extracts (*Dg-Ss-Lm*), demonstrating that the enzyme requires Ade[1]'s long carbon chain for insertion of the peptide into the enzyme active site (Figure 121-A). Stereochemistry can also impact the enzyme's ability to recognize the substrate. **2a-6a** have a particular structure with an alternation of L- and D-amino acids and are cleaved at the C-terminal end of D-amino acids (D-Thr, D-Leu and (2R,3S)-HyLeu). We therefore synthesized compound **9a**, an analogue of **5a**, that contained two L-Leu instead of the two D-Leu at the cleavage site (Figure 120). This peptide was not cleaved by the digestive gland extracts (*Dg-Ss-Lm*), emphasizing the importance of amino acid stereochemistry at the enzyme's recognition site (Figure 121-B).

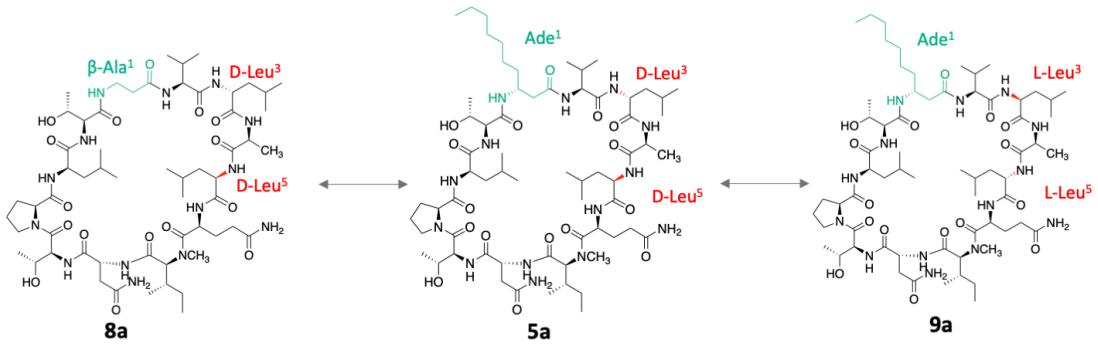

Figure 120. Structures of non-cleaved compounds 8a and 9a compared to 5a.

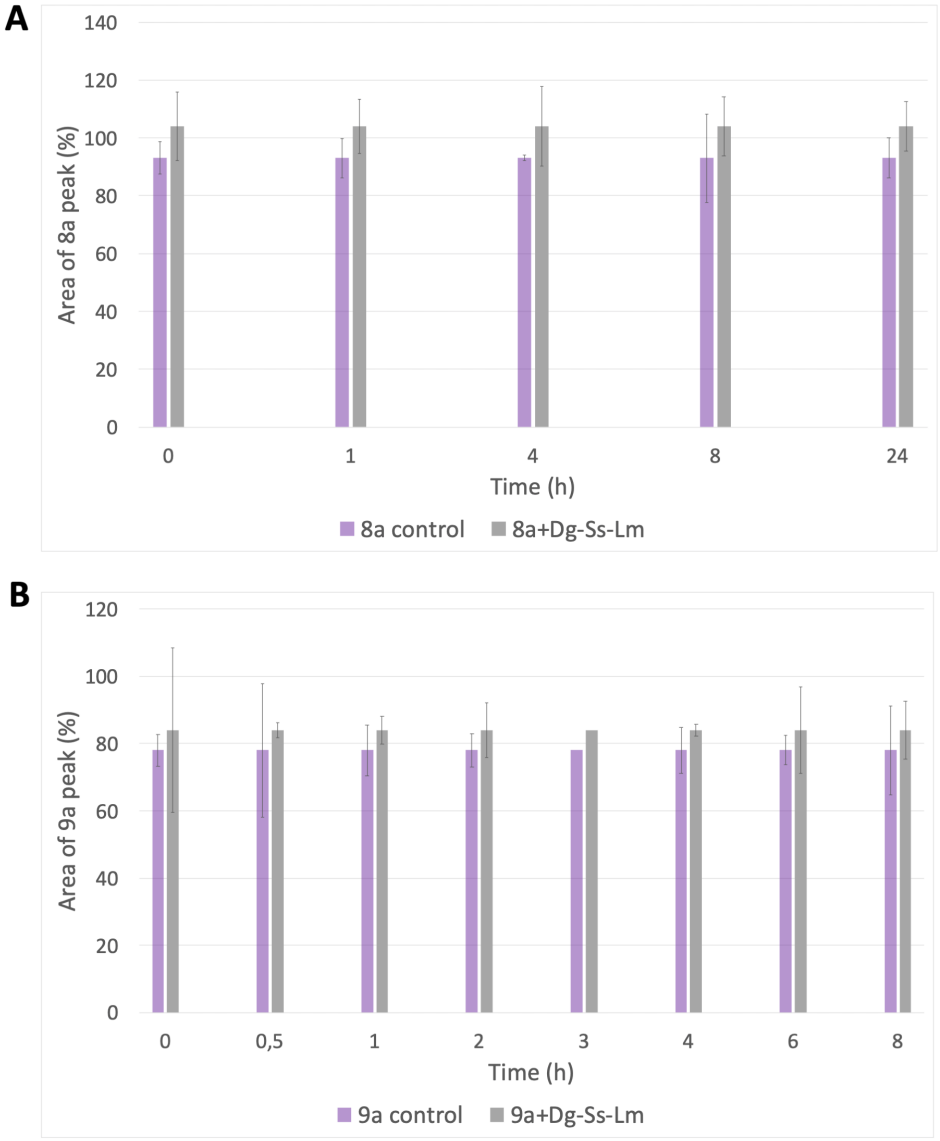

Figure 121. A) Cleavage rate of 8a with *Dg-Ss-Lm*. B) Cleavage rate of 9a with *Dg-Ss-Lm*. The control values (in purple) correspond to an average of all the values obtained during the kinetics.

To reinforce our findings, we replaced only one D-Leu with a L-Leu. Knowing that **7a** is recognized by the enzyme although it is a linear peptide, and that it is cleaved at the C-ter of the two D-Leu starting with D-Leu^5 then D-Leu^3, we synthesized the same peptide sequence by replacing D-Leu in position 3 by L-Leu, while keeping D-Leu in position 5, resulting in compound **10a** (Figure 122-A). LC-MS analysis showed that the peptide was cleaved at the C-ter of D-Leu^5 but no longer in position 3, where L-Leu was present (Figure 122-B). We also synthesized **11a**, having the same sequence as **10a** but with an opposite stereochemistry for the two leucines, i.e., a D-Leu in position 3 and an L-Leu in position 5 (Figure 123-A). Even though the cleavage kinetic is much slower than with **10a**, we can see the **11c** fragment corresponding to the C-ter cleavage of the D-Leu in position 3. However, its complementary fragment **11b** is not visible (Figure 123-B). As with **10a**, the cleavage of **11a** would have taken place in one step, at the C-ter of D-leu.

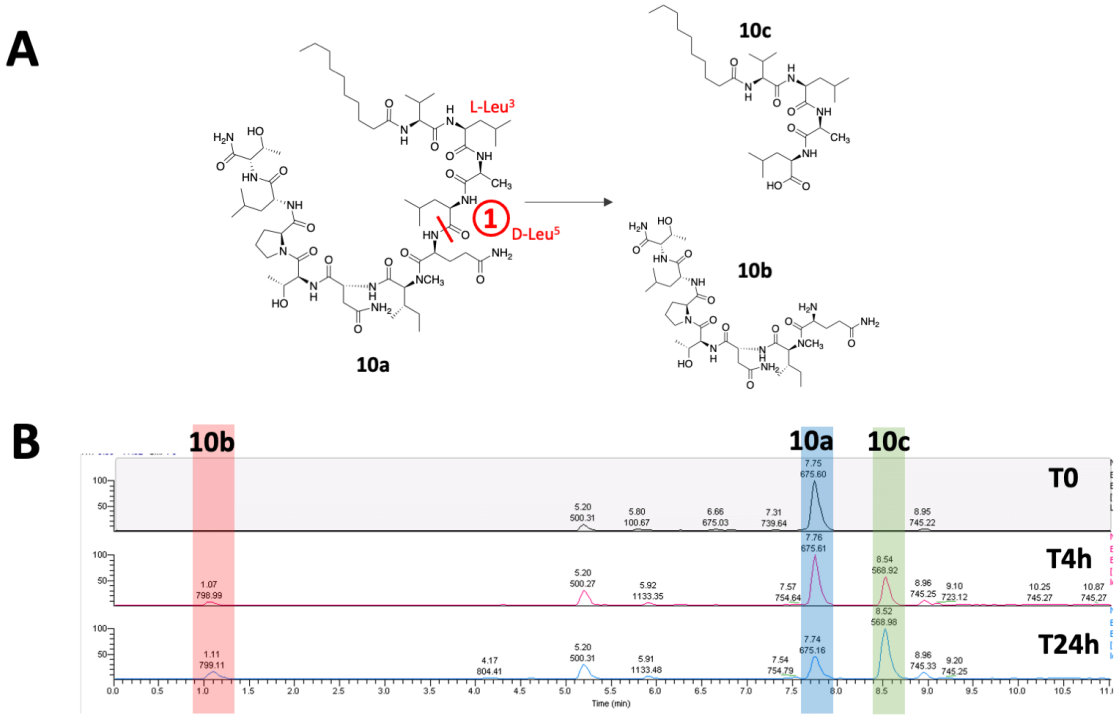

Figure 122. A) Cleavage observed by LC-MS for compound 10a. B) LC-MS kinetic monitoring of 10a cleavage with *Dg-Ss-Lm* extract at 30°C pH 8 and masses corresponding to the LC-MS peaks of 10a-c. Compounds 10d-e were not observed. The compound at 5.20 min belongs to the digestive gland extract.

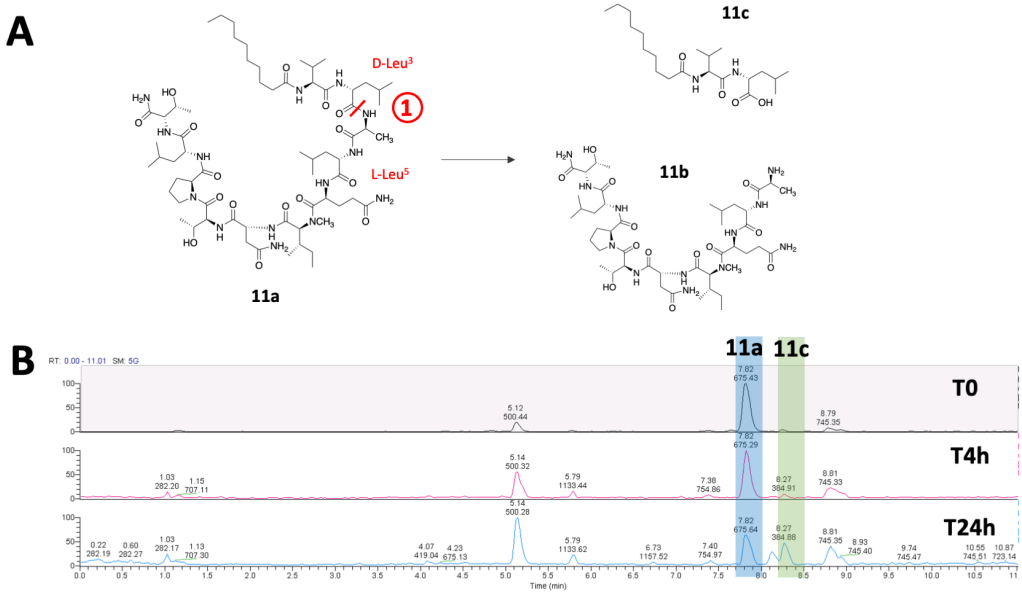

Figure 123. A) Cleavage observed by LC-MS for compound 11a. B) LC-MS kinetic monitoring of 11a cleavage with *Dg-Ss-Lm* extract at 30°C pH 8 and masses corresponding to the LC-MS peaks of 11a and 11c. Compounds 11b was not observed. The compound at 5.14 min belongs to the digestive gland extract.

Taken together, our results confirm that a D-peptidase within the digestive gland of *S. striatus* acts on cyclic lipopeptides in the laxaphycin B-type peptide family, but also on synthetic linear analogues if they contain D-leucine like amino acids with suitable surroundings. Indeed, the

D-leucine in position 11 does not constitute a preferred cleavage site. We also highlighted the importance of the long carbon chain of the Ade in position 1 for the recognition of the enzyme towards its substrate.

Recently D-peptidases have been found to act on newly introduced antibiotics biosynthesized by non-ribosomal peptide synthetases (NRPS) [168]. D-stereospecific resistant peptidases (DSRP) generally regulate the concentration of the antibiotic within the producer organism to avoid self-toxicity and are therefore closely associated with NRPS modules. A recent genome mining study reports the presence of DSRP in a large number of bacteria [168]. For example, BogQ and TriF are DSRPs in Firmicutes (mostly Gram-positive bacteria) and cleave the linear peptides bogorol and tridecaptin on the C-terminal side of D-amino acids (D-AA), but BogQ also cleaves the antibiotic bacitracin, a cyclic-non-ribosomal lipopeptide. Therefore, BogQ and TriF peptidases provide microbes with a potential of antibiotic resistance by having an enzymatic site that recognizes a minimal pattern containing D-amino acids. As such, D-peptidases might constitute a threat for the future of non-ribosomal lipopeptides used as antibiotics. However, these enzymes are poorly studied and their cleavage mechanisms are not well known.

Regarding this, we tested the stability of four antibiotics, the vancomycin glycopeptide, the CLPS daptomycin, bacitracin and colistin all containing D-amino acids as well as a cyclic structure like laxaphycins, against these same digestive gland extracts from *S. striatus*. None of these four peptides were cleaved in contact with the digestive gland extracts of the mollusk (Figure 124). No new fragments were observed and the peaks corresponding to the antibiotics remain stable over time. This result shows that the specificity of the investigated D-peptidase is restricted to the laxB family and that the D, L alternating stereochemistry observed may be an important prerequisite for the substrate-enzyme association.

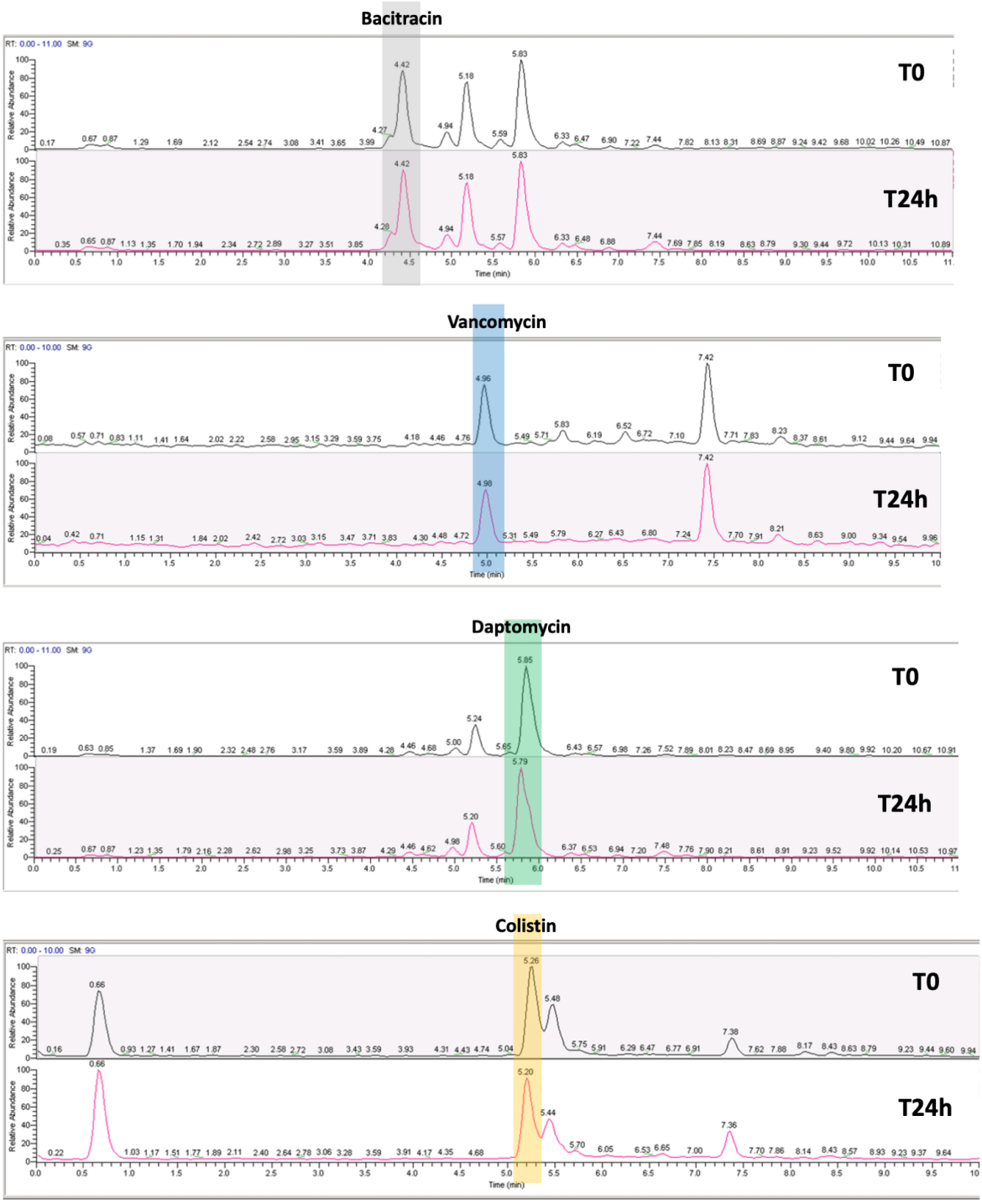

Figure 124. LC-MS kinetic monitoring of bacitracin, vancomycin, daptomycin and colistin potential cleavages with *Dg-Ss-Lm* extract at 30°C pH 8.

IV. Experimental part II

A. Peptide synthesis

Linear peptides were synthesized with an automated microwave peptide synthesizer (CEM Liberty One). The synthesis was performed at 50 °C under microwaves (25 W) and at 0.1 mmol scale with PyOxim (4.9 equiv)/DIEA (10 equiv) as coupling reagents. 20% piperidine in DMF were used for deprotection steps. Depending on the peptide to be synthesized, either Rink Amide resin (0.67 mmol/g) or 2-chlorotrityl chloride resin (1.6 mmol/g-Cl) preloaded with the first amino acid was used. For each amino acid the standard coupling cycle was as follows: after Fmoc deprotection of the amino acid supported by the resin, 2.5 mL of the requested amino acid at a concentration of 0.2 M in DMF was added to the resin, followed by 1 mL of PyOxim in DMF at 0.49 M and lastly by 0.5 mL 2M DIEA in NMP. The coupling of all amino acids was performed for 20 minutes except for difficult couplings which were carried out 2 or 3 times such as Fmoc-L-Gln(Trt)-OH that was coupled three times for 20 minutes, followed by capping with a solution of 100 mL of DMF, 5 mL of anhydride acetic (0.5 M, 1 equiv), 2 mL of DIEA (0.21 equiv) and 135 mg of HOBt (0.019 equiv) for 3 minutes. The Fmoc-group was deprotected by adding 20% piperidine solution in DMF for 3 minutes. At the end of the synthesis, the resin was washed three times with DMF and three times with DCM and then was dried under *vacuum*.

In the case of the linear peptides **5b**, **5d**, **7a**, **10a** and **11a**, a total cleavage was done using a solution of TFA/TIS/H_2O 95:2.5:2.5 (v/v) under agitation over 2 hours. The resin was then filtered and the filtrate was concentrated *in vacuo* with cyclohexane as a co-solvent. Peptides were precipitated in ice-cold diethyl ether and freeze-dried. Peptides were then purified by semi-preparative HPLC.

In the case of cyclic peptides **8a** and **9a**, a cleavage of the protected peptide from the resin was carried out using a solution of 20% TFE in DCM under agitation for 2 hours. The resin was then filtered and the filtrate was concentrated *in vacuo* with cyclohexane as a co-solvent. The peptide was then freeze-dried but not purified. The linear peptide (45 μmol) was dissolved in DMF (4.5 mL) into a syringe. EDC (3 equiv) was dissolved in the same amount of DMF (4.5 mL) into another syringe. OxymaPure (3 equiv) was dissolved in 4.5 mL of DMF into a three-neck round-bottom flask purged under nitrogen atmosphere. The two syringes were put on both sides of the flask and both solutions were added under a nitrogen atmosphere at a rate of 0.01 mL/min. Once the addition was complete, the mixture was stirred for 48 hours under a nitrogen atmosphere. DMF was evaporated using Genevac (T=36°C, Medium Boiling Point) over 3 hours and the resulting sediments were dissolved with 10 mL of ethyl acetate. The organic layer was washed three times with citric acid (1M), three times with $NaHCO_3$ (1M) and three times with brine in order to separate the cyclic peptide from any potential remaining linear ones. The organic layer was dried over magnesium sulfate and then concentrated *in vacuo*. To allow side-chain deprotection, the resulting solid was mixed with a solution of

TFA/TIS/H_2O 95:2.5:2.5 (v/v) over 2 hours. TFA was evaporated under *vacuum* and the peptide was precipitated using ice-cold diethyl ether. The peptide was then purified by semi-preparative HPLC.

Syntheses of trichormamide C (**4a**) and its two cyclic analogs **5a** and **6a** have been previously described in the precedent chapter.

B. Peptide stability in buffer solutions

Two buffer solutions were prepared and sterilized by autoclave: a pH 8 buffer (50 mM Tris, pH adjusted with HCl 1M) and a pH 3 buffer (citric acid 0.1 M, sodium citrate 0.1 M, pH adjusted with NaOH 1M). Stock solutions of peptides were prepared at 10 mg/mL in DMSO. These solutions were diluted 10 times in buffer pH 3 and pH 8. Peptide solutions at 1 mg/mL (10% DMSO in buffer) were diluted 10 times with the same buffer used for previous dilutions resulting in peptides at 0.1 mg/mL (1% DMSO in buffer) in both buffers. Solutions were incubated under agitation (different temperatures were tested to fit with enzyme specificities). For each kinetic point, the same procedure was applied: solutions were centrifuged for a few seconds, then part of the solution was removed to be quenched by 90% MeOH, resulting in 0.01 mg/mL peptide solutions (DMSO/buffer/MeOH, 0.1:9.9:90, v/v). The quenched solutions were centrifuged at 21,952 x *g* for 20 minutes at 4°C. The maximum amount of supernatant was recovered in a LC-MS vial for analysis. All tests were performed in triplicate.

C. Enzymatic cleavage of peptides by isolated known enzymes

Two buffers were prepared and sterilized by autoclave: a pH 8 buffer (50 mM Tris, pH adjusted with HCl 1 M) and a pH 3 buffer (citric acid 0.1 M, sodium citrate 0.1 M, pH adjusted with NaOH 1 M). Stock solutions of peptides were prepared at 10 mg/mL in DMSO. A stock solution of Pepsin (purchased from Promega) was prepared at 2 mg/mL in buffer pH 3 then was diluted 1.6 times in the same buffer to give a Pepsin solution at 1,24 mg/mL. A stock solution of Elastase (purchased from Promega) was prepared at 1 mg/mL in buffer pH 8 then was diluted 1.06 times in the same buffer to give an Elastase solution at 0.94 mg/mL. A stock solution of Thermolysin (purchased from Promega) was prepared at 2 mg/mL in buffer pH 8 then was diluted 1.5 times in the same buffer to give a Thermolysin solution at 1,3 mg/mL. A stock solution of Subtilisin (purchased from Sigma Aldrich, ref P8038) was prepared at 1 mg/mL in buffer pH 8 then was diluted 1.02 times in the same buffer to give a Subtilisin solution at 0.98 mg/mL.
Peptide solutions were diluted 10 times in buffer pH 3 and pH 8 to give peptide solutions at 1 mg/mL (10% DMSO in buffer). These solutions (1 mg/mL) were mixed with appropriate enzyme stock solutions to obtain an enzyme/substrate ratio of 1/20.
Solutions were incubated under agitation (37°C for Pepsin and Elastase, 75°C for Thermolysin and 60°C for Subtilisin). For each kinetic point, the same procedure was applied: solutions were centrifuged a few seconds, then part of the solution was taken off to be quenched by 90% MeOH, obtaining peptide solutions at 0.01 mg/mL (DMSO/buffer/MeOH, 0.1:9.9:90, v/v). The quenched solutions were centrifuged at 21,952 x g for 20 minutes at 4°C. The maximum

of supernatant was recovered in a LC-MS vial to be analyzed. All tests were performed in triplicate.

D.Peptide stability in the presence of *Dg-Ss-Lm* or rat serum

A pH 8 buffer was prepared and sterilized by autoclave (50 mM Tris, pH adjusted with HCl 1M). Stock solutions of peptides were prepared at 10 mg/mL in DMSO. These solutions were diluted 10 times in buffer pH 8 to give peptide solutions at 1 mg/mL (10% DMSO in buffer). These solutions (1 mg/mL) were mixed with *Dg-Ss-Lm* extracts (10 mg/mL) or rat serum (between 60 and 80 mg/mL) and completed with the same buffer resulting in peptides at 0.1 mg/mL (1% DMSO in buffer) and extracts at 1 mg/mL (concentration varying between 0.4 and 1 mg/mL depending on the extracts) or rat serum around 10 mg/mL. Solutions were incubated at 30°C under agitation. For each kinetic point, the same procedure was applied: solutions were centrifuged for a few seconds, then part of the solution was removed to be quenched by 90% MeOH, obtaining peptide solutions at 0.01 mg/mL (DMSO/buffer/MeOH, 0.1:9.9:90, v/v). The quenched solutions were centrifuged at 21,952 x *g* for 20 minutes at 4°C. The maximum amount of supernatant was recovered in a LC-MS vial for analysis. All the tests were carried out in triplicate on the same extract and in several replicates with other extracts.

E. Heating of the digestive gland of the mollusk

A pH 8 buffer (50 mM Tris, pH adjusted with HCl 1 M) was prepared and sterilized by autoclave. A stock solution of **2a** was prepared at 10 mg/mL in DMSO. This stock solution was diluted 10 times in buffer. *Dg-Ss-Lm* extract was heated at 90°C for 5 minutes while vortexing the solution from time to time and checking that there was no evaporation of the buffer. **2a** solution at 1 mg/mL was mixed with *Dg-Ss-Lm* extract previously heated (10 mg/mL) and completed with the same buffer to afford **2a** at 0.1 mg/mL and extract at 1 mg/mL. Solution was incubated at 30°C under agitation. For each kinetic point, the same procedure was applied: solution was centrifuged a few seconds, then part of the solution was taken off to be quenched by 90% MeOH, obtaining **2a** at 0.01 mg/mL. The quenched solution was centrifuged at 21,952 x g for 20 minutes at 4°C. The maximum of supernatant was recovered in a LCMS vial to be analyzed. In parallel, **2a** stability was test at 90°C.

F. Analyses

The peptides studied in this chapter are laxaphycin A (**1a**), B (**2a**) and B2 (**3a**) and their synthetic analogues **4a**, **5a**, **6a**, **8a** and **9a** as well as the linear peptides **5b**, **5d**, **7a**, **10a** and **11a**. Hereafter, the HRMS, LCMS and NMR analyses of the synthesized peptides are reported, except for **4a-6a** that were reported in the precedent chapter. Compounds **1a-3a** were isolated from cyanobacteria.

a) Compound 5b

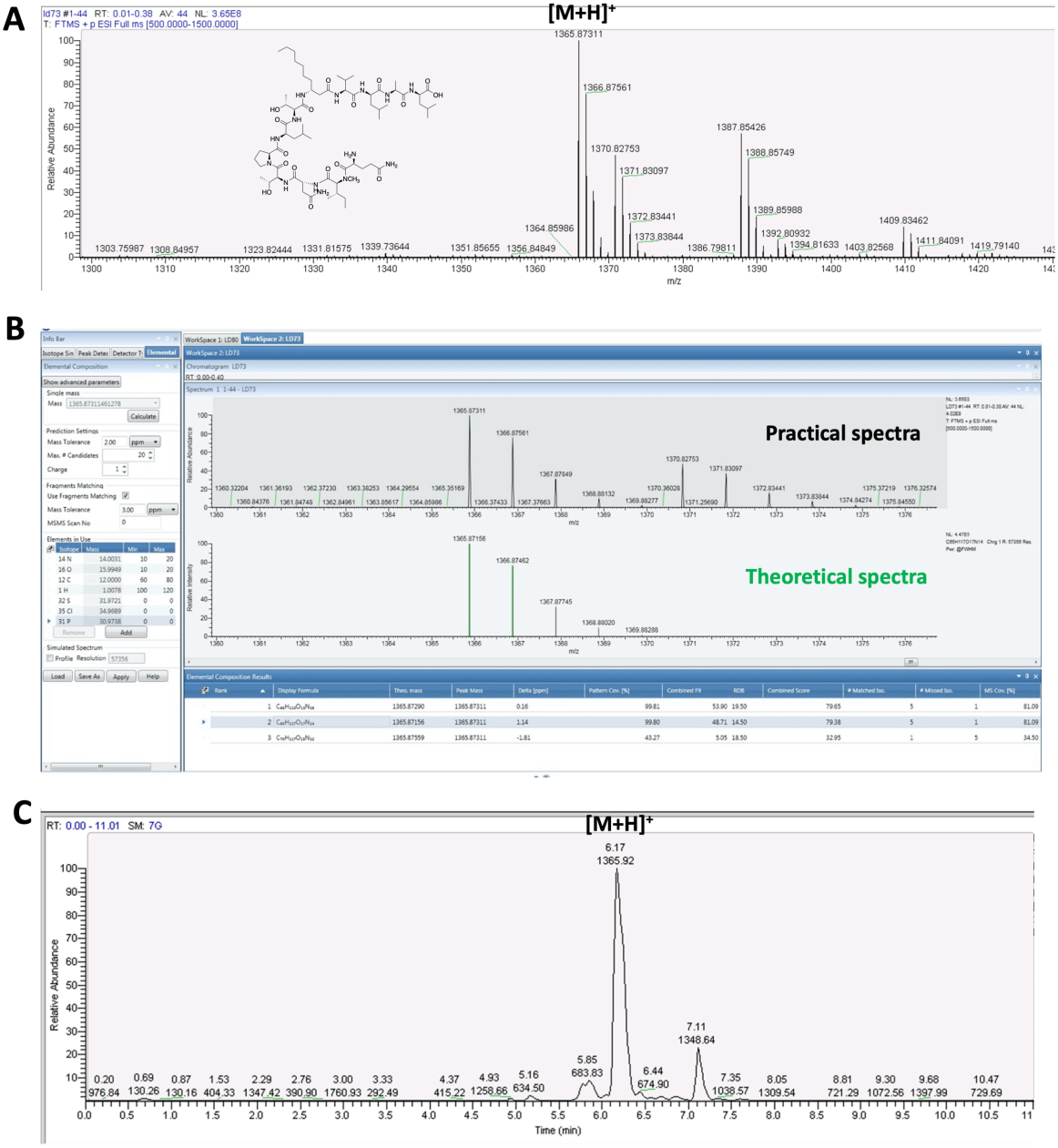

Figure 125. A) ESI-HRMS spectrum of 5b. B) Comparison with the theoretical spectrum. Calculated for $C_{65}H_{117}N_{14}O_{17}$ $[M+H]^+$ *m/z* 1365.87156; Found $[M+H]^+$ *m/z* 1365.87311; mass error = 1.14 ppm. C) LC-MS profile of 5b.

Table 14. NMR spectroscopic data of 5b in DMSO-d_6

entry	position	C, mult.	H, mult. (J in Hz)	entry	position	C, mult.	H, mult. (J in Hz)
Ade[1]	1	170.6, C	-		NH_2	-	7.29 & 6.99
	2	40.4, CH_2	2.36		NH_2-term	-	7.37 & 6.96
			2.25	N-MeIle[7]	1	171.2, C	-
	3	46.2, CH	4.04		2	59.8, CH	4.70, d (10.88)
	4	33.6, CH_2	1.31		3	31.7, CH	1.94
			1.39		3-Me	15.2, CH_3	0.82
	5	25.2, CH_2	1.26		4	24.1, CH_2	1.33
			1.16		5	10.7, CH_3	0.83
	6	28.8, CH_2	1.19		N-Me	30.2, CH_3	2.97
	7	28.8, CH_2	1.19	D-Asn[8]	1	171.2, C	-
	8	31.2, CH_2	1.19		2	49.6, CH	4.60, t (6.30)
	9	22.1, CH_2	1.24		3	36.8, CH_2	2.50
	10	13.9, CH_3	0.84				2.40
	NH	-	7.55, d (8.02)		4	171.6, C	-
Val[2]	1	171.2, C	-		NH	-	8.20, d (7.45)
	2	58.7, CH	4.06		NH_2	-	7.35 & 6.94
	3	30.0, CH	1.92	Thr[9]	1	168.8, C	-
	3-Me	19.08, CH_3	0.81		2	55.3, CH	4.54, t (7.45)
	4	18.4, CH_3	0.84		3	66.6, CH	3.93
	NH	-	7.97, d (9.16)		4	18.7, CH_3	1.05, d (6.30)
D-Leu[3]	1	170.7, C	-		3-OH	-	5.10
	2	51.1, CH	4.25		NH	-	7.84, d (7.45)
	3	40.5, CH_2	1.50	Pro[10]	1	171.6, C	-
	4	24.1, CH	1.57		2	59.8, CH	4.33
	4-Me	20.9-23.2, CH_3	0.81-0.87		3	29.1, CH_2	1.83
	5	20.9-23.2, CH_3	0.81-0.87				2.03
	NH	-	8.19, d (7.45)		4	24.2, CH_2	1.82
Ala[4]	1	172.0, C	-				1.89
	2	51.1, CH	4.32		5	47.4, CH_2	3.73
	3	18.4, CH_3	1.21				3.73
	NH	-	7.80, d (8.59)	D-Leu[11]	1	171.8, C	-
D-Leu[5]	1	173.9, C	-		2	48.2, CH	4.26
	2	50.0, CH	4.24		3	40.5, CH_2	1.50
	3	40.5, CH_2	1.50		4	24.1, CH	1.57
	4	24.1, CH	1.57		4-Me	20.9-23.2, CH_3	0.81-0.87
	4-Me	20.9-23.2, CH_3	0.81-0.87		5	20.9-23.2, CH_3	0.81-0.87
	5	20.9-23.2, CH_3	0.81-0.87		NH	-	7.90, d (7.45)
	NH	-	7.95, d (8.59)	Thr[12]	1	168.8, C	-
Gln[6]	1	171.9, C	-		2	58.0, CH	4.11
	2	49.6, CH	4.39		3	66.6, CH	3.96
	3	25.6, CH_2	1.91		4	19.6, CH_3	0.98, d (6.30)
	4	29.5, CH_2	2.23		3-OH	-	4.78
	5	173.6, C	-		NH	-	7.62, d (8.59)

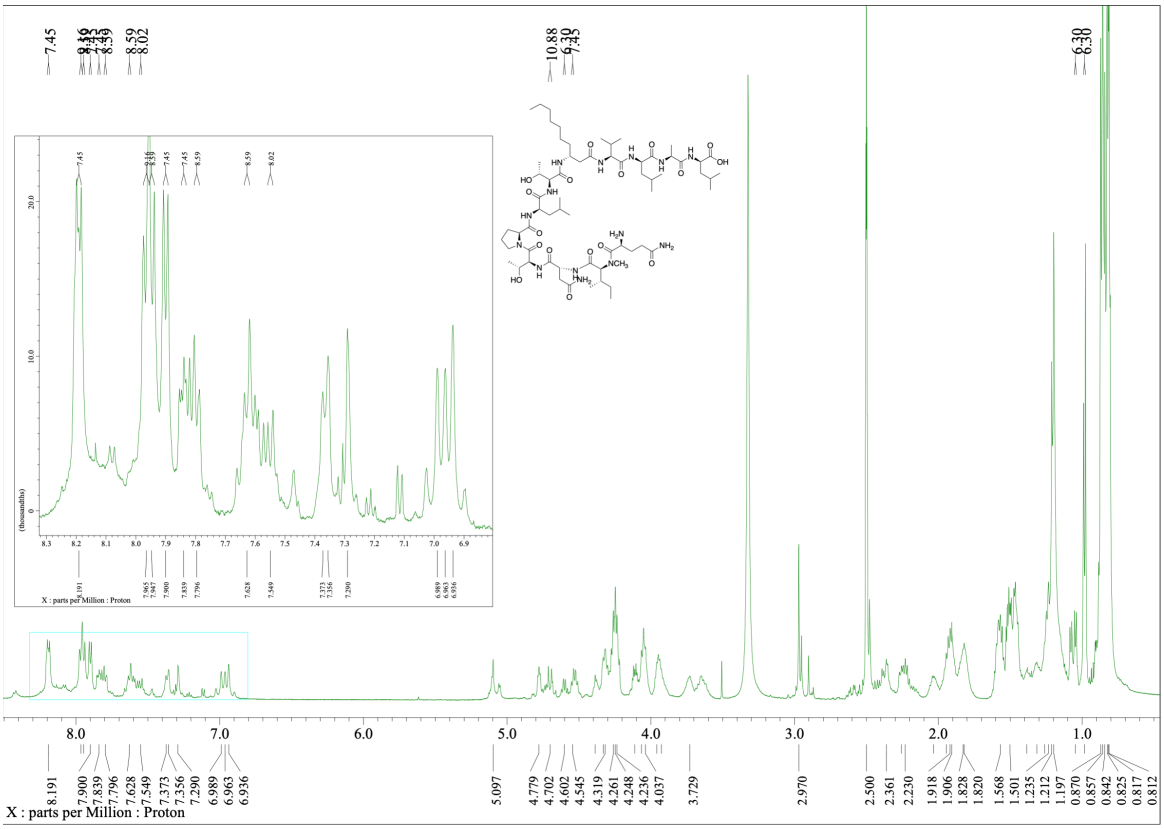

Figure 126. ^{1}H NMR spectrum of 5b. Solvent : dmso-d_6; T : 23°C; Scans : 32

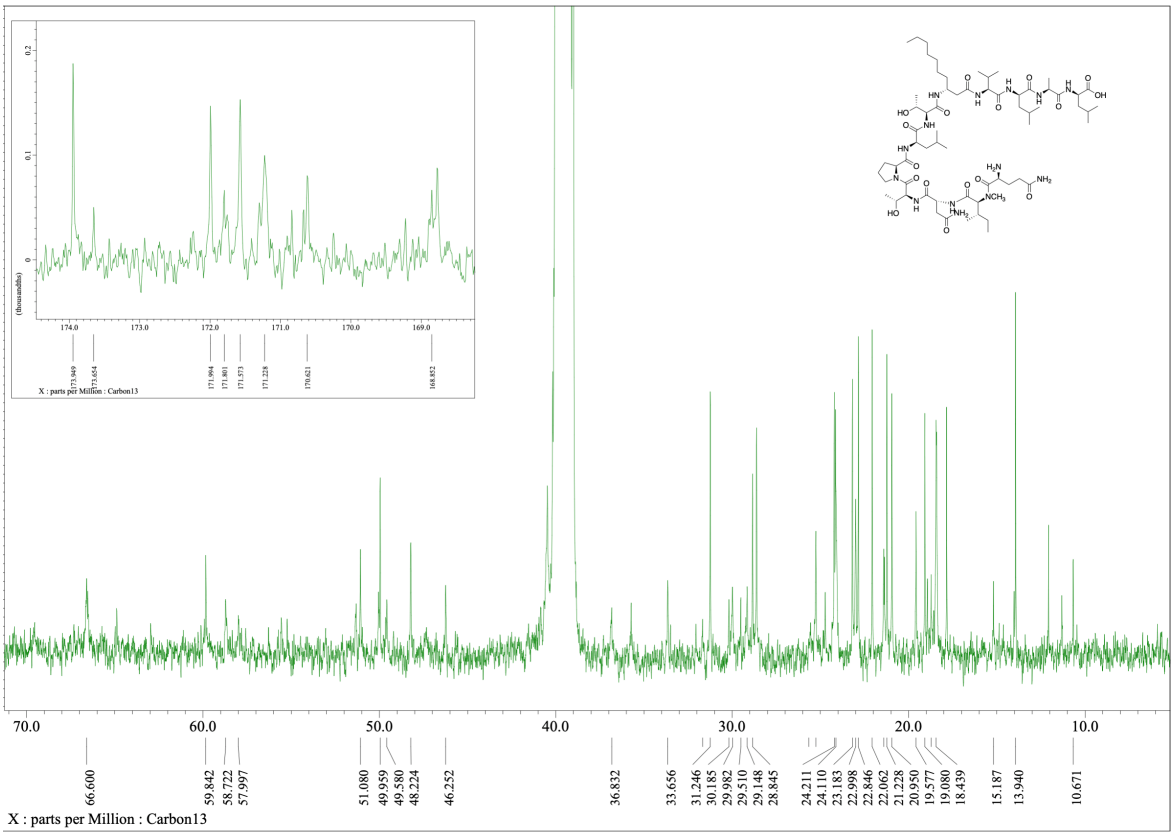

Figure 127. ^{13}C NMR spectrum of 5b. Solvent : dmso-d_6; T : 23°C; Scans : 20000

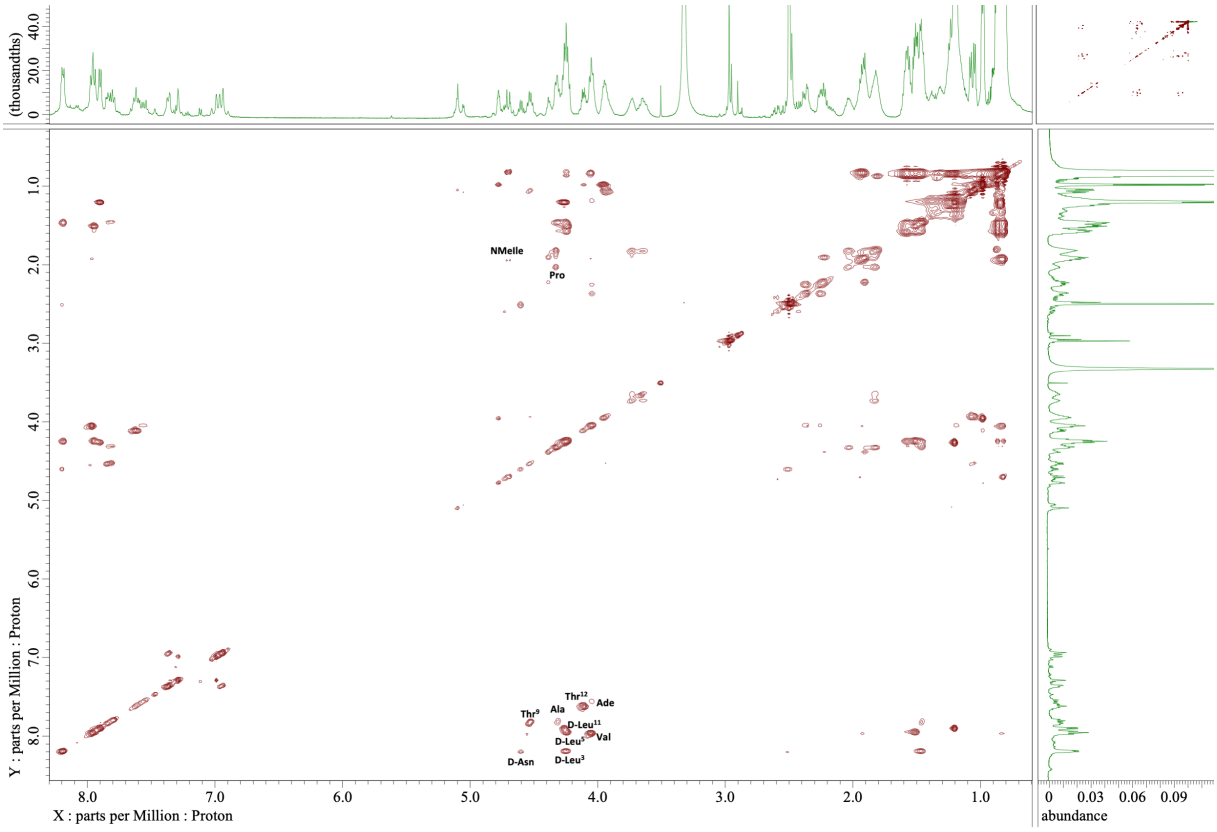

Figure 128. TOCSY spectrum of 5b. Solvent : dmso-d_6; T : 23°C; Scans : 8192

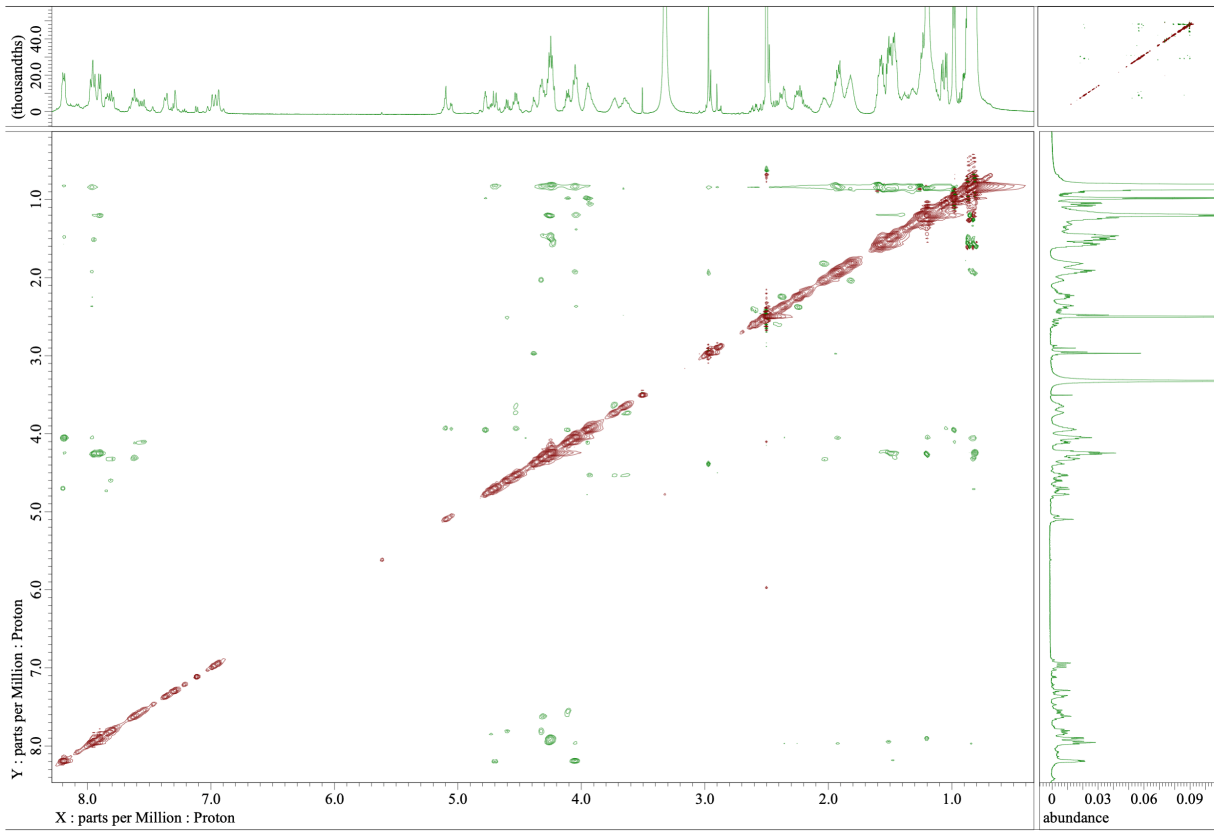

Figure 129. ROESY spectrum of 5b. Solvent : dmso-d_6; T : 23°C; Scans : 8192

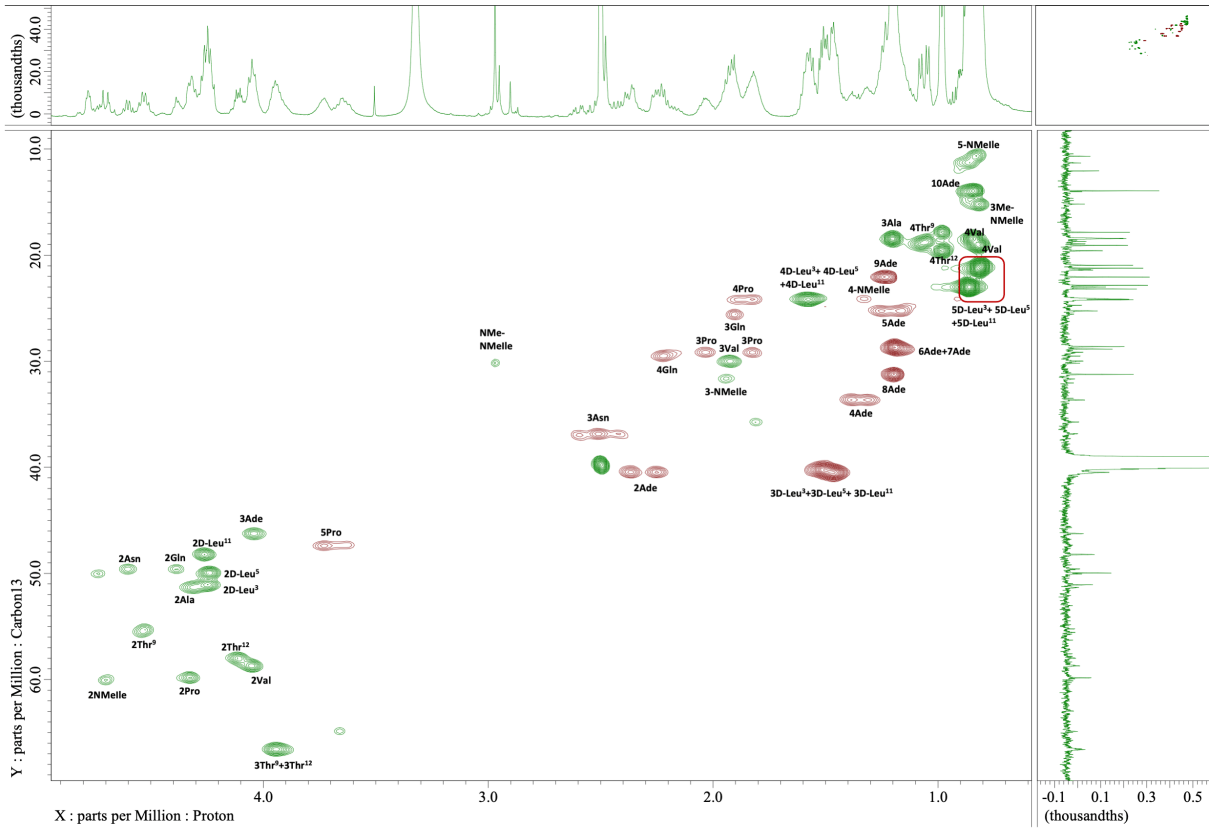

Figure 130. HSQC spectrum of 5b. Solvent : dmso-d_6; T : 23°C; Scans : 8192

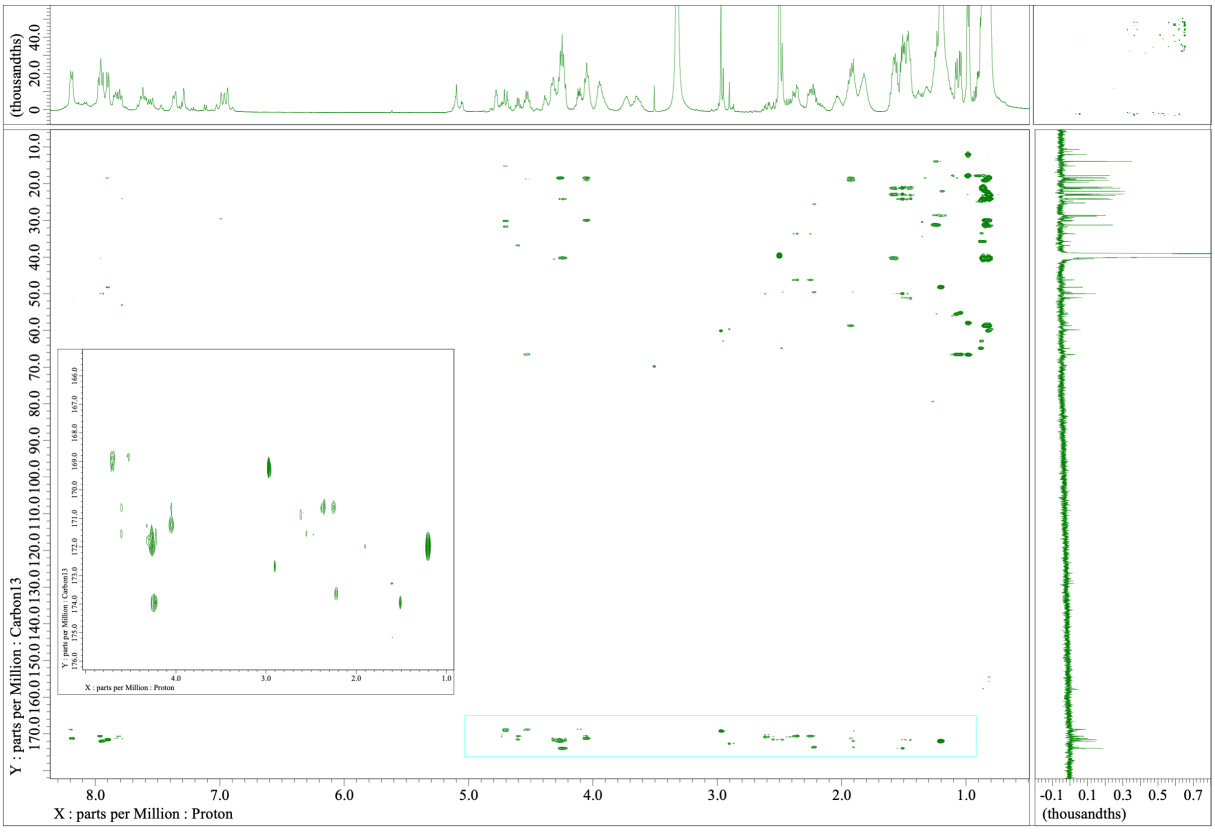

Figure 131. HMBC spectrum of 5b. Solvent : dmso-d_6; T : 23°C; Scans : 16384

b) Compound 5d

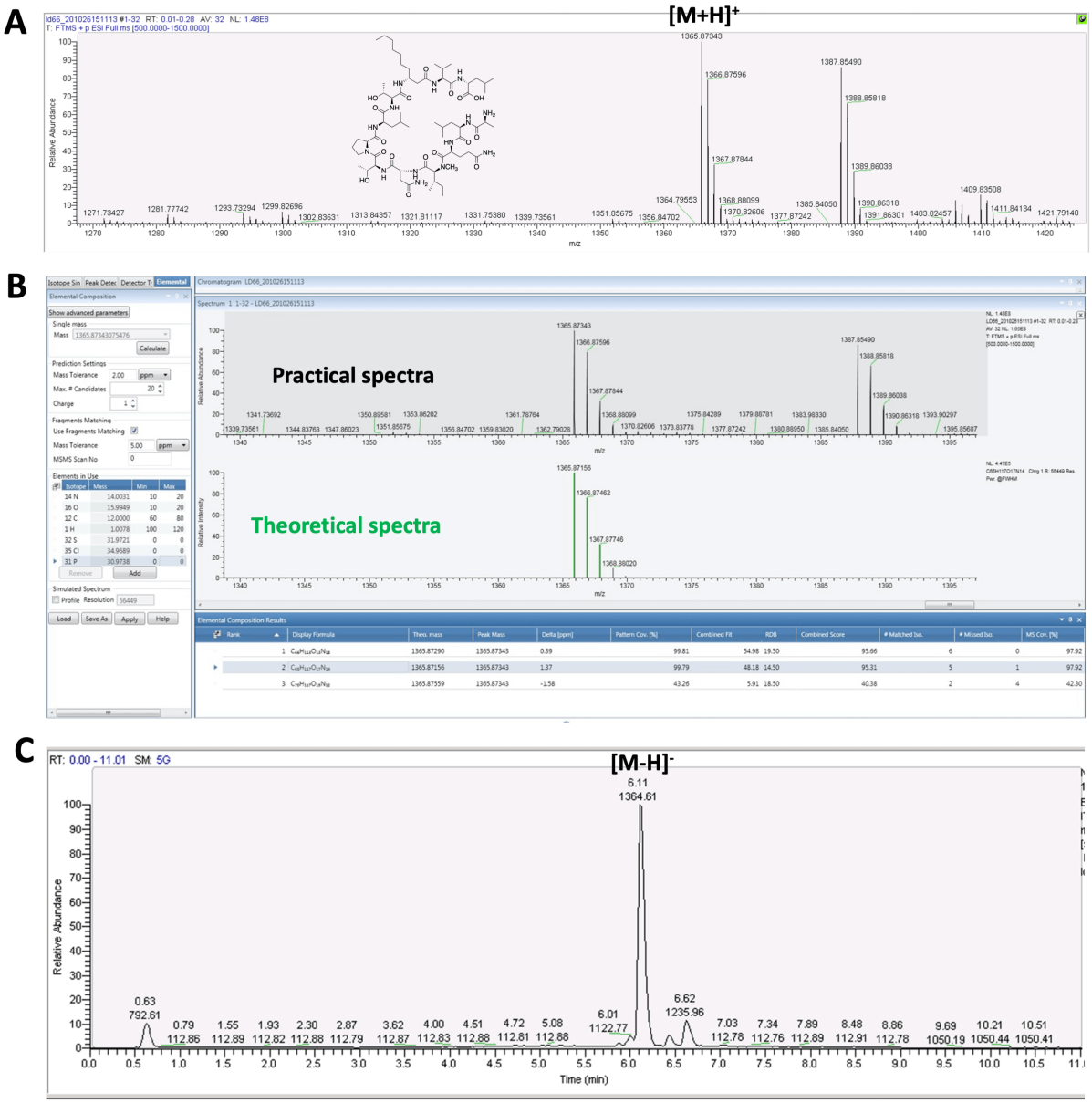

Figure 132. A) ESI-HRMS spectrum of 5d. B) Comparison with the theoretical spectrum. Calculated for $C_{65}H_{117}N_{14}O_{17}$ $[M+H]^+$ *m/z* 1365.87156; Found $[M+H]^+$ *m/z* 1365.87343; mass error = 1.37 ppm. C) LC-MS profile of 5d

Table 15. NMR spectroscopic data of 5d in DMSO-d_6

entry	position	C, mult.	H, mult. (J in Hz)	entry	position	C, mult.	H, mult. (J in Hz)
Ade[1]	1	*nd*, C	-	N-MeIle[7]	1	*nd*, C	-
	2	40.2, CH_2	2.47		2	59.5, CH	4.68, d (10.88)
			2.28		3	31.8, CH	1.90
	3	46.7, CH	3.93		3-Me	15.3, CH_3	0.78
	4	32.8, CH_2	1.40		4	24.1, CH_2	1.23
	5	25.9, CH_2	1.18		5	10.4, CH_3	0.75
	6	28.9, CH_2	1.18		N-Me	30.2, CH_3	3.00
	7	28.9, CH_2	1.18	D-Asn[8]	1	*nd*, C	-
	8	31.3, CH_2	1.18		2	49.8, CH	4.60, d (6.30)
	9	22.1, CH_2	1.22		3	37.1, CH_2	2.50
	10	13.9, CH_3	0.83		4	*nd*, C	-
	NH	-	7.77		NH	-	8.08, d (6.87)
Val[2]	1	*nd*, C	-		NH_2	-	7.34 & 6.90
	2	58.2, CH	4.06	Thr[9]	1	168.9, C	-
	3	*nd*, CH	2.03		2	55.6, CH	4.52
	3-Me	19.3, CH_3	0.79		3	66.6, CH	3.94
	4	17.8, CH_3	0.83		4	18.7, CH_3	1.05, d (6.30)
	NH	-	7.75		3-OH	-	
D-Leu[3]	1	*nd*, C	-		NH	-	7.75
	2	51.9, CH	3.96	Pro[10]	1	*nd*, C	-
	3	41.5, CH_2	1.44		2	60.3, CH	4.29
	4	24.0, CH	1.64		3	29.3, CH_2	1.82
	4-Me	21.4, CH_3	0.84				2.03
	5	21.4, CH_3	0.84		4	24.2, CH_2	1.74
	NH	-	7.66				1.88
Ala[4]	1	*nd*, C	-		5	47.5, CH_2	3.71
	2	*nd*, CH	4.03				3.71
	3	19.8, CH_3	1.14	D-Leu[11]	1	*nd*, C	-
	NH_2	-	nd		2	52.2, CH	4.18
D-Leu[5]	1	*nd*, C	-		3	39.5, CH_2	1.37
	2	50.7, CH	4.33		4	24.0, CH	1.62
	3	41.5, CH_2	1.44		4-Me	21.0, CH_3	0.80
	4	24.0, CH	1.55		5	21.0, CH_3	0.80
	4-Me	22.7-22.9, CH_3	0.86		NH	-	8.10
	5	22.7-22.9, CH_3	0.86	Thr[12]	1	169.7, C	-
	NH	-	7.76		2	59.1, CH	4.03
Gln[6]	1	*nd*, C	-		3	66.3, CH	4.01
	2	48.4, CH	4.61, d (6.87)		4	19.8, CH_3	0.97, d (5.73)
	3	26.7, CH_2	1.74		3-OH	-	
			1.84		NH	-	8.10
	4	30.7, CH_2	2.07				
	5	*nd*, C	-				
	NH	-	8.26, d (7.45)				
	NH_2	-	7.26 & 6.85			*nd* =	Not determined

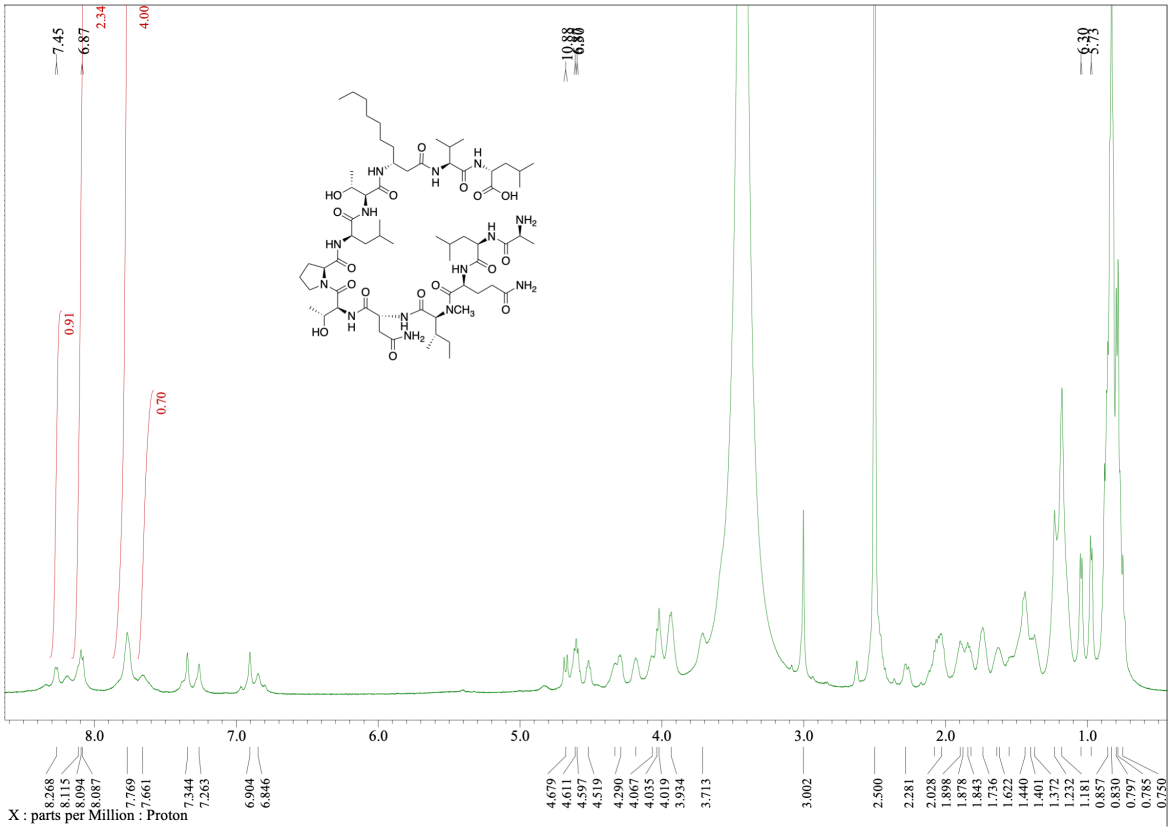

Figure 133. ^{1}H NMR spectrum of 5d. Solvent : dmso-d_6; T : 23°C; Scans : 32

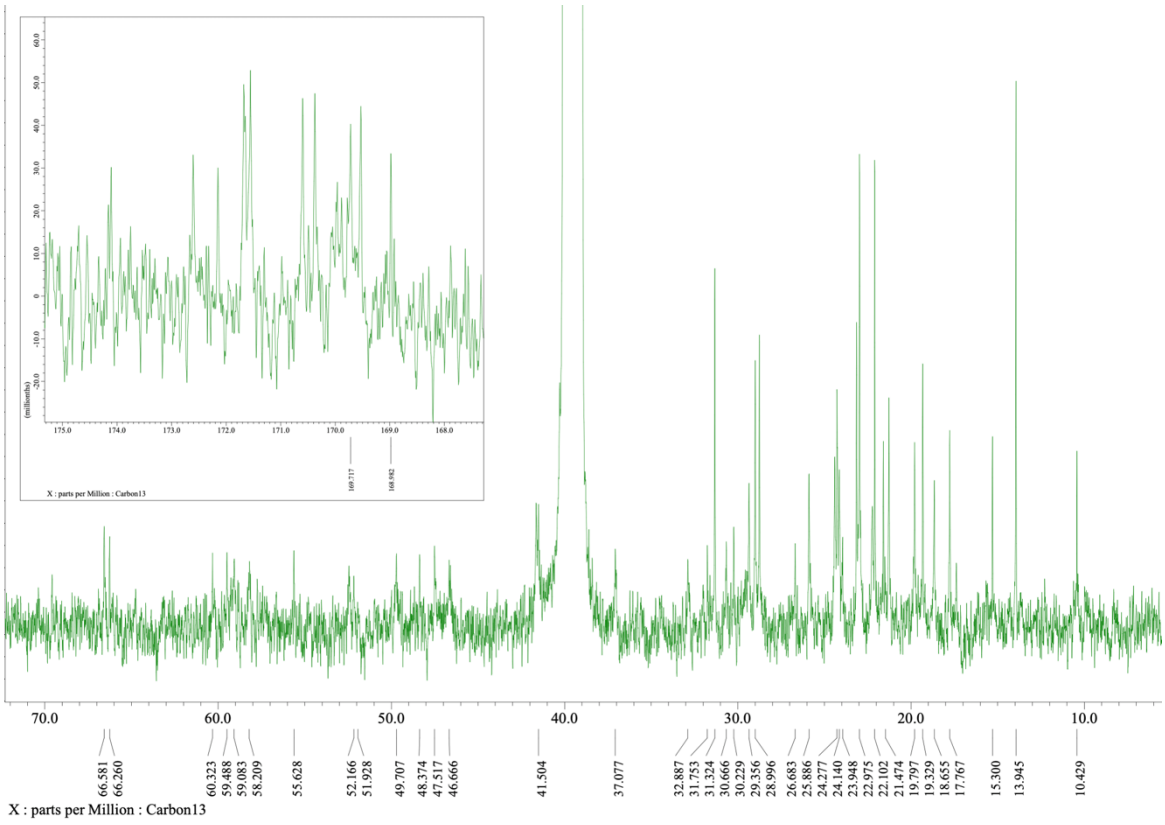

Figure 134. ^{13}C NMR spectrum of 5d. Solvent : dmso-d_6; T : 23°C; Scans : 20000

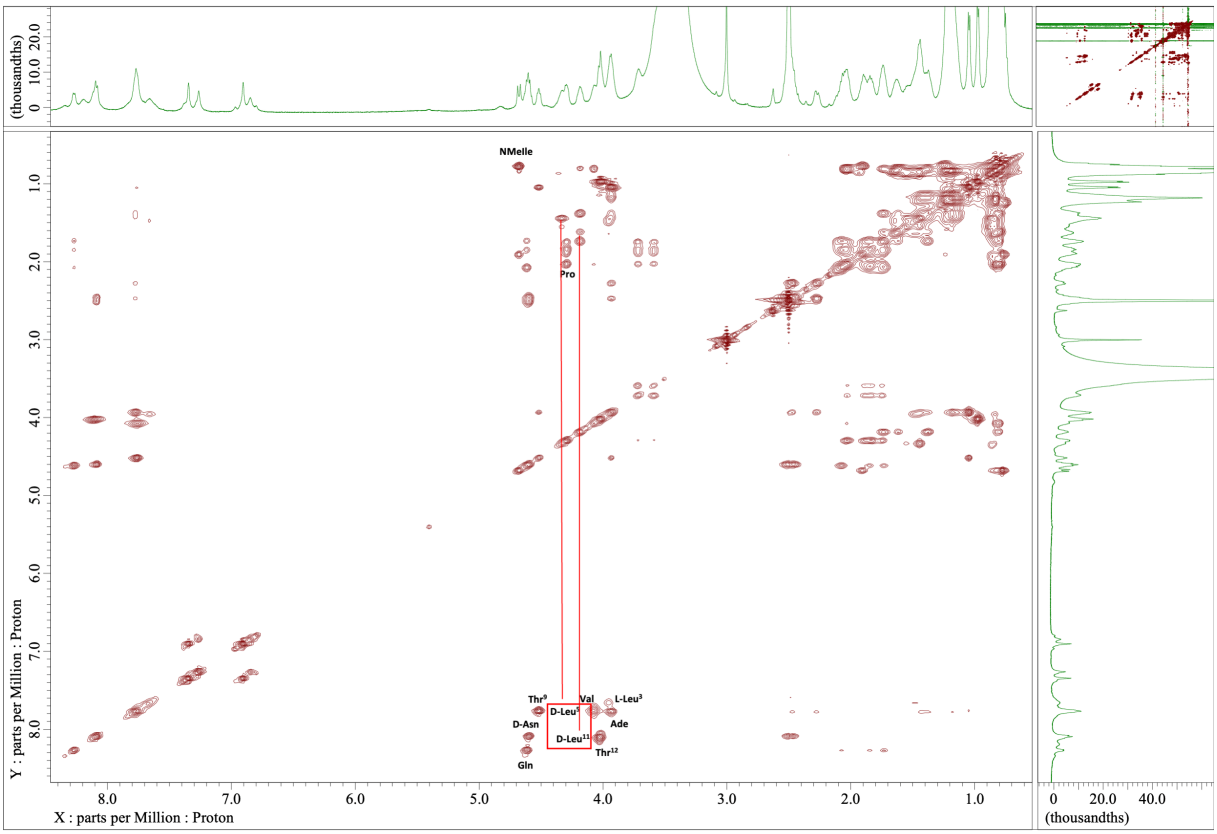

Figure 135. TOCSY spectrum of 5d. Solvent : dmso-d_6; T : 23°C; Scans : 8192

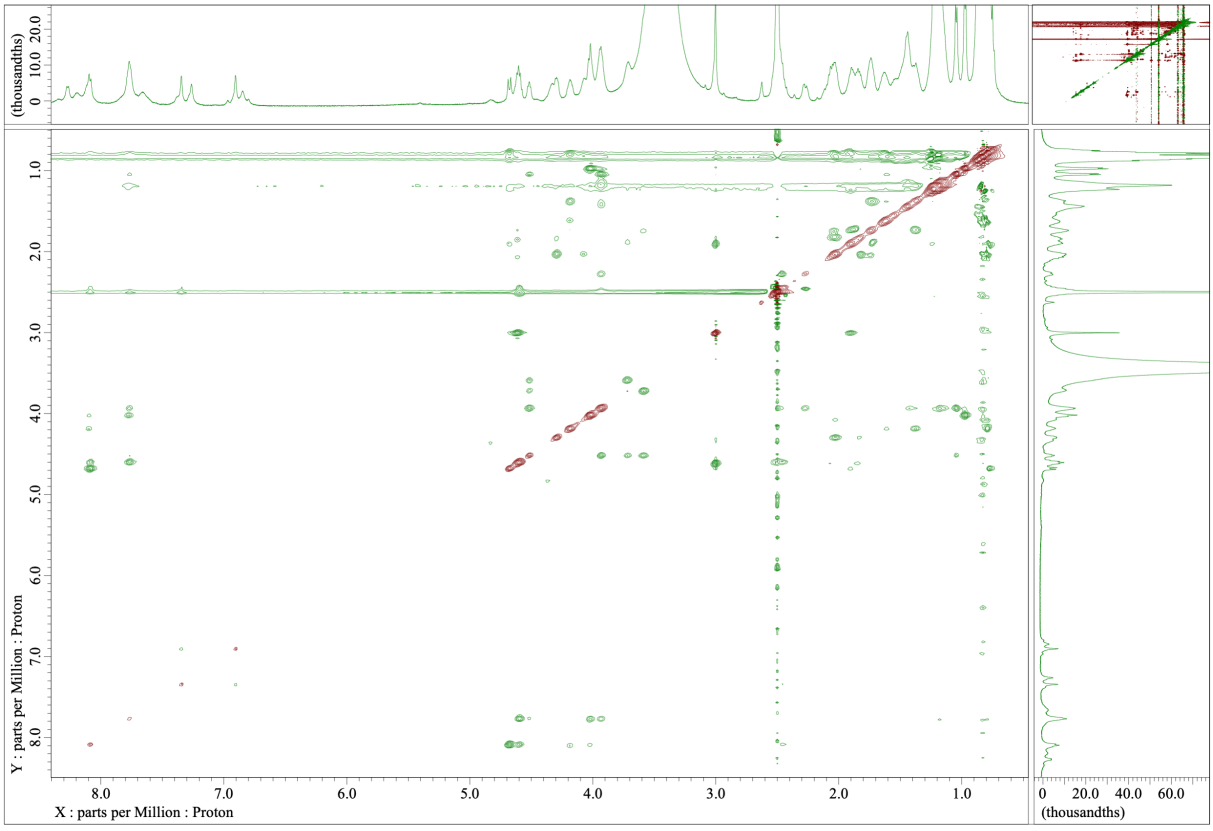

Figure 136. ROESY spectrum of 5d. Solvent : dmso-d_6; T : 23°C; Scans : 8192

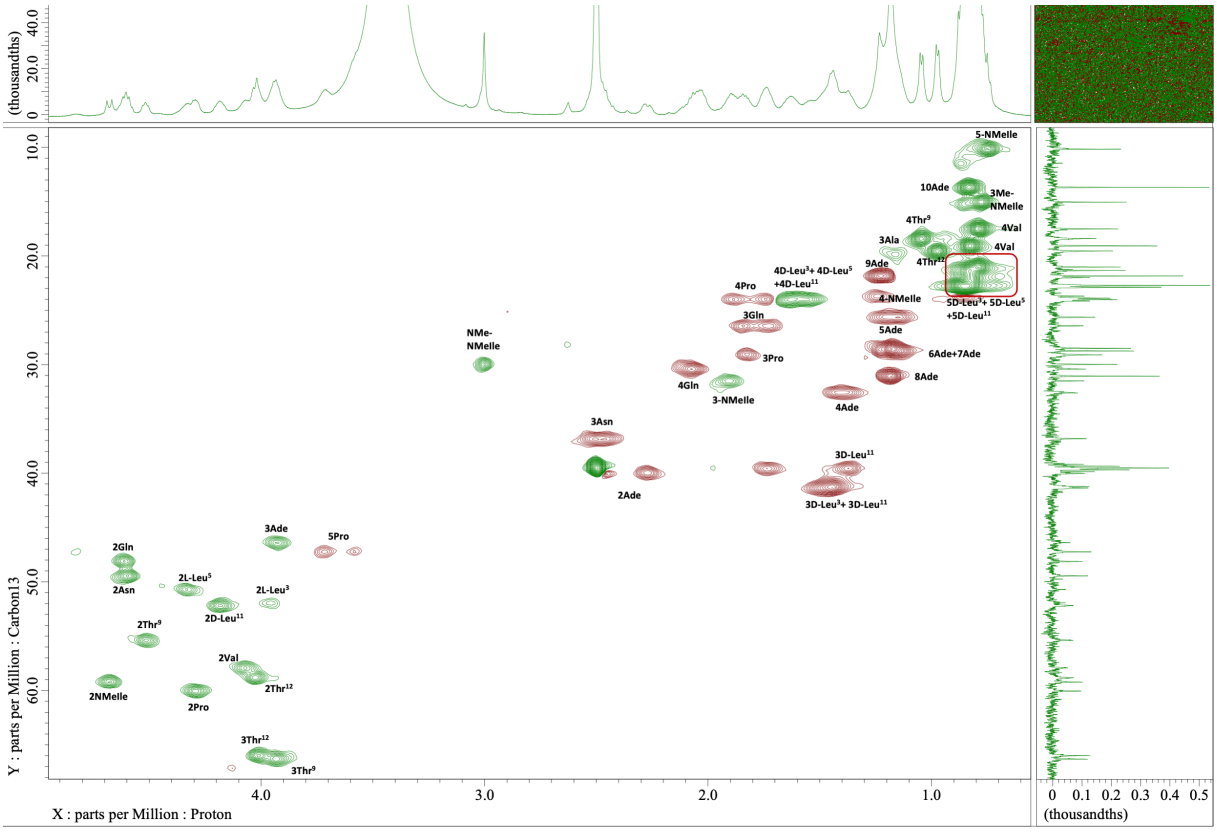

Figure 137. HSQC spectrum of 5d. Solvent : dmso-d_6; T : 23°C; Scans : 8192

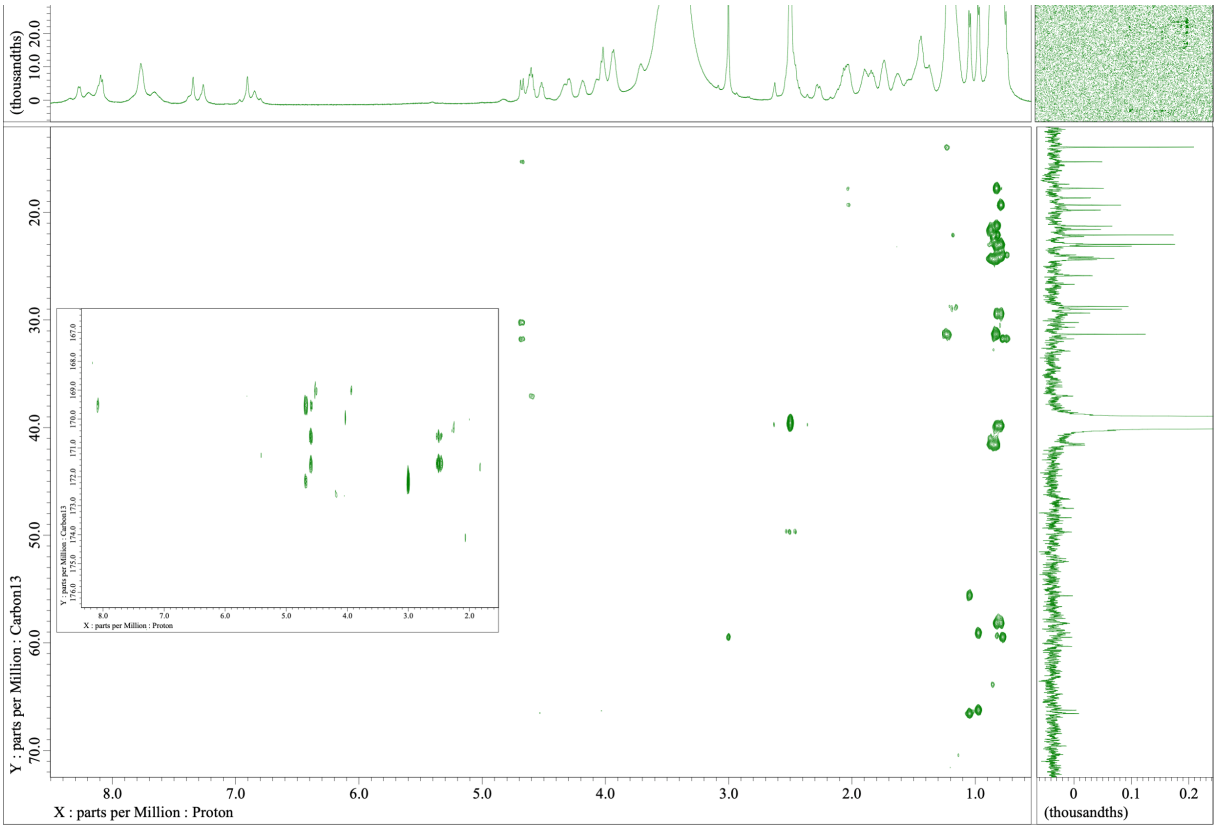

Figure 138. HMBC spectrum of 5d. Solvent : dmso-d_6; T : 23°C; Scans : 16384

c) Compound 7a

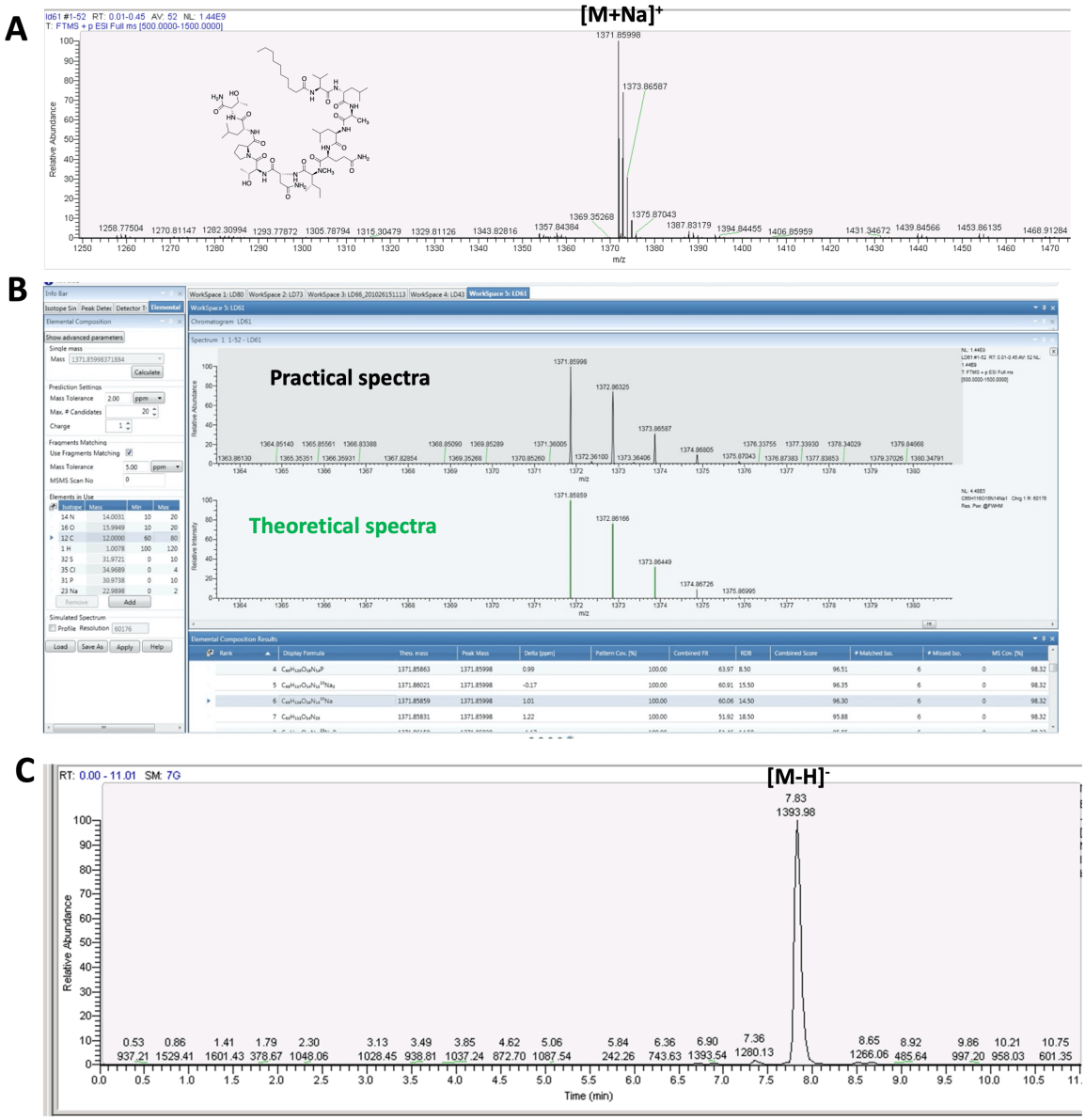

Figure 139. A) ESI-HRMS spectrum of 7a. B) Comparison with the theoretical spectrum. Calculated for $C_{65}H_{116}N_{14}O_{16}Na$ $[M+Na]^+$ *m/z* 1371.85859; Found $[M+Na]^+$ *m/z* 1371.85998; mass error = 1.01 ppm. C) LC-MS profile of 7a

Table 16. NMR spectroscopic data of 7a in DMSO-d_6

entry	position	C, mult.	H, mult. (J in Hz)	entry	position	C, mult.	H, mult. (J in Hz)
Decanoic acid[1]	1	173.0, C	-	N-MeIle[7]	1	169.6, C	-
	2	34.9, CH_2	2.18		2	59.5, CH	4.68, d (11.46)
			2.10		3	31.7, CH	1.90
	3	25.2, CH_2	1.45		3-Me	15.3, CH_3	0.78
	4	28.6-28.9, CH_2	1.21		4	23.9, CH_2	1.27
	5	28.6-28.9, CH_2	1.21		5	10.4, CH_3	0.78
	6	28.6-28.9, CH_2	1.21		N-Me	30.2, CH_3	3.01
	7	28.6-28.9, CH_2	1.21	D-Asn[8]	1	170.8, C	-
	8	31.2, CH_2	1.21		2	49.6, CH	4.60, t (6.30)
	9	22.1, CH_2	1.23		3	37.1, CH_2	2.50
	10	14.0, CH_3	0.84		4	171.6, C	-
Val[2]	1	171.8, C	-		NH	-	8.05, d (8.02)
	2	59.2, CH	3.99, t (7.45)		NH_2	-	7.32 & 6.92
	3	29.7, CH	1.90	Thr[9]	1	168.8, C	-
	3-Me	19.1, CH_3	0.83		2	55.5, CH	4.49, t (6.87)
	4	18.9, CH_3	0.89		3	66.6, CH	3.89
	NH	-	7.96, d (6.87)		4	18.9, CH_3	1.05, d (5.73)
D-Leu[3]	1	172.1, C	-		3-OH	-	5.06, d (4.58)
	2	51.3, CH	4.16		NH	-	7.75, d (8.02)
	3	40.2, CH_2	1.48	Pro[10]	1	171.6, C	-
	4	24.1, CH	1.59		2	59.9, CH	4.32
	4-Me	20.8-23.2, CH_3	0.83		3	29.2, CH_2	1.80
	5	20.8-23.2, CH_3	0.83				2.04
	NH	-	8.33, d (8.02)		4	24.2, CH_2	1.82
Ala[4]	1	172.1, C	-				1.89
	2	48.9, CH	4.13, t (7.45)		5	47.4, CH_2	3.68
	3	17.8, CH_3	1.20				3.68
	NH	-	7.91, d (6.87)	D-Leu[11]	1	172.1, C	-
D-Leu[5]	1	171.8, C	-		2	51.3, CH	4.32
	2	51.0, CH	4.29		3	40.1, CH_2	1.48
	3	41.2, CH_2	1.41		4	24.2, CH	1.55
	4	24.2, CH	1.53		4-Me	20.8-23.2, CH_3	0.87
	4-Me	20.8-23.2, CH_3	0.83		5	20.8-23.2, CH_3	0.87
	5	20.8-23.2, CH_3	0.83		NH	-	7.95, d (7.45)
	NH	-	7.80, d (8.59)	Thr[12]	1	172.2, C	-
Gln[6]	1	172.1, C	-		2	58.1, CH	4.05, d (6.87)
	2	48.2, CH	4.64, t (6.87)		3	66.1, CH	4.05, d (6.87)
	3	26.9, CH_2	1.73		4	20.1, CH_3	0.99, d (6.30)
			1.86		3-OH	-	4.80, d (5.73)
	4	30.6, CH_2	2.05		NH	-	7.63, d (8.59)
	5	174.0, C	-		NH_2	-	7.13 & 7.08
	NH	-	8.09, d (8.02)				
	NH_2	-	7.17 & 6.80				

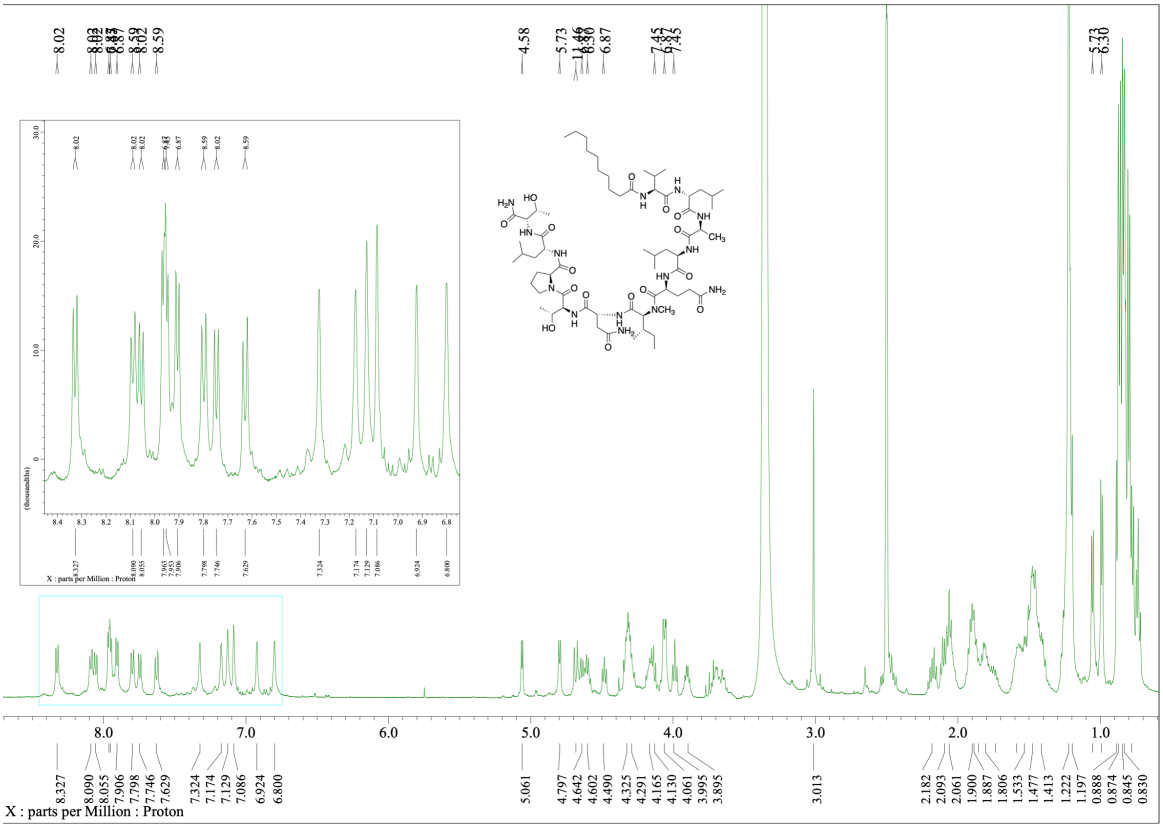

Figure 140. ^{1}H NMR spectrum of 7a. Solvent : dmso-d_6; T : 23°C; Scans : 32

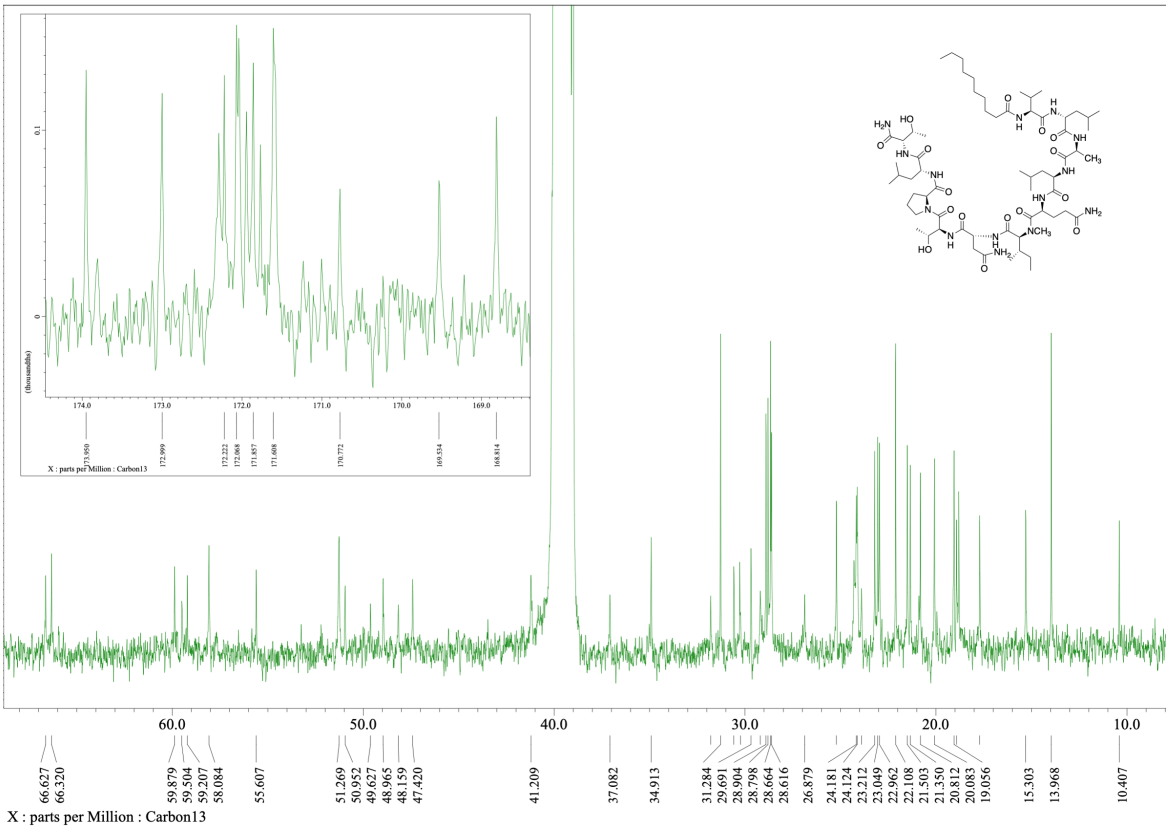

Figure 141. ^{13}C NMR spectrum of 7a. Solvent : dmso-d_6; T : 23°C; Scans : 20000

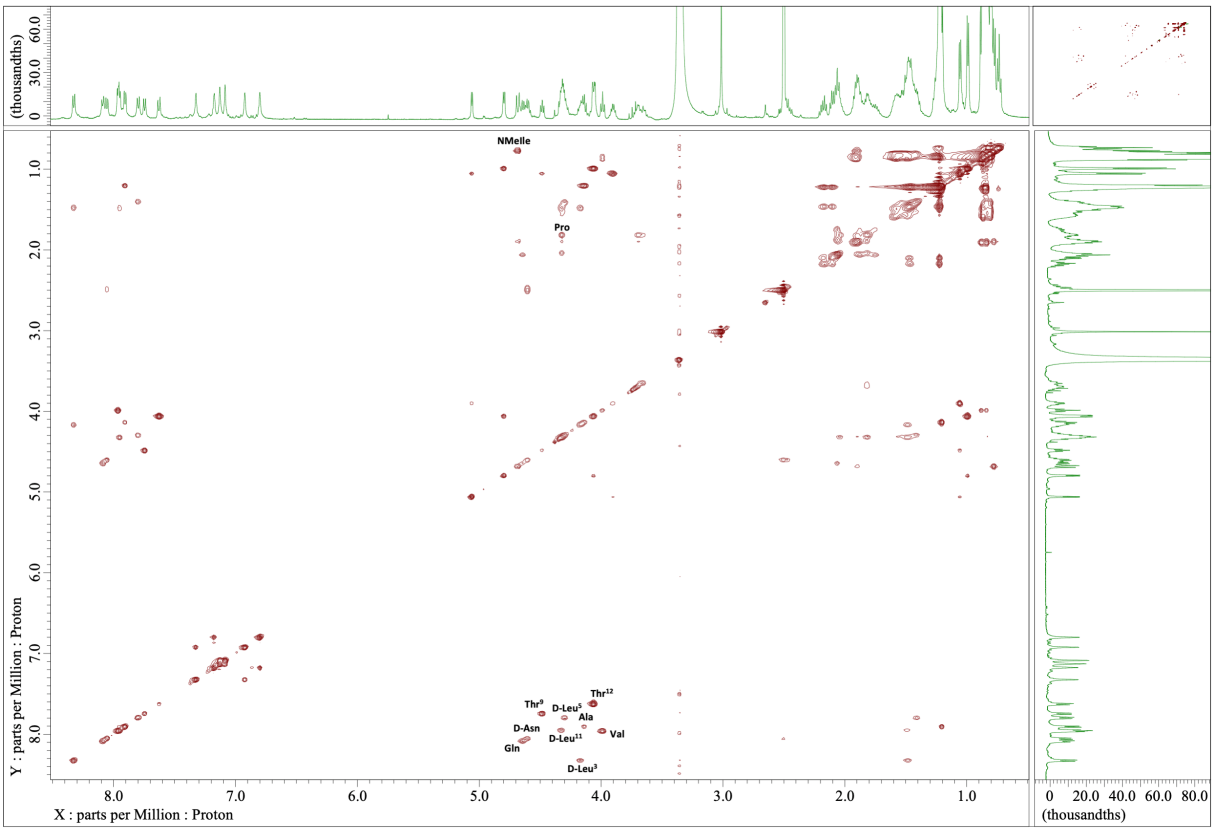

Figure 142. TOCSY spectrum of 7a. Solvent : dmso-d_6; T : 23°C; Scans : 8192

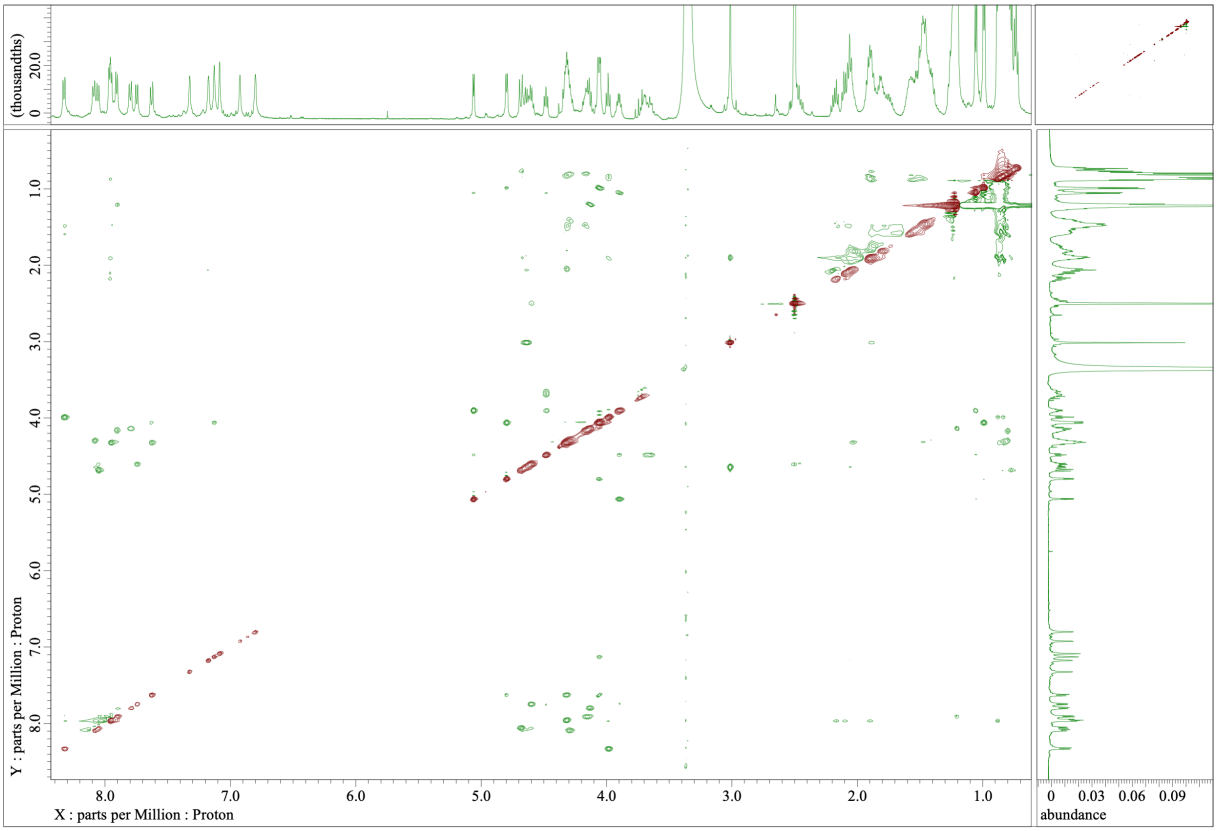

Figure 143. ROESY spectrum of 7a. Solvent : dmso-d_6; T : 23°C; Scans : 8192

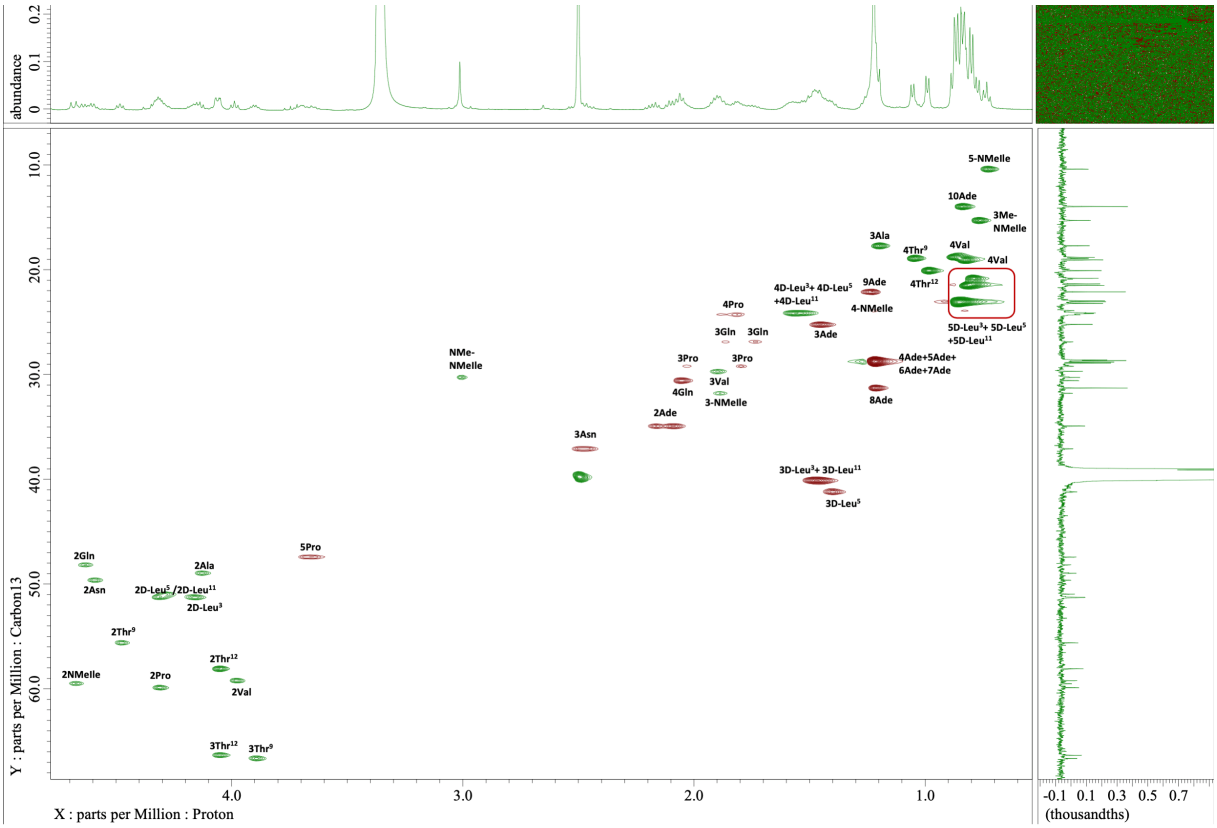

Figure 144. HSQC spectrum of 7a. Solvent : dmso-d_6; T : 23°C; Scans : 8192

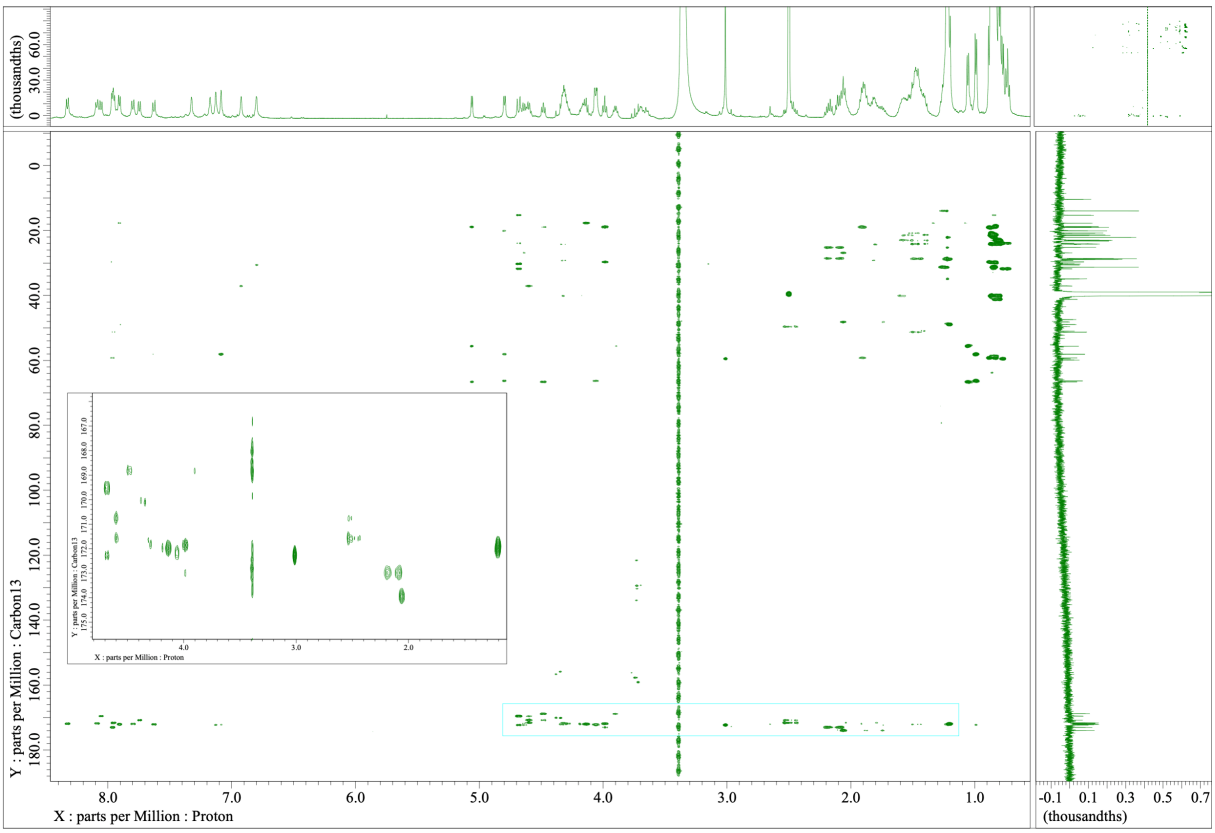

Figure 145. HMBC spectrum of 7a. Solvent : dmso-d_6; T : 23°C; Scans : 16384

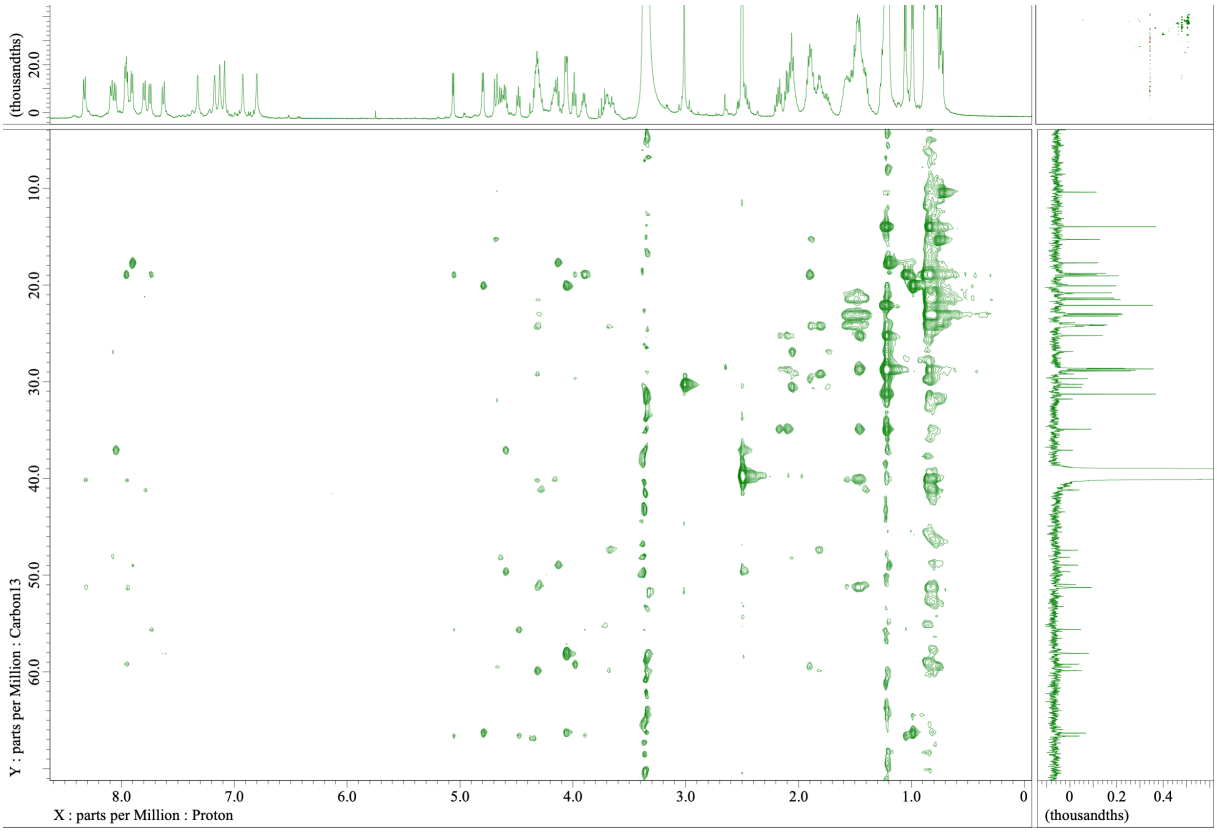

Figure 146. HSQC-TOCSY spectrum of 7a. Solvent : dmso-d_6; T : 23°C; Scans : 8192

d) Compound 8a

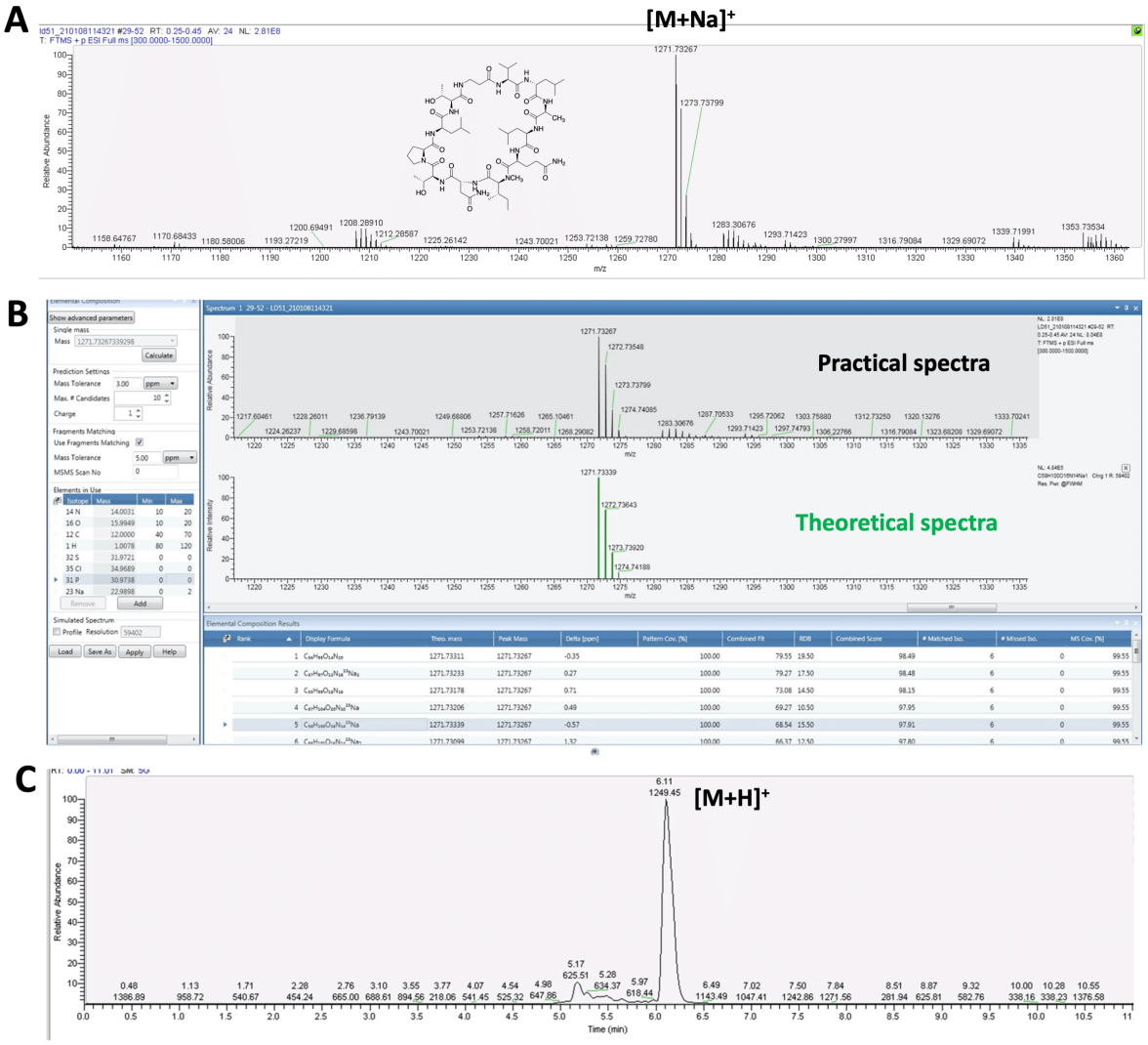

Figure 147. A) ESI-HRMS spectrum of 8a. B) Comparison with the theoretical spectrum. Calculated for $C_{58}H_{100}N_{14}O_{16}Na$ $[M+Na]^+$ *m/z* 1271.73339; Found $[M+Na]^+$ *m/z* 1271.73267; mass error = 0.57 ppm. C) LC-MS profile of 8a

Table 17. NMR spectroscopic data of 8a in DMSO-d_6

entry	position	C, mult.	H, mult. (J in Hz)	entry	position	C, mult.	H, mult. (J in Hz)
β-Ala[1]	1	*nd*, C	-	N-MeIle[7]	1	170.7, C	-
	2	35.0, CH_2	2.36		2	59.6, CH	4.66, d (10.88)
	3	34.4, CH_2	3.25		3	31.8, CH	1.90
	NH	-	7.80, t (5.15)		3-Me	15.4, CH_3	0.78
Val[2]	1	171.1, C	-		4	24.0, CH_2	1.24
	2	58.3, CH	4.15, t (7.45)		5	10.5, CH_3	0.76
	3	30.3, CH	1.95		N-Me	30.2, CH_3	2.96
	3-Me	19.1, CH_3	0.84	D-Asn[8]	1	171.5, C	-
	4	18.3, CH_3	0.85		2	49.6, CH	4.62
	NH	-	8.12, d (8.02)		3	36.0, CH_2	2.55
D-Leu[3]	1	*nd*, C	-				2.43
	2	51.1-51.4, CH	4.26		4	172.6, C	-
	3	40.5-41.1, CH_2	1.43		NH	-	8.22, d (7.45)
	4	24.2, CH	1.55		NH_2	-	7.30 & 6.87
	4-Me	21.1-23.2, CH_3	0.81	Thr[9]	1	168.6, C	-
	5	21.1-23.2, CH_3	0.81		2	56.1, CH	4.41, t (6.87)
	NH	-	8.34, d (7.45)		3	66.5, CH	3.87, t (6.30)
Ala[4]	1	171.9, C	-		4	19.1, CH_3	1.07, d (6.30)
	2	48.8, CH	4.20, t (7.45)		NH	-	7.45, d (7.45)
	3	18.1, CH_3	1.20, d (6.87)	Pro[10]	1	171.8, C	-
	NH	-	8.18, d (6.87)		2	59.8, CH	4.32
D-Leu[5]	1	*nd*, C	-		3	29.3, CH_2	1.75
	2	51.1-51.4, CH	4.24				2.07
	3	40.5-41.1, CH_2	1.43		4	24.4, CH_2	1.82
	4	24.2, CH	1.55				1.89
	4-Me	21.1-23.2, CH_3	0.86		5	47.6, CH_2	3.66
	5	21.1-23.2, CH_3	0.86	D-Leu[11]	1	*nd*, C	-
	NH	-	7.91, d (8.59)		2	51.1-51.4, CH	4.32
Gln[6]	1	*nd*, C	-		3	40.5-41.1, CH_2	
	2	48.3, CH	4.60		4	24.2, CH	
	3	26.8, CH_2	1.68		4-Me	21.1-23.2, CH_3	0.81
			1.85		5	21.1-23.2, CH_3	0.81
	4	30.6, CH_2	2.05		NH	-	8.06, d (7.45)
	5	174.2, C	-	Thr[12]	1	169.7, C	-
	NH	-	8.08, d (8.59)		2	58.4, CH	4.07
	NH_2	-	7.21 & 6.77		3	66.3, CH	4.02
					4	19.9, CH_3	0.99, d (6.30)
					NH	-	7.82, d (8.59)

nd = Not determined

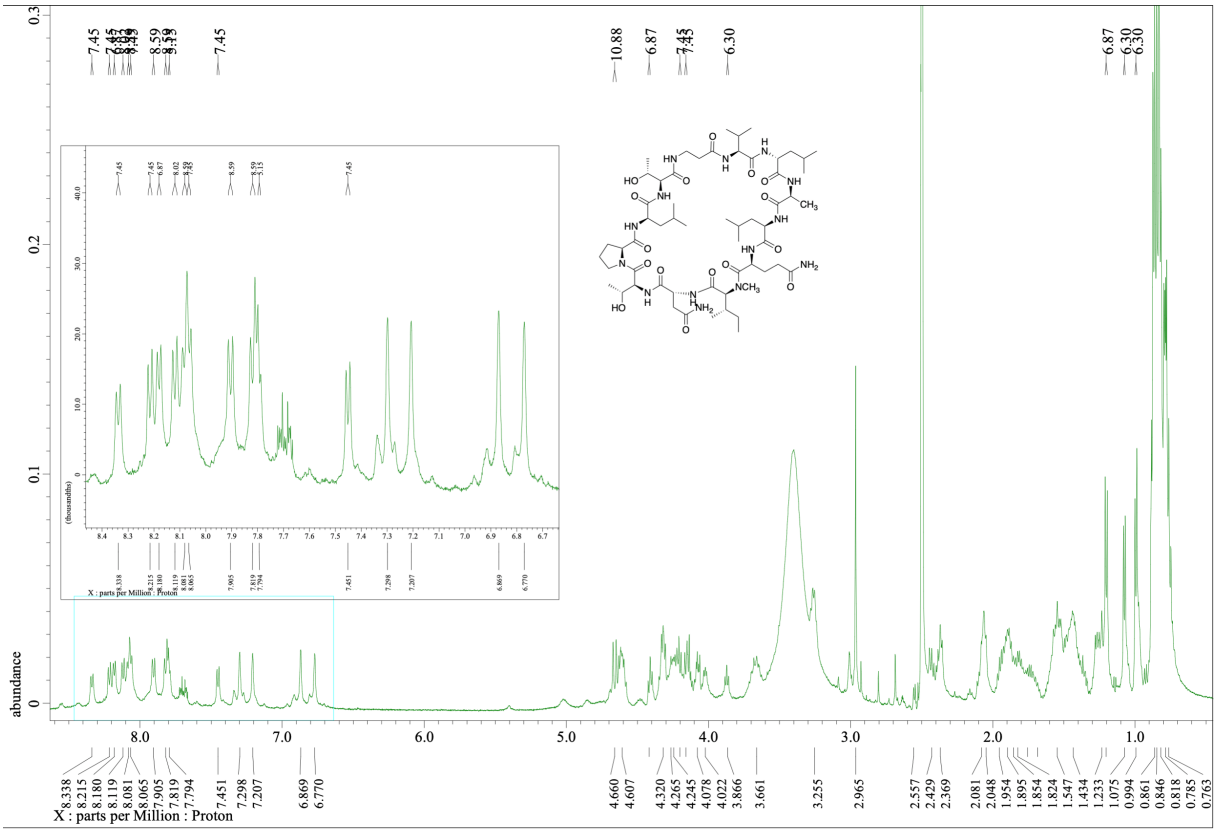

Figure 148. ^{1}H NMR spectrum of 8a. Solvent : dmso-d_6; T : 23°C; Scans : 32

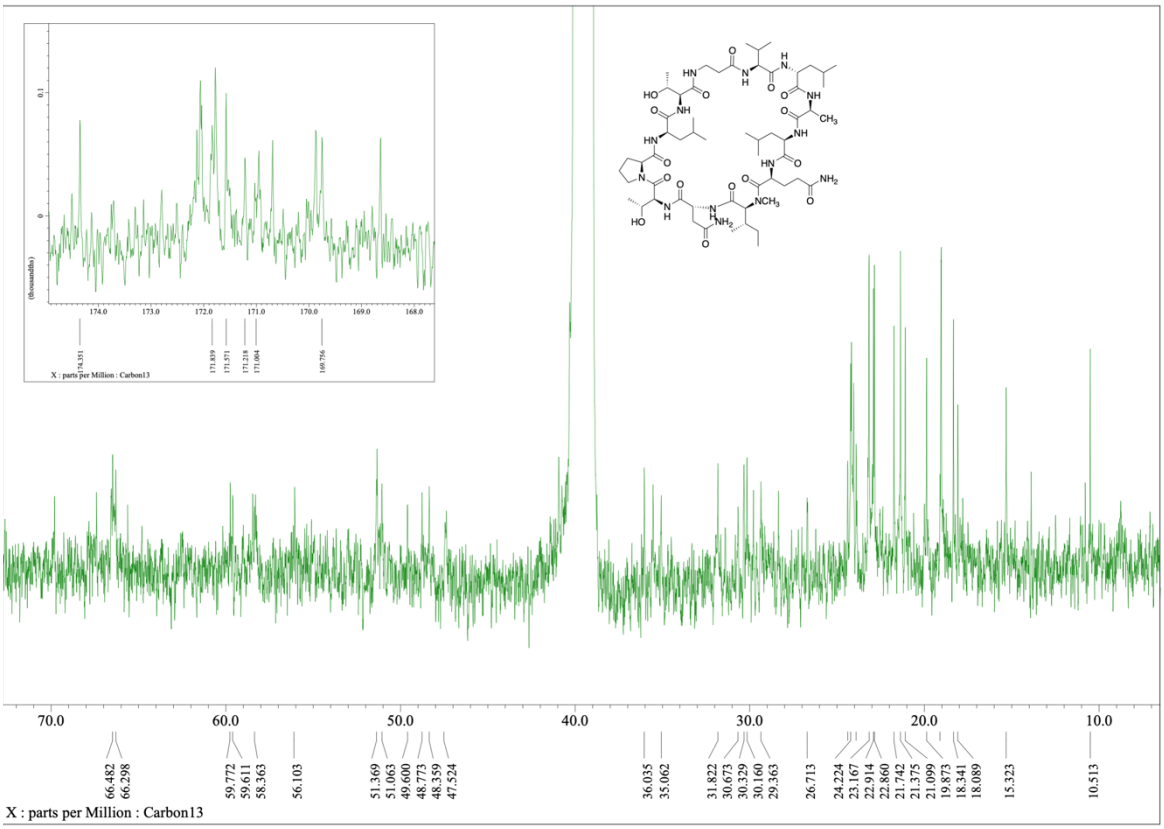

Figure 149. ^{13}C NMR spectrum of 8a. Solvent : dmso-d_6; T : 23°C; Scans : 20000

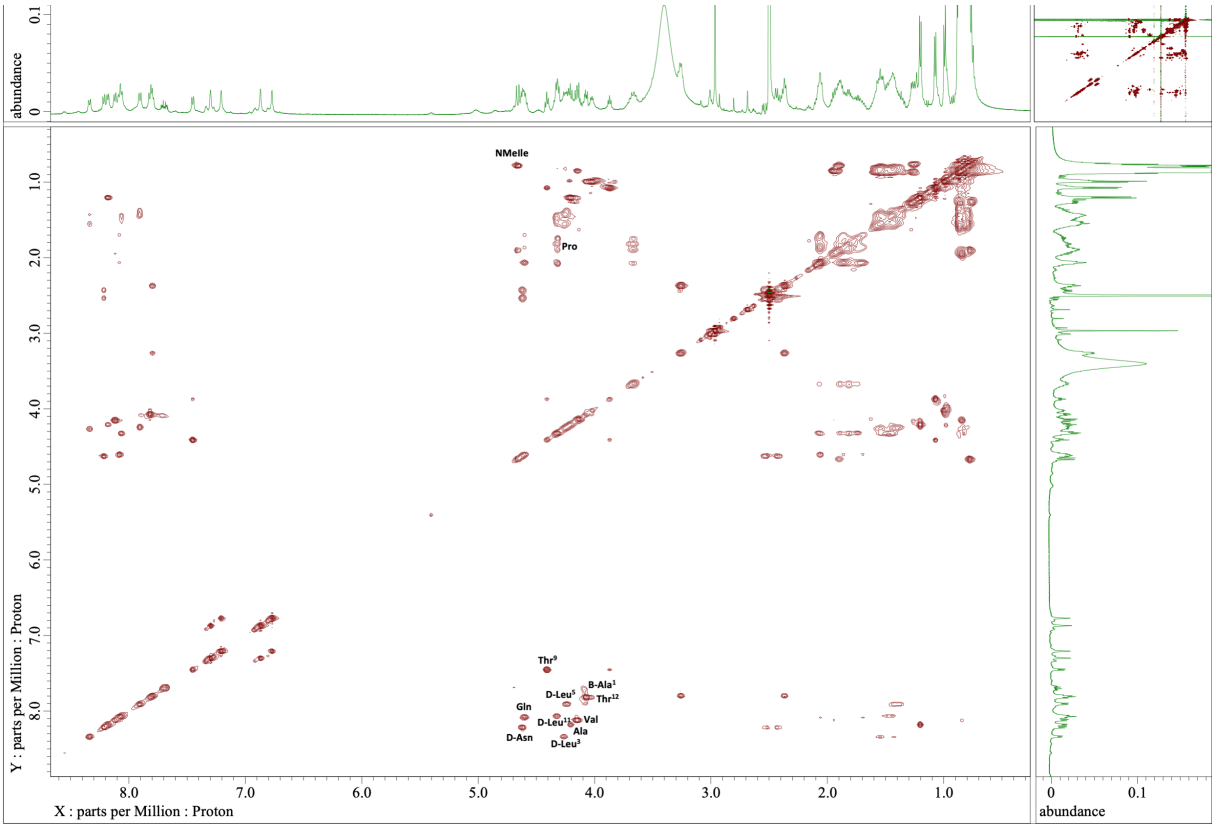

Figure 150. TOCSY spectrum of 8a. Solvent : dmso-d_6; T : 23°C; Scans : 8192

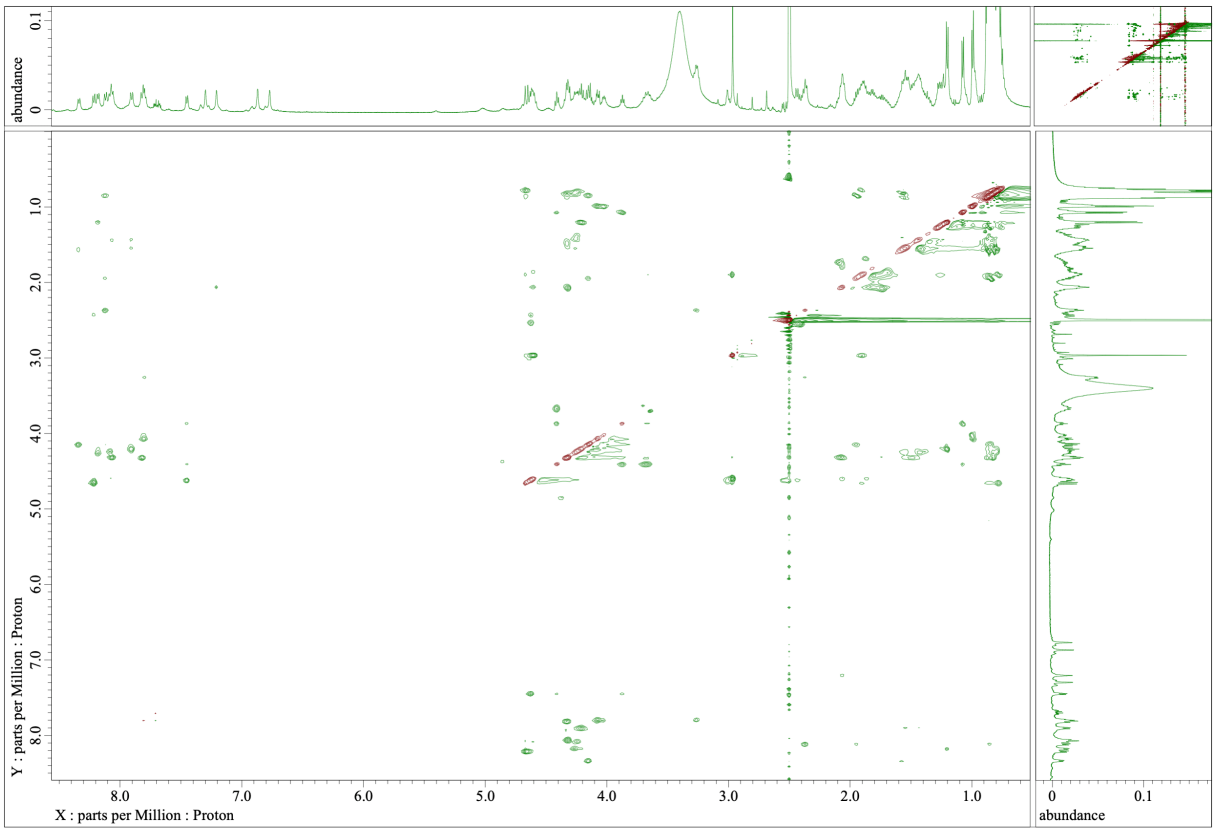

Figure 151. ROESY spectrum of 8a. Solvent : dmso-d_6; T : 23°C; Scans : 8192

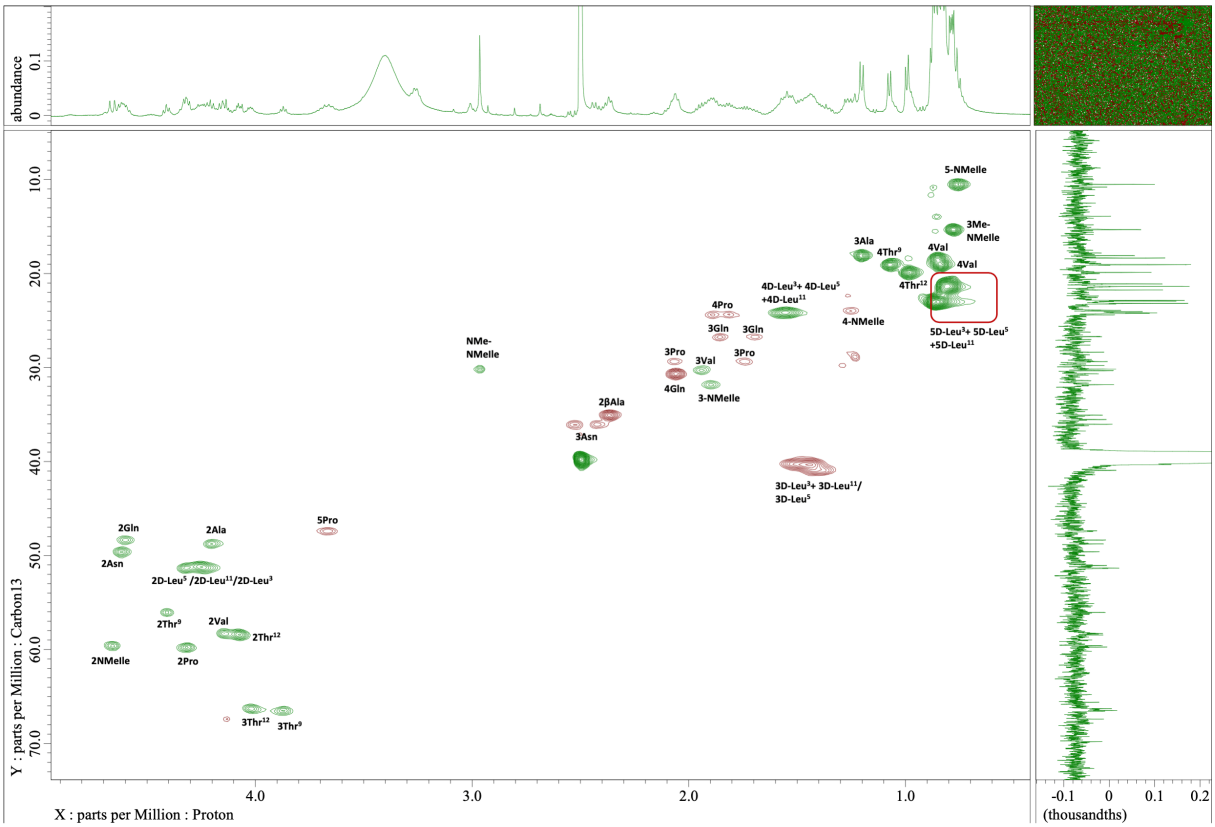

Figure 152. HSQC spectrum of 8a. Solvent : dmso-d_6; T : 23°C; Scans : 8192

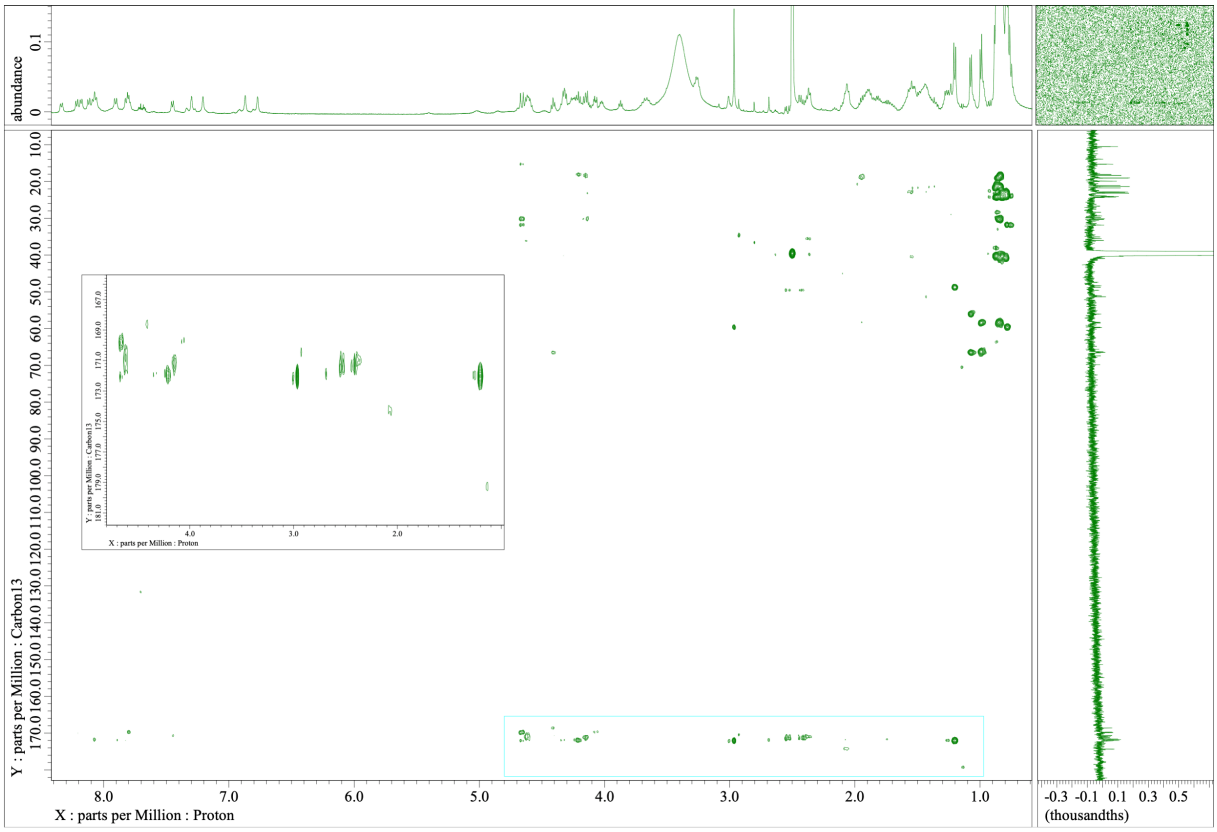

Figure 153. HMBC spectrum of 8a. Solvent : dmso-d_6; T : 23°C; Scans : 16384

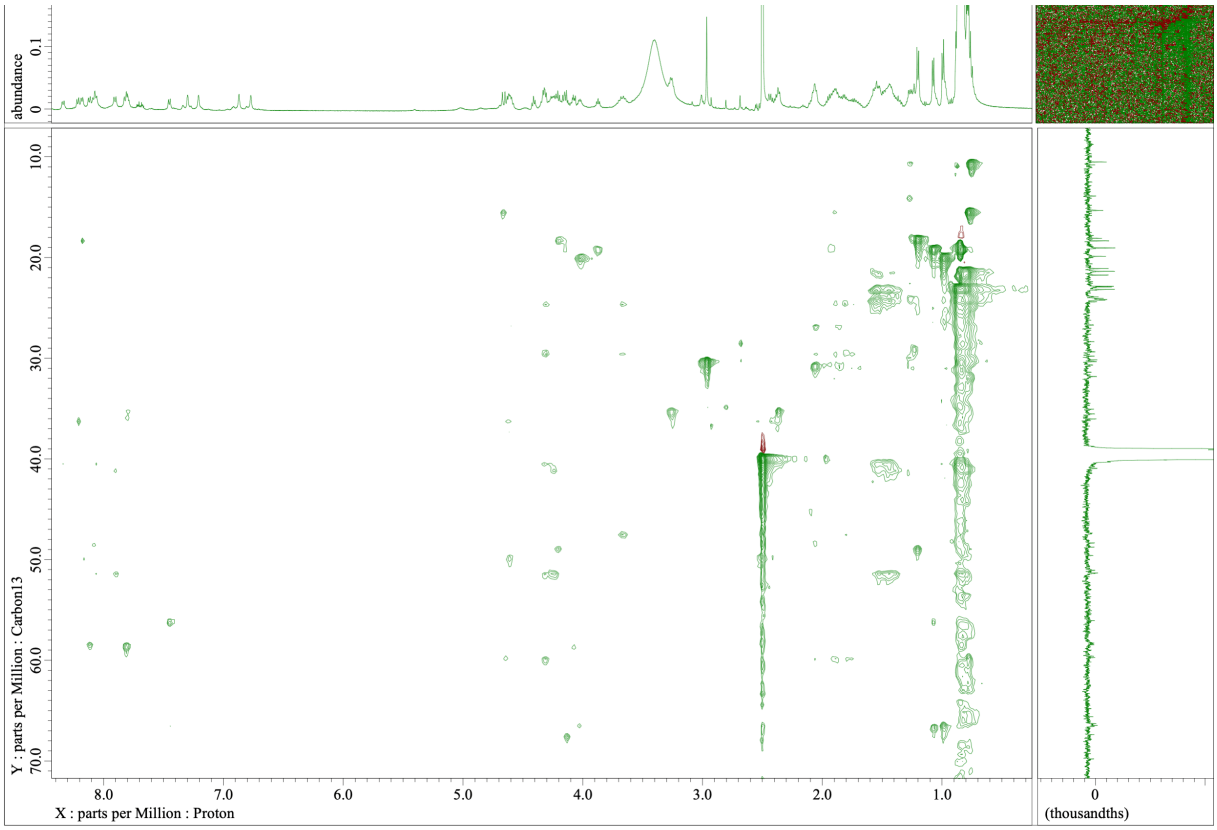

Figure 154. HSQC-TOCSY spectrum of 8a. Solvent : dmso-d_6; T : 23°C; Scans : 8192

e) Compound 9a

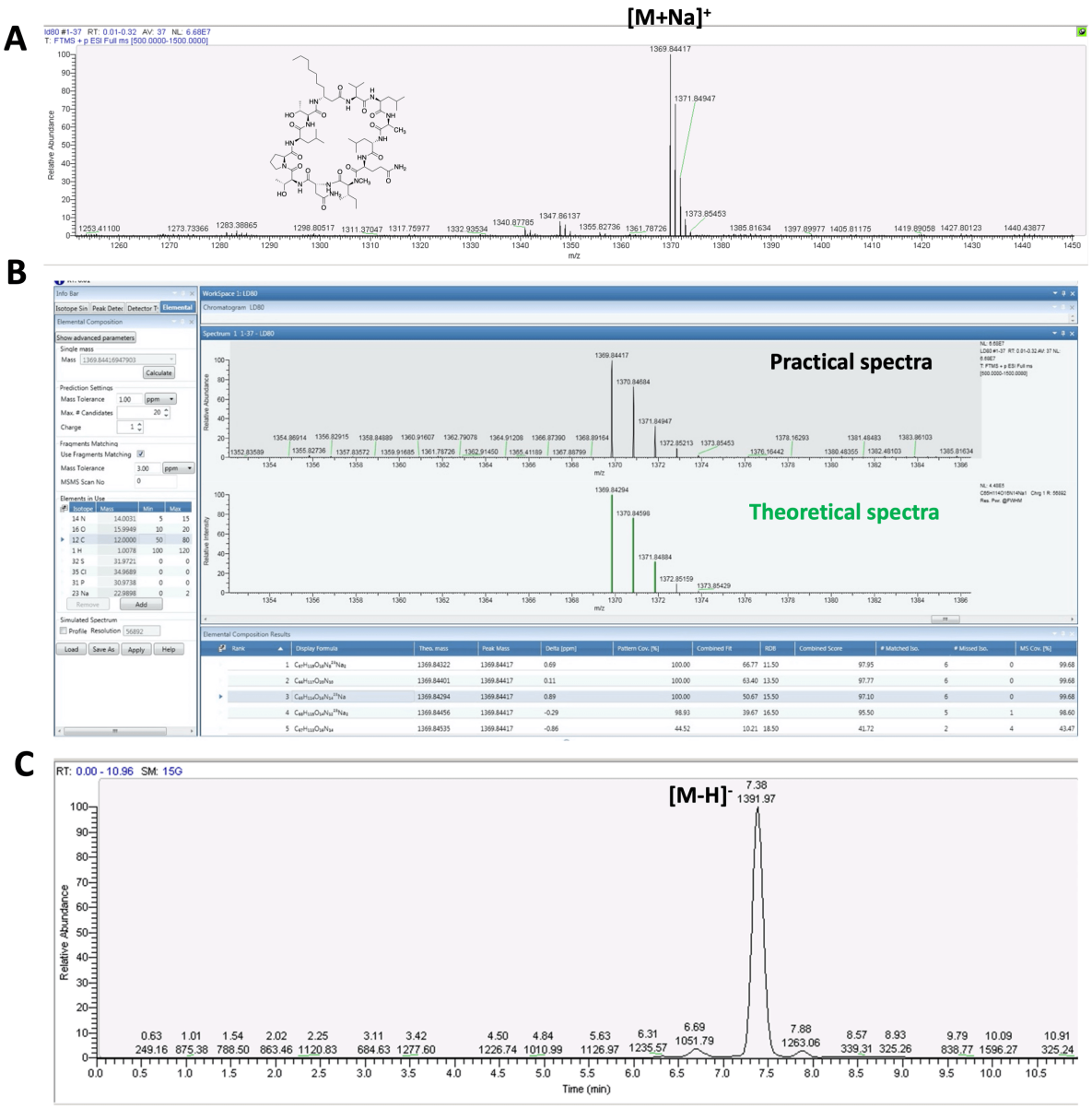

Figure 155. A) ESI-HRMS spectrum of 9a. B) Comparison with the theoretical spectrum. Calculated for $C_{65}H_{114}N_{14}O_{16}Na$ $[M+Na]^+$ *m/z* 1369.84294; Found $[M+Na]^+$ *m/z* 1369.84417; mass error = 0.89 ppm. C) LC-MS profile of 9a

Table 18. NMR spectroscopic data of 9a in DMSO-d_6

entry	position	C, mult.	H, mult. (J in Hz)	entry	position	C, mult.	H, mult. (J in Hz)
Ade[1]	1	*nd*, C	-	N-MeIle[7]	1	*nd*, C	-
	2	41.1, CH_2	2.37, d (8.59)		2	59.5, CH	4.66, d (10.31)
			2.37, d (8.59)		3	31.7, CH	1.90
	3	46.2, CH	4.10		3-Me	15.4, CH_3	0.78
	4	33.4, CH_2	1.38		4	23.9, CH_2	1.20
	5	25.5, CH_2	1.23		5	10.5, CH_3	0.77
	6	28.8, CH_2	1.19		N-Me	30.1, CH_3	2.93
	7	28.8, CH_2	1.19	D-Asn[8]	1	*nd*, C	-
	8	31.3, CH_2	1.19		2	49.2, CH	4.68
	9	22.2, CH_2	1.24		3	35.8, CH_2	2.54
	10	14.0, CH_3	0.84				2.42
	NH	-	7.56		4	*nd*, C	-
Val[2]	1	*nd*, C	-		NH	-	8.20, d (7.45)
	2	58.4, CH	4.06		NH_2	-	7.34 & 6.92
	3	29.8, CH	2.03	Thr[9]	1	*nd*, C	-
	3-Me	19.3, CH_3	0.80		2	55.2, CH	4.51
	4	18.1, CH_3	0.82		3	66.5, CH	3.93
	NH	-	8.07		4	18.7, CH_3	1.06, d (5.73)
L-Leu[3]	1	*nd*, C	-		3-OH	-	
	2	50.7, CH	4.29		NH	-	7.46, d (7.45)
	3	40.4, CH_2	1.46	Pro[10]	1	*nd*, C	-
	4	24.1, CH	1.56		2	59.7, CH	4.33
	4-Me	22.9-23.2, CH_3	0.84		3	29.3, CH_2	1.73
	5	22.9-23.2, CH_3	0.84				2.06
	NH	-	7.90		4	24.1, CH_2	1.82
Ala[4]	1	171.4, C	-				1.82
	2	48.2, CH	4.19, d (6.87)		5	47.4, CH_2	3.7
	3	17.3, CH_3	1.20				3.61
	NH	-	8.06, d (6.30)	D-Leu[11]	1	*nd*, C	-
L-Leu[5]	1	*nd*, C	-		2	51.5, CH	4.28
	2	50.7, CH	4.26		3	40.4, CH_2	1.46
	3	41.2, CH_2	1.37		4	24.1, CH	1.56
	4	24.1, CH	1.56		4-Me	22.9-23.2, CH_3	0.84
	4-Me	22.9-23.2, CH_3	0.84		5	22.9-23.2, CH_3	0.84
	5	22.9-23.2, CH_3	0.84		NH	-	7.97
	NH	-	7.61	Thr[12]	1	*nd*, C	-
Gln[6]	1	*nd*, C	-		2	59.1, CH	4.03, d (8.59)
	2	48.1, CH	4.59, dd (6.87)		3	66.3, CH	4.01
	3	27.1, CH_2	1.73		4	19.7, CH_3	0.99, d (5.73)
			1.86		3-OH	-	
	4	30.7, CH_2	2.04		NH	-	7.96(8.59)
	5	*nd*, C	-				
	NH	-	8.21, d (6.87)				
	NH_2	-	7.13 & 6.75				

nd = Not determined

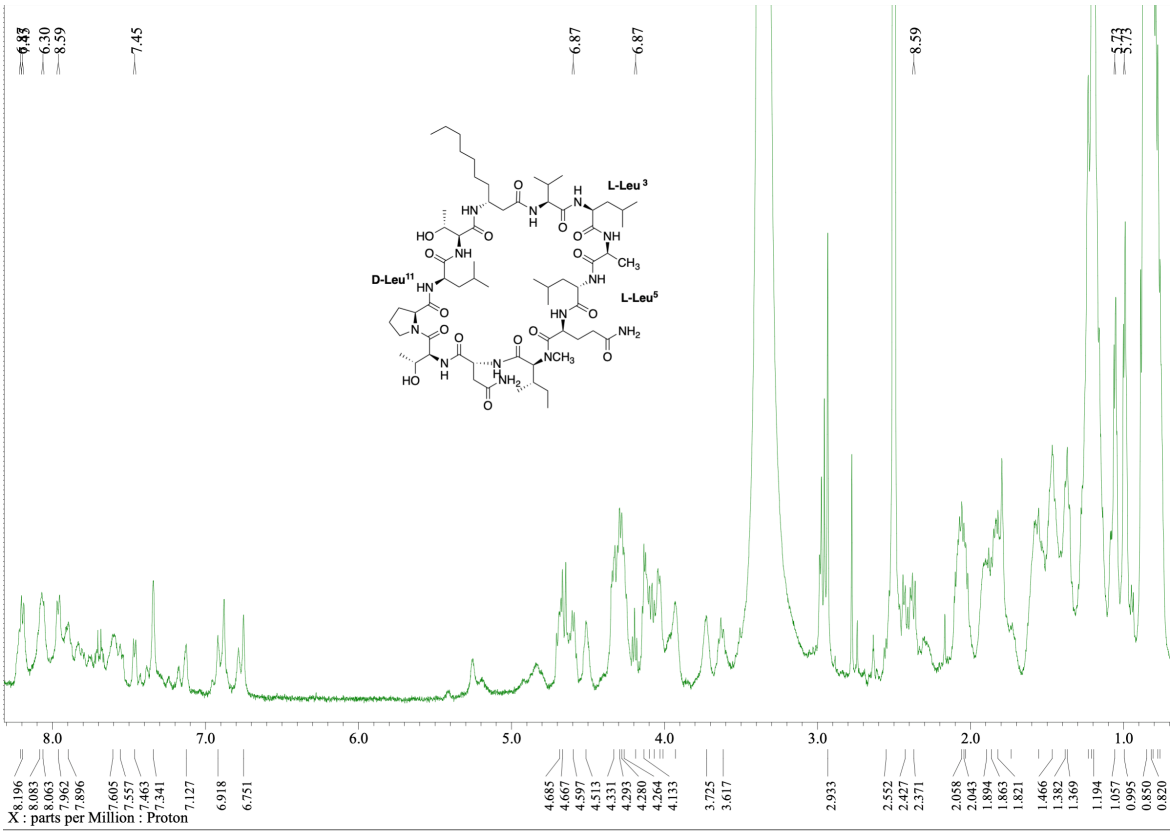

Figure 156. ^{1}H NMR spectrum of 9a. Solvent : dmso-d_6; T : 23°C; Scans : 32

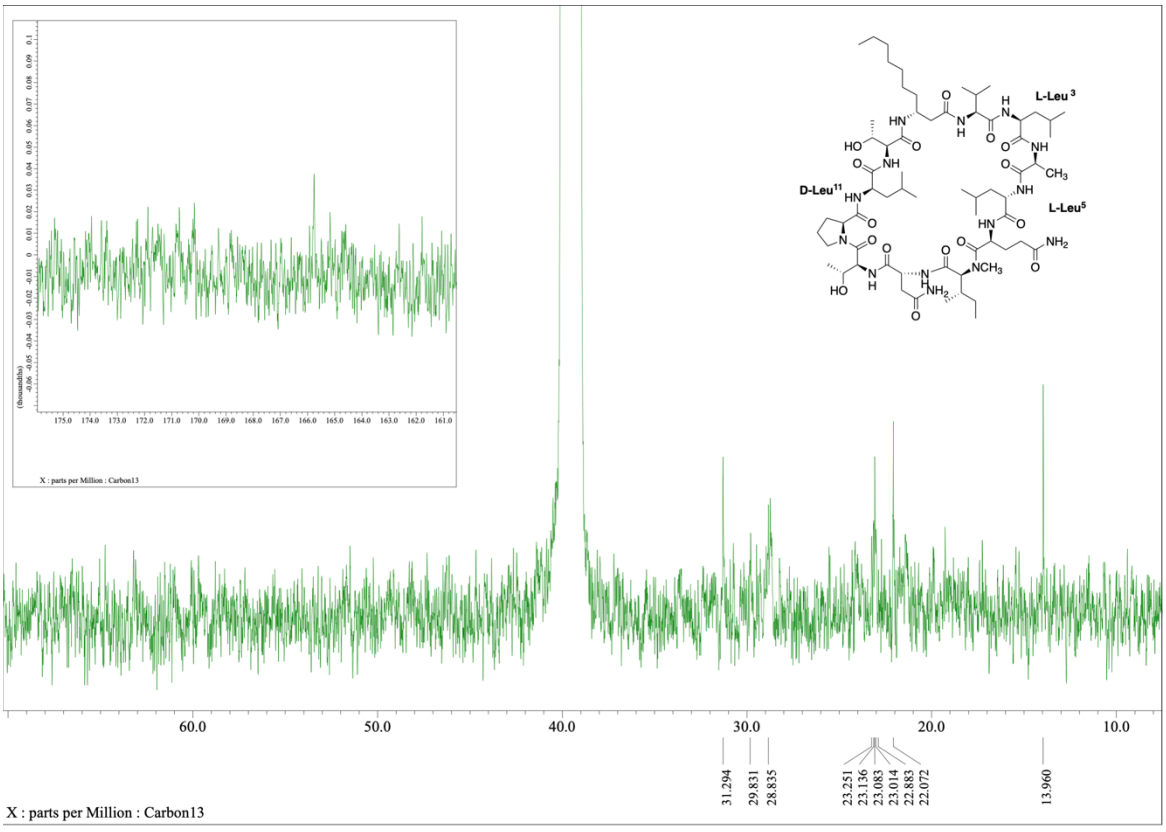

Figure 157. DEPT135 NMR spectrum of 9a. Solvent : dmso-d_6; T : 23°C; Scans : 10000

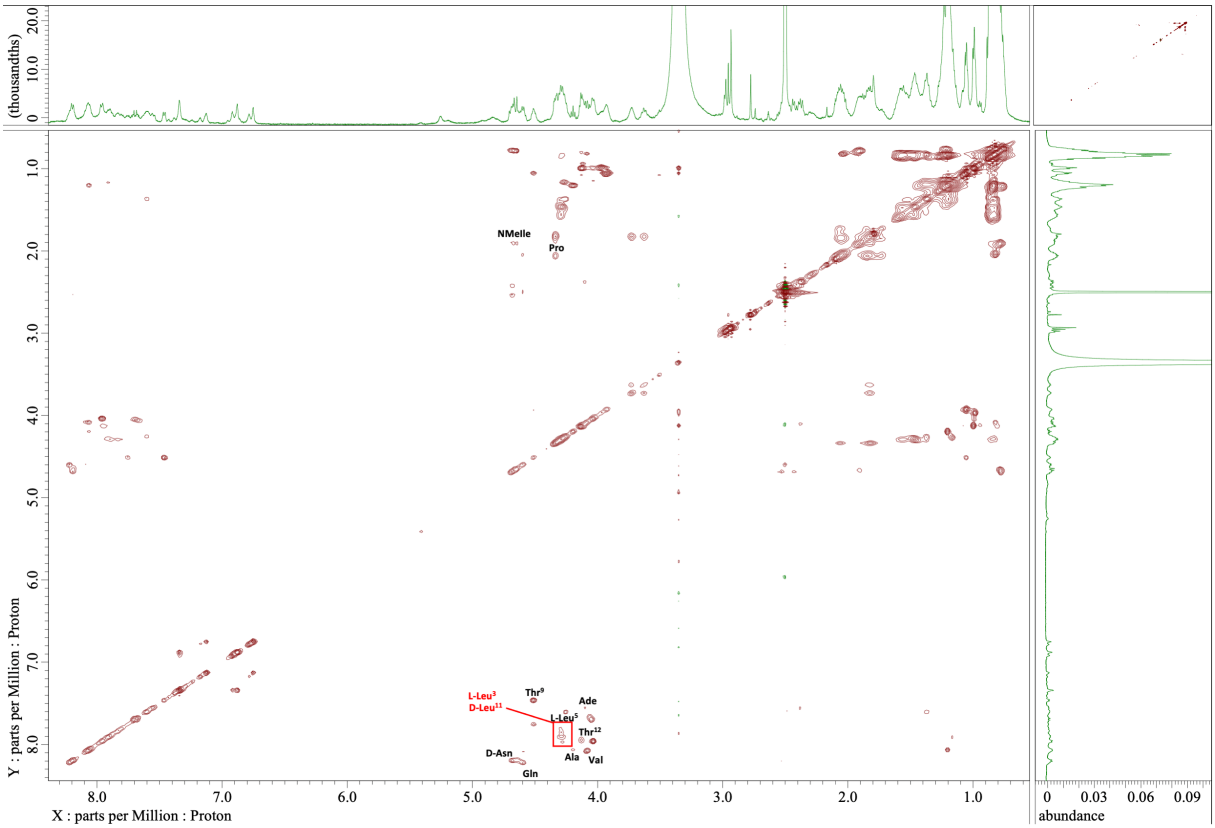

Figure 158. TOCSY spectrum of 9a. Solvent : dmso-d_6; T : 23°C; Scans : 8192

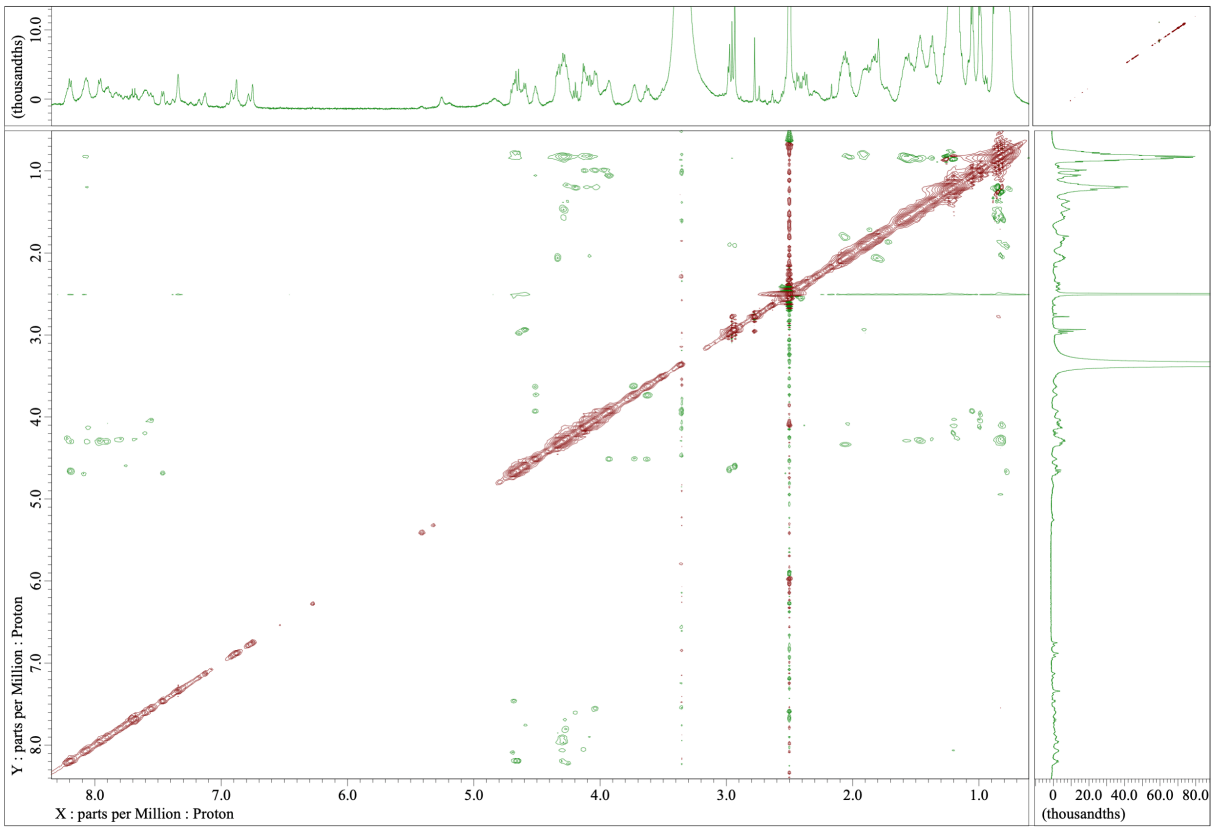

Figure 159. ROESY spectrum of 9a. Solvent : dmso-d_6; T : 23°C; Scans : 8192

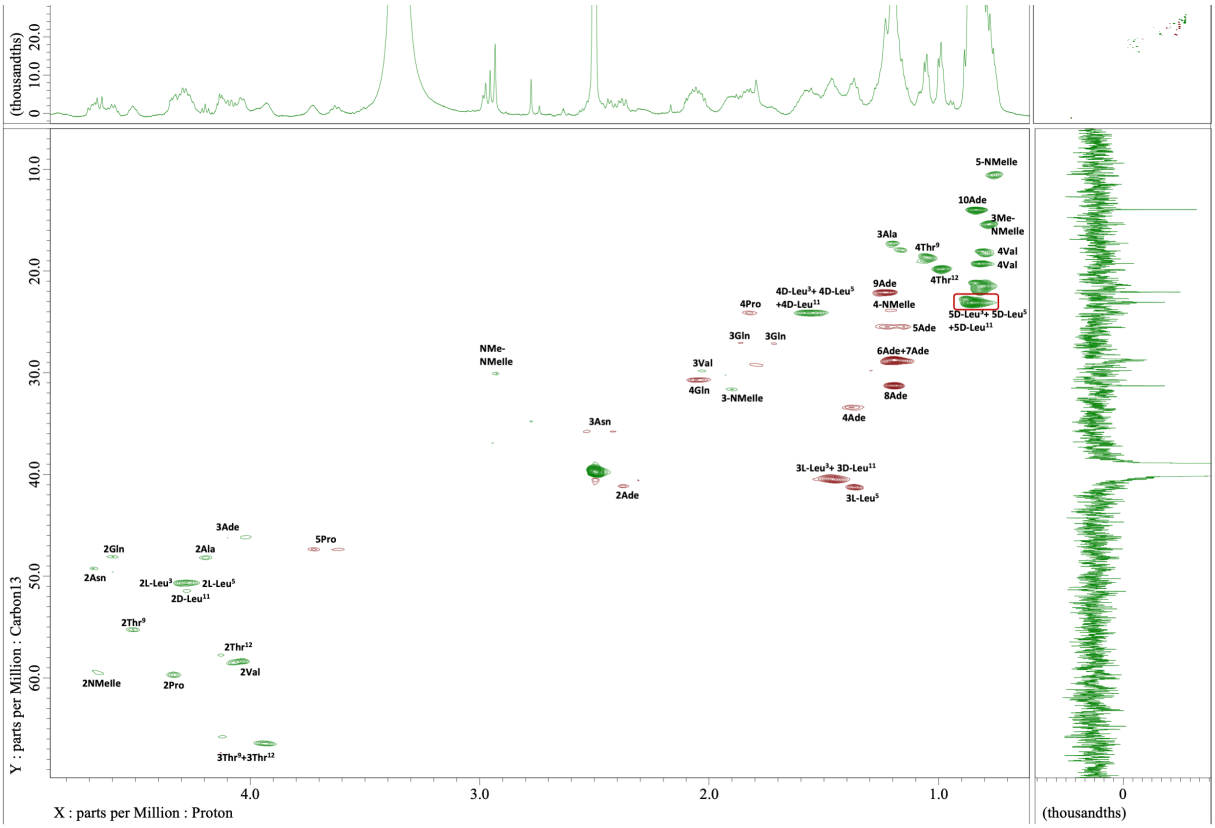

Figure 160. HSQC spectrum of 9a. Solvent : dmso-d_6; T : 23°C; Scans : 8192

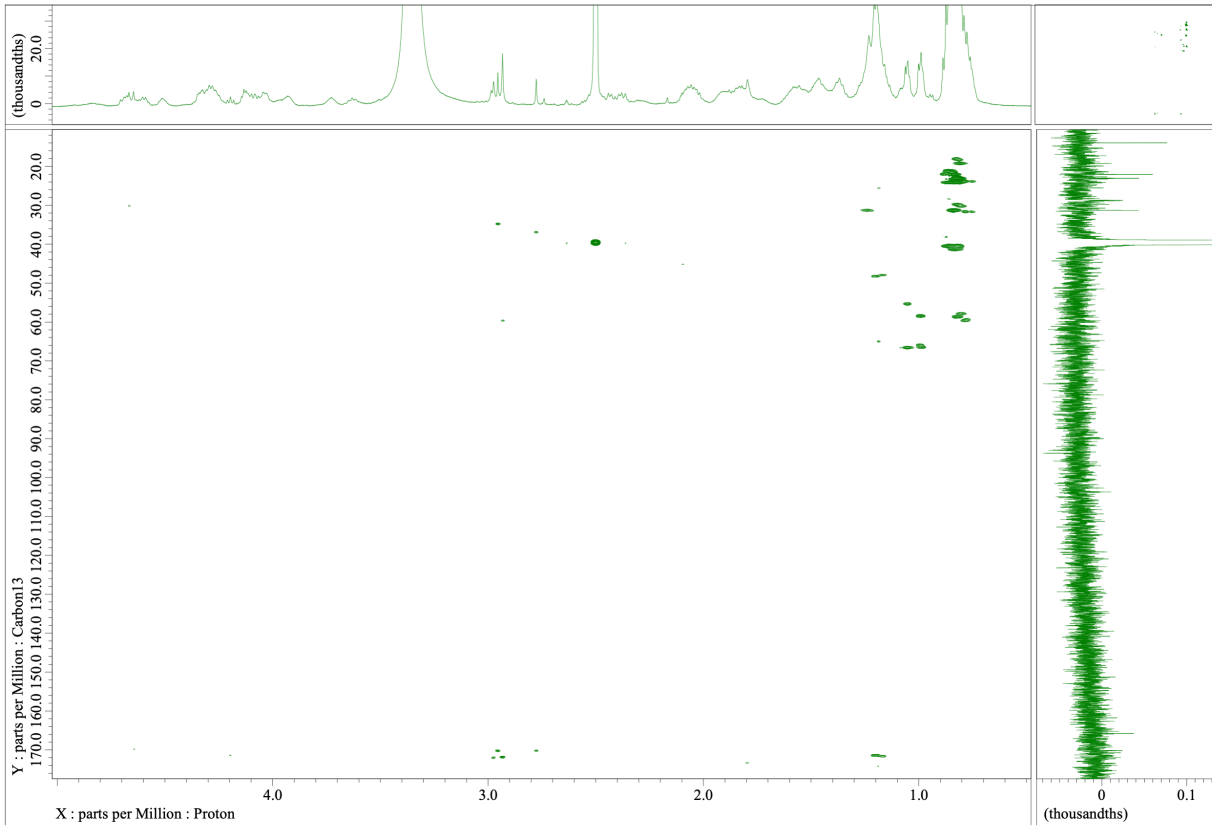

Figure 161. HMBC spectrum of 9a. Solvent : dmso-d_6; T : 23°C; Scans : 16384

f) Compound 10a

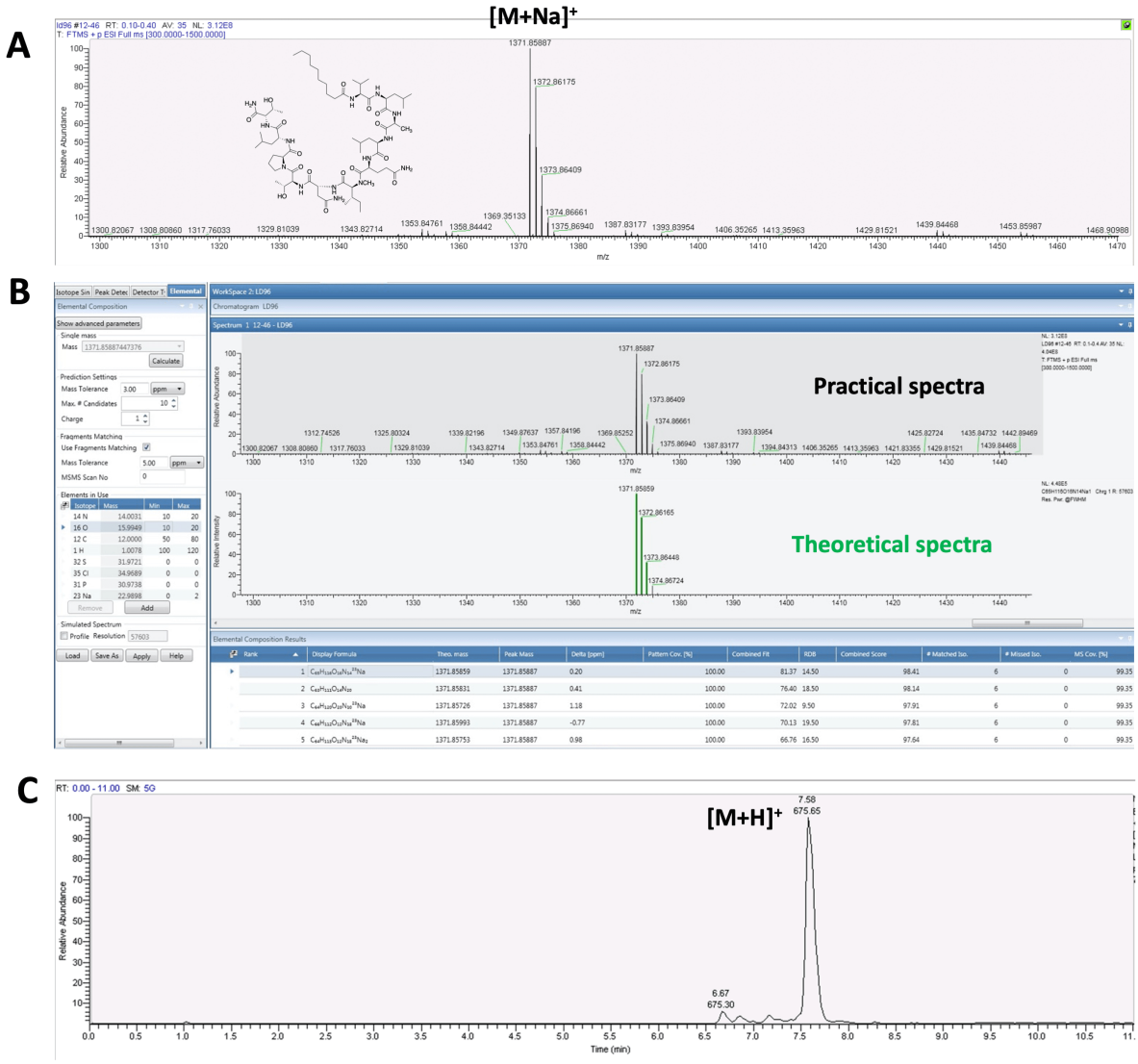

Figure 162. A) ESI-HRMS spectrum of 10a. B) Comparison with the theoretical spectrum. Calculated for $C_{65}H_{116}N_{14}O_{16}Na$ $[M+Na]^+$ *m/z* 1371.85859; Found $[M+Na]^+$ *m/z* 1371.85887; mass error = 0.2 ppm. C) LC-MS profile of 10a

Table 19. NMR spectroscopic data of 10a in DMSO-d_6

entry	position	C, mult.	H, mult. (J in Hz)	entry	position	C, mult.	H, mult. (J in Hz)
Decanoic acid[1]	1	172.3, C	-	N-MeIle[7]	1	169.3, C	-
	2	34.9, CH_2	2.14		2	59.1, CH	4.69, d (11.00)
			2.14		3	31.4, CH	1.89
	3	25.1, CH_2	1.46		3-Me	15.0, CH_3	0.77
	4	28.3-28.7, CH_2	1.23		4	23.8, CH_2	1.23
	5	28.3-28.7, CH_2	1.23		5	10.1, CH_3	0.73
	6	28.3-28.7, CH_2	1.23		N-Me	30.0, CH_3	3.00
	7	28.3-28.7, CH_2	1.23	D-Asn[8]	1	171.2, C	-
	8	31.0, CH_2	1.22		2	49.4, CH	4.60, t (6.42)
	9	21.8, CH_2	1.26		3	36.9, CH_2	2.49
	10	13.7, CH_3	0.85		4	*nd*, C	-
Val[2]	1	*nd*, C	-		NH	-	8.07, d (8.25)
	2	57.6, CH	4.12, t (8.25)		NH_2	-	7.33 & 6.92
	3	29.9, CH	1.94	Thr[9]	1	*nd*, C	-
	3-Me	19.0, CH_3	0.83		2	55.3, CH	4.48, t (7.34)
	4	18.0, CH_3	0.81		3	66.4, CH	3.90, t (5.96)
	NH	-	7.84, d (8.71)		4	18.6, CH_3	1.05, d (5.96)
L-Leu[3]	1	*nd*, C	-		NH	-	7.74, d (7.79)
	2	50.4-51.0, CH	4.30	Pro[10]	1	*nd*, C	-
	3	40.1-40.9, CH_2	1.43-1.47		2	59.6, CH	4.32
	4	23.8-24.0, CH	1.57		3	28.9, CH_2	1.80
	4-Me	21.0-23.0, CH_3	0.82-0.86				2.03
	5	21.0-23.0, CH_3	0.82-0.86		4	24.0, CH_2	1.87
	NH	-	7.94, d (7.79)				1.87
Ala[4]	1	171.6, C	-		5	47.1, CH_2	3.69
	2	48.4, CH	4.20, t (7.34)				3.69
	3	17.9, CH_3	1.18, d (6.88)	D-Leu[11]	1	*nd*, C	-
	NH	-	7.94, d (7.79)		2	50.4-51.0, CH	4.32
D-Leu[5]	1	171.6, C	-		3	40.1-40.9, CH_2	1.43-1.47
	2	50.4-51.0, CH	4.26		4	23.8-24.0, CH	1.57
	3	40.1-40.9, CH_2	1.43-1.47		4-Me	21.0-23.0, CH_3	0.82-0.86
	4	23.8-24.0, CH	1.57		5	21.0-23.0, CH_3	0.82-0.86
	4-Me	21.0-23.0, CH_3	0.82-0.86		NH	-	7.97, d (8.25)
	5	21.0-23.0, CH_3	0.82-0.86	Thr[12]	1	171.8, C	-
	NH	-	7.94, d (7.79)		2	57.9, CH	4.05, d (6.88)
Gln[6]	1	*nd*, C	-		3	66.0, CH	4.05, d (6.88)
	2	47.8, CH	4.63, t (6.88)		4	19.8, CH_3	0.99, d (5.96)
	3	26.6, CH_2	1.73		NH	-	7.66, d (8.71)
			1.84		NH_2	-	7.14 & 7.08
	4	30.3, CH_2	2.05				
	5	173.6, C	-				
	NH	-	8.04, d (8.25)				
	NH_2	-	7.20 & 6.80			*nd* =	Not determined

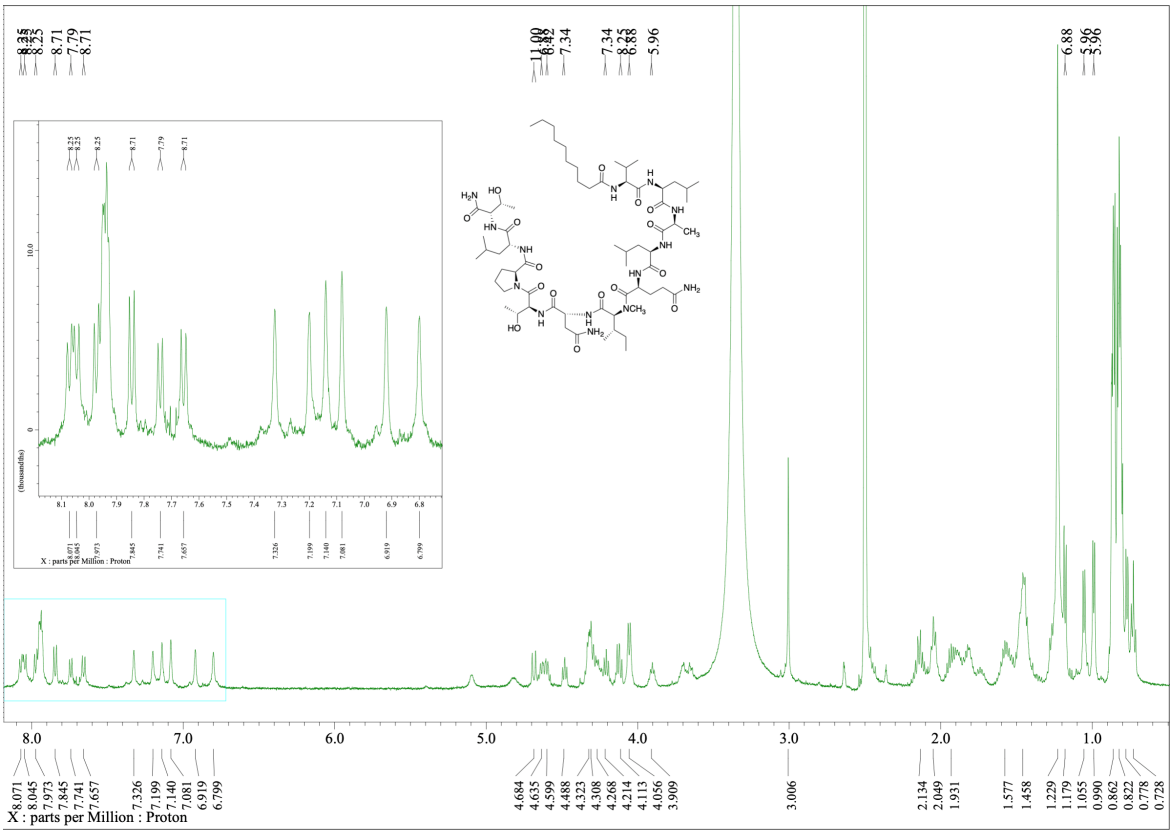

Figure 163. ^{1}H NMR spectrum of 10a

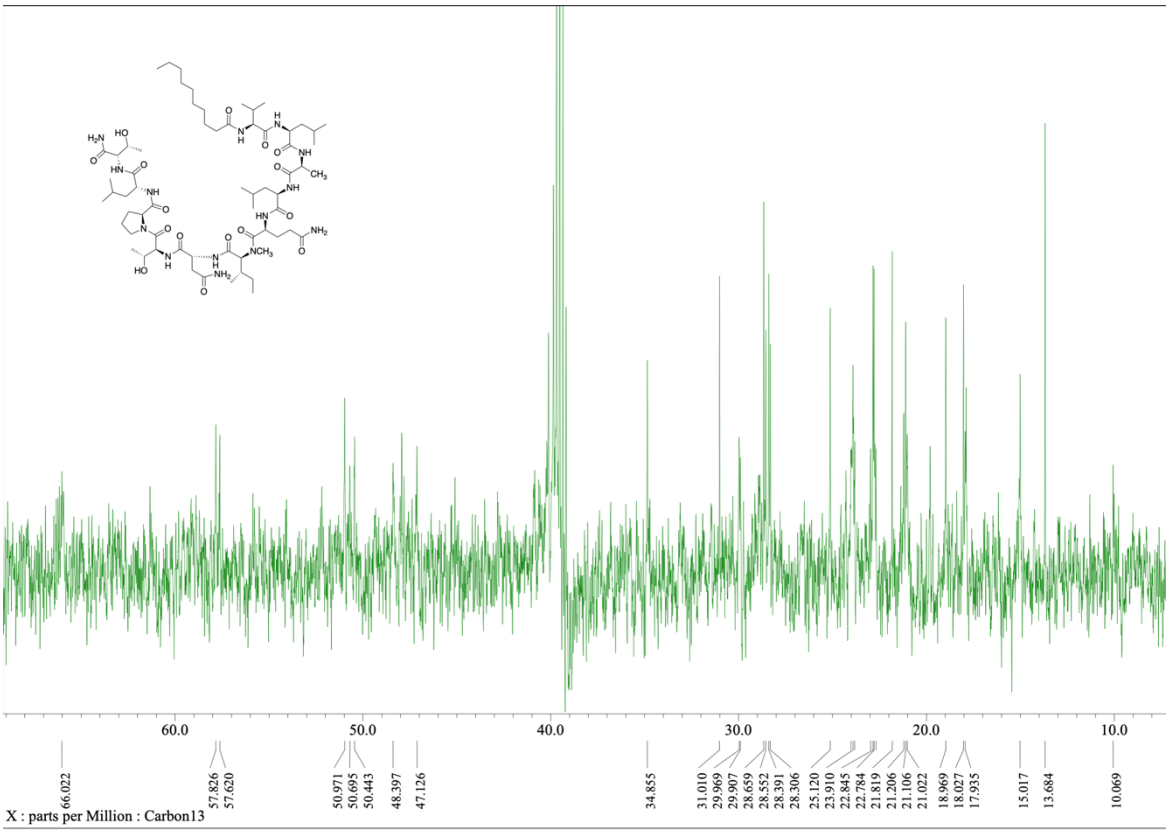

Figure 164. ^{13}C spectrum of 10a. Solvent : dmso-d_6; T : 23°C; Scans : 20000

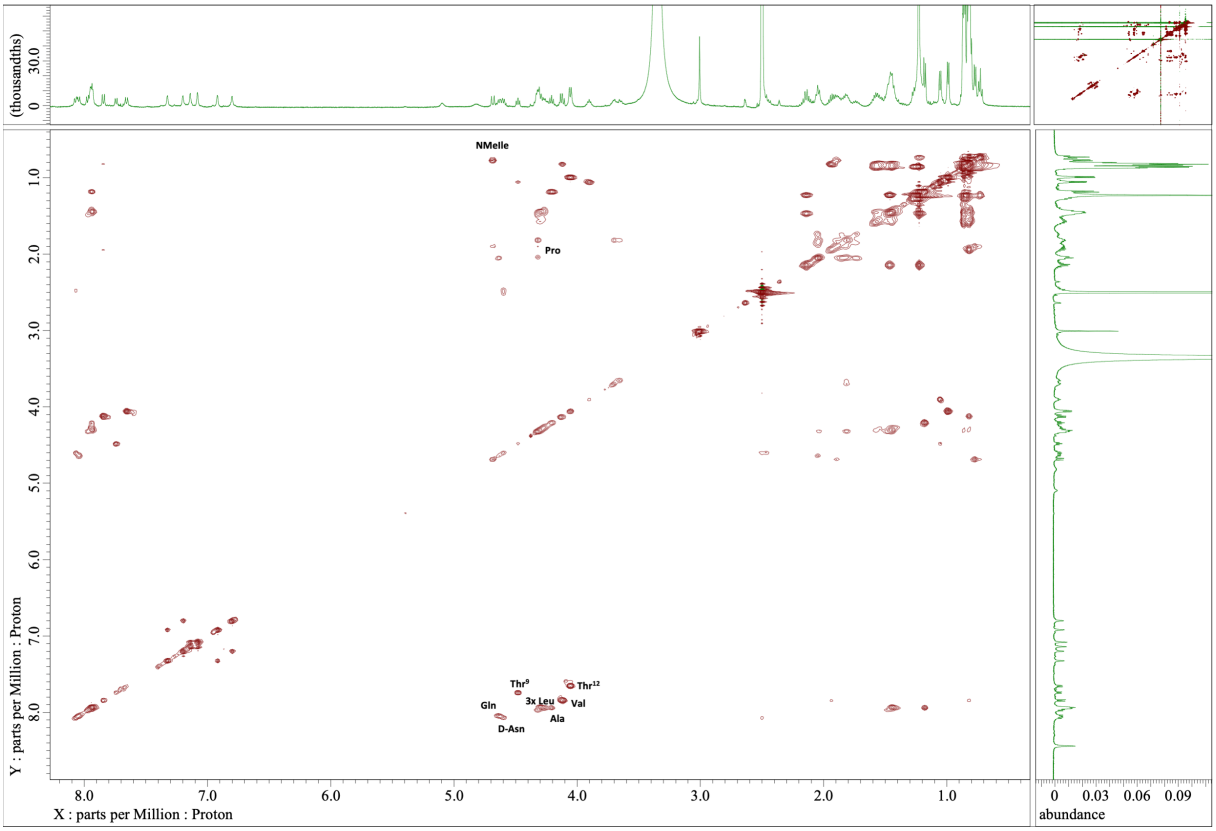

Figure 165. TOCSY spectrum of 10a. Solvent : dmso-d_6; T : 23°C; Scans : 8192

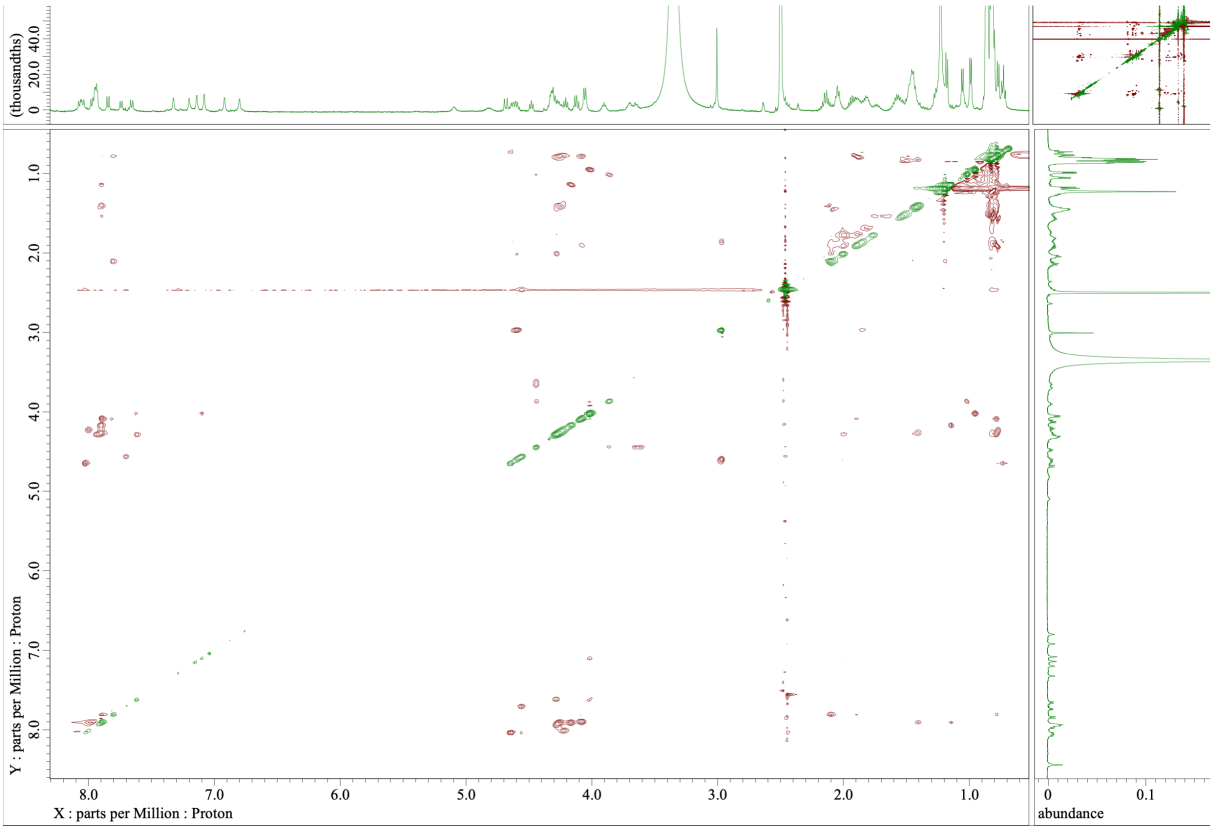

Figure 166. ROESY spectrum of 10a. Solvent : dmso-d_6; T : 23°C; Scans : 8192

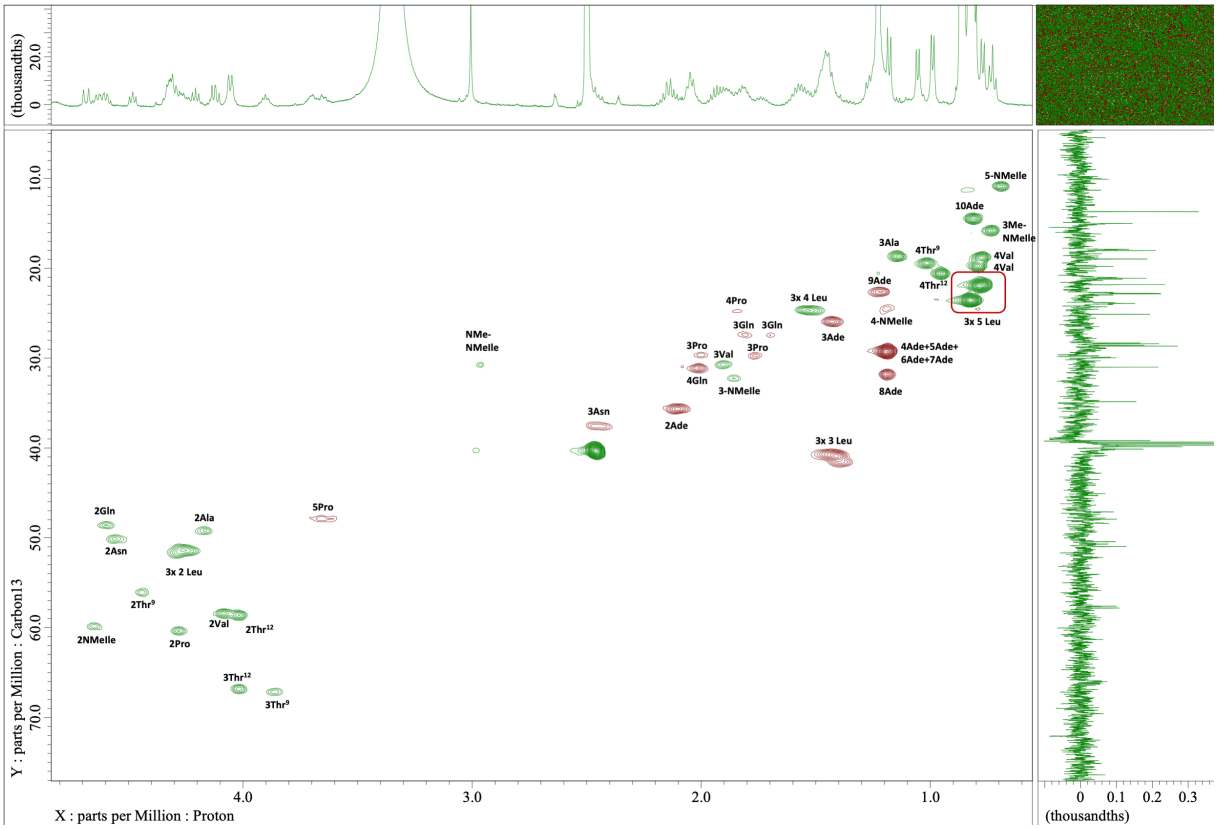

Figure 167. HSQC spectrum of 10a. Solvent : dmso-d_6; T : 23°C; Scans : 8192

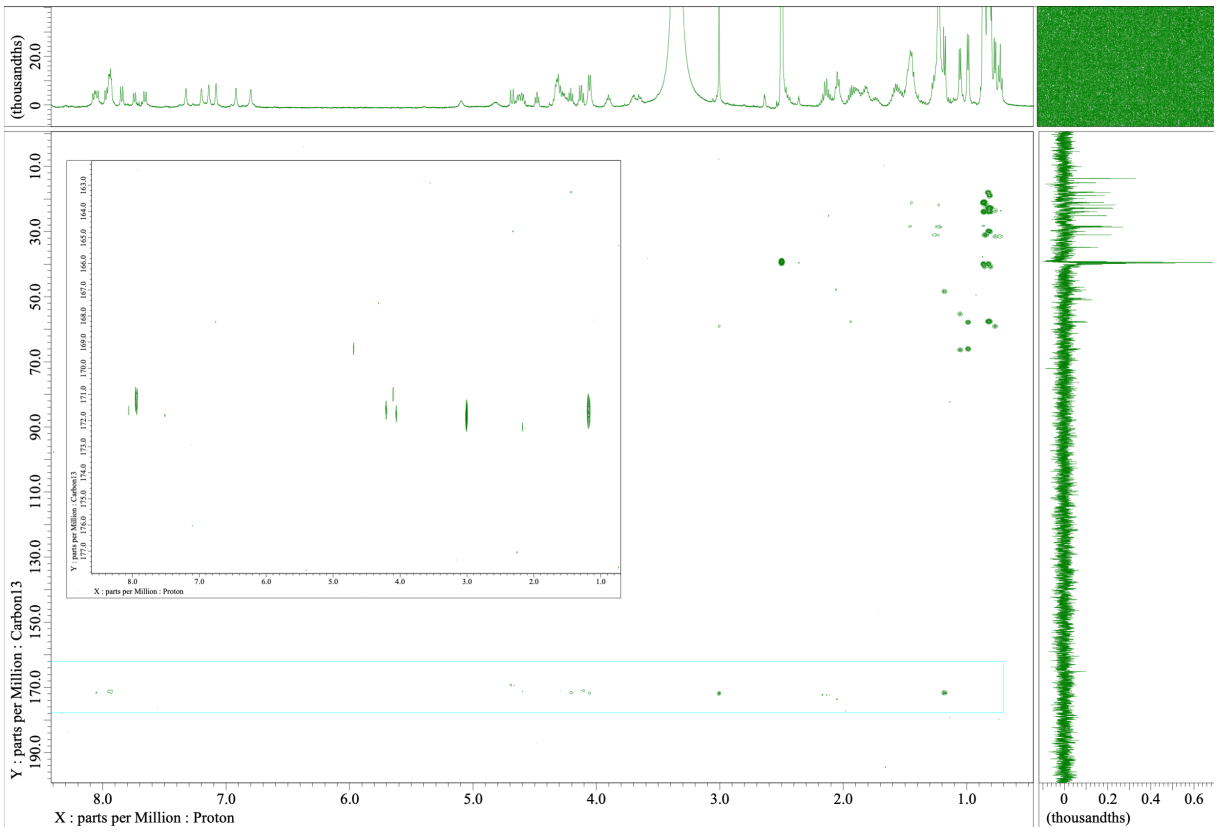

Figure 168. HMBC spectrum of 10a. Solvent : dmso-d_6; T : 23°C; Scans : 16384

g) Compound 11a

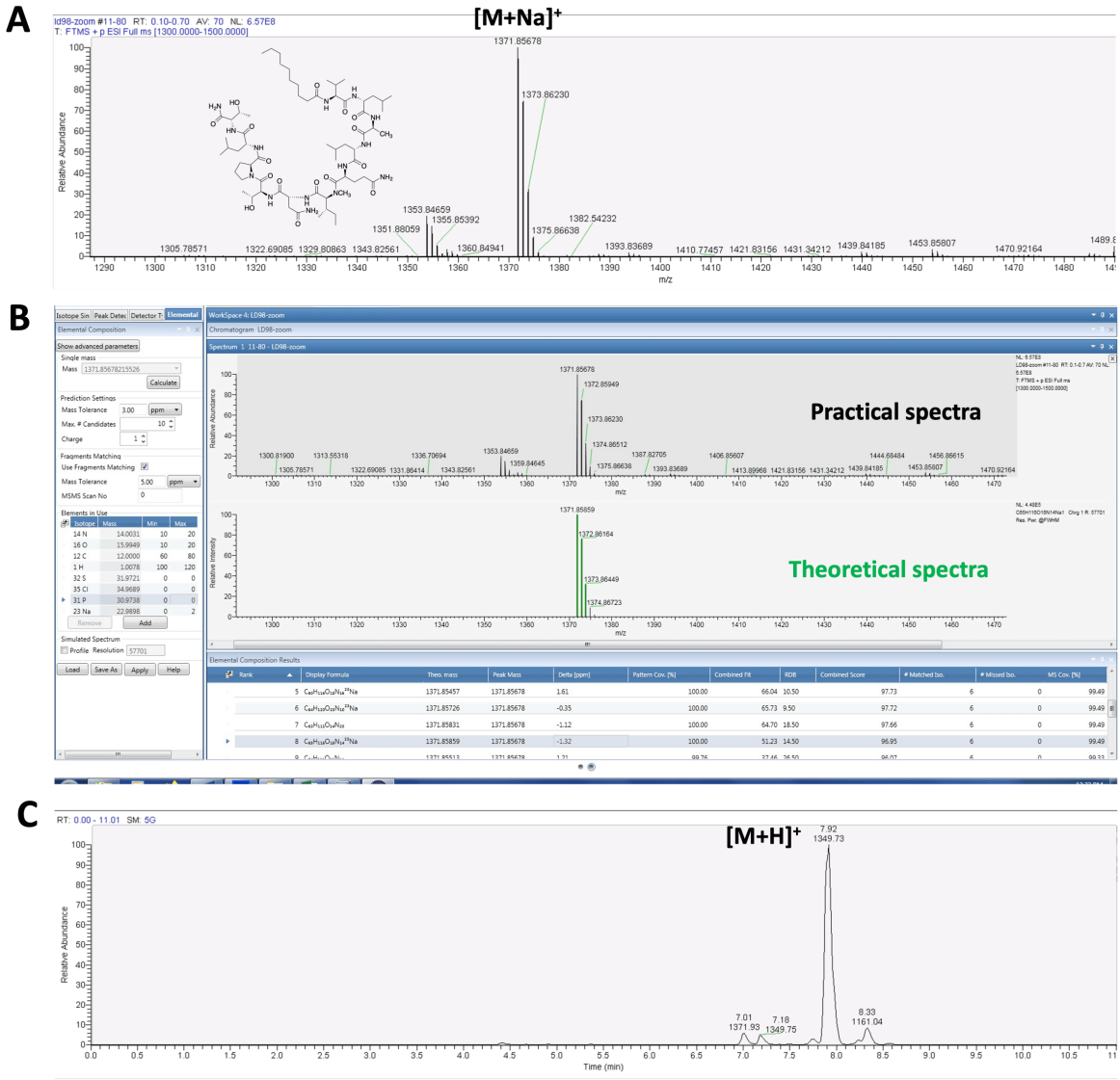

Figure 169. A) ESI-HRMS spectrum of 11a. B) Comparison with the theoretical spectrum. Calculated for $C_{65}H_{116}N_{14}O_{16}Na$ $[M+Na]^+$ *m/z* 1371.85859; Found $[M+Na]^+$ *m/z* 1371.85678; mass error = 1.32 ppm. C) LC-MS profile of 11a

Table 20. NMR spectroscopic data of 11a in DMSO-d_6

entry	position	C, mult.	H, mult. (J in Hz)	entry	position	C, mult.	H, mult. (J in Hz)
Decanoic acid[1]	1	173.2, C	-	N-MeIle[7]	1	170.1, C	-
	2	35.5, CH_2	2.11		2	59.7, CH	4.65
			2.06		3	32.3, CH	1.84
	3	25.8, CH_2	1.42		3-Me	15.7, CH_3	0.74
	4	29.1-29.4, CH_2	1.18		4	24.4, CH_2	1.18
	5	29.1-29.4, CH_2	1.18		5	10.8, CH_3	0.72
	6	29.1-29.4, CH_2	1.18		N-Me	30.6, CH_3	2.93
	7	29.1-29.4, CH_2	1.18	D-Asn[8]	1	168.6, C	-
	8	31.8, CH_2	1.18		2	49.5 or 50.1, CH	4.09 or 4.56
	9	22.6, CH_2	1.20		3	36.3 or 37.6, CH_2	2.53 or 2.43
	10	14.5, CH_3	0.81				2.67 or 2.43
Val[2]	1	171.9, C	-		4	*nd*, C	-
	2	59.3, CH	3.98		NH	-	8.02 or 8.09
	3	30.3, CH	1.86		NH_2	-	7.24 & 6.90
	3-Me	19.6, CH_3	0.78	Thr[9]	1	*nd*, C	-
	4	19.1, CH_3	0.81		2	56.8, CH	4.48, t (7.45)
	NH	-	7.85, d (7.45)		3	67.1, CH	3.84, t (6.87)
D-Leu[3]	1	172.1, C	-		4	19.6, CH_3	1.07, d (6.30)
	2	51.5, CH	4.18		NH	-	8.61, d (8.02)
	3	40.8-41.7, CH_2	1.35-1.44	Pro[10]	1	*nd*, C	-
	4	24.6-24.8, CH	1.53		2	60.4, CH	4.27
	4-Me	21.5-23.7, CH_3	0.78-0.82		3	29.8, CH_2	1.76
	5	21.5-23.7, CH_3	0.78-0.82				2.00
	NH	-	8.22, d (8.02)		4	24.9, CH_2	1.79
Ala[4]	1	172.1, C	-				1.89
	2	48.5, CH	4.20		5	48.0, CH_2	3.69
	3	18.2, CH_3	1.14, d (7.45)				3.69
	NH	-	7.89, d (6.87)	D-Leu[11]	1	172.4, C	-
L-Leu[5]	1	172.1, C	-		2	51.7, CH	4.30
	2	51.7, CH	4.25		3	40.8-41.7, CH_2	1.35-1.44
	3	40.8-41.7, CH_2	1.35-1.44		4	24.6-24.8, CH	1.53
	4	24.6-24.8, CH	1.53		4-Me	21.5-23.7, CH_3	0.78-0.82
	4-Me	21.5-23.7, CH_3	0.78-0.82		5	21.5-23.7, CH_3	0.78-0.82
	5	21.5-23.7, CH_3	0.78-0.82		NH	-	7.96, d (8.02)
	NH	-	7.74, d (8.59)	Thr[12]	1	172.4, C	-
Gln[6]	1	*nd*, C	-		2	58.5, CH	4.04
	2	48.5, CH	4.61		3	66.9, CH	4.01

3	27.5, CH_2	1.67
		1.80
4	31.3, CH_2	2.04
5	173.2, C	-
NH	-	8.15, d (8.02)
NH_2	-	7.14 & 6.77
4	20.5, CH_3	0.95, d (6.30)
NH	-	7.60
NH_2	-	7.12 & 7.05

nd = Not determined

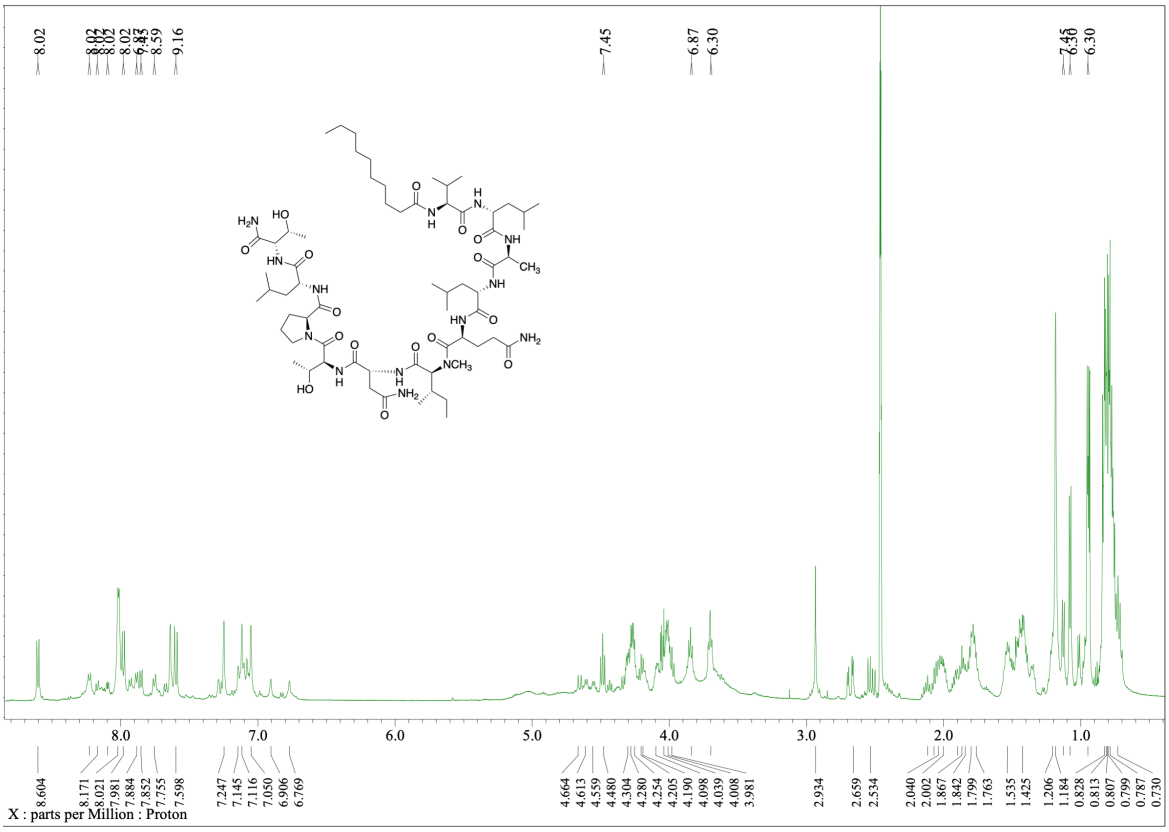

Figure 170. ^{1}H NMR spectrum of 11a. Solvent : dmso-d_6; T : 23°C; Scans : 32

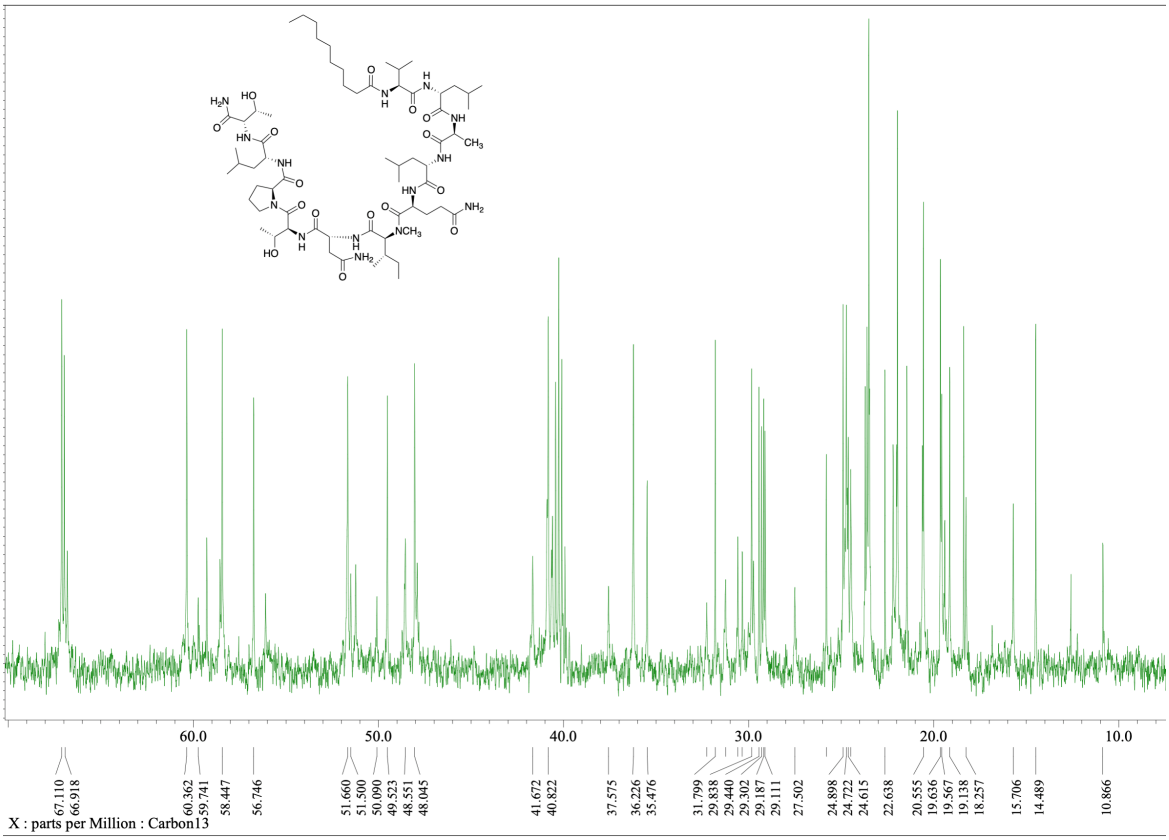

Figure 171. ^{13}C spectrum of 11a. Solvent : dmso-d_6; T : 23°C; Scans : 20000

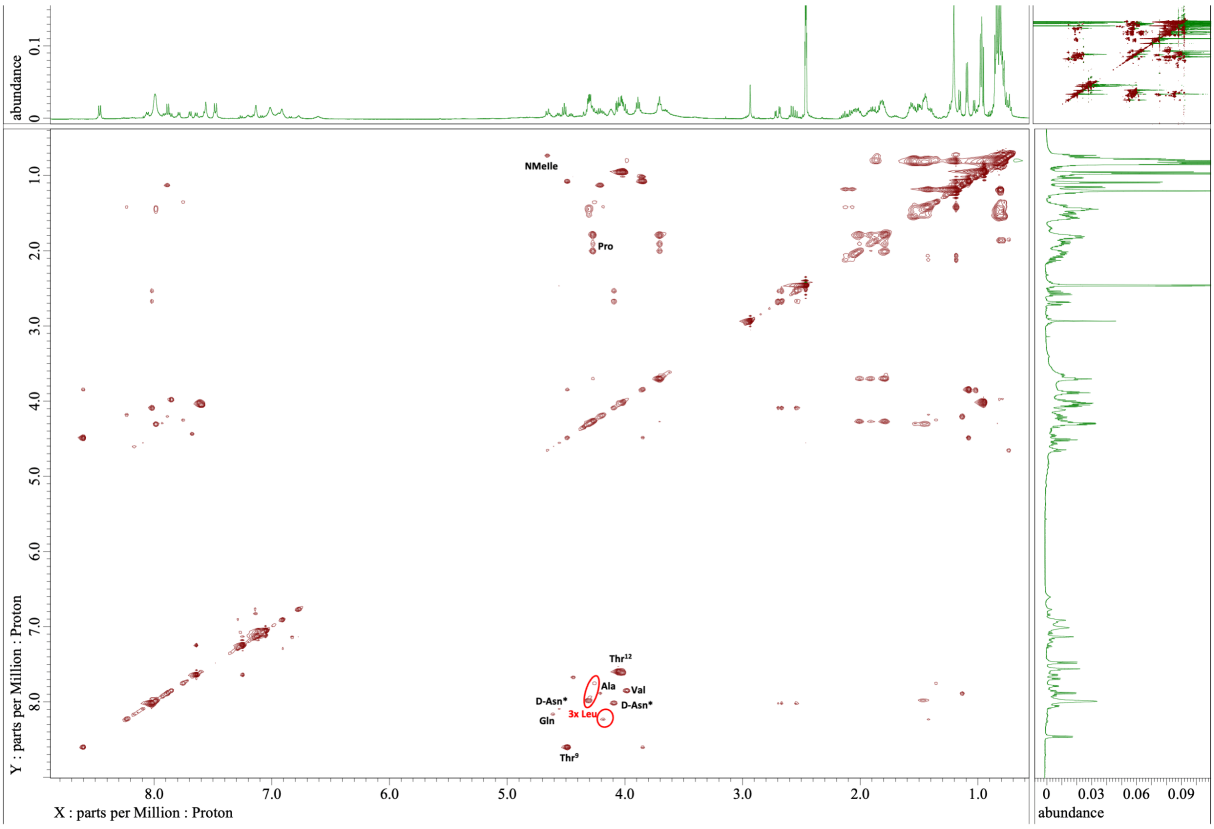

Figure 172. TOCSY spectrum of 11a. Solvent : dmso-d_6; T : 23°C; Scans : 8192

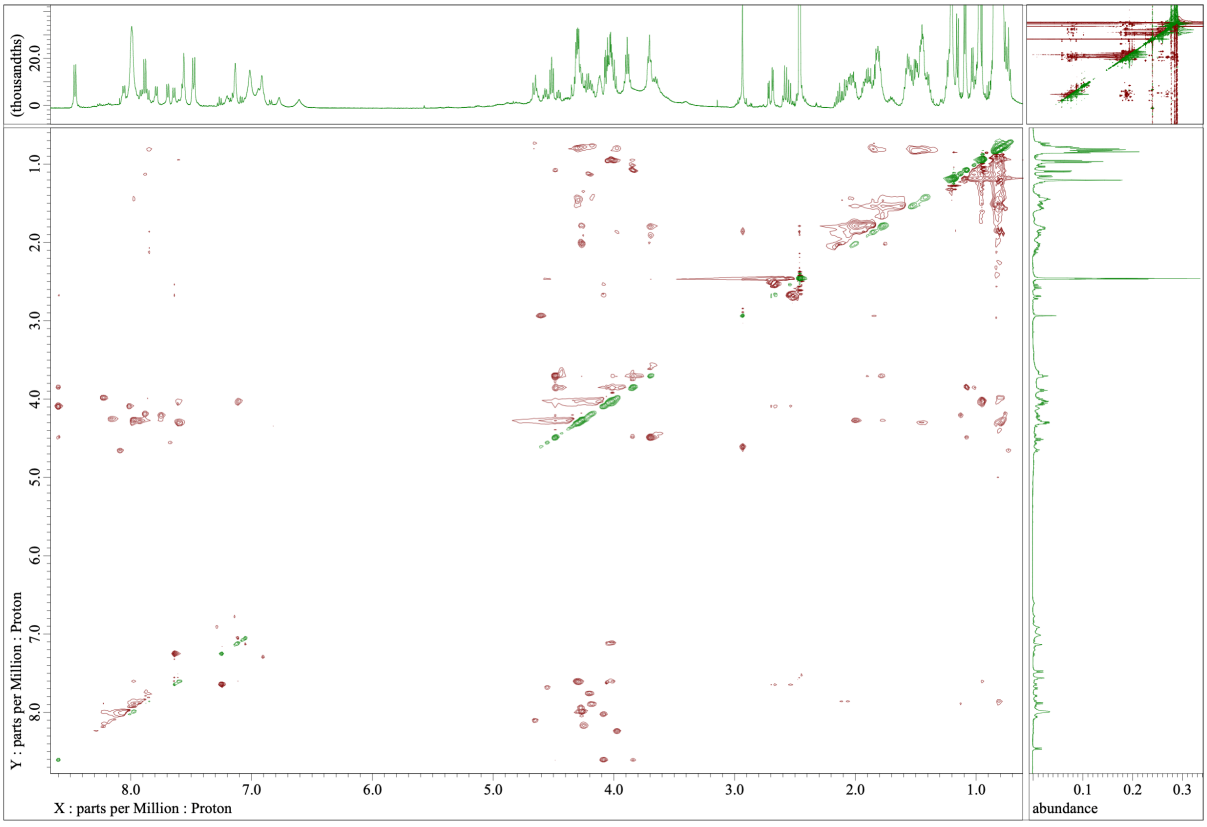

Figure 173. ROESY spectrum of 11a. Solvent : dmso-d_6; T : 23°C; Scans : 8192

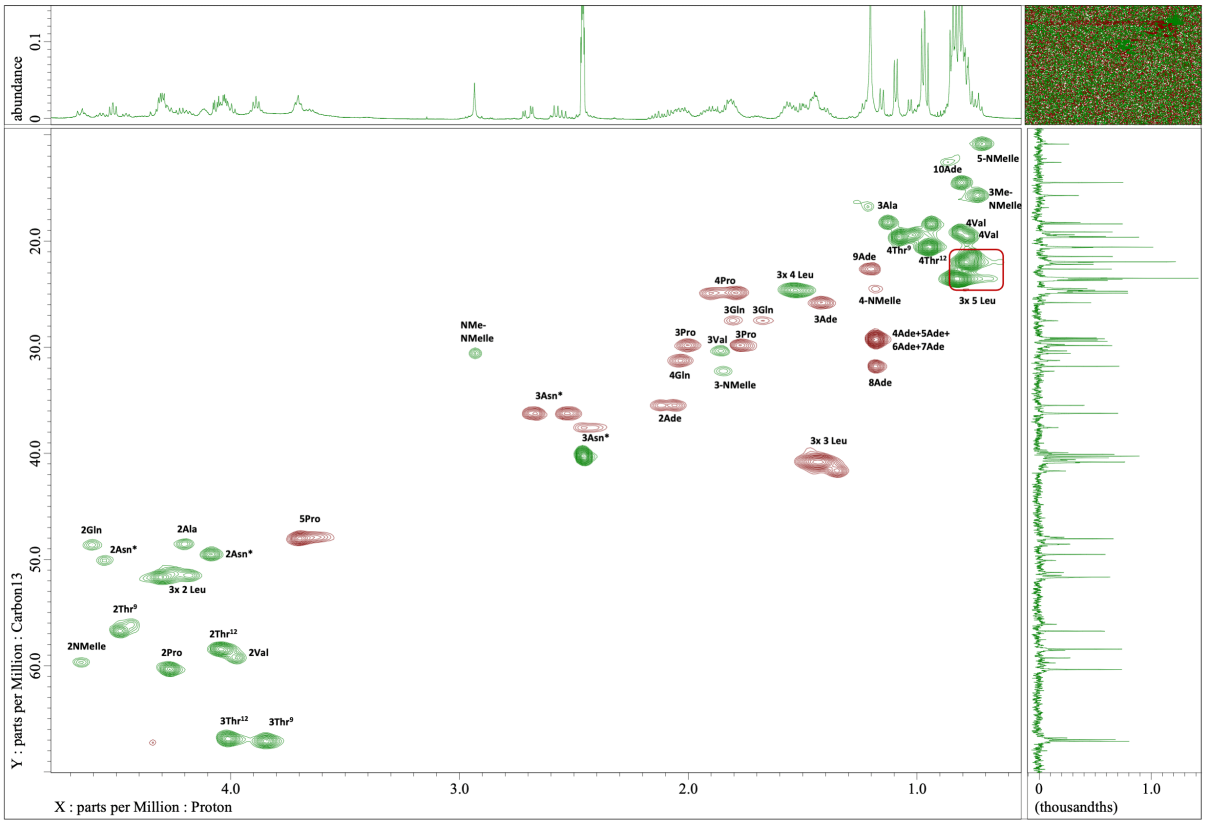

Figure 174. HSQC spectrum of 11a. Solvent : dmso-d_6; T : 23°C; Scans : 8192

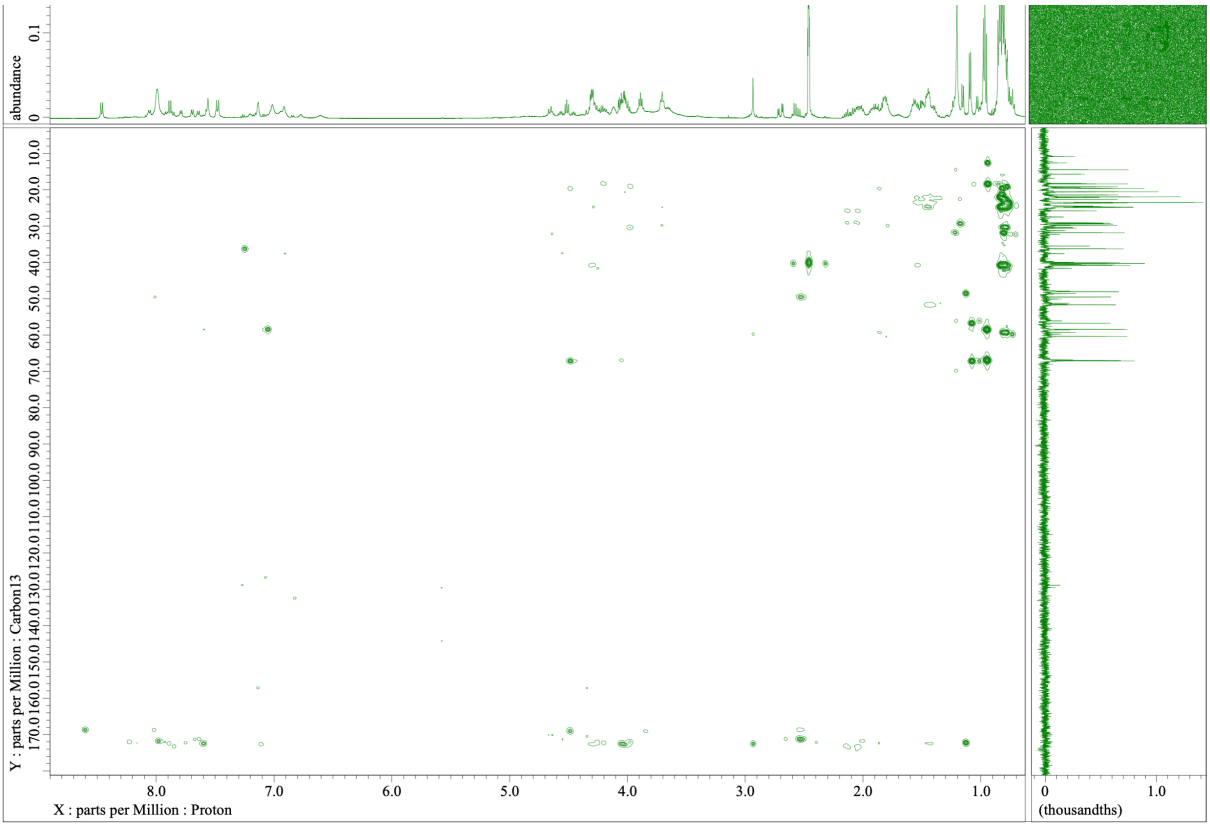

Figure 175. HMBC spectrum of 11a. Solvent : dmso-d_6; T : 23°C; Scans : 16384

Chapter 4.
Attempts to recover the D-peptidase

I.Determination of a less complex cleavable peptide sequence recognized by the enzyme

As we have seen in chapter 2, the synthesis of laxaphycin B type peptides is complex and gives low yields. First, there is a decrease in yield related to some difficult couplings such as glutamine to N-methylisoleucine. Secondly, the cyclization has a low conversion rate. Moreover, we know that the specificity of the enzyme subsites S relies on the recognition of a minimal part of the substrate sequence [169]. Indeed, the P1 and P1' pockets located at the N-ter and C-ter, respectively, determine the cleavage site and to a substantial level the protease specificity. The substrate amino acids fitting the more distant positions P2, P3 and P2', P3' surrounding the cleavage site can have more or less importance for the recognition with the enzyme (Figure 176). Guided by the fact that linear peptides were also proceeded by the enzyme, we examined the possibility to find a minimal peptide sequence recognized by the enzyme. A shorter and linear sequence will facilitate the synthesis and enables to study more easily the various properties of the enzyme. Furthermore, this shorter substrate is amenable to further modifications that will be helpful to implement a strategy for the enzyme recovery.

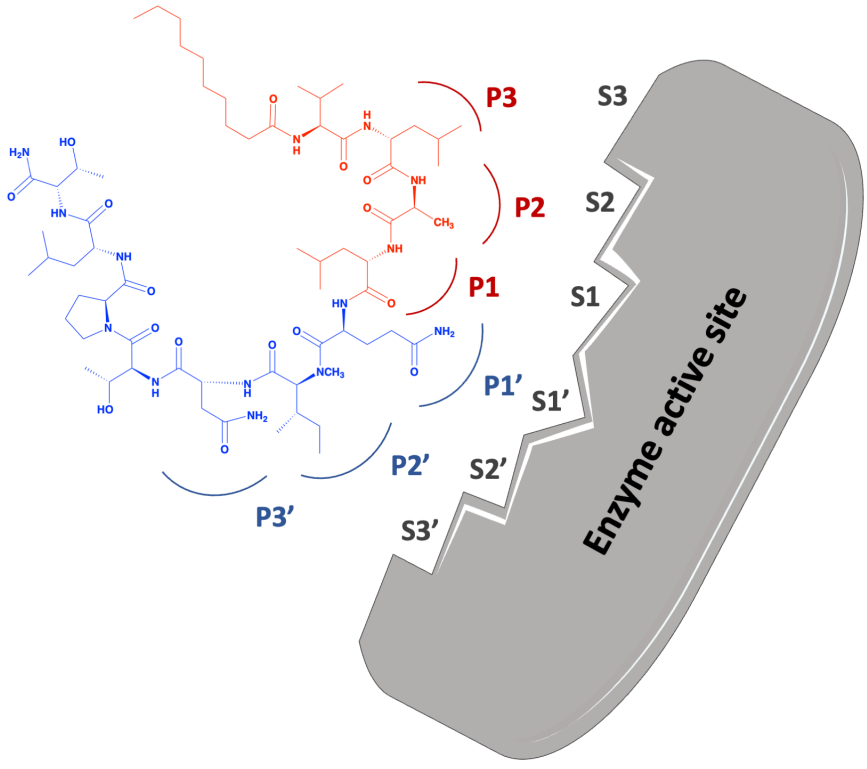

Figure 176. Enzyme binding sites S with potential sites of interaction P on the peptide substrate (7a sequence).

A. Study of short peptides

At first, we wanted to reduce the peptide sequence as much as possible by keeping only the two cleavage points, i.e., a part containing the amino acids in position 3 and 5. We thus synthesized compounds **12** and **13**, going from position 2 of the peptide sequence to position 5. Compound **12** has two D-Thr in position 3 and 5 while compound **13** has two D-Leu, these two types of amino acids being conceivable as we could see on the cyclic peptides **5a** and **6a** (Figure 177). Another short peptide was obtained, named compound **14**, containing this time only position 5 with a D-Thr and going from position 4 to position 7 (Figure 177). These 3 peptides were synthesized on a MBHA amide rink resin to obtain an amide function at C-ter, and the N-ter function was acetylated to mimic the following peptide bond.

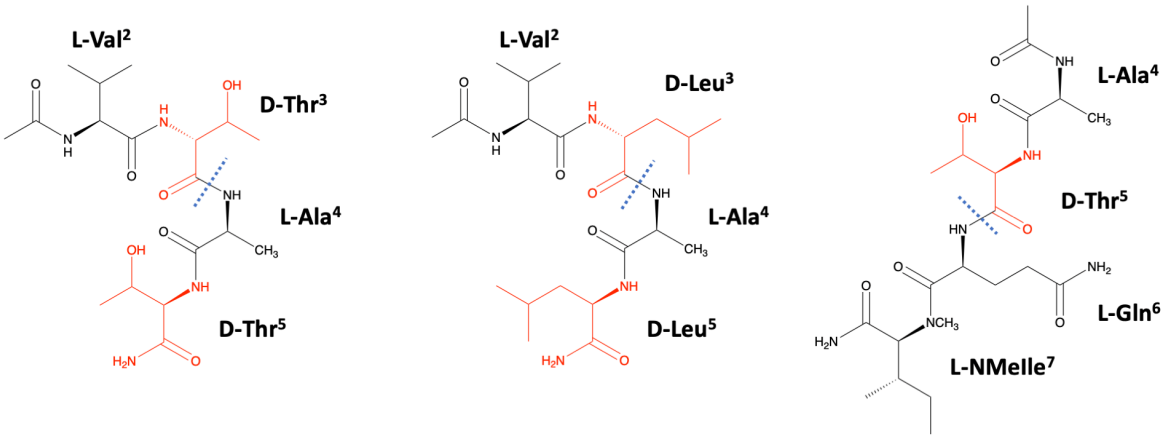

Figure 177. Structures of short peptides 12, 13 and 14, with potential cleavage points in blue.

The three short peptides were exposed to the digestive gland extract (*Dg-Ss-Lm*) and monitored by LC-MS. None of these peptides were impacted by the contact with the extract after a 24-hour period, with no new fragments appearing. At this stage of the study, we did not have any information on the recognition properties of the enzyme towards the substrate. We did not know the importance of the Ade in position 1. Moreover, the direction of cleavage between positions 3 and 5 was not yet determined, so amino acids could be missing around a cleavage point. These 3 peptides were therefore, in retrospect, too short to be recognized by the enzyme, both in C-ter and N-ter.

B. Extension of the minimum sequence

We therefore extended the minimal sequence from the Ade in position 1 to the D-Asn in position 8. We synthesized compound **15** with two D-Leu at position 3 and 5. In order to simplify the synthesis, the Ade in position 1 was replaced by decanoic acid, already used in compound **7a**. For comparison, compound **16**, an analogue of compound **15**, was obtained by

replacing the decanoic acid in position 1 by an acetylated β-alanine, in order to verify the importance of an acylated N-terminus on a linear peptide of medium size (Figure 178).

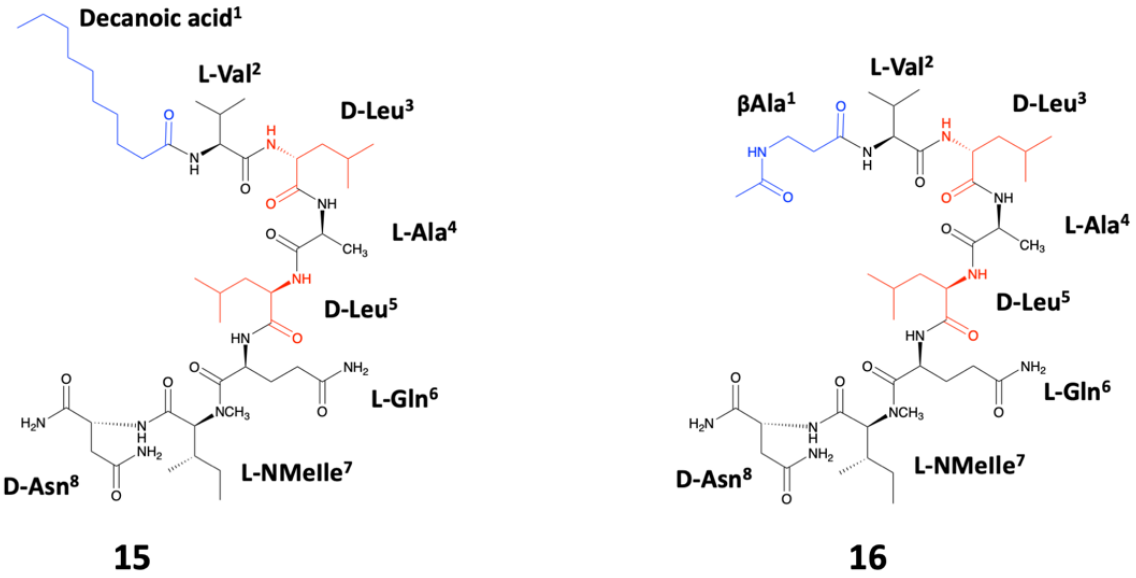

Figure 178. Structures of peptides 15 and 16.

Compound **15**, comprising a wide range of amino acids around the cleavage points, was indeed cleaved at the expected positions. The study of the fragments obtained by LC-MS shows that the first cleavage occurs at the C-ter of the D-Leu in position 5 and then a second cleavage takes place at the C-ter of the D-Leu in position 3. Using the same annotations as in the previous chapter, we obtain compounds **15b** and **15c** after the first cleavage of **15a**, then **15c** is split to deliver **15d** and **15e** following the second cleavage (Figure 179). This observation confirms the results obtained on compound **7a** including the complete peptide sequence (Figure 117). We could also observe the action of another enzyme, acting like a carboxypeptidase, on **15a** with the successive loss of asparagine (**15b'**) and N-methylisoleucine (**15c'**). The action of this other enzyme would stop at D-Leu^5, not being of L configuration like the previous amino acids removed. The cleavage kinetics is relatively fast since only 10% of the peptide remains after 30 minutes of incubation. On the other hand, compound **16** not containing decanoic acid is not cleaved by the enzyme, supporting again the importance of this acid in the sequence, and thus of Ade in type-B laxaphycins, just as observed previously with cyclic compound **8**.

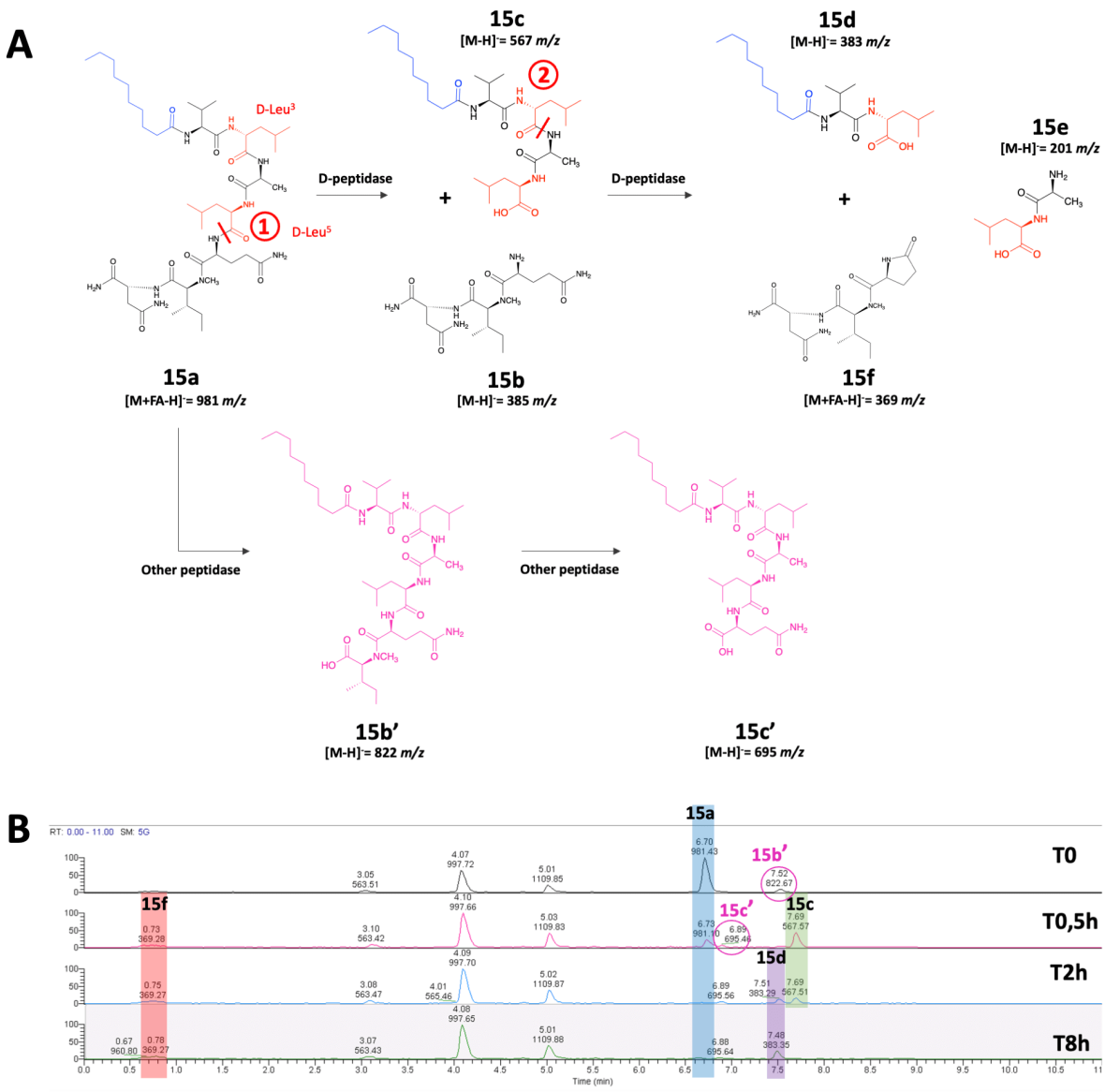

Figure 179. A) Successive cleavages of 15a by the D-peptidase and another enzyme, observed by LC-MS. B) LC-MS kinetic monitoring of 15a cleavage with *Dg-Ss-Lm* extract at 30°C pH 8 and masses corresponding to the LC-MS peaks of 15a-f. Pink circles correspond to parallel cleavages by the other enzyme. Compounds at 4.07 min and 5.02 min belong to the digestive gland extract.

Starting from the cleavage-positive sequence of compound **15** when exposed to *Dg-Ss-Lm*, we decreased the size of the peptide by starting the synthesis at glutamine in position 6 rather than at asparagine in position 8. Moreover, starting the synthesis at glutamine allows us to avoid the difficult coupling between glutamine and N-methylisoleucine. Compound **17** could then be synthesized, containing again two D-Leu in position 3 and 5 (Figure 180).

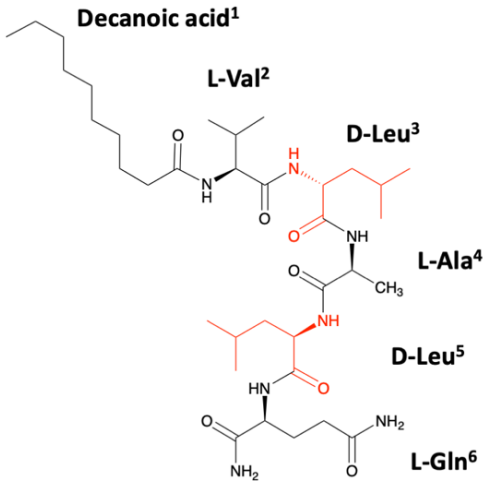

17

Figure 180. Structure of peptide 17.

When this peptide was exposed to *Dg-Ss-Lm*, the appearance of the expected fragments was observed but more slowly than for compound **15** with 10% of peptide still remaining at 8 hours of incubation. The first cleavage of **17a** at the C-ter of D-Leu^5 was then observed giving rise to **17b** and **17c** followed by a second cleavage at the C-ter of D-Leu^3 splitting **17c** into **17d** and **17e** (Figure 181). Moreover, this peptide is poorly soluble in the buffer used and precipitates over time. The disappearance of the peptide over time observed in LC-MS is therefore linked to both the precipitation of the peptide in the buffer and the cleavage of the latter by the enzyme, making the monitoring of the enzymatic activity more complex, although the new fragments **17c** and **17d** are observable.

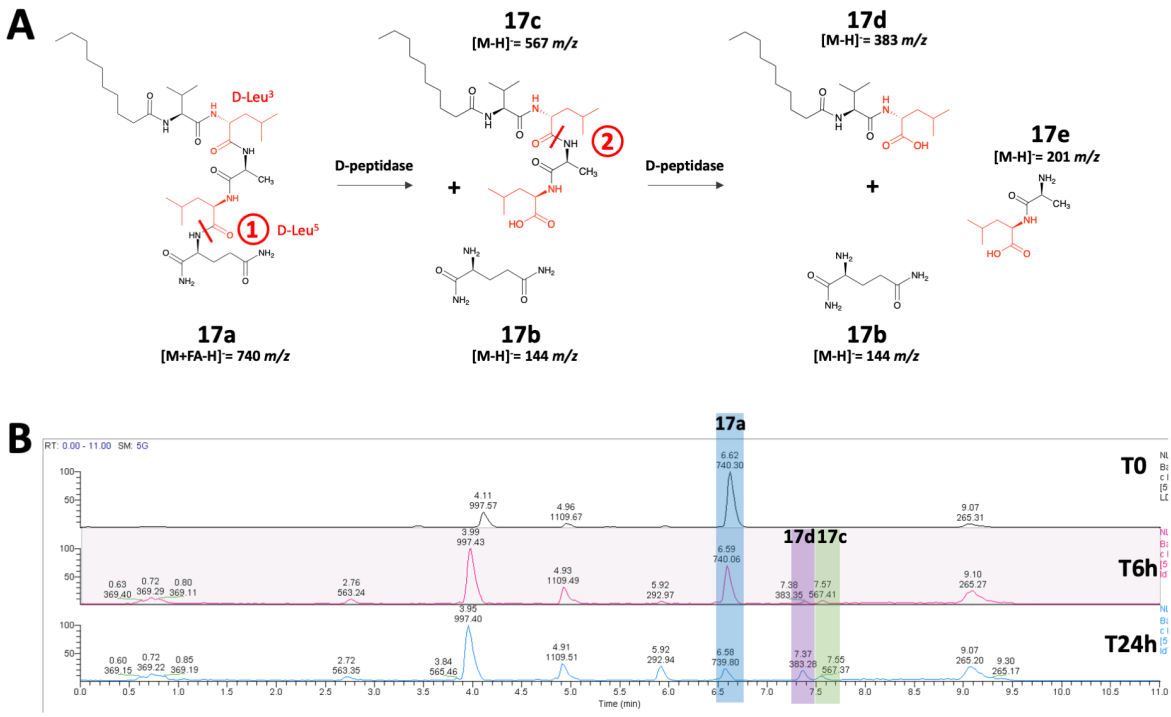

Figure 181. A) Successive cleavages of 17a by the D-peptidase, observed by LC-MS. B) LC-MS kinetic monitoring of 17a cleavage with *Dg-Ss-Lm* extract at 30°C pH 8 and masses corresponding to the LC-MS peaks of 17a-d. Compounds at 4.111 min and 4.96 min belong to the digestive gland extract.

In order to gain in solubility without affecting the positions P1 and P1', we added a lysine in C-ter of the peptide, upstream of the glutamine, as well as replaced the two D-Leu by two D-Thr, giving the compound **18** (Figure 182). This new compound **18** is indeed soluble in the buffer used. However, its cleavage is very slow, with 50% of peptide remaining after 5 days of incubation with *Dg-Ss-Lm*. Indeed, we could observe the difference in cleavage kinetics between peptides **5a** and **6a** containing respectively D-Leu and D-Thr in positions 3 and 5, with a slower cleavage in the presence of D-Thr. In this case, compound **18** is also cleaved more slowly than these D-Leu-containing analogues. Over this 5-day period, it is possible to observe the first **18c** fragment corresponding to the C-ter cleavage of **18a** from D-Leu^5, but it is not possible to visualize the second fragment corresponding to the C-ter cleavage of D-Leu^3 (Figure 183). As in the case of **15a**, the compound **18b'** corresponding to the loss of the lysine in C-ter position is also observed, due to the action of another enzyme present in the *Dg-Ss-Lm* extract (Figure 183).

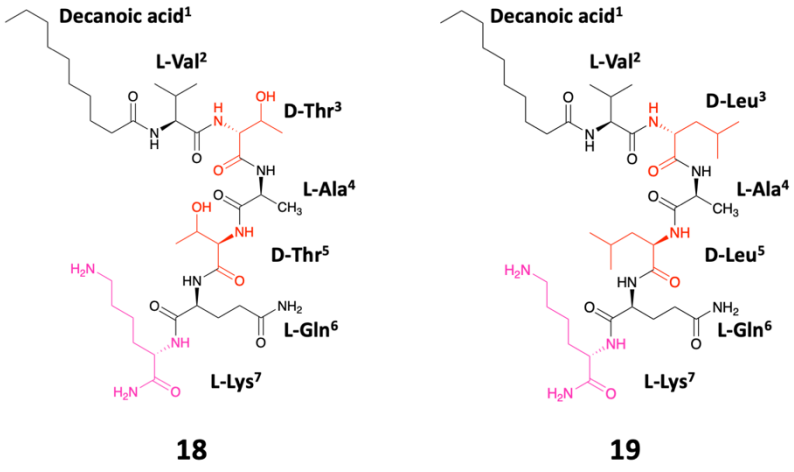

Figure 182. Structures of peptides 18 and 19.

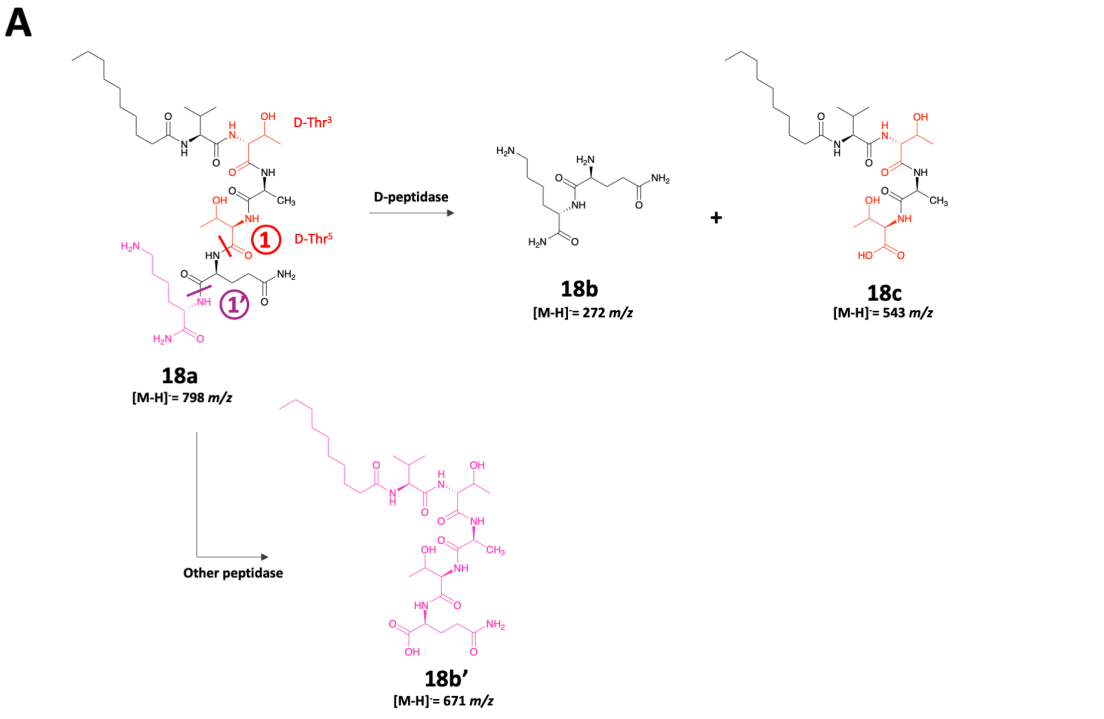

Figure 183. A) Cleavages of 18a by the D-peptidase and another enzyme, observed by LC-MS. B) LC-MS kinetic monitoring of 18a cleavage with *Dg-Ss-Lm* extract at 30°C pH 8 and masses corresponding to the LC-MS peaks of 18a-c. Pink circle corresponds to a parallel cleavage by the other enzyme. Compounds at 4.85 min and 5.55 min belong to the digestive gland extract.

As such a slow cleavage was not adequate for kinetic monitoring by LC-MS, we synthesized the equivalent of compound **18**, named compound **19**, containing D-Leu in position 3 and 5, but keeping the lysine in C-ter to maintain a higher solubility than compound **17** (Figure 182). Thus, although the solubility of the peptide in the buffer was lower than with compound **18**, it was slightly higher than with compound **17**. In addition, the cleavage kinetics were improved as compound **19** could be completely cleaved over a 24-hour period, with 50% of peptide remaining after 8 hours of incubation. With this peptide, it is possible to visualize in LC-MS, the disappearance of compound **19a** in favor of the fragment **19c** corresponding to the C-ter cleavage of D-Leu^5 in a first step, then the fragment **19d** corresponding to the C-ter cleavage of D-Leu^3 (Figure 184). We also visualized **19b'** which corresponds to the loss of lysine at C-ter position. The action of the other enzyme then stops because of the D-configuration of Leu^5 (Figure 184).

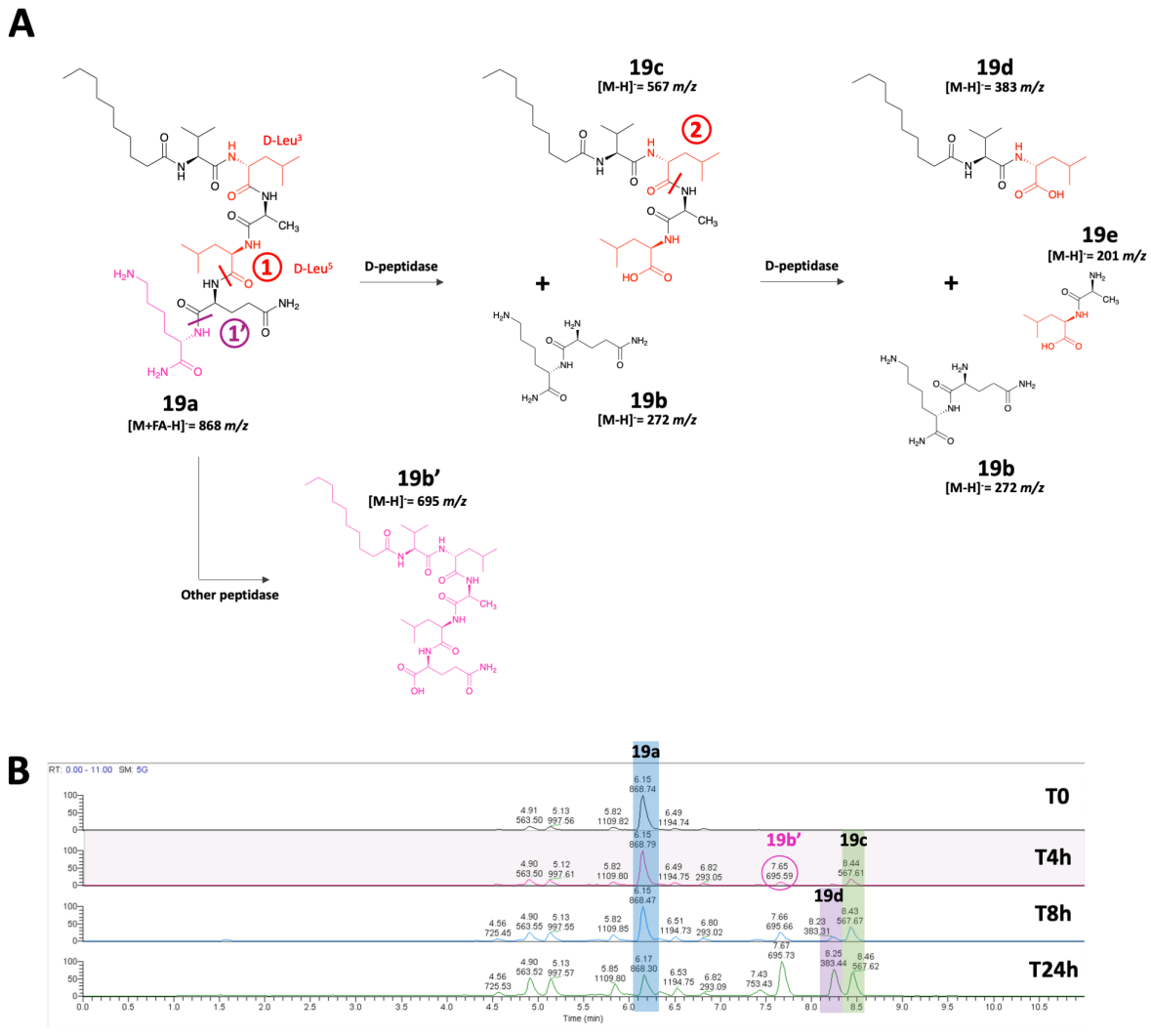

Figure 184. A) Successive cleavages of 19a by the D-peptidase and another enzyme, observed by LC-MS. B) LC-MS kinetic monitoring of 19a cleavage with *Dg-Ss-Lm* extract at 30°C pH 8 and masses corresponding to the LC-MS peaks of 19a-d. Pink circle corresponds to a parallel cleavage by the other enzyme. Compounds at 5.13 min and 5.82 min belong to the digestive gland extract.

We therefore hypothesized that two reactions were taking place in parallel, a cleavage by an enzyme present in the extract, hydrolyzing the peptide by its C-terminal side, and a cleavage by the D-peptidase we are studying, cleaving in C-ter of D-amino acids in positions 3 and 5.

Compound **19** showing more favorable kinetics, constitutes an interesting basis for the continuation of our study of the D-peptidase.

II. Perspectives for recovering the enzyme

A. Using a photoactivable amino acid

After determining a minimal peptide sequence recognized by the enzyme, we decided to took advantage of this substrate to set up a strategy enabling to trap the enzyme through a cross-linking between the enzyme and its substrate. One of the difficulties was to compensate for the fact that the enzyme acts at two different locations in the peptide sequence. We considered the use of photoactivatable amino acids, allowing the binding between the latter and an enzyme under UV irradiation. Indeed, the irradiation at 350 nm leads to the loss of nitrogen on the side chain of the photoactivatable amino acid, generating a carbene group. The two electrons can then form a bond with a function within the enzyme, such as an acid function, if it is close enough for that (Figure 185). It is possible to obtain commercially photo-leucine, which can then replace our leucines in the peptide. However, only the L-configuration photo-leucine is commercially available, while the two leucines of the peptide studied are of D-configuration.

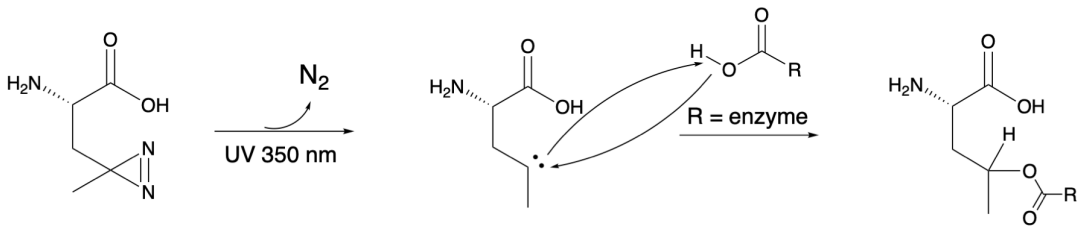

Figure 185. Schematic example of a photocrosslinking between a photoactivable amino acid (photoleucine) and an enzyme.

We could see with the compounds **10a** and **11a** previously studied, that the enzyme is able to cleave the peptide **10a** in position 5 and the peptide **11a** in position 3, where a D-Leu is present whereas a L-Leu is present on position 3 and 5 respectively for the two compounds. It is therefore possible to have a substrate cleaved by the enzyme with only one D-Leu in the sequence. We therefore wished to confirm this observation on linear peptides corresponding to the sequence optimized with peptide **19**. We thus synthesized compounds **20** and **21**, containing respectively a D-Leu^5 and a L-Leu^3 or a L-Leu^5 and a D-Leu^3 (Figure 186).

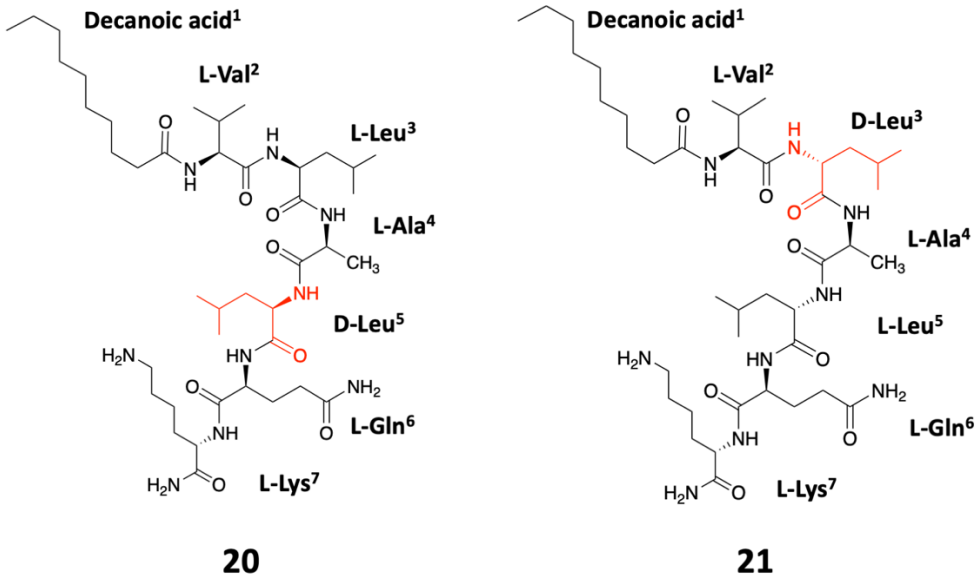

Figure 186. Structures of peptides 20 and 21.

In contact with *Dg-Ss-Lm*, peptide **20a** is indeed cleaved in the C-ter of D-Leu^5 only. However, the cleavage is very slow compared to compound **19a**, with about 75% of the peptide still present after 8 hours of incubation. However, the cleavage fragment **20c** is visible over an 8-hour study period. Again, the peptide **20b'** corresponding to the loss of the lysine at C-ter is also visualized (Figure 187).

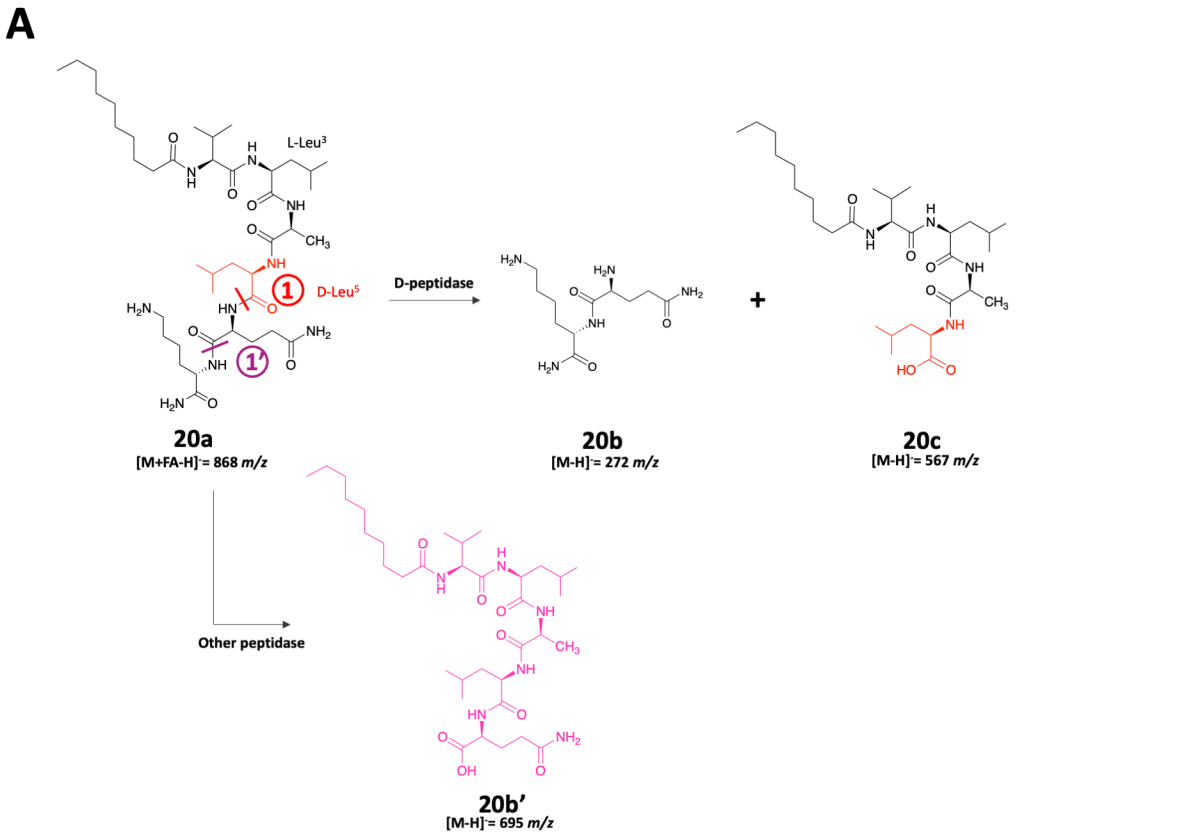

Figure 187. A) Cleavages of 20a by the D-peptidase and another enzyme, observed by LC-MS. B) LC-MS kinetic monitoring of 20a cleavage with *Dg-Ss-Lm* extract at 30°C pH 8 and masses corresponding to the LC-MS peaks of 20a-c. Pink circle corresponds to a parallel cleavage by the other enzyme. Compounds at 5.22 min and 5.97 min belong to the digestive gland extract.

Concerning compound **21**, the cleavage by the D-peptidase is slow and we mainly observe the successive cleavages made by the other enzyme from the C-ter side of the peptide. Indeed, 21a has successive amino acids of L configuration that could be remove from the sequence. We visualized in LC-MS, the successive loss of lysine (**21b'**), glutamine (**21c'**), L-Leu^5 (**21d'**). The fragment corresponding to the direct C-ter cleavage of D-Leu^3 (**21c**) is present from the beginning of the reaction (visible at T=2h), showing that the fragment is indeed obtained by a parallel pathway, through the action of the D-peptidase (Figure 188). The competition between these reactions impacts the kinetics of peptide cleavage, thus slower, with a cleavage in position 3 more difficult to observe. Indeed, thanks to the analysis of the direction of cleavage on peptides **5a** and **7a**, we could see that the D-peptidase we are looking for would

have a preference for position 5 for its first cleavage, compared to position 3. Thus, modifying position 3 as in the case of compounds **10** and **20** would have less impact on recognition than modifying position 5 as in the case of compounds **11** and **21**. The slower cleavage kinetics as well as the parallel reaction with another peptidase thus pushed us to keep compound **20** as a model peptide for the continuation of our study. It is then possible to have a peptide recognized by the enzyme and containing both a D-Leu and an L-Leu, thus leaving the possibility of inserting an L-photoleucine in position 3 of the peptide sequence.

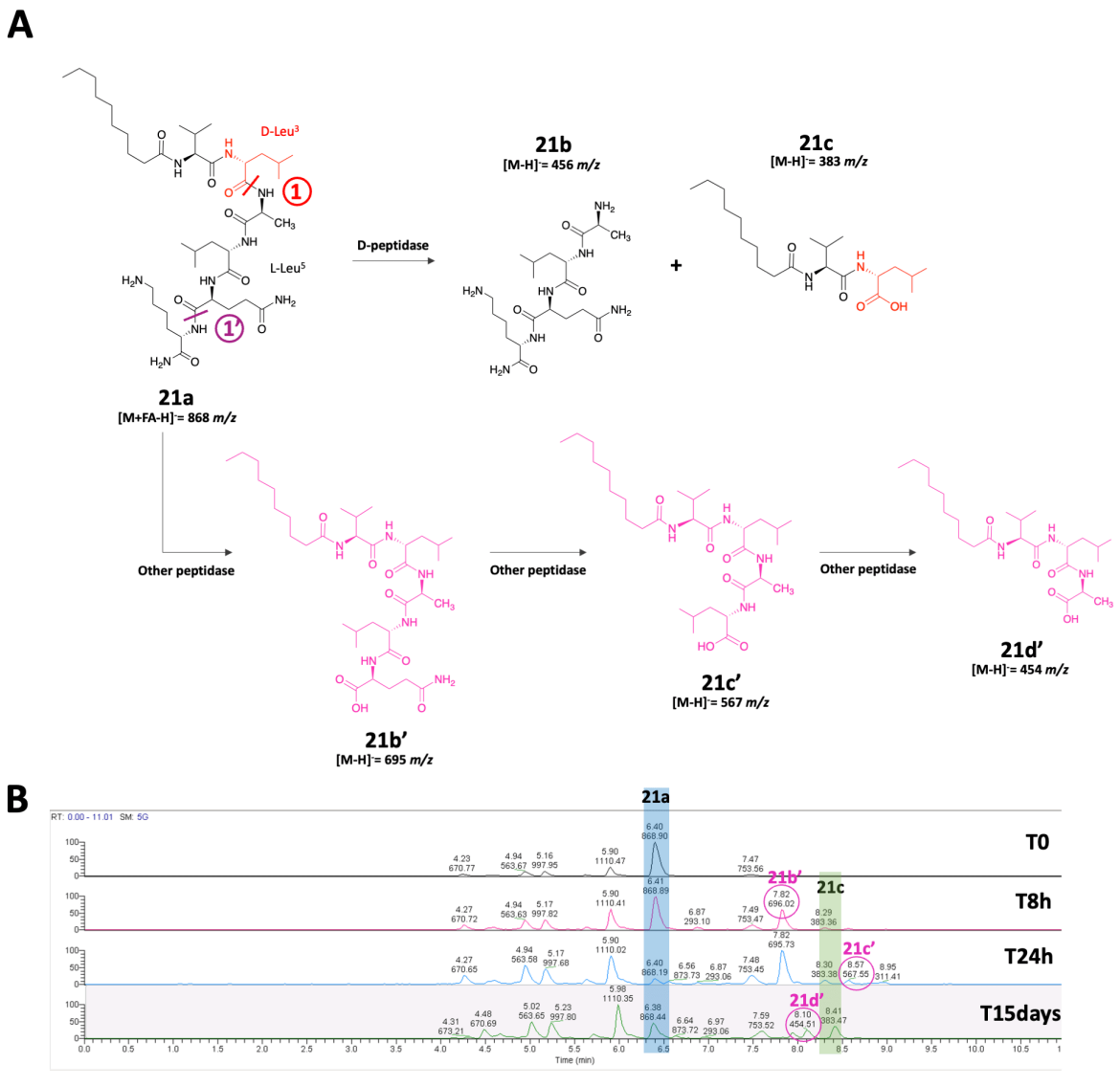

Figure 188. A) Cleavages of 21a by the D-peptidase and another enzyme, observed by LC-MS. B) LC-MS kinetic monitoring of 21a cleavage with *Dg-Ss-Lm* extract at 30°C pH 8 and masses corresponding to the LC-MS peaks of 21a-c. Pink circles correspond to parallel cleavages by the other enzyme. Compounds at 5.17 min and 5.90 min belong to the digestive gland extract.

Using a UV irradiation method, with a photo-leucine in position 3 and a D-Leu in position 5, the enzyme contained in *Dg-Ss-Lm* would then be bound to the substrate in position 3 while cleavage would take place in position 5. In order to visualize the remaining fragment coupled

to the enzyme, we considered the use of a fluorophore. This fluorophore could not be located on the C-ter side of the peptide since this part would be separated from the enzyme at position 3 following the cleavage at position 5, so it had to be integrated on the N-ter part of the peptide. The fatty chain of decanoic acid being important for the recognition of the enzyme, we replaced decanoic acid by 6-heptynoic acid in order to mimic the chain of Ade while adding an alkyne function. This acid is the longest commercialized acid containing a terminal alkyne. An alkyne function can thus react with an N_3 function by click chemistry, allowing the alkyne of the peptide to be linked to a fluorophore containing N_3 (Figure 189). The advantage of using this technique is that the click chemistry can be done after the binding of the enzyme under irradiation, thus avoiding that the peptide is hindered by the fluorophore upstream of the cleavage and thus taking the risk that the peptide is not recognized by the enzyme.

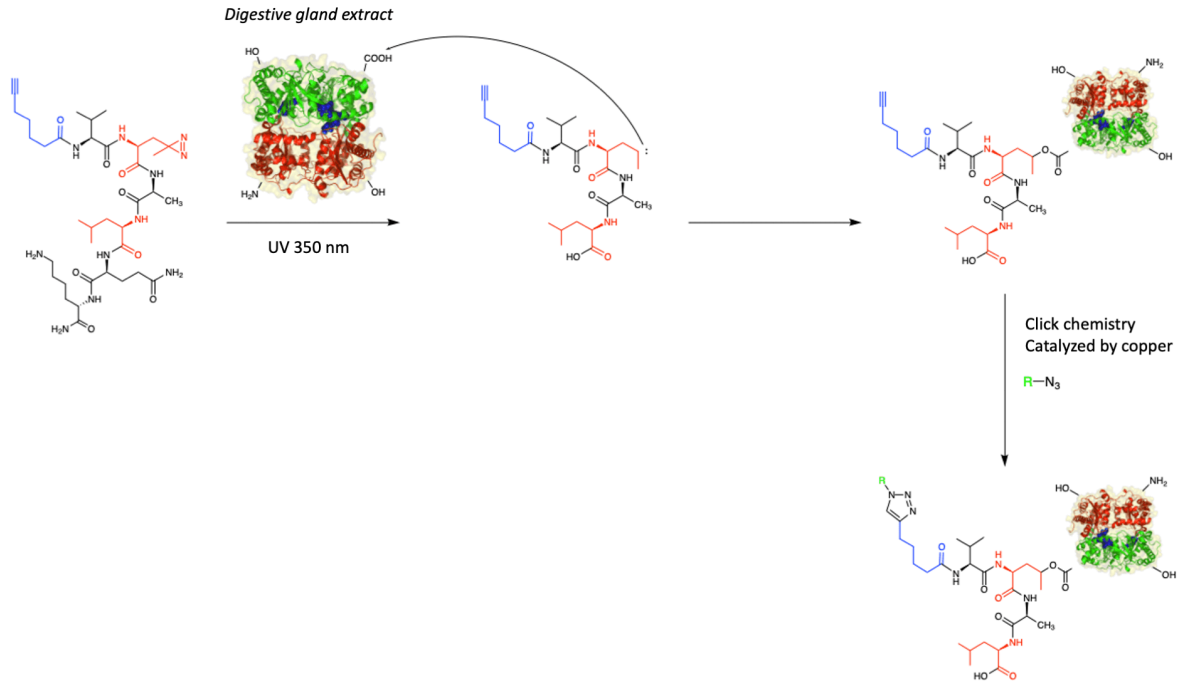

Figure 189. Schematic principle of photocoupling between a photoactivatable peptide and an enzyme, and addition of a fluorophore by click chemistry. R group is a fluorophore.

In order to consider this technique, it was necessary to verify the ability of the enzyme to cleave a peptide containing 6-heptynoic acid at N-ter. For this purpose, we synthesized compound **22**, an analogue of compound **20**, containing 6-heptynoic acid instead of decanoic acid (Figure 190).

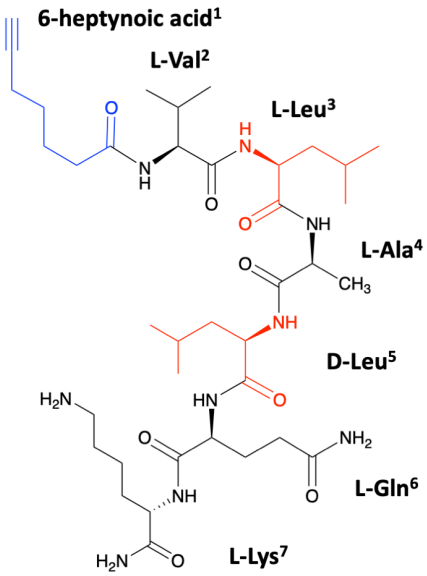

22

Figure 190. Structure of peptide 22.

Unfortunately, this peptide exposed to *Dg-Ss-Lm* is not cleaved by the enzyme. The expected fragments related to the C-ter cleavage of D-Leu[5] (**22b** and **22c**) are not visualized in LC-MS. On the other hand, after 24 hours of incubation, we observe the peptide **22b'** having lost the lysine at C-ter (Figure 191) through the action of another peptidase. We therefore decided to supplement the medium with digestive gland extract after 24 hours of reaction, with the idea that the reaction would be very slow. We thus followed the peptide until 3 days after the enzyme addition. We then observe the increase of the peak corresponding to the loss of lysine (**22b'**), without any other new fragments. It seems that the peptide is no longer cleaved by the enzyme. Indeed, the 3-aminodecanoic acid (Ade) in type-B laxaphycins contains 10 carbons within an alkane chain. In the case of type-A laxaphycins, not cleaved by the desired enzyme, 3-aminooctanoic acid (Aoc) contains 8 carbons with an alkane chain as well. Here, 6-heptynoic acid contains only 7 carbons with a terminal alkyne function. It is very likely that the loss of carbons in the chain impacts the recognition of the enzyme towards the substrate. This result is in agreement with the observations made with peptides **8** and **16** containing a β-alanine in position 1, not cleaved by the enzyme. In addition, an alkyne function has a linear and more rigid geometry than an alkane that can rotate more freely. The integration of the 6-heptynoic acid into the active site of the enzyme would therefore be less obvious than in the case of decanoic acid, causing the enzyme to lose its activity on the peptide substrate. The use of an alkyne replacing decanoic acid in order to integrate a fluorophore to visualize and recover the enzyme was therefore set aside. This technique could be re-evaluated, using the original Ade, allowing to functionalize the peptide on the amine of the latter.

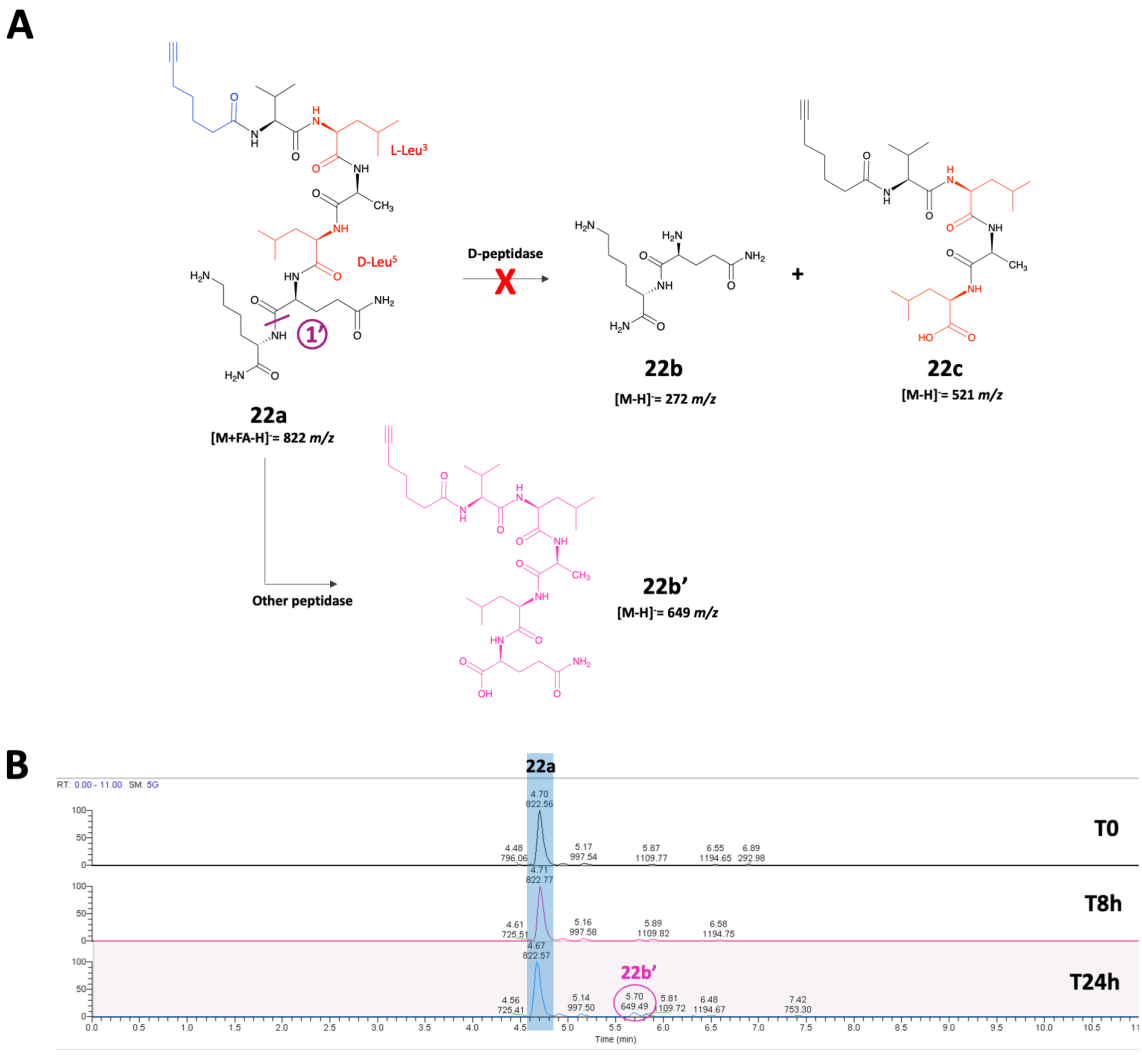

Figure 191. A) Cleavage of 22a by another enzyme, observed by LC-MS. B) LC-MS kinetic monitoring of 22a cleavage with *Dg-Ss-Lm* extract at 30°C pH 8 and masses corresponding to the LC-MS peaks of 22a. Pink circle corresponds to a parallel cleavage by the other enzyme. Compounds at 5.17 min and 5.87 min belong to the digestive gland extract.

B. Using its physico-chemical properties

a) Pre-concentration of the enzyme using ion exchange column

We considered the separation of proteins contained in the studied extract, using ion exchange columns. The objective was to fractionate the extract and to check the enzymatic activity of each fraction on laxaphycin B in order to pre-concentrate our enzyme in a fraction.

Ion exchange chromatography separates molecules based on their respective charges. The charges of each molecule interact with opposite charges attached to the stationary phase of the column allowing their retention, while the identical charges remain within the mobile phase to be eluted through the column. Thus, when using a cationic resin column, the analyte

ions retained by the resin are negatively charged and replace the negative counter ions initially in the stationary phase. Once the negative ions of the analyte are retained, they can be eluted and removed from the resin, notably by adding salts, whose negative ions will compete with the negative ions remaining on the resin and allow them to be removed (Figure 192).

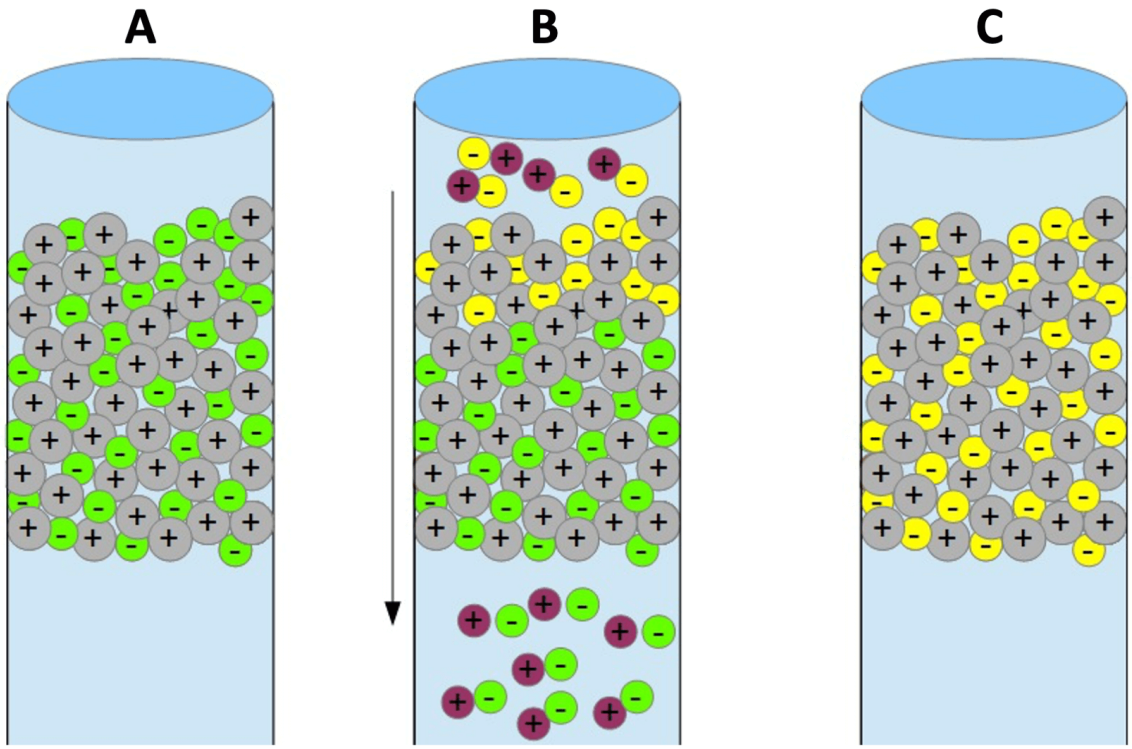

Figure 192. Steps of an anion exchange on an ion exchange column with a cationic resin. A) Cationic resin with negative counterion. B) Addition of an analyte containing a target anion replacing the negative counterion of the resin. C) The target anion is retained by the cationic resin.
This image was made by F. Bachelier on Wikipedia.org (License CC BY-SA 4.0).

As a preliminary experiment, we used Fast Flow type ion exchange columns with a total volume of 1 mL. The columns are first rinsed with milliQ water and then equilibrated with the same buffer used to prepare the extracts to be purified, a Tris buffer (50 mM) at pH 8. The extract is then loaded onto the column (160 uL). The column is then rinsed with the buffer in order to elute what does not bind to the stationary phase of the column. Then, the column is rinsed with a NaCl salt gradient, ranging from 0.1 M to 0.5 M, in order to create a competition between the extract ions blocked on the column and the salt ions. Thus, several fractions are recovered which are then filtered on Illustra Microspin G-50 columns to remove the salts. The fractions obtained before and after salt gradient can then be tested on laxaphycin B.

In a first step, we used a HiTrap DEAE (diethylaminoethyle) Fast Flow cationic column, which is a positively charged resin allowing weak anion exchanges. We first performed a binary test, with a first elution without salts with the buffer only, then in a second step the application of the buffer with 0.5 M NaCl. The fractions obtained before the addition of salts did not show any enzymatic activity on laxaphycin B. On the other hand, enzymatic activity is recovered

with the fractions obtained with 0.5 M in NaCl. After 24 hours of incubation, laxaphycin B is 93% cleaved with a final product corresponding to [des-(Ala^4-Hle^5)]acyclolaxaphycin B (compound **2c**, mass 1213 *m/z*) in the case of the control while in the case of the active fractions, there remains a mixture of first opened laxaphycin B (compounds **2b** or **2d**, mass 1413 *m/z*) and final [des-(Ala^4-Hle^5)]acyclolaxaphycin B (compound **2c**, mass 1213 *m/z*), with a 91% cleaved laxaphycin B (Table 21).

Table 21. Cleavage rate of laxaphycin B obtained with salted or unsalted fractions with DEAE column. Masses of the majority peaks observed in LC-MS.

Control **T=24h**	Cleavage 93% Majority peak = 1213 *m/z*
	DEAE column (+) **Weak anion exchange**
Non-salted fractions **T=24h**	-
Salted fractions at 0.5 M NaCl **T=24h**	Cleavage 91% Majority peaks = 1213 *m/z* + 1413 *m/z*

We then repeated the experiment, this time applying a salt gradient from 0.1 M to 0.5 M NaCl. As in the previous case, the non-salted fractions are not active on laxaphycin B. On the other hand, we recover the enzymatic activity on the fractions obtained at 0.1 M NaCl. Fractions with a higher salt concentration are not active. After 72 hours of incubation, laxaphycin B is completely cleaved with a final product corresponding to [des-(Ala^4-Hle^5)]acyclolaxaphycin B (compound **2c**, mass 1213 *m/z*) in the case of the control whereas in the case of the active fractions there remains a mixture of first opened laxaphycin B (compound **2b** or **2d**, mass 1413 *m/z*) and final [des-(Ala^4-Hle^5)]acyclolaxaphycin B (compound **2c**, mass 1213 *m/z*), although laxaphycin B is completely cleaved (Table 22). The enzyme or a co-factor would contain a set of negative charges allowing the enzyme to attach to the resin and the addition of a low concentration of salts is sufficient to unhook it. However, the enzymatic activity is not amplified in the fraction compared to the control extract.

Table 22. Cleavage rate of laxaphycin B obtained with the different salted or unsalted fractions with DEAE column. Masses of the majority peaks observed in LC-MS.

Control **T=72h**	Cleavage 100% Majority peak = 1213 *m/z*
	DEAE column (+) **Weak anion exchange**
Non-salted fractions **T=72h**	-
Salted fractions at 0.1 M NaCl **T=72h**	Cleavage 100% Majority peaks = 1213 *m/z* + 1413 *m/z*
Salted fractions at 0.2 M NaCl **T=72h**	Cleavage 3%
Salted fractions at 0.3 M NaCl **T=72h**	-
Salted fractions at 0.4 M NaCl **T=72h**	-
Salted fractions at 0.5 M NaCl **T=72h**	-

We then used 1 mL HiTrap CM (Carboxymethyl) Fast Flow and HiTrap SP (Sulfopropyl) Fast Flow anionic columns, negatively charged allowing weak and strong anion exchanges, respectively. Regardless of the column used, the enzyme activity was recovered from the unsalted fractions, obtained before the application of the salt gradient. The enzyme sought is therefore not able to bind to a negatively charged column.
However, as with DEAE column, the enzyme activity was not fully recovered within these fractions. Indeed, whereas the control sample showed 94% cleavage of laxaphycin B after 24 hours of incubation, only 73% and 65% cleaved laxaphycin B was observed in the case of the non-salted fractions of each column, respectively (Table 23).
Moreover, the cleavage stops mostly at the first opening of the peptide corresponding to a gain of H_2O in mass (compound **2b** or **2d**, mass 1413 *m/z*). Even if the majority compound observed in LC-MS remains the compound of mass 1413 *m/z*, the beginning of the appearance of compound **2c** (mass 1213 *m/z*) could be visualized.

The enzyme could be acting with a non-protein cofactor or a co-enzyme, which would be separated from it through the column, not allowing the cleavage to go through. There would then be an enzyme allowing the first cleavage giving rise to acyclic laxaphycin B of mass 1413 *m/z*, and another enzyme performing the second cleavage to obtain [des-(Ala^4-Hle^5)]acyclolaxaphycin B of mass 1213 *m/z*. Previously, we have demonstrated with peptides **10** and **11** that the cleavage activity could take place in position 3 or 5 independently, showing

that it would be possible to have different enzyme for each cleavage. However, the absence of a cofactor generally results in inactivity of the enzyme an no other enzymatic activity was observed in other fractions.

Moreover, the observation of the appearance of [des-(Ala^4-Hle^5)]acyclolaxaphycin B with mass 1213 *m/z* shows that the second cleavage is possible with the collected fraction but is simply much slower than in the control case. These results are not consistent with having two distinct enzymes.
The preferred hypothesis is that the enzyme concentration in the fractions used on laxaphycin B is not as high as that in the crude extract, implying an enzyme deficit that does not allow cleavage to proceed to completion. In fact, it is important to note that an approximation was made for the calculation of the volume of fractionated extract to be used with laxaphycin B. During the separation on column, the extract is diluted by the addition of eluent, and 500 µL are collected in different Eppendorf tubes. The recovery of these 500 µL is done visually and a dilution factor is approximated, between the initial volume of the extract deposited on the column and the volume recovered at the column outlet. In order to compare the activity of the fractionated extract to the initial extract on laxaphycin B, the volume of fractionated extract used was calculated with this same dilution factor. However, if the volume used with this approximation was too small, it could explain this slowing down of the cleavage kinetics.

These preliminary results did not allow us to amplify the enzymatic activity but brought us first information on the charges present in the enzyme, allowing to hang it on a cationic resin.

Table 23. Cleavage rate of laxaphycin B obtained with the different salted or unsalted fractions according to the type of column used. Masses of the majority peaks observed in LC-MS.

Control T=24h	Cleavage 94% Majority peaks = 1413 *m/z* + 1213 *m/z*	Cleavage 94% Majority peaks = 1413 *m/z* + 1213 *m/z*
	CM column (-) **Weak cation exchange**	**SP column (-)** **Strong cation exchange**
Non-salted fractions T=24h	Cleavage 73% Majority peak = 1413 *m/z*	Cleavage 65% Majority peak = 1413 *m/z*
Salted fractions at 0.1 M NaCl T=24h	-	-
Salted fractions at 0.2 M NaCl T=24h	-	-
Salted fractions at 0.3 M NaCl T=24h	-	-
Salted fractions at 0.4 M NaCl T=24h	-	-
Salted fractions at 0.5 M NaCl T=24h	-	-

b) Pre-concentration of the enzyme using filtration by molecular weight

We also tried to pre-concentrate the enzyme using Amicon mass filters. These filters allow to separate the molecules according to their molecular weight. We performed two experiments in parallel, with the same enzyme extract *Dg-Ss-Lm* (Figure 193). This extract was deposited in a 100 kDa filter. The C1 concentrate was set aside, and the F1 filtrate was redeposited in a 50 kDa filter and so on down to the 10 kDa filter. In parallel, the same extract was deposited in a 10 kDa filter first. The F1' filtrate was set aside while the C1' concentrate was reused in the 30 kDa filter and so on until the 100 kDa filter.

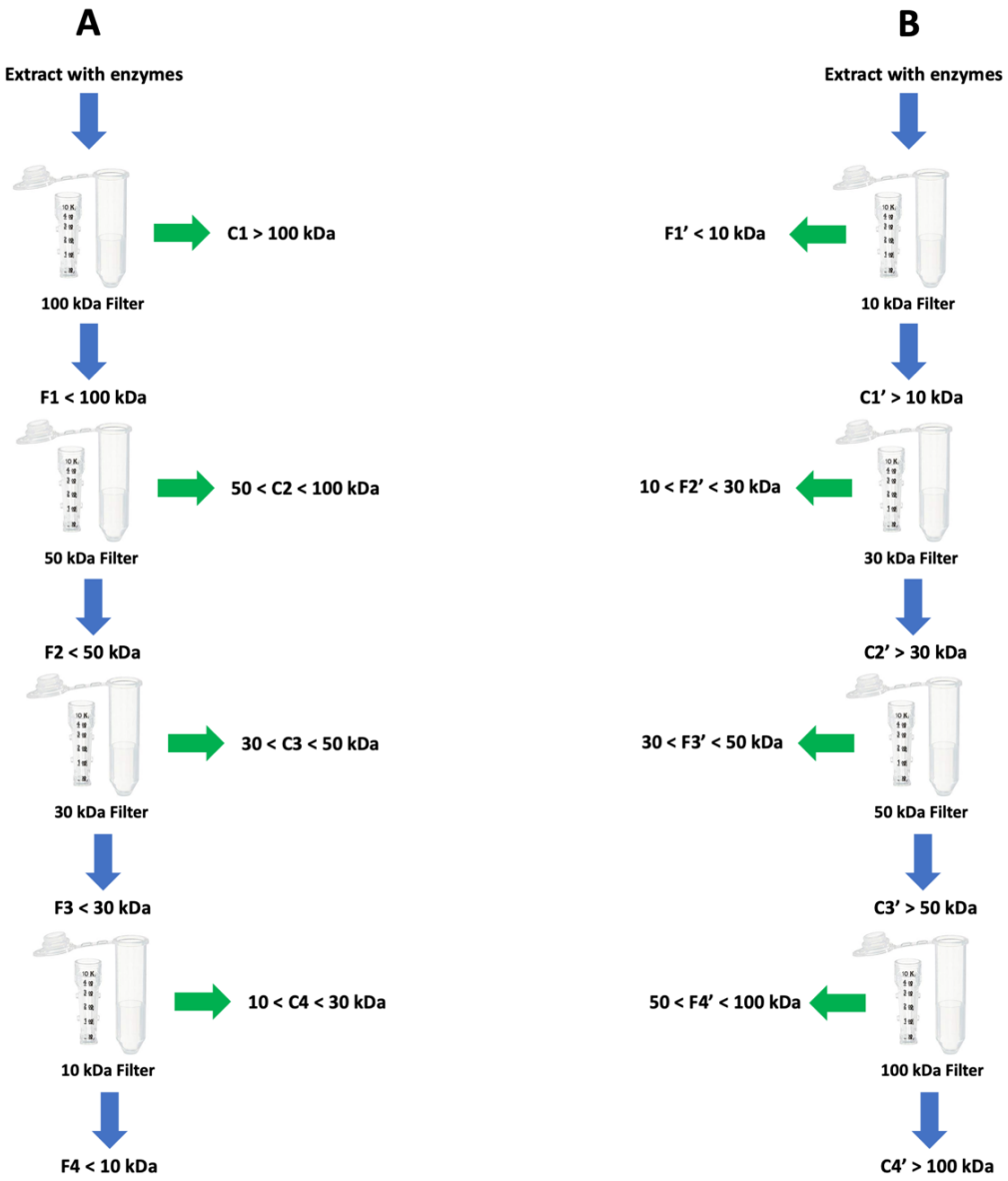

Figure 193. Schematic representation of the filtration protocol on Amicon filters. A) Use of filters by decreasing mass. B) Use of filters by increasing mass.

The different fractions were then tested for their activity on laxaphycin B, in comparison to the initial unfiltered extract (Table 24). Enzyme activity was fully recovered in the fractions corresponding to molecules with masses greater than 100 kDa, i.e., C1 in the case of decreasing mass filtration and C4' in the case of increasing mass filtration. No enzymatic activity was observed for the fractions of lower masses. The enzyme of interest would therefore have a mass greater than 100 kDa. In addition, the cleavage kinetics are slightly faster at the beginning of the reaction with laxaphycin B. After 24 hours of incubation, laxaphycin B is 95% and 98% cleaved with C1 and C4' respectively, whereas it is 93% cleaved in the unfiltered control extract. Filtration thus had a slight benefit on enzymatic activity, potentially removing other molecules that may impede it.

Table 24. Cleavage rate of laxaphycin B obtained with different mass fractions. Masses of the majority peaks observed in LC-MS.

	T=1h	**T=4h**	**T=24h**
Control (unfiltered extract)	Cleavage 48% Majority peak = 1413 *m/z*	*Not evaluated*	Cleavage 93% Majority peak = 1213 *m/z*
C1 (M>100 kDa)	Cleavage 66% Majority peak = 1413 *m/z*	Cleavage 89% Majority peak = 1413 *m/z* + 1213 *m/z*	Cleavage 95% Majority peak = 1213 *m/z*
C4' (M>100 kDa)	Cleavage 77% Majority peak = 1413 *m/z*	Cleavage 87% Majority peak = 1413 *m/z* + 1213 *m/z*	Cleavage 98% Majority peak = 1213 *m/z*
Other fractions (M < 100 kDa)	-	-	-

By summarizing all the results obtained in chapters 3 and 4, we could see that the long fatty chain of the Ade in position 1 is of strong importance for the peptide to be cleaved or not by the enzyme. Indeed, a residue of this size must take a particular conformation in the active site of the enzyme. The cleavage activity is then lost if this chain is modified, either in size or in terms of functions. The study of linear peptides allowed us to show that the cyclic structure of B-type laxaphycins is not a mandatory condition to visualize the same cleavages. Indeed, the enzyme is able to cleave in C-ter of D-amino acids in position 5 and then in position 3, as long as the amino acids neighboring these positions are suitable for the recognition of the enzyme. We have also shown that it is possible to cleave peptides at the C-ter of the D-amino acid in position 5 despite the presence of an L-amino acid in position 3. However, this change in stereochemistry strongly slows down the cleavage kinetics. The use of a more flexible linear peptide than a cyclic one, together with a change in absolute configuration, could make the peptide more sensitive to other enzymes present in the extract which may also have an enzymatic activity on this peptide to the detriment of the desired enzyme. However, the linear peptide 19 will constitute a good basis for the continuation of the project. Moreover, first information on the properties of the enzyme could be provided. This enzyme would have a mass higher than 100 kDa and will be fixable on a cationic resin column. These preliminary results will have to be deepened in the future.

III. Experimental part III

A. Peptide synthesis

Peptides were synthesized with an automated microwave peptide synthesizer (CEM Liberty One). The synthesis was performed at 50 °C under microwaves (25 W) and at 0.1 mmol scale with PyOxim (4.9 equiv)/DIEA (10 equiv) as coupling reagents. 20% piperidine in DMF were used for deprotection steps. Rink Amide resin (0.67 mmol/g) was used for every peptide syntheses. For each amino acid the standard coupling cycle was as follows: after Fmoc deprotection of the amino acid supported by the resin, 2.5 mL of the requested amino acid at a concentration of 0.2 M in DMF was added to the resin, followed by 1 mL of PyOxim in DMF at 0.49 M and lastly by 0.5 mL 2M DIEA in NMP. The coupling of all amino acids was performed for 20 minutes except for difficult couplings which were carried out 2 or 3 times such as Fmoc-L-Gln(Trt)-OH that was coupled three times for 20 minutes, followed by capping with a solution of 100 mL of DMF, 5 mL of anhydride acetic (0.5 M, 1 equiv), 2 mL of DIEA (0.21 equiv) and 135 mg of HOBt (0.019 equiv) for 3 minutes. The Fmoc-group was deprotected by adding 20% piperidine solution in DMF for 3 minutes. At the end of the synthesis, the resin was washed three times with DMF and three times with DCM and then was dried under *vacuum*.

A total cleavage was done using a solution of TFA/TIS/H_2O 95:2.5:2.5 (v/v) under agitation over 2 hours. The resin was then filtered and the filtrate was concentrated *in vacuo* with cyclohexane as a co-solvent. Peptides were precipitated in ice-cold diethyl ether and freeze-dried. Peptides were then purified by semi-preparative HPLC.

B. Peptide stability in buffer (pH 8) and with *Dg-Ss-Lm* at 30°C

A buffer solution at pH 8 (50 mM Tris, pH adjusted with HCl 1M) was prepared and sterilized by autoclave. Stock solutions of peptides were prepared at 50 mg/mL in DMSO. To assess peptide stability, these solutions were diluted 50 times in buffer pH 8. Peptide solutions at 1 mg/mL were diluted 10 times with the same buffer resulting in peptides at 0.1 mg/mL. Solutions were incubated at 30°C under agitation. For each kinetic point, the same procedure was applied: solutions were centrifuged for a few seconds, then part of the solution was removed to be quenched by 90% MeOH, resulting in 0.01 mg/mL peptide solutions. The quenched solutions were centrifuged at 21,952 x *g* for 20 minutes at 4°C. The maximum amount of supernatant was recovered in a LC-MS vial for analysis. All tests were performed in triplicate.

To evaluate peptide stability in presence of Dg-Ss-Lm, peptide solutions at 1 mg/mL in buffer were mixed with *Dg-Ss-Lm* extracts (10 mg/mL) and completed with the same buffer resulting in peptides at 0.1 mg/mL and extracts at 1 mg/mL. Solutions were incubated at 30°C under agitation. For each kinetic point, the same procedure was applied: solutions were centrifuged for a few seconds, then part of the solution was removed to be quenched by 90% MeOH,

obtaining peptide solutions at 0.01 mg/mL. The quenched solutions were centrifuged at 21,952 x *g* for 20 minutes at 4°C. The maximum amount of supernatant was recovered in a LC-MS vial for analysis. All the tests were carried out in triplicate on the same extract and in several replicates with other extracts.

C. Pre-concentration with ion exchange columns

Tris buffer (50 mM) is prepared at pH 8 and sterilized by autoclaving. Solutions containing Tris buffer (50 mM) and NaCl at 0.1 M, 0.2 M, 0.3 M, 0.4 M or 0.5 M are also prepared. These solutions are filtered on 0.45 µm filters. First, the column (Fast Flow 1 mL, HiTrap DEAE or CM or SP) is rinsed with 3 mL of milliQ water. The column is then equilibrated with the Tris buffer without salts, used to obtain the digestive gland extract. The extract (160 µL) is loaded on the column which is then rinsed with 3 mL of Tris buffer that is collected in 500 µL Eppendorf tubes. As the column volume is 1 mL, only the 500 µL fractions n°2 and n°3 will be considered hereafter. The column is then rinsed with 3 mL of Tris buffer (50 mM) and 0.1 M NaCl, and the fractions are also recovered in 500 µL Eppendorf tubes. The same procedure is performed for Tris buffer (50 mM) solutions containing 0.2 M NaCl then 0.3 M NaCl then 0.4 M NaCl then 0.5 M NaCl. Finally, the column is washed with Tris buffer (50 mM) without salts, then with milliQ water. The column is then washed with 20% ethanol in milliQ water to be stored in the freezer. The fractions obtained by adding salts are filtered on Illustra Microspin G-50 columns. To do this, the column resin is vortexed and then centrifuged at 750 x *g* for 1 minute to pack the column. 200 µL of the salted fraction is loaded onto the resin and then centrifuged at 750 x *g* for 1 minute to recover the filtrate. This filtrate will be used to check the enzymatic activity on laxaphycin B, along with the unsalted fraction and the initial extract for comparison.

D. Pre-concentration with Amicon mass filters

The filters are pre-rinsed with milliQ water. 1000 µL of digestive gland extract is divided into two 500 µL fractions. 500 µL of extract is placed on the 100 kDa filter and centrifuged at 14000 x *g* at 2°C for 8 minutes (Figure 193A). The C1 concentrate is collected in a new tube by inverting the filter upside down on this tube and centrifuging at 1500 x *g* at 2°C for 4 minutes. About 100 µL of C1 concentrate is recovered, leaving about 400 µL of F1 filtrate. F1 is diluted to 500 µL and inserted into the 50 kDa filter. F1 is centrifuged at 14000 x *g* at 2°C for 5 minutes. 30 µL of C2 concentrate is set aside and 460 µL of F2 filtrate is diluted to 500 µL and placed on the 30 kDa filter. F2 is centrifuged at 14000 x *g* at 2°C for 5 minutes. 50 µL of C3 concentrate is set aside and 450 µL of F3 filtrate is diluted to 500 µL and placed on the 10 kDa filter. F3 is centrifuged at 14000 x *g* at 2°C for 5 minutes. 150 µL of C4 concentrate and 350 µL of F4 filtrate are set aside.

In parallel, 500 µL of extract is placed on the 10 kDa filter and centrifuged at 14000 x *g* at 2°C for 8 minutes (Figure 193B). The C1 concentrate is collected in a new tube by inverting the filter upside down on this tube and centrifuging at 1500 x *g* at 2°C for 4 minutes. About 110

µL of C1' concentrate is recovered, leaving about 390 µL of F1' filtrate. F1' is set aside and C1' is diluted to 500 µL and inserted into the 30 kDa filter. C1' is centrifuged at 14000 x *g* at 2°C for 5 minutes. 400 µL of filtrate F2' is set aside and 100 µL of concentrate C2' is diluted to 500 µL and placed on the 50 kDa filter. C2' is centrifuged at 14000 x *g* at 2°C for 5 minutes. 390 µL of filtrate F3' is set aside and 110 µL of concentrate C3' is diluted to 500 µL and placed on the 100 kDa filter. C3' is centrifuged at 14000 x *g* at 2°C for 5 minutes. 110 µL of C4' concentrate and 390 µL of F4' filtrate are set aside.

The amount of protein in each fraction as well as in the initial extract is evaluated with the Bradford method, so that each fraction is used in the right proportions to compare their activity with that of the unfiltered extract. These fractions are then tested on laxaphycin B to verify that some contain enzymatic activity.

E. Analyses

The compound studied in this chapter are the synthetic peptides **12-22**. Hereafter, the HRMS, LCMS and NMR analyses of the synthesized peptides are reported. For products **12-14**, only the proton NMR spectrum is reported, because the quantities of these products were not sufficient to obtain other spectra.

a) Compound 12

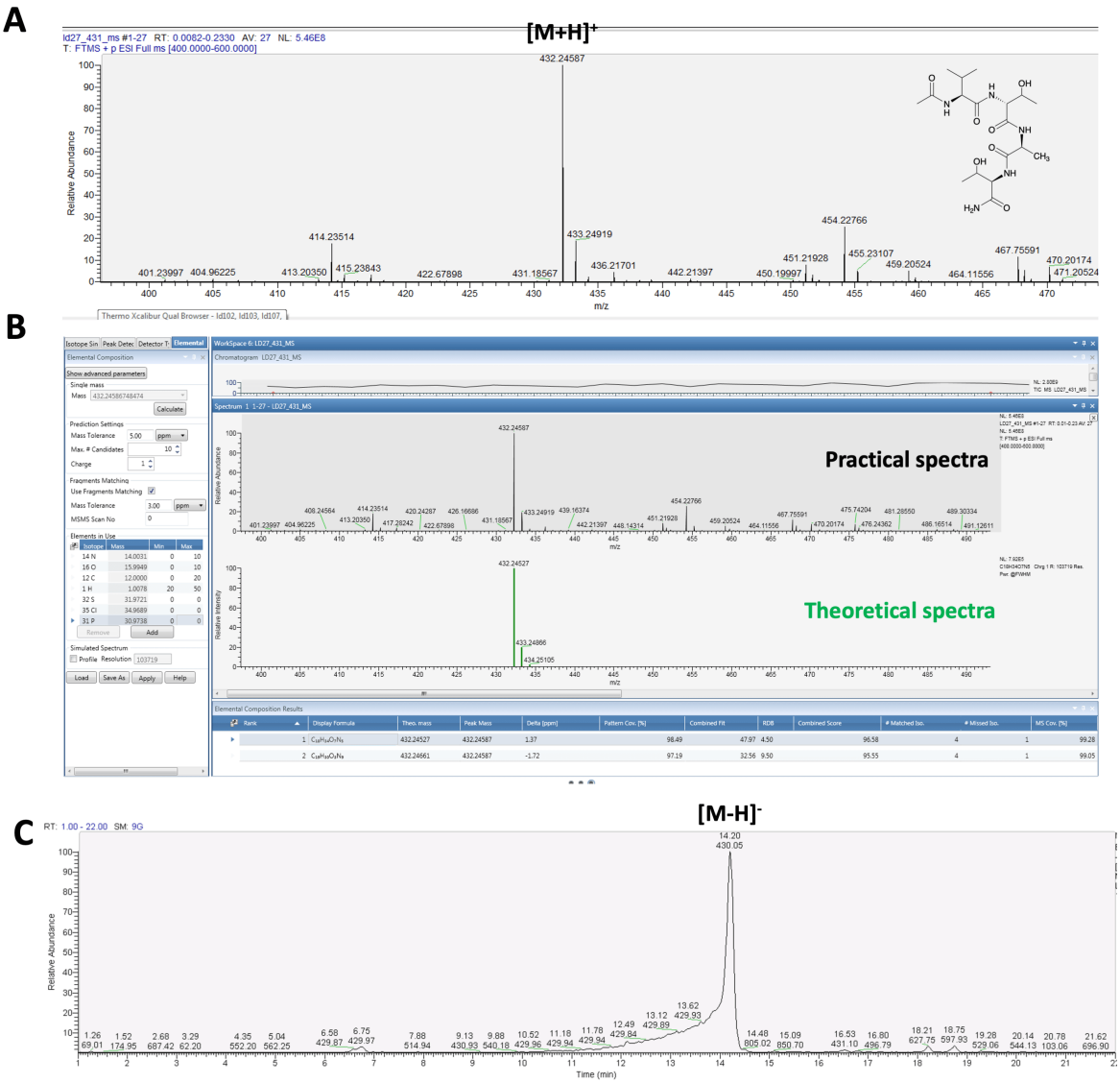

Figure 194. A) ESI-HRMS spectrum of 12. B) Comparison with the theoretical spectrum. Calculated for $C_{18}H_{34}N_5O_7$ [M+H]$^+$ *m/z* 432.24527; Found [M+H]$^+$ *m/z* 432.24587; mass error = 1.37 ppm. C) LC-MS profile of 12.

Table 25. NMR spectroscopic data of 12 in DMSO-d_6

entry	position	C, mult.	H, mult. (J in Hz)
Val[2]	1	*nd*, C	-
	2	59.4, CH	4.09
	3	30.1, CH	1.89
	3-Me	19.7, CH_3	0.83
	4	19.1, CH_3	0.85
	NH	-	8.02, d (7.45)
		nd, C acetylation	-
		22.8, CH_3 acetylation	1.83
D-Thr[3]	1	*nd*, C	-
	2	59.1, CH	4.07
	3	66.9, CH	4.02
	4	20.3-20.6, CH_3	0.96-1.00
	NH	-	7.99, d (8.31)
Ala[4]	1	*nd*, C	-
	2	49.3, CH	4.29, t (6.87)
	3	18.2, CH_3	1.20, d (6.87)
	NH	-	7.83, d (6.87)
D-Thr[5]	1	*nd*, C	-
	2	58.4, CH	4.03
	3	66.9, CH	4.02
	4	20.3-20.6, CH_3	0.96-1.00
	NH	-	7.62, d (8.59)
	$NH_{2\ C\text{-}ter}$	-	7.14 & 7.04
nd =	not determined		

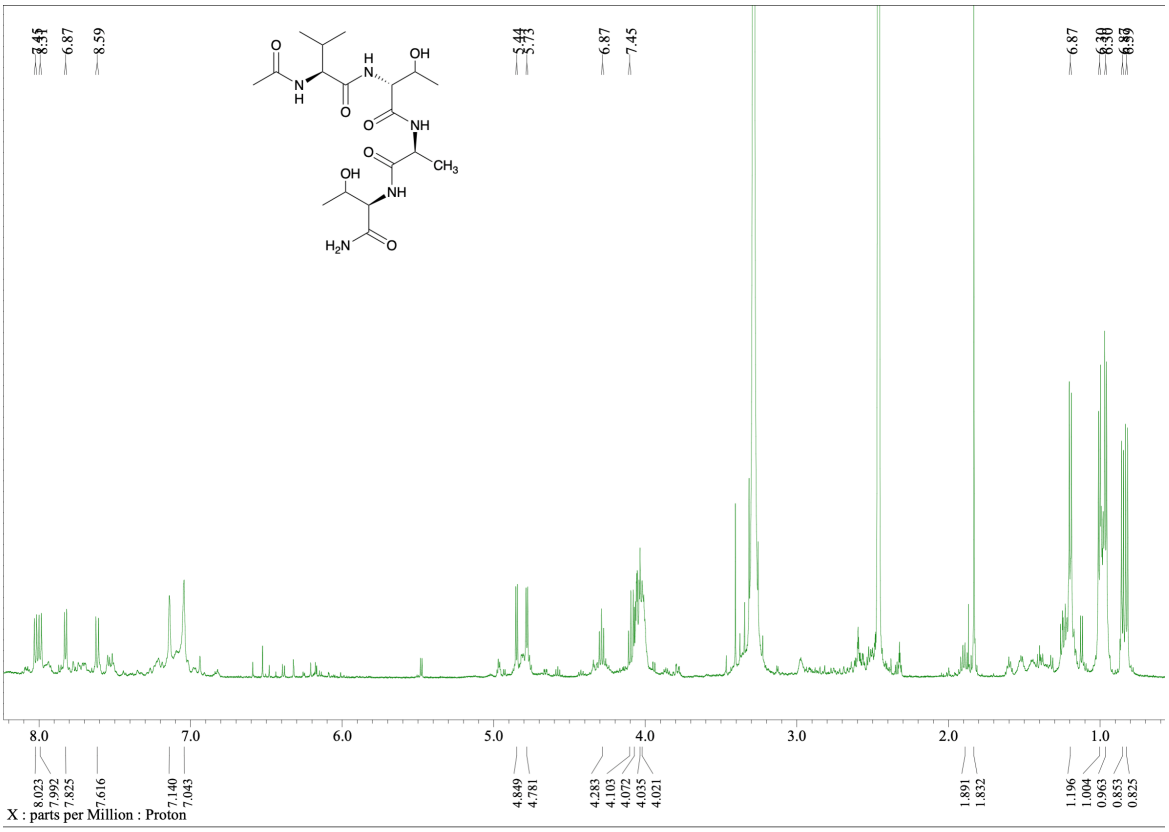

Figure 195. ^{1}H NMR spectrum of 12. Solvent : dmso-d_6; T : 23°C; Scans : 32

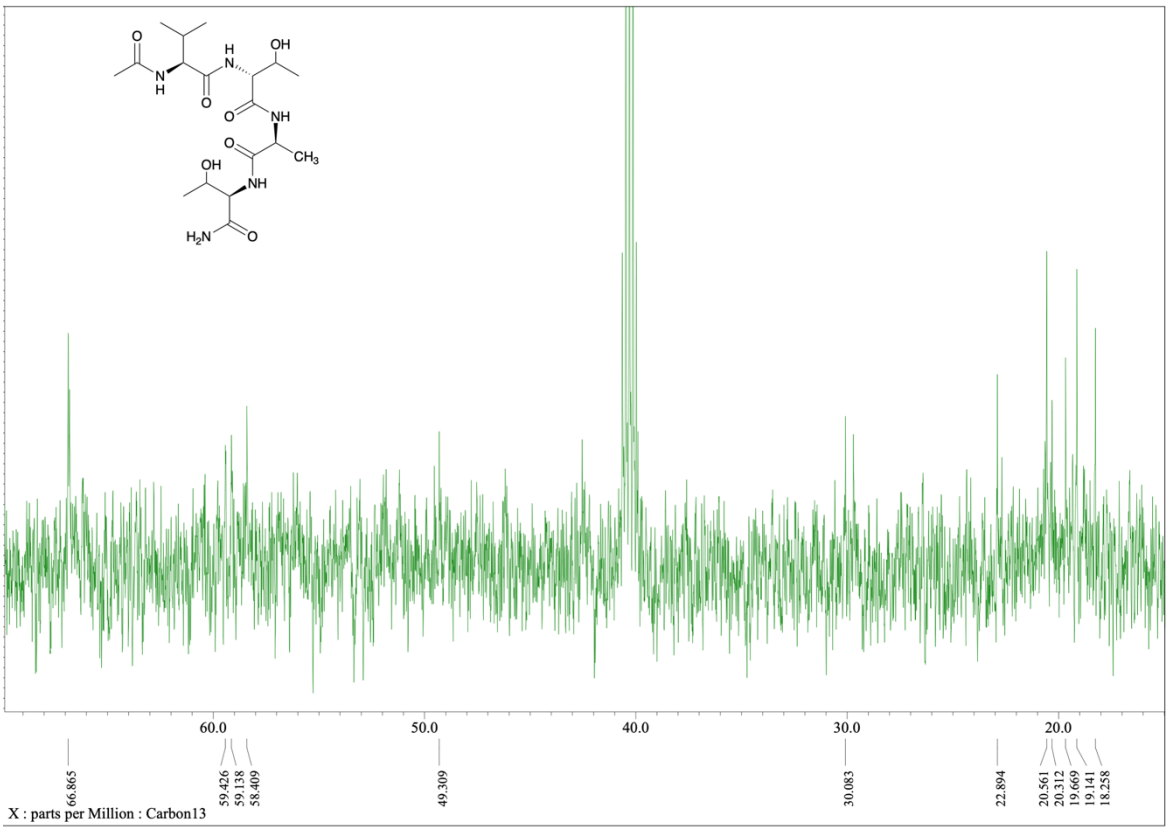

Figure 196. DEPT spectrum of 12. Solvent : dmso-d_6; T : 23°C; Scans : 10000

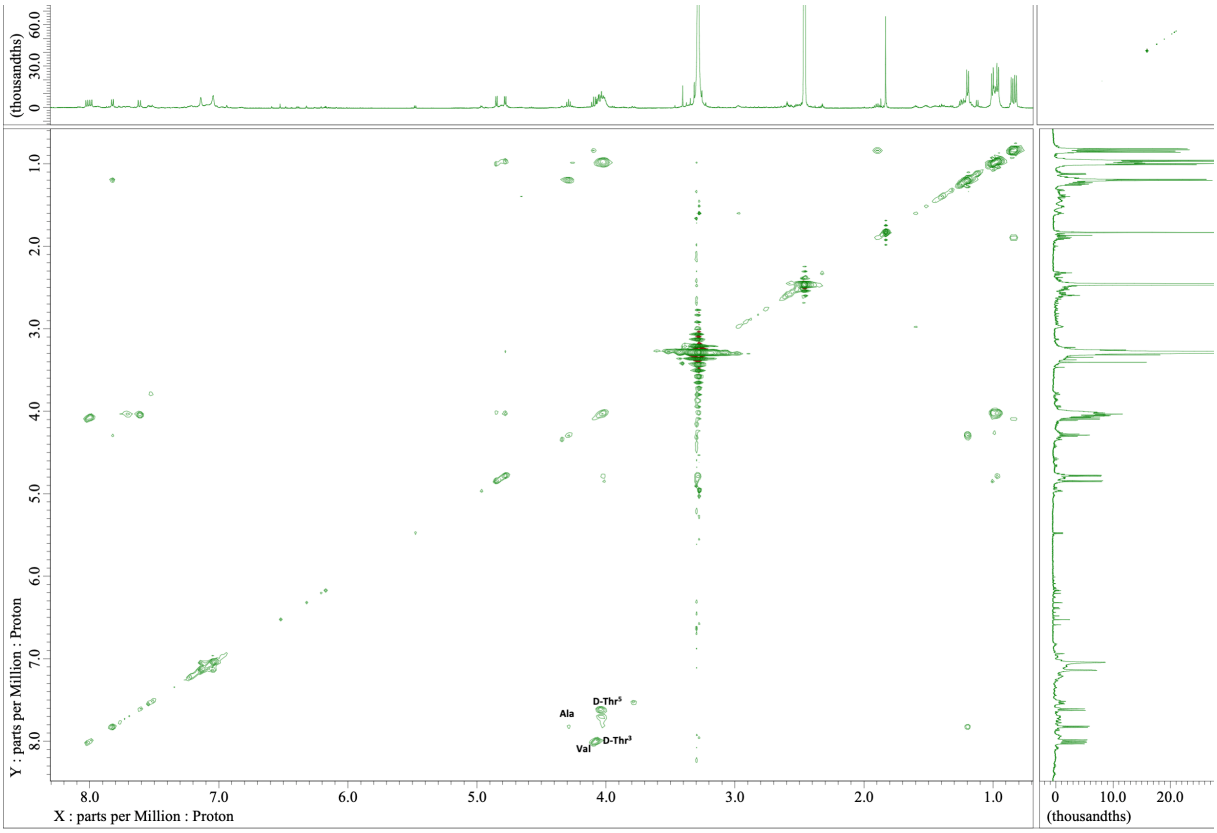

Figure 197. TOCSY spectrum of 12. Solvent : dmso-d_6; T : 23°C; Scans : 8192

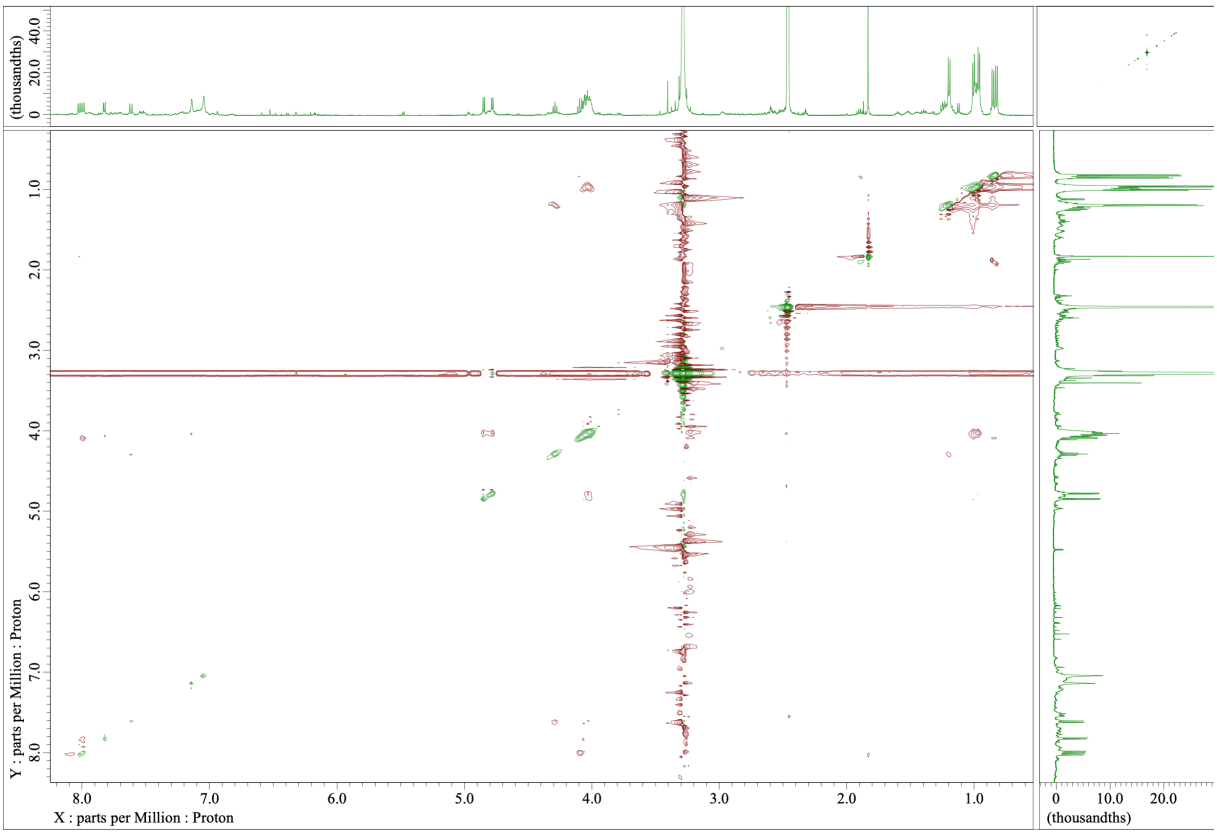

Figure 198. ROESY spectrum of 12. Solvent : dmso-d_6; T : 23°C; Scans : 8192

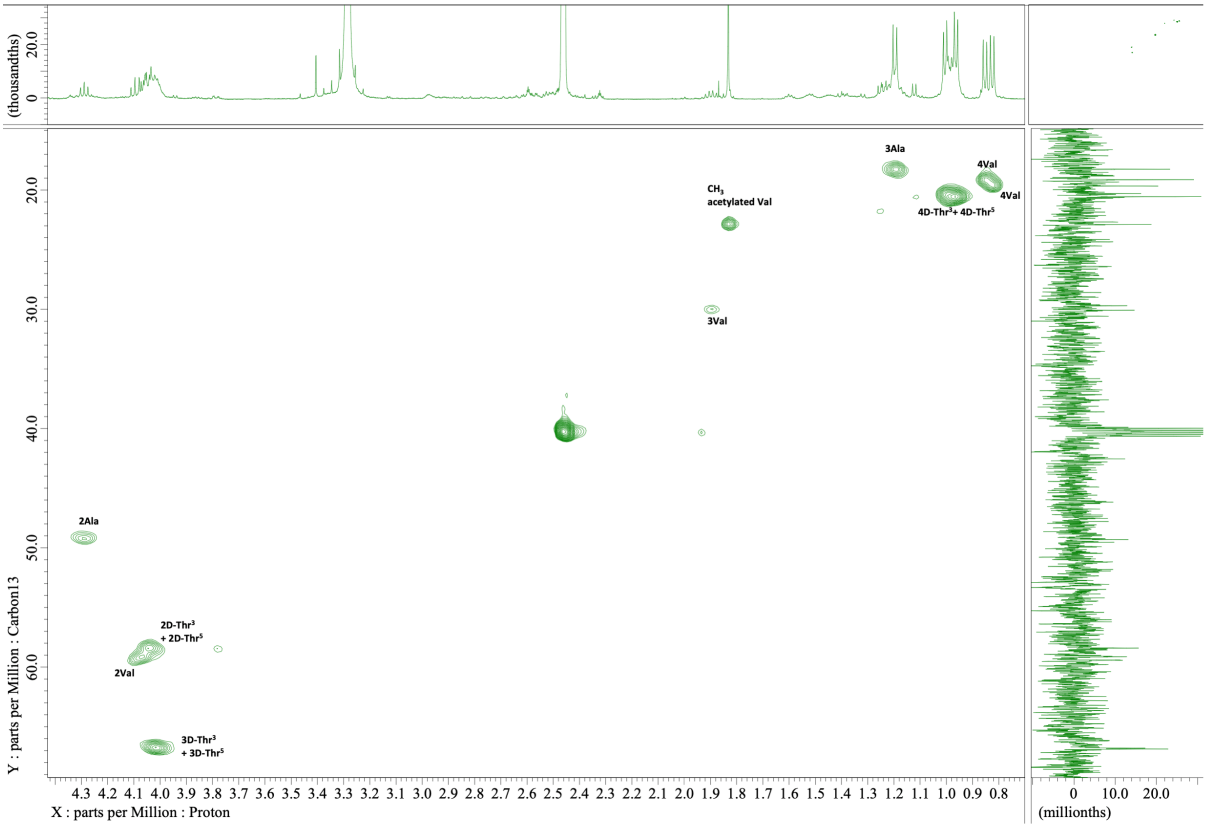

Figure 199. HSQC spectrum of 12. Solvent : dmso-d_6; T : 23°C; Scans : 8192

b) Compound 13

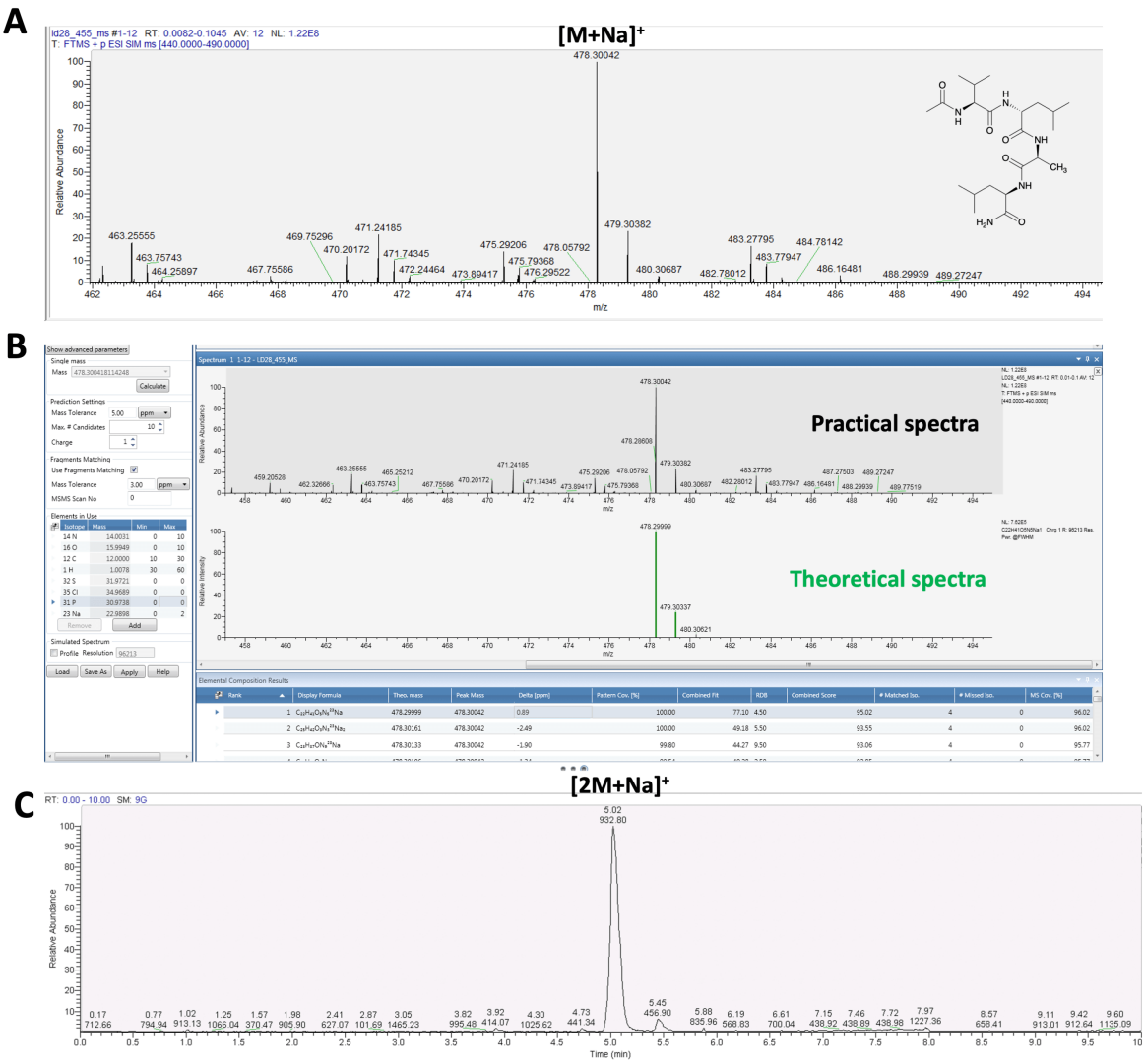

Figure 200. A) ESI-HRMS spectrum of 13. B) Comparison with the theoretical spectrum. Calculated for $C_{22}H_{41}N_5O_5Na$ $[M+Na]^+$ *m/z* 478.29999; Found $[M+Na]^+$ *m/z* 478.30044; mass error = 0.89 ppm. C) LC-MS profile of 13.

Table 26. NMR spectroscopic data of 13 in DMSO-d_6

entry	position	C, mult.	H, mult. (J in Hz)
Val[2]	1	*nd*, C	-
	2	59.5, CH	3.96
	3	30.2, CH	1.86
	3-Me	19.5, CH_3	0.79
	4	19.2, CH_3	0.83
	NH	-	7.99, d (7.73)
		nd, C acetylation	-
		22.9, CH_3	1.81
		acetylation	
D-Leu[3]	1	*nd*, C	-
	2	51.2-51.6, CH	4.15
	3	40.7-41.1, CH_2	1.44
	4	24.6-24.8, CH	1.54
	4-Me	21.4-23.7, CH_3	0.77-0.82
	5	21.4-23.7, CH_3	0.77-0.82
	NH	-	8.30, d (8.02)
Ala[4]	1	*nd*, C	-
	2	49.3, CH	4.12, t (6.59)
	3	18.2, CH_3	1.16, d (7.16)
	NH	-	7.89
D-Leu[5]	1	*nd*, C	-
	2	51.2-51.6, CH	4.14
	3	40.7-41.1, CH_2	1.44
	4	24.6-24.8, CH	1.54
	4-Me	21.4-23.7, CH_3	0.77-0.82
	5	21.4-23.7, CH_3	0.77-0.82
	NH	-	7.86, d (8.59)
	$NH_{2\ C\text{-}ter}$	-	7.23 & 6.95
nd =	Not determined		

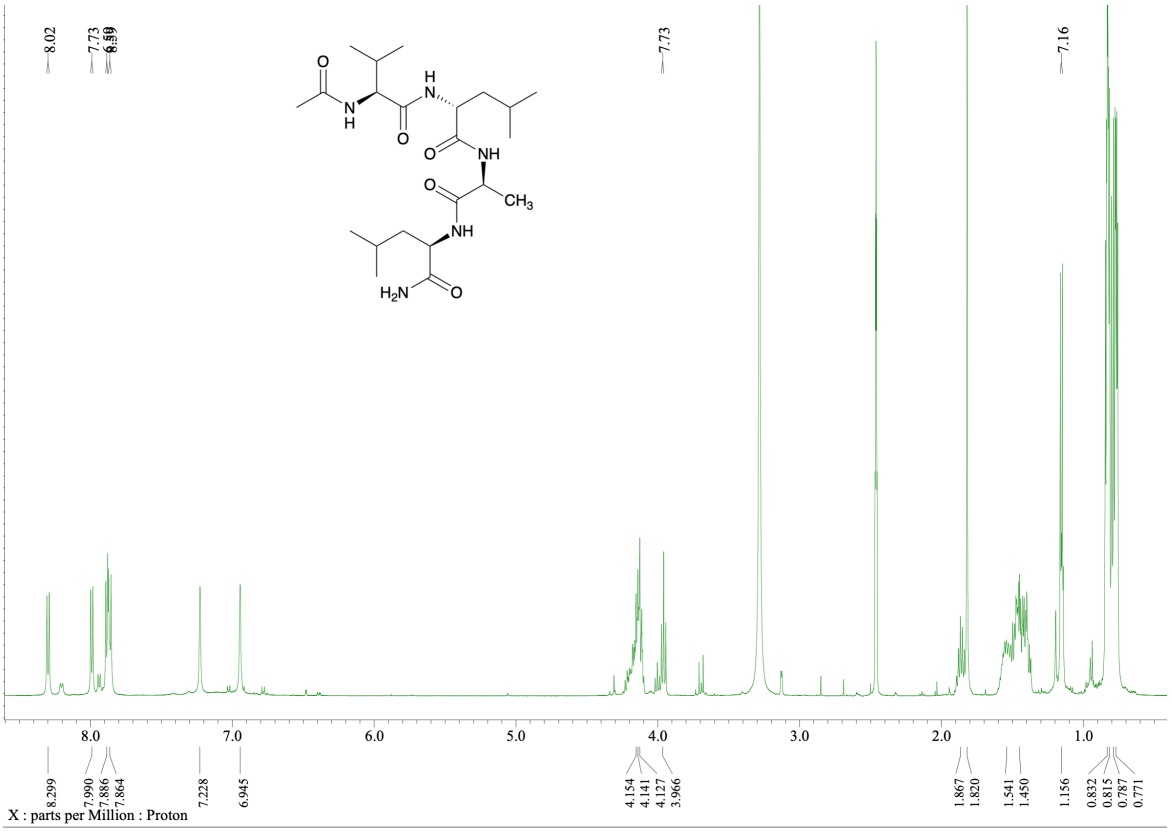

Figure 201. ^{1}H NMR spectrum of 13. Solvent : dmso-d_6; T : 23°C; Scans : 32

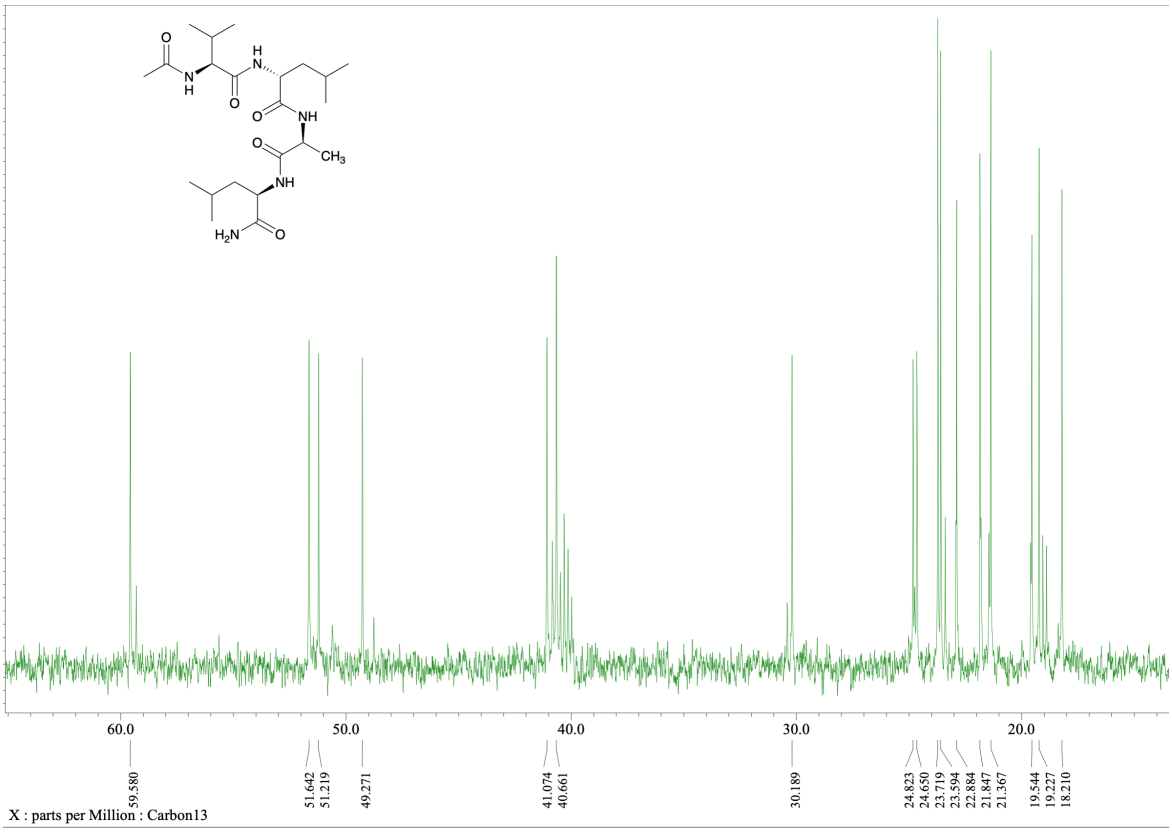

Figure 202. DEPT spectrum of 13. Solvent : dmso-d_6; T : 23°C; Scans : 10000

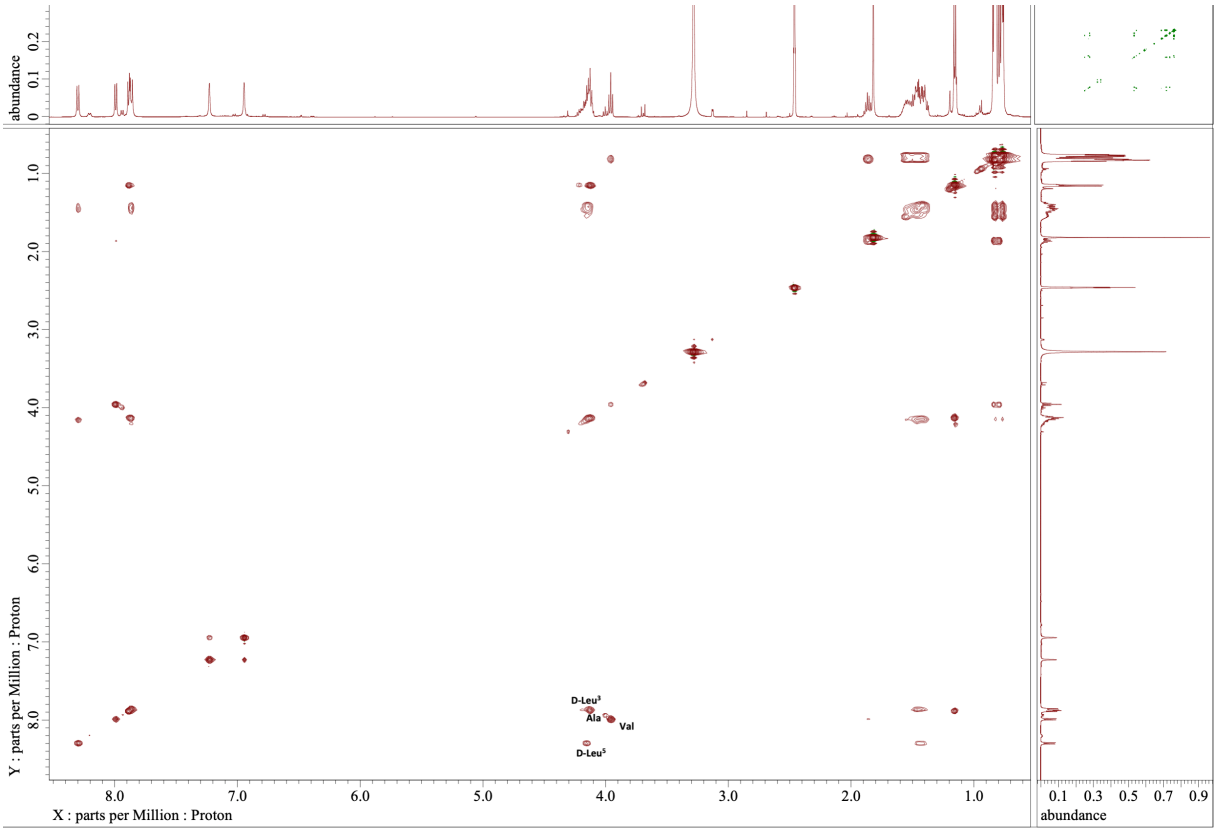

Figure 203. TOCSY spectrum of 13. Solvent : dmso-d_6; T : 23°C; Scans : 8192

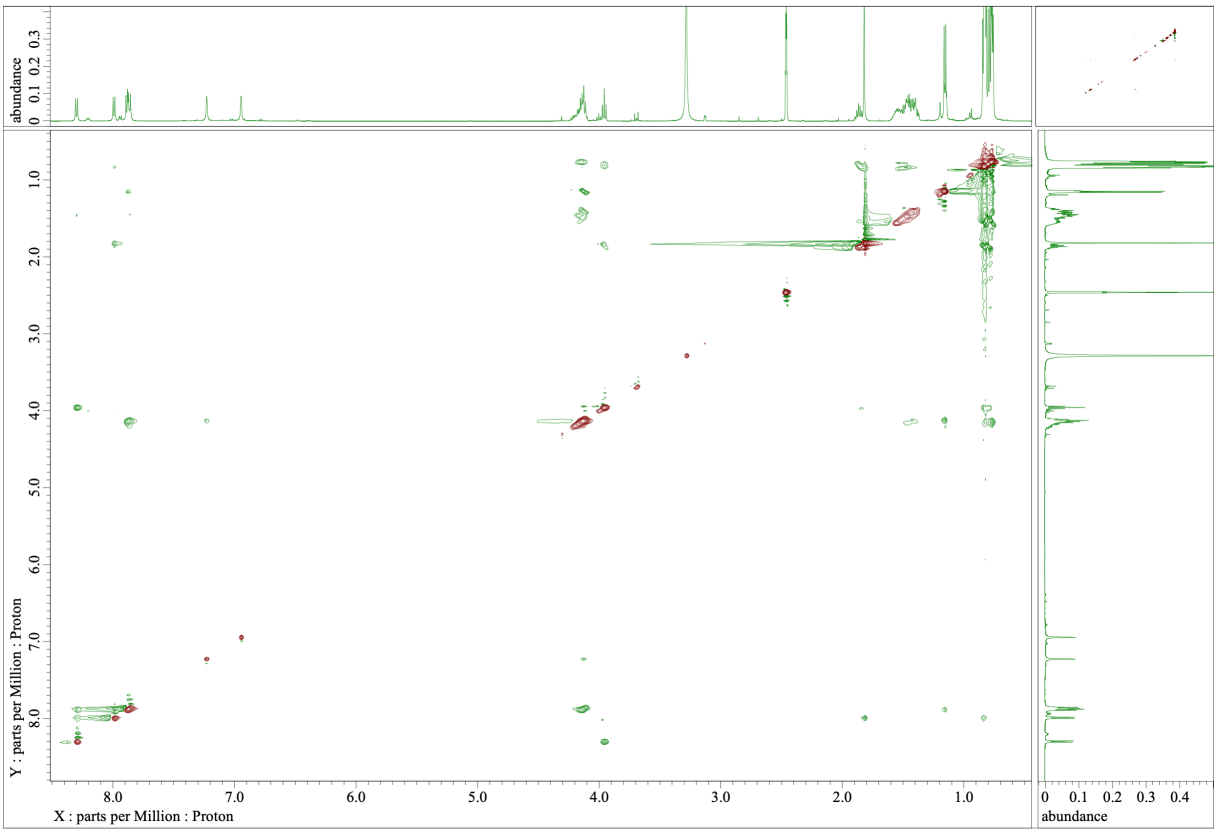

Figure 204. ROESY spectrum of 13. Solvent : dmso-d_6; T : 23°C; Scans : 8192

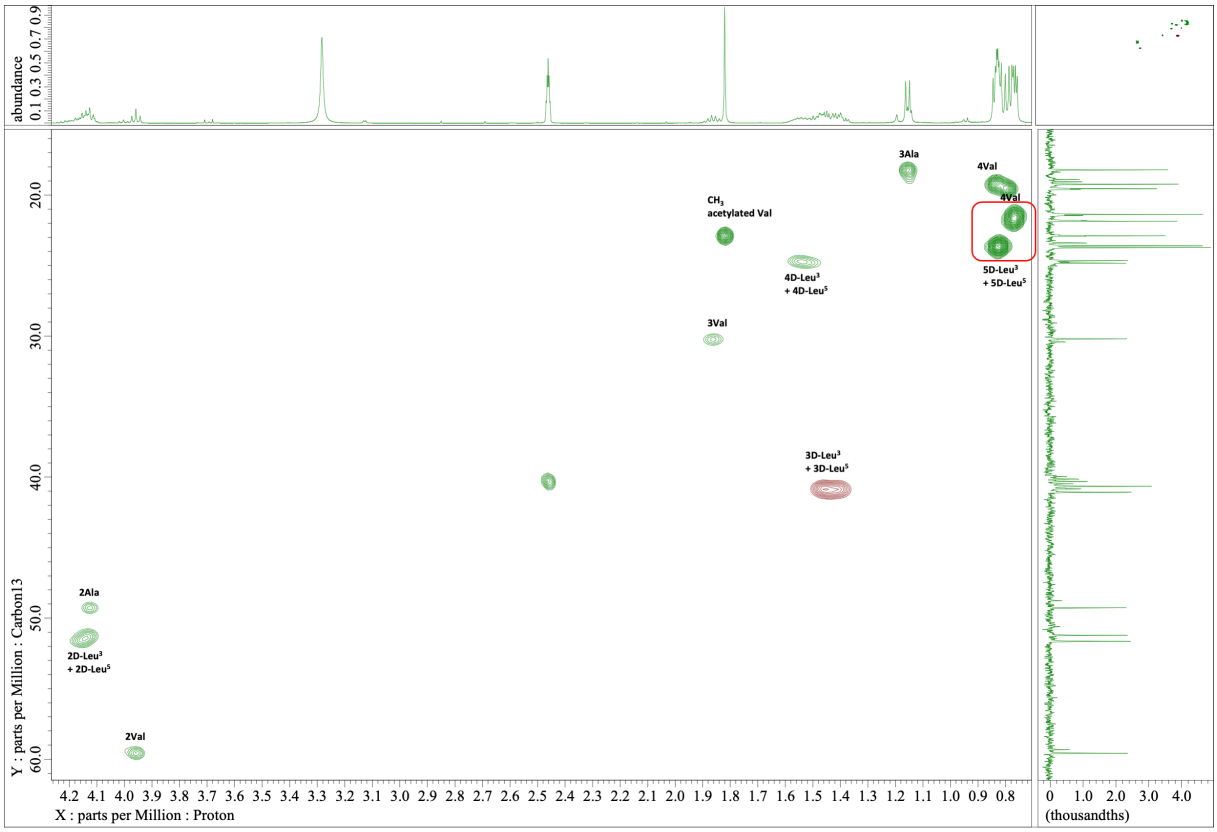

Figure 205. HSQC spectrum of 13. Solvent : dmso-d_6; T : 23°C; Scans : 8192

c) Compound 14

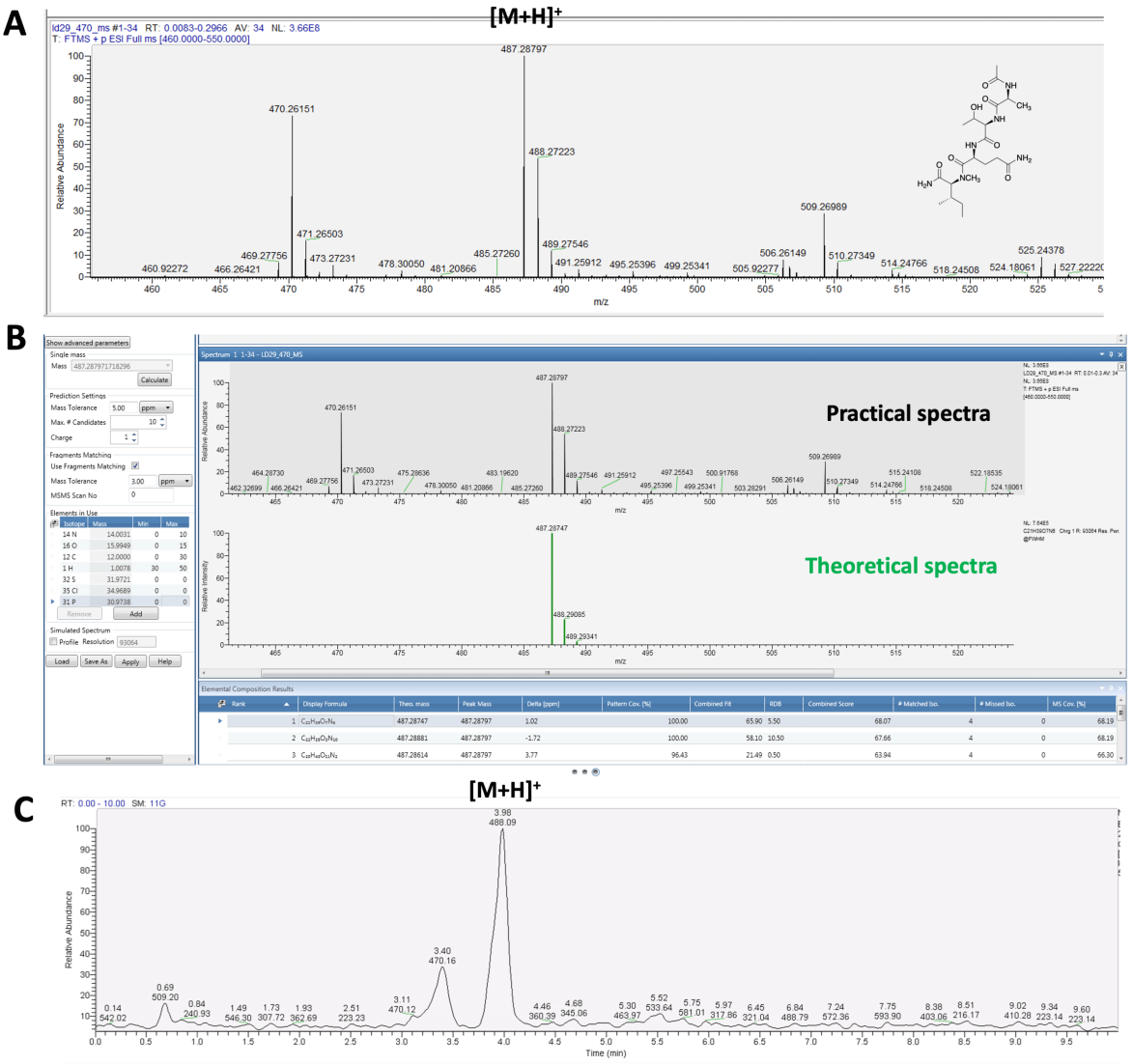

Figure 206. A) ESI-HRMS spectrum of 14. B) Comparison with the theoretical spectrum. Calculated for $C_{21}H_{39}N_6O_7$ $[M+H]^+$ *m/z* 487.28747; Found $[M+H]^+$ *m/z* 487.28797; mass error = 1.02 ppm. C) LC-MS profile of 14.

Table 27. NMR spectroscopic data of 14 in DMSO-d_6

entry	position	C, mult.	H, mult. (J in Hz)
Ala[4]	1	*nd*, C	-
	2	49.2, CH	4.28
	3	18.5, CH_3	1.16, d (7.16)
	NH	-	8.08, d (7.73)
		nd, C acetylation	-
		22.8, CH_3 acetylation	1.79
D-Thr[5]	1	*nd*, C	-
	2	58.6, CH	4.12
	3	*nd*, CH	*nd*
	4	20.4, CH_3	0.97
	NH	-	7.71, d (8.59)
Gln[6]	1	*nd*, C	-
	2	*nd*, CH	4.64
	3	*nd*, CH_2	*nd*
	4	31.3, CH_2	2.03
	5	*nd*, C	-
	NH	-	7.80, d (8.02)
	NH_2	-	7.13 & 6.72
N-MeIle[7]	1	*nd*, C	-
	2	*nd*, CH	4.56, d (10.88)
	3	*nd*, CH_2	*nd*
	3-Me	16.0, CH_3	0.79
	4	*nd*, CH_2	*nd*
	5	11.0, CH_3	0.73
	N-Me	40.3, CH_3	2.98
	NH_2 C-ter	-	7.27 & 6.93
nd =	Not determined		

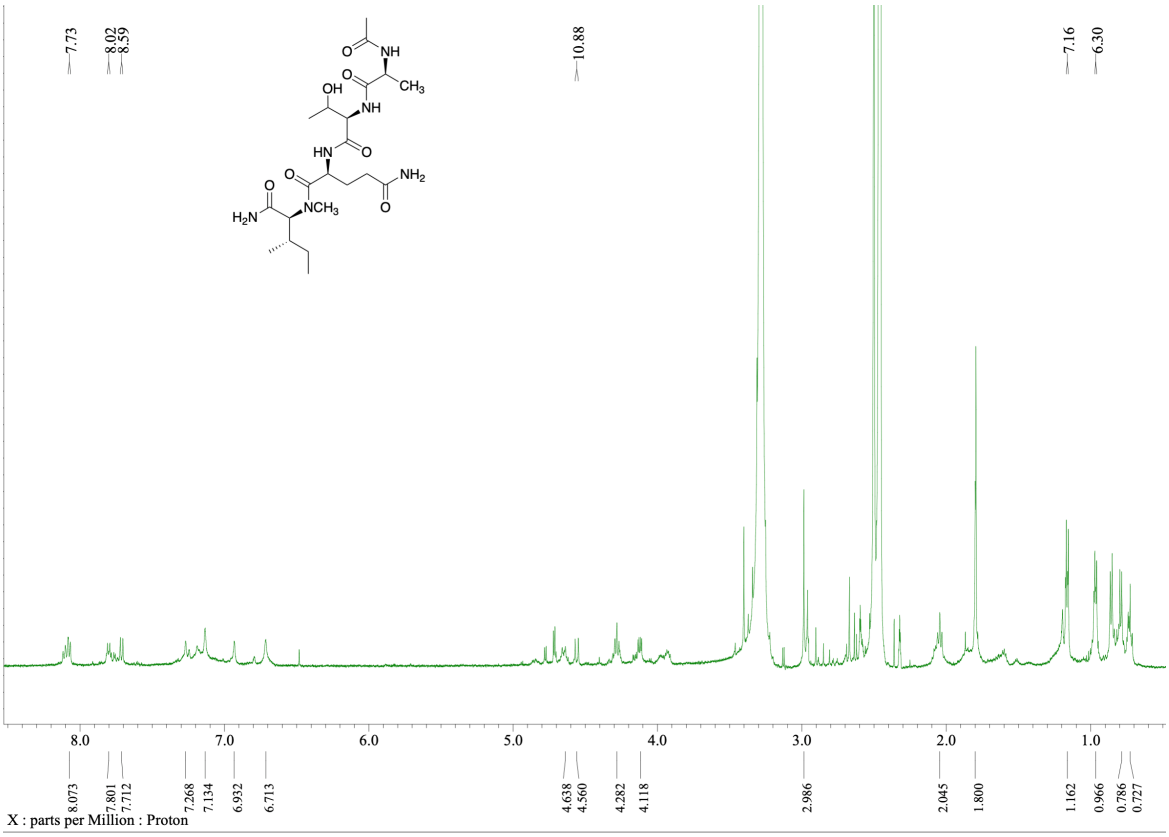

Figure 207. ^{1}H NMR spectrum of 14. Solvent : dmso-d_6; T : 23°C; Scans : 32

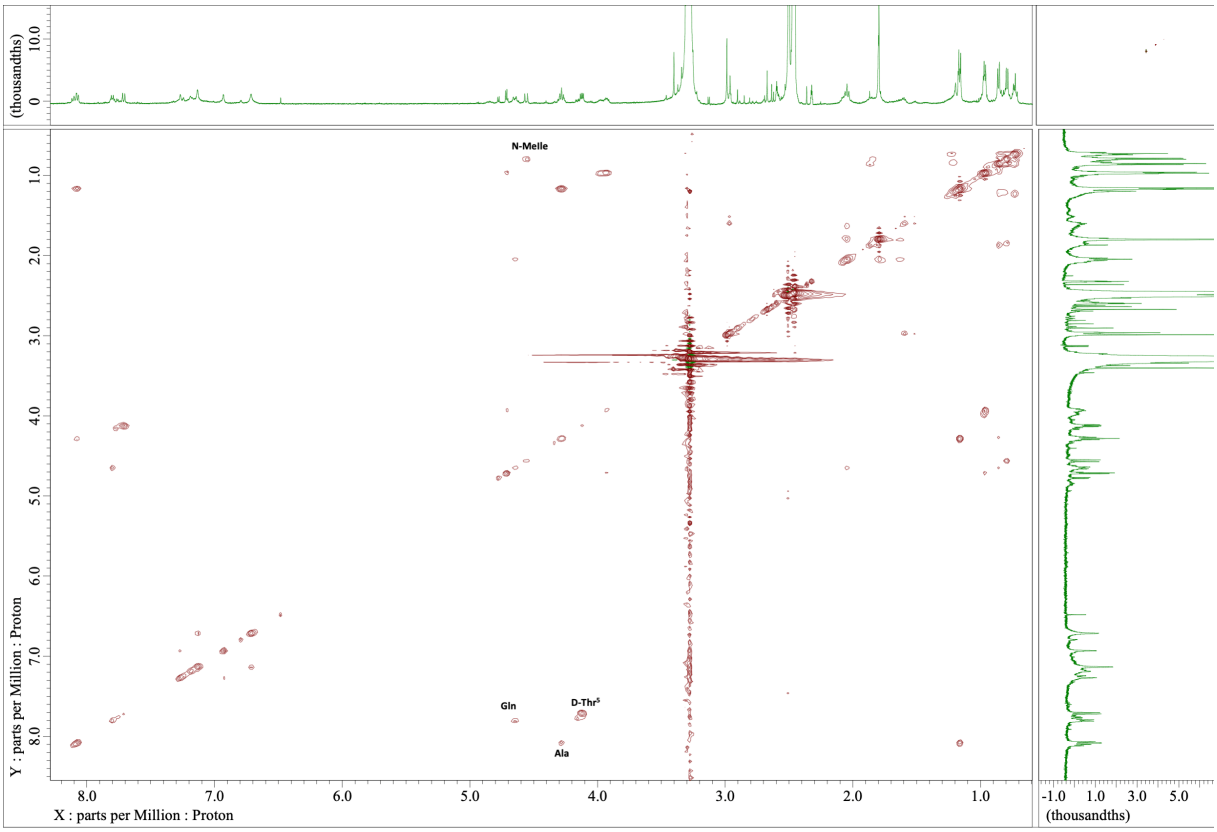

Figure 208. TOCSY spectrum of 14. Solvent : dmso-d_6; T : 23°C; Scans : 8192

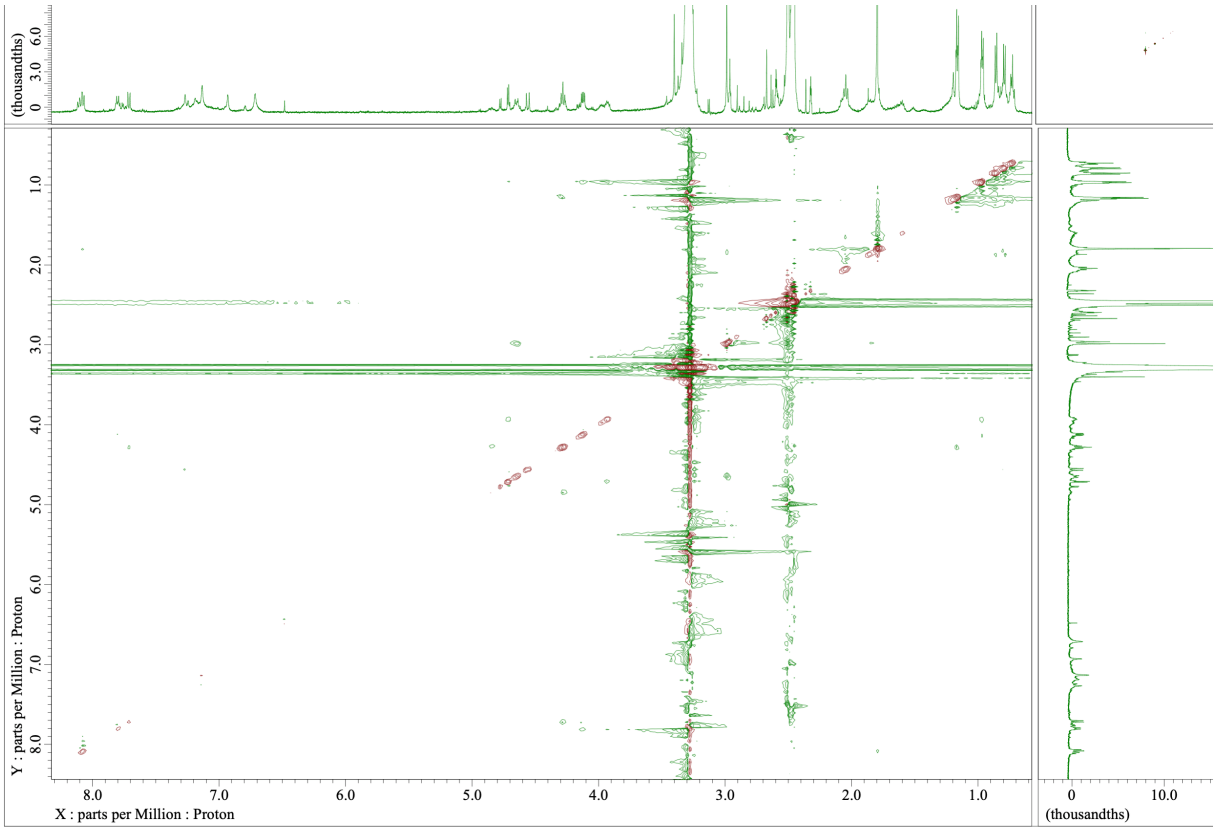

Figure 209. ROESY spectrum of 14. Solvent : dmso-d_6; T : 23°C; Scans : 8192

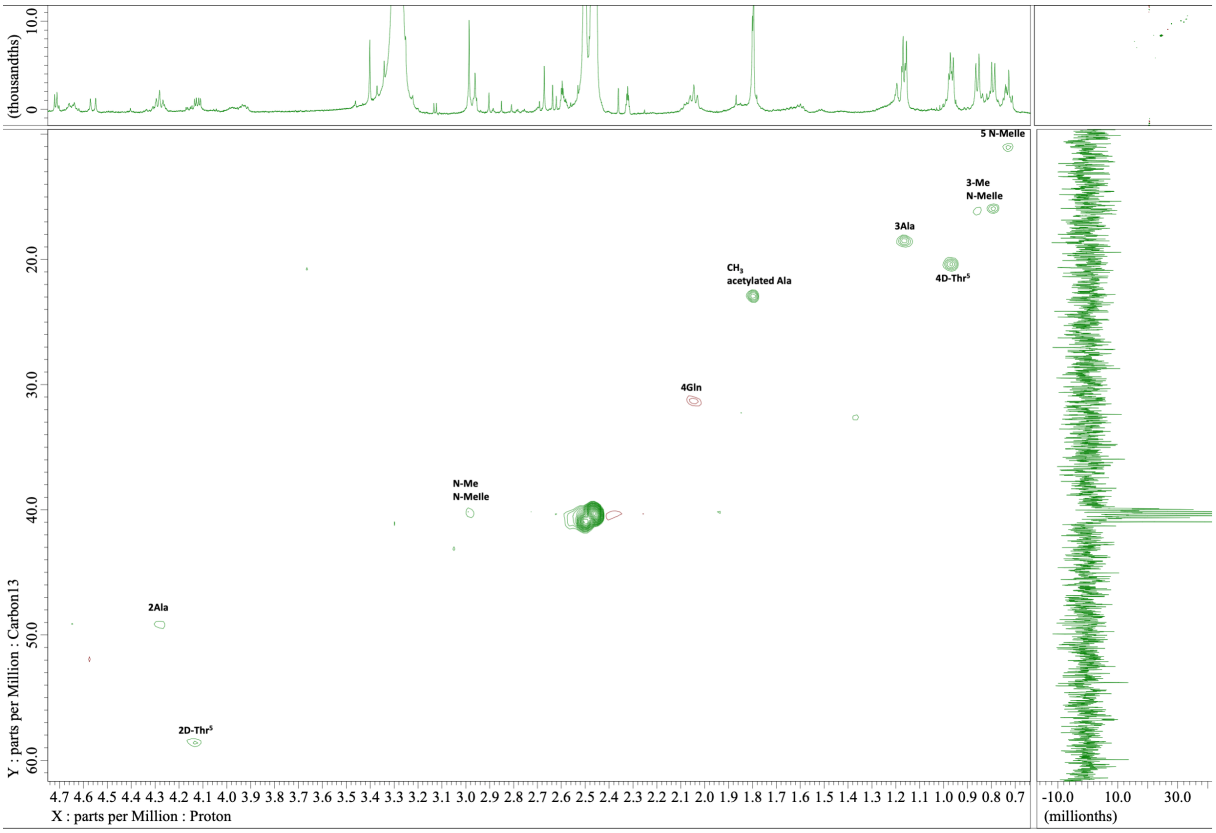

Figure 210. HSQC spectrum of 14. Solvent : dmso-d_6; T : 23°C; Scans : 8192

d) Compound 15a

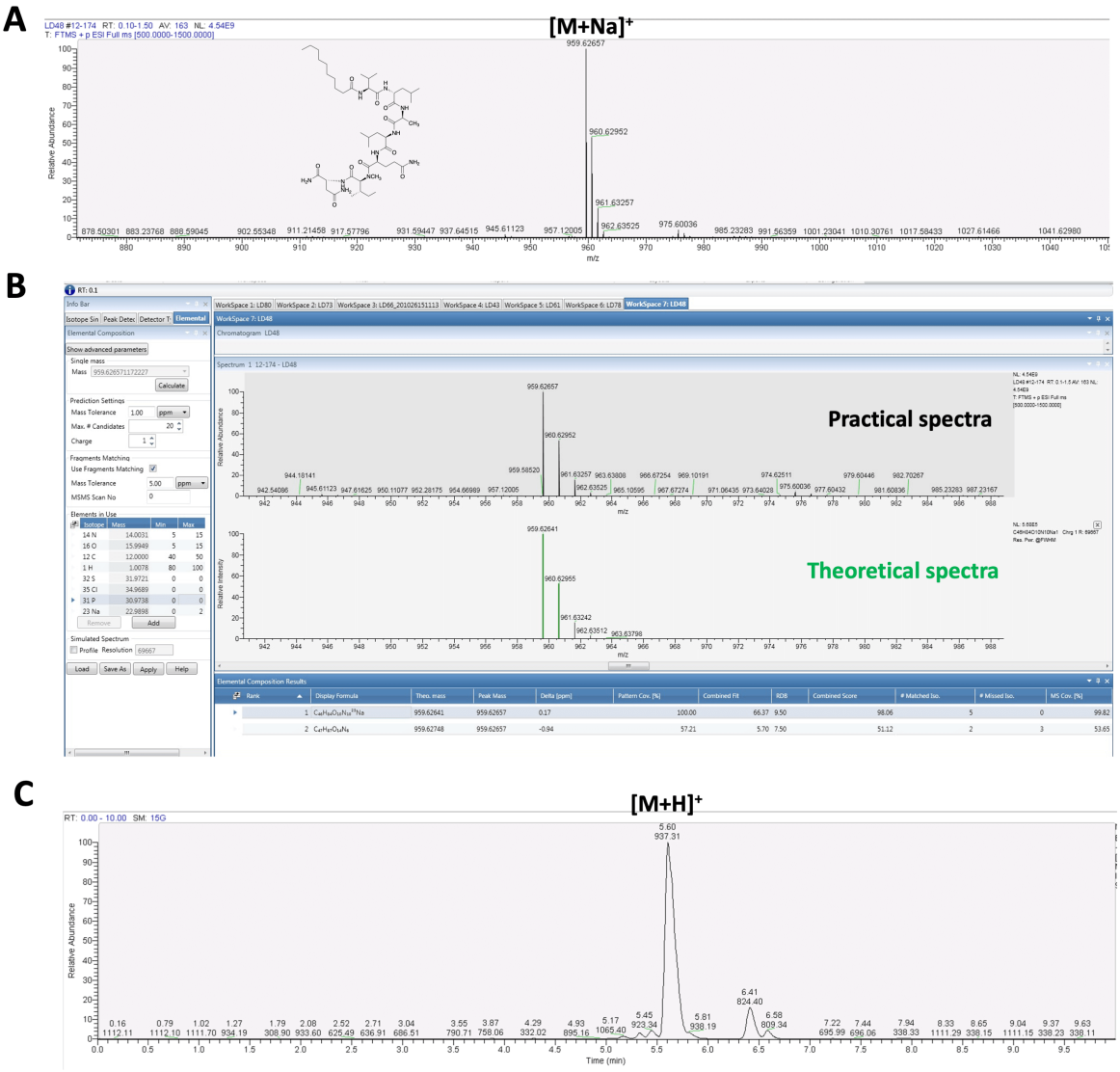

Figure 211. A) ESI-HRMS spectrum of 15a. B) Comparison with the theoretical spectrum. Calculated for $C_{48}H_{84}N_{10}O_{10}Na$ $[M+Na]^+$ *m/z* 959.62641; Found $[M+Na]^+$ *m/z* 959.62657; mass error = 0.17 ppm. C) LC-MS profile of 15a.

Table 28. NMR spectroscopic data of 15a in DMSO-d_6

entry	position	C, mult.	H, mult. (J in Hz)	entry	position	C, mult.	H, mult. (J in Hz)
decanoic acid[1]	1	*nd*, C	-	N-MeIle[7]	1	*nd*, C	-
	2	35.5, CH_2	2.13		2	60.5, CH	4.57, d (10.88)
			2.05		3	32.2, CH_2	1.86
	3	25.7, CH_2	1.43		3-Me	15.8, CH_3	0.74
	4	29.1-29.4, CH_2	1.19		4	24.8, CH_2	1.22
	5	29.1-29.4, CH_2	1.19		5	10.8, CH_3	0.71
	6	29.1-29.4, CH_2	1.19		N-Me	31.0, CH_3	2.99
	7	29.1-29.4, CH_2	1.19	D-Asn[8]	1	*nd*, C	-
	8	31.7, CH_2	1.19		2	49.9, CH	4.45
	9	22.6, CH_2	1.21		3	37.5, CH_2	2.42
	10	14.4, CH_3	0.81		4	*nd*, C	-
Val[2]	1	*nd*, C	-		NH	-	7.86, d (6.01)
	2	59.6, CH	3.97, t (7.45)		NH_2	-	7.21 & 6.81
	3	30.3, CH	1.87		NH_2 C-ter	-	7.07 & 7.01
	3-Me	19.6, CH_3	0.80				
	4	19.3, CH_3	0.84				
	NH	-	7.90, d (7.73)				
D-Leu[3]	1	*nd*, C	-				
	2	51.8, CH	4.14				
	3	40.7, CH_2	1.45				
	4	24.6, CH	1.55				
	4-Me	21.4-21.9, CH_3	0.76				
	5	21.4-21.9, CH_3	0.76				
	NH	-	8.26, d (8.02)				
Ala[4]	1	*nd*, C	-				
	2	49.4, CH	4.11, t (6.87)				
	3	18.2, CH_3	1.17				
	NH	-	7.88, d (8.02)				
D-Leu[5]	1	*nd*, C	-				
	2	51.4, CH	4.25				
	3	41.7, CH_2	1.37				
	4	24.6, CH	1.55				
	4-Me	23.5-23.7, CH_3	0.81				
	5	23.5-23.7, CH_3	0.81				
	NH	-	7.76, d (8.59)				
Gln[6]	1	*nd*, C	-				
	2	48.7, CH	4.61, t (6.87)				
	3	27.5, CH_2	1.69				
			1.83				
	4	31.0, CH_2	2.03				
	5	*nd*, C	-				
	NH	-	8.04, d (7.73)			*nd* =	Not determined
	NH_2	-	7.13 & 6.68				

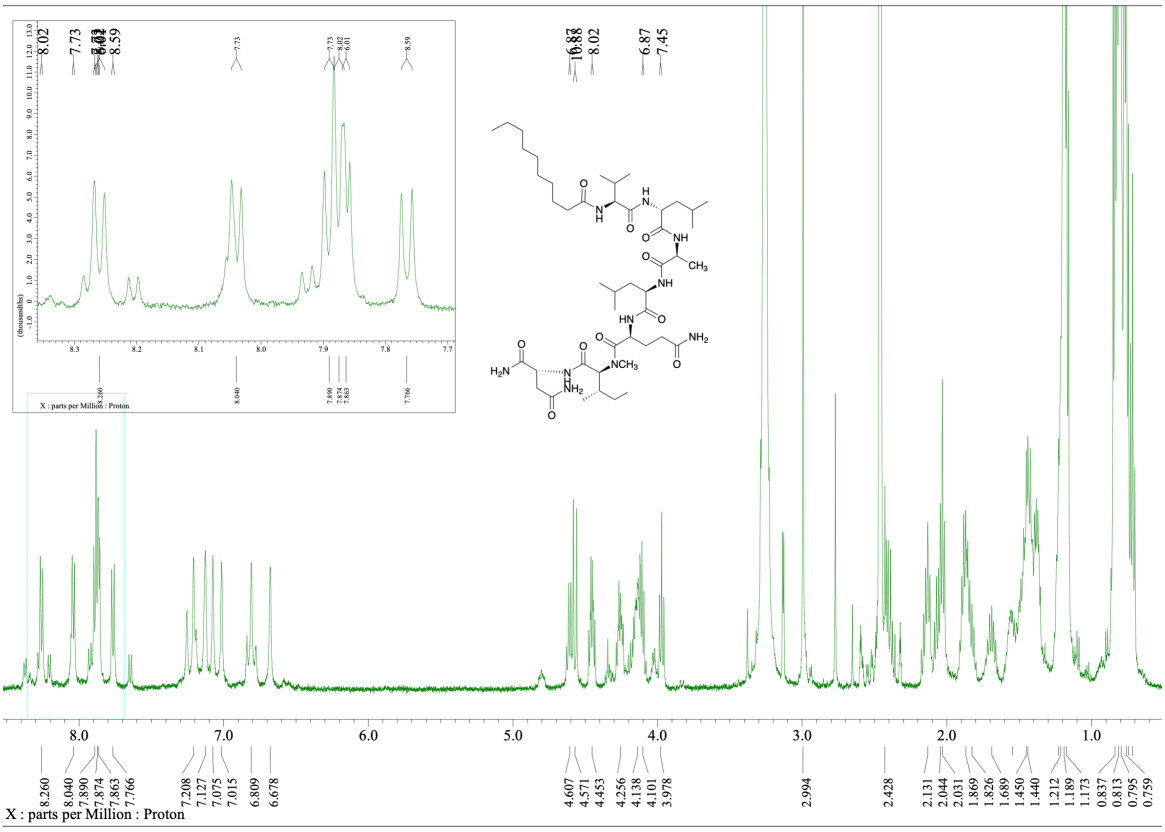

Figure 212. ^{1}H NMR spectrum of 15a. Solvent : dmso-d_6; T : 23°C; Scans : 32

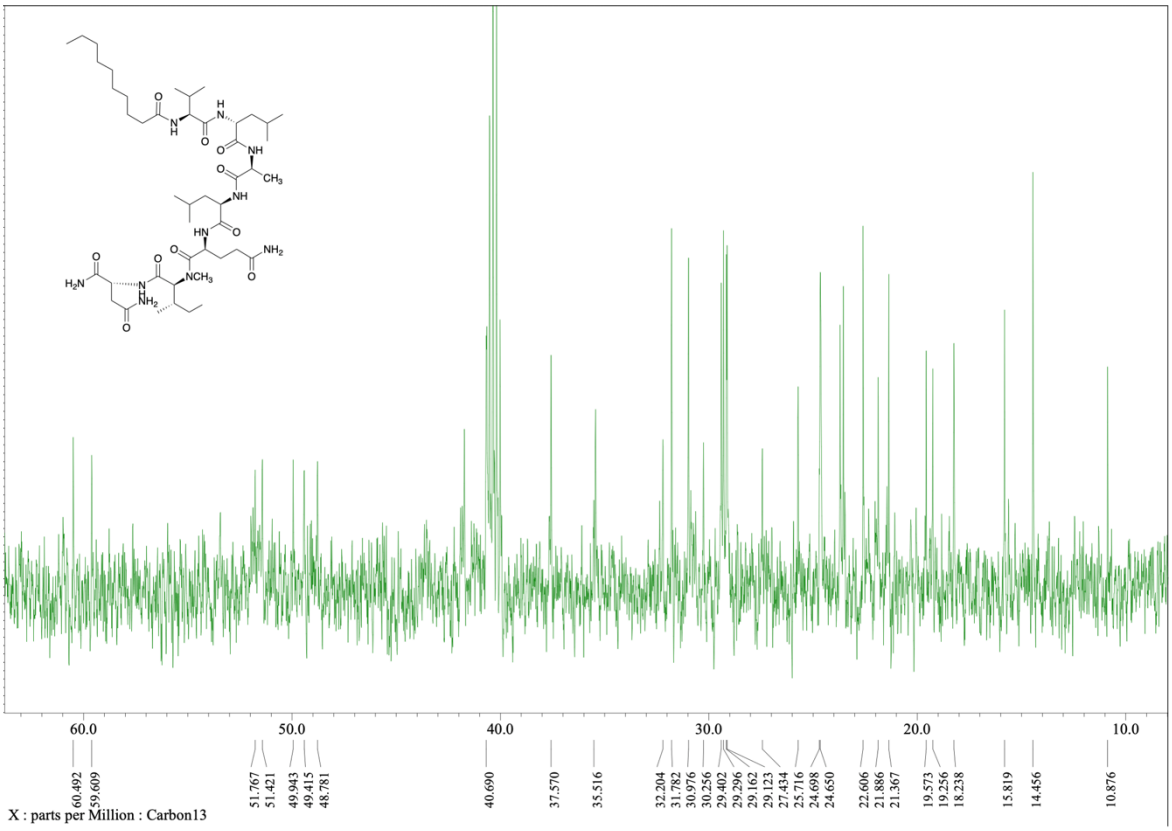

Figure 213. DEPT spectrum of 15a. Solvent : dmso-d_6; T : 23°C; Scans : 10000

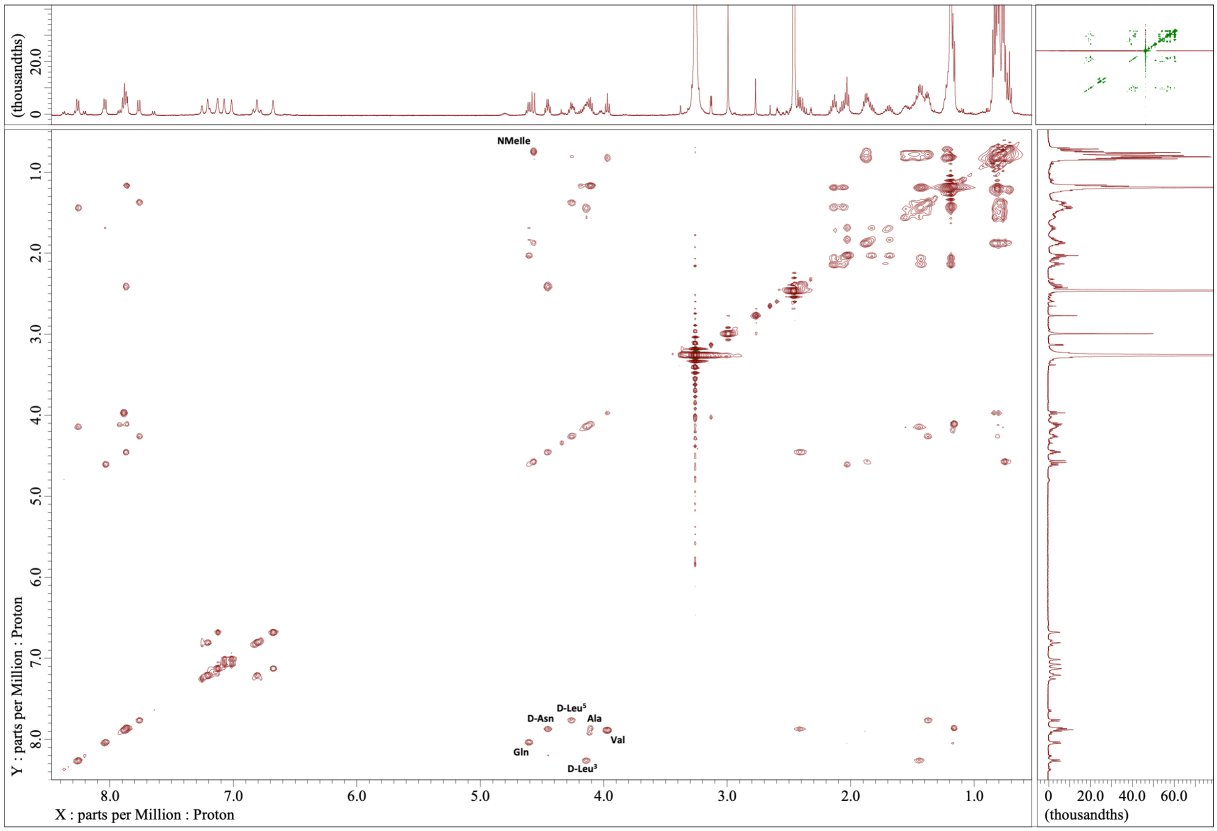

Figure 214. TOCSY spectrum of 15a. Solvent : dmso-d_6; T : 23°C; Scans : 8192

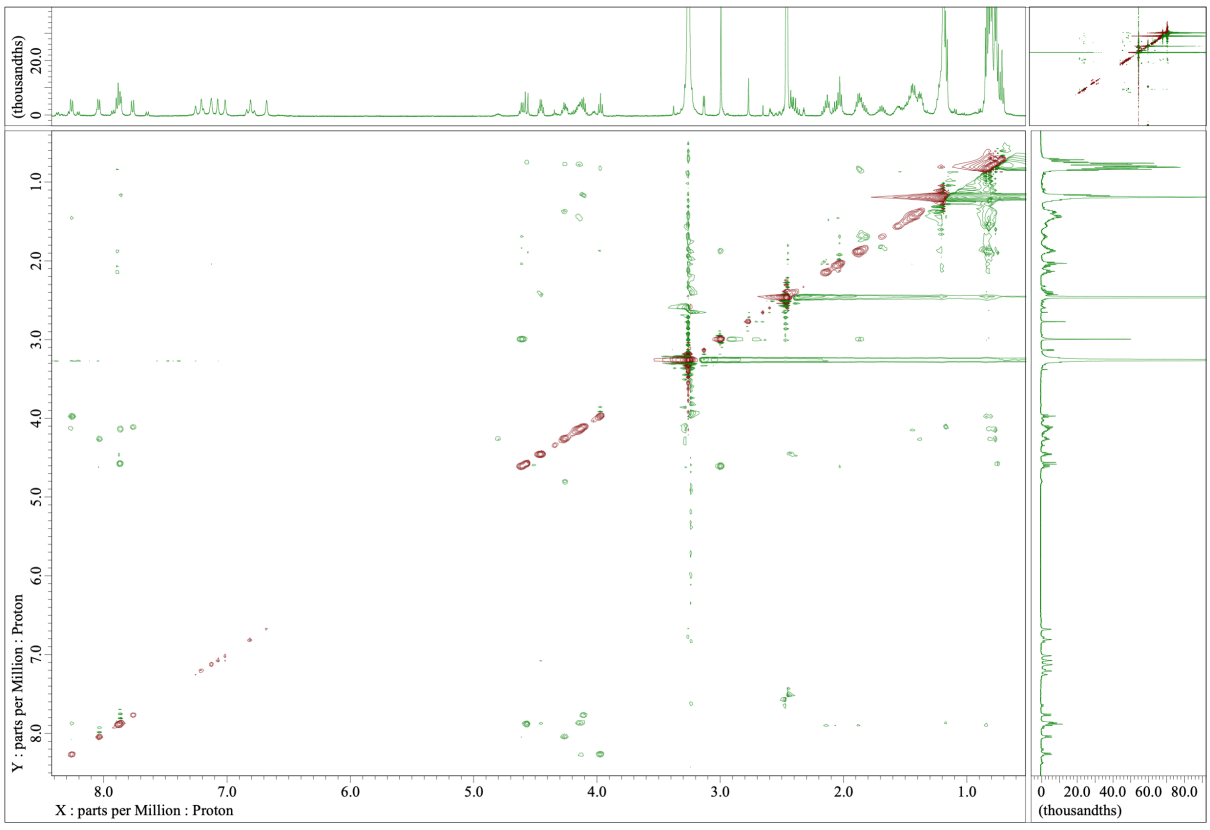

Figure 215. ROESY spectrum of 15a. Solvent : dmso-d_6; T : 23°C; Scans : 8192

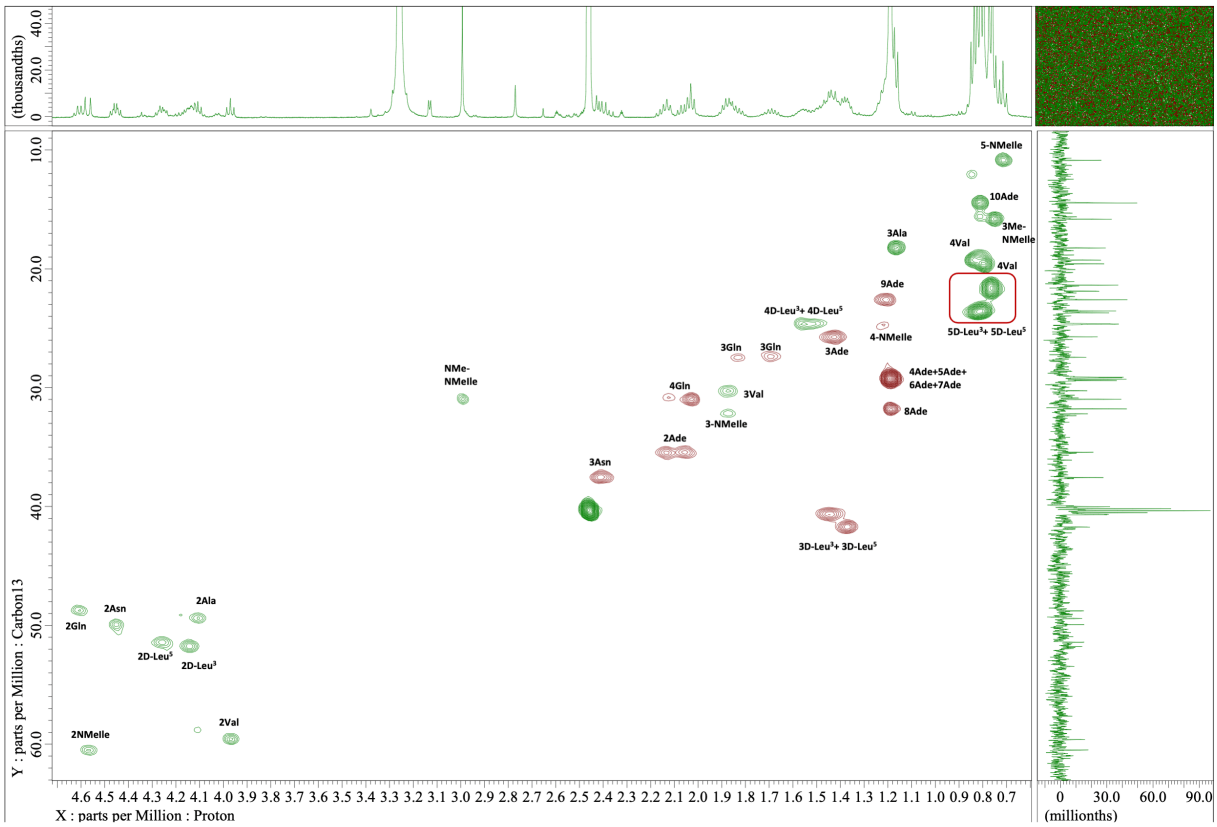

Figure 216. HSQC spectrum of 15a. Solvent : dmso-d_6; T : 23°C; Scans : 8192

e) Compound 16

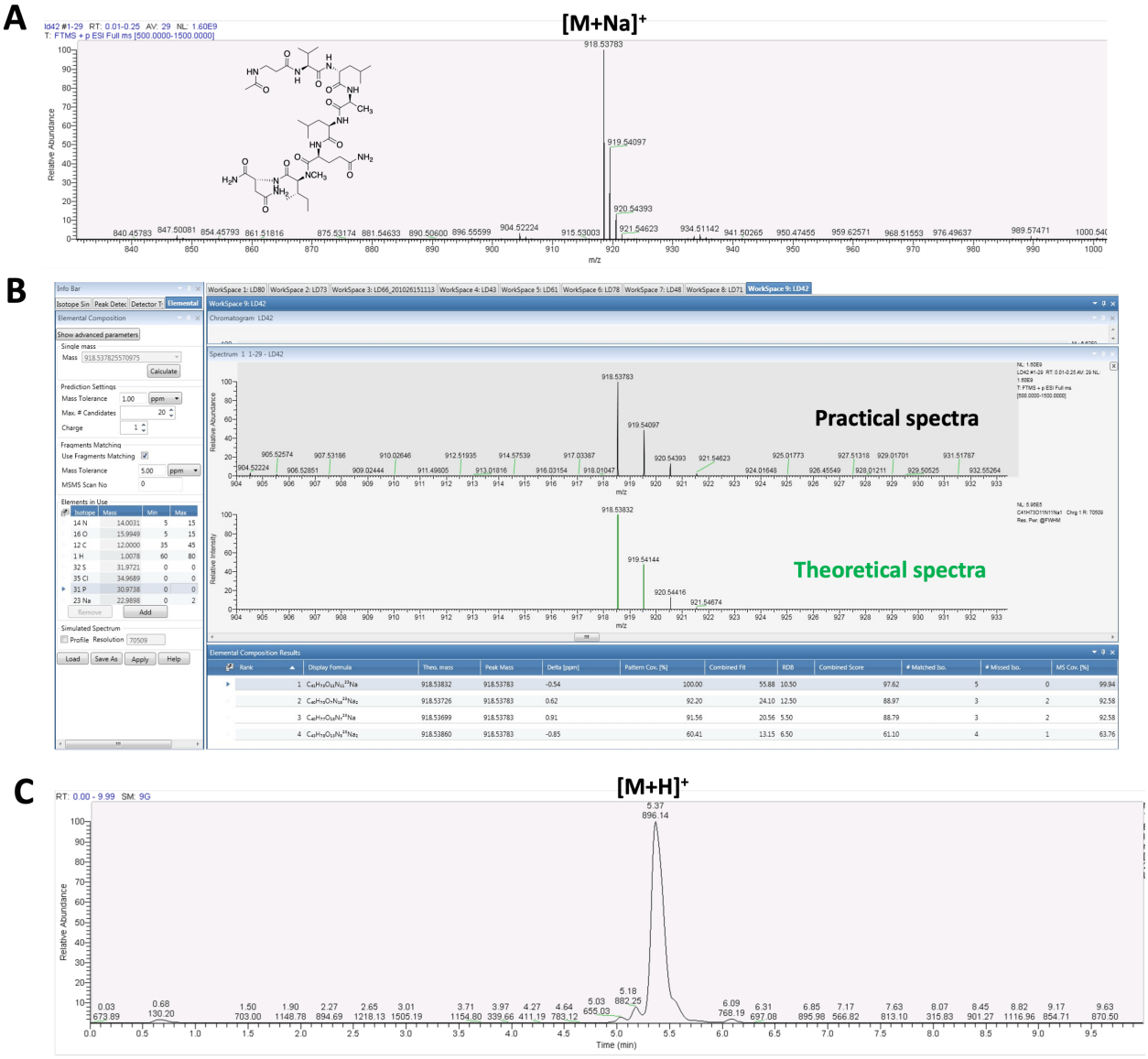

Figure 217. A) ESI-HRMS spectrum of 16. B) Comparison with the theoretical spectrum. Calculated for $C_{41}H_{73}N_{11}O_{11}Na$ $[M+Na]^+$ *m/z* 918.53832; Found $[M+Na]^+$ *m/z* 918.53783; mass error = 0.54 ppm. C) LC-MS profile of 16.

Table 29. NMR spectroscopic data of 16 in DMSO-d_6

entry	position	C, mult.	H, mult. (J in Hz)	entry	position	C, mult.	H, mult. (J in Hz)
βAla[1]	1	*nd*, C	-	N-MeIle[7]	1	*nd*, C	-
	2	35.6, CH_2	2.23		2	60.4, CH	4.58
			2.34		3	32.2, CH_2	1.84
	3	36.0, CH_2	3.15		3-Me	15.8, CH_3	0.75
	NH	-	7.77, t (6.01)		4	24.8, CH_2	1.22
		nd, C acetylation	-		5	10.9, CH_3	0.71
		23.1, CH_3 acetylation	1.73		N-Me	31.0, CH_3	3.00
Val[2]	1	*nd*, C	-	D-Asn[8]	1	*nd*, C	-
	2	59.2, CH	4.05, t (7.45)		2	50.0, CH	4.46
	3	30.5, CH	1.87		3	37.5, CH_2	2.41
	3-Me	19.6, CH_3	0.80		4	*nd*, C	-
	4	19.0, CH_3	0.82		NH	-	7.95, d (8.02)
	NH	-	7.99, d (7.45)		NH_2	-	7.22 & 6.82
D-Leu[3]	1	*nd*, C	-		NH_2 C-ter	-	7.09 & 7.03
	2	51.8, CH	4.16				
	3	40.7, CH_2	1.44				
	4	24.6, CH	1.53				
	4-Me	21.4-21.9, CH_3	0.76				
	5	21.4-21.9, CH_3	0.76				
	NH	-	8.30, d (7.73)				
Ala[4]	1	*nd*, C	-				
	2	49.2, CH	4.14				
	3	18.3, CH_3	1.16, d (7.16)				
	NH	-	7.90, d (6.87)				
D-Leu[5]	1	*nd*, C	-				
	2	51.4, CH	4.25				
	3	41.7, CH_2	1.36				
	4	24.6, CH	1.53				
	4-Me	23.5-23.7, CH_3	0.82				
	5	23.5-23.7, CH_3	0.82				
	NH	-	7.83, d (8.59)				
Gln[6]	1	*nd*, C	-				
	2	48.7, CH	4.60				
	3	27.3, CH_2	1.68				
			1.81				
	4	30.9, CH_2	2.03				
	5	*nd*, C	-				
	NH	-	8.05, d (7.73)			*nd* =	Not determined
	NH_2	-	7.16 & 6.71				

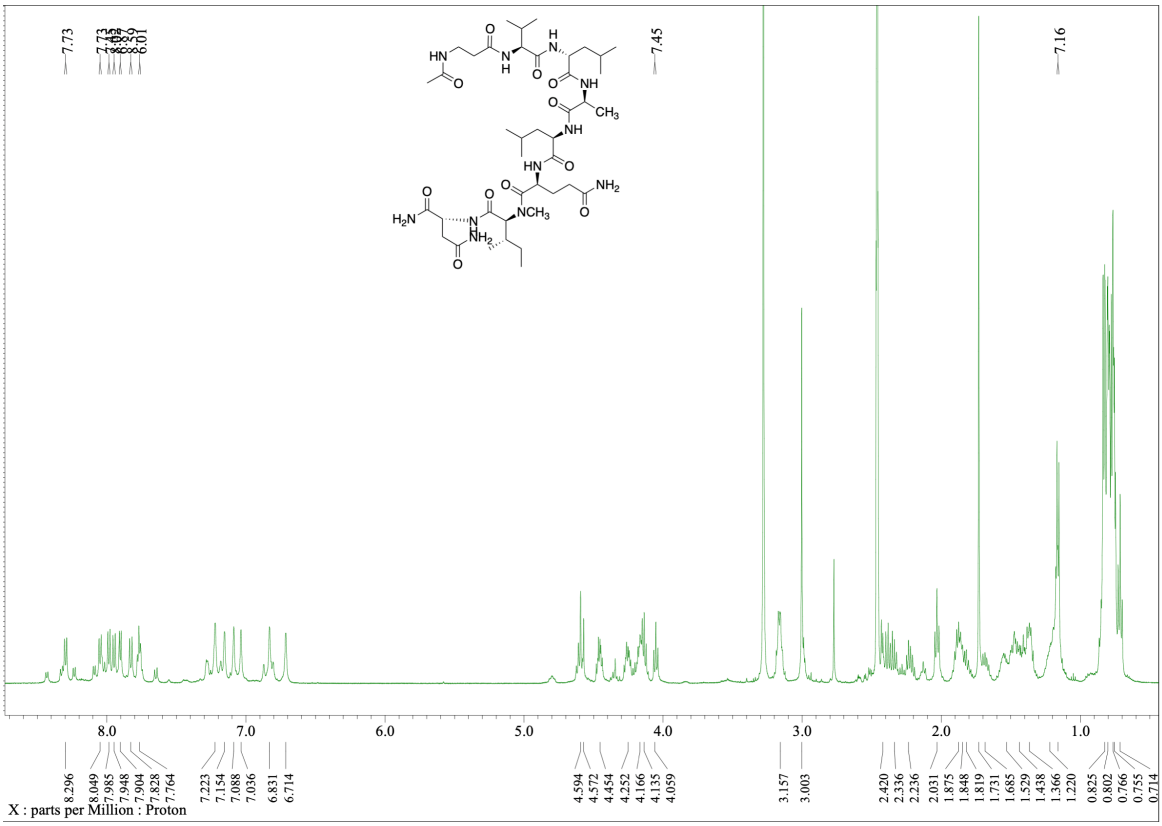

Figure 218. ^{1}H NMR spectrum of 16. Solvent : dmso-d_6; T : 23°C; Scans : 32

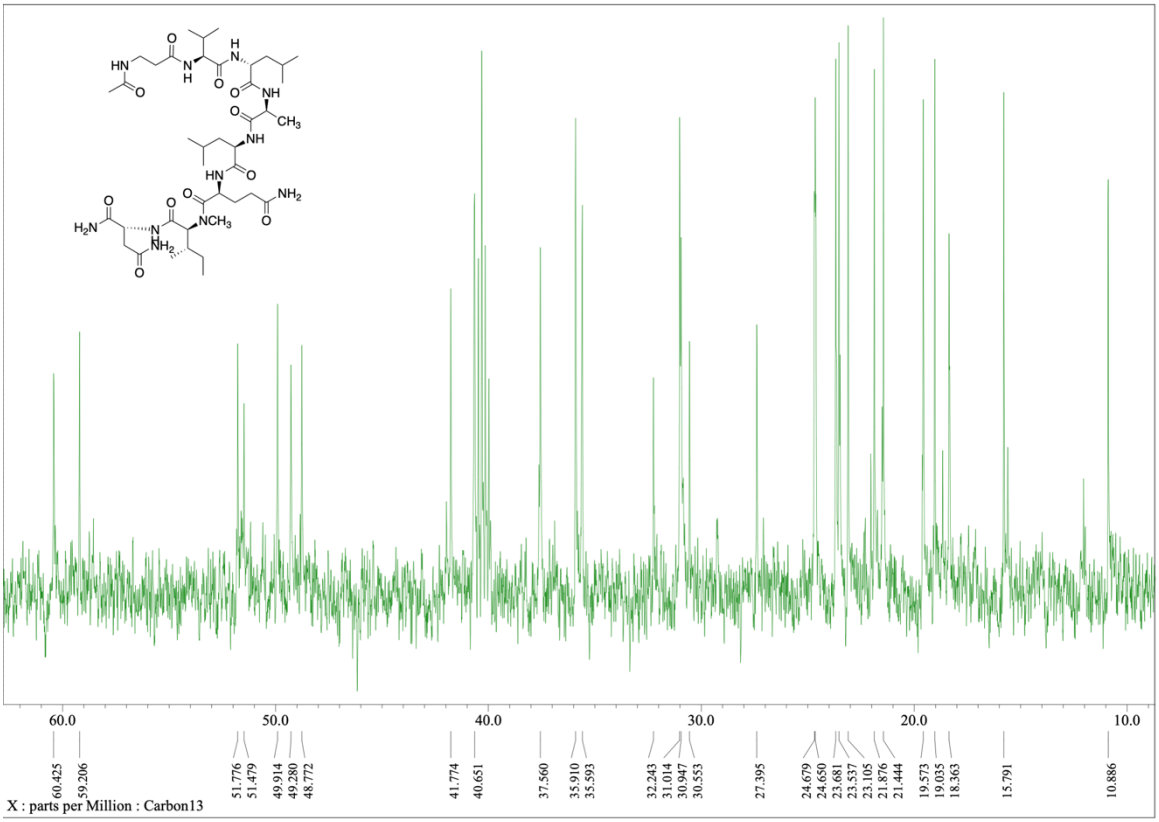

Figure 219. DEPT spectrum of 16. Solvent : dmso-d_6; T : 23°C; Scans : 10000

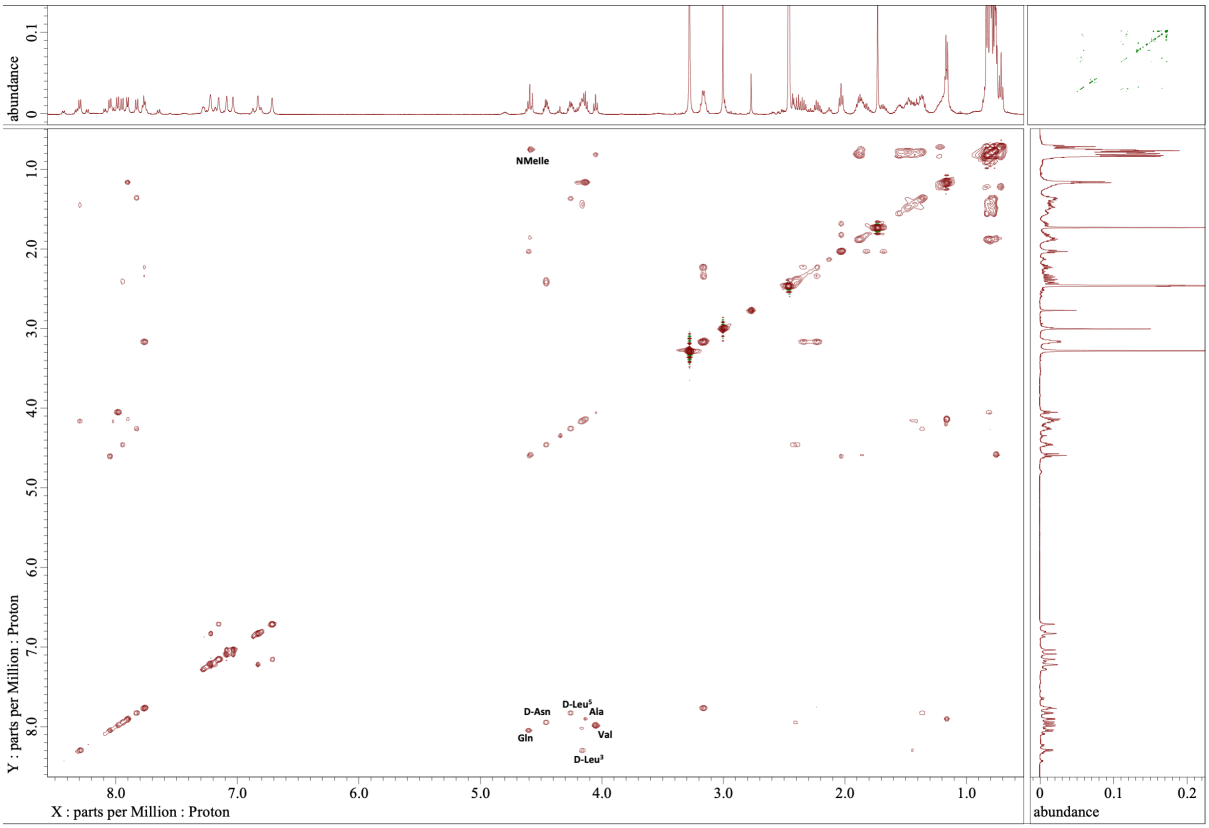

Figure 220. TOCSY spectrum of 16. Solvent : dmso-d_6; T : 23°C; Scans : 8192

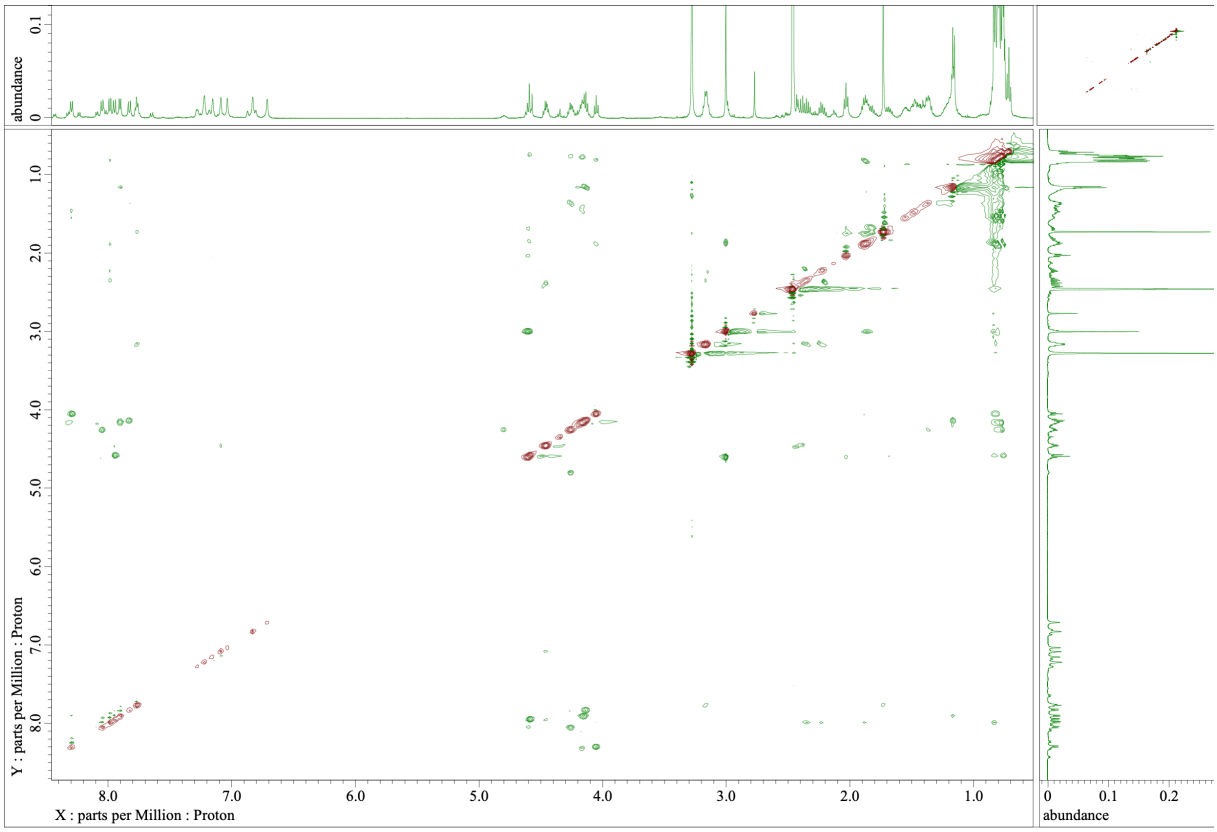

Figure 221. ROESY spectrum of 16. Solvent : dmso-d_6; T : 23°C; Scans : 8192

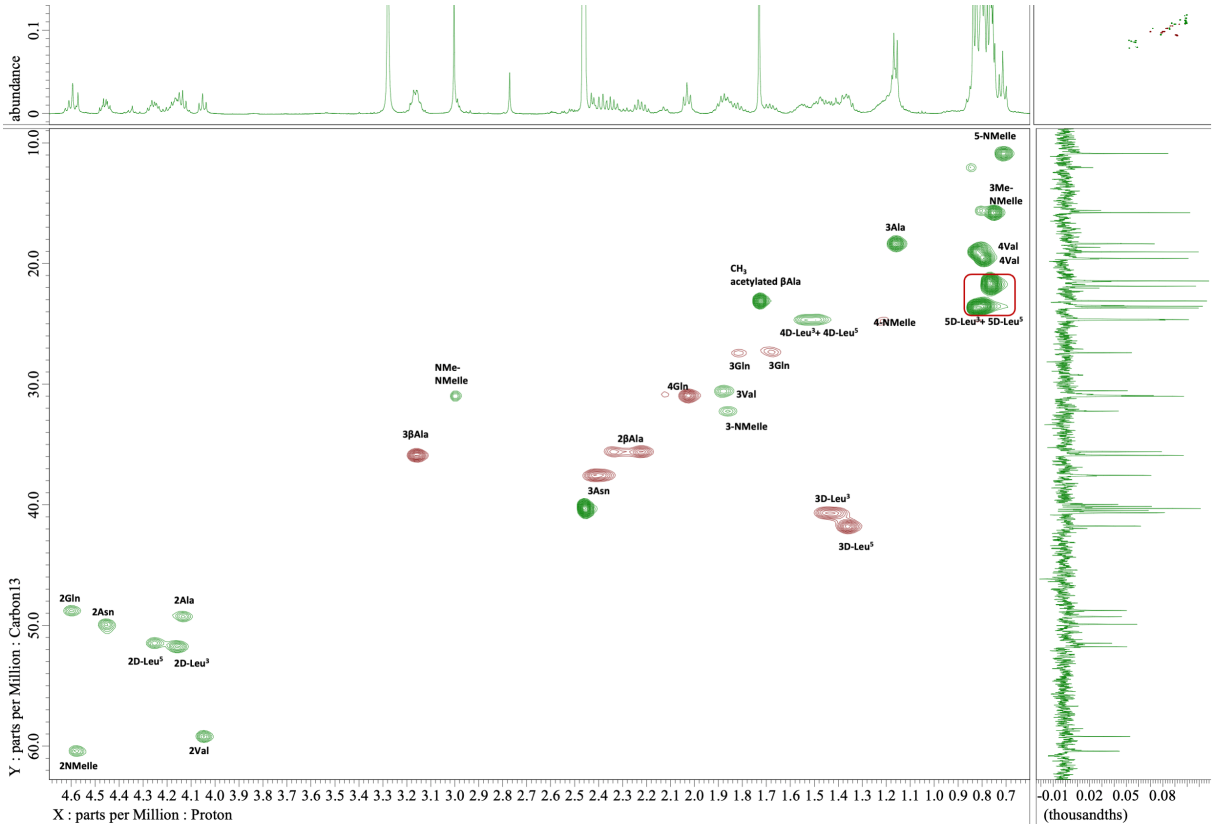

Figure 222. HSQC spectrum of 16. Solvent : dmso-d_6; T : 23°C; Scans : 8192

f) Compound 17a

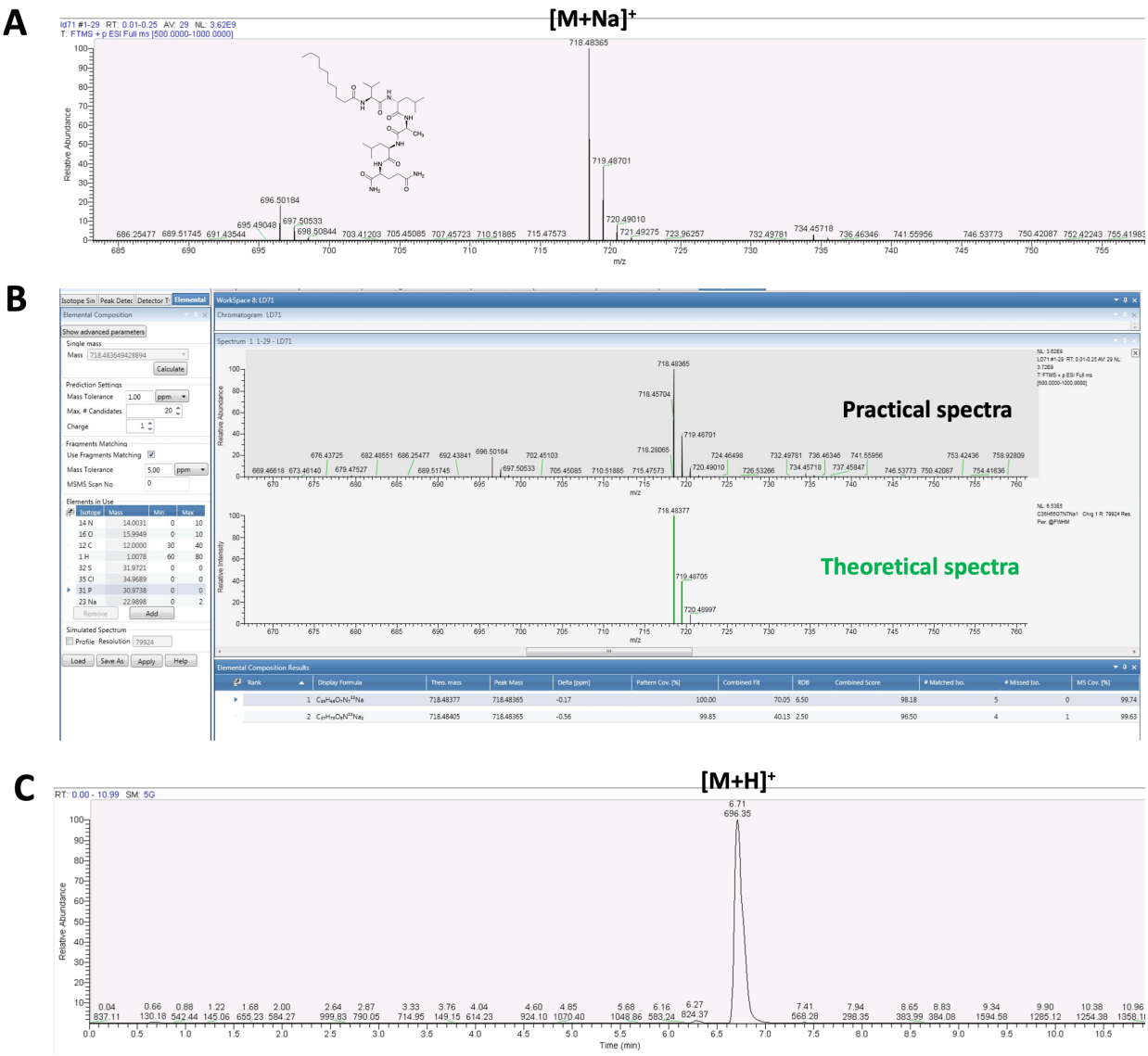

Figure 223. A) ESI-HRMS spectrum of 17a. B) Comparison with the theoretical spectrum. Calculated for $C_{35}H_{65}N_7O_7Na$ $[M+Na]^+$ *m/z* 718.48377; Found $[M+Na]^+$ *m/z* 718.48365; mass error = 0.17 ppm. C) LC-MS profile of 17a.

Table 30. NMR spectroscopic data of 17a in DMSO-d_6

entry	position	C, mult.	H, mult. (J in Hz)
Decanoic acid[1]	1	*nd*, C	-
	2	35.4, CH_2	2.06
			2.13
	3	25.8, CH_2	1.43
	4	29.1-29.4, CH_2	1.19
	5	29.1-29.4, CH_2	1.19
	6	29.1-29.4, CH_2	1.19
	7	29.1-29.4, CH_2	1.19
	8	31.8, CH_2	1.19
	9	22.6, CH_2	1.21
	10	14.5, CH_3	0.81
Val[2]	1	*nd*, C	-
	2	59.3, CH	4.01, t (7.73)
	3	30.3, CH	1.87
	3-Me	19.6, CH_3	0.80
	4	19.1, CH_3	0.82
	NH	-	7.92, d (7.73)
D-Leu[3]	1	*nd*, C	-
	2	51.8, CH	4.14, t (6.87)
	3	41.0, CH_2	1.43
	4	24.7, CH	1.55
	4-Me	21.4-23.7, CH_3	0.77-0.82
	5	21.4-23.7, CH_3	0.77-0.82
	NH	-	8.27, d (7.73)
Ala[4]	1	*nd*, C	-
	2	49.2, CH	4.12
	3	18.3, CH_3	1.17, d (7.16)
	NH	-	7.96, d (6.59)
D-Leu[5]	1	*nd*, C	-
	2	51.9, CH	4.22, t (7.45)
	3	41.0, CH_2	1.42
	4	24.7, CH	1.50
	4-Me	21.4-23.7, CH_3	0.77-0.82
	5	21.4-23.7, CH_3	0.77-0.82
	NH	-	7.88, d (8.31)
Gln[6]	1	*nd*, C	-
	2	52.7, CH	4.11
	3	28.2, CH_2	1.68
			1.87
	4	32.0, CH_2	2.02
	5	*nd*, C	-
	NH	-	8.00, d (8.31)
	NH_2	-	7.21 & 6.70
	NH_2 C-ter	-	7.23 & 7.02

nd = not determined

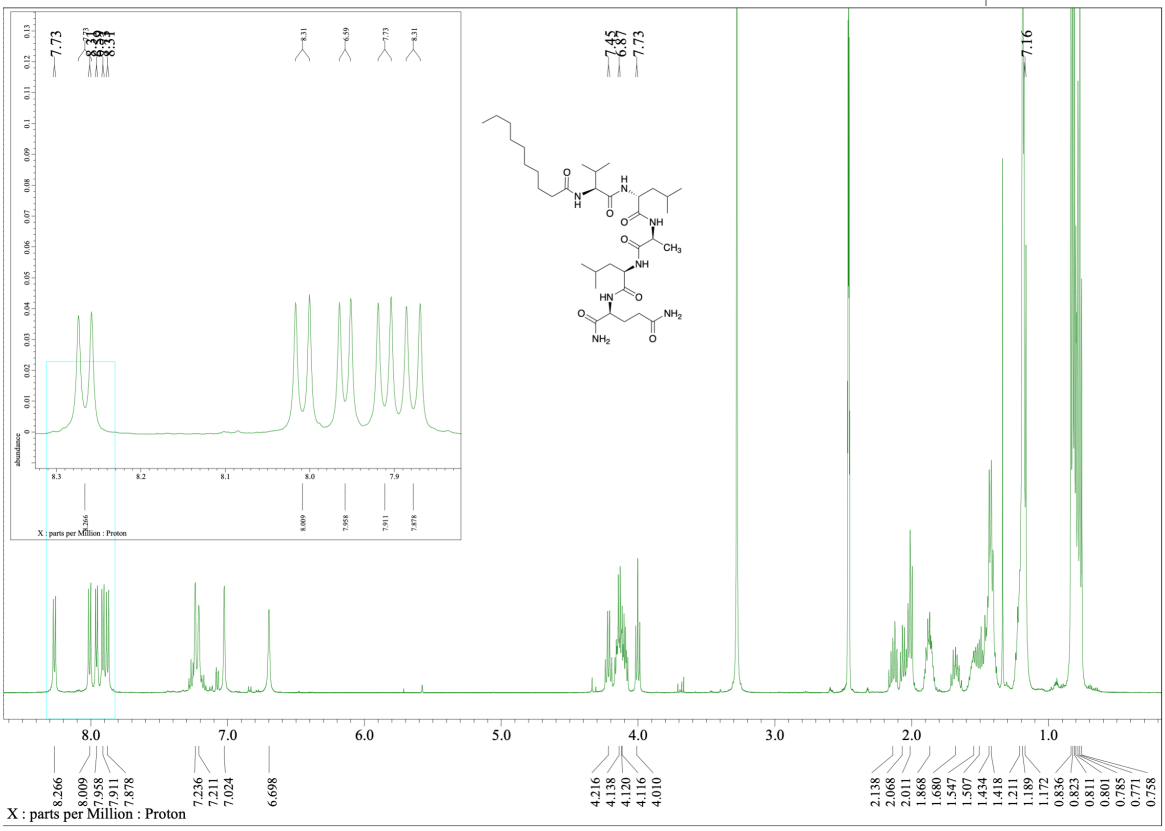

Figure 224. ^{1}H NMR spectrum of 17a. Solvent : dmso-d_6; T : 23°C; Scans : 32

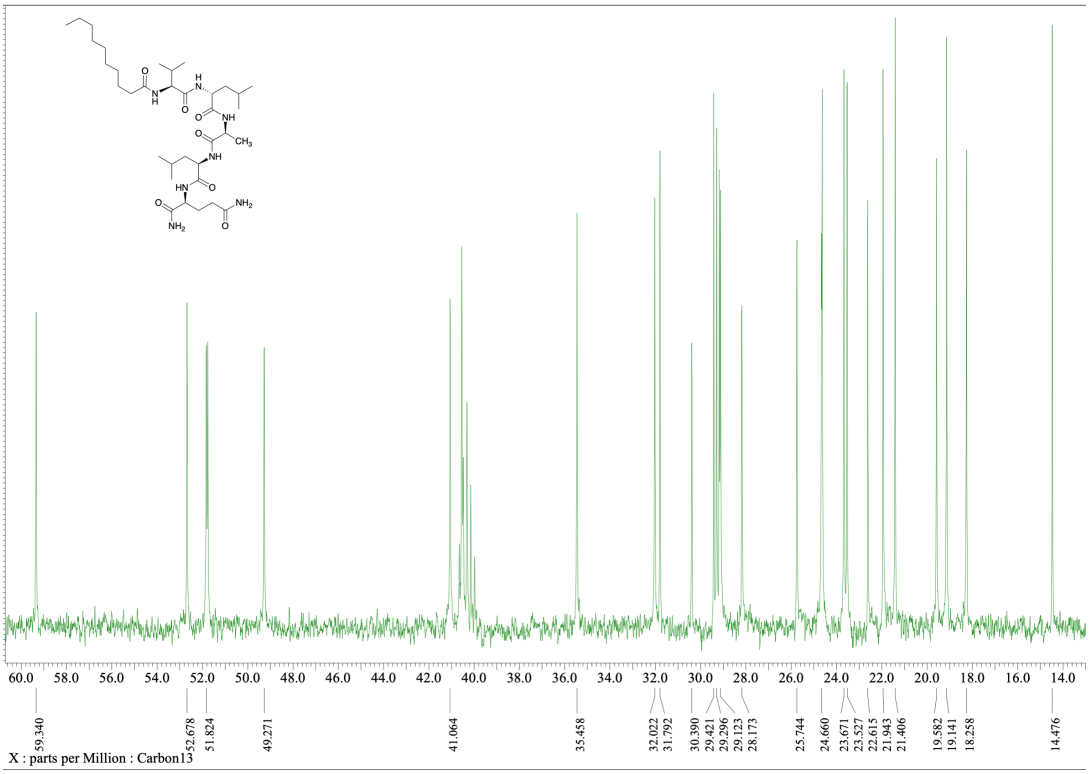

Figure 225. DEPT spectrum of 17a. Solvent : dmso-d_6; T : 23°C; Scans : 10000

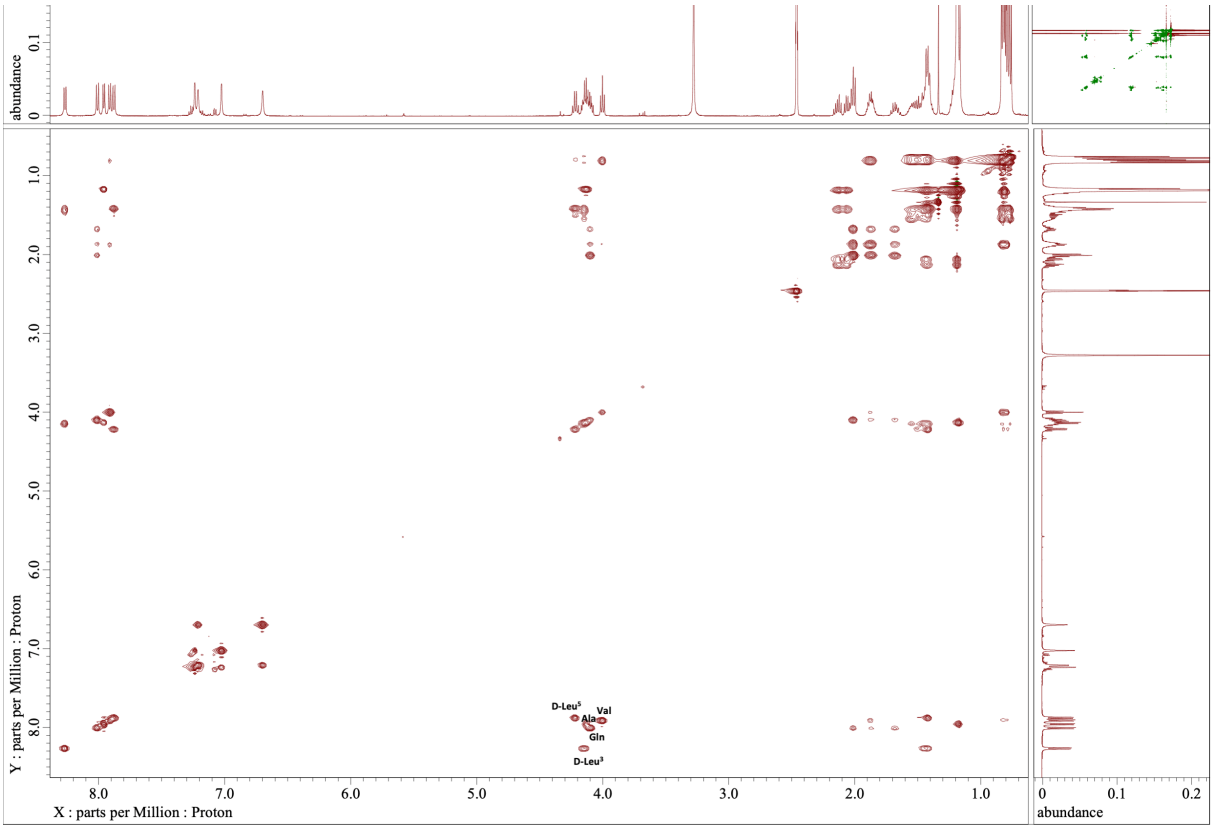

Figure 226. TOCSY spectrum of 17a. Solvent : dmso-d_6; T : 23°C; Scans : 8192

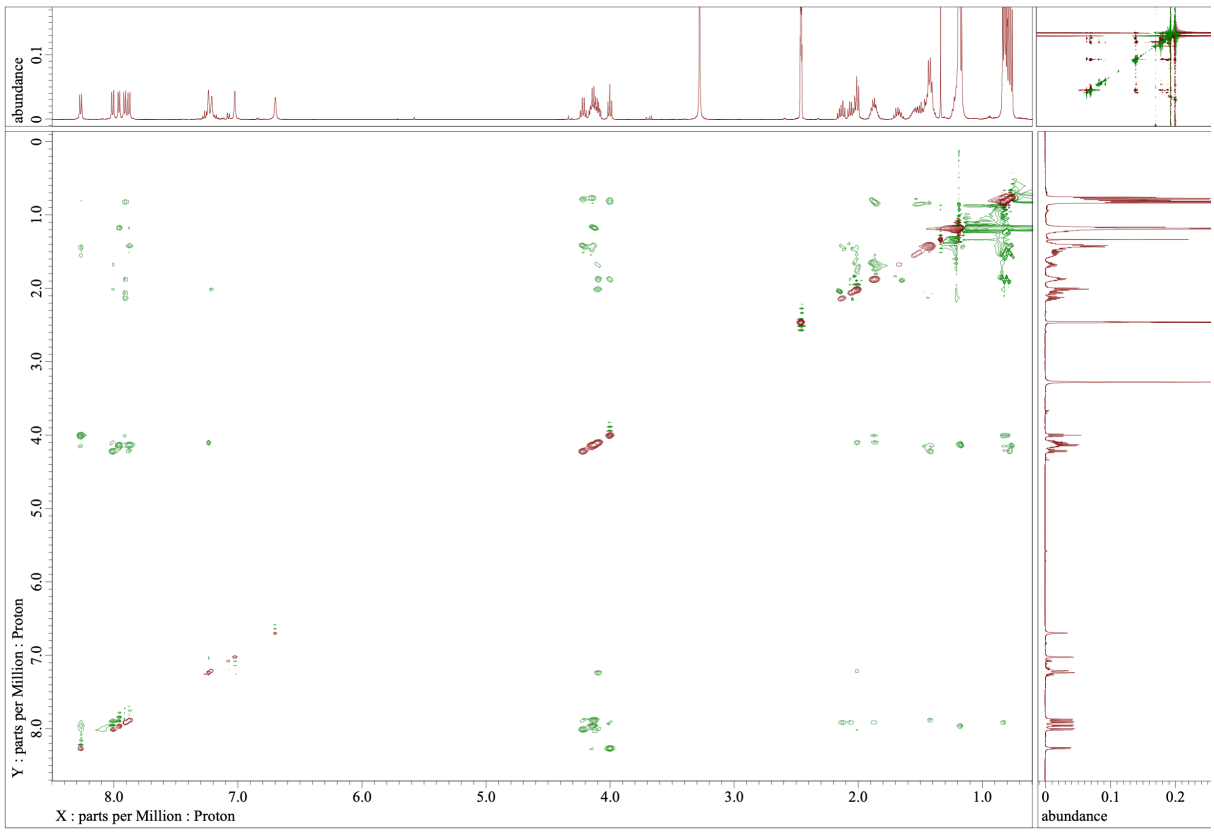

Figure 227. ROESY spectrum of 17a. Solvent : dmso-d_6; T : 23°C; Scans : 8192

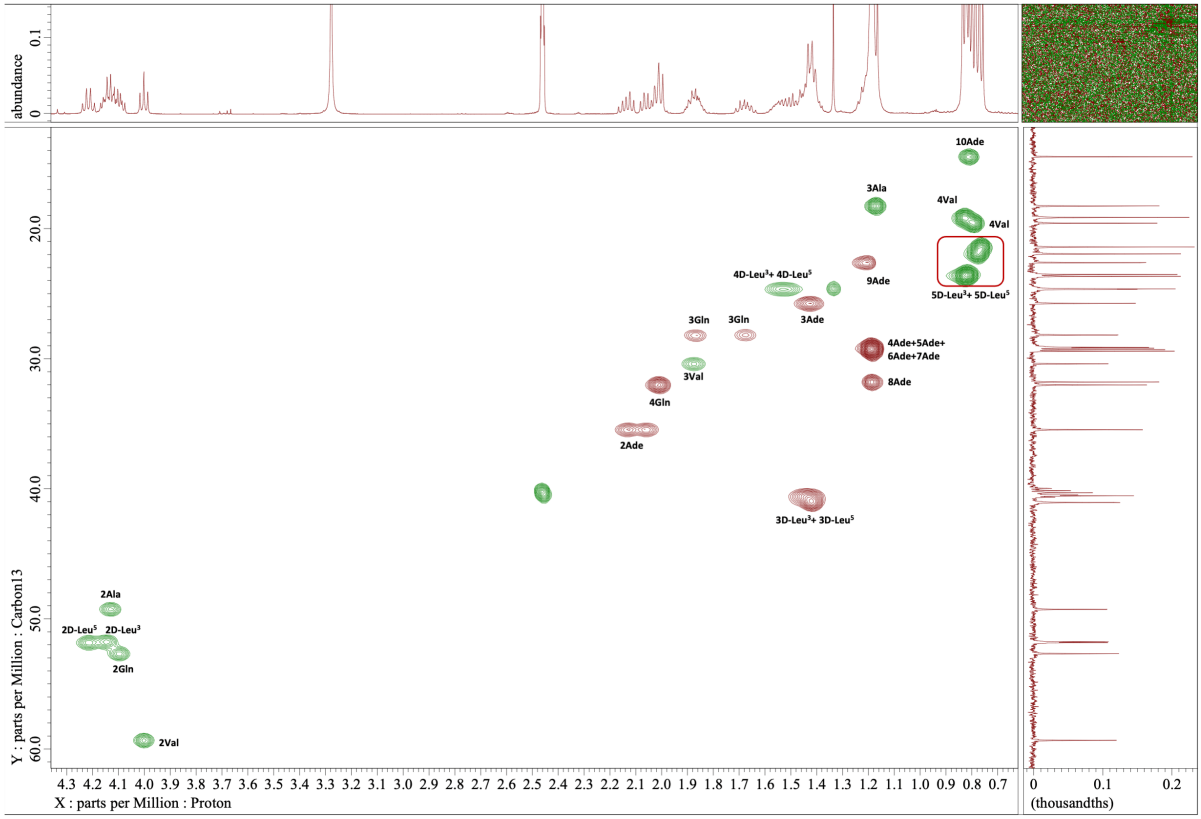

Figure 228. HSQC spectrum of 17a. Solvent : dmso-d_6; T : 23°C; Scans : 8192

g) Compound 18a

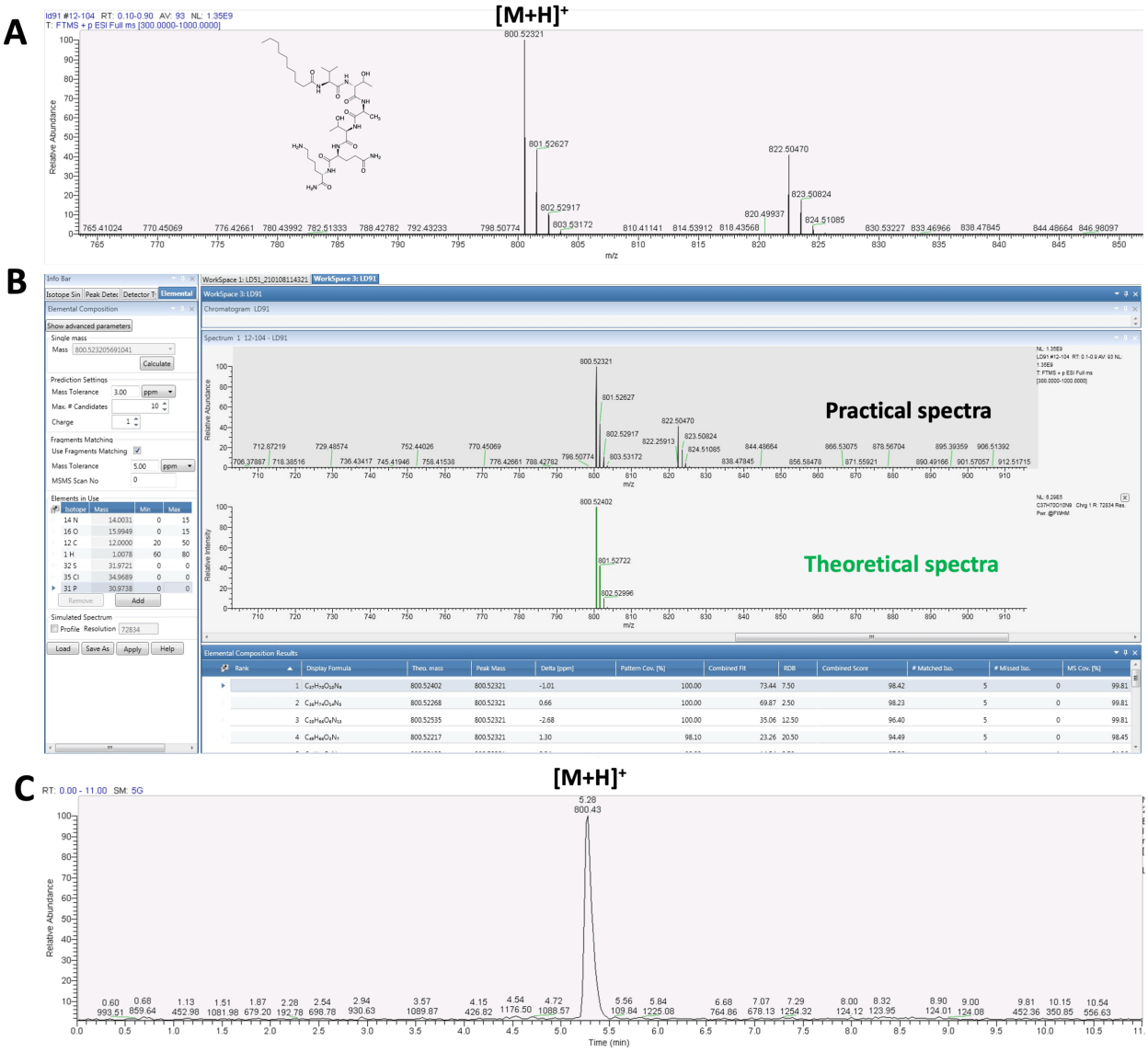

Figure 229. A) ESI-HRMS spectrum of 18a. B) Comparison with the theoretical spectrum. Calculated for $C_{37}H_{70}N_9O_{10}$ $[M+H]^+$ *m/z* 800.52402; Found $[M+H]^+$ *m/z* 800.52321; mass error = 1.01 ppm. C) LC-MS profile of 18a.

Table 31. NMR spectroscopic data of 18a in DMSO-d_6

entry	position	C, mult.	H, mult. (J in Hz)	entry	position	C, mult.	H, mult. (J in Hz)
Decanoic acid[1]	1	*nd*, C	-	Lys[7]	1	*nd*, C	-
	2	35.5, CH_2	2.13		2	52.7, CH	4.10
			2.08		3	31.5, CH_2	1.49
	3	25.8, CH_2	1.43				1.66
	4	29.1-29.4, CH_2	1.19		4	22.9, CH_2	1.26
	5	29.1-29.4, CH_2	1.19		5	27.1, CH_2	1.46
	6	29.1-29.4, CH_2	1.19		6	39.3, CH_2	2.72
					NH	-	7.81, d (8.31)
	7	29.1-29.4, CH_2	1.19		NH_2	-	7.61
	8	31.8, CH_2	1.18		NH_2 C-ter	-	7.09 & 7.03
	9	22.6, CH_2	1.21				
	10	14.5, CH_3	0.80				
Val[2]	1	*nd*, C	-				
	2	59.1-59.4, CH	4.09				
	3	30.1, CH	1.90				
	3-Me	19.7, CH_3	0.82				
	4	19.1, CH_3	0.84				
	NH	-	7.93, d (7.45)				
D-Thr[3]	1	*nd*, C	-				
	2	59.1-59.4, CH	4.09				
	3	66.8, CH	4.02				
	4	20.2-20.3, CH_3	1.00				
	NH	-	7.98, d (8.02)				
Ala[4]	1	*nd*, C	-				
	2	49.2, CH	4.29, t (7.16)				
	3	18.4, CH_3	1.20, d (7.45)				
	NH	-	7.84, d (6.87)				
D-Thr[5]	1	*nd*, C	-				
	2	59.1-59.4, CH	4.10				
	3	67.3, CH	3.91				
	4	20.2-20.3, CH_3	1.00				
	NH	-	7.76, d (7.73)				
Gln[6]	1	*nd*, C	-				
	2	53.4, CH	4.13, t (6.87)				
	3	28.1, CH_2	1.73				
			1.90				
	4	32.0, CH_2	2.08				
	5	*nd*, C	-				
	NH	-	8.16, d (7.16)			*nd* =	Not determined
	NH_2	-	7.22 & 6.75				

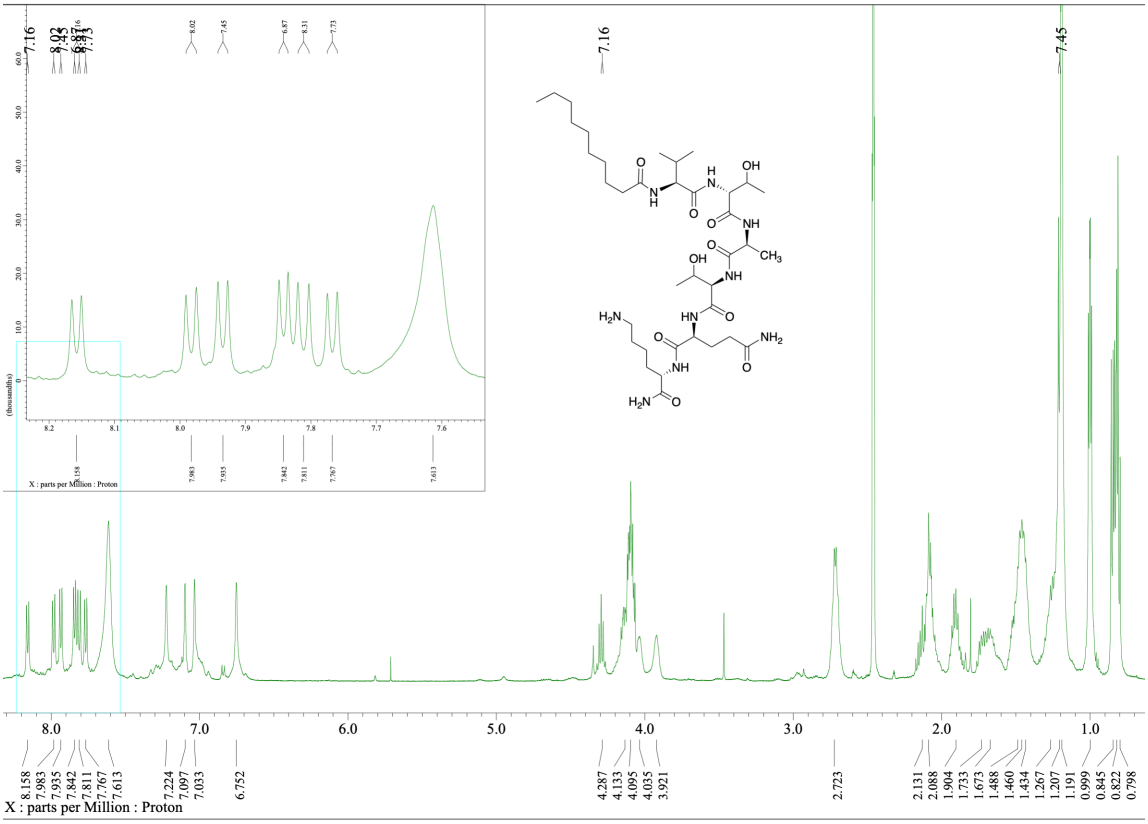

Figure 230. ^{1}H NMR spectrum of 18a. Solvent : dmso-d_6; T : 23°C; Scans : 32

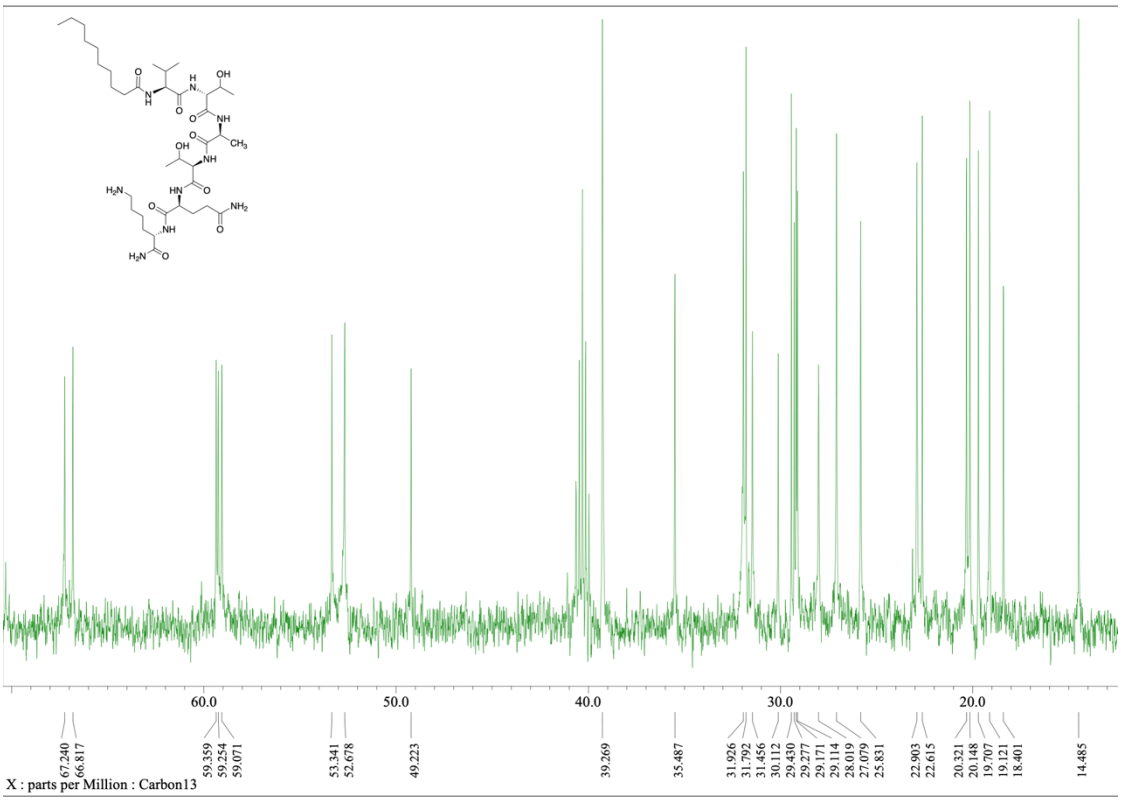

Figure 231. DEPT spectrum of 18a. Solvent : dmso-d_6; T : 23°C; Scans : 10000

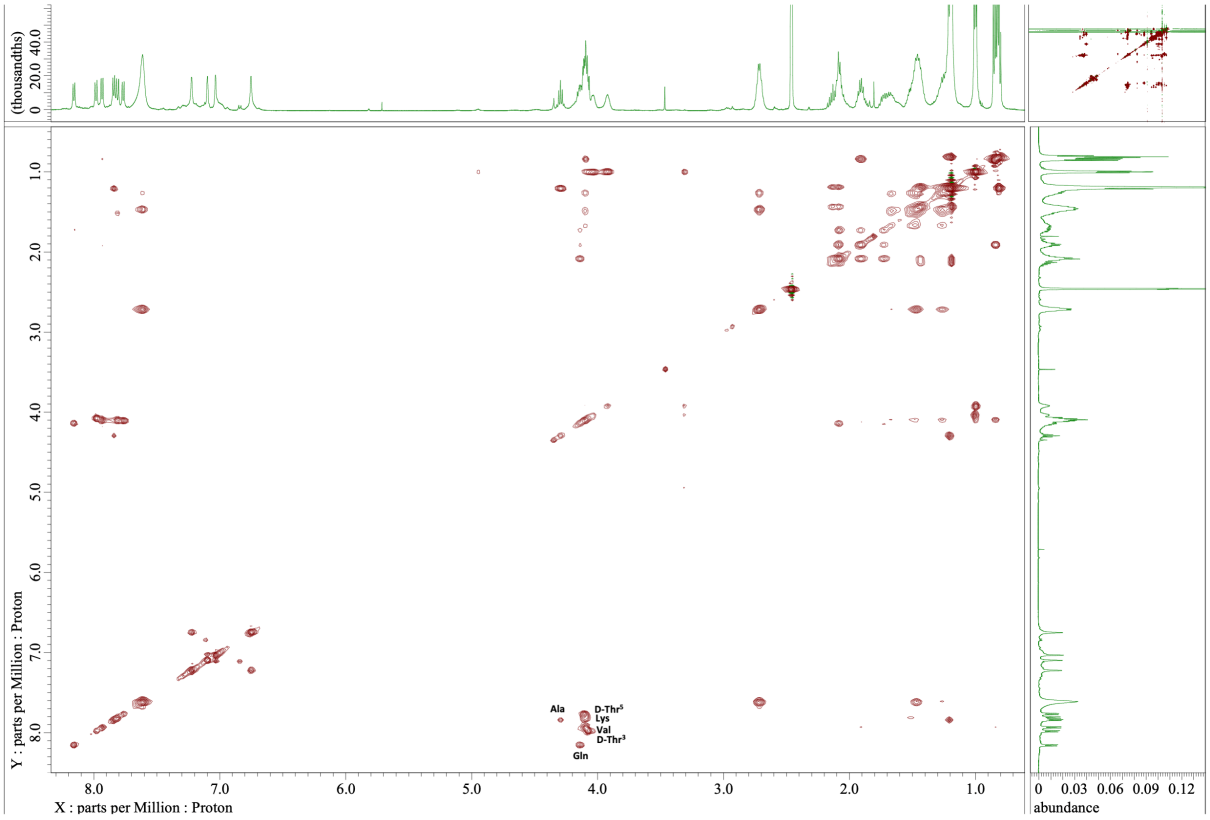

Figure 232. TOCSY spectrum of 18a. Solvent : dmso-d_6; T : 23°C; Scans : 8192

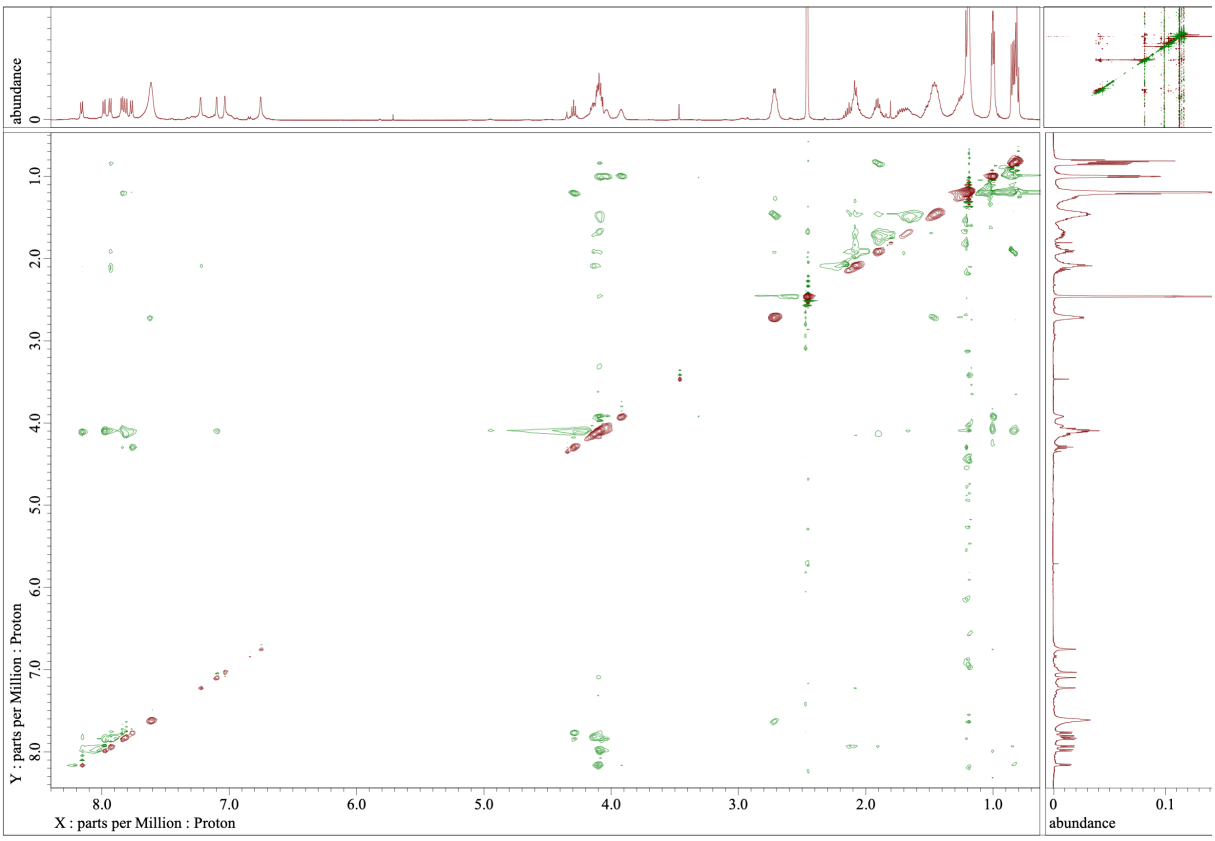

Figure 233. ROESY spectrum of 18a. Solvent : dmso-d_6; T : 23°C; Scans : 8192

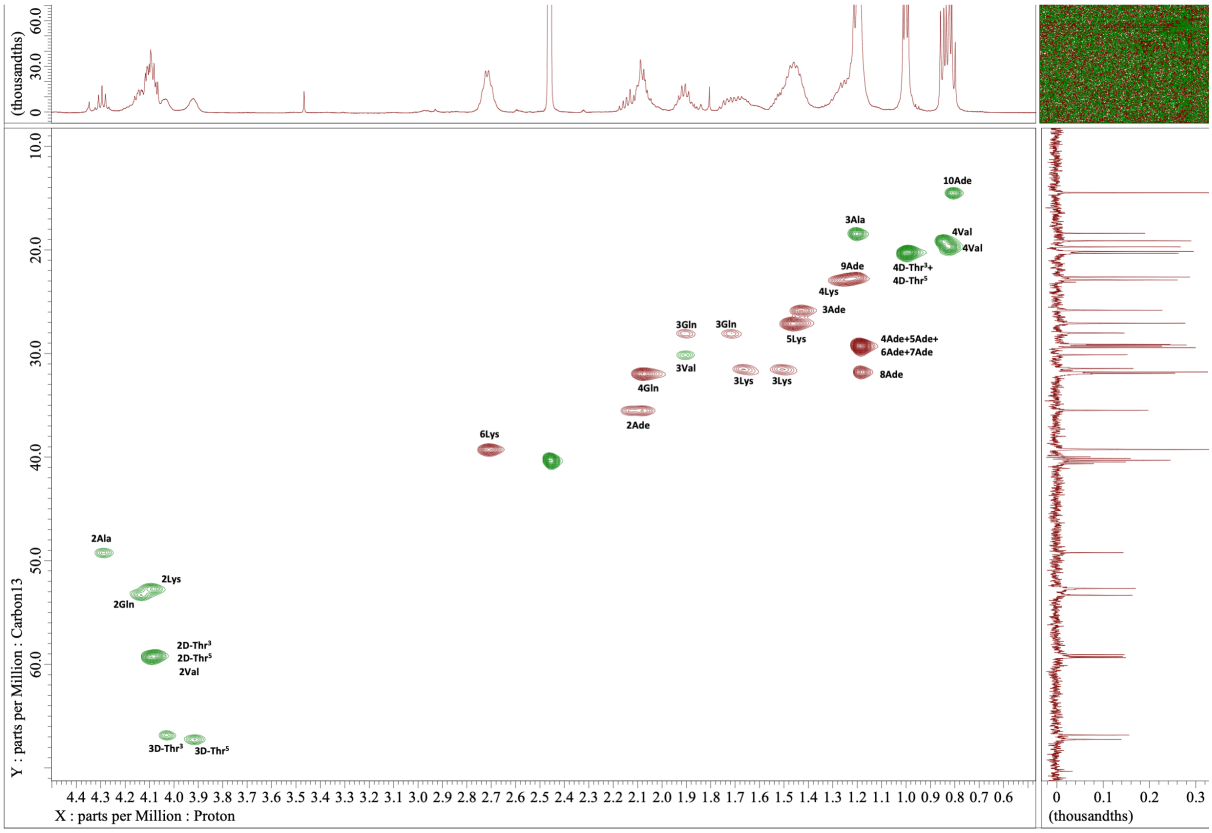

Figure 234. HSQC spectrum of 18a. Solvent : dmso-d_6; T : 23°C; Scans : 8192

h) Compound 19a

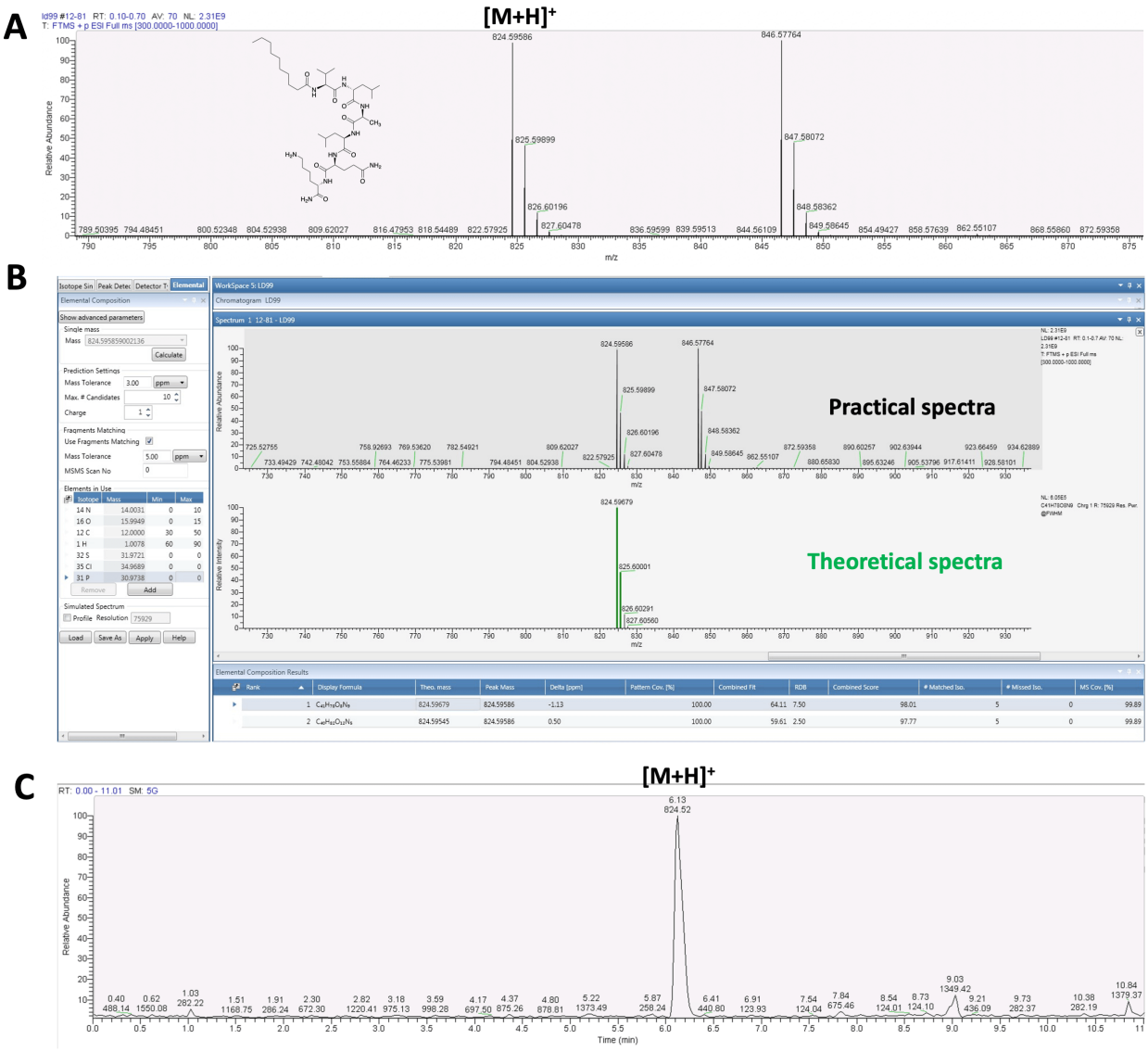

Figure 235. A) ESI-HRMS spectrum of 19a. B) Comparison with the theoretical spectrum. Calculated for $C_{41}H_{78}N_9O_8$ $[M+H]^+$ *m/z* 824.59679; Found $[M+H]^+$ *m/z* 824.59586; mass error = 1.13 ppm. C) LC-MS profile of 19a.

Table 32. NMR spectroscopic data of 19a in DMSO-d_6

entry	position	C, mult.	H, mult. (J in Hz)	entry	position	C, mult.	H, mult. (J in Hz)
Decanoic acid[1]	1	*nd*, C	-	Gln[6]	1	*nd*, C	-
	2	35.4, CH_2	2.14		2	53.2, CH	4.12
			2.07		3	28.0, CH_2	1.72
	3	25.8, CH_2	1.43				1.90
	4	29.1-29.4, CH_2	1.19		4	32.0, CH_2	2.05
	5	29.1-29.4, CH_2	1.19		5	*nd*, C	-
	6	29.1-29.4, CH_2	1.19		NH	-	8.19, d (7.45)
					NH_2	-	7.23 & 6.74
	7	29.1-29.4, CH_2	1.19	Lys[7]	1	*nd*, C	-
	8	31.8, CH_2	1.19		2	52.7, CH	4.09
	9	22.6, CH_2	1.21		3	31.5, CH_2	1.52
	10	14.5, CH_3	0.81				1.66
Val[2]	1	*nd*, C	-		4	22.9, CH_2	1.26
	2	59.5, CH	3.97, t (7.73)		5	27.1, CH_2	1.48
	3	30.3, CH	1.88		6	39.2, CH_2	2.72
	3-Me	19.6, CH_3	0.80		NH	-	7.79, d (8.31)
	4	19.2, CH_3	0.83		NH_2	-	7.61
	NH	-	7.92, d (7.45)		NH_2 C-ter	-	7.11 & 7.02
D-Leu[3]	1	*nd*, C	-				
	2	51.7-52.0, CH	4.17				
	3	40.6-41.0, CH_2	1.43				
	4	24.6, CH	1.54				
	4-Me	21.4-23.7, CH_3	0.78-0.83				
	5	21.4-23.7, CH_3	0.78-0.83				
	NH	-	8.23, d (7.73)				
Ala[4]	1	*nd*, C	-				
	2	49.3, CH	4.13				
	3	18.2, CH_3	1.18, d (7.45)				
	NH	-	7.94, d (6.87)				
D-Leu[5]	1	*nd*, C	-				
	2	51.7-52.0, CH	4.17				
	3	40.6-41.0, CH_2	1.43				
	4	24.6, CH	1.54				
	4-Me	21.4-23.7, CH_3	0.78-0.83				
	5	21.4-23.7, CH_3	0.78-0.83			*nd* =	Not determined
	NH	-	7.89, d (7.73)				

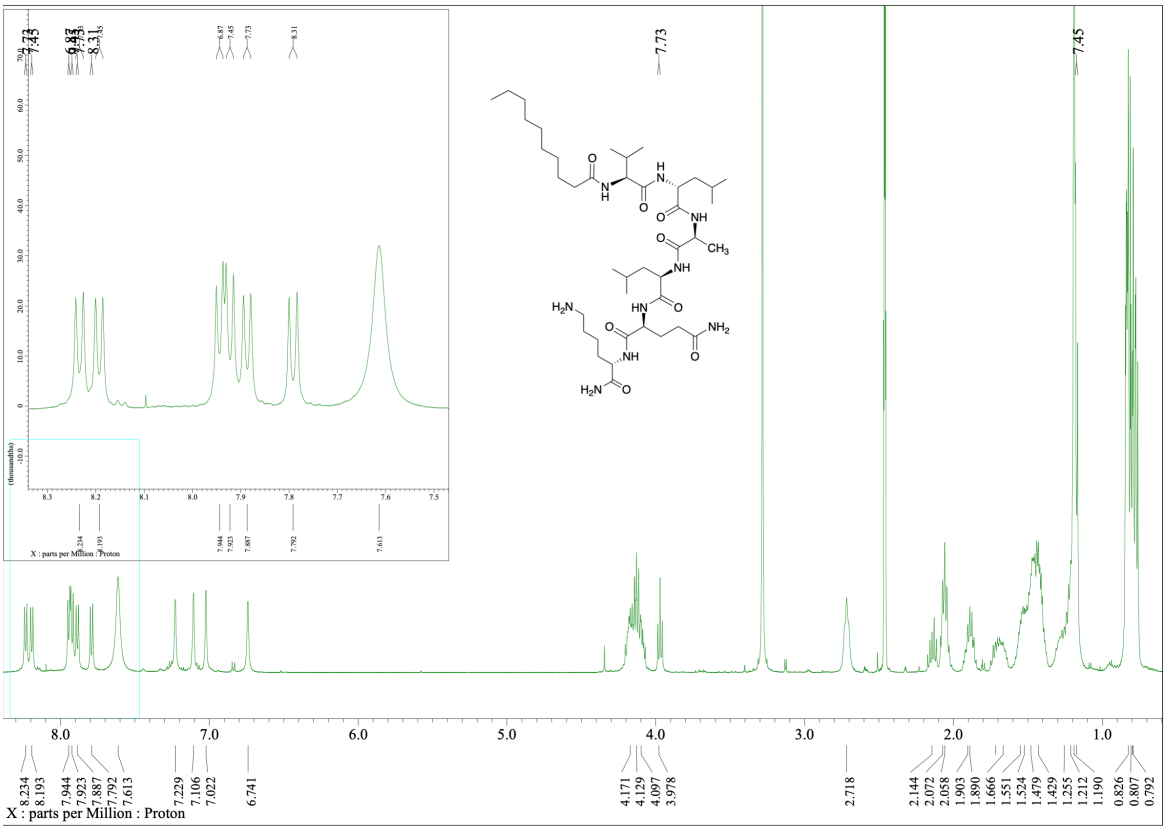

Figure 236. ^{1}H NMR spectrum of 19a. Solvent : dmso-d_6; T : 23°C; Scans : 32

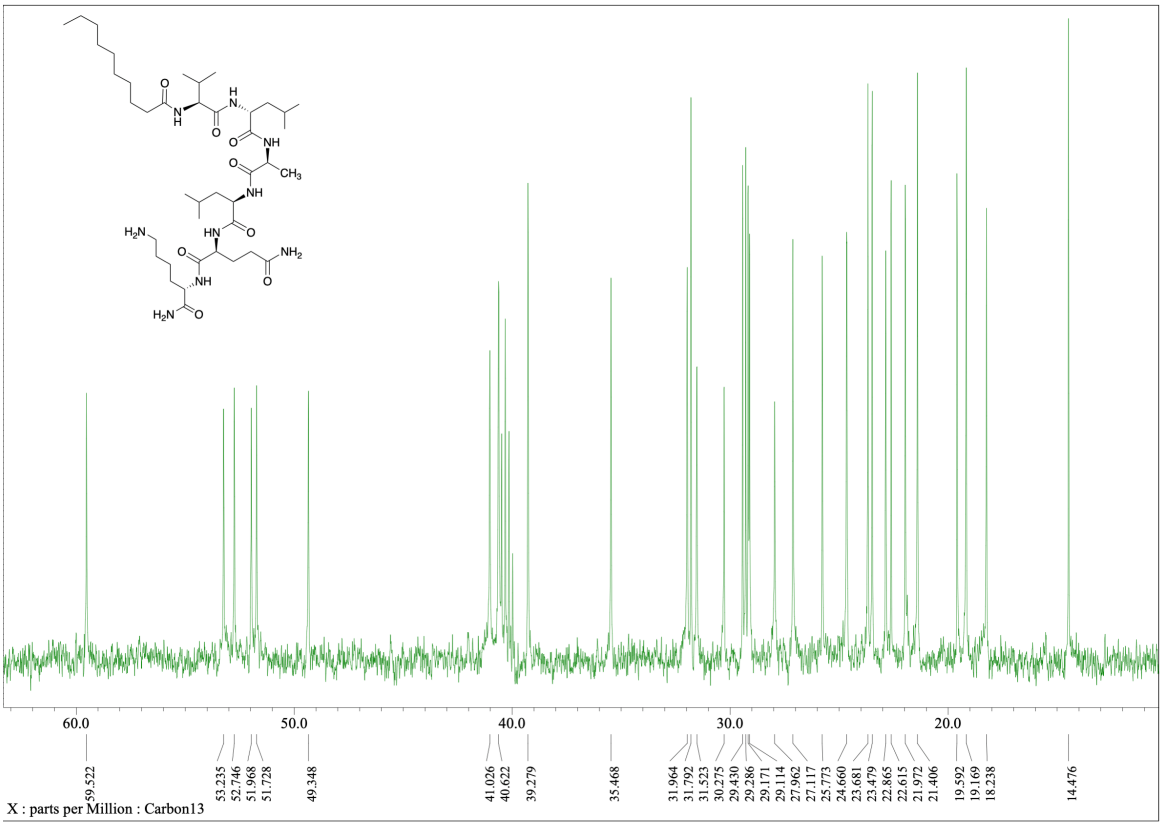

Figure 237. DEPT spectrum of 19a. Solvent : dmso-d_6; T : 23°C; Scans : 10000

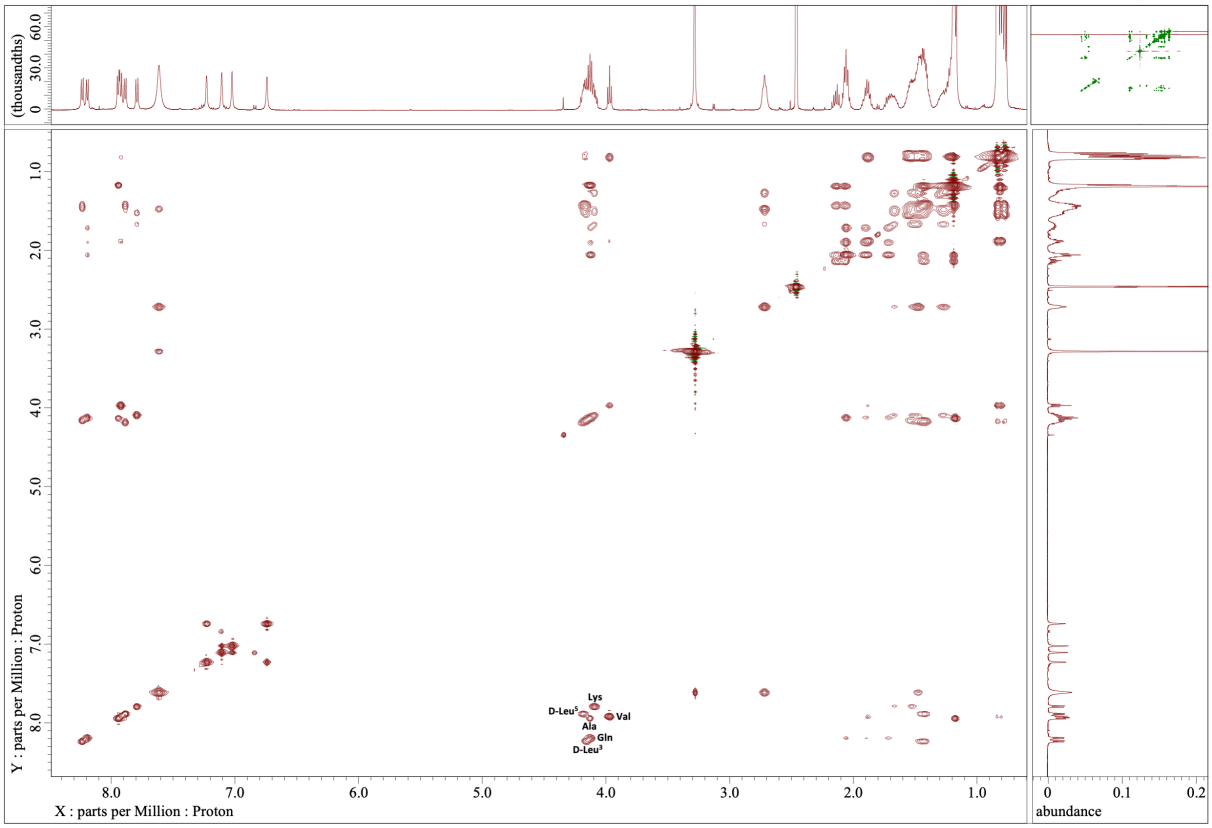

Figure 238. TOCSY spectrum of 19a. Solvent : dmso-d_6; T : 23°C; Scans : 8192

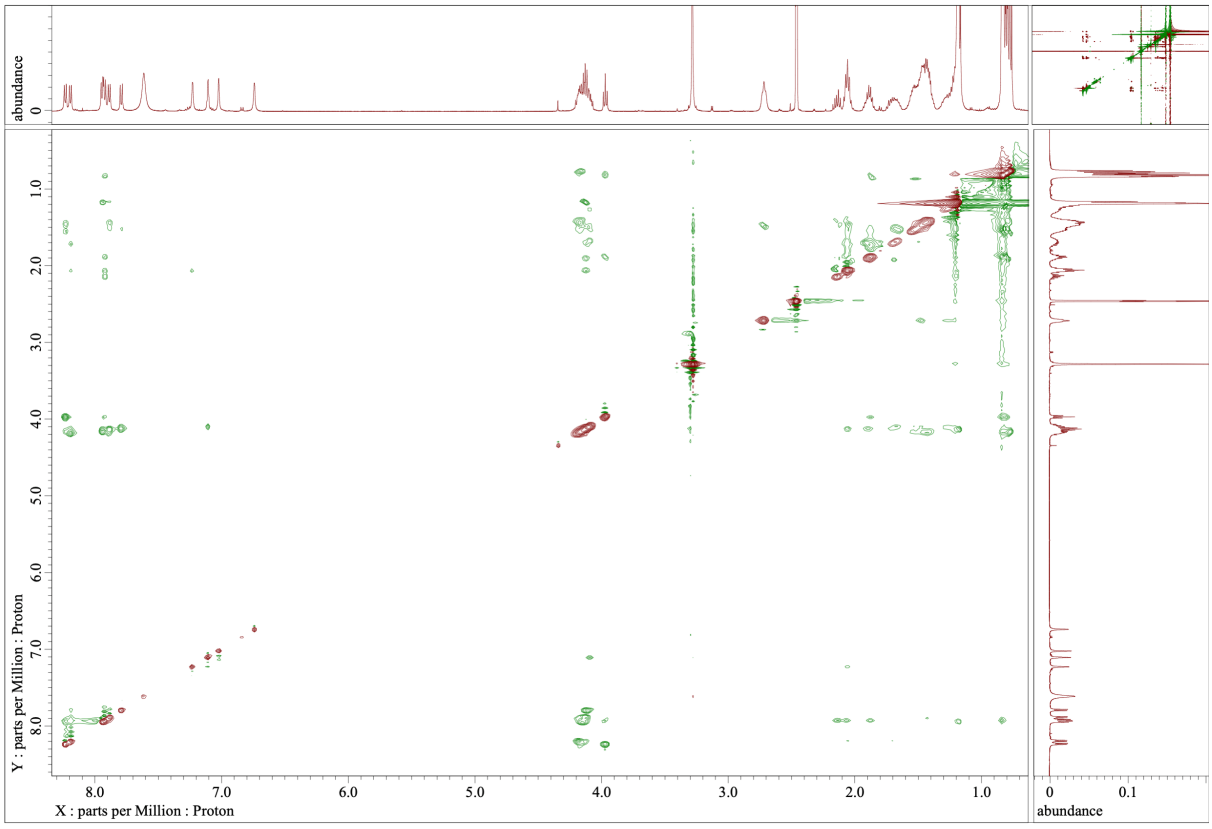

Figure 239. ROESY spectrum of 19a. Solvent : dmso-d_6; T : 23°C; Scans : 8192

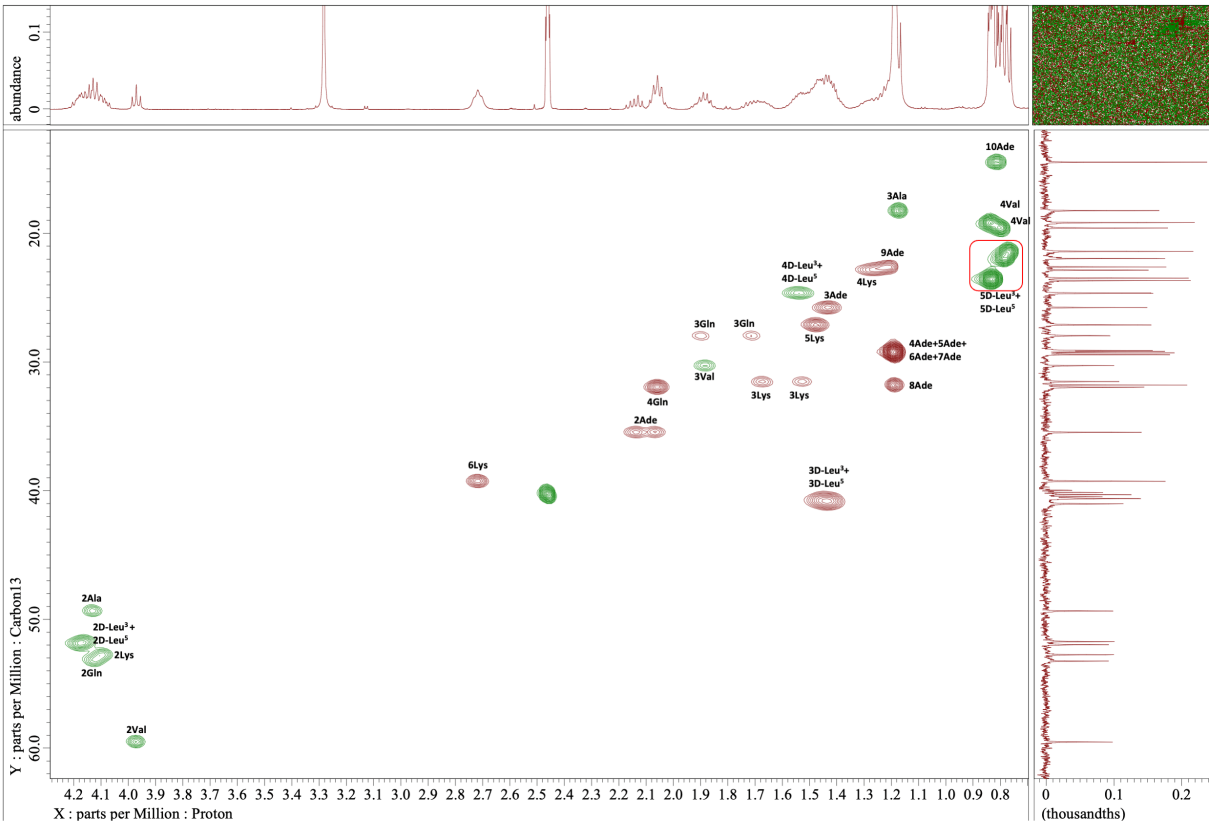

Figure 240. HSQC spectrum of 19a. Solvent : dmso-d_6; T : 23°C; Scans : 8192

i) Compound 20a

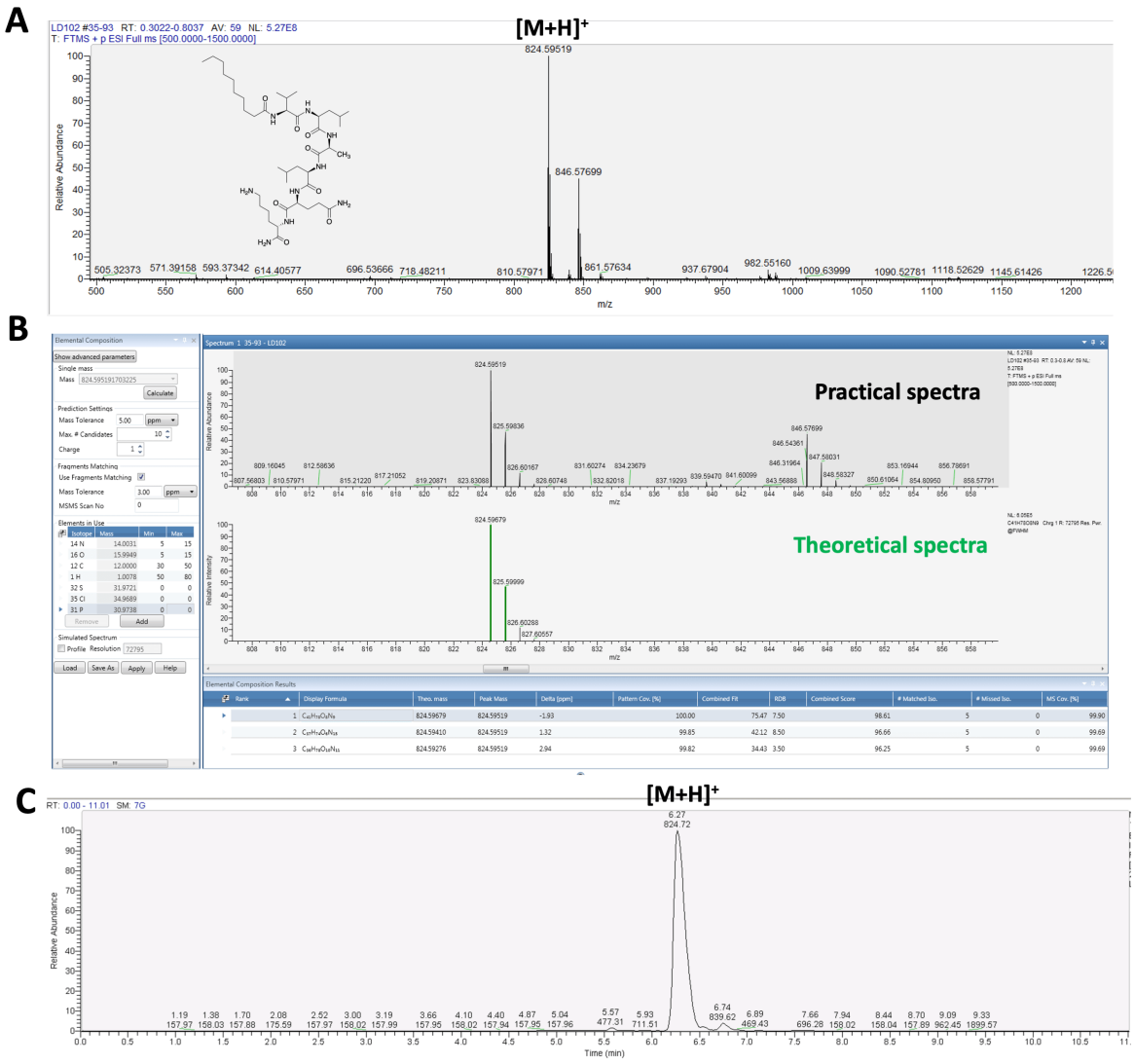

Figure 241. A) ESI-HRMS spectrum of 20a. B) Comparison with the theoretical spectrum. Calculated for $C_{41}H_{78}N_9O_8$ [M+H]$^+$ *m/z* 824.59679; Found [M+H]$^+$ *m/z* 824.59519; mass error = 1.93 ppm. C) LC-MS profile of 20a.

Table 33. NMR spectroscopic data of 20a in DMSO-d_6

entry	position	C, mult.	H, mult. (J in Hz)	entry	position	C, mult.	H, mult. (J in Hz)
Decanoic acid[1]	1	*nd*, C	-	Gln[6]	1	*nd*, C	-
	2	35.7, CH_2	2.10		2	53.2, CH	4.10
	3	25.9, CH_2	1.42		3	27.9, CH_2	1.75
							1.87
	4	29.1-29.5, CH_2	1.19		4	32.0, CH_2	2.05
	5	29.1-29.5, CH_2	1.19		5	*nd*, C	-
	6	29.1-29.5, CH_2	1.19		NH	-	8.10, d (7.45)
					NH_2	-	7.27 & 6.78
	7	29.1-29.5, CH_2	1.19	Lys[7]	1	*nd*, C	-
	8	31.8, CH_2	1.19		2	52.7, CH	4.09
	9	22.6, CH_2	1.21		3	31.6, CH_2	1.49
	10	14.5, CH_3	0.81				1.66
Val[2]	1	*nd*, C	-		4	22.8, CH_2	1.27
	2	58.4, CH	4.08		5	27.1, CH_2	1.47
	3	30.6, CH	1.90		6	39.2, CH_2	2.72
	3-Me	19.8, CH_3	0.79		NH	-	7.75, d (8.02)
	4	18.8, CH_3	0.78		NH_2	-	7.61
	NH	-	7.76, d (8.59)		$NH_{2\ C\text{-}ter}$	-	7.14 & 7.00
L-Leu[3]	1	*nd*, C	-				
	2	51.1, CH	4.29				
	3	40.8-41.0, CH_2	1.40				
	4	24.6-24.7, CH	1.54				
	4-Me	21.8-23.7, CH_3	0.78-0.83				
	5	21.8-23.7, CH_3	0.78-0.83				
	NH	-	7.87, d (8.02)				
Ala[4]	1	*nd*, C	-				
	2	49.3, CH	4.14				
	3	18.4, CH_3	1.16, d (7.16)				
	NH	-	7.92, d (6.59)				
D-Leu[5]	1	*nd*, C	-				
	2	51.8, CH	4.16				
	3	40.8-41.0, CH_2	1.40				
	4	24.6-24.7, CH	1.51				
	4-Me	21.8-23.7, CH_3	0.78-0.83				
	5	21.8-23.7, CH_3	0.78-0.83			*nd* =	not determined
	NH	-	7.97, d (7.45)				

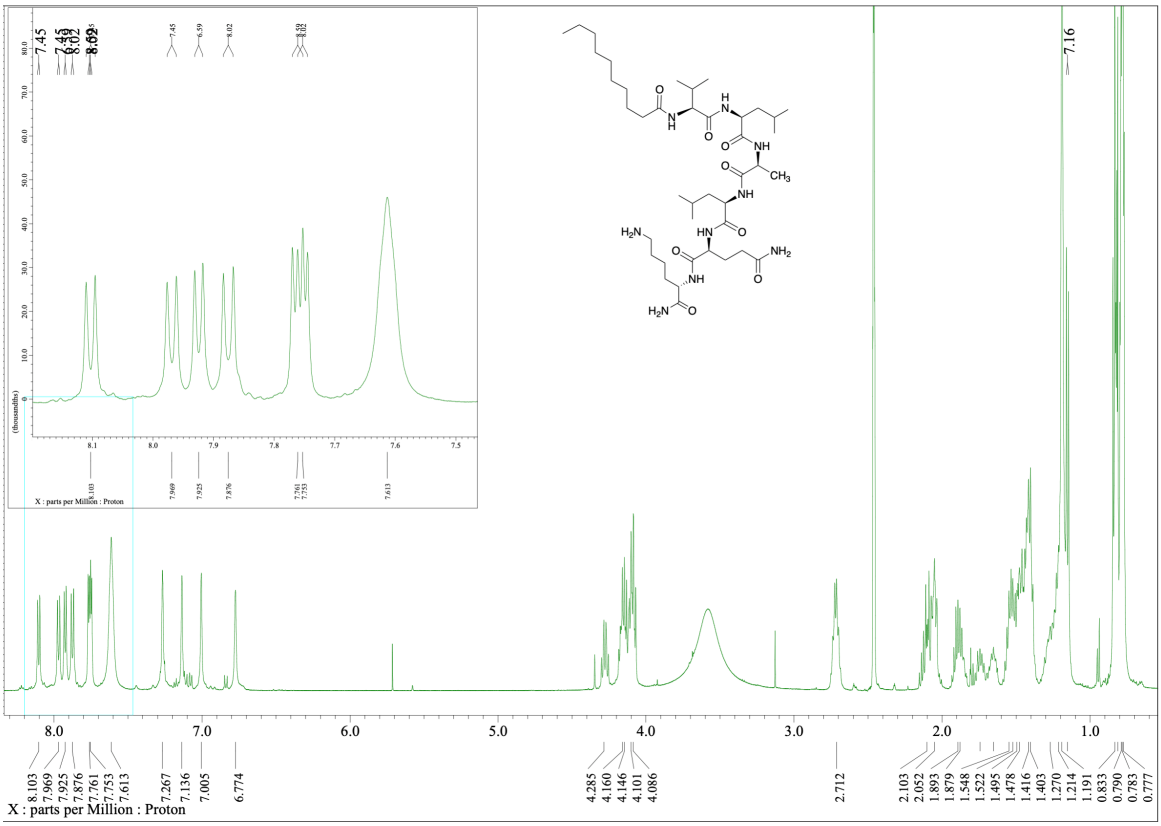

Figure 242. ^{1}H NMR spectrum of 20a. Solvent : dmso-d_6; T : 23°C; Scans : 32

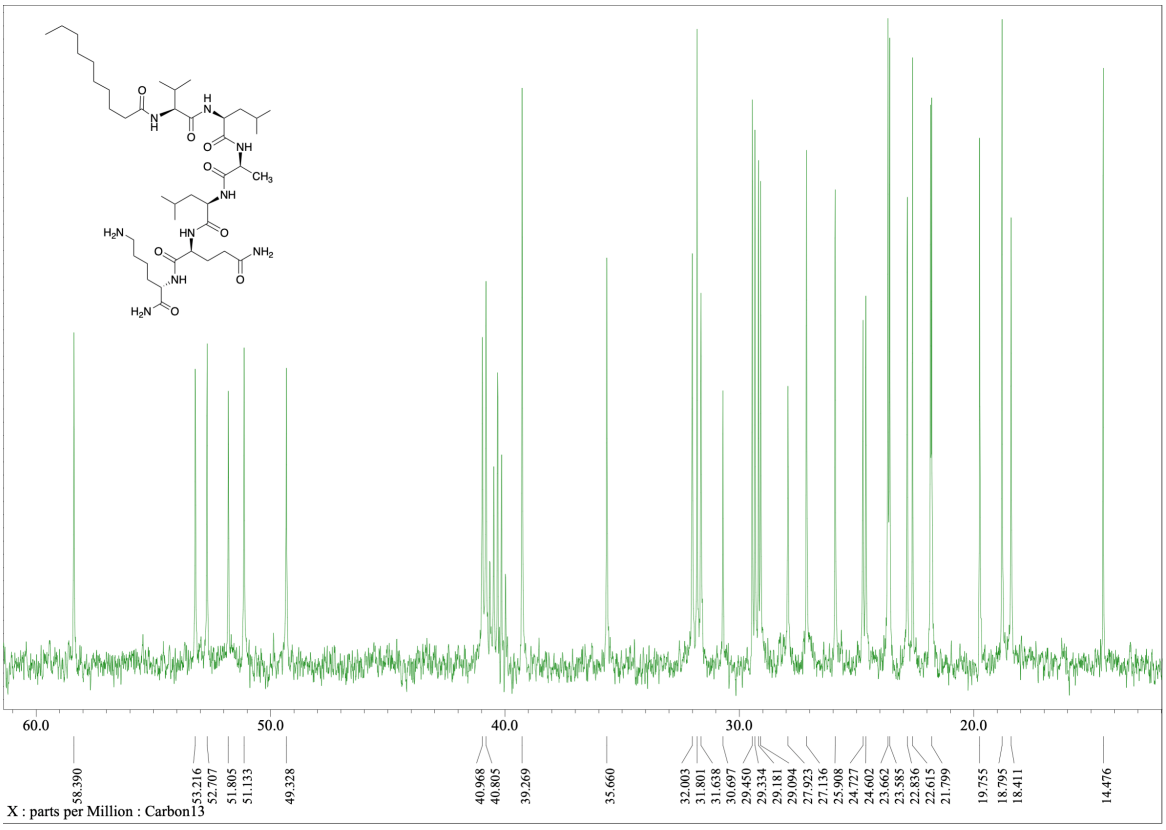

Figure 243. DEPT spectrum of 20a. Solvent : dmso-d_6; T : 23°C; Scans : 10000

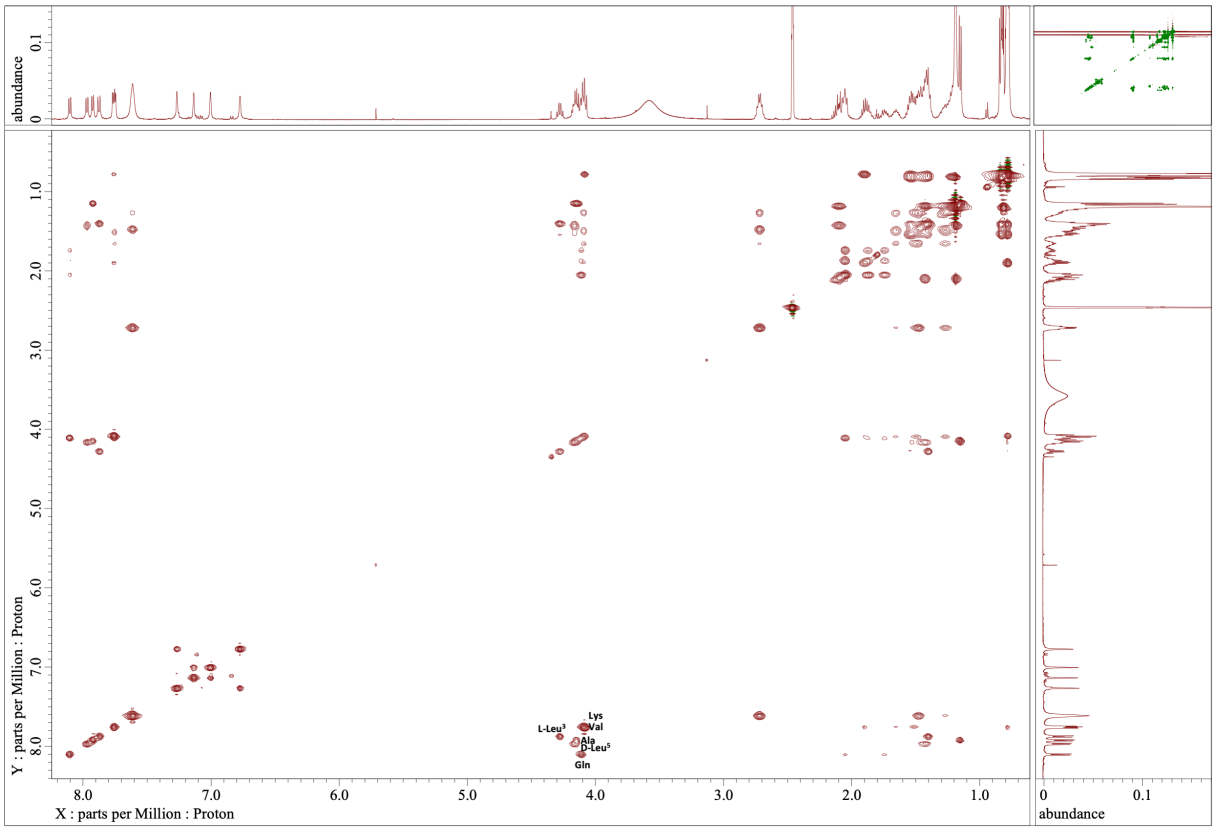

Figure 244. TOCSY spectrum of 20a. Solvent : dmso-d_6; T : 23°C; Scans : 8192

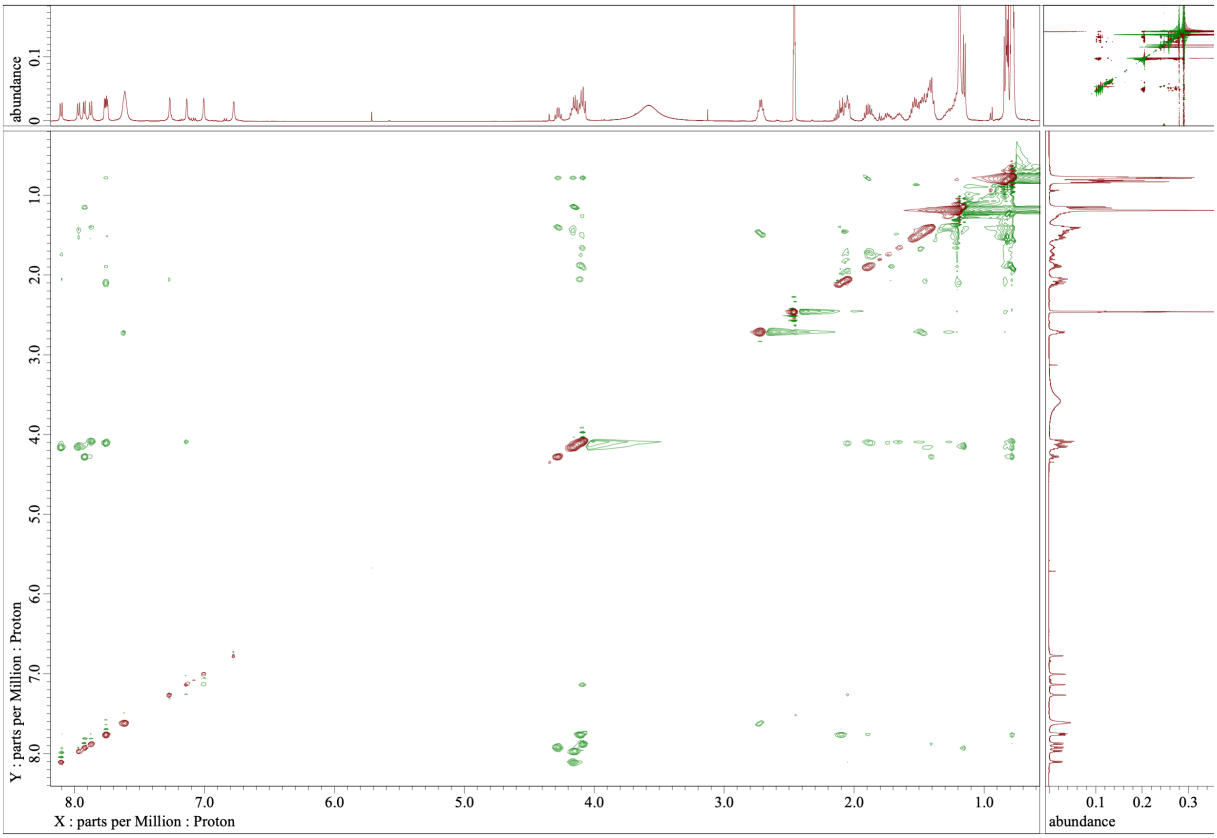

Figure 245. ROESY spectrum of 20a. Solvent : dmso-d_6; T : 23°C; Scans : 8192

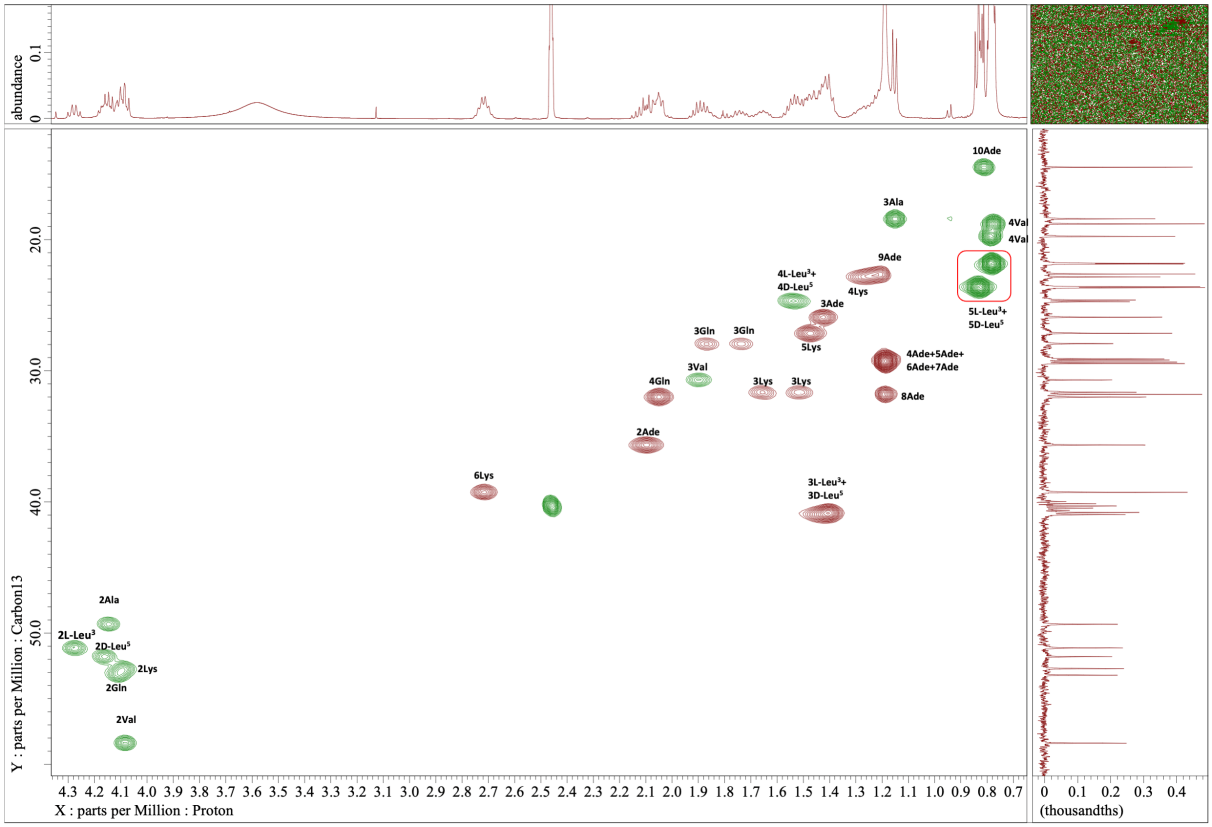

Figure 246. HSQC spectrum of 20a. Solvent : dmso-d_6; T : 23°C; Scans : 8192

j) Compound 21a

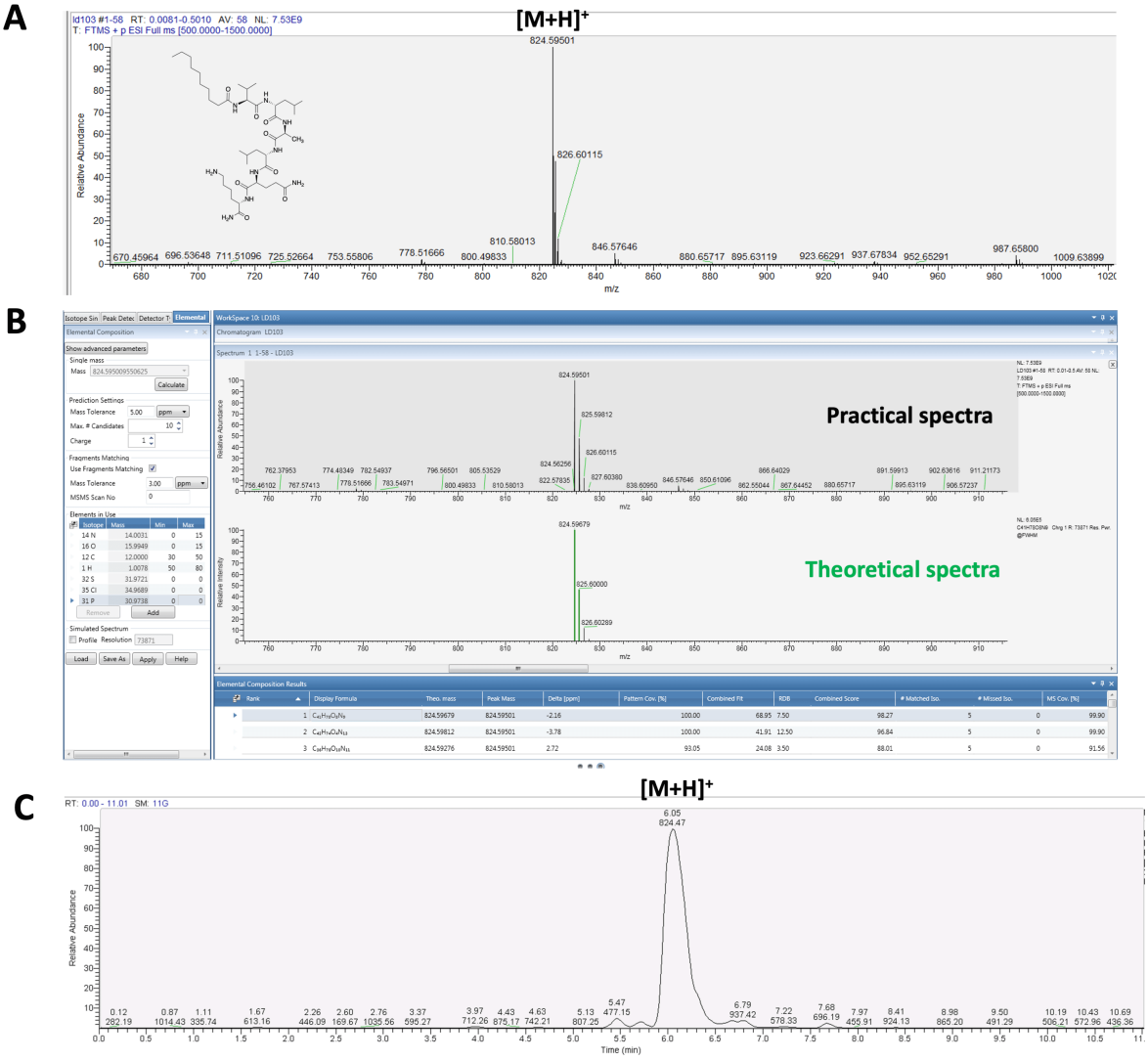

Figure 247. A) ESI-HRMS spectrum of 21a. B) Comparison with the theoretical spectrum. Calculated for $C_{41}H_{78}N_9O_8$ [M+H]$^+$ *m/z* 824.59679; Found [M+H]$^+$ *m/z* 824.59501; mass error = 2.16 ppm. C) LC-MS profile of 21a.

Table 34. NMR spectroscopic data of 21a in DMSO-d_6

entry	position	C, mult.	H, mult. (J in Hz)	entry	position	C, mult.	H, mult. (J in Hz)
Decanoic acid[1]	1	*nd*, C	-	Lys[7]	1	*nd*, C	-
	2	35.5, CH_2	2.13		2	52.6, CH	4.09
			2.06		3	31.8, CH_2	1.48
	3	25.8, CH_2	1.42				1.63
	4	29.1-29.4, CH_2	1.19		4	22.7, CH_2	1.25
	5	29.1-29.4, CH_2	1.19		5	27.2, CH_2	1.47
	6	29.1-29.4, CH_2	1.19		6	39.3, CH_2	2.72
					NH	-	7.72, d (8.02)
	7	29.1-29.4, CH_2	1.19		NH_2	-	7.62
	8	31.8, CH_2	1.19		NH_2 C-ter	-	7.22 & 7.02
	9	22.6, CH_2	1.21				
	10	14.5, CH_3	0.81				
Val[2]	1	*nd*, C	-				
	2	59.3, CH	3.98, t (7.73)				
	3	30.4, CH	1.87				
	3-Me	19.6, CH_3	0.79				
	4	19.1, CH_3	0.82				
	NH	-	7.83, d (7.73)				
D-Leu[3]	1	*nd*, C	-				
	2	51.6-51.8, CH	4.18				
	3	40.8-40.9, CH_2	1.42				
	4	24.6, CH	1.56				
	4-Me	21.5-23.7, CH_3	0.77-0.83				
	5	21.5-23.7, CH_3	0.77-0.83				
	NH	-	8.22, d (8.02)				
Ala[4]	1	*nd*, C	-				
	2	48.9, CH	4.19				
	3	18.0, CH_3	1.15, d (7.16)				
	NH	-	7.96, d (7.16)				
L-Leu[5]	1	*nd*, C	-				
	2	51.6-51.8, CH	4.18				
	3	40.8-40.9, CH_2	1.42				
	4	24.6, CH	1.56				
	4-Me	21.5-23.7, CH_3	0.78-0.83				
	5	21.5-23.7, CH_3	0.78-0.83				
	NH	-	7.83, d (7.73)				
Gln[6]	1	*nd*, C	-				
	2	52.9, CH	4.13				
	3	28.2, CH_2	1.70				
			1.85				
	4	32.0, CH_2	2.04				
	5	*nd*, C	-				
	NH	-	7.88, d (7.45)			*nd* =	Not determined
	NH_2	-	7.21 & 6.73				

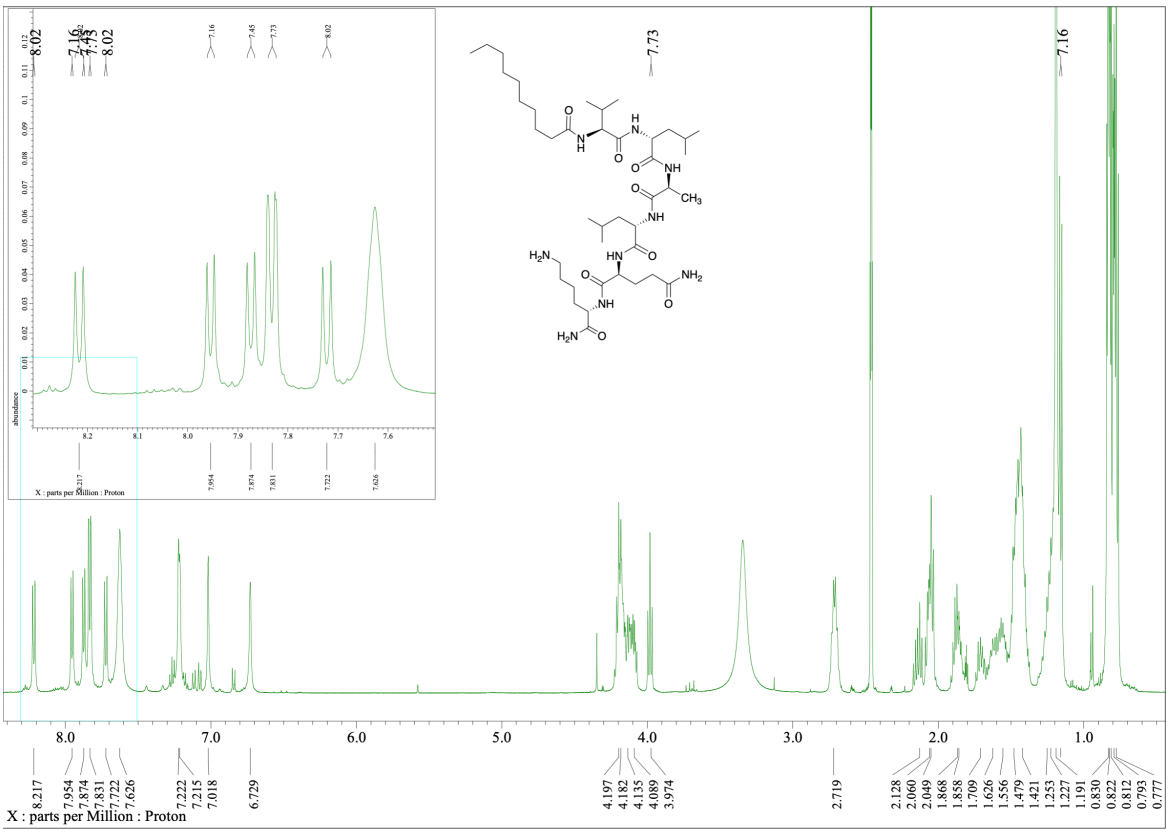

Figure 248. ^{1}H NMR spectrum of 21a. Solvent : dmso-d_6; T : 23°C; Scans : 32

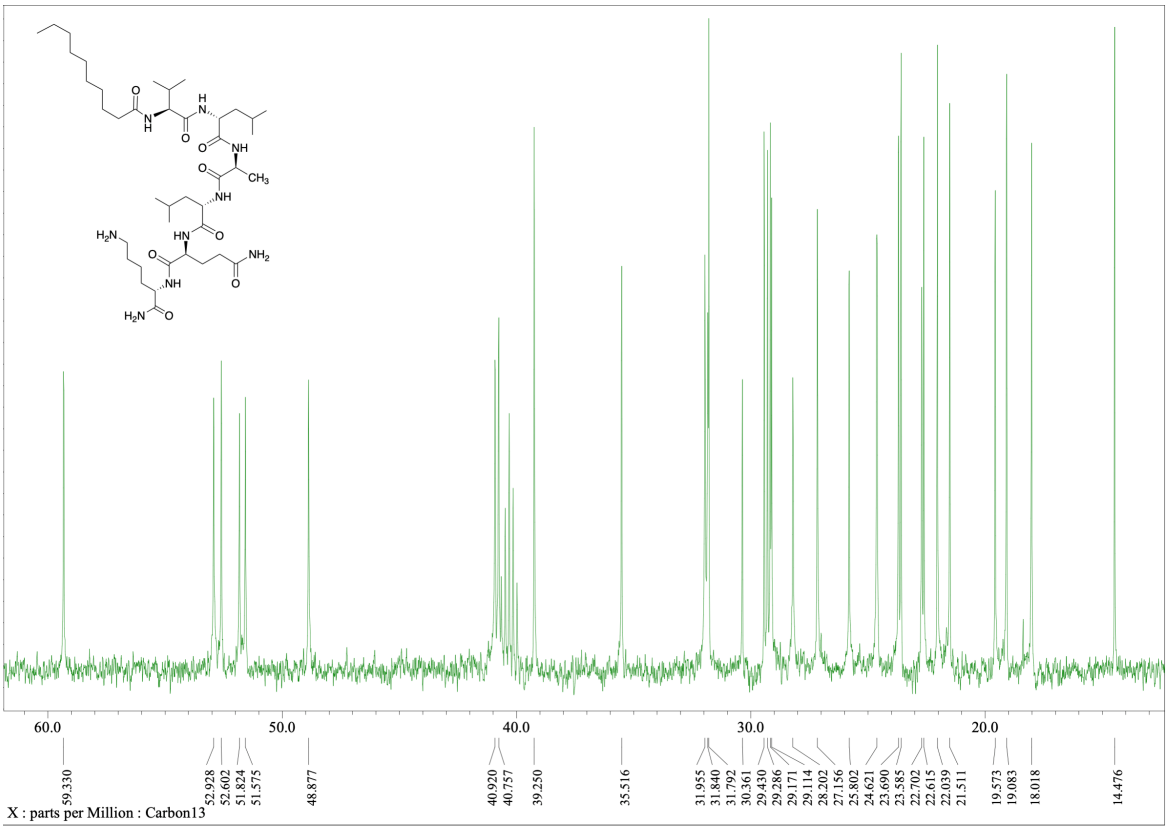

Figure 249. DEPT spectrum of 21a. Solvent : dmso-d_6; T : 23°C; Scans : 10000

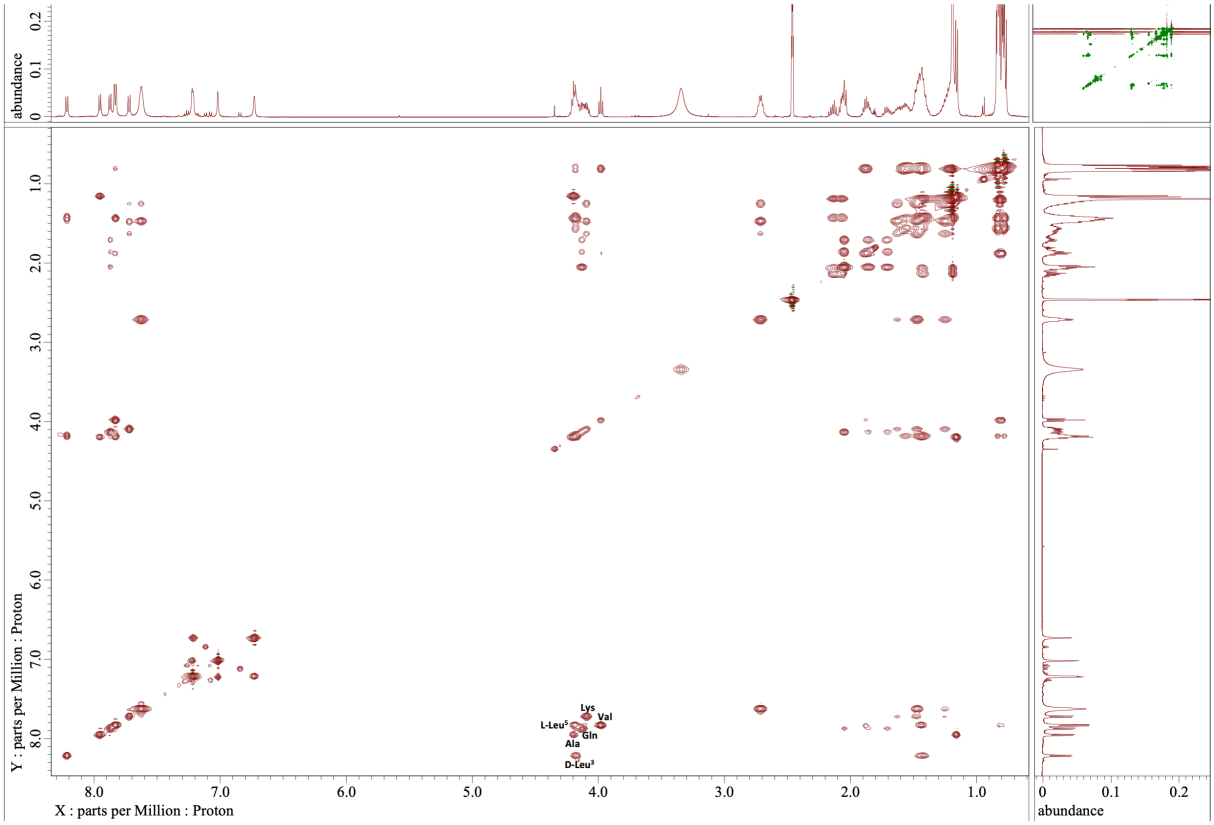

Figure 250. TOCSY spectrum of 21a. Solvent : dmso-d_6; T : 23°C; Scans : 8192

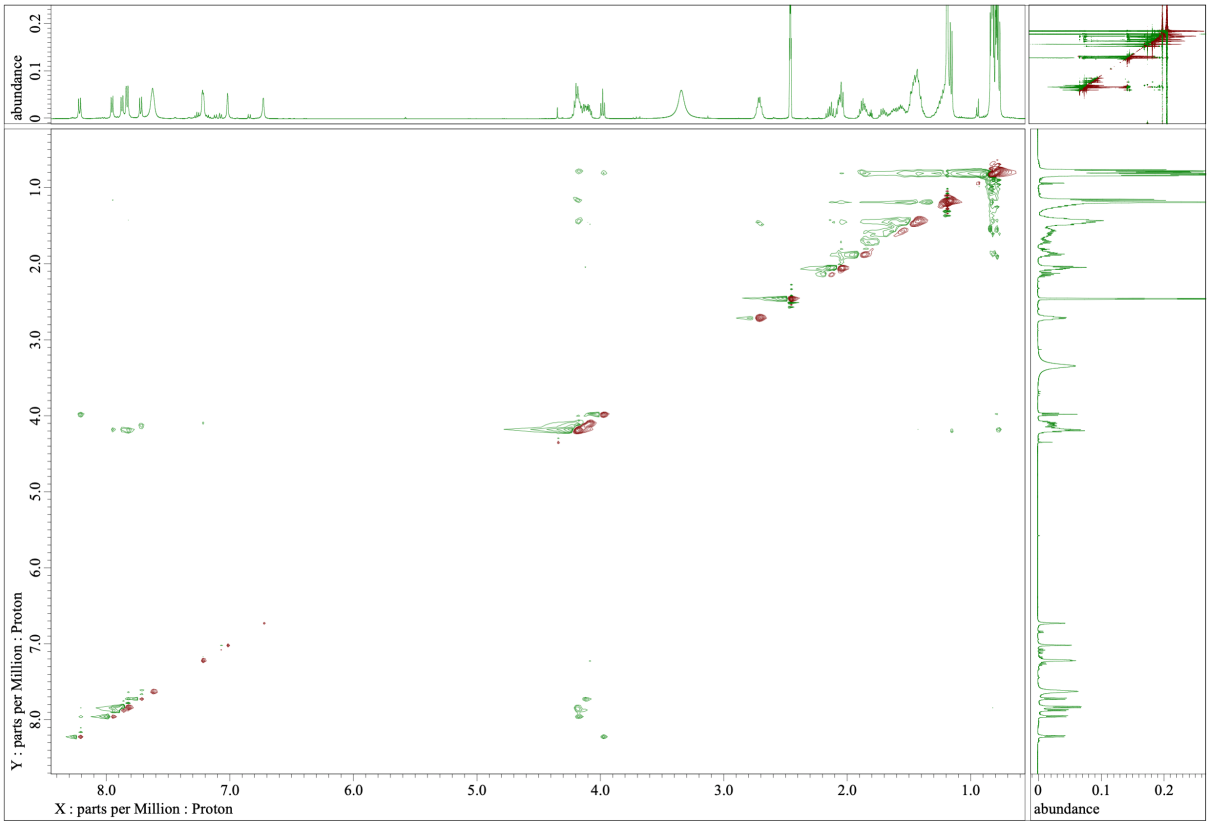

Figure 251. ROESY spectrum of 21a. Solvent : dmso-d_6; T : 23°C; Scans : 8192

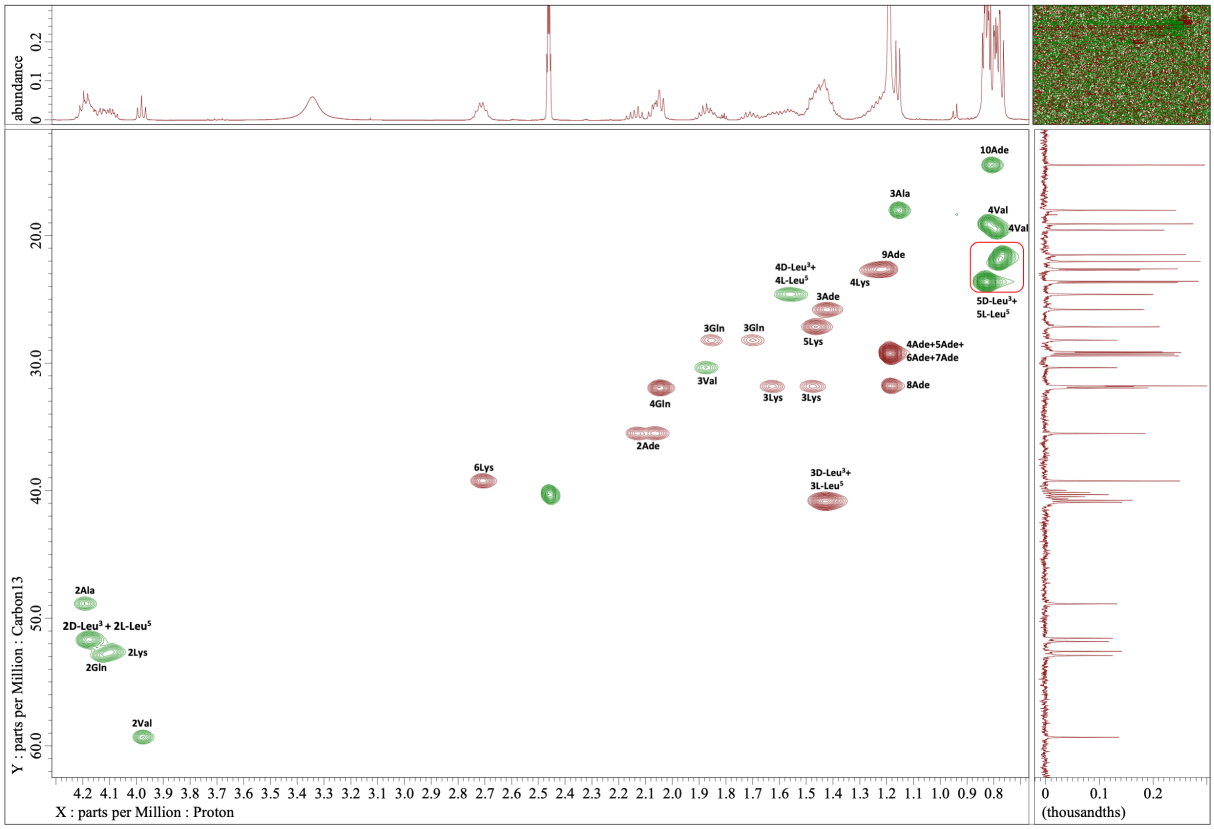

Figure 252. HSQC spectrum of 21a. Solvent : dmso-d_6; T : 23°C; Scans : 8192

k) Compound 22

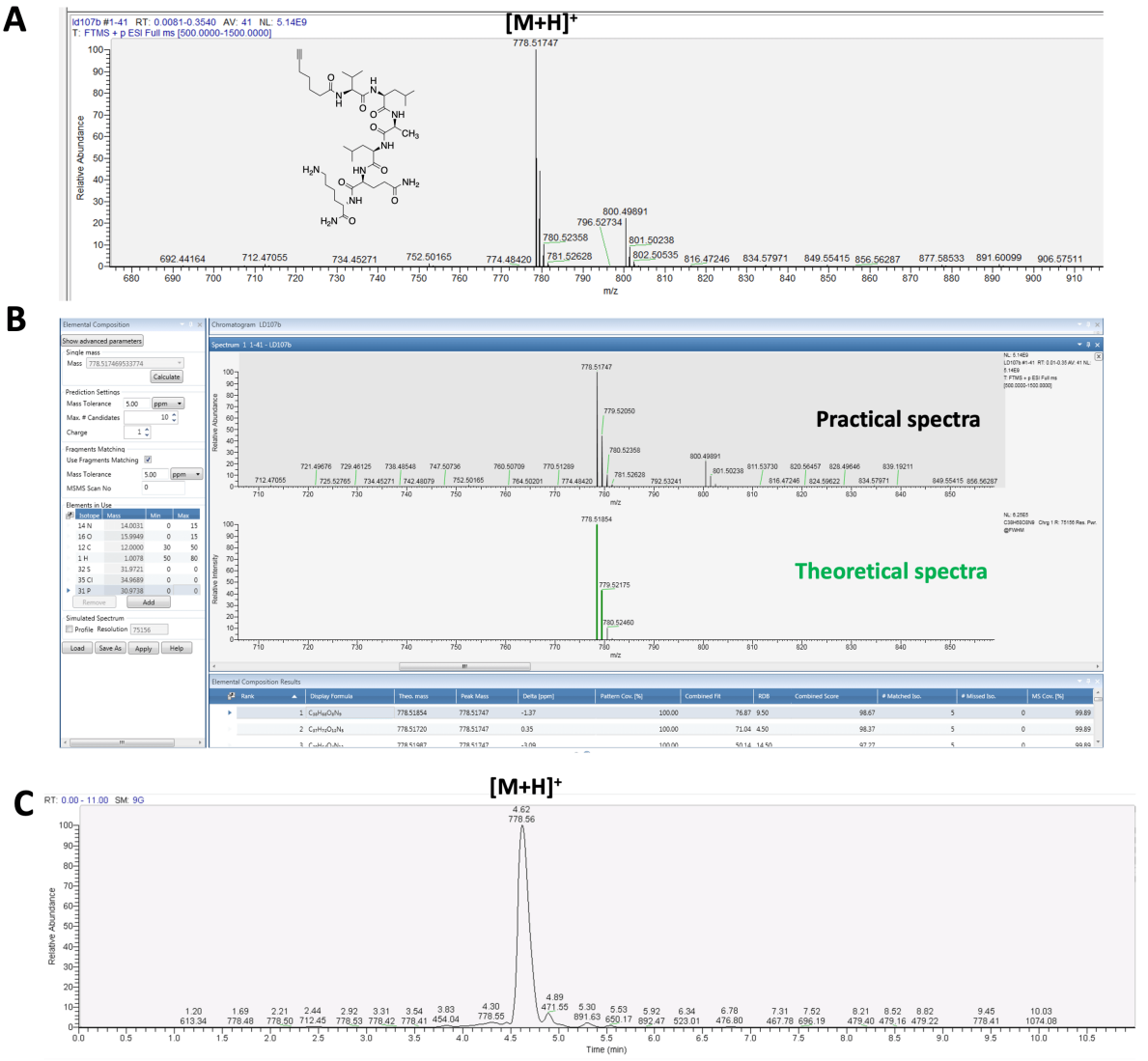

Figure 253. A) ESI-HRMS spectrum of 22. B) Comparison with the theoretical spectrum. Calculated for $C_{38}H_{68}N_9O_8$ $[M+H]^+$ *m/z* 778.51854; Found $[M+H]^+$ *m/z* 778.51747; mass error = 1.37 ppm. C) LC-MS profile of 22.

Table 35. NMR spectroscopic data of 22 in DMSO-d_6

entry	position	C, mult.	H, mult. (J in Hz)	entry	position	C, mult.	H, mult. (J in Hz)
6-heptynoic acid[1]	1	*nd*, C	-	Lys[7]	1	*nd*, C	-
	2	35.1, CH_2	2.13		2	52.7, CH	4.09
	3	25.1, CH_2	1.52		3	31.7, CH_2	1.50
	4	28.0, CH_2	1.37				1.66
	5	18.0, CH_2	2.10		4	22.8, CH_2	1.26
	6	*nd*, C	-		5	27.1, CH_2	1.48
	7	*nd*, CH	nd		6	39.3, CH_2	2.71
Val[2]	1	*nd*, C	-		NH	-	7.76, d (8.02)
	2	58.4, CH	4.09		NH_2	-	7.61
	3	30.7, CH	1.90		NH_2 C-ter	-	7.14 & 7.01
	3-Me	19.7, CH_3	0.79				
	4	18.8, CH_3	0.78				
	NH	-	7.79, d (8.59)				
L-Leu[3]	1	*nd*, C	-				
	2	51.1, CH	4.28				
	3	40.8-41.0, CH_2	1.40				
	4	24.6, CH	1.54				
	4-Me	21.8-23.7, CH_3	0.79-0.83				
	5	21.8-23.7, CH_3	0.79-0.83				
	NH	-	7.89, d (8.02)				
Ala[4]	1	*nd*, C	-				
	2	49.3, CH	4.14				
	3	18.4, CH_3	1.14, d (7.16)				
	NH	-	7.93, d (6.87)				
D-Leu[5]	1	*nd*, C	-				
	2	51.8, CH	4.16				
	3	40.8-41.0, CH_2	1.40				
	4	24.6, CH	1.54				
	4-Me	21.8-23.7, CH_3	0.79-0.83				
	5	21.8-23.7, CH_3	0.79-0.83				
	NH	-	7.98, d (7.45)				
Gln[6]	1	*nd*, C	-				
	2	53.2, CH	4.11				
	3	27.9, CH_2	1.74				
			1.88				
	4	32.0, CH_2	2.05				
	5	*nd*, C	-				
	NH	-	8.10, d (7.16)			*nd* =	not determined
	NH_2	-	7.27 & 6.78				

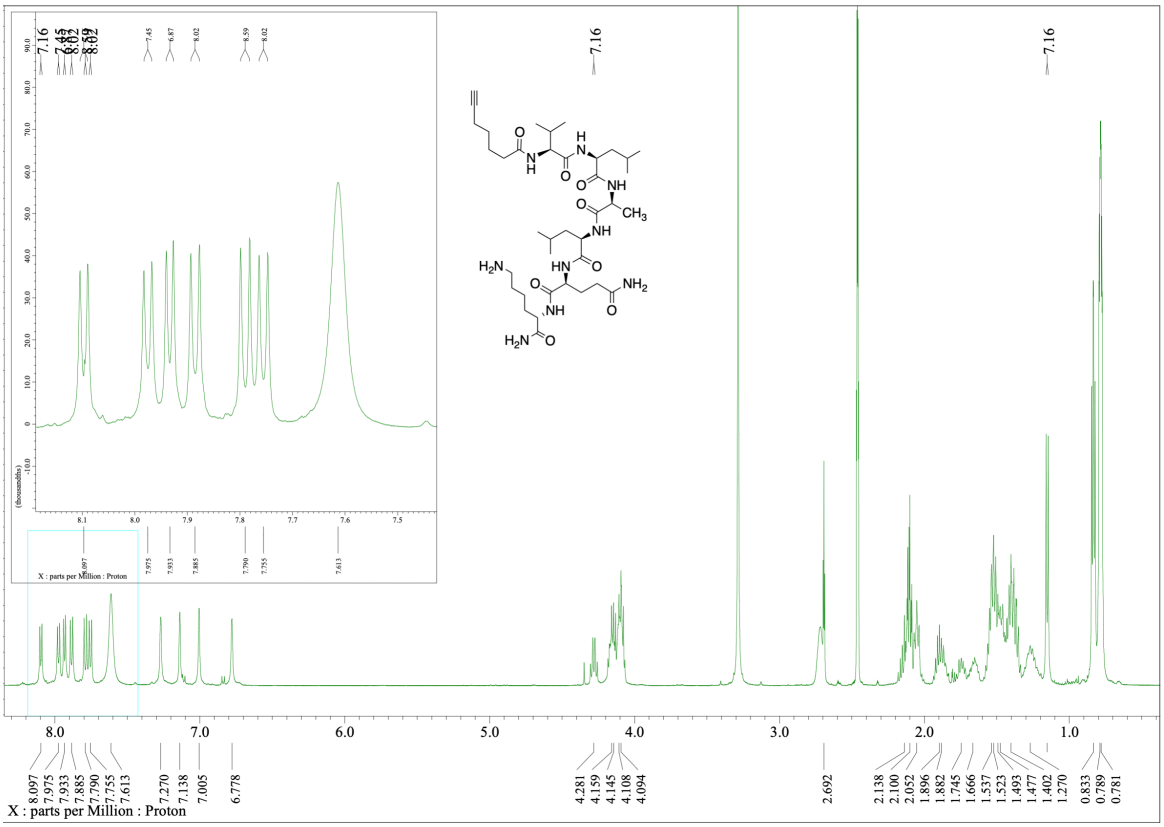

Figure 254. ^{1}H NMR spectrum of 22. Solvent : dmso-d_6; T : 23°C; Scans : 32

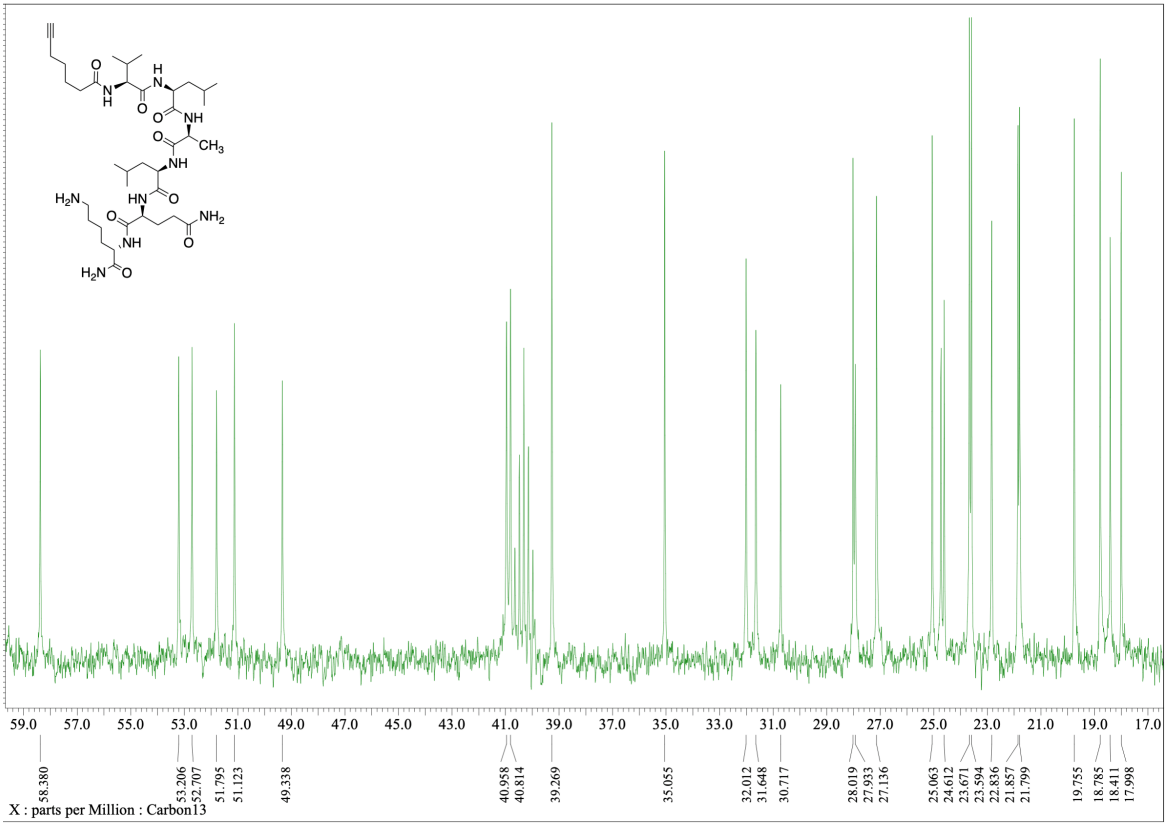

Figure 255. DEPT spectrum of 22. Solvent : dmso-d_6; T : 23°C; Scans : 10000

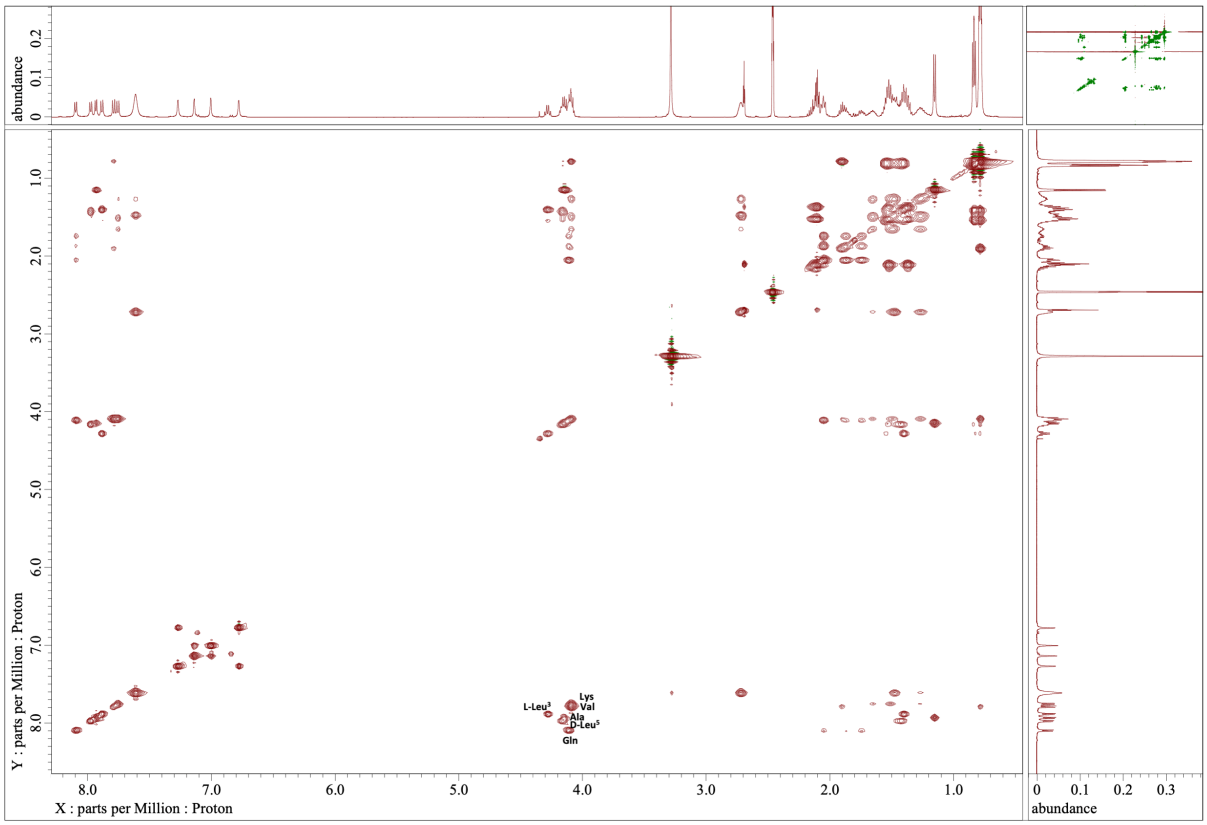

Figure 256. TOCSY spectrum of 22. Solvent : dmso-d_6; T : 23°C; Scans : 8192

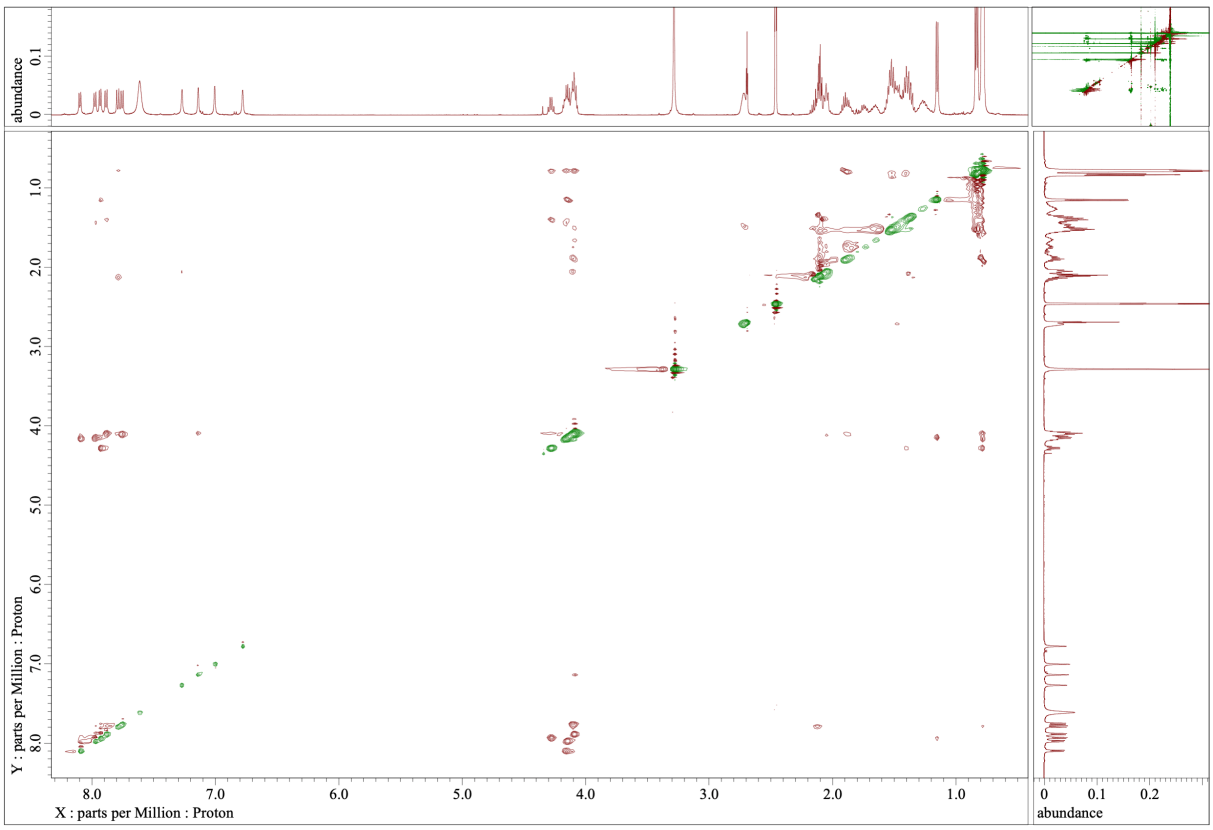

Figure 257. ROESY spectrum of 22. Solvent : dmso-d_6; T : 23°C; Scans : 8192

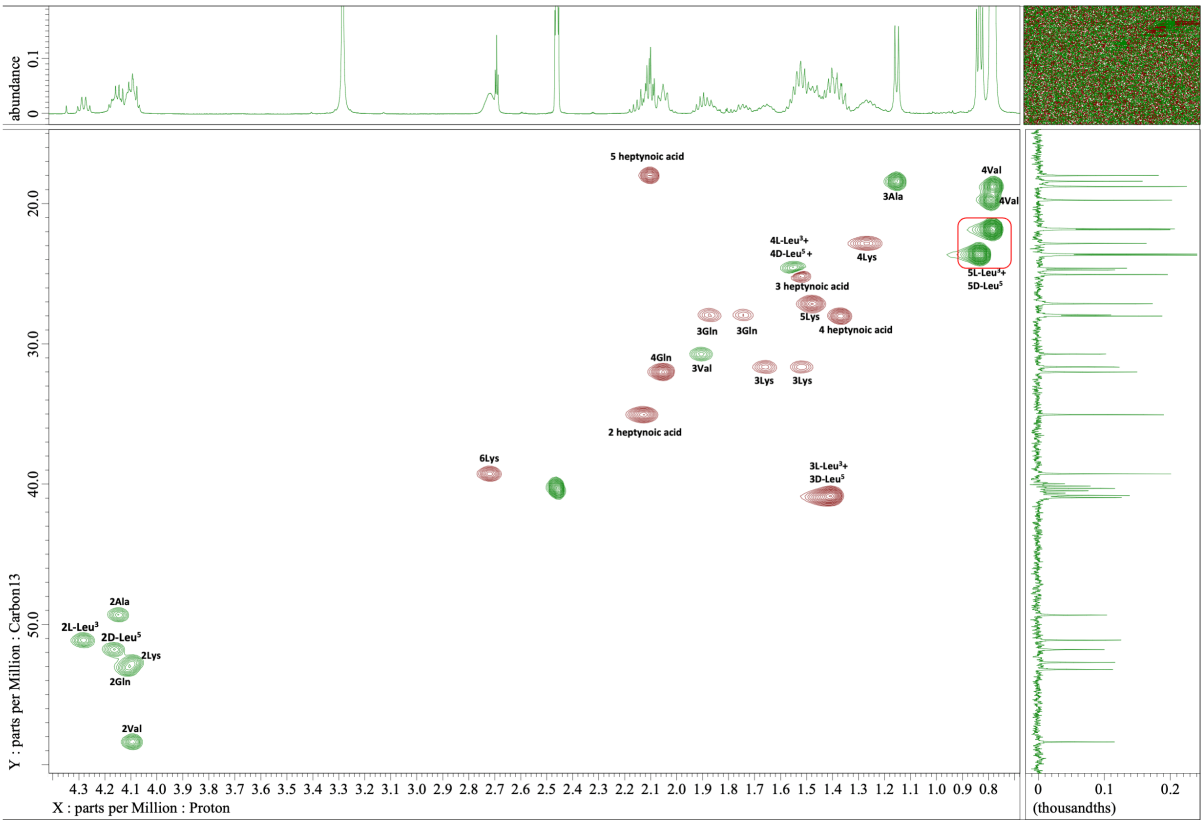

Figure 258. HSQC spectrum of 22. Solvent : dmso-d_6; T : 23°C; Scans : 8192

Chapter 5.
Conclusions and perspectives

I.General conclusion

This thesis project was devoted to the study of the biotransformation of cyclic lipopeptides from the B-type laxaphycin family. The laxaphycins were discovered about thirty years ago and widely characterized and studied for their various toxicological and ecological properties. We have written a synthesis of all these studies in the form of a scientific review published in the journal *Marine Drugs*.

In view of the preliminary results obtained in previous studies on the fate of laxaphycins within the digestive gland of *Stylocheilus striatus*, the hypothesis of the presence of a specific endopeptidase within the mollusk was formulated. The observation of a C-ter cleavage of the two hydroxyleucines of the peptide sequence supported this hypothesis. The primary objective of this thesis project was to build a library of laxaphycin B substrate analogues in order to characterize the activity and specificity of the peptidase. These analogues would allow us to verify the maintenance of the detoxification capacity of laxaphycin B at the identified enzymatic cleavage point. In a second step, the objective was to optimize a peptide sequence from these analogues, which could be used to isolate and characterize the enzyme.

In order to build up a library of laxaphycin B analogues, it was necessary to set up an adequate synthesis strategy. Although the synthesis of laxaphycin B was previously developed by France Boyaud in the same laboratory [47], it was problematic because of the excessive use of 3-aminodecanoic acid (Ade), which is expensive and complex to synthesize. Our goal was to reduce the amount of Ade used, and therefore to graft it first onto a resin in order to recover the ungrafted part. To do so, we grafted Ade on a chlorotrityl resin and we proceeded to the elongation of the peptide on a solid support. The optimization of this synthesis technique revealed a difficulty regarding the coupling of the first amino acids. A guanidylation of the first half of the amino acids of the sequence was observed with the use of classical coupling agents such as DIC or HATU. These coupling problems were solved with the use of PyOxim which does not allow guanidylation. Cyclization in solution was then performed on the unpurified linear peptide retaining its side chain protections. Despite low overall yields due to the complex structure of the peptides, cyclic analogues of laxaphycin B were obtained in yields between 2 and 8%, with purities allowing their use in our enzyme specificity study. The development of this synthesis pathway also allowed to obtain trichormamide C, a laxaphycin B analogue, which can also be isolated from *Oscillatoria* sp. cyanobacteria. The synthesis of this peptide allowed the confirmation of its structure by comparing the NMR analyses of the synthetic molecule with the NMR analyses of the natural molecule already characterized [61]. Our work on trichormamide C synthesis and its analogues led to an article in the journal *Organic Letters*, entitled "Trichormamide C structural confirmation through total synthesis and extension to analogs" and published in December 2019 [30].

This synthesis approach was then applied to obtain different cyclic and acyclic analogues of laxaphycin B. These molecules could be used to obtain first information on the specificity of the studied enzyme. Thus, through different modifications of amino acids within the peptide sequence, we were able to show that the enzyme was able to cleave the peptide in C-ter of two amino acids, in position 3 and 5 of the sequence. This double cleavage can take place in the presence of hydroxyleucine, leucine or threonine at these two positions 3 and 5. The enzyme we are looking for is therefore not specific to hydroxyleucine, and would have a broader spectrum of action, with cleavage on isosteric amino acids of hydroxyleucine. On the other hand, double cleavage occurs only at these two positions, and is not observed with other known classical enzymes used on laxaphycin B. The direction of cleavage could be determined by synthesizing the two possible intermediate peptides, with an opening in position 3 or 5. Thus, the enzyme cleaves first the C-ter of the amino acid in position 5 and then the C-ter of the amino acid in position 3. This result could be confirmed by cleaving linear peptides giving rise to fragments of different masses depending on the cleavage direction. Laxaphycin B would be cleaved first at position 5 and then at position 3. However, we observed the presence of Laxaphycin B cleaved in position 3 (acyclolaxaphycin B), within the cyanobacterium *Anabaena torulosa*, which is contrary to the results obtained. It should be noted that this acyclolaxaphycin B could only be isolated from a single collection of the cyanobacterium, covered by a mucous film suggesting the presence of bacteria. The same acyclolaxaphycin B could not be isolated from other harvesting of *Anabaena torulosa* afterwards. Therefore, it could be thought that bacteria present on the cyanobacterium with a mucous film were involved in the cleavage of laxaphycin B at position 3. However, it is not impossible that there was an error in the interpretation of the NMR spectra during the analysis of acyclolaxaphycin B. To address this hypothesis, acyclolaxaphycin B should be reanalyzed and the NMR spectra compared with synthetic peptides corresponding to the two possible openings.

The study of different synthetic peptides also demonstrated the importance of 3-aminodecanoic acid (Ade) in maintaining the ability of the enzyme to cleave the peptide.
Finally, modification of the stereochemistry of the amino acids at the cleavage sites showed that it was necessary that positions 3 and 5 of the sequence be occupied by amino acids of D configuration. This result allowed us to hypothesize that the enzyme we were looking for was a D-peptidase and this hypothesis could be confirmed by studying other peptides with alternating configurations (D-Leu^3/L-Leu^5 or L-Leu^3/D-Leu^5). D-peptidases are of increasing interest in research because they are suspected to be partly responsible for the increasing resistance of bacteria to antibiotics. This new enzyme is therefore a starting point to provide new information on these specific peptidases. All the important information obtained on the specificity of the enzyme allowed the writing of an article in the *Journal of Medicinal Chemistry*, entitled "D-peptidase activity in a marine mollusk detoxifies a nonribosomal cyclic lipopeptide: an ecological model to study antibiotic resistance" and published in May 2021 [31].

The use of linear peptides positive to cleavage by this enzyme having been demonstrated, we were able to optimize the peptide sequence so that it is as short and simple as possible to synthesize while remaining cleavable by the enzyme. We have thus obtained a sequence ranging from the decanoic acid in position 1 (N-terminal), necessary for the recognition of the substrate by the enzyme for the cleavage, to a lysine in position 7 (C-terminal), allowing a gain in solubility, and a L-Leu^3/D-Leu^5 combination (compound **20**). A first solution to visualize and isolate the enzyme was considered using this peptide optimized with a 6-heptynoic acid replacing the decanoic acid, in order to attach a fluorophore by click chemistry, and a photo-leucine in position 3, in order to attach the enzyme by UV irradiation. Unfortunately, the study of this compound **22** showed that the model peptide had to possess the unmodified decanoic acid comprising 10 carbons in order to be cleaved by the enzyme.

Nevertheless, peptides **19a** and **20a** constitute an interesting basis to consider other strategies to isolate the enzyme. Compound **19c**, obtained from the first cleavage of **19a** in position 5 but not chemically synthesized, is handled by the enzyme for the second cleavage in position 3. The shorter sequence of **19c** is therefore an interesting starting point, as are **19a** and **20a**.

II. Perspectives

Since this project is multidisciplinary, it is possible to consider parallel paths for the further study of this enzyme.

From a chemical point of view, we now have an optimized peptide sequence (compounds **19** and **20**) cleavable by the enzyme, which can allow us to consider different techniques to isolate the enzyme. In order to pursue the idea of coupling the enzyme to the substrate via UV activation of a photoleucine, we could consider adding a residue after the 3-aminodecanoic acid (Ade) to have an alkyne function. Thus, we would keep the long fatty chain of the Ade to ensure the cleavage by the enzyme and thus to consider the coupling of the enzyme with the photoleucine in position 3. The remaining cleaved fragment in position 5 would then be coupled to a fluorophore by click chemistry allowing its visualization by fluorescence. It is then possible to perform a gel purification to recover only the fluorescent part. Using this method, it is first necessary to verify that the peptide remains cleavable with an additional function in N-terminal position.

However, this method is based on whether cleavage is observed or not. But the fact that a peptide is not cleaved by the enzyme does not mean that the peptide is not recognized by the enzyme. It would then be interesting to use internally quenched fluorescent substrates, with competitive tests between inhibitors [170]. It would then be necessary to synthesize an analogue of peptides **19** or **20**, with a quencher in N-terminal position (e.g., Dabcyl or 3-nitrotyrosine) and a fluorescent molecule in C-ter position (e.g., 7-amino-4-carbamoylmethylcoumarin or o-aminobenzamine, respectively). Thus, since the fluorophore and the quencher have overlapping emission and absorption spectra, intramolecular energy

transfer can deactivate the fluorescence of the peptide. On the other hand, when the peptide is cleaved by the enzyme, the fluorophore and the quencher are separated and the fragment of the peptide containing the fluorescent molecule emits a fluorescent signal. This system can be used in solution or on solid support to visualize the fluorescence on resin beads (Figure 259). This peptide can then be deposited on resin beads together with a potential inhibitor peptide. If this peptide is a bad inhibitor, the peptide model will be cleaved by the enzyme and fluorescence will be observed (thanks to a microplate reader for example). If the peptide is a good inhibitor, the peptide will not be cleaved by the enzyme and no fluorescence will be observed. These competitive tests would then allow us to obtain a library of potential inhibitors of the enzyme that we could then functionalize with biotin for example, in order to deposit them on a column including streptavidin, and carry out a purification by affinity chromatography.

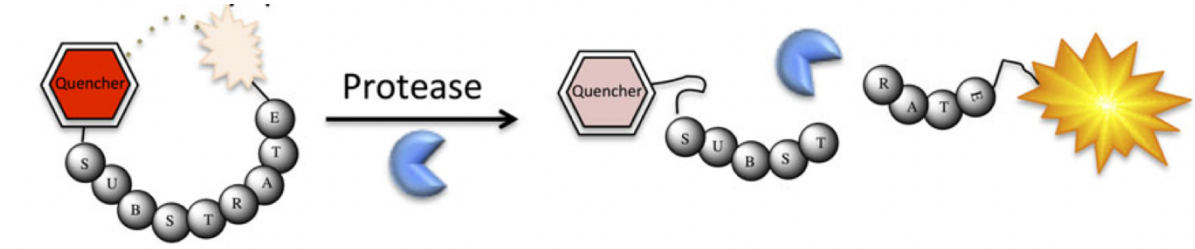

Figure 259. Schematic representation of the proteolysis mechanism of internally quenched fluorescent peptide.

This image was taken from the article of Kasperkiewicz *et al*. [171] (Kasperkiewicz, P.; Poreba, M.; Groborz, K.; Drag, M. Emerging Challenges in the Design of Selective Substrates, Inhibitors and Activity-Based Probes for Indistinguishable Proteases. *Febs J*. 2017, 284, 1518–1539, doi:10.1111/febs.14001.)

As a preliminary experiment, we competed laxaphycin B with some synthetic linear peptides against the enzyme contained in *Dg-Ss-Lm*. For this purpose, we added peptides **12** to **20** and **22** to laxaphycin B in 10-fold molar amounts. The cleavage kinetics of laxaphycin B were evaluated without competitors (control case), and in cases of competition with each peptide. At a 10-fold molar amount relative to laxaphycin B, none of the linear peptides used acted as a total inhibitor of the enzyme since laxaphycin B degradation was observed in all cases. On the other hand, the results obtained are not reported here because the comparison of the cleavage kinetics did not allow us to conclude about the potential competition of each peptide towards laxaphycin B. This experiment could only be performed once and we suspect possible problems related to the analytical equipment, we will therefore have to repeat it in replicate.

From an enzymatic point of view, we plan to study the kinetic constants of the enzyme, K_m and k_{cat}. K_m is the Michaelis constant representing the substrate concentration for which the initial reaction rate is half of the maximum initial rate. The lower K_m is, the more enzymatic activity is reached for a low substrate concentration and thus the higher the affinity of the enzyme for the substrate. K_{cat} is the catalytic constant characterizing the maximum number of substrate molecules transformed per second and per enzyme molecule. For this purpose, the substrate concentration will be varied relative to the enzyme concentration and the increase

in product concentration will be plotted over time. The quasi-steady state will be studied to evaluate the initial rates as a function of each substrate concentration. These results will allow to determine the maximum speed v_{max} as well as the constant K_m corresponding to the concentration when the speed is equal to half of v_{max}. K_{cat} is proportional to v_{max} and to the enzyme concentration. In order to determine the affinity of the enzyme towards different substrates, this study will be performed on laxaphycin B but also on previously synthesized linear peptides.

From a biological point of view, it would be interesting to investigate the origin of the enzyme. Initially, we thought that *Stylocheilus striatus* recovered the enzyme from the cyanobacteria on which it grazed. Indeed, we could observe on some of cyanobacteria a mucous film which could be composed of bacteria. The mollusk being able to detoxify laxaphycin B whether it is harvested on *Anabaena torulosa* (*At*) or on *Lyngbya majuscula* (*Lm*), it would thus be a common bacterium to these cyanobacteria. We verified the cleavage capacity of the digestive gland of a mollusk harvested on algal turf (*Dg-Ss-Turf*), not having been in contact with these two cyanobacteria. The use of *Dg-Ss-Turf* allows indeed to cleave laxaphycin B in the same way as *Dg-Ss-Lm* or *Dg-Ss-At*. The enzyme would therefore be either harvested by the mollusk from its environment, and not necessarily from the cyanobacteria, or produced directly by himself. Furthermore, we cannot be entirely certain that the mollusk collected from the algal turf has never been in contact with cyanobacteria. Therefore, it would be interesting to compare the cleavage capacity of *Stylocheilus striatus* from Moorea in French Polynesia with other *Stylocheilus striatus* from different locations, for example from Réunion where they can also be found, so that the mollusks have a completely different environment.

To go further, the main idea would be to study the microbiome associated with the digestive gland of *Stylocheilus striatus*. To date, there is no study in the literature that deals with the microbial diversity of the digestive gland of *Stylocheilus striatus*. As a first step, the idea will be to verify if the digestive gland of the mollusk has an associated microbiota and to monitor its diversity.

As preliminary results, we compared the enzymatic activity within the different compartments of the mollusk once dissected. For this purpose, we studied the cleavage rate of laxaphycin B when it was mix with the digestive gland of *Stylocheilus striatus* harvested from *Lyngbya majuscula* (*Dg-Ss-Lm*) or with the gizzard of this same mollusk (*Gizz-Ss-Lm*) or with the part containing the mouth and the esophagus (*Mouth-Ss-Lm*). Most of the enzymatic activity was found in the gizzard and the digestive gland, with a slightly faster cleavage rate in the gizzard. Indeed, after 2 hours of incubation, laxaphycin B was cleaved at 92% with *Gizz-Ss-Lm*, at 80% with *Dg-Ss-Lm* and at 43% with *Mouth-Ss-Lm* (Figure 260).

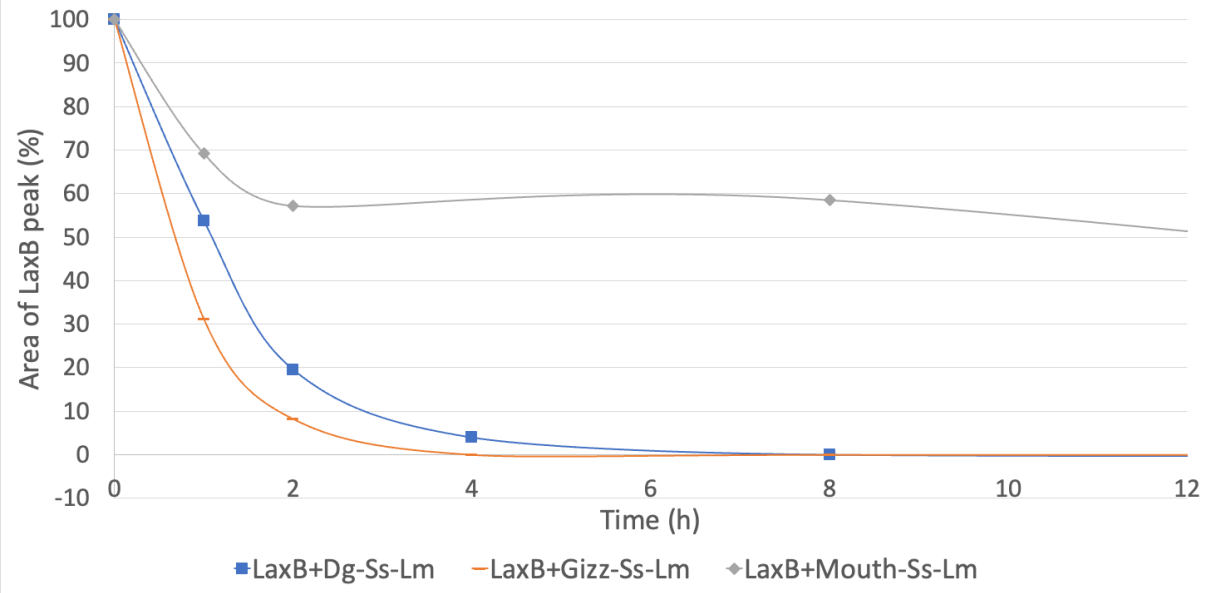

Figure 260. Cleavage rate of laxaphycin B in contact with different organs of the mollusk (Digestive gland, Gizzard or Mouth) as a function of incubation time.

These first results, which will have to be reproduced, will be useful to compare the microbial richness of each organ and to see if it is possible to reveal important differences between the bacteria found.
Furthermore, we would like to compare the bacteria found in the mollusk with the potential bacteria found on the cyanobacteria. Finally, if it is possible to collect mollusks from a different location than Moorea, and if these mollusks are not able to detoxify laxaphycin B, it would also be interesting to compare the bacteria present or not in the digestive tract of these mollusks coming from different places, in order to discriminate some bacteria.

It is possible that sequencing brings us many different data that are difficult to process and discriminate since we have no information about the enzyme we are looking for. To date, very few peptidases capable of cleaving cyclic peptides have been described in the literature [172,173]. To our knowledge, only microcystinase, cleaving cyclopeptides of the microcystin family, has been more extensively described [25,26]. Concerning D-peptidases, they are found in a large number of bacteria, according to a recent genome mining study [168]. This is the case of BogQ and TriF presented in chapter 3, which cleave the linear peptides bogorol and tridecaptin in C-ter of D-amino amides. BogQ is also able to cleave bacitracin, a cyclic lipopeptide. Without deactivating the peptide itself, D-peptidases have been described as modifying the target of the vancomycin peptide. Vancomycin binds to lipid II consisting of a D-Ala-D-Ala region, thus preventing the maturation of the peptidoglycan layer composing the bacterial cell wall. The described D-peptidases VanX and VanY cleave this region composed of D-Ala, thus preventing vancomycin from binding to its target [174]. The few D-peptidases described are of bacterial origin, with a predominance of Firmicutes [168]. In case the bacterial pool contained in the mollusk digestive gland would be consequent, the research priority would therefore be on these Firmicutes, if present.

Supporting Information

This appendix includes information on the chromatographic and analytical equipments used and their parameters of use, as well as the protocols generalized to all the previous chapters (preparation of the extracts of digestive gland of the mollusk, quantification of proteins).

Instruments used

Peptide synthesizer

Linear peptides were synthesized thanks to an automated Microwave Peptide Synthesizer CEM Liberty One equipped with a UV detector to monitor coupling rates.

LCMS

LC-MS analyses were carried out with a Thermo Fisher Scientific LC-MS device, Accela HPLC coupled to a LCQ Fleet fitted with an electrospray ionization source and a 3D ion-trap analyzer. Columns used were Phenomenex BioZen™ and Aeris™ 2.6 µm Peptide XB-C18 (LC Column 50x2.1 mm). Elution was made with ACN (0.1 % FA) in H_2O (0.1 % FA) at a flow rate of 0.5 mL/min for a 10 µL injection.

Tune parameters for LC-MS injections are as follows:

ESI Source	**Values**	**Ions optics**	**Values**
Sheath Gas Flow Rate (arb)	25	RF Lens offset (V)	-2.75
Aux Gas Flow Rate (arb)	10	Lens 0 Voltage (V)	-5.5
Sweep Gas Flow Rate (arb)	1	Multipole 0 offset (V)	-8.5
Spray Voltage (kV)	4.5	Lens 1 Voltage (V)	-13
Spray current (µA)	0.12	Gate Lens Voltage (V)	-48
Capillary Temperature (°C)	290	Multipole 1 offset (V)	-19
Capillary Voltage (V)	33	Multipole RF Amplitude (V p.p)	400
Tube Lens (V)	80	Front Lens (V)	-65.93

Here are parameters of the method used for LC-MS analysis of purified compounds:

Autosampler	**Values**	**Pump**	**Values**
Injection volume (μL)	10	Pressure (bar)	From 10 to 600
Flush volume (μL)	400	Pressure stability (bar)	10
Wash volume (μL)	1000	**MS detector**	**Values**
Tray temperature (°C)	20	Mass range (m/z)	From 100 to 2000
Column oven temperature (°C)	30	Scan Type	Full
PDA Detector	**Values**	Polarity	Positive/Negative
Wavelength (nm)	From 200 to 600	Data Type	Centroid
Channels (nm)	214 and 254	Source Fragmentation	NO

Intermediate compounds were analyzed by direct infusion on the same LC-MS device with a flow rate of 10 μL/min. Tune parameters for LC-MS direct infusions are as follows:

ESI Source	**Values**	**Ions optics**	**Values**
Sheath Gas Flow Rate (arb)	5	RF Lens offset (V)	-7.25
Aux Gas Flow Rate (arb)	1	Lens 0 Voltage (V)	-7.5
Sweep Gas Flow Rate (arb)	0	Multipole 0 offset (V)	-7.75
Spray Voltage (kV)	4.5	Lens 1 Voltage (V)	-10
Spray current (μA)	0.02	Gate Lens Voltage (V)	-46
Capillary Temperature (°C)	290	Multipole 1 offset (V)	-10
Capillary Voltage (V)	33	Multipole RF Amplitude (V p.p)	400
Tube Lens (V)	80	Front Lens (V)	-55.93

HRESI-MS

High resolution mass spectra were recorded through direct infusion on a ThermoFisher Q Exactive Plus spectrometer.

Tune parameters for HRESI-MS direct infusions are as follows:

HESI Source	**Values**	**Scan parameters**	**Values**
Sheath Gas Flow Rate (arb)	10	Scan type	Full MS
Aux Gas Flow Rate (arb)	0	Scan range	500 to 2000
Sweep Gas Flow Rate (arb)	0	Fragmentation	NO
Spray Voltage (kV)	3.2	Resolution	140000
Spray current (μA)	0.02	Polarity	Positive
Capillary Temperature (°C)	300	Microscans	1
Aux Gas Heater Temperature (°C)	50	AGC target	10^6

Semi-preparative HPLC purification

Semi-preparative purification of cyclic peptides was performed using a Waters 1525 chromatography system fitted with a Waters 2487 tunable absorbance detector with detection at 214 nm and 254 nm. Purification was performed by eluting ACN (0.1% FA) in H_2O (0.1% FA). The column used was a GRACE Vydac C-18 column (250x10 mm, 5 μm) at a flow rate of 3 mL/min.

NMR

All spectra were recorded on a JEOL JNM-ECZR 500 MHz spectrometer equipped with the ROYAL probe covering the frequency ranges from ^{1}H / ^{19}F to ^{109}Ag and ^{31}P. Peptides were all analyzed in DMSO-d_6 purchased from Eurisotop. The concentration of peptides was around 7 mg/mL, but only 2.5 mg/mL for the most complex compounds to obtain, such as cyclic peptides. The field strength used was 11.7 T and the analysis temperature was 23°C.

Number of scans for each analysis :
1H : 32 scans
13C : 20000 scans
DEPT : 10000 scans
COSY-TOCSY-ROESY-HSQC : 8192 scans
HMBC : 16384 scans

Spectra were processed and visualized with JEOL software Delta 5.3.0.

Mollusk harvesting, dissection and solid-liquid extraction

Adult specimens of *Stylocheilus striatus* were collected from either the lagoon of Moorea Island (Society Archipelago, French Polynesia) or from populations residing in flow-through aquaria at the University of California Gump Field Research Station situated in Moorea. Specimens obtained from the lagoon were collected at depths of 1-4 m within large cyanobacterial blooms of either *Lyngbya majuscula* or *Anabaena torulosa* on sandy substrates. Animals were transferred in cool boxes within 3 hours of collection into outdoor, flow-through aquaria (40 L) supplied with oxygenated running seawater (0.5 L/min) at CRIOBE. Sea hares were starved for 48 hours prior to dissection to ensure that all food items had been digested and excreted.

Opisthobranches were dissected following cold anesthesia at 4 °C for 20 minutes. A shallow incision was made through the mantle, ventrally from the head to tail. The mantle was removed to expose all internal organs (Figure 261 (A)). The internal organs were then dissected to expose the mouth and buccal mass, gizzard, digestive gland, ovo-testis, hermaphroditic duct, and mucus and albumin gland (Figure 261 (B)). Each body segment was placed individually into labeled 1.5 mL Eppendorfs and immediately frozen and stored at −20 °C. Ethical approval for the study was granted from The Animal Ethics Committee, Centre National de la Recherche Scientifique (permit number 006725).

Dissected digestive glands were stored into Eppendorfs tubes and immersed in liquid nitrogen. Eppendorfs tubes were then placed in a Silamat S6 mill (from Ivoclar vivadent) with 8 glass beads. 4 minimum cycles of alternation between liquid nitrogen and grinding were chained. After several cycles of 8 seconds, the whole sample was completely ground. The buffer (50 mM Tris, pH 8) was added and then solutions were mixed by vortexing. Mixtures were centrifuged at 4°C for 20 minutes at 21,952 x *g*. The supernatants of the centrifuged solutions were recovered and placed in aliquots. Solutions were stored at −25°C.

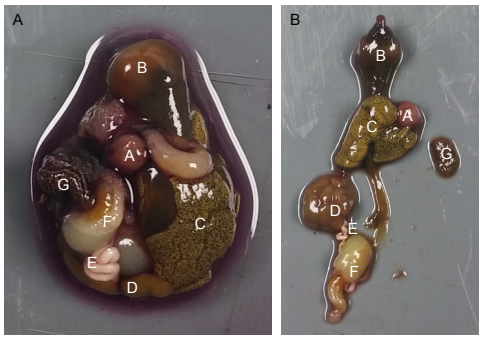

Figure 261. External (A) and internal (B) structures of the sea hare *Stylocheilus striatus*. A) Mouth and buccal mass. B) Gizzard. C) Digestive gland. D) Ovo-testis. E) hermaphroditic duct. F) Mucus and albumin gland. G) Mantle.

Protein quantification by the Bradford method

Preparation of the standard range:

We have at our disposal a stock solution of BSA (bovine serum albumin) at 10 mg/mL.

The stock solution of BSA was diluted 50 times in H_2O milliQ (4 µL of stock BSA +196 µL of H_2O milliQ). The new BSA solution is therefore 0,2 mg/mL.

We used disposable plastic cuvettes for spectrophotometer (Plastibrand, 70 L micro, 12.5 x 12.5 x 45 mm). The preparation of the BSA standard range was as follows (amount of BSA solution at 0.2 mg/mL in red, amount of H_2O milliQ in green, amount of Bradford's solution in blue, resulted BSA concentration in cuvettes in black):

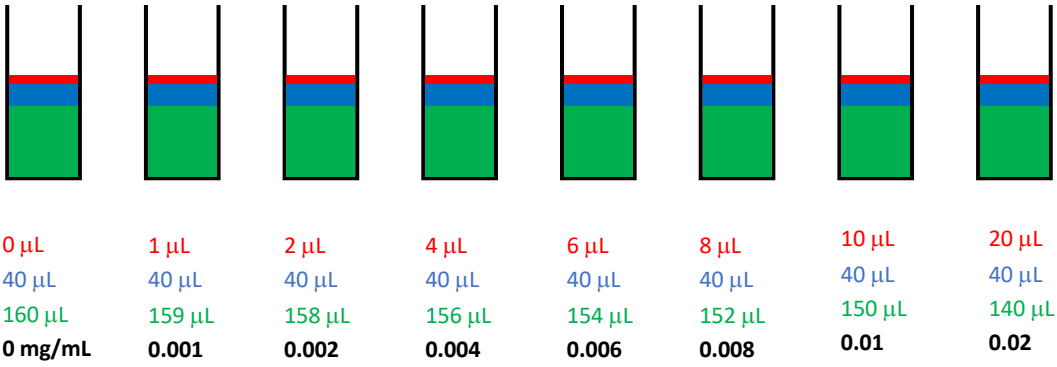

Figure 262. Preparation of the BSA standard range

Bradford's solution was purchased from Bio-Rad.

The cuvettes must be well mixed and bubble-free for measurement. The spectrophotometer used is an Eppendorf BioPhotometer with a single beam. In a first step, it is necessary to calibrate the instrument with standard solutions containing BSA that were prepared earlier. The first cuvette that does not contain BSA was analyzed and assimilated to the "blank" solution. Then other cuvettes of the range were analyzed one by one and represent "standard" solutions. The instrument displays the absorbance of the solutions contained in the cuvettes and assimilates it to the protein quantities indicated previously in the parameters of the spectrophotometer. Absorbance values obtained provide a linear calibration curve.

Preparation of the samples to be assayed:

Each digestive gland extract is diluted 50 times (1 µL in 50 µL of H_2O milliQ). The cuvettes are then prepared as follows (amount of extract diluted solution in red, H_2O milliQ in green, amount of Bradford's solution in blue). If the results obtained are outside the linearity of the model, amounts of extract are adjusted:

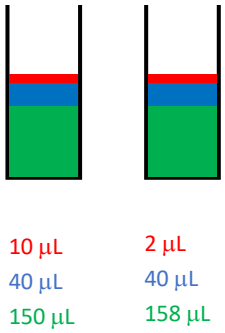

Figure 263. Preparation of the samples to be assayed.

It is then possible to determine the amount of protein contained in the digestive gland extracts.

Structures of studied peptides

Hereafter is a summary table of the structures of all the peptides studied in this manuscript. The amino acid sequences are reported from positions 1 to 12 as presented in the structures throughout the manuscript. All peptides were obtained by chemical synthesis, except peptides 1, 2 and 3, directly isolated from cyanobacteria. Laxaphycin A is the negative control, which is not cleaved by the enzyme, since this peptide has a completely different structure from B-type laxaphycins. Laxaphycin B is the positive control and all analogues are derived from this starting peptide. A "cleavage" column indicates whether the peptide could be cleaved upon contact with *Dg-Ss-Lm* or not.

Table 36. Summary of amino acid sequences of all peptides studied.

Orange boxes show amino acids that were never modified, compared to the laxaphycin B sequence. Striped boxes show amino acids in the N-ter and C-ter positions of linear peptides. Aoc: 3-aminooctanoic acid, Ade: 3-aminodecanoic acid, Hse: homoserine, Dhb: dehydrobutyrine, Hyp: hydroxyproline. Hle: hydroxyleucine, (N)-MeIle: N-methylisoleucine, Hasn: hydroxyasparagine.

Compounds	1	2	3	4	5	6	7	8	9	10	11	12	Cyclic/Linear	Cleavage
1 = Laxaphycin A	Aoc	Hse	E-Dhb	(2S,4R)Hyp	Hse	(2R)Phe	(2R)Leu	Ile	(2R,3S)Ile	Leu	Gly		Cyclic	NO
2 = Laxaphycin B	Ade	Val	(2R,3S)Hle	Ala	(2R,3S)Hle	Gln	(N)-MeIle	(2R,3R)Hasn	Thr	Pro	(2R)Leu	Thr	Cyclic	YES
3 = Laxaphycin B2	Ade	Val	(2R,3S)Hle	Ala	(2R)Leu	Gln	(N)-MeIle	(2R,3R)Hasn	Thr	Pro	(2R)Leu	Thr	Cyclic	YES
4 = Trichormamide C	Ade	Val	(2R,3S)Hle	Ala	(2R,3S)Hle	Gln	(N)-MeIle	(2R)Asn	Thr	Pro	(2R)Leu	Thr	Cyclic	YES
5	Ade	Val	(2R)Leu	Ala	(2R)Leu	Gln	(N)-MeIle	(2R)Asn	Thr	Pro	(2R)Leu	Thr	Cyclic	YES
5b	Ade	Val	(2R)Leu	Ala	(2R)Leu	Gln	(N)-MeIle	(2R)Asn	Thr	Pro	(2R)Leu	Thr	Linear	YES
5d	Ade	Val	(2R)Leu	Ala	(2R)Leu	Gln	(N)-MeIle	(2R)Asn	Thr	Pro	(2R)Leu	Thr	Linear	YES
6	Ade	Val	(2R)Thr	Ala	(2R)Thr	Gln	(N)-MeIle	(2R)Asn	Thr	Pro	(2R)Leu	Thr	Cyclic	YES
7	Decanoic acid	Val	(2R)Leu	Ala	(2R)Leu	Gln	(N)-MeIle	(2R)Asn	Thr	Pro	(2R)Leu	Thr	Linear	YES
8	β-Ala	Val	(2R)Leu	Ala	(2R)Leu	Gln	(N)-MeIle	(2R)Asn	Thr	Pro	(2R)Leu	Thr	Cyclic	NO
9	Ade	Val	Leu	Ala	Leu	Gln	(N)-MeIle	(2R)Asn	Thr	Pro	(2R)Leu	Thr	Cyclic	NO
10	Decanoic acid	Val	Leu	Ala	(2R)Leu	Gln	(N)-MeIle	(2R)Asn	Thr	Pro	(2R)Leu	Thr	Linear	YES
11	Decanoic acid	Val	(2R)Leu	Ala	Leu	Gln	(N)-MeIle	(2R)Asn	Thr	Pro	(2R)Leu	Thr	Linear	YES
12		Ac-Val	(2R)Thr	Ala	(2R)Thr								Linear	NO
13		Ac-Val	(2R)Leu	Ala	(2R)Leu								Linear	NO
14				Ac-Ala	(2R)Thr	Gln	(N)-MeIle						Linear	NO
15	Decanoic acid	Val	(2R)Leu	Ala	(2R)Leu	Gln	(N)-MeIle	(2R)Asn					Linear	YES
16	β-Ala	Val	(2R)Leu	Ala	(2R)Leu	Gln	(N)-MeIle	(2R)Asn					Linear	NO
17	Decanoic acid	Val	(2R)Leu	Ala	(2R)Leu	Gln							Linear	YES
18	Decanoic acid	Val	(2R)Thr	Ala	(2R)Thr	Gln	Lys						Linear	YES
19	Decanoic acid	Val	(2R)Leu	Ala	(2R)Leu	Gln	Lys						Linear	YES
20	Decanoic acid	Val	Leu	Ala	(2R)Leu	Gln	Lys						Linear	YES
21	Decanoic acid	Val	(2R)Leu	Ala	Leu	Gln	Lys						Linear	YES
22	6-heptynoic acid	Val	Leu	Ala	(2R)Leu	Gln	Lys						Linear	NO

Table 37. Structures of the studied peptides 1-6 according to their cleavage state.

The blue boxes show peptides isolated from natural extracts but not synthesized. The orange boxes represent synthesized peptides. The green boxes are the peptides observed in LC-MS. The yellow boxes are the peptides assumed according to the results obtained on other peptides.

	a	b	c	d
1	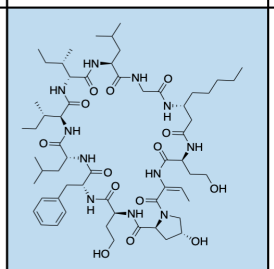			
2	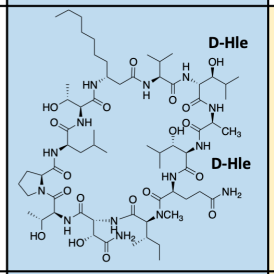	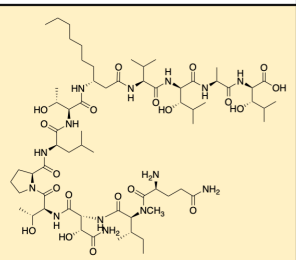	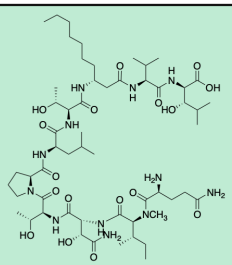	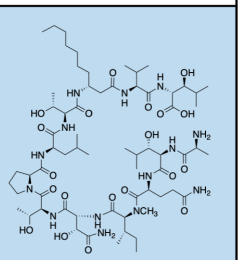
3	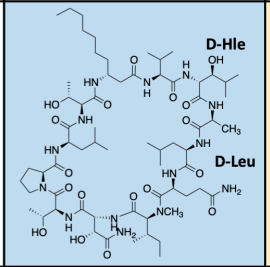	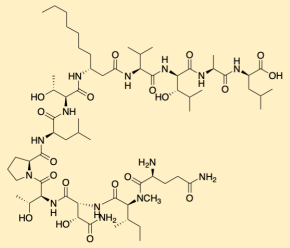	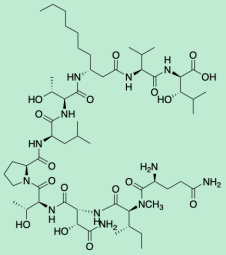	
4	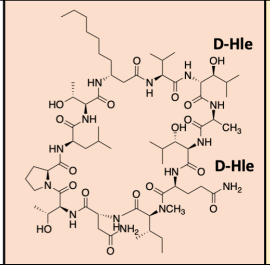	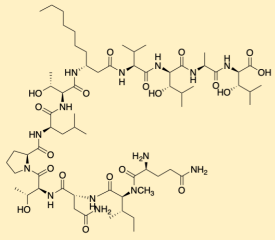	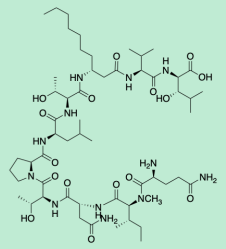	
5	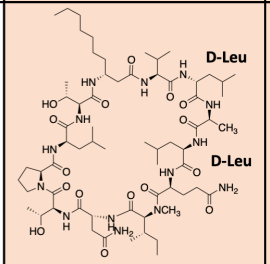	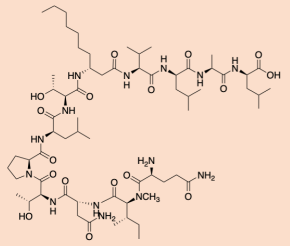	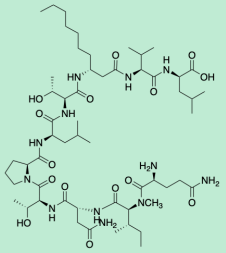	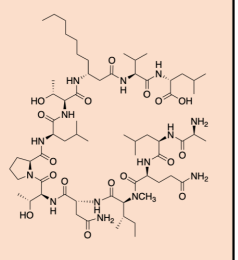
6	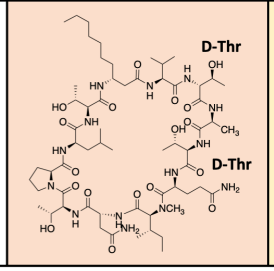	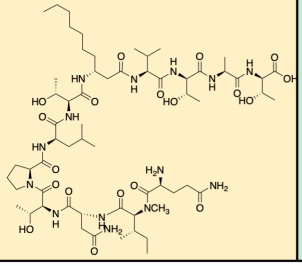	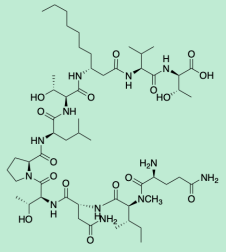	

Table 38. Structures of the studied peptides 7-14 according to their cleavage state.

The orange boxes represent synthesized peptides. The green boxes are the peptides observed in LC-MS.

	a	b	c	d	e
7	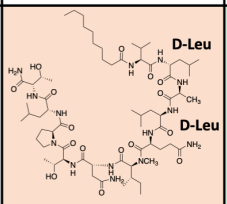	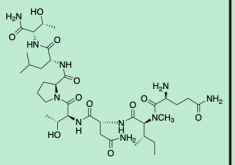	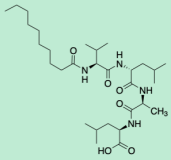	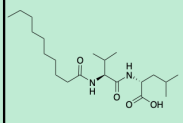	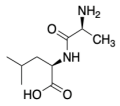
8	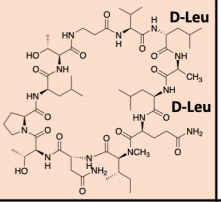				
9	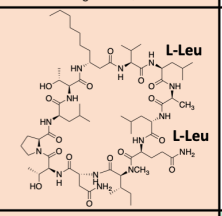				
10	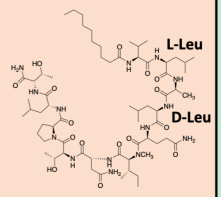	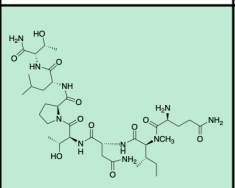	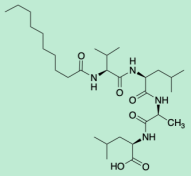		
11	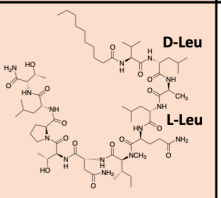	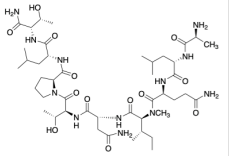	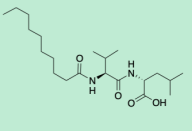		
12	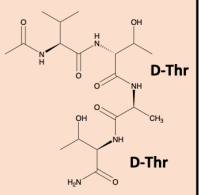				
13	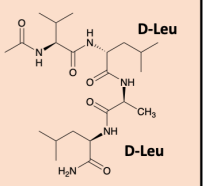				
14	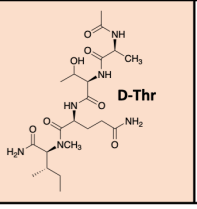				

Table 39. Structures of the studied peptides 15-22 according to their cleavage state.

The orange boxes represent synthesized peptides. The green boxes are the peptides observed in LC-MS.

	a	b	c	d	e
15	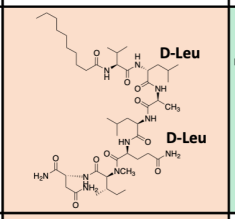	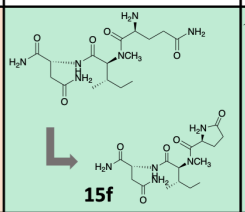	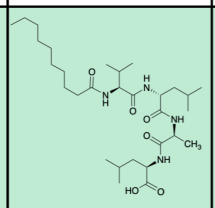	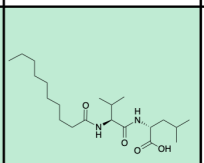	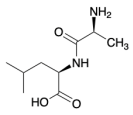
16	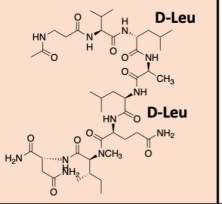				
17	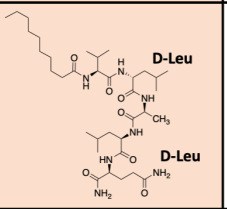	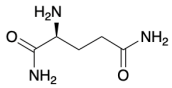	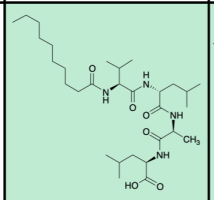	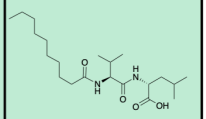	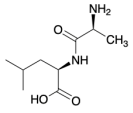
18	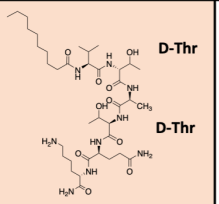	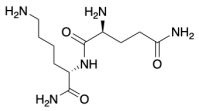	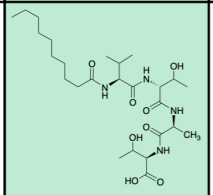		
19	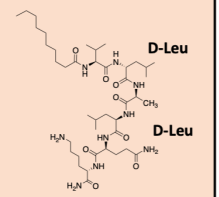	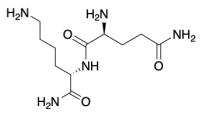	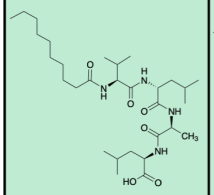	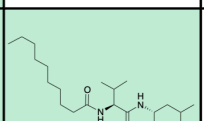	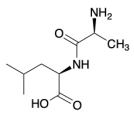
20	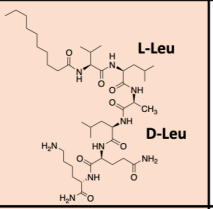	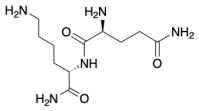	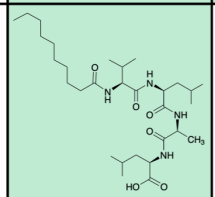		
21	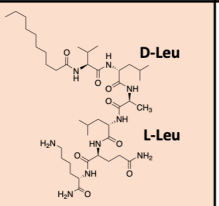	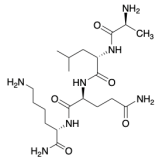	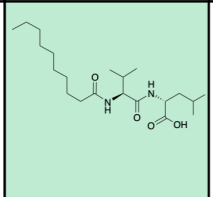		
22	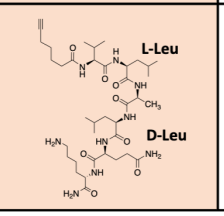				

References

1. Holtrop, T.; Huisman, J.; Stomp, M.; Biersteker, L.; Aerts, J.; Grébert, T.; Partensky, F.; Garczarek, L.; Woerd, H.J. van der Vibrational Modes of Water Predict Spectral Niches for Photosynthesis in Lakes and Oceans. *Nat. Ecol. Evol.* **2021**, *5*, 55–66, doi:10.1038/s41559-020-01330-x.

2. Paerl, H.W.; Hall, N.S.; Calandrino, E.S. Controlling Harmful Cyanobacterial Blooms in a World Experiencing Anthropogenic and Climatic-Induced Change. *Sci. Total Environ.* **2011**, *409*, 1739–1745, doi:10.1016/j.scitotenv.2011.02.001.

3. Jochimsen, E.M.; Cookson, S.T. Liver Failure and Death after Exposure to Microcystins at a Hemodialysis Center in Brazil. *N. Engl. J. Med.* **1998**, *338*, 873–878, doi:10.1056/NEJM199803263381304.

4. Stewart, I.; Webb, P.M.; Schluter, P.J.; Shaw, G.R. Recreational and Occupational Field Exposure to Freshwater Cyanobacteria – a Review of Anecdotal and Case Reports, Epidemiological Studies and the Challenges for Epidemiologic Assessment. *Environ. Health* **2006**, *5*, doi:10.1186/1476-069X-5-6.

5. Giannuzzi, L.; Sedan, D.; Echenique, R.; Andrinolo, D. An Acute Case of Intoxication with Cyanobacteria and Cyanotoxins in Recreational Water in Salto Grande Dam, Argentina. *Mar. Drugs* **2011**, *9*, 2164–2175, doi:10.3390/md9112164.

6. Hay, M.E.; Dufy, J.E.; Paul, V.J.; Renaud, P.E.; Fenical, W. Specialist Herbivores Reduce Their Susceptibility to Predation by Feeding on the Chemically Defended Seaweed Avrainvillea Longicaulis. *Limnol. Oceanogr.* **1990**, *35*, 1734–1743, doi:10.4319/lo.1990.35.8.1734.

7. Baumgartner, F.; Motti, C.; de Nys, R.; Paul, N. Feeding Preferences and Host Associations of Specialist Marine Herbivores Align with Quantitative Variation in Seaweed Secondary Metabolites. *Mar. Ecol. Prog. Ser.* **2009**, *396*, 1–12, doi:10.3354/meps08359.

8. Bonnard, I.; Bornancin, L.; Dalle, K.; Chinain, M.; Zubia, M.; Banaigs, B.; Roué, M. Assessment of the Chemical Diversity and Potential Toxicity of Benthic Cyanobacterial Blooms in the Lagoon of Moorea Island (French Polynesia). *J. Mar. Sci. Eng.* **2020**, *8*, 406, doi:10.3390/jmse8060406.

9. Osborne, N.J.T.; Webb, P.M.; Shaw, G.R. The Toxins of Lyngbya Majuscula and Their Human and Ecological Health Effects. *Environ. Int.* **2001**, *27*, 381–392, doi:10.1016/S0160-4120(01)00098-8.

10. Cruz-Rivera, E.; Paul, V.J. Coral Reef Benthic Cyanobacteria as Food and Refuge: Diversity, Chemistry and Complex Interactions.; Bali, Indonesia, October 2000; Vol. 1.

11. Cruz-Rivera, E.; Paul, V.J. Chemical Deterrence of a Cyanobacterial Metabolite against Generalized and Specialized Grazers. *J. Chem. Ecol.* **2006**, *33*, 213–217, doi:10.1007/s10886-006-9212-y.

12. Capper, A.; Tibbetts, I.R.; O'Neil, J.M.; Shaw, G.R. The Fate of *Lyngbya Majuscula*

Toxins in Three Potential Consumers. *J. Chem. Ecol.* **2005**, *31*, 1595–1606, doi:10.1007/s10886-005-5800-5.

13. Capper, A.; Cruz-Rivera, E.; Paul, V.J.; Tibbetts, I.R. Chemical Deterrence of a Marine Cyanobacterium against Sympatric and Non-Sympatric Consumers. *Hydrobiologia* **2006**, *553*, 319–326, doi:10.1007/s10750-005-1129-x.

14. Kamio, M.; Derby, C.D. Finding Food: How Marine Invertebrates Use Chemical Cues to Track and Select Food. *Nat. Prod. Rep.* **2017**, *34*, 514–528, doi:10.1039/C6NP00121A.

15. Hay, M.E.; Pawlik, J.R.; Duffy, J.E.; Fenical, W. Seaweed-Herbivore-Predator Interactions: Host-Plant Specialization Reduces Predation on Small Herbivores. *Oecologia* **1989**, *81*, 418–427, doi:10.1007/BF00377093.

16. Bornancin, L. Lipopeptides from Cyanobacteria : structure and role in a trophic cascade. Doctoral dissertation, University of Montpellier, 2016.

17. Bornancin, L.; Bonnard, I.; Mills, S.C.; Banaigs, B. Chemical Mediation as a Structuring Element in Marine Gastropod Predator-Prey Interactions. *Nat. Prod. Rep.* **2017**, *34*, 644–676, doi:10.1039/C6NP00097E.

18. Bornancin, L.; Boyaud, F.; Mahiout, Z.; Bonnard, I.; Mills, S.C.; Banaigs, B.; Inguimbert, N. Isolation and Synthesis of Laxaphycin B-Type Peptides: A Case Study and Clues to Their Biosynthesis. *Mar. Drugs* **2015**, *13*, 7285–7300, doi:10.3390/md13127065.

19. Bornancin, L.; Alonso, E.; Alvariño, R.; Inguimbert, N.; Bonnard, I.; Botana, L.M.; Banaigs, B. Structure and Biological Evaluation of New Cyclic and Acyclic Laxaphycin-A Type Peptides. *Bioorg. Med. Chem.* **2019**, *27*, 1966–1980, doi:10.1016/j.bmc.2019.03.046.

20. Bonnard, I.; Rolland, M.; Salmon, J.-M.; Debiton, E.; Barthomeuf, C.; Banaigs, B. Total Structure and Inhibition of Tumor Cell Proliferation of Laxaphycins. *J. Med. Chem.* **2007**, *50*, 1266–1279, doi:10.1021/jm061307x.

21. Jones, A.C.; Monroe, E.A.; Eisman, E.B.; Gerwick, L.; Sherman, D.H.; Gerwick, W.H. The Unique Mechanistic Transformations Involved in the Biosynthesis of Modular Natural Products from Marine Cyanobacteria. *Nat. Prod. Rep.* **2010**, *27*, 1048, doi:10.1039/c000535e.

22. Vitalis, T.Z.; Spence, M.J.; Carefoot, T.H. The Possible Rôle of Gut Bacteria in Nutrition and Growth of the Sea Hare *Aplysia*. *The Veliger* **1988**, *30*, 333–341.

23. Bourne, D.G.; Jones, G.J.; Blakeley, R.L.; Jones, A.; Negri, A.P.; Riddles, P. Enzymatic Pathway for the Bacterial Degradation of the Cyanobacterial Cyclic Peptide Toxin Microcystin LR. *Appl. Environ. Microbiol.* **1996**, *62*, 4086–4094, doi:10.1128/AEM.62.11.4086-4094.1996.

24. Dziga, D.; Wladyka, B.; Zielińska, G.; Meriluoto, J.; Wasylewski, M. Heterologous Expression and Characterisation of Microcystinase. *Toxicon* **2012**, *59*, 578–586, doi:10.1016/j.toxicon.2012.01.001.

25. Xu, Q.; Fan, J.; Yan, H.; Ahmad, S.; Zhao, Z.; Yin, C.; Liu, X.; Liu, Y.; Zhang, H. Structural Basis of Microcystinase Activity for Biodegrading Microcystin-LR. *Chemosphere* **2019**, *236*, doi:10.1016/j.chemosphere.2019.07.012.

26. Dexter, J.; McCormick, A.J.; Fu, P.; Dziga, D. Microcystinase – a Review of the Natural Occurrence, Heterologous Expression, and Biotechnological Application of MlrA. *Water Res.* **2021**, *189*, doi:10.1016/j.watres.2020.116646.

27. Choi, J.-M.; Han, S.-S.; Kim, H.-S. Industrial Applications of Enzyme Biocatalysis: Current Status and Future Aspects. *Biotechnol. Adv.* **2015**, *33*, 1443–1454, doi:10.1016/j.biotechadv.2015.02.014.

28. Li, Q.; Yi, L.; Marek, P.; Iverson, B.L. Commercial Proteases: Present and Future. *FEBS Lett.* **2013**, *587*, 1155–1163, doi:10.1016/j.febslet.2012.12.019.

29. Arnold, F.H. The Nature of Chemical Innovation: New Enzymes by Evolution. *Q. Rev. Biophys.* **2015**, *48*, 404–410, doi:10.1017/S003358351500013X.

30. Darcel, L.; Djibo, M.; Gaillard, M.; Raviglione, D.; Bonnard, I.; Banaigs, B.; Inguimbert, N. Trichormamide C Structural Confirmation through Total Synthesis and Extension to Analogs. *Org. Lett.* **2020**, *22*, 145–149, doi:10.1021/acs.orglett.9b04064.

31. Darcel, L.; Bornancin, L.; Raviglione, D.; Bonnard, I.; Mills, S.C.; Sáez-Vásquez, J.; Banaigs, B.; Inguimbert, N. D-Peptidase Activity in a Marine Mollusk Detoxifies a Nonribosomal Cyclic Lipopeptide: An Ecological Model to Study Antibiotic Resistance. *J. Med. Chem.* **2021**, *64*, 6198–6208, doi:10.1021/acs.jmedchem.1c00249.

32. Montaser, R.; Luesch, H. Marine Natural Products: A New Wave of Drugs? *Future Med. Chem.* **2011**, *3*, 1475–1489, doi:10.4155/fmc.11.118.

33. Martins, A.; Vieira, H.; Gaspar, H.; Santos, S. Marketed Marine Natural Products in the Pharmaceutical and Cosmeceutical Industries: Tips for Success. *Mar. Drugs* **2014**, *12*, 1066–1101, doi:10.3390/md12021066.

34. Singh, R.K.; Tiwari, S.P.; Rai, A.K.; Mohapatra, T.M. Cyanobacteria: An Emerging Source for Drug Discovery. *J. Antibiot. (Tokyo)* **2011**, *64*, 401–412, doi:10.1038/ja.2011.21.

35. Tan, L.T. Pharmaceutical Agents from Filamentous Marine Cyanobacteria. *Drug Discov. Today* **2013**, *18*, 863–871, doi:10.1016/j.drudis.2013.05.010.

36. Banaigs, B.; Bonnard, I.; Witczak, A.; Inguimbert, N. Marine Peptide Secondary Metabolites. In *Outstanding Marine Molecules*; La Barre, S., Kornprobst, J.-M., Eds.; Wiley-VCH Verlag GmbH & Co. KGaA: Weinheim, Germany, 2014; pp. 285–318 ISBN 978-3-527-68150-1.

37. Kehr, J.-C.; Gatte Picchi, D.; Dittmann, E. Natural Product Biosyntheses in Cyanobacteria: A Treasure Trove of Unique Enzymes. *Beilstein J. Org. Chem.* **2011**, *7*, 1622–1635, doi:10.3762/bjoc.7.191.

38. Clark, R.J.; Fischer, H.; Dempster, L.; Daly, N.L.; Rosengren, K.J.; Nevin, S.T.; Meunier, F.A.; Adams, D.J.; Craik, D.J. Engineering Stable Peptide Toxins by Means of Backbone Cyclization: Stabilization of the -Conotoxin MII. *Proc. Natl. Acad. Sci.* **2005**, *102*, 13767–13772, doi:10.1073/pnas.0504613102.

39. Cardillo, G.; Gentilucci, L.; Tolomelli, A. Unusual Amino Acids: Synthesis and Introduction into Naturally Occurring Peptides and Biologically Active Analogues. *Med. Chem.* **2006**, 293–304.

40. Gentilucci, L.; De Marco, R.; Cerisoli, L. Chemical Modifications Designed to Improve Peptide Stability: Incorporation of Non-Natural Amino Acids, Pseudo-Peptide Bonds, and Cyclization. *Curr. Pharm. Des.* **2010**, *16*, 3185–3203, doi:10.2174/138161210793292555.

41. Dennison, S.; Wallace, J.; Harris, F.; Phoenix, D. Amphiphilic Alpha-Helical Antimicrobial Peptides and Their Structure / Function Relationships. *Protein Pept. Lett.* **2005**, *12*, 31–39, doi:10.2174/0929866053406084.

42. Molinski, T.F. NMR of Natural Products at the 'Nanomole-Scale.' *Nat. Prod. Rep.* **2010**, *27*, 321–329, doi:10.1039/B920545B.

43. Fujii, K.; Ikai, Y.; Mayumi, T.; Oka, H.; Suzuki, M.; Harada, K. A Nonempirical Method Using LC/MS for Determination of the Absolute Configuration of Constituent Amino Acids in a Peptide: Elucidation of Limitations of Marfey's Method and of Its Separation Mechanism. *Anal. Chem.* **1997**, *69*, 3346–3352, doi:10.1021/ac9701795.

44. Frankmolle, W.P.; Larsen, L.K.; Caplan, F.R.; Patterson, G.M.L.; Knubel, G.; Levine, I.A.; Moore, R.E. Antifungal Cyclic Peptides from the Terrestrial Blue-Green Alga *Anabaena Laxa*. I. Isolation and Biological Properties. *J. Antibiot. (Tokyo)* **1992**, *45*, 1451–1457, doi:10.7164/antibiotics.45.1451.

45. Frankmolle, W.P.; Knubel, G.; Moore, E.; Patterson, G.M.L. Antifungal Cyclic Peptides from the Terrestrial Blue-Green Alga *Anabaena Laxa*. II. Structures of Laxaphycins A, B, C, D and E. *J. Antibiot. (Tokyo)* **1992**, *45*, 1458–1466, doi:10.7164/antibiotics.45.1458.

46. Bonnard, I.; Rolland, M.; Francisco, C.; Banaigs, B. Total Structure and Biological Properties of Laxaphycins A and B, Cyclic Lipopeptides from the Marine Cyanobacterium *Lyngbya Majuscula*. *Lett. Pept. Sci.* **1997**, *4*, 289–292, doi:10.1007/BF02442891.

47. Boyaud, F.; Mahiout, Z.; Lenoir, C.; Tang, S.; Wdzieczak-Bakala, J.; Witczak, A.; Bonnard, I.; Banaigs, B.; Ye, T.; Inguimbert, N. First Total Synthesis and Stereochemical Revision of Laxaphycin B and Its Extension to Lyngbyacyclamide A. *Org. Lett.* **2013**, *15*, 3898–3901, doi:10.1021/ol401645m.

48. Yoo, H.-D.; Nam, S.-J.; Chin, Y.-W.; Kim, M.-S. Misassigned Natural Products and Their Revised Structures. *Arch. Pharm. Res.* **2016**, *39*, 143–153, doi:10.1007/s12272-015-0649-9.

49. Cai, W.; Matthew, S.; Chen, Q.-Y.; Paul, V.J.; Luesch, H. Discovery of New A- and B-

Type Laxaphycins with Synergistic Anticancer Activity. *Bioorg. Med. Chem.* **2018**, *26*, 2310–2319, doi:10.1016/j.bmc.2018.03.022.

50. Sullivan, P.; Krunic, A.; Burdette, J.E.; Orjala, J. Laxaphycins B5 and B6 from the Cultured Cyanobacterium UIC 10484. *J. Antibiot. (Tokyo)* **2020**, *73*, 526–533, doi:10.1038/s41429-020-0301-x.

51. Gerwick, W.H.; Mrozek, Ch.; Moghaddam, M.F.; Agarwal, S.K. Novel Cytotoxic Peptides from the Tropical Marine Cyanobacterium *Hormothamnion Enteromorphoides* 1. Discovery, Isolation and Initial Chemical and Biological Characterization of the Hormothamnins from Wild and Cultured Material. *Experientia* **1989**, *45*, 115–121, doi:10.1007/BF01954842.

52. MacMillan, J.B.; Ernst-Russell, M.A.; de Ropp, J.S.; Molinski, T.F. Lobocyclamides A−C, Lipopeptides from a Cryptic Cyanobacterial Mat Containing *Lyngbya Confervoides*. *J. Org. Chem.* **2002**, *67*, 8210–8215, doi:10.1021/jo0261909.

53. Zhaxybayeva, O. Phylogenetic Analyses of Cyanobacterial Genomes: Quantification of Horizontal Gene Transfer Events. *Genome Res.* **2006**, *16*, 1099–1108, doi:10.1101/gr.5322306.

54. Alvariño, R.; Alonso, E.; Bornancin, L.; Bonnard, I.; Inguimbert, N.; Banaigs, B.; Botana, L.M. Biological Activities of Cyclic and Acyclic B-Type Laxaphycins in SH-SY5Y Human Neuroblastoma Cells. *Mar. Drugs* **2020**, *18*, 364, doi:10.3390/md18070364.

55. Gerwick, W.H.; Jiang, Z.D.; Agarwal, S.K.; Farmer, B.T. Total Structure of Hormothamnin A, a Toxic Cyclic Undecapeptide from the Tropical Marine Cyanobacterium *Hormothamnion Enteromorphoides*. *Tetrahedron* **1992**, *48*, 2313–2324, doi:10.1016/S0040-4020(01)88753-6.

56. Gerwick, W.H.; Jiang, Z.D.; Agarwal, S.K.; Farmer, B.T. Total Structure of Hormothamnin A, A Toxic Cyclic Undecapeptide from the Tropical Marine Cyanobacterium *Hormothamnion Enteromorphoides*. *Tetrahedron* **1992**, *48*, 5755, doi:10.1016/S0040-4020(01)90171-1.

57. Grewe, J.C. Cyanopeptoline und Scytocyclamide: Zyklische Peptide aus *Scytonema hofmanni* PCC 7110 Struktur und biologische Aktivität. Doctoral dissertation, Universität Freiburg im Breisgau, 2005.

58. Heinilä, L.M.P.; Fewer, D.P.; Jokela, J.K.; Wahlsten, M.; Jortikka, A.; Sivonen, K. Shared PKS Module in Biosynthesis of Synergistic Laxaphycins. *Front. Microbiol.* **2020**, *11*, doi:10.3389/fmicb.2020.578878.

59. Maru, N.; Ohno, O.; Uemura, D. Lyngbyacyclamides A and B, Novel Cytotoxic Peptides from Marine Cyanobacteria *Lyngbya* Sp. *Tetrahedron Lett.* **2010**, *51*, 6384–6387, doi:10.1016/j.tetlet.2010.06.105.

60. Luo, S.; Krunic, A.; Kang, H.-S.; Chen, W.-L.; Woodard, J.L.; Fuchs, J.R.; Swanson, S.M.; Orjala, J. Trichormamides A and B with Antiproliferative Activity from the Cultured

Freshwater Cyanobacterium *Trichormus* Sp. UIC 10339. *J. Nat. Prod.* **2014**, *77*, 1871–1880, doi:10.1021/np5003548.

61. Luo, S.; Kang, H.-S.; Krunic, A.; Chen, W.-L.; Yang, J.; Woodard, J.L.; Fuchs, J.R.; Hyun Cho, S.; Franzblau, S.G.; Swanson, S.M.; et al. Trichormamides C and D, Antiproliferative Cyclic Lipopeptides from the Cultured Freshwater Cyanobacterium Cf. *Oscillatoria* Sp. UIC 10045. *Bioorg. Med. Chem.* **2015**, *23*, 3153–3162, doi:10.1016/j.bmc.2015.04.073.

62. Gaillard, M.; Das, S.; Djibo, M.; Raviglione, D.; Roumestand, C.; Legrand, B.; Inguimbert, N. Towards the Total Synthesis of Trichormamide A, a Cyclic Undecapeptide. *Tetrahedron Lett.* **2018**, *59*, 3713–3718, doi:10.1016/j.tetlet.2018.09.010.

63. Heinilä, L.M.P.; Fewer, D.P.; Jokela, J.K.; Wahlsten, M.; Ouyang, X.; Permi, P.; Jortikka, A.; Sivonen, K. The Structure and Biosynthesis of Heinamides A1–A3 and B1–B5, Antifungal Members of the Laxaphycin Lipopeptide Family. *Org. Biomol. Chem.* **2021**, *19*, 5577–5588, doi:10.1039/D1OB00772F.

64. Yue, Q.; Chen, L.; Zhang, X.; Li, K.; Sun, J.; Liu, X.; An, Z.; Bills, G.F. Evolution of Chemical Diversity in Echinocandin Lipopeptide Antifungal Metabolites. *Eukaryot. Cell* **2015**, *14*, 698–718, doi:10.1128/EC.00076-15.

65. Gang, D.; Kim, D.; Park, H.-S. Cyclic Peptides: Promising Scaffolds for Biopharmaceuticals. *Genes* **2018**, *9*, 557, doi:10.3390/genes9110557.

66. Rezai, T.; Yu, B.; Millhauser, G.L.; Jacobson, M.P.; Lokey, R.S. Testing the Conformational Hypothesis of Passive Membrane Permeability Using Synthetic Cyclic Peptide Diastereomers. *J. Am. Chem. Soc.* **2006**, *128*, 2510–2511, doi:10.1021/ja0563455.

67. Xue, Y.; Zhao, P.; Quan, C.; Zhao, Z.; Gao, W.; Li, J.; Zu, X.; Fu, D.; Feng, S.; Bai, X.; et al. Cyanobacteria-Derived Peptide Antibiotics Discovered since 2000. *Peptides* **2018**, *107*, 17–24, doi:10.1016/j.peptides.2018.08.002.

68. Ghareeb, M.A.; Tammam, M.A.; El-Demerdash, A.; Atanasov, A.G. Insights about Clinically Approved and Preclinically Investigated Marine Natural Products. *Curr. Res. Biotechnol.* **2020**, *2*, 88–102, doi:10.1016/j.crbiot.2020.09.001.

69. Buron, F.; Turck, A.; Plé, N.; Bischoff, L.; Marsais, F. Towards a Biomimetic Synthesis of Barrenazine A. *Tetrahedron Lett.* **2007**, *48*, 4327–4330, doi:10.1016/j.tetlet.2007.04.108.

70. Boyaud, F. Synthèse totale de la laxaphycine B : un lipopeptide cyclique d'origine marine : extension à d'autres peptides apparentés. Doctoral dissertation, Montpellier University, 2013.

71. J. Hale, K.; Manaviazar, S.; M. Delisser, V. A Practical New Asymmetric Synthesis of (2S,3S)- and (2R,3R)-3-Hydroxyleucine. *Tetrahedron* **1994**, *50*, 9181–9188, doi:10.1016/S0040-4020(01)85384-9.

72. MacMillan, J.B.; Molinski, T.F. Lobocyclamide B from *Lyngbya Confervoides* . Configuration and Asymmetric Synthesis of β-Hydroxy-α-Amino Acids by (−)-Sparteine-Mediated Aldol Addition. *Org. Lett.* **2002**, *4*, 1883–1886, doi:10.1021/ol025876k.

73. Giltrap, A.M.; Haeckl, F.P.J.; Kurita, K.L.; Linington, R.G.; Payne, R.J. Total Synthesis of Skyllamycins A-C. *Chem. - Eur. J.* **2017**, *23*, 15046–15049, doi:10.1002/chem.201704277.

74. Ries, O.; Büschleb, M.; Granitzka, M.; Stalke, D.; Ducho, C. Amino Acid Motifs in Natural Products: Synthesis of *O*-Acylated Derivatives of (2*S*,3*S*)-3-Hydroxyleucine. *Beilstein J. Org. Chem.* **2014**, *10*, 1135–1142, doi:10.3762/bjoc.10.113.

75. Laib, T.; Chastanet, J.; Zhu, J. A Highly Stereoselective Synthesis of (2S,3S)-Beta-Hydroxyleucine. *Tetrahedron Lett.* **1997**, *38*, 1771–1772.

76. Davis, F.A.; Srirajan, V.; Fanelli, D.L.; Portonovo, P. Concise Asymmetric Synthesis of β-Hydroxy α-Amino Acids Using the Sulfinimine-Mediated Asymmetric Strecker Synthesis: Phenylserine and β-Hydroxyleucine. *J. Org. Chem.* **2000**, *65*, 7663–7666, doi:10.1021/jo000559h.

77. Nagamitsu, T.; Sunazuka, T.; Tanaka, H.; Ōmura, S.; Sprengeler, P.A.; Smith, A.B. Total Synthesis of (+)-Lactacystin. *J. Am. Chem. Soc.* **1996**, *118*, 3484–3590, doi:10.1021/ja9541544.

78. Kaur, H.; Harris, P.W.R.; Little, P.J.; Brimble, M.A. Total Synthesis of the Cyclic Depsipeptide YM-280193, a Platelet Aggregation Inhibitor. *Org. Lett.* **2015**, *17*, 492–495, doi:10.1021/ol503507g.

79. Makino, K.; Goto, T.; Hiroki, Y.; Hamada, Y. Stereoselective Synthesis of Anti -β-Hydroxy-α-amino Acids through Dynamic Kinetic Resolution. *Angew. Chem. Int. Ed.* **2004**, *43*, 882–884.

80. Boyaud, F.; Viguier, B.; Inguimbert, N. Synthesis of a Protected Derivative of (2R,3R)-β-Hydroxyaspartic Acid Suitable for Fmoc-Based Solid Phase Synthesis. *Tetrahedron Lett.* **2013**, *54*, 158–161, doi:10.1016/j.tetlet.2012.10.120.

81. Charvillon, F.B.; Amouroux, R. Synthesis of 3-Hydroxylated Analogues of D-Aspartic Acid β-Hydroxamate. *Synth. Commun.* **1997**, *27*, 395–403, doi:10.1080/00397919708006039.

82. Spengler, J.; Pelay, M.; Tulla-Puche, J.; Albericio, F. Synthesis of Orthogonally Protected L-Threo-β-Ethoxyasparagine. *Amino Acids* **2010**, *39*, 161–165, doi:10.1007/s00726-009-0389-6.

83. Inoue, M.; Shinohara, N.; Tanabe, S.; Takahashi, T.; Okura, K.; Itoh, H.; Mizoguchi, Y.; Iida, M.; Lee, N.; Matsuoka, S. Total Synthesis of the Large Non-Ribosomal Peptide Polytheonamide B. *Nat. Chem.* **2010**, *2*, 280–285, doi:10.1038/nchem.554.

84. Boger, D.L.; Lee, R.J.; Bounaud, P.-Y.; Meier, P. Asymmetric Synthesis of Orthogonally Protected L - *Threo* -β-Hydroxyasparagine. *J. Org. Chem.* **2000**, *65*, 6770–6772,

doi:10.1021/jo000628s.

85. Cardillo, G.; Gentilucci, L.; Tolomelli, A.; Tomasini, C. A Practical Method for the Synthesis of B-Amino a-Hydroxy Acids. Synthesis of Enantiomerically Pure Hydroxyaspartic Acid and Isoserine. *Synlett* **1999**, 1727–1730, doi:10.1055/s-1999-2927.

86. Kurokawa, N.; Ohfune, Y. Synthetic Studies on Antifungal Cyclic Peptides, Echinocandins. Stereoselective Total Synthesis of Echinocandin D via a Novel Peptide Coupling. *Tetrahedron* **1993**, *49*, 6195–6222, doi:10.1016/S0040-4020(01)87959-X.

87. Langlois, N.; Rakotondradany, F. Diastereoselective Synthesis of (2S,3S,4S)-3-Hydroxy-4-Methylproline, a Common Constituent of Several Antifungal Cyclopeptides. *Tetrahedron* **2000**, *56*, 2437–2448, doi:10.1016/S0040-4020(00)00117-4.

88. Carlsen, P.H.J.; Katsuki, T.; Martin, V.S.; Sharpless, K.B. A Greatly Improved Procedure for Ruthenium Tetroxide Catalyzed Oxidations of Organic Compounds | The Journal of Organic Chemistry. *J. Org. Chem.* **1981**, *46*, 3936–3938, doi:10.1021/jo00332a045.

89. Siodłak, D. α,β-Dehydroamino Acids in Naturally Occurring Peptides. *Amino Acids* **2015**, *47*, 1–17, doi:10.1007/s00726-014-1846-4.

90. Patel, H.C.; Singh, T.P.; Chauhan, V.S.; Kaur, P. Synthesis, Crystal Structure, and Molecular Conformation of Peptide N-Boc-L-Pro-Dehydro-Phe-L-Gly-OH. *Biopolymers* **1990**, *29*, 509–515, doi:https://doi.org/10.1002/bip.360290306.

91. Jain, R.; Chauhan, V.S. Conformational Characteristics of Peptides Containing α,β-Dehydroamino Acid Residues. *Biopolym. Pept. Sci.* **1996**, *40*, 105–119.

92. Goodall, K.; Parsons, A.F. A New and Efficient Preparation of α,β-Dehydroamino Acids. *Tetrahedron Lett.* **1995**, *36*, 3259–3260, doi:10.1016/0040-4039(95)00459-P.

93. Jiménez, J.C.; Nicolas, E.; Giralt, E.; Albericio, F. Synthesis of Peptides Containing α, β-Didehydroamino Acids. Scope and Limitations. *Lett. Pept. Sci.* **2002**, *9*, 135–141, doi:10.1007/BF02576876.

94. López-Macià, À.; Jiménez, J.C.; Royo, M.; Giralt, E.; Albericio, F. Synthesis and Structure Determination of Kahalalide F. *J. Am. Chem. Soc.* **2001**, *123*, 11398–11401, doi:10.1021/ja0116728.

95. Das, S. Methodological Development in Peptide Chemistry for Synthesis of Antimicrobial and Antifungal Derivatives of Marine Natural Peptides. Doctoral dissertation, University of Perpignan Via Domitia: Perpignan, 2018.

96. Ferreira, P.M.T.; Maia, H.L.S.; Monteiro, L.S.; Sacramento, J. High Yielding Synthesis of Dehydroamino Acid and Dehydropeptide Derivatives. *J. Chem. Soc. Perkin 1* **1999**, 3697–3703, doi:10.1039/a904730a.

97. Ferreira, P.M.T.; Monteiro, L.S.; Pereira, G.; Ribeiro, L.; Sacramento, J.; Silva, L. Reactivity of Dehydroamino Acids and Dehydrodipeptides TowardsN-Bromosuccinimide:

Synthesis of β-Bromo- and β,β-Dibromodehydroamino Acid Derivatives and of Substituted 4-Imidazolidinones. *Eur. J. Org. Chem.* **2007**, *2007*, 5934–5949, doi:10.1002/ejoc.200700669.

98. Tian, X.; Li, L.; Han, J.; Zhen, X.; Liu, S. Stereoselectively Synthesis and Structural Confirmation of Dehydrodipeptides with Dehydrobutyrine. *SpringerPlus* **2016**, *5*, doi:10.1186/s40064-016-2005-z.

99. Webster, A.M.; Coxon, C.R.; Kenwright, A.M.; Sandford, G.; Cobb, S.L. A Mild Method for the Synthesis of a Novel Dehydrobutyrine-Containing Amino Acid. *Tetrahedron* **2014**, *70*, 4661–4667, doi:10.1016/j.tet.2014.05.031.

100. Nagano, T.; Kinoshita, H. A New and Convenient Method for the Synthesis of Dehydroamino Acids Starting from Ethyl N-Boc- and N-Z-α-Tosylglycinates and Various Nitro Compounds. *Bull. Chem. Soc. Jpn.* **2000**, *73*, 1605–1613.

101. Bonauer, C.; Walenzyk, T.; König, B. α,β-Dehydroamino Acids. *SYNTHESIS* **2006**, 1–20, doi:10.1055/s-2005-921759.

102. Kim, E.; Moore, B.S.; Yoon, Y.J. Reinvigorating Natural Product Combinatorial Biosynthesis with Synthetic Biology. *Nat. Chem. Biol.* **2015**, *11*, 649–659, doi:10.1038/nchembio.1893.

103. Süssmuth, R.D.; Mainz, A. Nonribosomal Peptide Synthesis-Principles and Prospects. *Angew. Chem. Int. Ed.* **2017**, *56*, 3770–3821, doi:10.1002/anie.201609079.

104. Walsh, C.T.; O'Brien, R.V.; Khosla, C. Nonproteinogenic Amino Acid Building Blocks for Nonribosomal Peptide and Hybrid Polyketide Scaffolds. *Angew. Chem. Int. Ed.* **2013**, *52*, 7098–7124, doi:10.1002/anie.201208344.

105. Kim, W.E.; Patel, A.; Hur, G.H.; Tufar, P.; Wuo, M.G.; McCammon, J.A.; Burkart, M.D. Mechanistic Probes for the Epimerization Domain of Nonribosomal Peptide Synthetases. *Chembiochem Eur. J. Chem. Biol.* **2019**, *20*, 147–152, doi:10.1002/cbic.201800439.

106. Cryle, M.J.; Brieke, C.; Haslinger, K. Oxidative transformations of amino acids and peptides catalysed by Cytochromes P450. In *Amino Acids, Peptides And Proteins*; Farkas, E., Ryadnov, M., Eds.; Royal Society of Chemistry: Cambridge, 2013; Vol. 38, pp. 1–36 ISBN 978-1-84973-585-8.

107. Winn, M.; Fyans, J.K.; Zhuo, Y.; Micklefield, J. Recent Advances in Engineering Nonribosomal Peptide Assembly Lines. *Nat. Prod. Rep.* **2016**, *33*, 317–347, doi:10.1039/C5NP00099H.

108. Miyanaga, A.; Kudo, F.; Eguchi, T. Protein–Protein Interactions in Polyketide Synthase–Nonribosomal Peptide Synthetase Hybrid Assembly Lines. *Nat. Prod. Rep.* **2018**, *35*, 1185–1209, doi:10.1039/C8NP00022K.

109. Wang, H.; Fewer, D.P.; Holm, L.; Rouhiainen, L.; Sivonen, K. Atlas of Nonribosomal Peptide and Polyketide Biosynthetic Pathways Reveals Common Occurrence of Nonmodular

Enzymes. *Proc. Natl. Acad. Sci.* **2014**, *111*, 9259–9264, doi:10.1073/pnas.1401734111.

110. Hou, J.; Robbel, L.; Marahiel, M.A. Identification and Characterization of the Lysobactin Biosynthetic Gene Cluster Reveals Mechanistic Insights into an Unusual Termination Module Architecture. *Chem. Biol.* **2011**, *18*, 655–664, doi:10.1016/j.chembiol.2011.02.012.

111. Strieker, M.; Kopp, F.; Mahlert, C.; Essen, L.-O.; Marahiel, M.A. Mechanistic and Structural Basis of Stereospecific Cβ-Hydroxylation in Calcium-Dependent Antibiotic, a Daptomycin-Type Lipopeptide. *ACS Chem. Biol.* **2007**, *2*, 187–196, doi:10.1021/cb700012y.

112. Strieker, M.; Nolan, E.M.; Walsh, C.T.; Marahiel, M.A. Stereospecific Synthesis of *Threo* - and *Erythro* -β-Hydroxyglutamic Acid During Kutzneride Biosynthesis. *J. Am. Chem. Soc.* **2009**, *131*, 13523–13530, doi:10.1021/ja9054417.

113. Uhlmann, S.; Süssmuth, R.D.; Cryle, M.J. Cytochrome P450 $_{sky}$ Interacts Directly with the Nonribosomal Peptide Synthetase to Generate Three Amino Acid Precursors in Skyllamycin Biosynthesis. *ACS Chem. Biol.* **2013**, *8*, 2586–2596, doi:10.1021/cb400555e.

114. Fu, C.; Keller, L.; Bauer, A.; Brönstrup, M.; Froidbise, A.; Hammann, P.; Herrmann, J.; Mondesert, G.; Kurz, M.; Schiell, M.; et al. Biosynthetic Studies of Telomycin Reveal New Lipopeptides with Enhanced Activity. *J. Am. Chem. Soc.* **2015**, *137*, 7692–7705, doi:10.1021/jacs.5b01794.

115. Parkinson, E.I.; Tryon, J.H.; Goering, A.W.; Ju, K.-S.; McClure, R.A.; Kemball, J.D.; Zhukovsky, S.; Labeda, D.P.; Thomson, R.J.; Kelleher, N.L.; et al. Discovery of the Tyrobetaine Natural Products and Their Biosynthetic Gene Cluster *via* Metabologenomics. *ACS Chem. Biol.* **2018**, *13*, 1029–1037, doi:10.1021/acschembio.7b01089.

116. Li, Y.; Lan, N.; Xu, L.; Yue, Q. Biosynthesis of Pneumocandin Lipopeptides and Perspectives for Its Production and Related Echinocandins. *Appl. Microbiol. Biotechnol.* **2018**, *102*, 9881–9891, doi:10.1007/s00253-018-9382-x.

117. Mattay, J.; Houwaart, S.; Hüttel, W. Cryptic Production of *Trans*-3-Hydroxyproline in Echinocandin B Biosynthesis. *Appl. Environ. Microbiol.* **2018**, *84*, doi:10.1128/AEM.02370-17.

118. Gu, G.; Smith, L.; Liu, A.; Lu, S.-E. Genetic and Biochemical Map for the Biosynthesis of Occidiofungin, an Antifungal Produced by *Burkholderia Contaminans* Strain MS14. *Appl. Environ. Microbiol.* **2011**, *77*, 6189–6198, doi:10.1128/AEM.00377-11.

119. Freeman, M.F.; Gurgui, C.; Helf, M.J.; Morinaka, B.I.; Uria, A.R.; Oldham, N.J.; Sahl, H.-G.; Matsunaga, S.; Piel, J. Metagenome Mining Reveals Polytheonamides as Posttranslationally Modified Ribosomal Peptides. *Science* **2012**, *338*, 387–390, doi:10.1126/science.1226121.

120. McAuliffe, O.; Ross, R.P.; Hill, C. Lantibiotics: Structure, Biosynthesis and Mode of Action. *FEMS Microbiol. Rev.* **2001**, *25*, 285–308, doi:10.1111/j.1574-6976.2001.tb00579.x.

121. Willey, J.M.; van der Donk, W.A. Lantibiotics: Peptides of Diverse Structure and Function. *Annu. Rev. Microbiol.* **2007**, *61*, 477–501, doi:10.1146/annurev.micro.61.080706.093501.

122. You, Y.O.; van der Donk, W.A. Mechanistic Investigations of the Dehydration Reaction of Lacticin 481 Synthetase Using Site-Directed Mutagenesis. *Biochemistry* **2007**, *46*, 5991–6000, doi:10.1021/bi602663x.

123. Wieland Brown, L.C.; Acker, M.G.; Clardy, J.; Walsh, C.T.; Fischbach, M.A. Thirteen Posttranslational Modifications Convert a 14-Residue Peptide into the Antibiotic Thiocillin. *Proc. Natl. Acad. Sci.* **2009**, *106*, 2549–2553, doi:10.1073/pnas.0900008106.

124. Malcolmson, S.J.; Young, T.S.; Ruby, J.G.; Skewes-Cox, P.; Walsh, C.T. The Posttranslational Modification Cascade to the Thiopeptide Berninamycin Generates Linear Forms and Altered Macrocyclic Scaffolds. *Proc. Natl. Acad. Sci.* **2013**, *110*, 8483–8488, doi:10.1073/pnas.1307111110.

125. Kelly, W.L.; Pan, L.; Li, C. Thiostrepton Biosynthesis: Prototype for a New Family of Bacteriocins. *J. Am. Chem. Soc.* **2009**, *131*, 4327–4334, doi:10.1021/ja807890a.

126. Liao, R.; Duan, L.; Lei, C.; Pan, H.; Ding, Y.; Zhang, Q.; Chen, D.; Shen, B.; Yu, Y.; Liu, W. Thiopeptide Biosynthesis Featuring Ribosomally Synthesized Precursor Peptides and Conserved Posttranslational Modifications. *Chem. Biol.* **2009**, *16*, 141–147, doi:10.1016/j.chembiol.2009.01.007.

127. Yu, Y.; Duan, L.; Zhang, Q.; Liao, R.; Ding, Y.; Pan, H.; Wendt-Pienkowski, E.; Tang, G.; Shen, B.; Liu, W. Nosiheptide Biosynthesis Featuring a Unique Indole Side Ring Formation on the Characteristic Thiopeptide Framework. *ACS Chem. Biol.* **2009**, *4*, 855–864, doi:10.1021/cb900133x.

128. Moffitt, M.C.; Neilan, B.A. Characterization of the Nodularin Synthetase Gene Cluster and Proposed Theory of the Evolution of Cyanobacterial Hepatotoxins. *Appl. Environ. Microbiol.* **2004**, *70*, 6353–6362, doi:10.1128/AEM.70.11.6353-6362.2004.

129. Scholz-Schroeder, B.K.; Soule, J.D.; Lu, S.-E.; Grgurina, I.; Gross, D.C. A Physical Map of the Syringomycin and Syringopeptin Gene Clusters Localized to an Approximately 145-Kb DNA Region of *Pseudomonas Syringae* Pv. *Syringae* Strain B301D. *Mol. Plant-Microbe Interactions®* **2001**, *14*, 1426–1435, doi:10.1094/MPMI.2001.14.12.1426.

130. McIntosh, J.A.; Donia, M.S.; Schmidt, E.W. Ribosomal Peptide Natural Products: Bridging the Ribosomal and Nonribosomal Worlds. *Nat. Prod. Rep.* **2009**, *26*, 537, doi:10.1039/b714132g.

131. Tillett, D.; Dittmann, E.; Erhard, M.; von Döhren, H.; Börner, T.; Neilan, B.A. Structural Organization of Microcystin Biosynthesis in Microcystis Aeruginosa PCC7806: An Integrated Peptide–Polyketide Synthetase System. *Chem. Biol.* **2000**, *7*, 753–764, doi:10.1016/S1074-5521(00)00021-1.

132. Liu, W.-T.; Lamsa, A.; Wong, W.R.; Boudreau, P.D.; Kersten, R.; Peng, Y.; Moree, W.J.; Duggan, B.M.; Moore, B.S.; Gerwick, W.H.; et al. MS/MS-Based Networking and Peptidogenomics Guided Genome Mining Revealed the Stenothricin Gene Cluster in *Streptomyces Roseosporus*. *J. Antibiot. (Tokyo)* **2014**, *67*, 99–104, doi:10.1038/ja.2013.99.

133. Mareš, J.; Hájek, J.; Urajová, P.; Kopecky, J.; Hrouzek, P. A Hybrid Non-Ribosomal Peptide/Polyketide Synthetase Containing Fatty-Acyl Ligase (FAAL) Synthesizes the b-Amino Fatty Acid Lipopeptides Puwainaphycins in the Cyanobacterium *Cylindrospermum Alatosporum*. *PLoS ONE* **2014**, *9*, doi:10.1371/journal.pone.0111904.

134. Mareš, J.; Hájek, J.; Urajová, P.; Kust, A.; Jokela, J.; Saurav, K.; Galica, T.; Čapková, K.; Mattila, A.; Haapaniemi, E.; et al. Alternative Biosynthetic Starter Units Enhance the Structural Diversity of Cyanobacterial Lipopeptides. *Appl. Environ. Microbiol.* **2018**, *85*, e02675-18, /aem/85/4/AEM.02675-18.atom, doi:10.1128/AEM.02675-18.

135. Nishizawa, T.; Asayama, M.; Fujii, K.; Harada, K. -i.; Shirai, M. Genetic Analysis of the Peptide Synthetase Genes for a Cyclic Heptapeptide Microcystin in *Microcystis* Spp. *J. Biochem. (Tokyo)* **1999**, *126*, 520–529, doi:10.1093/oxfordjournals.jbchem.a022481.

136. Duitman, E.H.; Hamoen, L.W.; Rembold, M.; Venema, G.; Seitz, H.; Saenger, W.; Bernhard, F.; Reinhardt, R.; Schmidt, M.; Ullrich, C.; et al. The Mycosubtilin Synthetase of *Bacillus Subtilis* ATCC6633: A Multifunctional Hybrid between a Peptide Synthetase, an Amino Transferase, and a Fatty Acid Synthase. *Proc. Natl. Acad. Sci.* **1999**, *96*, 13294–13299, doi:10.1073/pnas.96.23.13294.

137. Markolovic, S.; Leissing, T.M.; Chowdhury, R.; Wilkins, S.E.; Lu, X.; Schofield, C.J. Structure–Function Relationships of Human JmjC Oxygenases—Demethylases versus Hydroxylases. *Curr. Opin. Struct. Biol.* **2016**, *41*, 62–72, doi:10.1016/j.sbi.2016.05.013.

138. Liu, L.; Budnjo, A.; Jokela, J.; Haug, B.E.; Fewer, D.P.; Wahlsten, M.; Rouhiainen, L.; Permi, P.; Fossen, T.; Sivonen, K. Pseudoaeruginosins, Nonribosomal Peptides in *Nodularia Spumigena*. *ACS Chem. Biol.* **2015**, *10*, 725–733, doi:10.1021/cb5004306.

139. Leão, P.N.; Engene, N.; Antunes, A.; Gerwick, W.H.; Vasconcelos, V. The Chemical Ecology of Cyanobacteria. *Nat. Prod. Rep.* **2012**, *29*, 372–391, doi:10.1039/c2np00075j.

140. Gbankoto, A.; Vigo, J.; Dramane, K.; Banaigs, B.; Aina, E.; Salmon, J.-M. Cytotoxic Effect of Laxaphycins A and B on Human Lymphoblastic Cells (CCRF-CEM) Using Digitised Videomicrofluorometry. *In Vivo* **2005**, *19*, 577–582.

141. Dussault, D.; Vu, K.D.; Vansach, T.; Horgen, F.D.; Lacroix, M. Antimicrobial Effects of Marine Algal Extracts and Cyanobacterial Pure Compounds against Five Foodborne Pathogens. *Food Chem.* **2016**, *199*, 114–118, doi:10.1016/j.foodchem.2015.11.119.

142. Xie, Y.; Wang, B.; Liu, J.; Zhou, J.; Ma, J.; Huang, H.; Ju, J. Identification of the Biosynthetic Gene Cluster and Regulatory Cascade for the Synergistic Antibacterial Antibiotics Griseoviridin and Viridogrisein in *Streptomyces Griseoviridis*. *ChemBioChem* **2012**, *13*, 2745–

2757, doi:10.1002/cbic.201200584.

143. Pennings, S.C.; Pablo, S.R.; Paul, V.J. Chemical Defenses of the Tropical, Benthic Marine Cyanobacterium *Hormothamnion Enteromorphoides*: Diverse Consumers and Synergisms. *Limnol. Oceanogr.* **1997**, *42*, 911–917, doi:10.4319/lo.1997.42.5.0911.

144. Capper, A.; Erickson, A.A.; Ritson-Williams, R.; Becerro, M.A.; Arthur, K.A.; Paul, V.J. Palatability and Chemical Defences of Benthic Cyanobacteria to a Suite of Herbivores. *J. Exp. Mar. Biol. Ecol.* **2016**, *474*, 100–108, doi:10.1016/j.jembe.2015.09.008.

145. Hoffmann, D.; Hevel, J.M.; Moore, R.E.; Moore, B.S. Sequence Analysis and Biochemical Characterization of the Nostopeptolide A Biosynthetic Gene Cluster from *Nostoc* Sp. GSV224. *Gene* **2003**, *311*, 171–180, doi:10.1016/S0378-1119(03)00587-0.

146. Montalbetti, C.A.G.N.; Falque, V. Amide Bond Formation and Peptide Coupling. *Tetrahedron* **2005**, *61*, 10827–10852, doi:10.1016/j.tet.2005.08.031.

147. Valeur, E.; Bradley, M. Amide Bond Formation: Beyond the Myth of Coupling Reagents. *Chem Soc Rev* **2009**, *38*, 606–631, doi:10.1039/B701677H.

148. Chandrudu, S.; Simerska, P.; Toth, I. Chemical Methods for Peptide and Protein Production. *molecules* **2013**, *18*, 4373–4388, doi:10.3390/molecules18044373.

149. Okada, Y. Synthesis of Peptides by Solution Methods. *Curr. Org. Chem.* **2001**, *5*, 1–43, doi:10.2174/1385272013375733.

150. du Vigneaud, V.; Ressler, C.; Swan, J.M.; Roberts, C.W.; Katsoyannis, P.G. The Synthesis of Oxytocin. *J. Am. Chem. Soc.* **1954**, *76*, 3115–3121, doi:doi.org/10.1021/ja01641a004.

151. Jou, G.; Gonzalez, I.; Albericio, F.; Lloyd-Williams, P.; Giralt, E. Total Synthesis of Dehydrodidemnin B. Use of Uronium and Phosphonium Salt Coupling Reagents in Peptide Synthesis in Solution. *J. Org. Chem.* **1997**, *62*, 354–366, doi:10.1021/jo961932h.

152. Maurin, O.; Verdié, P.; Subra, G.; Lamaty, F.; Martinez, J.; Métro, T.-X. Peptide Synthesis: Ball-Milling, in Solution, or on Solid Support, What Is the Best Strategy? *Beilstein J. Org. Chem.* **2017**, *13*, 2087–2093, doi:10.3762/bjoc.13.206.

153. Pawlas, J.; Antonic, B.; Lundqvist, M.; Svensson, T.; Finnman, J.; Rasmussen, J.H. 2D Green SPPS: Green Solvents for on-Resin Removal of Acid Sensitive Protecting Groups and Lactamization. *Green Chem.* **2019**, *21*, 2594–2600, doi:10.1039/C9GC00898E.

154. Ferrazzano, L.; Corbisiero, D.; Martelli, G.; Tolomelli, A.; Viola, A.; Ricci, A.; Cabri, W. Green Solvent Mixtures for Solid-Phase Peptide Synthesis: A Dimethylformamide-Free Highly Efficient Synthesis of Pharmaceutical-Grade Peptides. *ACS Sustain. Chem. Eng.* **2019**, *7*, 12867–12877, doi:10.1021/acssuschemeng.9b01766.

155. Declerck, V.; Nun, P.; Martinez, J.; Lamaty, F. Solvent-Free Synthesis of Peptides. *Angew. Chem. Int. Ed.* **2009**, *48*, 9318–9321, doi:https://doi.org/10.1002/anie.200903510.

156. Mahindra, A.; Patel, N.; Bagra, N.; Jain, R. Solvent-Free Peptide Synthesis Assisted by Microwave Irradiation: Environmentally Benign Synthesis of Bioactive Peptides. *RSC Adv.* **2013**, *4*, 3065–3069, doi:10.1039/C3RA46643D.

157. Thapa, P.; Zhang, R.-Y.; Menon, V.; Bingham, J.-P. Native Chemical Ligation: A Boon to Peptide Chemistry. *molecules* **2014**, *19*, 14461–14483, doi:10.3390/molecules190914461.

158. Amblard, M.; Fehrentz, J.-A.; Martinez, J.; Subra, G. Methods and Protocols of Modern Solid Phase Peptide Synthesis. *Mol. Biotechnol.* **2006**, *33*, 16.

159. Davies, J.S. The Cyclization of Peptides and Depsipeptides. *J. Pept. Sci.* **2003**, *9*, 471–501, doi:10.1002/psc.491.

160. C. Hayes, H.; P. Luk, L.Y.; Tsai, Y.-H. Approaches for Peptide and Protein Cyclisation. *Org. Biomol. Chem.* **2021**, *19*, 3983–4001, doi:10.1039/D1OB00411E.

161. Malesevic, M.; Strijowski, U.; Bächle, D.; Sewald, N. An Improved Method for the Solution Cyclization of Peptides under Pseudo-High Dilution Conditions. *J. Biotechnol.* **2004**, *112*, 73–77, doi:10.1016/j.jbiotec.2004.03.015.

162. Bornancin, L.; Boyaud, F.; Mahiout, Z.; Bonnard, I.; Mills, S.C.; Banaigs, B.; Inguimbert, N. Isolation and Synthesis of Laxaphycin B-Type Peptides: A Case Study and Clues to Their Biosynthesis. *Mar. Drugs* **2015**, *13*, 7285–7300, doi:10.3390/md13127065.

163. Gude, M.; Ryf, J.; White, P.D. An Accurate Method for the Quantitation of Fmoc-Derivatized Solid Phase Supports. *Lett. Pept. Sci.* **2002**, *9*, 203–206, doi:10.1007/BF02538384.

164. Echalier, C.; Al-Halifa, S.; Kreiter, A.; Enjalbal, C.; Sanchez, P.; Ronga, L.; Puget, K.; Verdié, P.; Amblard, M.; Martinez, J.; et al. Heating and Microwave Assisted SPPS of C-Terminal Acid Peptides on Trityl Resin: The Truth behind the Yield. *Amino Acids* **2013**, *45*, 1395–1403, doi:10.1007/s00726-013-1604-z.

165. Albericio, F.; El-Faham, A. Choosing the Right Coupling Reagent for Peptides: A Twenty-Five-Year Journey. *Org. Process Res. Dev.* **2018**, *22*, 760–772, doi:10.1021/acs.oprd.8b00159.

166. El-Faham, A.; Albericio, F. Peptide Coupling Reagents, More than a Letter Soup. *Chem. Rev.* **2011**, *111*, 6557–6602, doi:10.1021/cr100048w.

167. Bradford, M.M. A Rapid and Sensitive Method for the Quantitation of Microgram Quantities of Protein Utilizing the Principle of Protein-Dye Binding. *Anal. Biochem.* **1976**, *72*, 248–254, doi:10.1016/0003-2697(76)90527-3.

168. Li, Y.-X.; Zhong, Z.; Hou, P.; Zhang, W.-P.; Qian, P.-Y. Resistance to Nonribosomal Peptide Antibiotics Mediated by D-Stereospecific Peptidases. *Nat. Chem. Biol.* **2018**, *14*, 381–387, doi:10.1038/s41589-018-0009-4.

169. Schechter, I.; Berger, A. On the Size of the Active Site in Proteases. I. Papain. *Biochem. Biophys. Res. Commun.* **1967**, *27*, 157–162, doi:10.1016/S0006-291X(67)80055-X.

170. Poreba, M.; Drag, M. Current Strategies for Probing Substrate Specificity of Proteases. *Curr. Med. Chem.* **2010**, *17*, 3968–3995, doi:10.2174/092986710793205381.

171. Kasperkiewicz, P.; Poreba, M.; Groborz, K.; Drag, M. Emerging Challenges in the Design of Selective Substrates, Inhibitors and Activity-Based Probes for Indistinguishable Proteases. *Febs J.* **2017**, *284*, 1518–1539, doi:10.1111/febs.14001.

172. Kato, H.; Imanishi, S.Y.; Tsuji, K.; Harada, K. Microbial Degradation of Cyanobacterial Cyclic Peptides. *Water Res.* **2007**, *41*, 1754–1762, doi:10.1016/j.watres.2007.01.003.

173. Toruńska-Sitarz, A.; Kotlarska, E.; Mazur-Marzec, H. Biodegradation of Nodularin and Other Nonribosomal Peptides by the Baltic Bacteria. *Int. Biodeterior. Biodegrad.* **2018**, *134*, 48–57, doi:10.1016/j.ibiod.2018.08.004.

174. Meziane-Cherif, D.; Stogios, P.J.; Evdokimova, E.; Savchenko, A.; Courvalin, P. Structural Basis for the Evolution of Vancomycin Resistance D,D-Peptidases. *Proc. Natl. Acad. Sci.* **2014**, *111*, 5872–5877, doi:10.1073/pnas.1402259111.

Résumé

En raison du changement climatique, le lagon de Moorea en Polynésie Française est impacté par des efflorescences de cyanobactéries asphyxiant les coraux, causant la dégradation de récif et diminuant les ressources en nourriture. *Lyngbya majuscula* et *Anabaena torulosa* sont deux cyanobactéries benthiques filamenteuses qui prolifèrent sur le sable et les coraux. Elles produisent de nombreux métabolites secondaires pouvant être toxiques. *Anabaena torulosa* produit notamment des lipopeptides cycliques tels que les laxaphycins A et B, composés de 11 et 12 acides aminés, respectivement. Cette cyanobactérie a pu développer des stratégies chimiques de protection contre les brouteurs, pouvant être repoussés par les molécules toxiques produites telle que la laxaphycin B. A leur tour, les herbivores doivent contourner ces défenses et dans certains cas, ils en profitent même pour se mettre à l'abri de leurs propres prédateurs. C'est le cas de *Stylocheilus striatus*, un lièvre de mer qui se nourrit de *Lyngbya majuscula* et *Anabaena torulosa* et qui semble moins exposé à la prédation sur *Anabaena torulosa*. *Stylocheilus striatus* consomme cette dernière sans être affecté par la toxicité de la laxaphycin B. Afin de contourner cette toxicité, le lièvre de mer a mis en place un mécanisme d'adaptation permettant la biotransformation de la laxaphycin B en laxaphycin B acyclique non toxique. Alors que la laxaphycin A non toxique est bio-accumulée dans sa glande digestive, la laxaphycin B subit deux clivages successifs en position C-terminale de deux hydroxyleucines. Afin d'étudier le mécanisme enzymatique engagé dans cette biotransformation, nous avons synthétisé divers analogues de la laxaphycin B. Dans un premier temps, nous avons optimisé leur synthèse chimique, nous permettant également de confirmer la structure du trichormamide C, un peptide naturel analogue à la laxaphycin B. Dans un second temps, les analogues synthétisés ont pu être soumis à l'enzyme étudiée et ont montré la reproductibilité du clivage sur différentes séquences. Des premières caractéristiques de l'enzyme ont pu être identifiées, telles que ses spécificités de clivage. Enfin, nos efforts se sont concentrés sur le design d'une séquence peptidique minimale pour la reconnaissance de l'enzyme, afin d'envisager différentes stratégies pour l'isoler.

Mots-clés: Biotransformation ; Peptidase ; Lipopeptide cyclique ; Synthèse peptidique ; Cyanobactérie

Abstract

Due to climate change, the lagoon of Moorea in French Polynesia is impacted by cyanobacteria blooms asphyxiating corals, causing reef degradation and decreasing food resources. *Lyngbya majuscula* and *Anabaena torulosa* are two filamentous benthic cyanobacteria that proliferate on sand and corals. They produce many secondary metabolites that can be toxic. *Anabaena torulosa* produces cyclic lipopeptides such as laxaphycins A and B, composed of 11 and 12 amino acids, respectively. This cyanobacterium has been able to develop chemical strategies of protection against grazers, which can be repelled by the toxic molecules produced such as laxaphycin B. In turn, herbivores must circumvent these defenses and in some cases even take advantage of them to protect themselves from their own predators. This is the case of *Stylocheilus striatus*, a sea hare that feeds on *Lyngbya majuscula* and *Anabaena torulosa*, and appears to be less susceptible to predation on *Anabaena torulosa*. *Stylocheilus striatus* consumes the latter without being affected by laxaphycin B toxicity. To overcome this toxicity, the sea hare has developed an adaptive mechanism that allows the biotransformation of laxaphycin B into non-toxic acyclic laxaphycin B. While non-toxic laxaphycin A is bioaccumulated in its digestive gland, laxaphycin B undergoes two successive cleavages at the C-terminal position of two hydroxyleucines. In order to study the enzymatic mechanism involved in this biotransformation, we have synthesized various analogues of laxaphycin B. First, we optimized their chemical synthesis, allowing us to confirm the structure of trichormamide C, a natural peptide analogous to laxaphycin B. In a second step, the synthesized analogues could be submitted to the studied enzyme and showed the reproducibility of the cleavage on different sequences. First characteristics of the enzyme could be identified, such as its cleavage specificities. Finally, our efforts focused on the design of a minimal peptide sequence for the recognition of the enzyme, in order to consider different strategies to isolate it.

Keywords: Biotransformation ; Peptidase ; Cyclic lipopeptide ; Peptide synthesis ; Cyanobacteria